LANDUSE IMPACTS ON WATER RESOURCES MANAGEMENT IN A DATA-SCARCE WATERSHED OF THE EQUATORIAL NILE: CASE STUDY OF THE SEMLIKI.

Jean-Marie Kileshye Onema

A thesis submitted to the Faculty of Engineering and the Built Environment, University of the Witwatersrand, Johannesburg, in fulfillment of the requirements for the degree of Doctor of Philosophy.

Johannesburg, 2011

DECLARATION

I declare that this thesis is my own unaided work. It is being submitted to the degree of Doctor of Philosophy to the University of the Witwatersrand, Johannesburg. It has not been submitted before for any degree or examination to any other University.

DEDICATION

To my Mother Thérèse Yvonne Kileshye Nakunda and my late father Jean-Marie Onema Omanga. Thank you for the gift of life, your continued support and unwavering love.

To Yvon, Gracia, Sophie and those to come, may this work ignite your passion in the search for excellence.

To my wife Jolie and Sister Gracia, your love, support, advises and prayers kept me going.

ABSTRACT

Data availability in developing countries for water management, planning and design constitutes a challenge for comprehensive spatial and temporal studies. Prediction in Ungauged Basin (PUB) is an on-going area of research of modern hydrology.

The Nile is the world's longest stream which, depending on the time of the year, water travels for about 20 days in the Blue Nile tributary and more than 45 days for in White Nile tributary. Intermediate and long term flow prediction for the Nile is crucial for the management and operation of the existing water control infrastructures from the Central and Eastern parts of Africa up to Egypt via the middle reaches (Sudan). An effective and appropriate way to study the vast Nile is to work at subbasin level and this study aims at providing a rational approach for flow prediction in the Semliki watershed- one of the waterheads of the White Nile.

This thesis deals with the assessment of landscape interactions with water resources in the data scarce Semliki watershed of the Equatorial Nile. Using a combination of limited ground information, remotely sensed acquired datasets, GIS and statistical techniques, conceptual deterministic, mesoscale hydrologic models for the catchment were developed.

One of the outputs from this work is the development of a new equation for the correction of the FEWS-NOAA satellite generated rainfall for the Semliki watershed. It takes into account the spatial and temporal dynamics of rainfall for the catchment. This is valuable for planners and managers of the water resources of the watershed who hitherto had relied only on one rainfall gauging station at Beni.

The identification and grouping of similar subcatchments of the Semliki watershed from landscape attributes using ordination techniques and clustering analysis was performed. The ordination technique, namely the Principal Component Analysis, was further used in identifying data structure and redundant variables (landscape attributes) and subsequently guided the development of optimal model dimensions.

Using regression-based techniques, monthly linear and non-linear deterministic prediction models were developed to predict flows within Semliki subcatchments from the physiographic attributes.

Step-wise temporal and spatial sensitive analysis of the monthly flow on the variation of physiographic attributes was carried out for both the linear and non linear predictive models. The stream length of catchment was found to be generally most sensitive.

While providing water managers and planners with useful tools in a data-poor watershed, this study calls for urgent steps to be taken in acquiring Hydro meteorological data that can support further investigations into physically based modelling approaches that explicitly account for the interaction between landscape attributes and water resources in the Semliki watershed of the equatorial Nile region.

ACKNOWLEDGEMENTS

I would like to express my heartfelt thanks to the many people who have helped me to complete this thesis, either materially or with encouragements. First and foremost, to my supervisor Professor Akpofure Taigbenu for your valuable, detailed and careful guidance and contributions in helping me with the final production, none of it would have happened without your dedication.

To the Applied Training Project of the Nile Basin Initiative and the Post Graduate Merit Award Committee of the University of the Witwatersrand, and lately WaterNet for providing adequate funding support throughout. I hope that both others and I will find this work useful in supporting NBI's, WaterNet's and University's noble goals of capacity building in the society.

To Dr. John Ndiritu and Professor Vincent Lukanda for your critical and constructive inputs.

To Fundiswa Rula, for your endless encouragements, availability and patience in the production of my thesis, you have been a key person to me, thank you.

Data used in this study were provided by the Regional Remote Sensing Unit of the Southern African Development Community (RRSU/SADC), the National Oceanic and Atmospheric Administration of the American National Aeronautics and Space Administration (NOAA/NASA), the Ugandan Water Directorate and the Congolese meteorological services in Beni. The assistance provided by these organizations is gratefully acknowledged.

To my brother Jean-Marc Mwenge Kahinda, friends and colleagues Zacharia Katambara and Paul Kagoda for the fruitful discussions and the encouragement. I

hope that you all gained as much from these interactions as I have gained from working with you. May God bless your lives and all your efforts.

CONTENTS

LIST OF FIGURES

LIST OF TABLES

LIST OF EQUATIONS

LIST OF SYMBOLS

A	Area
Dd	Drainage density
df	degree of freedom
E	Evapotranspiration rate
ET	Evapotranspiration
ET_a	actual evapotranspiration
G_0	soil heat flux
H	sensible heat flux
I	Inflow
L	Length of stream
Λ	instantaneous evaporative fraction
L'	Fractal stream length
λ	latent heat of vaporization
λE	instantaneous latent heat flux
O	Outflow
Phi	Glaeson – Staelin index
r	correlation coefficient
R^2	coefficient of multiple determinations
R^2_{adj}	adjusted R^2
R_n	Net Radiation
R_{n24}	24-h averaged net radiation
ρ_ω	density of water
Sc	Stream slope
SS	sum of squares
σ_i	standard deviation of the original variable
μ_i	mean of the original variable
x_i	scaled variable
X_i	original variable
$\frac{\delta S}{\delta t}$	Change in storage for a given time step

ACRONYMS AND ABBREVIATIONS

ANFIS	Adaptive Neuro-Fuzzy Inference System
AVHRR	Advanced Very High Resolution Radiometer
CA	Correspondence Analysis
CCA	Canonical Correspondence Analysis
DCA	Detrended Correspondence Analysis
DCCA	Detrended Canonical Correspondence Analysis
DEM	Digital Elevation Model
DRCs	Dynamic Response Characteristics
EOF	Empirical Orthogonal Function
ESA	European Space Agency
FAO	Food and Agriculture Organisation of the United Nations
FDCs	Flow Duration Curves
FEWS	Famine Early Warning Systems
GIMMS	Global Inventory Monitoring and Modeling Studies
GIS	Geographical Information Systems
GLS	General Least square
GLUE	Generalised Likelihood Uncertainty Estimation
HPEM	Harr's Point Estimation Method
IAHS	Internatioanal Association of Hydrological Sciences
ITCZ	Inter Tropical Convergence Zone
LAI	Leaf Area Index
LHS	Latin Hypercube Simulation
MCS	Monte Carlo Simulation
MIRA	Microwave Infrared Algorithm
MODIS	Moderate Resolution Imaging Spectroradiometer
MPA-RT	Multi-Satellite Precipitation Analysis-Real Time
NDVI	Normal Difference Vegetation Index
NIR	Near Infrared
NOAA/NASA	National Oceanic and Atmospheric Administration / National

	Aeronautics and Space Administration
NOAA's CPC RFE	National Oceanic and Atmospheric Administration Climate Prediction Center Rainfall Estimation Algorithm
NSE	Nash-Sutcliffe Efficiency
PBIAS	Percent BIAS
PCA	Principal Component Analysis
PCDs	Physical Catchment Descriptors
PERSIANN	Precipitation Estimation from Remotely Sensed Information using Artificial Neural Network
PUB	Prediction in Ungauged Basins
RDA	Redundancy Analysis
RMSE	Root Mean Square Error
RPEM	Rosenblueth's Point Estimation Method
RRSU/ SADC	Regional Remote Sensing Unit/ Southern African Development Community
RSR	Root Mean Square Error-observations standard deviation ratio
SEBAL	Surface Energy Balance for Land
SOTERCAF	Soil and Terrain digital database for Central Africa
SPOT	Système Probatoire d'Observation de la Terre
SRTM	Shuttle Radar Topography Mission
SWAT	Soil and Water Assessment Tool
TRMM	Tropical Rainfall Measuring Mission
UNEP	United Nations Environmental Programme

1 INTRODUCTION

1.1 General background of the study

Over the years, water professionals have developed several predictive tools that provide rational and sound decision-making with respect to water resources management, development and planning. The most widely used approaches, such as unit hydrographs, flood frequency curves, flow duration curves are fundamentally data driven, and are estimated from hydrometric (gauged) measurements at catchment scale. The past three decades have seen attempts to make some of these approaches more robust and realistic representations of hydrological processes at the appropriate scale, though lack of data continues to be a major limiting factor. Mazvimavi (2003) reported that most of the sub-Saharan countries lack financial, human and technical resources for developing and maintaining networks that can provide reliable data for sustainable water resources planning, design and management. Similarly, Oyebande (2001) noted that the needs for hydrological data for Africa are increasing, while for the past 30 years most countries have experienced a decrease in the number of hydro meteorological stations (Sutcliffe and Parks, 1999). Though efforts are currently being put in place to extend available hydro meteorological networks, it will take 10 to 30 years before adequate data, of use for rigorous hydrological analyses, can be collected. Then again, Chiang *et al.* (2002) and Kundzewicz (2007) reported that it is not just realistic to establish hydrometric stations on every drainage basin. Furthermore Sivapalan (2003) reported that the underlying causes of difficulties in prediction for ungauged basins is the high heterogeneity in land surface conditions and the space-time variability of climatic inputs happening over vast range of spatial and temporal scales, and not only lack of flow measurements. In the short and medium terms therefore, water resources planning and management that rely on comprehensive hydrological analysis will be plagued by the lack of consistent data.

Hydrological processes at river catchment scale are mainly dependent on climatic controls such as rainfall, temperature and evaporation, and as well as landscape changes. However, these factors are modified by development and impoundments, and the extent to which each of these factors influence the surface water resource varies in time and space (Holmes *et al.*, 2002).

Changes in landscape can strongly influence runoff, and quantitatively predicting the extent of such influence is a major challenge of modern hydrology (Ott and Uhlenbrook, 2004). Runoff and infiltration coefficients change with changing land-use. These effects may be very significant and can dominate small catchment hydrology (Butterworth *et al.*, 1999). It is these land uses such as afforestation, human settlement, irrigation, agricultural practices, grazing, reservoirs and riparian vegetation that, according to Schulze (2003), have become associated with certain mechanisms of water utilisation and runoff generation.

Most hydrological tools are usually developed on the deductive cause-effect relationships experienced in temperate regions (Mutua and Klik, 2007). However, the effective and sustainable water resources management in other regions such as the tropics and equatorials requires a holistic methodology relying on in-situ hydrological principles and integrated landscape patterns (Gumbricht *et al.*, 1997*).*

Taking into account the huge data requirement of most models and their limited capabilities to forecast hydrological changes with landuse transformations, Paturel *et al.* (2007), Mutua and Klik (2007) reported that traditional approaches and models are not readily applicable in most of the developing world. The availability of remote sensing datasets and GIS applications has been documented to successfully overcome lack of data for hydrological applications (Moore *et al.*, 1991; Tsihrintzsis *et al.*, 1996; Ritchie and Rango, 1996; Aspinall and Pearson, 2000; McKinney and Cai, 2002; Jena and Tiwari, 2006; Collischonn *et al.*, 2008). In summary, the hydrology of sub-Saharan Africa is plagued by two major challenges. One arises from the lack of adequate and consistent hydro-meteorological data, while the other is appropriate predictive tools for long-term forecasts.

This research study therefore is an attempt to develop a methodology to assess landscape interactions with water resources in a data scarce watershed of the Equatorial Nile - the Semliki. The study makes use of a combination of limited ground information, remotely sensed acquired datasets, GIS and statistical techniques for the development of deterministic mesoscale hydrologic models for the catchment.

The Semliki River is part of the upper drainage of the Albert Nile. For part of its course, it forms the boundary between Semliki National Park and Virunga National Park. The Semliki watershed (Figure 1-1) is one of the headwaters of the White Nile.

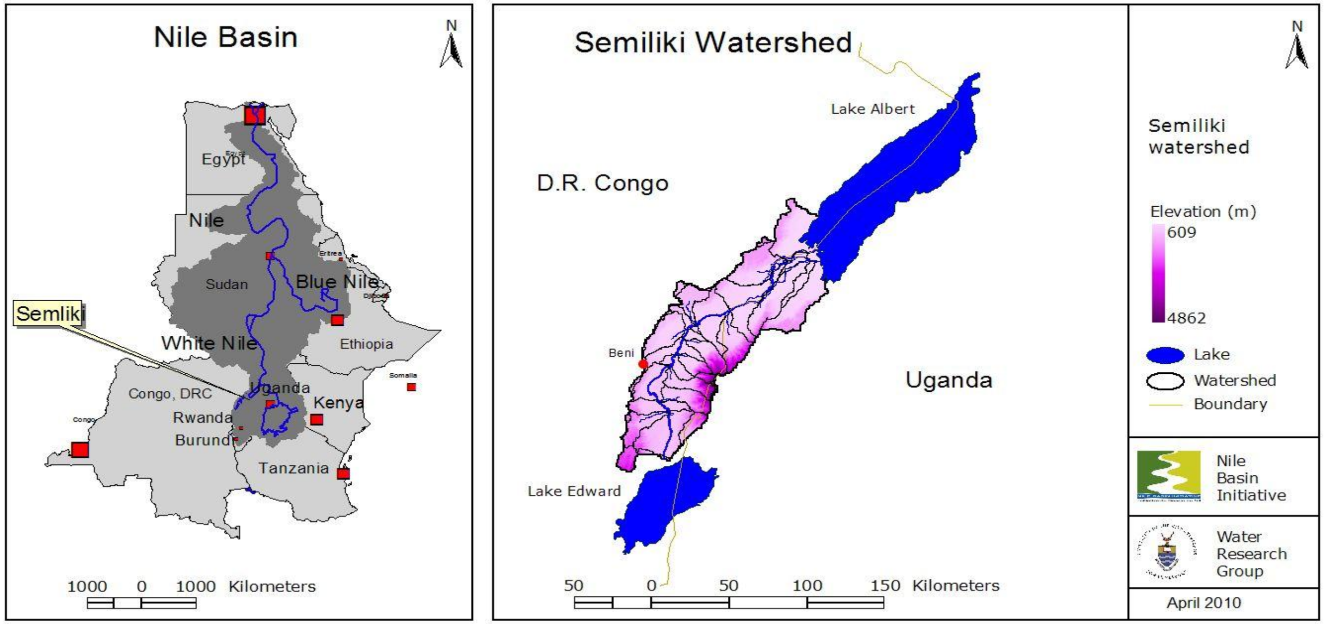

Figure 1-1 Semliki Watershed and the Nile Basin

The Nile is one of the world's great assets. Throughout history, the river has nourished livelihoods, an array of ecosystems, and a rich diversity of cultures (Rzòska, 1976; Said, 1993; Waterbury, 2002; Nicol, 2003). The following ten countries share the Nile: Burundi, Democratic Republic of Congo, Egypt, Ethiopia, Eritrea, Kenya, Rwanda, Sudan, Tanzania, and Uganda. From Lake Victoria to the Mediterranean Sea, the length of the Nile is 5584 Km. From its remotest headstream, the Ruvyironza River in Burundi, the river is 6671 km long. The basin comprises an area of 3 million Km^2- one tenth of Africa's total land mass -and the countries of the Nile serve as home to an estimated 300 million people (Karyabwite, 2000; Nicol, 2003).

The Nile Basin is very complex in terms of its size, geography, history and political divisions. Therefore, although there are several projects operating in the region, it is still difficult to obtain reliable data, at detailed scales for each area of the vast basin.

The Nile is the world's longest stream with water travel times varying from 20 days (Blue Nile tributary) to more than 45 days (White Nile tributary) depending on the seasons (Koutsoyiannis *et al*., 2008). The Nile River is utilised for numerous water uses that include energy generation, water supply for agricultural, industrial and domestic use, flood mitigation and management as well as the provision of other environmental and ecosystem services (Said, 1993; Waterbury, 2002). Intermediate and long term Nile flow prediction is crucial for the management and operation of the existing water control infrastructures from the Eastern part of Africa up to Egypt via the middle reaches (Sudan). This indicates the need for spatially and temporally appropriate monthly forecast of the flow of the widespread Nile River. An effective and appropriate way to study the vast Nile is to work at subbasin level as recommended by previous scholars and researchers. And this study aims at providing a rational approach for flow prediction in the Semliki watershed - one of the waterheads of the White Nile.

Moreover, the Semliki region is important because it harbours the rare and endangered mountain gorilla and it supports large numbers of montane plant and animal species endemic to the Albertine Rift. Human population density in the region is high, exceeding 300 persons per square kilometre; pressure on natural resources is consequently also high. In addition, since 1990 the region has been gripped by a horrifying genocidal civil war, and continues to be infested by cross-border military and civil conflicts, thereby further increasing pressure on natural resources.

1.2 Problem statement

The flow in the Nile River is generated by 20% of the drainage area with most of the downstream watersheds located in arid and semi-arid regions characterised by little contribution to the flow but with substantial losses through evaporation (Karyabwite, 2000; Senay *et al.*, 2009). The White Nile is one of the two major rivers that form the main Nile. Its headwaters are located in the highlands of the Eastern and Equatorial regions that enclose Lake Victoria and other water bodies such as Lake Albert, Edward and George. During the dry season in the Sudan and the Ethiopian Highlands, the White Nile provides the main base flow to the main

Nile. Several hydrological studies of the White Nile (Kite, 1981; Said, 1993; Sutcliffe and Parks, 1999, Tate *et al.*, 2001) indicated that Lake Victoria is the key feature in the behaviour of flows from the Equatorial region. However after the Victoria Nile, the Semliki River is the second tributary of the White Nile with a contribution up to 20% (Sene, 2000).

If direct rainfall on the Victoria Lake's surface is the key factor controlling its outflow (Tate *et al*, 2004; Sene, 2000; Sutcliffe and Parks, 1999; Nicholson, 1998; Piper *et al.*, 1986) very little is documented on the water flowing in the Semliki River from Lake Edwards and George. Several authors (Sahin, 1985; Sutcliffe and Parks, 1999; Conway, 2005; Kebede *et al*., 2006; Georgakakos, 2007) have called for more detailed investigations at spatially relevant scale for greater understanding of hydrological processes of the complex and wide spread Nile basin. Moreover, due to the complexity and diversity in the climate and landscape attributes of the sub basins of the Nile, improvement in the existing water resources models requires sub basin scale approaches which can be combined to produce sound and robust models for the entire Nile basin. This modelling process, however, for the Semliki watershed is characterised by a lack of adequate hydro meteorological records, posing a huge challenge for the quantification of the effects of specific landscape attributes on water resources. The region is densely populated and characterized by rapid population growth, refugee influxes and deforestation arising from the demand for wood for household and commercial fuel, resulting in more pressure on natural resources (Kileshye Onema *et al.*, 2006b).

1.3 Significance of the study

This research work is based on the premise that considerable interactions take place between landscape attributes and water resources of the Semliki catchment that is faced with inadequate hydro-meteorological records. The usefulness of such study will then be to extend it to physically similar basins in sub-Saharan Africa which experience the same challenge.

1.4 Research Objective

1.4.1 General Objective

The main objective is to develop and evaluate a methodology at the sub basin scale in order to identify, assess and evaluate the impacts of the landscape attributes on the water resources of the Semliki watershed of the Equatorial Nile that is inadequately resourced in terms of hydro-meteorological data

1.4.2 Specific objectives

The specific objectives are:

a) To identify and derive catchment characteristics that can be used to predict flows.

b) To identify zones with similar hydrological response

c) To determine temporal and spatial dynamics of landscape attributes in the studied watershed.

d) To develop models for predicting river flow characteristics from drainage basin attributes.

e) To identify the best model in terms of performance for flow prediction.

1.5 Research hypotheses

- Landscape attributes have impacts on water resources of a basin.
- Upstream hydrological conditions of a basin affect downstream flows.
- Lack of adequate information about the quantity of water resources can be overcome by a suitable combination of predictive methodologies.

1.5.1 Research questions

- What suite of methodologies is most appropriate for the prediction of flow, taking into cognizance data scarcity of the basin?
- What are the dominant catchment descriptors and critical driving parameters (biophysical) behind hydrological flow shifts at various spatial scales in the Semliki river basin?
- What are the impacts of catchment landscape attributes on catchment flows?

- How and where does landscape influence local scale hydrological responses in the Semliki basin?

- What are the potentials and limitations of public domain low to medium resolution remotely sensed acquired data in assessing landscape dynamics in the Semliki basin?

1.6 Terminology

The terminology related to hydrological modelling and forecasting is relatively well established, but it is worth mentioning that one may also observe certain changes in terminology over time, and certain preferences of various authors and scholars. The landuse alluded to in the title of this study is covered under landscape attributes throughout the thesis.

1.7 Outline of the thesis

The thesis is outlined as follows:

Chapter 1 introduces the context of the research, background and objectives.

Chapter 2 provides an extensive literature survey on water resources management in data scarce environment. Aspects of remotely sensed acquired data, watershed balance, water resources modelling and predictions in ungauged river basins are reviewed.

Chapter 3 covers the description of the study area and reports on the generation of catchments descriptors retained for this study.

Chapter 4 describes the analytical, statistical and predictive methodologies that are applied in subsequent chapters.

Chapter 5 reports on landform characterization and hydrological similarities identified within sub catchments from the generated physiographic attributes.

Chapter 6 presents the modelling approaches developed for flow predictions in the data scarce Semliki. The results of applying these techniques are compared and discussed.

Chapter 7 covers the uncertainty and sensitivity analyses associated with the predictive models

Chapter 8 presents conclusions and recommendations.

Appendix A provides details of the generated monthly NDVI from satellite imagery for the Semliki watershed.

Appendix B presents results from aerial rainfall datasets extracted from remotely sensed acquired FEWS-NOAA data.

Appendix C reports details on the step-wise sensitivity analyses.

2 RESEARCH BACKGROUND AND LITERATURE REVIEW

This chapter provides a comprehensive review on water resources management especially in data-poor environments. Aspects pertaining to Geographical Information Systems (GIS) and remotely sensed acquired data, watershed balance, water resources modelling, predictions in ungauged subcatchments and uncertainty in hydrological modelling are reviewed and related to this study.

2.1 Water management in data-scarce environment

Most basins in the developing world are characterized by little or no runoff data and hydrological measurements. The application of hydrological models in data-scarce basins has received substantial attention in the research community in recent years through the International Association of Hydrological Sciences (IAHS) Decade on Prediction in Ungauged Basins (PUB) (Sivapalan *et al*., 2003). This remains a complex area in hydrological research (Wagener and Wheater, 2006; Kundzewicz, 2007; Wagener and Kollat, 2007). It is therefore proper to carry on research on all aspects of this scientific endeavour.

For instance, the application of hydrological models to ungauged basins demands that model parameters are estimated by other methods, and these are discussed extensively by Duan *et al.* (2001). The model parameters are either estimated by deductions from field measurements or remote sensing (a priori estimation) or by parameter regionalisation (transposing calibrated parameters from similar gauged basins or using the notion of hydrological similarity) approaches. In theory, the estimation of the parameters should be a simple assignment, but the enormous heterogeneity of basin physical conditions coupled with the spatial and temporal variability of climate variables and model structure constraints limit the approximation of the appropriate parameters in data-poor basins (Beven, 1993). The next section introduces the concept of Geographical Information Systems and remotely sensed acquired data in water resources management especially in the context of data scarcity.

2.1.1 GIS and remotely sensed data

2.1.1.1 Evaporation and transpiration

Evaporation and transpiration are important components of hydrological processes in a catchment. Their estimation in catchments with multiple land use is complicated. It is, however, possible to model the effect of variations in topography and vegetation cover on evapotranspiration. Evaporation and transpiration can be determined using ground measurements, hydrological models or remotely-sensed acquired data. Hydrological processes can be modelled at field scale, such as SWAP (Soil-Water-Atmosphere-Plant model: climatic controls, soil attributes and agronomic characteristics are used to derive water use) or basin scale, such as SLURP (Semi-distributed Land-Use-based Runoff Process).

Under ground conditions scientists and water managers are still finding challenging the estimation of actual evapotranspiration (ET_a), especially where information is needed over a wide area (Ahmad *et al.*, 2005). Though, during the last two to three decades, substantial development has taken place in the computation of ET_a using satellite and remotely sensed acquired information (Kustas and Norman, 1996; Bastiaanssen *et al.*, 1998, 2002). These techniques provide authoritative ways to estimate ET_a from the local scale of an individual pixel right up to an entire raster image.

The Surface Energy Balance for Land (SEBAL) is one of such techniques; it works out a complete radiation and energy balance along with the resistances for momentum, heat and water vapour transport for each pixel (Bastiaanssen *et al.*, 1998; Bastiaanssen, 2000, Zwart and Bastiaanssen, 2007). The fundamental input for SEBAL comprises of spectral radiance in the visible, near-infrared and thermal infrared part of the spectrum. Further to satellite images, the following routine weather data parameters, wind speed, humidity, solar radiation, air temperature are required for the SEBAL model (Ahmad *et al.*, 2005).

Evaporation is computed from the instantaneous evaporative fraction Λ, and the daily averaged net radiation, R_{n24}. The evaporative fraction Λ is computed from the instantaneous surface energy balance at satellite overpass on a pixel-by-pixel basis (Ahmad *et al.*, 2005):

$$\lambda E = R_n - (G_0 + H)$$ **Equation 2-1**

Where: λE is the latent heat flux, R_n is the net radiation, G_0 is the soil heat flux and H is the sensible heat flux.

The latent heat flux defines the quantity of energy consumed to maintain a certain crop evaporation rate. The surface albedo, surface temperature and vegetation index are generated from satellite measurements, and are used together to compute R_n, G_0 and H. The instantaneous latent heat flux, λE, is the measured residual term of the energy budget, and it is then used to compute the instantaneous evaporative fraction Λ (Ahmad *et al.*, 2005)*:*

$$\Lambda = \frac{\lambda E}{\lambda E + H} = \frac{\lambda E}{R_n - G_0}$$ **Equation 2-2**

The instantaneous evaporative fraction Λ describes the ratio of the actual to the crop evaporative demand when the atmospheric moisture conditions are in balance with the soil moisture conditions. The instantaneous rate can be used to compute the daily value because evaporative fraction tends to be constant during daytime hours, although the H and λE fluxes vary considerably. The difference between the instantaneous evaporative fraction at satellite overpass and the evaporative fraction derived from the 24-hour integrated energy balance is marginal and may be neglected (Crago, 1996; Farah, 2004). For time scales of 1 day or longer, G_0 can be ignored and net available energy (R_n - G_0) reduces to net radiation (R_n). At daily timescales, ET_{24} (mm/day) can be computed as (Ahmad *et al.*, 2005):

$$ET_{24} = \frac{86400 \times 10^3}{\lambda \, \rho_w} \Lambda \, R_{n24}$$ **Equation 2-3**

Where: R_{n24} (W/m^2) is the 24-h averaged net radiation, λ (J/kg) is the latent heat of vaporization, and ρ_w (kg/m^3) is the density of water.

In the data scarce Krishna river basin of India, Ahmad *et al*. (2006) used a combination of satellite imagery and SEBAL to more accurately estimate ET_a. Landsat SEBAL results were put in the framework of the annual vegetation and cropping cycles established with the Moderate Resolution Imaging Spectroradiometer (MODIS) time series of Normal Difference Vegetation Index (NDVI). Recently, while considering turbulent heat exchange and the convective process, Koloskov *et al.* (2007) indicated the key role of the Monin–Obukhov length in the determination of evapotranspiration from remotely sensed data using SEBAL.

An alternative method uses subsurface soil moisture and surface energy flux measurements from the NASA Hydrosphere State mission and the European Space Agency (ESA) Soil Moisture and Ocean Salinity mission (Dunne and Entekhabi, 2006). Soil moisture can also be determined from radar imaging, where ground cover is not too dense (Thoma *et al.*, 2006). NDVI, one of the landscape attribute of this study, has also been documented to have relationship with regional evapotranspiration. Dibella *et al.* (2000) in the Pampa region of Argentina used multiple linear regression analysis to relate NDVI to evapotranspiration (ET) estimated from water balance technique. The study revealed that the relationship between spectral datasets and ET was more sensitive temporally than spatially for the generated models. Similarly, Bastiaanssen (1998) combined NDVI, surface temperature and hemispherical surface reflectance to infer surface energy balance and land wetness indicators for a wide spectrum of land type. A comparative evaluation of each of the cited sources and their proposed methods is beyond the scope of this study and reference can be made to the literature sources given above for more details. Furthermore, Boegh *et al.* (2004) documented the calculation of evapotranspiration rates (*E)* for Denmark using Normal Difference Vegetation Index (NDVI), global albedo and the surface temperature from the Advance Very High Resolution Radiometer provided by the National Oceanic and Atmospheric Administration (NOAA) satellite. Results have indicated the benefits of using remotely sensed acquired data in the calculation of evapotranspiration rates, especially since the effect of sea breezes on air temperature and air humidity could be determined.

2.1.1.2 Rainfall[1]

For many hydrological applications and models, high temporal resolution rainfall intensity data is required, and can sometimes be challenging to have. However, rainfall depth and depth-averaged rainfall intensity from tipping-bucket rain gauges can provide a reasonable rainfall intensity distribution (Van Dijk *et al.*, 2005). In the absence of ground measurement, remotely sensed acquired precipitation data from METEOSAT (Andersen *et al.*, 2002) or NOAA AVHRR could be used. In this approach, large droplets and/or ice in the clouds is associated with large effective radius of cloud particles. This is computed for highly reflective clouds in the visible wavelength. No distinction between water and ice is required, since the existence of either near the top of a thick cloud contributes to precipitation. In addition, a rain estimation algorithm, that is in good agreement with radar data is generated from the fraction of rain cloud coverage and cloud spatial structure. Furthermore, several satellite-derived

[1]Sourced partly from Kileshye Onema and Taigbenu, 2009a

rainfall dataset exist to date and extensive literature has documented the algorithms used to derive the final product. For instance, the Precipitation Estimation from Remotely Sensed Information uses Artificial Neural Network (PERSIANN; Hsu *et al.*, 1999; Sooroshian *et al.*, 2000), the Microwave Infrared Algorithm (MIRA; Todd *et al.*, 2001), the Multi-Satellite Precipitation Analysis-Real Time (MPA-RT; Laws *et al.*, 2004) and the National Oceanic and Atmospheric Administration Climate Prediction Center Rainfall Estimation Algorithm (NOAA's CPC RFE2.0; Xie *et al*., 2002). The NOAA satellite-derived rainfall dataset can be downloaded from the following link ftp://ftp.cpc.ncep.noaa.gov/fews/newalgo_est. These data are part of NOAA's effort to develop continuous and consistent rainfall dataset under the Famine and Early Warning Systems (FEWS).

2.1.1.3 Land use types

The use of remotely sensed acquired data and satellite image compositing and classification (supervised and unsupervised) to derive land use covers and dynamics is well recognized and widespread (Ludwig *et al.*, 2003). Leaf area index can also be remotely sensed, e.g. using NOAA AVHRR (Andersen *et al.*, 2002) as well as the NDVI (Normalised Difference Vegetation Index) (Mazvimavi, 2003). Numerous studies have documented the use of satellite imagery in combination with GIS packages as tools for studying land use dynamics in several regions of the world (Wittig *et al.*, 2007; Sesnie *et al.* 2008; Zhou *et al.*, 2008; Stehman 2009; Fraser *et al.* 2009; Dewan and Yamaguchi 2009). Land use is closely related to land cover, and progress made in terms of accessing low to medium resolutions satellite images has contributed substantially in undertaking studies on land use especially in areas where accessibility remains a challenge like in most regions of the developing world.

2.1.1.4 Hydrogeology

Hoffman (2005) documented the fact that radar-based and residual gravity approaches present some promising options in characterising surface subsidence and depth of weathering, which, when used in association with ground measurements of hydraulic head, allow storage parameters to be estimated. Futhermore, he reported that indirect remote sensing methods, such as those computing soil moisture and vegetation changes could be use in the estimatation of water table levels. Faults and fractures, which play a dominant role in controlling groundwater flow and yield in crystalline aquifers, can be readily identified using satellite imagery.

Satellite-based remote sensing techniques can also be used to characterize recharge and discharge zones within an aquifer or aquifer group (Bobba *et al.*, 1992) although Shaban *et al.* (2006) suggest that such methods be treated as indicative, rather than providing a reliable characterization.

2.2 Watershed balance

This study focuses on the interaction between landscape attributes and water resources, investigation that will provide the basis and documentation for greater understanding of the Semliki basin water balance. This section provides a general review of climatic controls, storage and utilisation and other aspects associated with watershed balance. The general approach in a water balance can be defined as:

$$O = I + \frac{\delta S}{\delta t}$$ **Equation 2-4**

O: Outflow

I: Inflow

$\frac{\delta S}{\delta t}$: Change in storage for a given time step

In a river basin inflows include rainfall and discharges. Outflows include flow into downstream basins (or the sea), abstractions, evaporation and transpiration. Flows include both surface and subsurface. Storage includes surface water bodies and deep, stable regional aquifers.

2.2.1 Climatic controls

The lake plateau region of the Nile basin receives in general adequate rainfall as presented in table 2.1. The incidence of rainfall in the Semliki watershed is associated with the seasonal migration of the Inter Tropical Convergence Zone

(ITCZ) which gives rise to two rainy seasons in about March-May and October-December. Todd *et al.* (1999), Conway (2005) and Asadullah *et al.* (2008) reported however that a lot of uncertainty still prevails in terms of rainfall origins and future trends for the equatorial region of the Nile.

Table 2-1 Rainfall for Congolese Nile basin

	Average annual rainfall in the sub-basin area (mm) / a[1]		
DR Congo	Minimum	Maximum	Mean
	875	1 915	1 245

[1]FAO, 1997

The probabilistic character of rainfall trends has been investigated and documented using (i) Markov chains (De Groen, 2002), although they tend to under-estimate seasonal variations; or (ii) Neymann-Scott rectangular pulses (Rodriguez-Iturbe *et al.*, 1984), although the approach is very limited in its ability to reproduce the probability of days without rain; or (iii) using an entropy-based approach (Koutsoyiannis, 2006).

Mean annual rainfall and runoff processes spatial distribution are the major factors in determining the homogeneity or heterogeneity of a catchment (Jothityangkoon and Sivapalan, 2001). The coefficient of variation in maximum annual floods is strongly influenced by rainfall intensity and duration, and channel travel times, as related to catchment size (Blöschl and Sivapalan, 1997).

In the Semliki watershed, there is little variation throughout the year in the mean temperature, which ranges from 16º C to 30º C on average depending on locality and altitude as the ice-capped mountains are frozen throughout the year. Limited studies have documented evaporation and evapotranspiration in this region. Sutcliffe and Parks (1999) reported on comparisons of Penman estimates of potential transpiration for the region. Results indicated a surplus during the rainy seasons. Detailed climatic controls for the Semliki watershed is documented in the subsequent chapter three.

2.2.2 Storage and water utilization

Where alluvial deposits are developed, alluvial aquifers play a significant role in the river basin water balance. An alluvial aquifer can be described as a groundwater unit, generally unconfined, that is hosted in laterally discontinuous layers of sand, silt and clay, deposited by a river in a river channel, banks or flood plain. They are recharged either continuously if the river is fully perennial, or, more usually, seasonally (Barker and Molle, 2004). Because of their shallow depth and vicinity to the streambed, alluvial aquifers have an intimate relationship with stream flow. Surface water bodies, or reaches thereof, can be classified as discharge water bodies if they receive a groundwater contribution to baseflow, or as recharge water bodies if they recharge a shallow aquifer below the streambed (Townley, 1998).

On the other hand, dams are also storage structures that store and capture runoff water, securing water for various uses like drinking water, domestic use, livestock watering and irrigation. Thus where dams are numerous, they have the potential to strongly influence downstream water quality and availability (Meigh, 1995; Kileshye Onema *et al.*, 2006a). The Semliki river watershed is characterized by no impoundment developments and limited information is available on groundwater potentials.

2.3 Water resources modelling

Hydrological systems can be described by either a purely deterministic approach in which process equations are analysed, or by a stochastic approach in which statistical distributions are handled (Dooge, 2005). Water resources modelling can be considered as that part of modelling that deals primarily with water resources systems, rather than focussing on hydrological processes. Modelling is based on a river basin, or a hydrologically definable portion thereof.

Modelling can be carried out at various depths of analysis, in terms of model structure (deterministic vs. stochastic) and spatial control (lumped vs. distributed):

- Conceptual models, comprising mutually interrelated storage elements representing the physical elements of the catchment, averaging inputs and outputs over the catchment area.
- Stochastic models are tools for estimating probability distributions of potential outcomes by allowing for random variation in one or more inputs over time. The random variation is usually based on fluctuations observed in historical data for a selected period using standard time-series techniques.
- Lumped models consider a catchment to be spatially homogeneous.

- Distributed or semi-distributed models consider a catchment to be spatially heterogeneous, dividing the catchment into hydrological response units with similar properties, and focusing on processes, calculating flows from governing equations (Calder *et al.*, 1995; Gallart and Llorens, 2004; Huisman *et al.*, 2004; Ott and Uhlenbrook, 2004), including ones operating in combination with a Geographical Information System (Nyabeze, 2003; 2005; Wegehenkel, 2003).

Models must be calibrated, either spatially by calibrating a model developed in a test catchment against a calibration catchment, or against stations outside the test catchment (Andersen *et al.*, 2001). Alternatively, models can be calibrated temporally, by calibrating a model developed with one time series against another time series from the same catchment (Lørup *et al.*, 1998).

Distinction can be drawn between three scales of catchment: (i) small catchments of farmer-field scale and under 1 km^2, (ii) meso-scale catchments of 1 - 1000 km^2 and (iii) large-scale catchments and basins of thousands or tens of thousands of square kilometres (Uhlenbrook *et al.*, 2002). Modelling of meso-scale catchments can be very challenging as most modelling methodologies have been developed for small catchments, often in headwaters (Uhlenbrook *et al.*, 2002).

The river basin is the appropriate scale for models that are used for decision-making in water resources management (Boughton, 2005). However basin scale models run the risk of over-simplicity – and therefore not accommodating system complexity sufficiently (Dent, 2000). However, modelers have tried to address that limitation with physically based approaches to models that are characterised with a significant number of parameters. At the same time, simple water balance models are easy for decision-makers to understand and use (Boughton, 2005). A balance must therefore be struck between the risk of over-simplification and the risk of over-parameterisation.

Water resources management in a basin is based on the operation of reservoir systems, aquifers, and conjunctive surface water and groundwater systems. A river basin water balance model must therefore include all these components.

It is possible to use distributed parameter value estimation techniques to estimate runoff on small scale ungauged catchments and aggregate to larger scale ungauged catchments (Nyabeze, 2005).

Water balance modelling can be defined as that branch of water resources modelling that operates through the continuous simulation of catchment water balance through dry periods as well as wet (Boughton, 2005). Simple water balance models can be derived by developing and combining models describing evaporation, soil moisture and overland flow (Finch, 1998; Gallart and Llorens, 2004). The rivers draining the basin area are divided into cells. The water balance is then determined by finite difference at each cell for each timestep (Nkomo and van der Zaag, 2004; Symphorian *et al.*, 2003; Winsemius *et al.*, 2006). This can be done using a spreadsheet model or a distributed water balance model such as SWAT (Soil and Water Assessment Tool) (Arnold and Foster, 2005).

Most catchments have heterogeneous landscape properties (topography, land cover, soils, etc) and this heterogeneity is scale-dependent (Shankar *et al.*, 2002). Such catchments require models that capture a variety of such landscape parameters. Flow partitioning at the soil surface and within the soil is especially sensitive to these parameters (Finch, 1998; Huisman *et al.*, 2004). The models must operate at the spatial and temporal scales applicable to the processes to be studied. This adds further complexity to any water balance modelling attempt, requiring a greater number of interacting water balance equations (Nyabeze, 2003). Such models can be satisfactorily calibrated (Nyabeze, 2005), but the equifinality problem arises: a variety of different calibrations could produce the same predicted response, where a large number of possible parameters sets may each calibrate well, but introduce high parameter uncertainty (Winsemius *et al.*, 2006). A further problem in defining equations for flow pathways is that evapotranspiration is better considered as a number of separate but interacting processes, such as evaporation from interception, transpiration and soil evaporation (Savenije, 2004), but most modelling systems do not allow this separation.

2.4 Landscape/use attributes and predictions of flows in watershed hydrology

Changes in land use can strongly influence runoff, and quantitatively predicting the extent of such influence is a major challenge of modern hydrology (Ott and Uhlenbrook, 2004). Runoff and infiltration coefficients change with changing land-use. These effects may be very significant and can dominate small catchment hydrology (Butterworth *et al.*, 1999a). The effects may relate to changes in soil properties or to changes in soil-vegetation interactions (Huisman *et al.*, 2004).

The hydrology of small, headwater catchments is often largely a factor of rainfall; with runoff contributing less to the water cycle, although in the wettest years, saturated overland flow makes a major contribution to runoff (Mugabe, 2005). Thus, the effects of land use change on runoff are likely to be felt strongly in the wetter years. At the same time, it is likely that occurrence of low flows is affected by land use changes in any year. Land degradation can also affect precipitation: the atmosphere can only generate rainfall downwind if the precipitable moisture is replenished by evaporation. Land degradation decreases the replenishment and hence the rainfall downwind (De Groen and Savenije, 1995). Conversion of forest and savannah vegetation to agricultural land or cleared land has been shown to result in an increase in runoff (Bari and Smettem, 2004; Calder *et al.*, 1995; Melesse, 2004). This is due to reduced transpiration and increased infiltration to shallow groundwater, contributing to baseflow (Bari and Smettem, 2004).

The effects of afforestation may be complex, both increasing groundwater recharge immediately following rainfall, and then increasing evapotranspiration in the longer term, thus altering the time dependent availability of groundwater and long term groundwater recharge, but often decreasing runoff (Iroumé *et al.*, 2005; Gallart and Llorens, 2004; Ott and Uhlenbrook, 2004; Wegehenkel, 2003). Plantations of species with high water consumption, such as the blue gum, can lower groundwater levels in the vicinity of the plantation during the day, when transpiration is taking place, and raise it at night, as the water is replenished from the local aquifer flowing down the hydraulic gradient (Engel *et al.*, 2005). This process can result in a medium term decline in local groundwater levels, and a consequent decrease in baseflow. The extent of specific land use changes and the effects of such changes on hydrology can be evaluated from field measurements in paired catchments (Bishop *et al.*, 2005; Iroumé *et al.*, 2005; Mugabe, 2005), which can be used as input to a conceptual water balance model (Bari and Smettem, 2004), or by comparisons of field or remotely-sensed measurements over time (Calder *et al.*, 1995; Gallart and Llorens, 2004; Kileshye Onema, 2004), or modelled using hydrological principles in a distributed model (Nyabeze, 2003; Ott and Uhlenbrook, 2004). Mazvimavi (2003) provides a review of studies that linked landscape attributes to flow characteristics and Table 2.2 summarizes those studies in addition to more recents works.

Table 2-2 : Previous studies on catchments descriptors and flow estimation

Catchment Characteristic	**Study**
Area	Tasker (1982), NERC (1975), Bullock (1988), Gustard et *al*. (1989), Gan et *al*.(1990), Bullock et *al*.(1990), Burn and Boorman (1993), Sefton and Howarth (1998), Jena and Tiwari (2006), Laudon et al.(2007)
Elevation	Tasker (1982),, Gustard et *al*. (1989), Nathan and McMahon (1990), Jena and Tiwari (2006) Getirana et *al*. (2009)
Main stream length	Nathan and McMahon (1990), Gustard

	et *al*. (1989), Burn and Boorman (1993)
Slope	Nathan and McMahon (1990), Gustard et *al*. (1989), Sefton and Howarth,(1998) Burn and Boorman (1993), Lacey and Grayson (1998), Berger and entekhabi (2001), Mazvimavi (2003), Jena and Tiwari (2006)
Stream frequency	Sefton and Howarth (1998), Nathan and McMahon (1990), Gustard et *al*. (1989), Burn and Boorman (1993), Jena and Tiwari (2006)
Drainage density	Nathan and McMahon (1990), Lacey and Grayson (1998), Berger and entekhabi (2001), Mazvimavi (2003), Jena and Tiwari (2006)
Proportion of catchment under various soil types	Sefton and Howarth (1998), Burn and Boorman (1993), Gustard et *al*. (1989), Tasker (1982), Laudon et al.(2007)
Land cover	Sefton and Howarth (1998), Nathan and McMahon (1990), Lacey and Grayson (1998), Mazvimavi (2003), Croke et *al*.(2004), Laudon et al.(2007)

Proportion of catchment under various types of geological formations	Sefton and Howarth (1998), Nathan and McMahon (1990), Gustard et *al*. (1989), Yokoo et *al*.(2001).
Location-latitude and longitude	Sefton and Howarth (1998), Nathan and McMahon (1990).
NDVI	Mazvimavi (2003).

2.5 Overview of predictions in ungauged basins[2]

With the use of simple approaches such as the rational method, the modeling of ungauged and data-scarce basins began a long time ago. Progress made in terms of the increased availability of workstations and computers in the sixties encouraged the development of continuous watershed models (Nash and Sutcliffe, 1970). Since then one of the key areas of research has been efforts to estimate parameters in ungauged basins. Different approaches have been developed temporally and at different subbasin scales which include the proxy-basin method (Klemeš, 1986), linear interpolation methods (Bergström, 1990), multiple regression approaches (Fernandez *et al*., 2000; Mazvimavi, 2003), parameter mapping (Midgley *et al*., 1994) and a priori estimation methods (Duan et *al*., 2001). However, the problem is far from being solved given that regionalisation of parameters of most of these predictive tools is not adequate for prediction in

[2]Partially sourced from Kileshye Onema et al., 2011(submitted)

ungauged basins. While continuous developments strive at enhancing our predictive capability for streamflow, we are often faced with the challenge of predictions in ungauged basin as stated by Sivapalan *et al*. (2003). Numerous approaches exist for flow prediction in natural river reaches. Flow prediction has significant interest both from research as well as from an operational point of view. The choice of methods depends on data availability and the type of application. Reliable and accurate estimates of hydrologic components are not only important for water resources planning and management but are also increasingly relevant to environmental studies (Schröder, 2006). Several studies have reported on the use of catchment descriptors and regionalization of parameters for flow prediction in ungauged basins. One of the studies is that of Sefton and Howard (1998) who worked on 60 catchments to obtain a set of dynamic response characteristics (DRCs) describing the hydrological behaviour within the regions of England and Wales. They used Physical catchment descriptors (PCDs) indexing topography, soil type, climate and land cover to collate and link to the hydrological model by overlaying catchment limits with a Geographical Information System (GIS).

Sanborn and Bledsoe (2006) provided useful information for water resources planning and management as well as ecohydrological applications for an ungauged stream in Colorado. Their approach indicated that a wide range of ecologically appropriate streamflow characteristics can be accurately modeled across large heterogeneous regions. Kwon *et al.* (2009) reported on the forecasting of seasonal and annual streamflow for the operation of dams in the Yangtze river basin of China; They made use of sea surface temperature and upland snow cover, uncertainty was estimated through a Bayesian approach and their results indicated great adaptive capability towards water resources management. In their comparison of linear regression with artificial neural networks, Heuvelmans *et al.* (2006) indicated the need for well-informed choice of physical catchment descriptors as a first condition for a successful parameter regionalization. Cheng *et al.* (2006) reported on the importance and usefulness of parsimonious models for runoff prediction in data-poor environment as these models are characterized by few numbers of parameters. Reducing uncertainty associated with prediction in ungauged basins is critical as reported by Uhlenbrook and Siebert (2003) Koutsoyiannis, (2005a, 2005b) as well as Zhang *et al.* (2008).

Lately, Koutsoyiannis *et al.* (2008) indicated that analogue modeling techniques for simulation are also used for prediction with impressive performance due to the advances achieved with non linear dynamical systems (chaotic systems). The major drawback is the fact that these approaches are data intensive and work as black boxes, thus no process insight is provided.

Relevant spatial and temporal scale to flow prediction continues to be a subject of discussions and investigations in watershed hydrology (Kundzewicz, 2007). This study attempts therefore to develop some modeling approaches for flow prediction in a data-scarce and medium size watershed of the equatorial Nile region. These approaches intend to provide tools that will ultimately contribute towards better water resources planning in a humid and data-poor environment.

2.5.1 Regionalization techniques

Regionalisation can be defined as deriving model parameters by linking them to physical catchment descriptors (Heuvelmans *et al.*, 2006). It is a process which transfers small-scale (or meso-scale) measurements to a large scale (or basin or regional) model, or from gauged catchments to ungauged catchments. It is particularly important in African river basins, which suffer from limited data and process knowledge (Bormann and Diekkrüger, 2003). This is relatively straightforward for climate parameters like precipitation, but much more complex for flows, vegetation-evaporation and transpiration relationships. Regionalisation could become a misleading hydrological modelling approach if it focuses only on the output (e.g. streamflow) without an attempt at incorporating the main salient hydrological process such as catchment drying time, slow flow response decay time, and proportional contribution of slow flow to total streamflow. Spatial heterogeneities in landscape parameters must be captured in the regionalization process, e.g. through areal variance/covariance.

Regionalisation can be undertaken through determining regression or multivariate statistical relationships between each of the model parameters (Heuvelmans *et al.*, 2004). The equations for such relationships are calibrated through a series of model runs on catchments which are controlled, or which have a long time series of data (Heuvelmans *et al.*, 2004; Nyabeze, 2005).

A simpler alternative is "geographic regionalisation", where point scale measurements are transferred to large-scale areas (Heuvelmans *et al.*, 2004). This can be via simple statistical methods, such as direct weighted averages, geometrically-derived measures, such as Thiessen polygons (Dingman, 2002), geostatistical methods, such as kriging (Dingman, 2002), or multifractal analysis approaches (Zeleke and Si, 2005). For developing reliable regionalization approaches, a good understanding of a particular model and a sound acquaintance of hydrological processes within a natural system is essential (Madsen *et al.*, 2002).

In ungauged catchments, extensive literature exists on regionalization applications. Niadas (2005) worked in small catchments (less than 50km^2) of the mountainous areas of Greece. Non-linear Regional Flow Duration Curves (FDC) were developed and used in hydrologically similar catchments with reasonable performance. Griffis and Stedinger (2007) equally illustrated the use of General Least Square (GLS) regression procedure in the estimation of model parameters in South Carolina. Sauquet (2006) made use of an interpolation system based on ordinary and residual kriging in producing chloropleth maps of average runoff at basin scale in France. The uncertainty analysis revealed however that traditional approaches for interpolation gave satisfactory results while the introduction of hydrological properties of the variables under investigation improved the outcomes. In Austria, Laaha and Blöschl (2006) compared the performance of four catchments grouping methods for predicting low flow. The seasonality effects-based approach captured more adequately the catchments' characteristics utilized in the regionalization. Furthermore, Merz and Blöschl (2004) documented that best estimates in regionalization of parameters of a lumped model for 308 Austrian catchments were provided by the average parameters of immediate upstream and downstream neighbours for kriging techniques. In the Mexican tropical regions the comparison of regional estimates for ungauged sites undertaken by Ouarda *et al.* (2008) indicated advantages of the neighborhood characteristics as well as the robustness of Canonical correlation investigation based techniques. Substantial progress has been made in terms of regionalization of statistical flow properties; Wagener and Wheater (2006) acknowledged however the fact that estimation of continuous streamflow time-series remains very uncertain. In addition, Kling and Gupta (2009) cautioned on the impact of ignoring the sub-basin scale variability during the regionalization exercise in lumped modeling. Developments in data driven approaches have substantially contributed to further applications of hydrological regionalization. Dawson *et al.* (2006) reported on the use of split validation method of neural networks in medium size catchments of the Great Britain. In the operational applications of hydrological models in the Flemish part of the Scheldt River in Belgium, Heuvelmans *et al.* (2006) indicated better results from artificial neural networks in comparison to linear regression. More recently, Shu and Ouarda (2008) documented the use of adaptive neuro-fuzzy inference system in regional flood frequency analysis on 151 catchments of Canada. The adaptive neuro-fuzzy inference system (ANFIS) was reported to have more flexibility and capability of including both the regionalization and estimation steps for ungauged basins in Quebec region of Canada.

Studies have also been undertaken on regionalization in sub-Saharan Africa. Reference can be made to studies undertaken by Hughes (1989) who estimated model parameters from physical catchment characteristics in South Africa. Servat and Dezetter (1993) attempted in the Western Ivory Coast to extend two conceptual models to ungauged catchments using a stepwise, forward regression. In South Western Tanzania, Mwakalila (2003) made use of Geographical Information System in order to link physical catchment properties to calibrated model parameters in the estimation of flows in data poor environment. Hughes *et al*. (2006) documented with satisfactory performance a regional approach of the Pitman model in the Southern African region. And lately, Kaluarachchi and Kim (2008) documented the use of global and subbasin mean in combination with multiple regression for regionalization of parameters in the Ethiopian upper Blue Nile river basin. Hydro meteorological data availability continues to be a challenge to investigations in Africa. Therefore, studies on physically-based parameter estimation methodologies which do not require calibration to observed flow data and which are gaining further recognizance (Gupta *et al*., 2006; Kundzewicz, 2007; Yadav *et al*., 2007) are adequate for modeling ungauged basins. Current developments comprise advancement in the application of physically-based approaches to approximate model parameters directly from watershed physical characteristics (Kapangaziwiri and Hughes, 2008) or utilisation of remotely sensed acquired data to calibrate physically-based models (Baumgartner *et al*., 1997; Nandagiri, 2007; Cole and Moore, 2008; Parajka and Blöschl, 2008; Immerzeel and Droogers, 2008).

2.5.2 Uncertainty[3] and sensitivity analysis

Uncertainty is everywhere and affects everyone. However, as Lindley (2006) states it is only in the twentieth century that the concept has been comprehensively studied and better understood. Table 2-3 presents a typology of uncertainty as suggested by the British Environmental Agency. The inclusion of uncertainty assessment in hydrological modelling is an up-and-coming notion not only for researchers but for all water practitioners who rely on the results of hydrological models and decision support systems as it has important impact on the value of the decisions taken.

Table 2-3 Typology of uncertainty as formulated by the British Environmental Agency (2000)

<table>
<tr><th colspan="2">Type</th><th>Examples of sources</th></tr>
<tr><td colspan="2">a. Real world environmental uncertainty
(e.g. Natural variability)
(non reducible form of uncertainty)</td><td>• Randomness observed in nature (climate data)
• Inherent variation in natural hydrological response systems</td></tr>
<tr><td rowspan="3">b. Knowledge Uncertainty

(This is a reducible form of uncertainty and is associated with ignorance or incomplete information)</td><td>i. Model input data uncertainty</td><td>Climate data and hydrological data
-missing/inaccurate records
-non-representative data (spatial and temporal)
-inappropriate temporal/spatial resolution
-data processing</td></tr>
<tr><td>ii. Model structural uncertainty</td><td>- Incomplete conceptual frameworks
-Spatial and temporal averaging of a model
-Ambiguous boundary conditions
-Wrong process representation</td></tr>
<tr><td>iii. Parameter uncertainty</td><td>-Lumping of parameters and scale issues
-Parameter estimation process</td></tr>
</table>

[3] Sourced partly from Kileshye Onema and Taigbenu, 2008

Regardless of its significance, a considerable part of the society is still unwilling to adopt uncertainty estimation in hydrological modelling. Pappenberger and Beven (2006) reported on the seven common causes behind the fact that uncertainty analysis is not an usual and accepted part of modelling exercise, but highlighted that there should be no justification for not integrating uncertainty in water resources estimations. Gourley and Vieux (2006) documented the fact that it is still a challenge for water resources development, planning and management to identify the major causes of uncertainty.

Taking into account the fact that rainfall is the primary driving force behind most hydrological processes, extensive and abundant literature is available to date on how uncertainty associated with rainfall input does affect the modeling of hydrological processes. Among the most recent studies, for example, Koutsoyannis (2006) indicated that uncertainty in statistical estimates and long term predictions could be attributed to the conceptual approach chosen to capture multi-scale variability. He attempted also to link the uncertainty concept to the well-established physical and mathematical principle of entropy in order to explain the distributional and autocorrelation properties of hydrological processes at both temporal and spatial scales (Koutsoyiannis, 2005a, 2005b). Ewen *et al.* (2006) documented that incomplete, erroneous or misused forcing rainfall data contributes to the runtime error and to the overall uncertainty of the system. Yadav *et al.* (2007), in their attempt to improve regionalization of constraints in ungauged basins, noted that among the three physical characteristics that influence streamflow behaviour the most, rainfall was a key parameter and should be consider as such in uncertainty management. Ajami *et al.* (2007) further demonstrated that not accounting for existing error in the input and model conceptual framework could produce spurious parameter estimations leading to inaccurate and unreliable uncertainty bounds of the model prediction. Habib *et al.* (2008) who worked in a humid mid size catchment and used radar-rainfall estimates provide insight into the complex spatio-temporal behaviours of radar errors at hydrologically relevant scales and how they impact our definitions of uncertainties in stream flow modeling. Immerzeel and Droogers (2008) recommended a monthly rainfall increment in calibration per subbasin as a way of optimization of the NASA-TRMM (Tropical Rainfall Measuring Mission) rainfall data. Along the same line, Sawunyama and Hughes (2008) have also indicated the potential of using NOAA-derived rainfall for hydrological modeling in data-poor southern Africa with some local calibration of the remotely sensed-acquired rainfall data set as prerequisite. Using four different model structures with varying degrees of spatial resolution, Das *et al.* (2008) concluded that finely resolved input (rainfall data included) does not significantly improve the model performance in distributed and semi-distributed structures.

Following the analyses of Conway (2005), Koutsoyannis *et al.* (2008) indicated that due to uncertainty associated with climate change and consequently future rainfall patterns over the Nile Basin; its future behavior is unclear. While continuing along the lines of improving techniques for estimating rainfall from remotely sensed acquired data, this study underscores the challenges of uncertainty in the quality of the estimates. In other words, reliable and accurate hydrologic predictions are not possible unless the uncertainty associated with satellite-derived data can be quantified and corrected for. Several approaches exist for addressing the problem of uncertainty in hydrological modelling varying from Bayesian, fractals, fuzzy-sets, time series, random fields, risk criteria and non-parametric methods (Kundzewicz, 1995). The review from Sawunyama (2008) on approaches to estimate uncertainty associated with model outputs is reported in table 2-4.

Table 2-4 Summary of uncertainty estimation methods

Method	Description	Reference
a. The Monte Carlo Simulation (MCS)	uniform random sampling of parameters and subsequently the computation of model output	Beven and Binley, 1992
b. The Latin Hypercube Simulation (LHS)	step-wise approach that determines the statistics of an output by dividing a probability distribution of each basic variable into N ranges with an equal probability of occurrence (1/N)	Melching, 1995 Helton and Davis, 2003
c. The Rosenblueth's point estimation method (RPEM)	point-probability distribution to estimate the statistical moments of an output.	Rosenblueth, 1981 Binley et al., 1991
d. The Harr's Point Estimation Method (HPEM)	the statistical moments of the model output are estimated for a given number of parameters and model runs	Harr Milton, 1989
e. The first-order uncertainty analysis method	Taylor series expansion approximate linearization using the mean of a parameter range	Melching et al. 1990 Melching, 1992
f. Bayesian uncertainty analysis methods	assessement by combination of prior information associated with the uncertainty of model inputs with the ability of different parameter sets to describe the available data on state	Vrugt et al. 2003 Gupta et al. 2006

	variables	
g. Multi-objective approaches	assess uncertainty using predictions based on some Pareto "optimal" parameter sets	Gupta et al. 1998 Yapo et al. 1998
h. The Generalised Likelihood Uncertainty Estimation (GLUE) method	Built from the equifinality concept and allows multiple acceptable models or parameter sets based on some likelihood measures and performance thresholds.	Beven and Binley, 1992 Freer et al. 1996

The limitation of the MCS and LHS approaches is that they are computer intensive because they require many model simulations to establish acceptable parameter sets (Beven, 2001). The point-estimation approaches (c-e) are limited by the linearity approximation assumption of the model. Having recognised the limitations of those methods, advanced numerical simulation approaches such as Bayesian and multi-objective methods were developped.

Montanari (2007) grouped methods of estimating uncertainty into analytical methods, formal statistical methods, approximate numerical methods and non probabilistic methods. The recognized use of uncertainty and sensitivity analyses in hydrology provides answers to the following points: (a) the examination of the performance of a model, (b) the identification of the key model input data or parameters, and the interactions between them, guiding the calibration process, (c) the identification of input data or parameters that should be measured or estimated more accurately to reduce uncertainty of model outputs and (d) the quantification of the uncertainty in the model results (Saltelli, 2000).

Sensitivity analyses aim at determining how a model relates to its inputs, parameters, structure and underlying assumptions. As a result, sensitivity analysis can be part of uncertainty estimation methods by indicating where emphasis should be focussed in order to reduce uncertainty. The local techniques allow the response of outputs to deviation of individual inputs or variables, while fixing the other variables at their initial values. The global techniques allow for changes of all inputs or variables and implicitly account for parameter interactions (Muleta and Nicklow, 2005). The sensitivity analysis studies documented in this review of hydrological modelling and processes relate mainly to the sensitivity to rainfall input data (Andréassian *et al.*, 2001; Fekete *et al.*, 2004; Xu *et al.*, 2006), the sensitivity to potential evapotranspiration input data (Andréassian *et al*., 2004; Oudin *et al*., 2005) and the sensitivity to model structure and parameter values (Butts *et al*., 2004; Vrugt *et al*., 2005).

3 STUDY AREA AND DATASETS

3.1 Hydro-climatic and physical characteristics

3.1.1 Climate and hydrology

The Semliki drains the basins of lakes Edwards and George, and a contributing area downstream that includes the western slopes of the Ruwenzori range. The watershed receives an average rainfall of 1245mm per annum, with peaks occurring in April-May (95mm/month) and October (205mm/month). An average annual local runoff of 4.622 km^3 has been estimated from records at Bweramule (Sutcliffe and Parks, 1999). The Semliki River (Figures 3-1 & 3-2) joins Lake Edward to Lake Albert, after a flowing distance of about 250 km down the Rift Valley to the west of the Ruwenzori Mountain. The difference in water level is 295 m (Sahin, 1985). Most of the go down takes place over the fast-moving water that exists in the upper section of the river course. In the mid section the river has a width of 150 m at flood stage and reduces to 50 m at low stage. The average depth of water in these two seasons is 5 m and 3 m respectively (Sahin, 1985).

The chain formed by Lakes Albert and Edward constitutes a part of the Great Rift Valley. Lake Albert formerly called Lake Mobutu-Sese Seko, has a surface area of 5,300 km^2 at an elevation of 617 m. The depth of the water reaches 50 m at some places in the water body. The runoff from the lake drainage area plus the direct rainfall on the lake itself are all depleted by evaporation from the lake surface. The net gain is a result of the inflow of River Semliki, which comes into the lake from the southwest.

Lake Edward lies in the western Rift Valley, at an altitude of about 2,200 m. The lake basin area is traversed by a number of streams often obstructed by dense forest at their low ends. The lake is connected to Lake George in Uganda by the Kazinga channel, which is practically only a carrier.

3.1.2 Landform, lithology, soils and vegetation [4]

The flora and fauna of the watershed constitute one of a kind unique and distinct ecosystems of the Albertine Rift ecosystem. The flora is part of the Guineo-congolian, Afromontane and Zambesian phytochoria (Plumptre et *al.,* 2003). The vegetation predominantly comprises medium altitude moist evergreen to semi deciduous forest. Five distinct vegetation zones have been documented for mount Ruwenzori and they occur with ranges in altitude (savanna sites, woodland sites with lower altitude scrubby forest, low-mid altitude forests, medium altitude forests, high altitude forests) (UNEP, 2003). Landform, lithology and soils of the Semliki watershed sourced from the Soil and Terrain digital database for Central Africa (SOTERCAF) project are presented in Table 3.1 and Figures 3-3; 3-4; 3-5 Subcatchments (S5, S8 and part of S10 and S14) that are located in Uganda were not covered by the SOTERCAF project, hence no data are available. The Semliki subcatchments consist of diverse landform types with the depressions (LD) and plains (LP) representing the level land (Gradient <10%; relief intensity <50 m km^{-2}), the medium-gradient escarpments (SE), the medium-gradient hill (SH) and the medium-gradient mountain (SM) representing the sloping land (Gradient 10-30%; relief intensity 100-300m km^{-2}). The steep land in the watershed occurs as high

---

[4] Sourced from Kileshye Onema and Taigbenu, 2009b.

gradient mountain landform (TM) characterized by gradient higher than 30% and relief intensity above 300m km^{-2}. The major lithological classes of the Semliki subcatchments are acidic igneous rocks (IA), basic igneous rocks (dolerite\diabase), acidic metamorphic rocks (MA) and lacustrine sedimentary rocks (UL). Diverse soil types are found in this basin; the waterlogged cambisols (CMo) characterized by weak to moderate horizon development, acrisols (ACh) that are strongly acidic with high concentration of quartz or other resistant minerals in sand and silt sizes. Ferrasols (FRu) are excessively weathered with low fertility. Luvisols (LXh) that occur only in humid and sub humid environment, have high clay content that allows for good water storage. Nitosols (NTh) present an argillic horizon with a slight increase of clay in the profile. Phaeozems (Phi) are mostly grasslands with some broadleaf forest-covered soils with relatively deep and dark horizons.

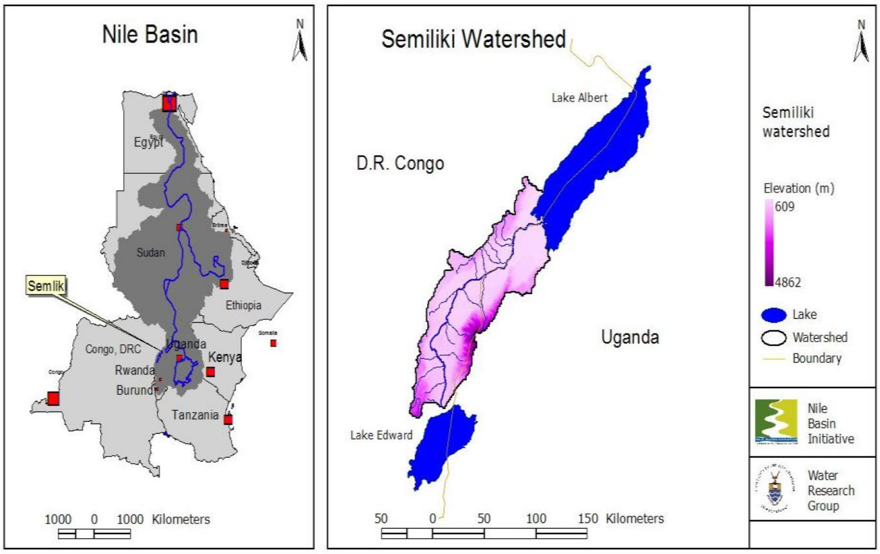

Figure 3-1 Semliki watershed and the Nile Basin

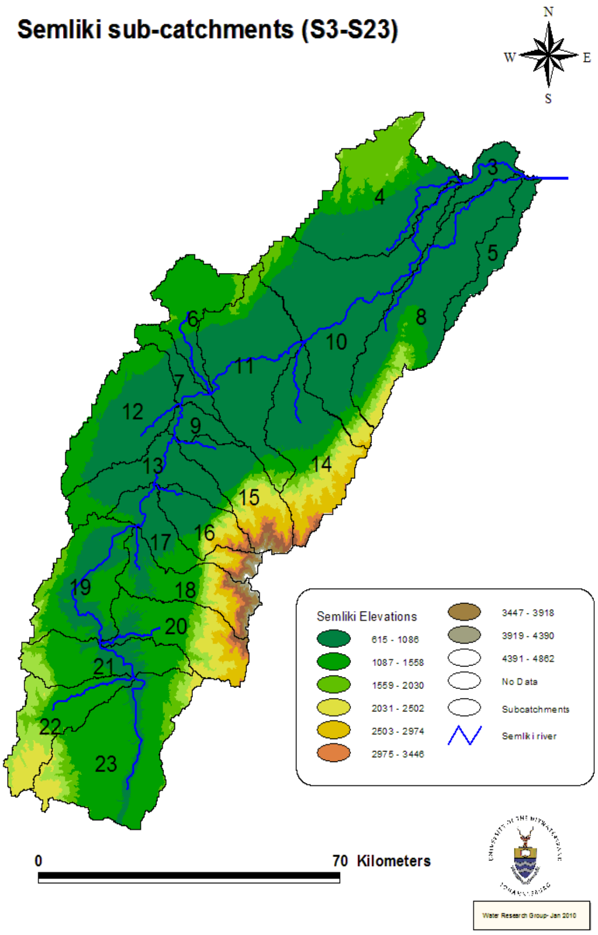

Figure 3-2 Semliki subcatchments (S3 to S23)

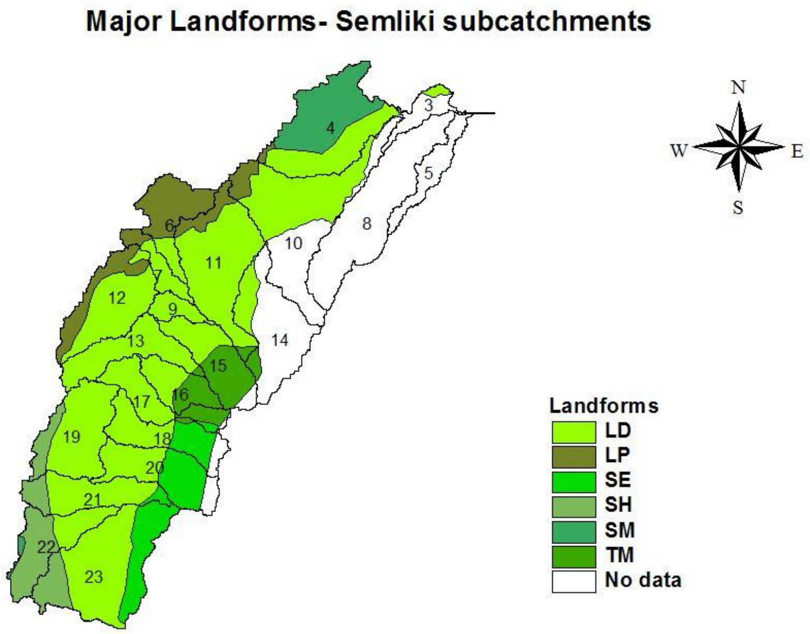

Figure 3-3 Semliki subcatchments Landforms

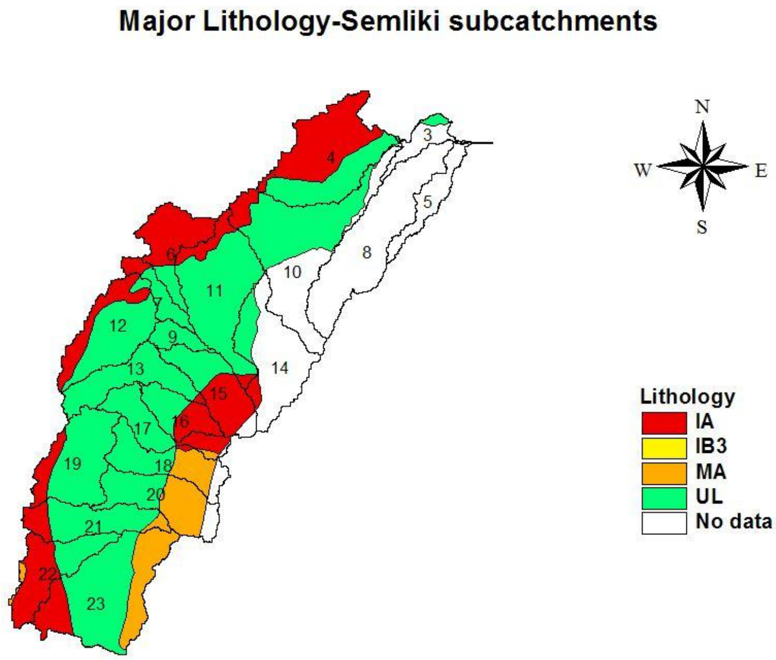

Figure 3-4 Semliki Subcatchments Lithology

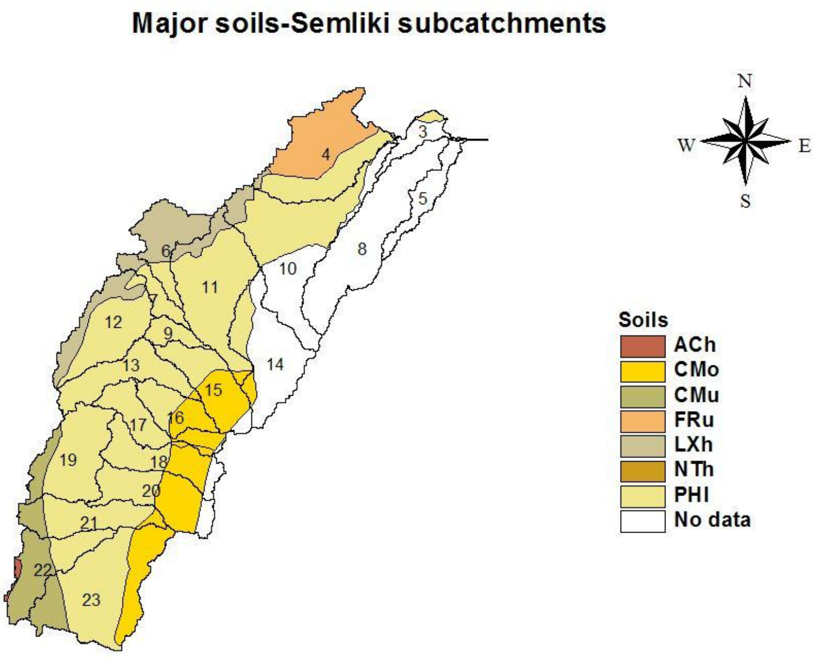

Figure 3-5 Semliki Subcatchments Soils

Table 3-1 Landform, lithology and soils for the Semliki subcatchments (S3-S23)

Id	Watershed Area (Km^2)	Watershed %	Landform	Lithology	Soils
S3	18.34	16.83	LD	UL	PHl
S4	10.42	1.68	LP	IA	LXh
S4	364.20	58.65	SM	IA	FRu
S4	245.89	39.60	LD	UL	PHl
S6	214.98	81.74	LP	IA	LXh
S6	48.79	18.55	LD	UL	PHl
S7	28.13	25.81	LP	IA	LXh
S7	80.69	74.03	LD	UL	PHl
S8	0.22	0.03	LD	UL	PHl
S9	81.64	99.56	LD	UL	PHl

S10	54.59	6.88	LP	IA	LXh
S10	421.83	53.19	LD	UL	PHI
S11	67.84	11.68	LP	IA	LXh
S11	501.30	86.28	LD	UL	PHI
S11	12.45	2.14	TM	IA	CMo
S12	145.56	32.49	LP	IA	LXh
S12	303.11	67.66	LD	UL	PHI
S13	0.04	0.01	LP	IA	LXh
S13	282.87	97.88	LD	UL	PHI
S13	6.02	2.08	TM	IA	CMo
S14	84.08	17.74	LD	UL	PHI
S14	22.69	4.79	TM	IA	CMo
S15	128.23	41.77	LD	UL	PHI
S15	156.16	50.87	TM	IA	CMo
S16	102.64	54.89	LD	UL	PHI
S16	84.85	45.37	TM	IA	CMo
S17	166.21	72.58	LD	UL	PHI
S17	50.13	21.89	TM	IA	CMo
S17	9.42	4.11	SE	MA	CMo
S18	152.75	52.49	LD	UL	PHI
S18	6.02	2.07	TM	IA	CMo
S18	97.46	33.49	SE	MA	CMo
S19	346.60	83.12	LD	UL	PHI
S19	0.74	0.18	SH	IB3	NTh
S19	69.64	16.70	SH	IA	CMu
S20	155.75	44.63	LD	UL	PHI
S20	155.27	44.49	SE	MA	CMo

S21	224.48	74.83	LD	UL	PHI
S21	55.89	18.63	SH	IA	CMu
S21	19.55	6.52	SE	MA	CMo
S22	106.21	35.05	LD	UL	PHI
S22	185.34	61.17	SH	IA	CMu
S22	11.89	3.92	SM	MA	ACh
S23	420.40	58.55	LD	UL	PHI
S23	102.96	14.34	SH	IA	CMu
S23	195.54	27.23	SE	MA	CMo

Landform

TM: High Gradient Mountain Zone

SE: Medium Gradient Escarpement Zone

SH: Medium Gradient Hill

SM: Medium Gradient Mountain

LD: Depression

LP: Plain

Lithology

IA: Acid Igneous Rock

IB3 :Dolerite\Diabase

MA: Acid Metamorphic Rock

UL: Lacustrine

Soils

ACh: Haplic Acrisols

CMo : Ferralic Cambisols

CMu: Humic Cambisols

FRu: Humic Ferrasols

LXh: Haplic luvisols

NTh: Haplic Nitosols

PHi: Luvic PhaeozemsT

3.2 Generation of catchments descriptors

3.2.1 Elevations

Meijerink *et al.* (1994) reported on how time consuming it is to estimate watershed attributes such as elevation from traditional relief maps. The 90m Digital Elevation Model (DEM) from the Shuttle Radar Topography Mission (SRTM) was used to derive maximum, weighted-average and minimum elevations for each of the 21 sub catchments (S3-S23) that constitute the study area (Figure 3-2). The maximum elevations in subcatchments vary from 640 metres to 4862 metres. Subcatchments S14, S15, S16, S17, S18, S20 are characterised by the highest relief. The minimum elevations of the 21 subcatchments range between 615 m and 901 m. The weighted average elevations were computed for each subcatchments using the equation 3-1:

$$weigthed\ elevation = \frac{\sum_{i=1}^{n} E_i\ C_i}{\sum_{i=1}^{n} C_i}$$ **Equation 3-1**

With

E_i representing elevation values of subcatchments.

C_i representing the count or the frequency of occurrences per elevation within subcatchments.

The weighted elevations for the Semliki subcatchments vary between 625 m and 1,915 m.

Hypsometric curves, also called Hypsographic Curves, which represent an empirical cumulative distribution function of elevations for each subcatchments, were also produced from the 90 m DEM. Gordon *et al.* (2004) indicated their usefulness in the analysis of hydrological variables that vary with altitude. Luo and Harlins (2003) successfully established a theoretical travel time based on watershed hypsometry of 23 fluvial basins in the United States of America. Recently Huang and Niemann (2008) documented the effects of streamflow generation mechanisms on basin hypsometry by using a numerical model. Furthermore, Vivoni *et al.*, (2008) related the Peacheater Creek basin hydrological response to its geomorphologic characteristics. The hypsometric distribution applies control over surface and subsurface runoff separation.

Hypsometric curves for the Semliki watershed (Figure 3-6) have indicated that 30% of elevation for sub catchments S14, S15, S16, S17, S18, and S20 are located above 2000 m.

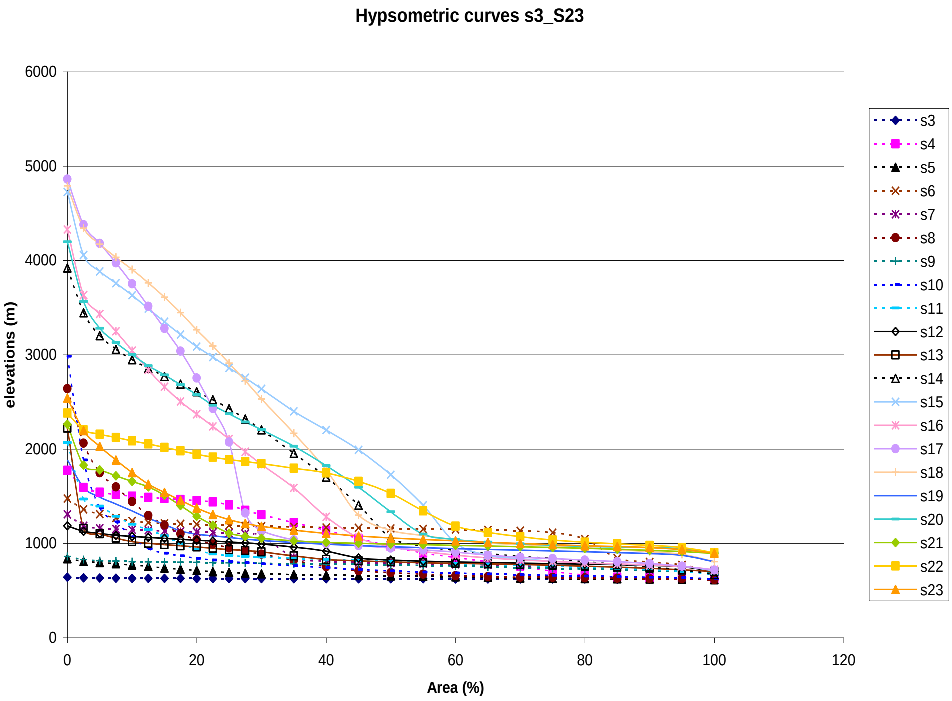

Figure 3-6 Hypsometric curves of the Semliki subcatchments (S3-S23)

3.2.2 Stream length

The stream length is one of the catchment characteristics which influences the travel time of water in the watershed as well as the quantity of stream habitat area in a drainage system (Gordon *et al.*, 2004). Measurements of stream length may be made by following the line with a ruler or scale graduated in map units, a digitizer or a pair of dividers. Map wheels (opisometers) are also recommended for measuring distance as they are rolled across the map. Their limitation is that they are not suitable for highly tortuous stream lines. Debate on the true stream length is still on. On one hand, the thalweg distance (distance measured down the central point of the stream channel or down its deepest path) is believed to be the true stream length. On the other hand, Gan *et al.* (1992) suggests the use of a fractal stream length as a more consistent measure. Using maps of the same scale, the stream is stepped off repetitively with dividers set at diverse intervals. Hence, a stream length (L) is computed for each interval (X). With simple regression, the information are represented with a log-log equation of the form

$$L = uX^{v} \qquad \textbf{Equation 3-2}$$

with u and v being the regression constants. The fractal stream length (L') is then simply equal to the constant u.

$$L' = u \qquad \textbf{Equation 3-3}$$

The stream lengths of the Semliki watershed were obtained from measurements of the blue lines on the 1:50 000 topographical map of the area. The real length of channel conveying flows varies over time, hence this map measurement should be considered as standardized index.

3.2.3 Drainage density

Drainage density (*Dd*) was defined by Horton (1945) as the sum of the lengths of all streams in a basin divided by the basin area. It is an essential characteristic of natural landscape that is related to local climate, relief and geology (Tucker *et al.*, 2001). It is an attribute that indicates how dissected a basin is. It has been documented that Drainage density (*Dd*) affects the transformation of rainfall into runoff (Pitlick, 1994; Tucci *et al.*, 1995; Berger and Entekhabi, 2001). Oguchi (1997) reported on previous studies that indicated relationship between drainage density (*Dd)* and climate, vegetation and hypsometric integral. He further indicated that the climatic and geologic controls on the drainage density (*Dd)* are widely documented and well established: The drainage density (*Dd)* has been reported also to be large in arid environments of light vegetation, in temperate to tropical subject to regular significant rains, and in regions underlain by lithology with low infiltration capacity or transmissibility (Madduma Bandara, 1974; Gardiner *et al.*,1977; Day, 1978; Tarborton *et al.*, 1992; Naden, 1992; Lin and Oguchi, 2004; Krause *et al.*, 2007). This study used a combination of stream as generated by the preprocessor of SWAT from the 90m SRTM Digital Elevation Model together with a 1:50 000 topographical map of the area to establish the stream network. While drainage densities estimated from this approach may not be precise in an absolute sense, they allow a comparison of the effects of differing intensities of dissection on runoff among sub catchments.

The drainage density (*Dd)* is defined as (Horton, 1945):

$$Dd = \frac{\sum L}{A}$$ **Equation 3-4**

Where L is the length of the stream and A the drainage area

3.2.4 Stream slope

The channel slope is important, first because streams control not only the shape of hill-slopes adjacent to the channel but also the coarse morphology of the whole catchment and landscape. Secondly, the stream channel is that part of the catchment which is most geomorphologically active under current climatic conditions (Penning-Rowsell and Tonshend, 1977; Acreman, 1985). It is therefore more likely that channel slope is accustomed to current processes, so that a meaningful analysis of interrelationships with other catchment attributes is possible. Stream discharge, represented by the contributory drainage basin area to each stream site examined by Hack (1957), showed a moderate negative relationship with slope but for each site the quotient of particle size and drainage area illustrated a high correlation with stream slope over all lithologies. Channel slopes are measured with a clinometer in gradually sloped sites and with a rod and level in steeply sloped sites, measurements are then averaged over sites and subsections and, in some instances, over shorter stream lengths (Adams *et al.*, 2000). For this study, the channel slope was computed with the equation 3-5 as recommended by Gordon *et al.* (2004).

The channel slope generated for Semliki subcatchment is actually the mean stream slope (*Sc*) and is given by:

$$Sc = \frac{(Es - Eo)}{L}$$ **Equation 3-5**

Sc Stream slope (%)

Es Elevation at source (m)

Eo Elevation at outfall (m)

L Length of stream (Km)

3.2.5 Rainfall[5]

Several satellite-derived rainfall datasets exist to date and extensive literature has documented the algorithms used to derive the final product. A review of some of the approaches is provided under section 2.1.1.2. The NOAA satellite-derived rainfall dataset was used for this study and was downloaded from the following link ftp://ftp.cpc.ncep.noaa.gov/fews/newalgo_est. As mentioned previously, these data are part of NOAA's effort to develop continuous and consistent rainfall dataset under the Famine and Early Warning Systems (FEWS). These data are currently available from 2001 and the derived gridded daily rainfall has a spatial resolution of 0.1 degree. The binary format of the dataset was converted into text using a Delphi data extraction program. The area-weighted average was used to calculate the total daily rainfall for each of the 21 subcatchments (S3 to S23) of the study area (Figure. 3-7).

The observed rainfall (August 1973 to date) measured at Beni station were the only data available for validation. The satellite-derived rainfall of neighboring grids to the only observed rainfall station were found at 95% confidence level to be significantly correlated in the range from 0.43 to 0.48 (Table 3-2). The non-linear optimization method, originally developed by Smakhtin and Hughes (1996) to patch and extend streamflow records and more recently documented by Sawunyama and Hughes (2008) in their attempt to correct satellite-derived rainfall data for hydrological modeling in South Africa, was used to locally calibrate the dataset for the Semliki subcatchments. The approach is an attempt to try to match

[5] Sourced from Kileshye Onema and Taigbenu, 2009b

the predictions against the observed. Figure 3-8 presents a summary of satellite derived rainfall of Semliki subcatchments.

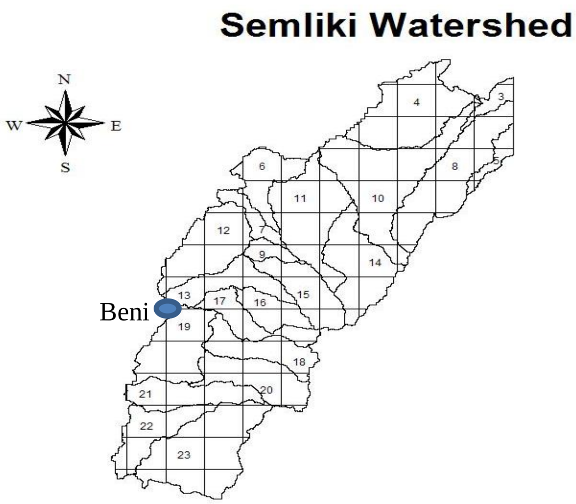

Figure 3-7 Semliki watershed subcatchments (S3 to S23 polygons) (NOAA spatial daily rainfall was generated and monthly aggregated and corrected for every grid)

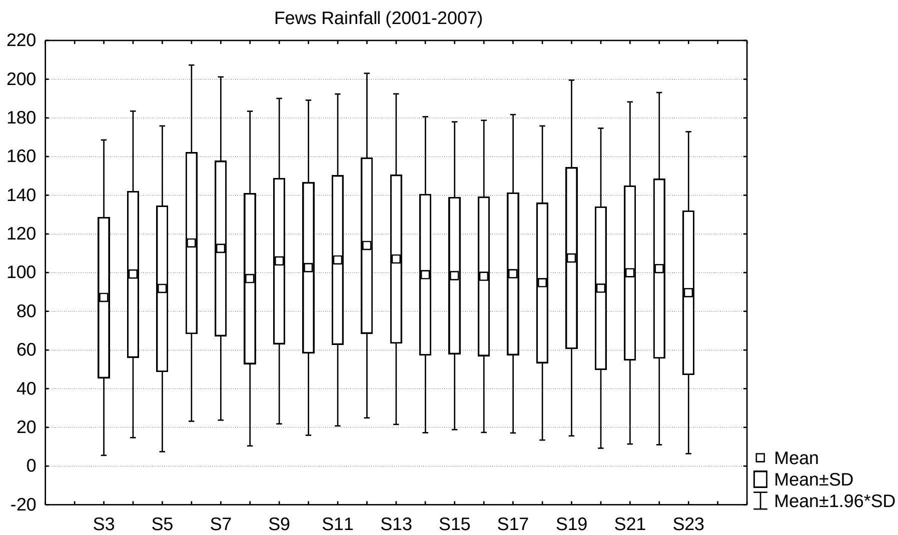

Figure 3-8 Whisker- box of Satellite derived monthly rainfall of the Semliki subcatchments (S3 to S23) from 2001 to 2007.

The correction of satellite derived rainfall approach relies on frequency of exceedance curves with the underlying assumption of cyclostationarity in variability of time series. From the NOAA dataset frequency exceedance values, a power relationship with the observed represented in equation (3-6) ($r^2 = 0.97$) was established for Beni and used to correct satellite derived rainfall over the Semliki Basin.

$$v = 0.73 \cdot u^{1.12}$$ **Equation 3-6**

With u = NOAA measured monthly rainfall and v = corrected NOAA-measured monthly rainfall

Table 3-2 Correlation between observed rainfall at Beni and satellite derived rainfall

Underlined correlations are significant at $p < .05$										
	P13a	P13b	P13c	P13d	P13e	P13f	P13g	P13h	P13i	P13j
Pobs	0.45	0.46	0.44	0.46	0.47	0.47	0.45	0.44	0.45	0.44
	P19a	P19b	P19c	P19d	P19e	P19f	P19g	P19h	P19i	
Pobs	0.43	0.47	0.45	0.47	0.48	0.44	0.46	0.46	0.46	

3.2.6 NDVI[6].

The normalized difference vegetation index (NDVI) is an indirect measurement of the photosynthetic activity. It ranges between -1 for low and +1 for high photosynthetic activity. The NDVI is defined as

$$NDVI = \frac{NIR - RED}{NIR + RED}$$ **Equation 3-7**

It uses the underlying principle that for vegetated surface, red (RED) and near-infrared (NIR) wavelengths are characterized by high and low absorption, respectively (Chen *et al.,* 2003; Groeneveld and Baugh 2007). Chlorophyll reflectance is about 20% in the red (RED) and 60% in the near infrared (NIR) and the contrast between the responses of both bands allows the quantification of the energy absorbed by chlorophyll, thereby providing indicative levels of different vegetation surfaces (Tucker and Sellers, 1986).

Many studies have investigated the relationship between NDVI and other physiographic attributes in different regions of the world. Reports have indicated positive linear relationship between rainfall and NDVI (Kawabata *et al.,* 2001; Wang *et al*., 2003; Ji and Peters, 2003; Groeneveld and Baugh, 2007). NDVI has been reported to also have relationship with other landscape physiographic attributes such as leaf area index (LAI) (Andersen *et al*., 2002; Wang *et al.,* 2005), land surface emissivities (Sobrino *et al*., 2006), and regional evapotranspiration (Bastiaanssen *et al.,* 1998; Jiang and Islam, 2001; Bastiaanssen *et al.,* 2002;

[6] Sourced from Kileshye Onema and Taigbenu, 2009b.

Dibella *et al.*, 2000; Boegh and Soegaard, 2004). For more detailed discussions on NDVI, see Groeneveld and Baugh (2007).

The Regional Remote Sensing Unit of SADC provided NDVI decadal images that were processed with WinDisp 5.1 to derive monthly NDVI. WinDisp 5.1 is a map and image display analysis software for satellite images, maps and associated databases, with an emphasis on early warning for food security. It was originally developed for the FAO Global Information and Early Warning System. The NDVI generated for this study is originally a product of the Advanced Very High Resolution Radiometers (AVHRR) on the National Oceanic and Atmospheric Administration satellites (NOAA7-16). The Global Inventory Monitoring and Modeling Studies (GIMMS) group ensures the dissemination of the images around the world. The dataset is inter-calibrated with the Système Probatoire d'Observation de la Terre (SPOT) Vegetation NDVI and further processing includes the maximum value compositing, artifacts removal as well as stratospheric aerosol corrections (Pinzon *et al.*, 2004; Tucker *et al.*, 2005). The data has also been corrected for sensor degradation, global cloud cover contamination, viewing angle effects due to satellite drift and low signal-to-noise ratios due to sub-pixel cloud contamination and water vapor (Tarnavsky *et al.*, 2008).

The 10-day NDVI dataset acquired from RRSU\SADC has a spatial resolution of 0.1 degrees (8 km under equal area conic projection) and a radiometric resolution of 8 bits per pixel. The consistency and the quality of these data have already been documented by several authors in Africa and other regions of the world as reported by Martiny *et al.* (2006).

To date it is widely acknowledged that remotely sensed acquired rainfall estimates are linked to significant uncertainties that originate from several elements such as hardware calibration, spatial representation, meteorological conditions as well as the pre-processing of the acquired information. Figure 3-9 provides a summary of the generated NDVI values for all the subcatchments of the Semliki watershed.

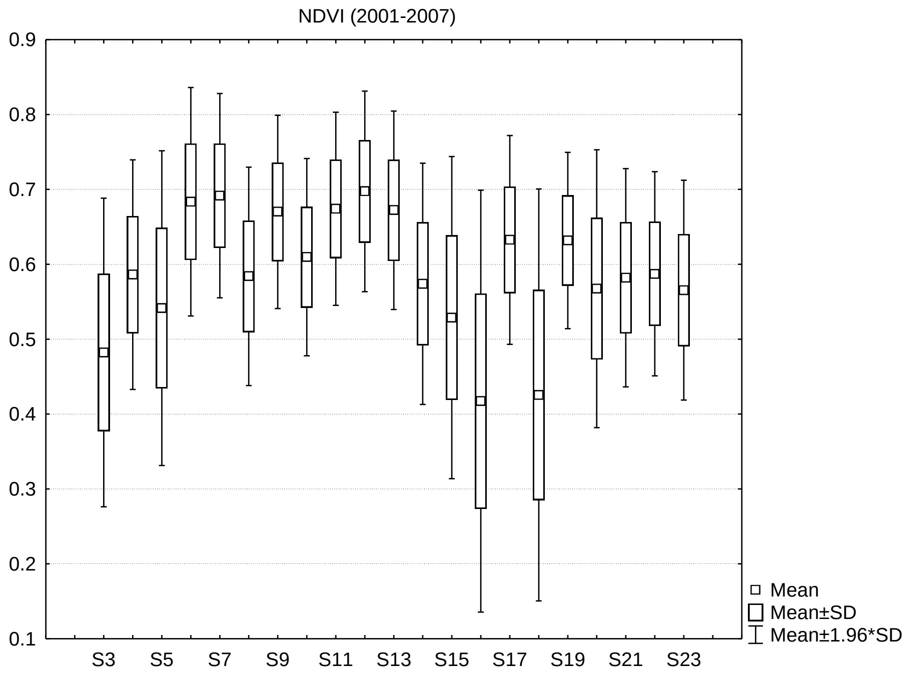

Figure 3-9 Whisker box of monthly NDVI of the Semliki subcatchments (S3 to S23) from 2001 to 2007.

This study highlights the challenge of hydrological data availability for rigorous water studies in data-poor watershed like in most regions of the developing world. Hence this research work started by generating data for the Semliki watershed from mainly remotely sensed acquired datasets and quasi-inexistant ground measurements. Table 3-3 summarises all the sources and data that have been generated and used for this research work.

Table 3-3 Data generated for the research work in the Semliki watershed

Description	Source	Observation
Landform	SOTERCAF	GIS processing (WINDISP, ARC View3.3, Excel 07-10, Statistica 8.0)
Lithology	SOTERCAF	GIS processing (WINDISP, ARC View3.3, Excel 07-10, Statistica 8.0)
Soils	SOTERCAF	GIS processing (WINDISP, ARC View 3.3, Excel 07-10, Statistica 8.0)
Drainage Density (Dd)	SRTM 90m-DEM, SWAT pre-processor	Subcatchments areas generated from SWAT preprocessor (WINDISP, ARC View3.3, Excel 07-10, Statistica 8.0, SWAT)
Stream Length	SRTRM 90m-DEM, topographical map (1/50,000), SWAT pre-processor	Generated from the SWAT preprocessor and cross validation with traditional map (WINDISP, ARC View3.3, Excel 07-10, Statistica 8.0, SWAT)
Stream slope	SRTM 90m DEM	Remotely sensed acquired (ARC View 3.3, Excel 07-10, Statistica 8.0)
Rainfall	FEWS NOAA / RFE (2001-2007) rain gauge (1973 to 2008)	Remotely sensed acquired and Locally corrected and calibrated (WINDISP, ARC view3.3, Excel 07-10, Statistica 8.0)
Elevations: Minimum Maximum Area-weighted average	SRTM 90m-DEM, topographical map (1/50,000)	Remotely sensed acquired and cross validation with traditional map. (Arc View 3.3, Excel 07-10, Statistica 8.0)
NDVI	NOAA-AVHRR (1982- 2008)	Remotely sensed acquired and correlated with rainfall. (WINDISP, ARC View3.3, excel 07-10, Statistica 8.0)

4 GENERAL METHODOLOGY OF THE STUDY

Variation of flow characteristics in time and space are influenced by catchment characteristics such as climate, catchment morphometry, lithology and land cover (Mazvimavi, 2003). Catchment characteristics differently affect the flow characteristics. Consequently, land cover/land use is not the only influential characteristic on flow characteristics to be examined. Multiple regression methods can be used to identify influential catchment characteristics for flows that are generated within a watershed. The following assumptions are made:

- There is a linear relationship between the dependant variable and catchment characteristics
- Those variables have distributions that approximate a normal.

These assumptions are not always verified, thus polynomial regression that are capable of modelling non-linear relationship and do not assume a specific underlying distribution for the data will be explored as well.

The landscape of any watershed is constituted of numerous combinations of physiographic attributes. These combinations are usually uneven among catchments, resulting in different hydrological responses. The effect on flow characteristics of a change in single catchment attribute such as land use or other morphometric characteristic is prone to be recognized (Mazvimavi, 2003; Bosch and Hewlett, 1982; Mumeka, 1986). However, effects of changes of a combination of watershed attributes are not easily identifiable. Multivariate analysis (ordination) and cluster analysis were then used to explore the structure of the data and guided the determination of optimal dimension of model for flow prediction in the Semliki watershed of the equatorial Nile region.

4.1 Ordination

Ordination techniques fall into two categories, namely indirect or direct gradient analysis. Table 4-1 as reported in Mazvimavi (2003) presents these techniques.

Table 4-1 Methods for indirect and direct gradient analysis

Indirect Gradient Analysis	Direct Gradient Analysis
Principal component analysis (PCA)	Redundancy Analysis (RDA)
Correspondence analysis (CA)	Canonical correlation (CanCor)
Detrended correspondence analysis (DCA)	Canonical correspondence analysis (CCA)
	Detrended Canonical correspondence analysis (DCCA)

The objective of indirect gradient analysis is to describe the structure between dependent and independent variables which in our case is that between flow characteristics and catchment descriptors.

From the regression equation

$$y = \boldsymbol{X}\beta + \varepsilon \qquad \textbf{Equation 4-1}$$

Let ***y*** *be* a vector of *n* observations on the dependent variable, measured about their mean, **X** is a (*n* x *p*) matrix whose (i, j) th element is the value of the j^{th}

predictor variable for the i^{th} observation, measured about its mean as well, β is a vector of p regression coefficients and ε is a vector of error terms; ε is made of independent elements. The value of the Prinipal Components (PCs) for each observation are computed by

$$\boldsymbol{Z} = \boldsymbol{XA} \qquad \textbf{Equation 4-2}$$

Where the $(i, k)^{th}$ element of **Z** is the value of the k^{th} Principal Component for the i^{th} observation, and **A** is a (p x p) matrix whose k^{th} column is the eigenvector of $\mathbf{X}^T\mathbf{X}$.

A is orthogonal (AA^T=I), hence $\mathbf{X\beta}$ can be represented as $\mathbf{XA}\mathbf{A}^T\boldsymbol{\beta} = \mathbf{Z}\boldsymbol{\gamma}$ with $\boldsymbol{\gamma}=\mathbf{A}^T\boldsymbol{\beta}$. Equation 4-1 then becomes

$$\boldsymbol{y} = \boldsymbol{Z\gamma} + \boldsymbol{\varepsilon} \qquad \textbf{Equation 4-3}$$

This is just the replacement of the predictor variables by their PCs in the regression expression (Jolliffe, 2002).

In the current study, Let y_i be the flow characteristic and i=1,2,…,n_c (where n_c denotes the number of catchments). Changes in flow characteristics y_i is explained by an unknown explanatory variable or landscape attribute x_{ik} and $k=1,2, \ldots n_q$ (Where n_q is the number of explanatory variables).

$$\boldsymbol{Y_i = a_i + x_{ik}\, b_k} \qquad \textbf{Equation 4-4}$$

Where a_k and b_k are unknown regression coefficients which relate the variation of $\boldsymbol{x_{ik}}$ with respect to $\boldsymbol{Y_i}$. The flow characteristic investigated is the volume of water generated within each subcatchment of the Semliki watershed.

A direct gradient analysis seeks to provide the fundamental structure in a dataset by investigating the relationship between the predicted variable (flow characteristics) and explanatory or predictor variables (physiographic attributes).

4.1.1 Principal Component Analysis

Mathematically, the PCA is defined as an orthogonal linear transformation that provides a new system of coordinate for data such that the greatest variance by any projection of the data lies on the first coordinates with the second greatest variance lying on the second coordinate and so forth. In meteorology, the PCA is referred to as the empirical orthogonal function (EOF). The Principal Component Analysis is theoretically the optimum transform for given data in least square terms. The output of a PCA is unique and independent of any underlying assumptions about the data probability distribution.

The Principal component analysis (PCA) as Indirect Gradient Analysis was used as the exploratory technique to study the structure of the data. The PCA was further utilised in the identification of similarities among sub catchments. Multi linear and polynomial regressions were performed on the eight physiographic attributes selected to derive the models as illustrated in figure 4-1 except that the normality test was not performed for polynomial optimization.

4.2 Clustering analysis[7]

Cluster analysis includes a number of different procedures and algorithms that aim at grouping objects of similar kind into respective categories. A shared problem that researchers faced in their respective work and domains is how to organize data into expressive and comprehensive structures, that is, to develop

[7] Partly sourced from www.statsoft.com , Electronic statistics textbook

classifications. Cluster analysis is the exploratory technique that allows data analysis that subsequently result into sorting different objects into groups in a way that the level of association between two objects is maximal if they belong to the same category and minimal otherwise. From the above, cluster analysis is used to ascertain structures in data without explanations or interpretations. However, unlike several other statistical techniques, cluster analysis methods are meant to be used when we do not have any a priori hypotheses, but are still in the exploratory phase of the investigation. In a sense, cluster analysis finds the "most significant solution possible." The review of the general categories of cluster analysis methods indicates the following approaches :

- Joining (Tree Clustering)
- Two-way Joining (Block Clustering)
- k-Means Clustering

4.2.1 Joining / Tree clustering

The purpose of this technique is to join together data into sequentially larger clusters, using some measure of similarity or distance. A typical result of this type of clustering is the hierarchical tree. The joining or tree clustering method uses the similarities or distances between objects when establishing the categories. Similarities are defined as set of rules that serve as criteria for grouping or separating items. These distances can be built on a single dimension or multiple dimensions, with each dimension representing a rule or condition for grouping objects. The following methods are computed to find distances between objects:

Euclidean distance: This is one of the most generally chosen type of distance. It is the geometric distance in the multidimensional space. It is computed as:

$$\boldsymbol{Distance}(\boldsymbol{x},\boldsymbol{y}) = \left\{\sum_{\boldsymbol{i}} (\boldsymbol{x}_{\boldsymbol{i}} - \boldsymbol{y}_{\boldsymbol{i}})^2\right\}^{\frac{1}{2}}$$ **Equation 4-5**

With *x* and *y* being the coordinates

The Euclidean distances are usually computed from raw data, and not from standardized data. This method presents certain robustness that includes for instance that the distance between any two objects is not influenced by the build up of new objects to the analysis, which may be outliers.

4.2.2 Two-way joining / block clustering

When the research design is uncertain on whether to cluster cases or variables, the two-way joining technique presents the opportunity to cluster both simultaneously. Two-way joining is useful in circumstances when one expects that both cases and variables will simultaneously contribute to the uncovering of meaningful patterns of clusters. The difficulty with interpreting these results may arise from the fact that the similarities between different clusters may pertain to (or be caused by) somewhat different subsets of variables. Thus, the resulting structure (clusters) is by nature not homogeneous. This may seem a bit confusing at first, and, indeed, compared to the other clustering methods described and k-Means Clustering, two-way joining is probably the one least commonly used.

4.2.3 K-Means clustering

This method of clustering differs substantially from the Tree Clustering and Two-way Joining. This technique supposes that one have predefined hypotheses with regard to the number of clusters for cases or variables. The overall objective is to set exactly the number of clusters to be computed. This is the type of research question that can be addressed by the k- means clustering algorithm. In general, the k-means method will generate exactly k different clusters of greatest possible distinction.

Tree clustering and block clustering are the two methods that have been used together with the PCA to explore Semliki landscape attributes association in this study.

4.3 Multilinear and polynomial regressions

4.3.1 Multilinear regression

The general purpose of multiple regressions (the term was first used by Pearson, 1908) is to learn more about the relationship between several independent or predictor variables and a dependent or criterion variable. To date several examples have documented the approach, for instance an estate company might be interested in documenting for each product the size of the house, the number of rooms, the mean income in the respective neighborhood according to survey data, and an idiosyncratic (subjective) rating of request of the property. Once this information has been compiled for various products, it would be informative to identify whether and how these factors relate to the price for which a specific product is being sold. One of the probable results is that the number of rooms is a fairly good and representative predictor of the price for which a property goes for in a specific market. In addition, it will also be interesting to see why some products are marginalized (outliers). Other examples come from natural and social sciences, the multiple regression approach have been extensively documented. The procedure of multiple regression provides the researcher with an answer on the more suitable or appropriate predictor. Cases in educational studies have documented the search for the most appropriate variable in the prediction of success or failure. Similarly, psychologists have tried to identify the kind of profile that is the most related to social responses and behaviors. Equally, sociologists may be interested in identifying the social parameter that is the most significant with regards to immigration group behaviors for instance. First of all, as is evident in the name multiple linear regression, it is assumed that the relationship between variables is linear as alluded to in the introduction of this chapter. In practice, this underlying assumption can almost never be established; on the other hand, multiple regression techniques are not significantly affected by negligible deviations from this basic supposition. When the evidence of curvature in relationships is reported, the researcher may decide on either to perform the transformation of predictors, or to explicitly provide room for nonlinear constituents. The other assumption in multiple regression is that the residuals (predicted minus observed values) follow a normal distribution. Despite the report that tests are significantly powerful and versatile especially the F-test with regards to the violation of the normality assumption, it is recommended however to undertake some normality test before drawing final conclusions. The main theoretical drawback of all regression techniques is to be found in the fact that you can only establish some relationships, but no insight is provided on the underlying causal mechanism.

4.3.2 Polynomial regression

Higher-order effects for continuous variables that do not account for effects between variables in the prediction of a dependent variable can be modeled through Polynomial regression. The polynomial regression (degree 2) for instance for a set of three continous variables *P, Q,* and *R* equation (4-10) would comprise the core effects of *P*, *Q*, and *R* and their second order effects (quadratic), however the 2-way or 3-way interaction effect between variables will not be catered for the three predictors.

$$Y = b_0 + \begin{Bmatrix} b_1 \\ b_3 \\ b_5 \end{Bmatrix} \{P\ Q\ R\} + \begin{Bmatrix} b_2 \\ b_4 \\ b_6 \end{Bmatrix} \{P^2\ Q^2\ R^2\}$$ **Equation 4-6**

In practice, polynomial regression set up does not have to contain all effects up to the identical level (degree) for each and every variable. Quadratic and cubic degree for example could be incorporated in the modeling of some predictors, and effects up the fourth level (degree) could be considered in the model development of other predictor variables. Polynomial (or 'fixed nonlinear') regression computes the relationship between a dependent variable with one or more independent (predictor) variables, and those independent variables squared, cubed, etc. For example, for one independent variable one could estimate the regression equation (4-11):

$$Y = a + b_1X + \ b_2X^2$$ **Equation 4-7**

Here, the dependent variable Y is a linear function of X and X^2. Polynomial regression is common in studies when reserachers aim at investigating some curvilinearity in relationships between predictor variables and the dependant. The case of stress as the predictor or independent variable, for instance to performance of some duty might have a curvilinear relationship. Hence, minimal to moderate stress may increase the performance. However, beyond a certain threshold of stress, performance will be affected. If that is the case, the quadratic (nonlinear) component or regression coefficient in the regression equation would be significant. Figure 4-1 summarises the methodology which was undertaken in the development of the Multilinear and the polynomial models of this study.

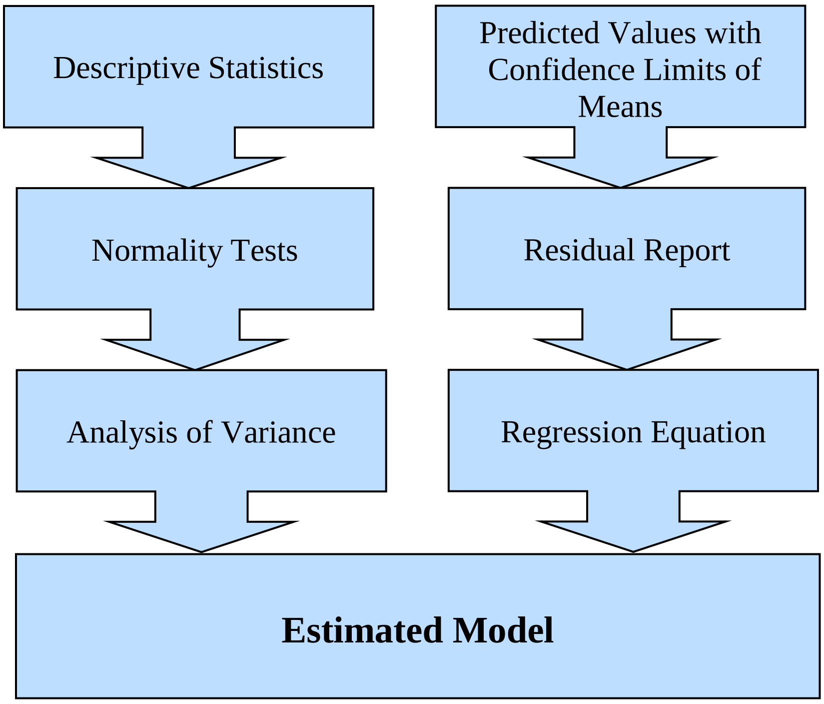

Figure 4-1 summary of the statistical approaches

4.4 Statistical performance measures

The performance ratings for prediction accuracy were the following dimensionless evaluation statistics. The Nash-Sutcliffe efficiency (NSE), the Percent bias (PBIAS), the Root Mean Square Error-observations standard deviation ratio (RSR), The coefficient of multiple correlation (*Multiple R*), The R^2 and the adjusted R^2_{adj}.

The coefficient of multiple correlations (*Multiple R*) is the positive square root of R-square (the coefficient of multiple determinations). This statistic is useful in multivariate regression to describe the relationship between the variables.

The R^2 equation (4-8) field contains the coefficient of multiple determinations, which measures the reduction in the total variation of the dependent variable due to the (multiple) independent variables.

$$R^2 = 1 - \left(\frac{Residual\ SS}{Total\ SS} \right)$$ **Equation 4-8**

SS: Sum of squares

The adjusted R_{adj}^2 equation (4-9) is interpreted similarly to the R^2 value except the adjusted R^2 takes into account the number of degrees of freedom. It is adjusted by dividing the error sum of squares and total sums of square by their respective degrees of freedom.

$$R_{adj}^2 = 1 - \left(\frac{(Residual\ SS)/df}{(Total\ SS)/df} \right)$$ **Equation 4-9**

SS: Sum of squares

df Degrees of freedom

The Nash-Sutcliffe Efficiency (NSE) is a normalized index that defines the relative magnitude of the residual variance (“noise”) compared to the measured data variance (“information”) (Nash and Sutcliffe, 1970). NSE shows how well the graph of observed versus simulated data fits the 1:1 line. NSE is calculated as shown in equation 4-10:

$$NSE = 1 - \left[\frac{\sum_{i=1}^{n} (Y_i^{obs} - Y_i^{sim})^2}{\sum_{i=1}^{n} (Y_i^{obs} - Y^{mean})^2} \right]$$ **Equation 4-10**

where Y_i^{obs} is the *i*th observation for the constituent being evaluated, Y_i^{sim} is the *i*th simulated value for the constituent being evaluated, Y^{mean} is the mean of observed data for the constituent being evaluated, and *n* is the total number of observations.

NSE ranges between -1.0 and 1.0 (1 inclusive), with NSE 1 being the optimal value. Values between 0.0 and 1.0 are generally viewed as acceptable levels of performance, whereas values <0.0 indicates that the observed mean value is a better predictor than the simulated value, which indicates unacceptable performance (Moriasi *et al.,* 2007).

Percent bias (PBIAS) as reviewed in Moriasi *et al.,* (2007) is defined as the index evaluating the average tendency of the simulated data to be larger or smaller than their observed counterparts (Gupta *et al*., 1999). The optimal value of PBIAS is 0.0, with low-magnitude values showing accurate model simulation. Positive values indicate model underestimation bias, and negative values indicate model overestimation bias (Gupta *et al.,* 1999). PBIAS is calculated with equation 4-11:

$$PBIAS = \left[\frac{\sum_{i=1}^{n} (Y_i^{obs} - Y_i^{sim}) * 100}{\sum_{i=1}^{n} (Y_i^{obs})} \right]$$ **Equation 4-11**

where PBIAS is the deviation of data being evaluated, expressed as a percentage.

where Y_i^{obs} is the *i*th observation for the constituent being evaluated and Y_i^{sim} is the *i*th simulated value for the constituent being evaluated.

Percent streamflow volume error (Singh *et al.,* 2004), prediction error (Fernandez et *al.,* 2005), and percent deviation of stream flow volume are computed similarly to the PBIAS. The deviation factor is used to measure the accumulation of differences in streamflow volume between forecasted and measured data for a particular period of analysis. PBIAS has the ability to clearly indicate poor model performance (Gupta *et al.,* 1999). PBIAS values for streamflow tend to vary more, among different autocalibration methods, during dry years than during wet years (Gupta *et al.,* 1999).

The RMSE-observations standard deviation ratio (RSR) standardizes RMSE using the observations standard deviation. The Root Mean Square Error (RMSE) is one of the frequently used error index statistics and the lower the RMSE the better the model performance. However most of the time guidelines are not available on what to accept as a low RMSE based on the observations standard deviation. Therefore, the RSR is calculated as the ratio of the RMSE and standard deviation of measured data, as shown in equation 4-12 (Moriasi *et al.,* 2007).

$$RSR = \frac{RMSE}{STDEV_{obs}} = \frac{\left[\sqrt{\sum_{i=1}^{n}(Y_i^{obs} - Y_i^{sim})^2}\right]}{\left[\sqrt{\sum_{i=1}^{n}(Y_i^{obs} - Y^{mean})^2}\right]} \quad \textbf{Equation 4-12}$$

Where Y_i^{obs} is the ith observation for the constituent being evaluated, Y_i^{sim} is the ith simulated value for the constituent being evaluated, Y^{mean} is the mean of observed data for the constituent being evaluated, and n is the total number of observations.

The RSR integrates the benefits of error index statistics and includes a scaling/normalization factor, so that the resulting statistic and reported values can apply to various constituents. RSR varies from the optimal value of 0, which indicates zero RMSE or residual variation and therefore perfect model simulation, to a large positive value.

4.5 Summary

This chapter reports on the different approaches that were used for this research work

- An indirect ordination technique namely the Principal Component Analysis (PCA) in conjunction with the clustering analysis (tree diagram and two-way joining) were used to detect data structure and similiraties.
- The Principal Component Analyis (PCA) provided variables (landscape attributes) structure as well hence guiding the model development in identifying redundant variables and optimal dimension.
- Multilinear and polynomial regressions together with all the statistical techniques linked with the two approaches were performed to developped the mesoscale deterministic prediction model for the Semliki watershed.
- Several statistical performance indices were computed for the calibration of the developed models

5 LANDFORM CHARACTERIZATION AND CLASSIFICATION OF SIMILAR SUBCATCHMENTS

5.1 Identification of similar catchment descriptors and sub-catchments

5.1.1 Principal Components Analysis (PCA)

The descriptive statistics below (Table 5.1) show that the variables included in the PCA are measured at significantly varying scales. However this does not affect the results of the analysis as the matrix analyzed is the scale invariant correlation matrix of the variables (as opposed to the covariance matrix).

Table 5-1 Descriptive statistics of stationary variables

Variables	Variable	Count	Mean	Standard Deviation	Units
Stream Length	X_1	21	29.46	20.66	Km
Drainage density	X_2	21	7.85×10^{-2}	3.52×10^{-2}	$Km.Km^{-2}$
Average Slope	X_3	21	0.2	0.23	%
Maximum elevation	X_4	21	2577.9	1273.84	m
Minimum elevation	X_5	21	733.18	99.78	m
Average elevation	X_6	21	1164.82	392.54	m

The other two variables X_7 and X_8 are respectively the NDVI and the precipitation which vary spatially and temporally.

The correlations between the variables are summarized in table 5.2. There are some high correlations (greater than 0.5), implying that there is a correlation structure that can potentially be assessed or further explored using PCA. If all the correlations were low there would be no need to try to assess the correlation structure using principal components analysis.

The value of phi (ϕ) for this data (0.4) (Table 5-3) suggests that there is considerable redundancy or complexity in the group of variables which warrants further examination using PCA. Bartlett's sphericity test is used to test the null hypothesis that the correlation matrix of the group of variables is a zero identity matrix i.e. none of the variables are correlated. If we obtain a p-value for the Bartlett's test which is greater than 0.05 we should not carry out PCA. The p-value obtained (Table 5-3) is very low indicating that we can carry out the PCA.

Table 5-2 Coefficients of correlations between variables

	Stream Length	Drainage Density	Average Slope	Maximum elevation	Minimum Elevation	Average elevation	Monthly precipitation	Monthly NDVI
Stream Length	1	0.344	-0.2	-0.05	-0.29	-0.29	-0.08	0.07
Drainage Density		1	-0.19	-0.46	-0.24	-0.45	0.07	0.16
Average Slope			1	0.37	0.13	0.54	0.08	-0.15
Maximum Elevation				1	0.23	0.87	-0.5	-0.63
Minimum Elevation					1	0.46	-0.25	-0.23
Average Elevation						1	-0.45	-0.64
Monthly Precipitation							1	0.78
Monthly NDVI								1

Table 5-3 Bartlett test and Glaeson – Staelin (Phi)

Bartlett Test	DF	P-Value	Glaeson –Staelin (Phi)
81.98	28	0.000	0.395

According to the Kaiser criterion when the principal components have been calculated using correlation coefficients those components with an eigenvalue greater than 1 are retained. Therefore, based on the results shown in table 5-4, we would retain the first 3 principal components. These 3 principal components account for 76% of the variation in the data.

Table 5-4 Eigenvalues of components

No.	Eigenvalue	Individual Percent	Cumulative Percent
1	3.49	43.59	43.59
2	1.56	19.46	63.04
3	1.02	12.71	75.75
4	0.78	9.80	85.55
5	0.64	7.97	93.51
6	0.30	3.74	97.25
7	0.17	2.13	99.38
8	0.05	0.62	100.00

The Eigenvectors are the coefficients that relate the scaled original variables to the derived factors. The scaled original variables are defined as follows:

$$x_i = \frac{X_i - \mu_i}{\sigma_i}$$ **Equation 5-1**

where; x_i = the scaled variable; X_i = the original variable; μ_i = the mean of the original variable and σ_i = the standard deviation of the original variable

For instance, the first principal component is:

Factor1 = $-0.16x_1 - 0.28x_2 + 0.24x_3 + 0.47x_4 + 0.27x_5 + 0.51x_6$ - **Equation 5-2**

$0.42x_7 - 0.34x_8$

Where the x_i in Equation (5-2) represents the scaled form of the variables

X_1: Stream Length (Strm_len)

X_2: Drainage density (Drainage)

X_3: Mean Stream slope (avg_slope)

X_4: Maximum elevation of the subcatchments (Max_elev)

X_5: Minimum elevation of the subcatchments (Min_elev)

X_6: Weighted average elevation of the area (avg_elv)

X_7: Monthly NDVI (monthly_NDVI)

X_8: Monthly precipitation (monthly_prec)

Inspection of the eigenvectors for the first factor shows that avg_slope, max_elev, min_elev and avg_elev play contrasting roles to strm_len, drainage, monthly__prec and monthly_NDVI. This factor explains 44% of the variation in the data. The eigenvectors of the three factors are shown in Table 5-5.

Table 5-5 Eigenvectors of principal components

Variables	Factor1	Factor2	Factor3
Strm_len	-0.16	-0.52	-0.42
Drainage	-0.28	-0.36	-0.10
avg_slope	0.24	0.37	-0.60
Max_elev	0.47	-0.08	-0.27
Min_elev	0.27	0.17	0.56
avg_elev	0.51	0.10	-0.14
monthly__prec	-0.34	0.52	-0.22
monthly_NDVI	-0.42	0.37	-0.05

The factor loadings are the correlations between the variables and the factors. Factor 1 is most highly correlated to the maximum elevation and the average elevation; whereas factor 3 is most highly correlated to the average slope and the minimum elevation (Table 5-6).

Table 5-6 Factor loadings of principal components

Variables	Factor1	Factor2	Factor3
Strm_len	-0.29	-0.65	-0.42
Drainage	-0.53	-0.45	-0.10
avg_slope	0.45	0.46	-0.60
Max_elev	0.87	-0.10	-0.27
Min_elev	0.50	0.21	0.56
avg_elev	0.94	0.12	-0.14
monthly__prec	-0.63	0.65	-0.22
monthly_NDVI	-0.78	0.46	-0.05

Figure 5-1 provides an illustration of the projection of the variables on a factor plane using an alternative criteria for the PCA of variables. Each quadrant represents a similar group of variables in terms of changes in variance in the datasets

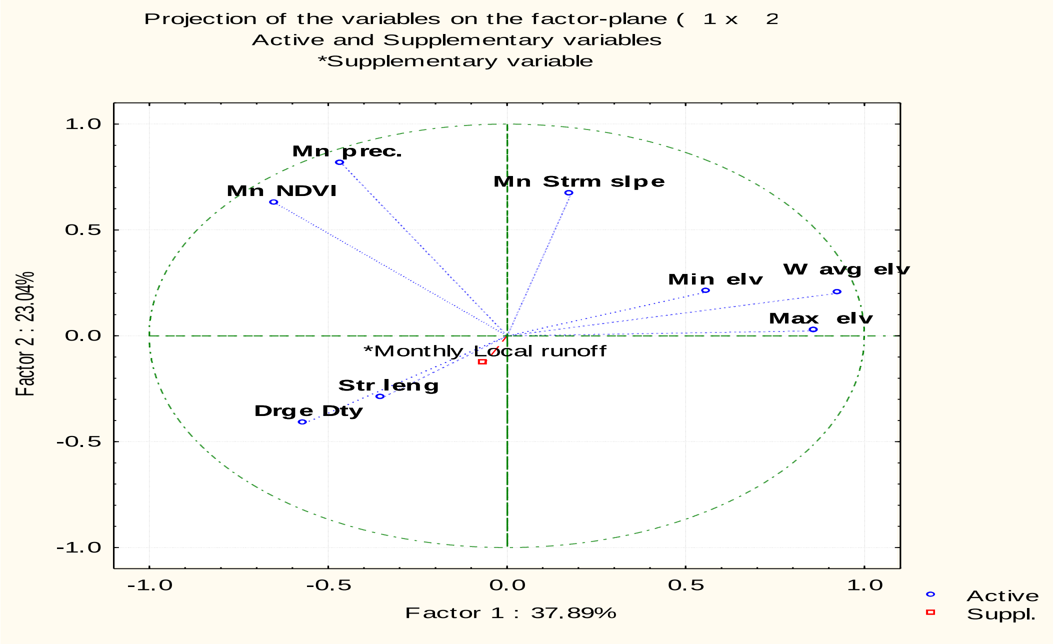

Figure 5-1 PCA of variables

Further use of the PCA is made in order to identify groupings of subcatchments by assessing the projection of cases onto the factor plane (Figure 5-2)

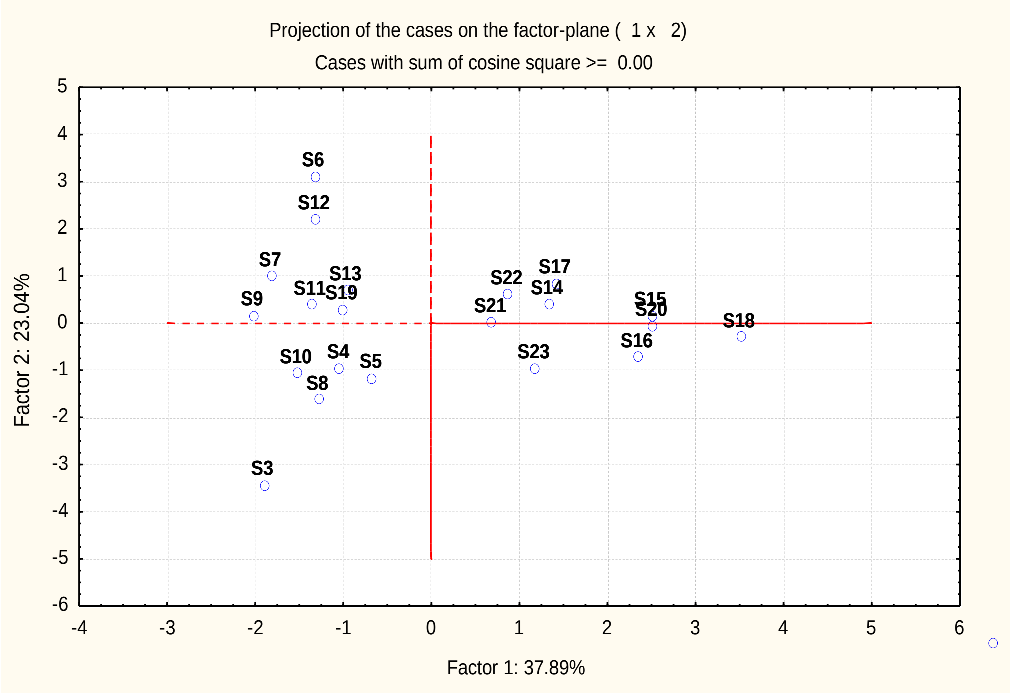

Figure 5-2 Projection of cases from the PCA of variables

The figure distinguishes four groups of similar subcatchments in terms of variability of catchment descriptors. However, these groupings are reduced to two (2) main groups or categories (Table 5-7) so as to simplify the prediction equations of the runoff, which is the main goal of this study. The physiographic attributes, namely mean stream slope, minimum elevation, maximum elevation, weighted average elevation that provide this major categorization from the PCA are located in the first quadrant of figure 5-1. The two main categories of subcatchments identified through the PCA are further illustrated in table 5-8.

Table 5-7 Grouping of Semliki subcatchments from the PCA

Category I	Category II
S3	S14
S4	S15
S5	S16
S6	S17
S7	S18
S8	S20
S9	S21
S10	S22
S11	S23
S12	
S13	
S19	

All subcatchments in group I for instance are characterized by elevations whose minimum values do not exceed 703m, while Group II subcatchments on the other hand show weighted average of elevations that are above 1122m. These similarities in physiographic attributes further support the grouping of subcatchments that is produced by the PCA.

5.1.2 Clustering analysis

The clustering analysis was performed with the single linkage as the amalgation rule and the Euclidean distance since all the data were considered to be raw. The outcome of the analysis produced the tree diagram (Figure 5-3) that further supports the grouping of subcatchments (S14, S16, S20, S15, S18, S17) which clearly constitutes a cluster. Subcatchments (S21, S22, S23) on the other hand are more related to the other cluster under this tree diagram.

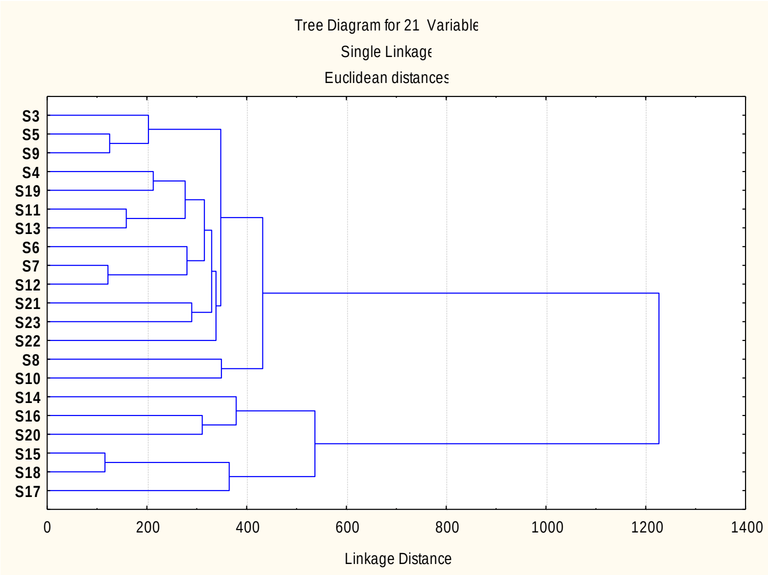

Figure 5-3 Tree Diagram-clustering of Semliki subcatchments

The two-way joining results (Figure 5-4) are in agreement with the PCA on grouping of subcatchments (S3, S4, S5, S6, S7, S8, S9, S10, S11, S12, S13 and S19) that constitutes the first group of similar subcatchments in terms of their hydrological conditions. Similarly, the classification of the second group of related subcatchments under this clustering analysis further supports the output of the tree diagram graph as reported in Figure 5-3. From Figure 5-4, three (C_6, C_5 and C_4) of the eight classes identified (C_1 to C_8) exhibit the most dissimilarities in terms of landscape attributes. This is evident with subcatchments S14, S15, S16 and S20 that are characterised by elevation values higher than 4000 m above the sea level.

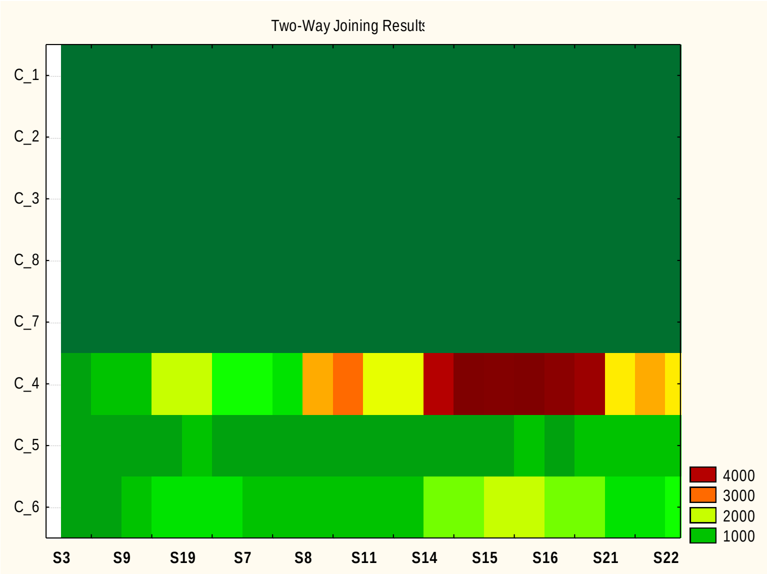

Figure 5-4 Two-way joining results of Semliki subcatchments

Table 5-8 further presents the grouping of sub-catchments as identified through the Principal Component Analysis. In fact, the two groups of subcatchments can be identified from the color code used in the first column of the table 5-8. Further subdivision of the subcatchments is illustrated for the two groups. For the category of subcatchments denoted by light blue (Category I), there exist two sub-groups that are identified by yellow and green shade in their repective rows. While for the second category denoted by purple colour, there exist two sub-groups denoted by white and brown rows. For instance, sub-grouping for S3, S4, S5, S8 and S10 is largely determined by similarities of these landscape attributes namely, stream slope, minimum elevation and NDVI.

Table 5-8 Physiographic attributes of the two groups of Semliki subcatchments as identified by the PCA and the clustering analysis

	Str. leng(Km)	Drain. Dsity	Strm slope (%)	Max elev. (m)	Min elev. (m)	W avge elev. (m)	Monthly prec.(mm)	Monthly NDVI
S3	24.9	0.2284	**0.0121**	640	**617**	625	87.1	**0.48**
S4	55.0	0.0886	**0.0909**	1774	**624**	1040	99.1	**0.59**
S5	7.3	0.0482	**0.0953**	836	**615**	675	91.7	**0.54**
S6	29.4	0.1118	1.3927	1476	692	1111	115.3	0.68
S7	10.9	0.1007	0.0365	1307	690	888	112.5	0.69
S8	74.4	0.1148	**0.0632**	2640	**615**	877	96.9	**0.58**
S9	10.8	0.1328	0.0739	861	695	767	106.0	0.67
S10	82.4	0.1039	**0.0594**	2983	**624**	812	102.5	**0.61**
S11	39.0	0.0671	0.0564	2069	667	879	106.6	0.67
S12	15.7	0.0351	0.4454	1186	703	891	114.0	0.70
S13	16.7	0.0577	0.0240	2221	701	858	107.0	0.67
S14	25.7	0.0543	0.4667	3920	669	1600	98.9	0.57
S15	14.0	0.0457	0.2705	4727	710	1915	98.4	0.53
S16	10.1	0.0541	0.2470	4329	719	1502	98.1	0.41
S17	17.7	0.0772	0.5196	4862	717	1566	99.4	0.63
S18	12.9	0.0441	0.4280	4792	806	1913	94.6	0.43
S19	47.6	0.1143	0.1953	1887	804	1036	107.6	0.63
S20	22.0	0.0630	0.3048	4197	899	1718	92.0	0.57
S21	17.0	0.0567	0.0118	2264	894	1122	99.8	0.58
S22	29.3	0.0965	0.4238	2382	901	1499	102.1	0.59
S23	36.5	0.0508	0.0329	2542	895	1201	89.6	0.57

6 FLOW PREDICTION IN THE SEMLIKI WATERSHED

6.1 Methodology

6.1.1 Multi-linear and polynomial regression

Multi-linear and polynomial regressions were the modeling approaches used for the determination of the monthly local runoff equations. The multi-linear approach assumed linearity between catchments descriptors and the volume generated within the watershed. Therefore, several normality tests were performed and the results, reported in Table 6-1, show that the Anderson Darling test was the only one that rejected the null hypothesis at 20%.

Table 6-1 Normality test

Test name	Test value	Prob level	Reject H_0 At Alpha = 20%
Shapiro Wilk	0.96	0.44	No
Anderson Darling	0.53	0.18	Yes
D'Agostino Skewness	0.64	0.52	No
D'Agostino Kurtosis	0.35	0.73	No
D'Agostino Omnibus	0.54	0.76	No

The general models generated from the multi-linear and polynomial regressions are represented in equations (6-1) and (6-2). The ordination technique, namely the Principal Component Analysis, identified redundant variables and was used in the determination of the optimal dimension of the predictive models. The reduction of model dimension for the multilinear model equation (6-1), did not indicate any improvement in performance indexes (NSE, PBIAS, RSR) Table (6-2). In other words, the optimal performance of the multilinear model required the use of all eight landscape attibutes. However, the equation 6-2 illustrating the non-linear relationship between the landscape attributes and the flow generated provided optimal performance indexes after reduction of variables as guided by the PCA. The optimal dimension for the non-linear model has respectively six and five variables for the first and second group of subcatchments. The optimum monthly parameters for each category and the two models are reported in Tables 6-3 and 6-4.

$$Y = a_o + A_i^T X_i$$ **Equation 6-1**

T denotes the transpose

Where :

$$A_i = \begin{Bmatrix} \alpha_1 \\ \alpha_2 \\ . \\ . \\ . \\ \alpha_8 \end{Bmatrix} \quad \text{and} \quad X_i = \begin{Bmatrix} x_1 \\ x_2 \\ . \\ . \\ . \\ x_8 \end{Bmatrix}$$

$$Y = a_0 + A_{ij}^T Z_{ij}$$ **Equation 6-2**

$$A_{ij} = \begin{bmatrix} \alpha_{11} & \alpha_{12} \\ \alpha_{21} & \alpha_{22} \\ . & . \\ . & . \\ . & . \\ \alpha_{71} & \alpha_{72} \\ \alpha_{81} & \alpha_{82} \end{bmatrix} \quad \text{and} \quad Z_{ij} = \begin{bmatrix} x_1 & x_1^2 \\ x_2 & x_2^2 \\ . & . \\ . & . \\ . & . \\ x_7 & x_7^2 \\ x_8 & x_8^2 \end{bmatrix}$$

With a_o: the intercept and other variables X_i are as defined earlier.

Table 6-2 Performance indexes and model dimension

Model	NSE	PBIAS	RSR	Dimension & observation
Multilinear- January- C1	0.79	-0.0044	0.46	4 predictors (stream length, w-average elevation, NDVI and precipitation)
Multilinear- January- C1	0.933	0.097	0.259	8 predictors (all the landscape attributes selected)
Multilinear- April- C1	0.799	-0.001	0.449	4 predictors (stream length, w-average elevation, NDVI and precipitation)
Multilinear- April- C1	0.932	-0.030	0.260	8 predictors (all the landscape attributes selected)
Multilinear- July- C1	0.804	0.003	0.443	4 predictors (stream length, w-average elevation, NDVI and precipitation)
Multilinear- July- C1	0.934	0.020	0.256	8 predictors (all the landscape attributes selected)
Multilinear- Oct- C1	0.797	0.002	0.450	4 predictors (stream length, w-average elevation, NDVI and precipitation)
Multilinear- Oct- C1	0.934	0.025	0.257	8 predictors (all the landscape attributes selected)
Multilinear- Jan- C2	0.699	-0.430	0.549	4 predictors (stream length, w-average elevation, NDVI and precipitation)
Multilinear- Jan- C2	0.997	-1.060	0.057	8 predictors (all the landscape attributes selected)
Multilinear- April- C2	0.712	-0.003	0.536	4 predictors (stream length, w-average elevation, NDVI and precipitation)
Multilinear- April- C2	0.998	-0.015	0.050	8 predictors (all the landscape attributes selected)
Multilinear- Jul- C2	0.717	0.007	0.532	4 predictors (stream length, w-average elevation, NDVI and precipitation)
Multilinear- Jul- C2	0.9975	0.0076	0.0495	8 predictors (all the landscape attributes selected)
Multilinear- Oct- C2	0.716	0.006	0.533	4 predictors (stream length, w-average elevation, NDVI and precipitation)
Multilinear- Oct- C2	0.998	0.001	0.049	8 predictors (all the landscape attributes selected)

Table 6-3 Monthly equations parameters from multi-linear regression optimization for Semliki subcatchments

		a_0 (10^5)	α_1 (10^4)	α_2 (10^6)	α_3 (10^4)	α_4	α_5 (10^2)	α_6	α_7 (10^4)	α_8
Group 1	Jan	56.01	16.48	-35.53	-38.21	-719.88	-14.00	-201.95	150.01	1222.84
	Feb	47.30	14.83	-31.33	-36.16	-642.21	-9.88	-112.01	127.40	520.72
	Mar	53.90	16.08	-32.70	-42.33	-892.36	-22.72	-607.55	319.28	957.68
	Apr	48.70	17.08	-36.28	-39.13	-753.17	-10.80	-334.74	196.1	1535.05
	May	64.00	18.82	-41.39	-40.67	-708.66	-8.29	-10.07	6.02	1800.68
	Jun	37.02	16.78	-35.29	-34.38	-725.02	-8.79	-508.86	374.50	2821.7
	Jul	46.78	17.70	-37.45	-35.58	-791.07	-8.06	-553.03	259.50	5097.92
	Aug	52.58	18.22	-38.60	-29.86	-757.17	-15.04	-317.23	284.80	1160.25
	Sep	47.31	19.19	-38.54	-46.60	-1098.71	-28.99	-1020.17	599.10	1544.80
	Oct	52.66	19.60	-40.86	-45.63	-893.83	-22.71	-771.69	427.00	2983.79
	Nov	31.05	20.99	-41.82	-74.25	-1097.14	-25.40	-796.84	787.60	3515.37
	Dec	49.29	19.71	-40.81	-59.94	-927.30	-20.72	-252.88	436.20	1411.49
Group 2	Jan	51.14	33.54	-90.44	-40.88	322.03	-2.79	-872.59	-13.15	10.57
	Feb	40.09	27.02	-73.36	-30.08	258.47	-1.53	-700.24	2.10	250.21
	Mar	44.52	29.951	-81.58	-31.94	283.73	-1.66	-773.52	6.96	30.78
	Apr	49.45	33.26	-90.33	-37.20	317.06	-2.03	-855.94	4.15	48.04
	May	55.15	37.47	-102.95	-36.29	350.33	-2.00	-961.26	32.87	224.64
	Jun	48.73	32.69	-88.79	-36.16	311.26	-1.97	-841.62	2.76	33.69
	Jul	51.09	34.34	-93.25	-38.65	326.76	-2.06	-881.12	2.89	131.12
	Aug	53.36	35.70	-97.01	-41.57	336.48	-2.57	-902.37	8.37	13.27
	Sep	52.06	35.21	-95.96	-39.75	332.06	-2.22	-888.41	13.12	83.98
	Oct	55.17	37.63	-103.09	-38.74	358.54	-1.99	-980.17	26.12	175.35
	Nov	57.42	39.37	-107.70	-38.50	373.67	-1.76	-1015.20	19.92	220.07
	Dec	56.28	38.10	-103.68	-41.36	365.54	-2.11	-988.24	7.84	349.41

Table 6-4 Monthly equations parameters from polynomial regression optimization for Semliki subcatchments

		$a_0(10^5)$	α_{11} (10^4)	α_{12} (10^2)	α_{21} (10^6)	α_{22} (10^6)	α_{31} (10^5)	α_{32} (10^5)	α_{61} (10^3)	α_{62}	α_{71} (10^5)	α_{72} (10^5)	α_{81} (10^2)	α_{82}
Group 1	Jan	-179.33	27.42	-13.19	-79.98	203.10	25.40	-11.35	54.10	-32.40	9.09	-3.73	19.61	14.40
	Feb	-118.54	25.06	-12.12	-68.99	168.03	24.14	-12.38	42.10	-25.58	-40.51	50.03	-241.12	185.93
	Mar	-150.17	25.52	-12.17	-74.31	188.10	22.86	-10.63	45.30	-27.38	7.84	1.42	48.26	-18.41
	Apr	-143.93	28.52	-13.61	-81.86	205.83	26.53	-13.22	47.70	-28.95	-50.78	53.93	52.32	-10.81
	May	-169.92	32.11	-15.57	-90.91	227.42	30.58	-14.14	62.60	-37.59	-111.9	87.66	-7.12	4.14
	Jun	-163.19	27.80	-13.29	-80.49	203.69	24.94	-11.58	49.40	-29.83	-4.82	21.71	30.39	-5.31
	Jul	-163.99	29.33	-14.19	-81.02	198.27	29.47	-14.09	54.90	-33.12	-88.71	78.21	216.21	-95.50
	Aug	-204.07	30.54	-14.79	-86.94	218.71	28.42	-12.83	57.80	-34.80	-12.30	17.66	299.44	-116.12
	Sep	-117.78	29.73	-13.55	-89.93	228.62	24.60	-12.54	42.60	-26.01	-68.60	82.39	118.95	-46.91
	Oct	-209.42	31.78	-14.87	-96.46	250.31	27.53	-12.79	55.80	-33.69	93.60	-52.37	-10.49	-1.30
	Nov	-179.07	33.17	-15.59	-95.83	240.55	29.50	-14.41	58.50	-35.32	-48.37	55.26	34.17	-8.54
	Dec	-161.32	31.65	-14.66	-94.94	241.92	28.57	-13.92	57.60	-34.48	-104.8	96.09	205.63	-145.43
Group 2	Jan	56.68	18.73	30.28	20.14	-750.34	-	-	-4.68	1.65	-11.55	15.65	20.96	-14.76
	Feb	46.88	14.52	25.53	16.31	-607.02	-	-	-3.73	1.31	8.53	-5.78	-178.52	167.26
	Mar	45.09	17.08	26.54	9.61	-616.86	-	-	-3.92	1.37	-11.43	16.03	109.56	-41.38
	Apr	47.44	17.20	32.51	8.26	-673.04	-	-	-3.49	1.26	16.45	-8.55	-32.64	13.57
	May	62.60	21.45	32.78	9.48	-764.34	-	-	-4.23	1.52	-17.01	21.49	-14.79	5.19
	Jun	56.65	18.60	28.81	8.66	-666.08	-	-	-4.12	1.46	-14.27	18.72	-17.87	20.93
	Jul	60.49	19.63	30.52	9.05	-697.21	-	-	-4.83	1.70	-11.85	18.07	26.76	-2.25
	Aug	49.50	19.76	32.64	15.67	-766.07	-	-	-4.46	1.58	12.78	-10.72	87.65	-37.73
	Sep	53.42	19.54	31.86	9.54	-718.87	-	-	-4.09	1.47	4.43	1.31	10.27	-4.31
	Oct	52.32	20.60	34.65	15.74	-803.16	-	-	-4.44	1.58	19.72	-13.31	18.25	-8.99
	Nov	60.45	22.26	35.03	21.00	-870.98	-	-	-5.18	1.85	15.39	-8.48	-47.82	18.46
	Dec	60.70	20.72	35.53	21.76	-850.59	-	-	-4.99	1.78	-21.07	25.22	125.89	-82.99

The deterministic models developed in the previous section using multilinear regression and polynomial regression for the two category of subcatchments identified in the Semliki watershed are evaluated under the following section against historical data. From the model parameters, monthly equations are defined for the two types of subcatchments and for the two modeling approaches. This defines 48 equations which calibration results are presented from Figure 6-1 to Figure 6-48. The historical monthly flow measurements at the outlet of the Semliki watershed for 1950-1978 were used for the calibration of both the linear and the non- linear models. For each subcatchments, an historical 28-years monthly mean volume was computed proportionally to the subcathment area and was labeled as “control”. This approach is supported by the fact that, in general, flow estimation at ungauged sites depends on watershed characteristics of the drainage area. This is particularly applicable in humid basins like the Semliki as opposed to arid and semi-arid regions, where “stream flows increase in the downstream direction, and the spatial distribution of average monthly or seasonal rainfall is more or less the same from one part of the river basin to another, hence the runoff per unit land area is assumed constant over space. In these situations, estimated flows are usually based on the watershed areas, as contributing flow to those sites, and the corresponding streamflows and watershed areas above the nearest or most representative gauge sites” (Loucks et al., 1981 and Loucks and Van Beek, 2005).

Table 6-5 presents a summary of statistical indexes (NSE, PBIAS and RSR) which were evaluated during the calibration.

6.2 Model calibration

6.2.1 Multilinear regression model

The spatial performance of Multilinear model has indicated for category I of subcatchments that the predictions were underestimated in subcatchments S3, S4, S11, S12 and S13 while the remaining subcatchments (S5, S6, S7, S8, S9, S10 and S19) were overestimated. (Figure 6-1 to 6-12). The optimal prediction for multilinear model in category I of subcatchments occurred in S4 and S10 while S3 and S5 provided the less accurate performance between the predicted and the control. The common physiographic attributes for S4 and S10 is that the drainage area is greater than 600 km^2 and their minimum elevations and average monthly rainfall have similar ranges (624 m, 99-102 mm/month). On the other hand the similarity among S3 and S5 is that they are flatter (maximum elevation below 850 m) than all the other subcatchments of this category and that their respective drainage area is not greater than 160 km^2

The temporal performance of the Multilinear model in category I especially in terms of statistical indexes (Table 6-5) have indicated that the model is overestimating flows for March, April and August while the remaining months predictions are underestimated for this group of subcatchments (PBIAS). The Nash-Sutcliffe Efficiency index varies between 0.929 in March to a maximum of 0.938 in November. The RSR values ranges are comprised between 0.265 in March to 0.249 in November. Over time the month of November indicates the best performance for the multilinear model for this category of subcatchments. November is one of the wettest months of the Semliki watershed.

In the second group of subcatchments, the multilinear model (Figure 6-25 to Figure 6-36) is underestimated flows for S15, S17, S18 and S23 while flows are being overestimated for the remaining subcatchments. The multilinear optimum predictions for these subcatchments are spatially occurring in subcatchments S21 and S22. S20 predictions for the multilinear model are the least accurate for this group of subcatchments. Temporally, the PBIAS (Table 6-5) indicated that flows are overestimated for the following months, January, April, May, June and December while the other months are underestimated. The point worth mentioning in this case is that April and May coincide with one of the peak period of the bi-modal rainfall occurrences in the watershed and December and January and the driest months. The NSE value for this group of subcatchments varies temporally from a minimum of 0.991 in June to a maximum of 0.998 in September. The RSR extremes are 0.049 and 0.097 respectively associated with the months of September and June.

These results indicate that the multilinear model in the second group of subcatchments out performed predictions in the first group of subcatchments of the Semliki watershed.

6.2.2 Polynomial regression model

The polynomial model predictions in the first group of subcatchments (Figure 6-13 to 6-24) report spatially the following, flows are overestimated for these subcatchments (S3, S5, S6, S7, S8, S13 and S19) while underestimation occurs with the predictions of the remaining subcatchments (S4, S9, S10, S11, S12). Better flow predictions are obtained for subcatchments S3, S6 and S7 when compared to the remaining subcatchments of this category. The similarity in terms of catchment attributes between these subcatchments are the geographical location, the drainage density between 0.228 and 0.112 km\km^2, minimum elevations of between 617 and 690m and the maximum elevations ranges comprised between 1307 and 1476 m above the sea level for S6 and S7.

Temporally, the PBIAS in Table 6-5 indicates that predictions are overestimated for the months of January, June, September and December while the predictions for the remaining months are underestimated. The range of the NSE for the polynomial prediction model in the first group of subcatchments lies between 0.976 for the month of January to 0.982 for the month of February. The RSR extreme values for these predictions are 0.132 and 0.152 for February and January respectively (Table 6-5).

These results also indicate the fact that the polynomial model over time and space provide better flow predictions than the multilinear model in this first group of subcatchments.

The polynomial model in the second group of subcatchments shows that predictions are spatially overestimated mainly in subcatchments S16, S20 and S22 (Figure 6-37 to 6-48). For S20 predictions over time are the least accurate when compared to the remaining subcatchments. Spatially, the results of the predictions of the polynomial model outperformed those of the multilinear model in this group of subcatchments.

Temporally, the PBIAS (Table 6-5) indicates that the predictions from the polynomial model overestimate values for the months of January, July, October, November and December while the opposite is observed in the remaining months.

The month of May indicates the lowest performance in terms of the NSE and the RSR, while the month of July shows the best performance both in terms of the NSE and the RSR.

This model highlighted also the limitations of performance indexes, namely the NSE and the RSR, their values were found to be very close (Table 6-5) hence not handy for the assessment of the model temporal performances. The PBIAS index on the other hand, provided very unambiguous values and was used in the assessment of the temporal dynamics. The polynomial model results for the second group of subcatchments outperformed spatially and temporally all the results of predictions obtained using the multilinear model.

There is however similarities in model results; spatially, the polynomial model and multilinear models predict less accurately the flows in subcatchment S20 that belongs to the second group of subcatchments. Temporally, the predictions for the month of January which is one of the driest months is overestimated in three of the four scenarios, indicating that these models appears more suited for very humid watersheds. On the other hand this findings also indicate that these models are not versatile enough to cater for extreme conditions characteristics, shortfall that is foreseeable due to the deterministic and conceptual approach of the two models.

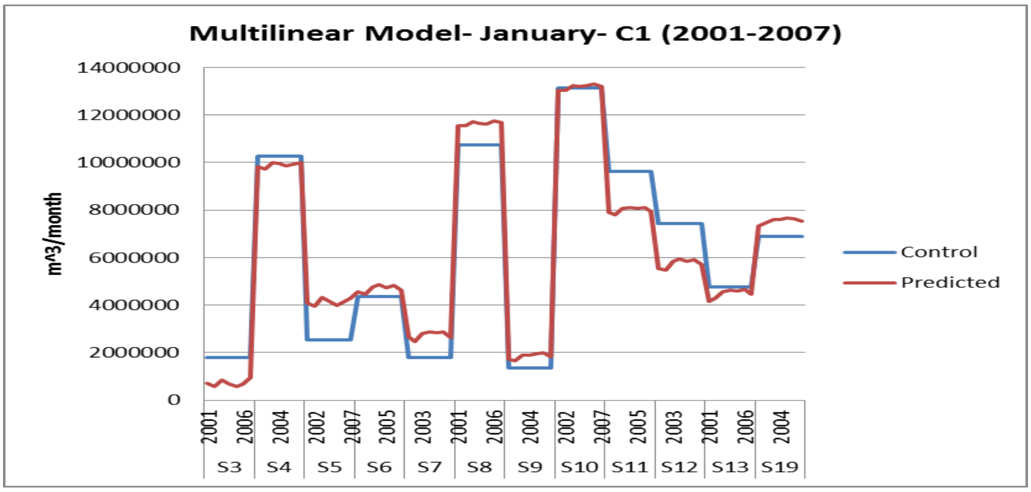

Figure 6-1 Multilinear Model- January- C1

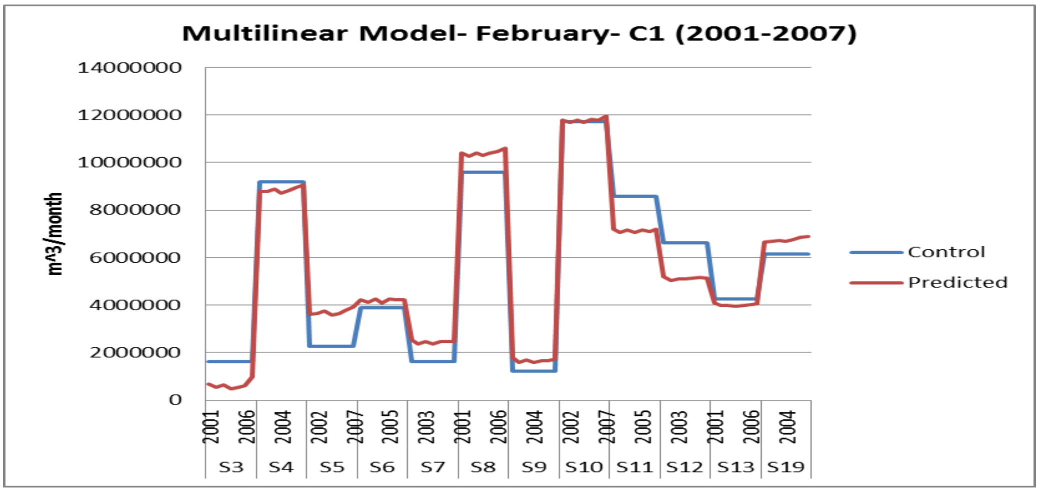

Figure 6-2 Multilinear Model- February-C1

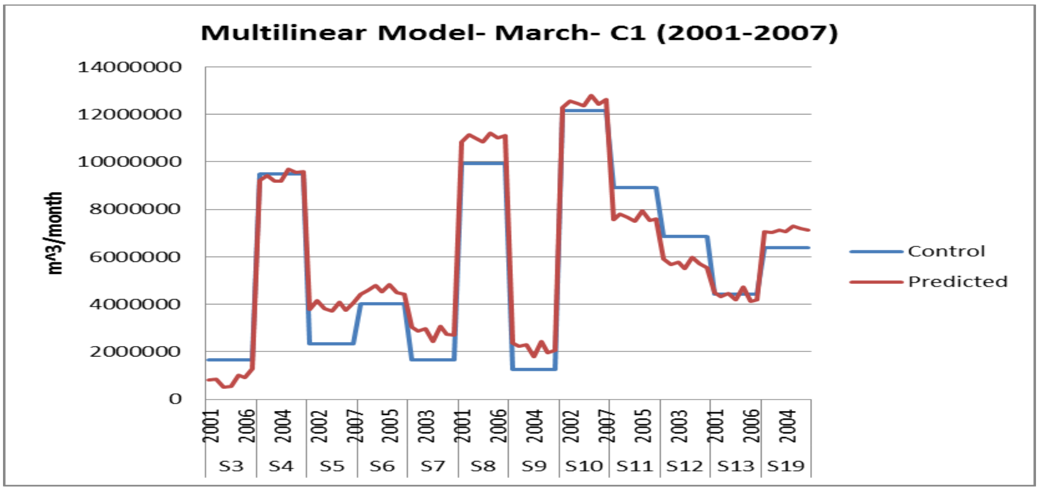

Figure 6-3 Multilinear Model- March- C1

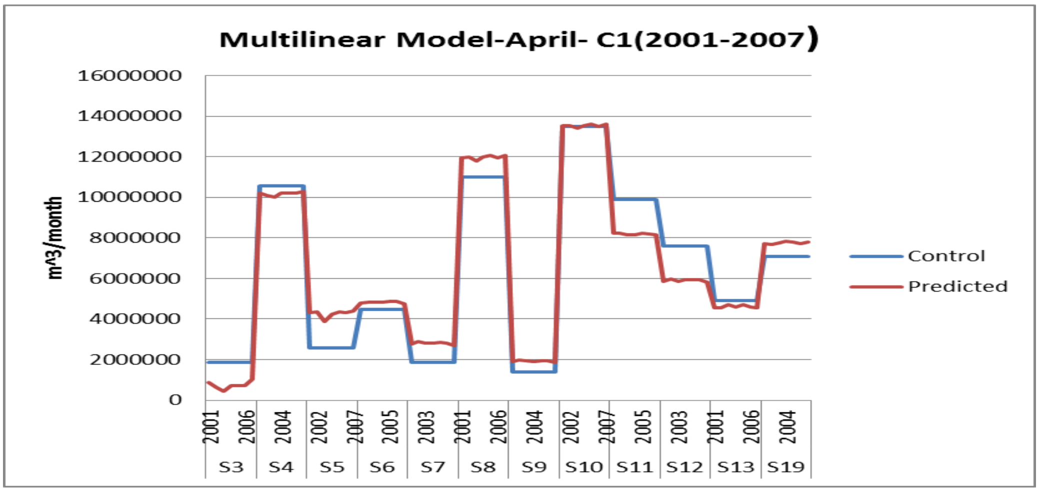

Figure 6-4 Multilinear Model April- C1

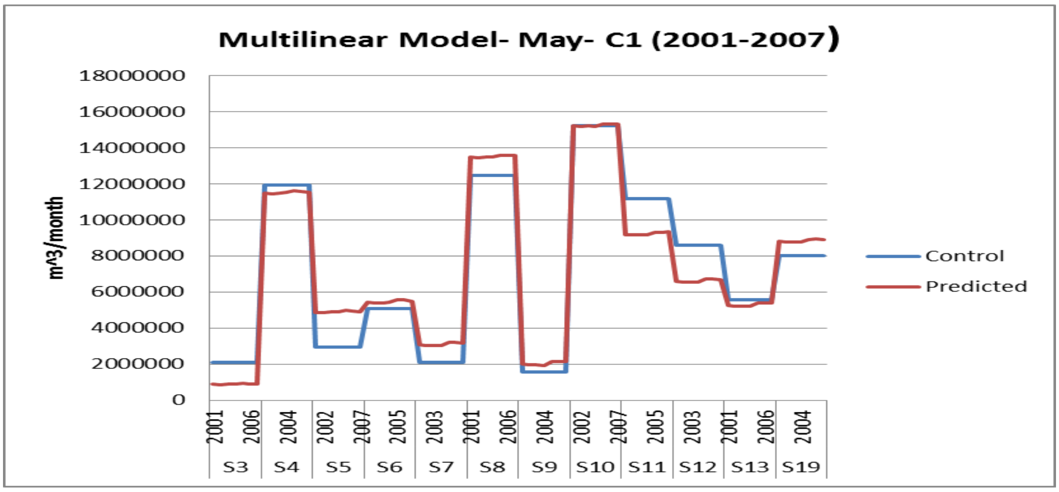

Figure 6-5 Multilinear Model- May- C1

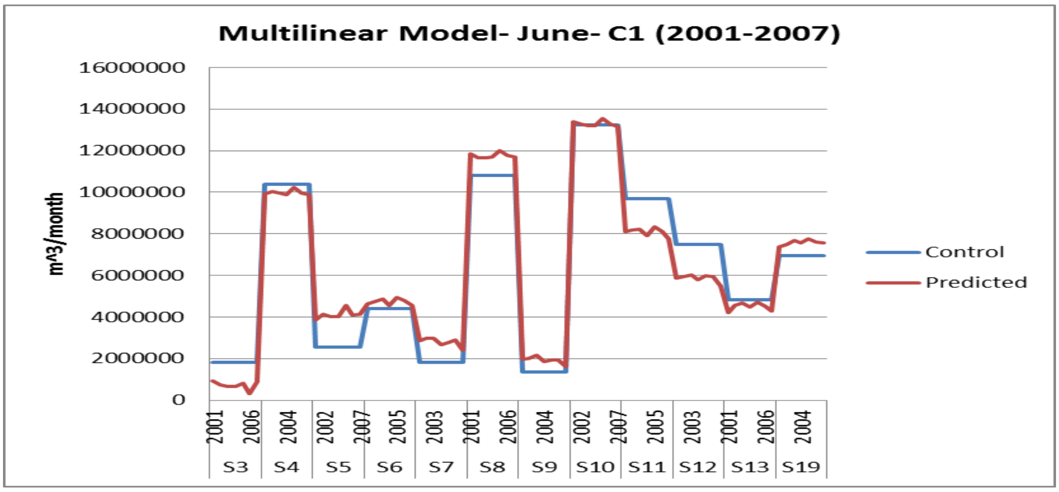

Figure 6-6 Multilinear Model- June-C1

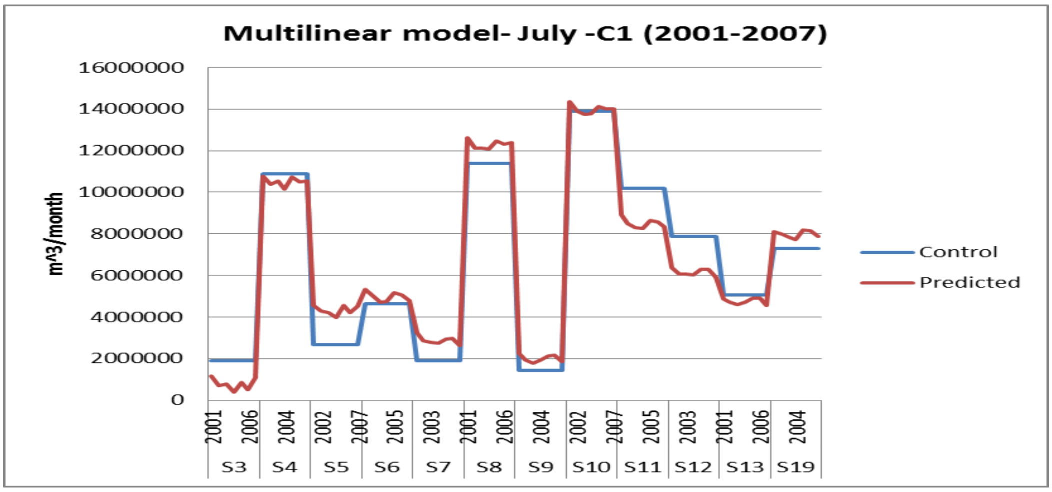

Figure 6-7 Multilinear Model- July-C1

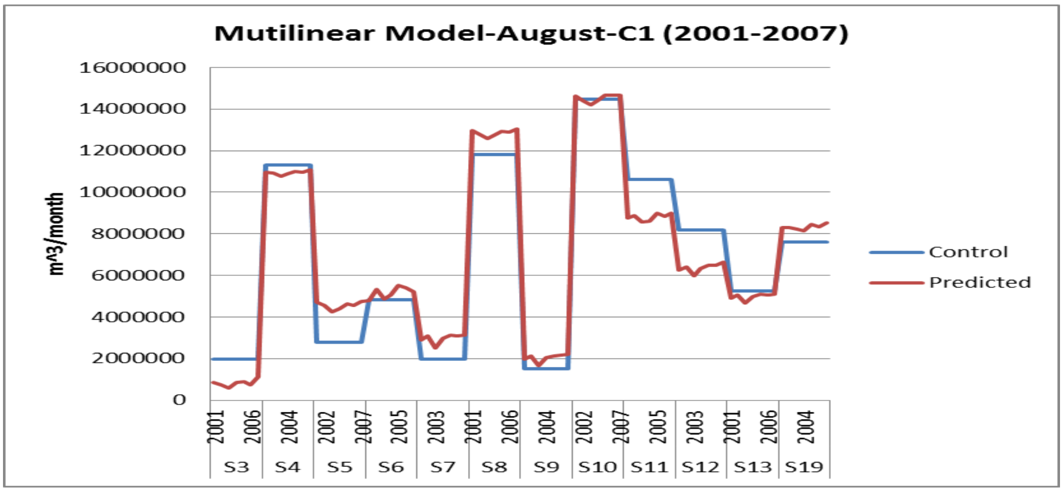

Figure 6-8 Multilinear Model-August-C1

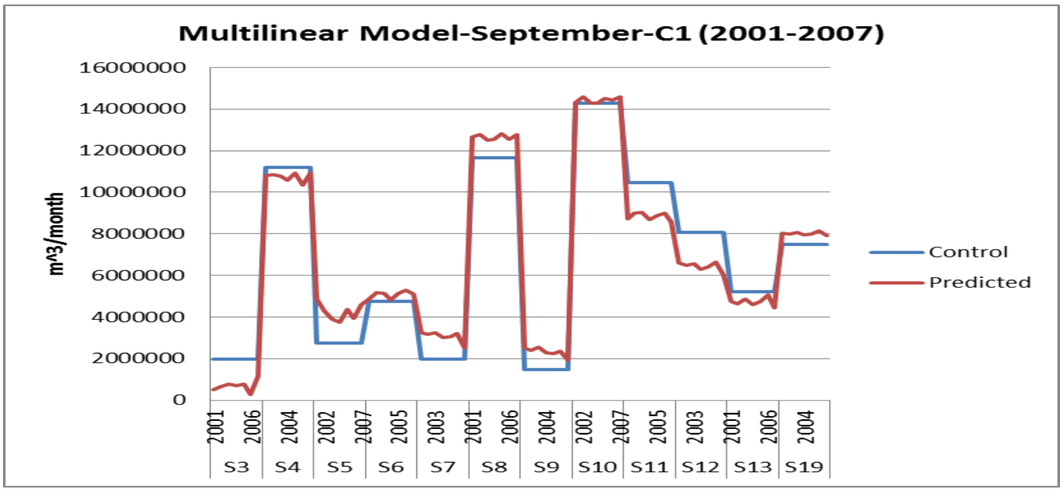

Figure 6-9 Multilinear Model-September-C1

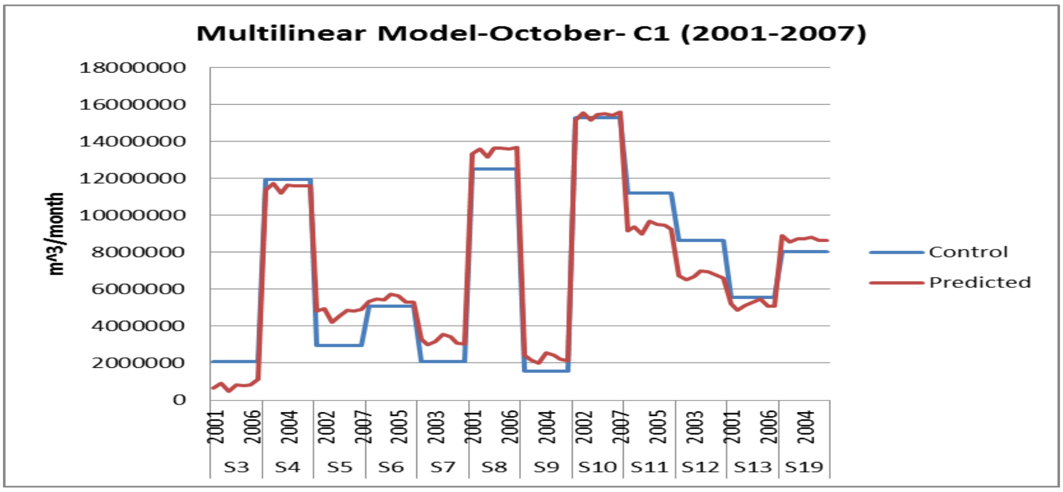

Figure 6-10 Multilinear Model- October-C1

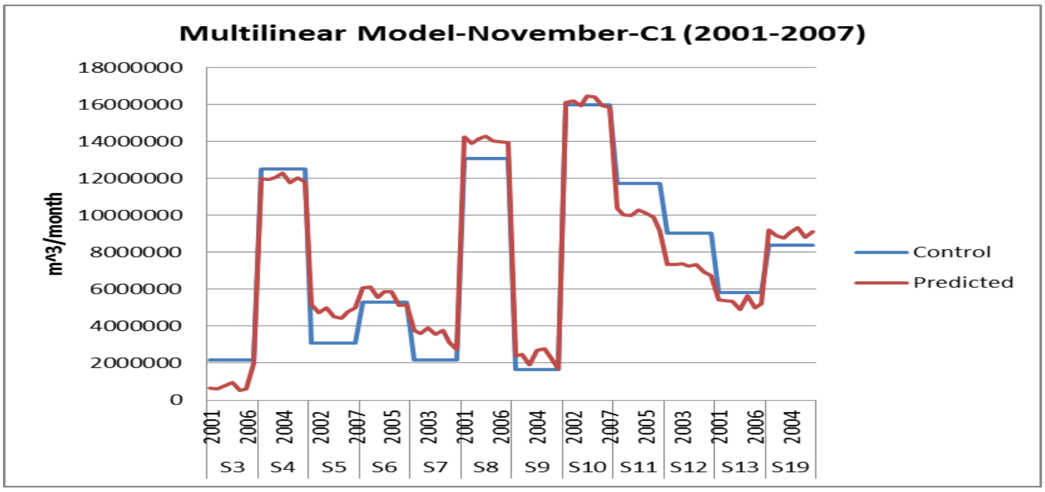

Figure 6-11 Multilinear Model- November-C1

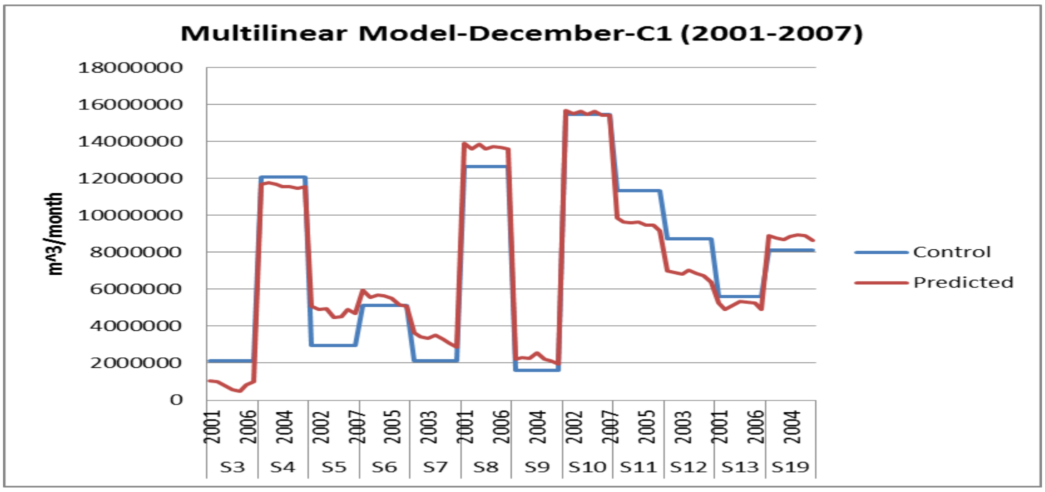

Figure 6-12 Multilinear Model- December- C1

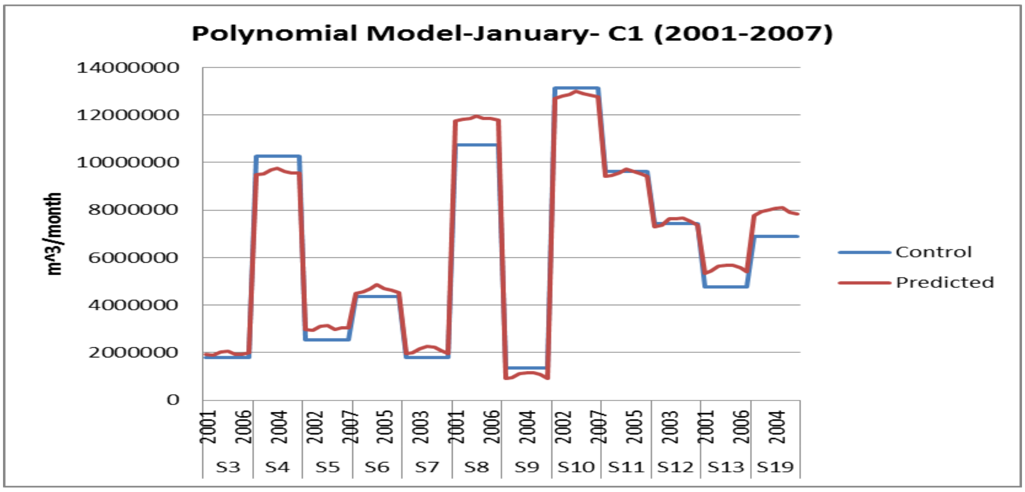

Figure 6-13 Polynomial Model- January- C1

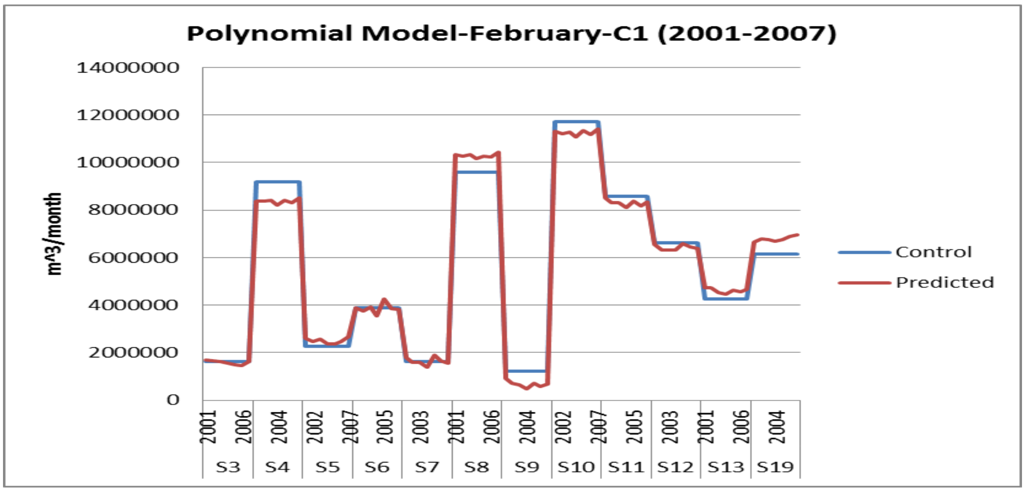

Figure 6-14 Polynomial Model- February –C1 (2001-2007)

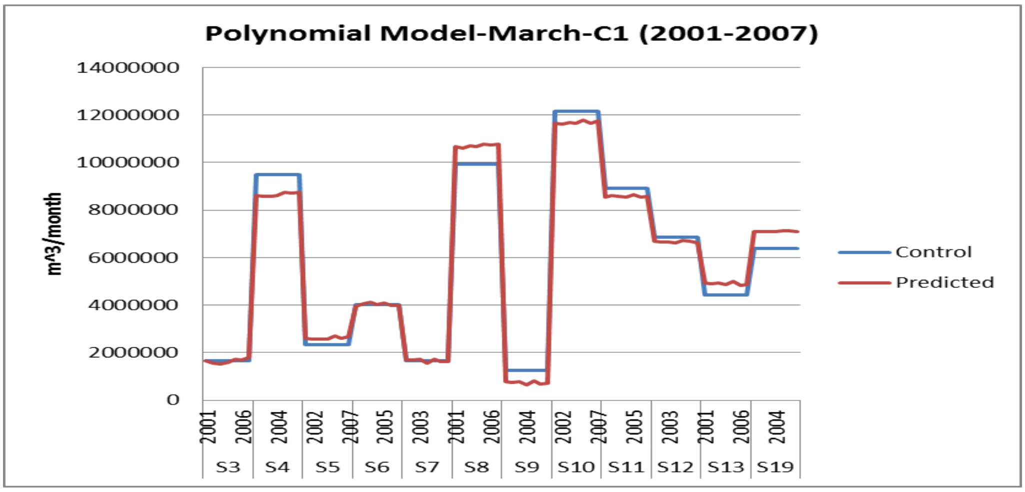

Figure 6-15 Polynomial Model- March- C1 (2001-2007)

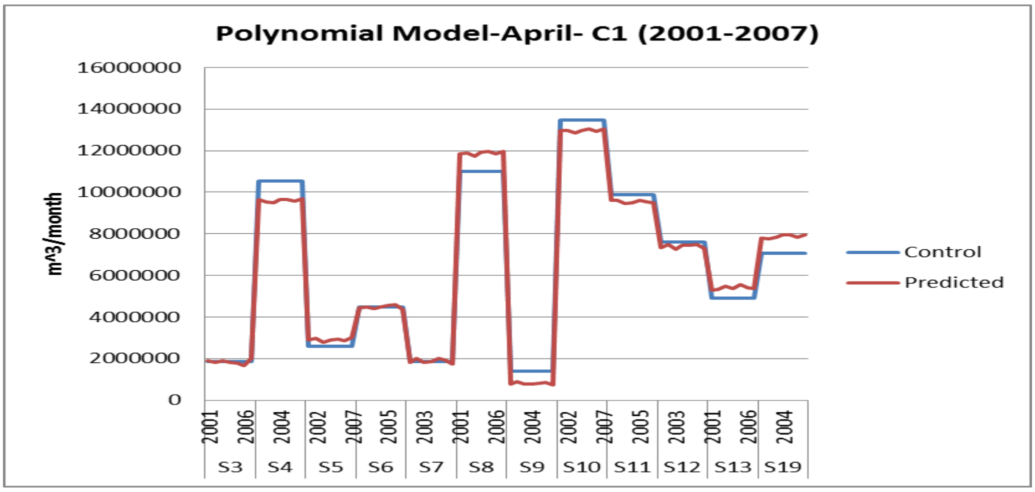

Figure 6-16 Polynomial Model- April-C1

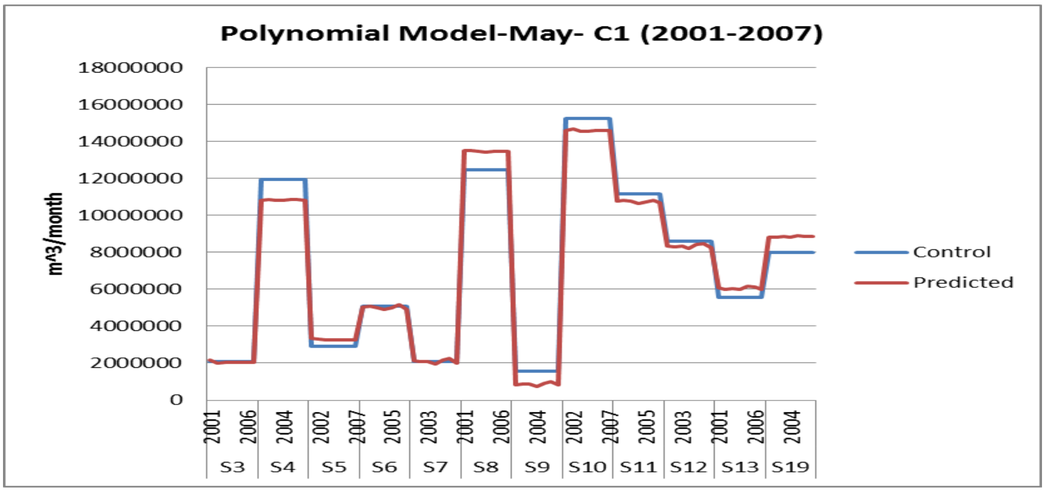

Figure 6-17 Polynomial Model- May-C1

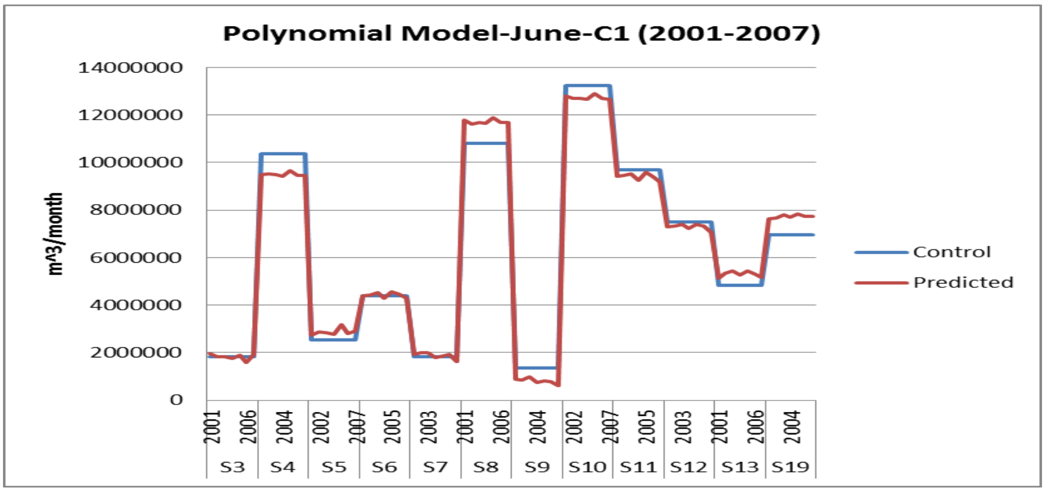

Figure 6-18 Polynomial Model- June- C1

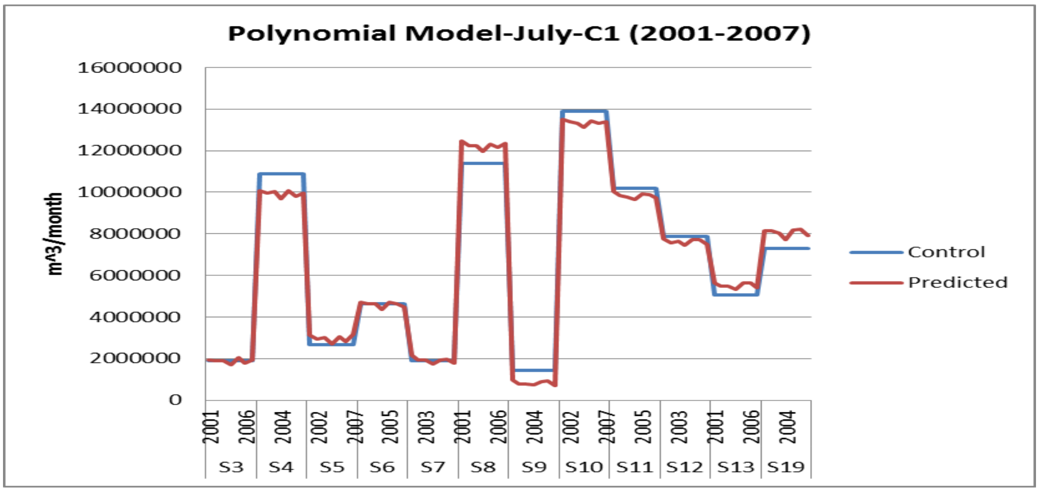

Figure 6-19 Polynomial Model- July-C1

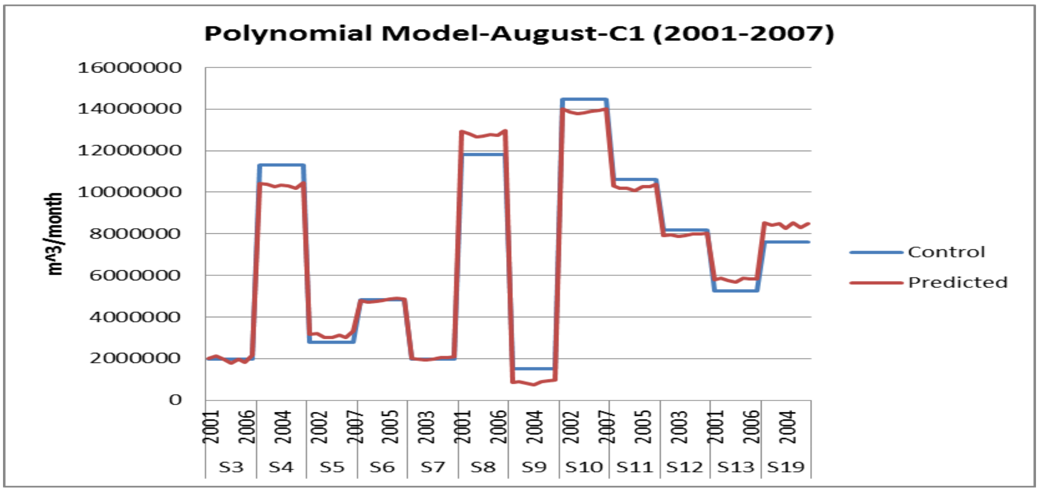

Figure 6-20 Polynomial Model- August- C1

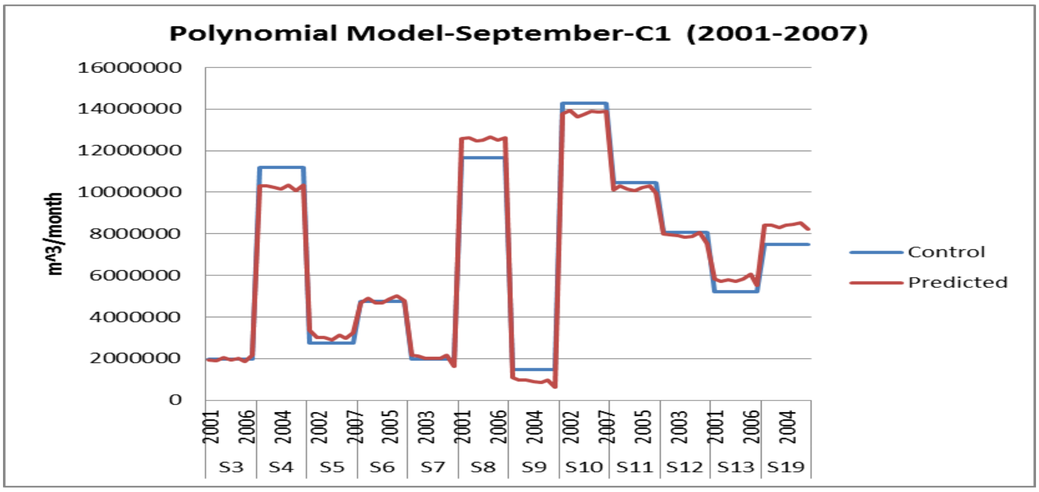

Figure 6-21 Polynomial Model-September-C1

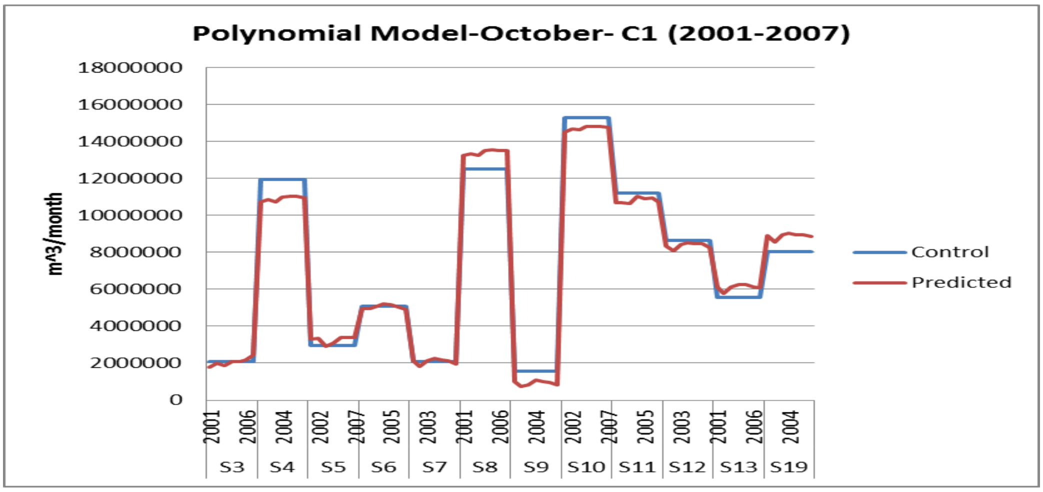

Figure 6-22 Polynomial Model- October –C1

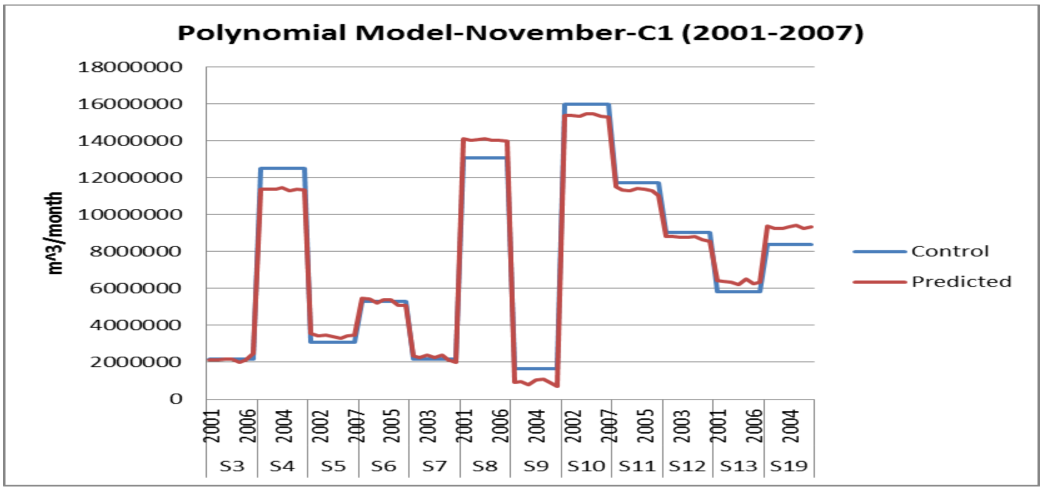

Figure 6-23 Polynomial Model- November- C1

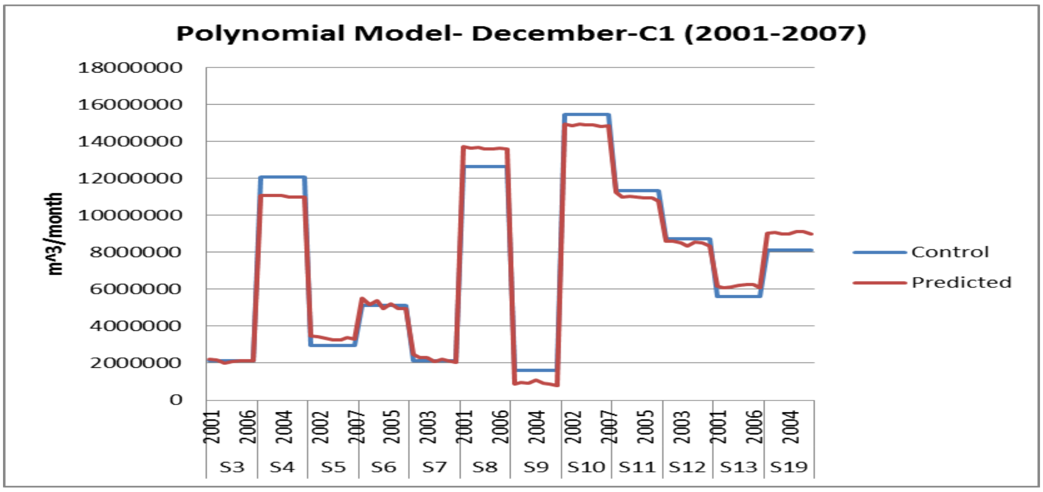

Figure 6-24 Polynomial Model –December-C1

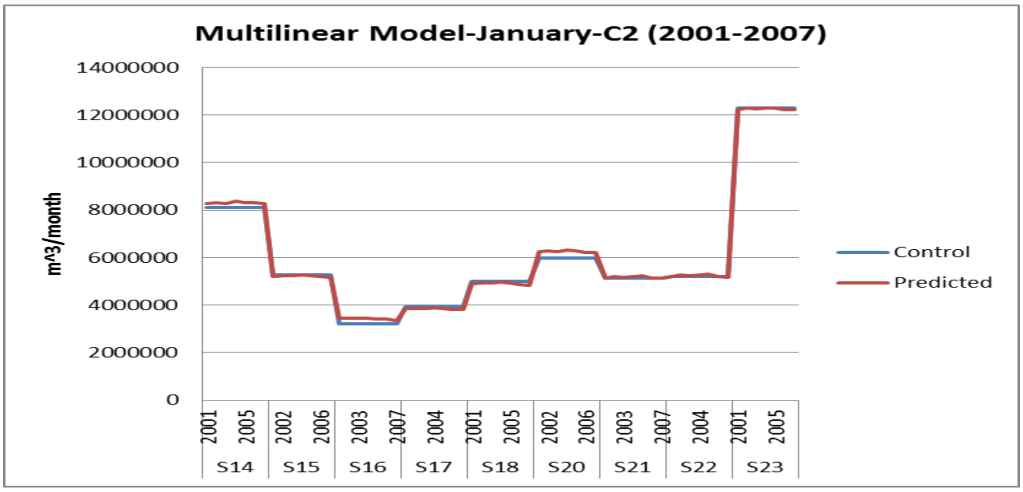

Figure 6-25 Multilinear Model- January- C2

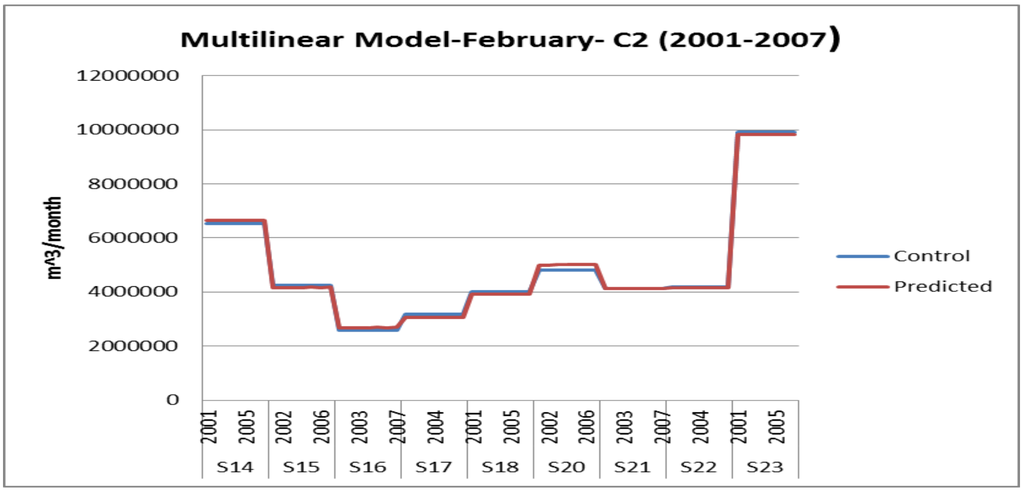

Figure 6-26 Multilinear Model- February- C2

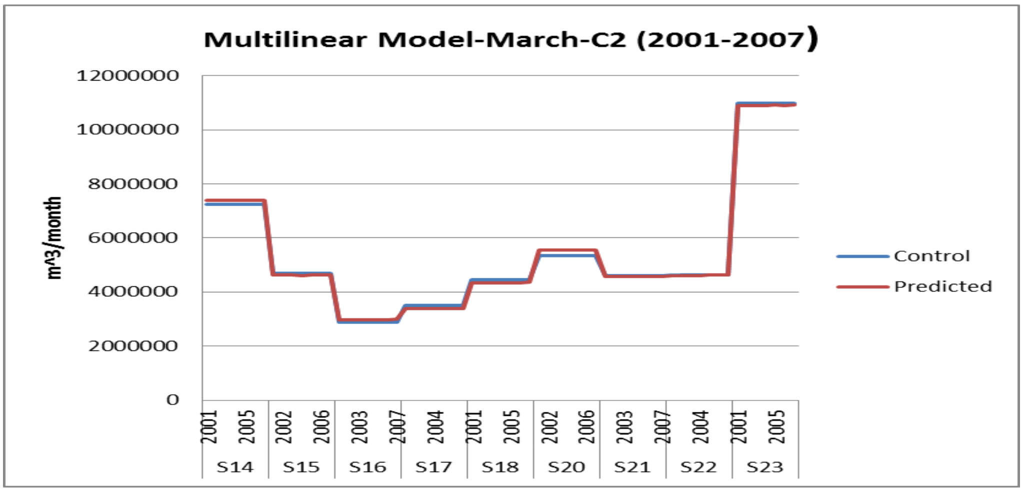

Figure 6-27 Multilinear Model- March –C2

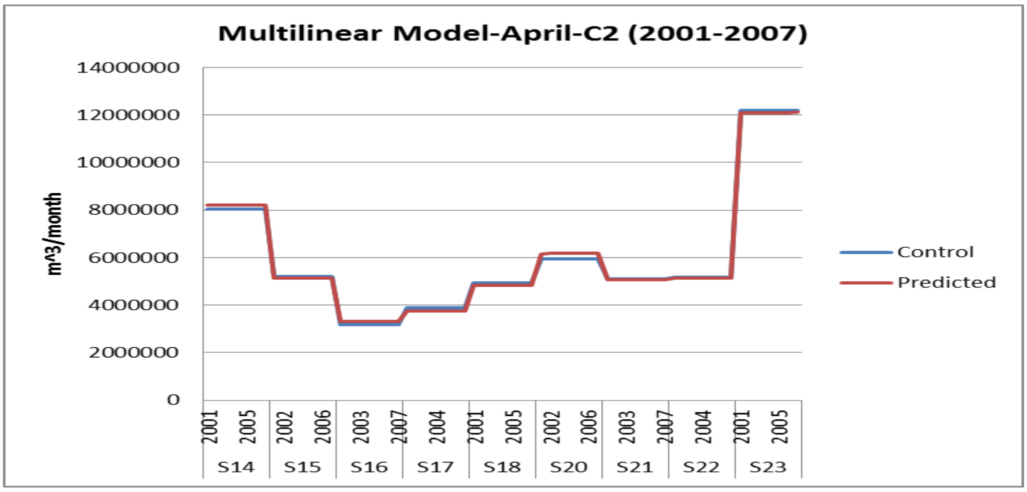

Figure 6-28 Multilinear Model- April- C2

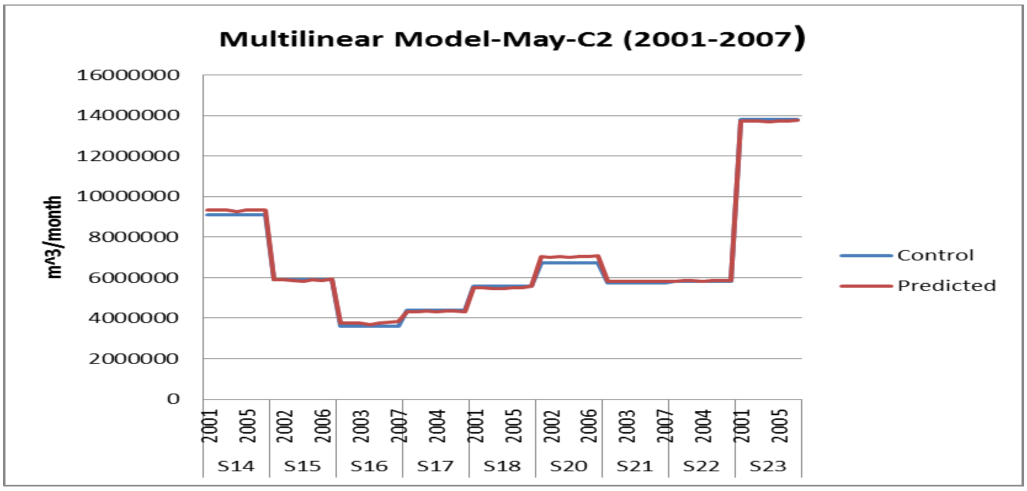

Figure 6-29 Multilinear Model- May- C2

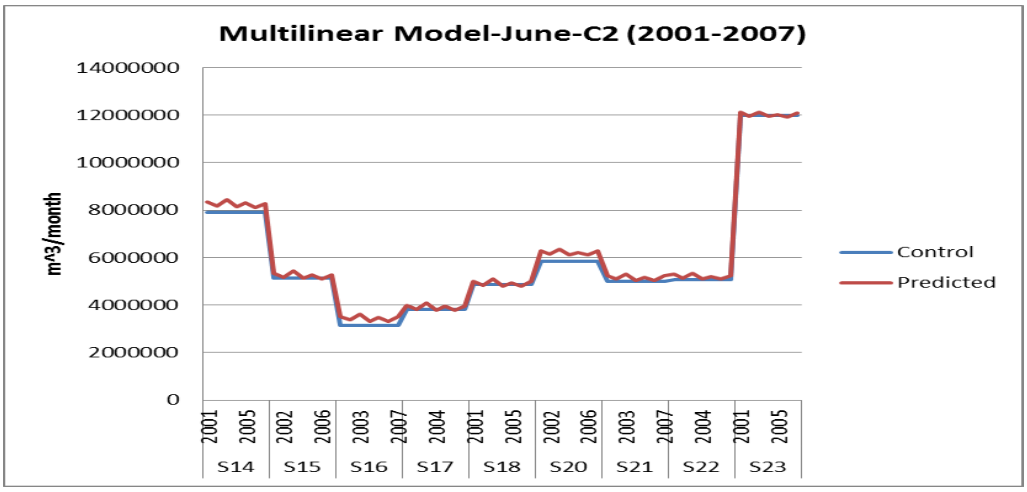

Figure 6-30 Multilinear Model- June- C2

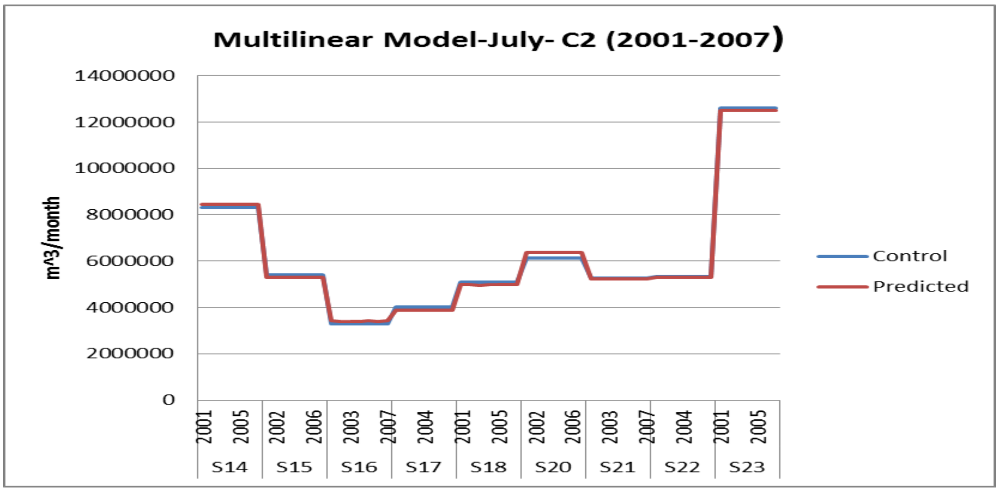

Figure 6-31 Multilinear Model- July- C2

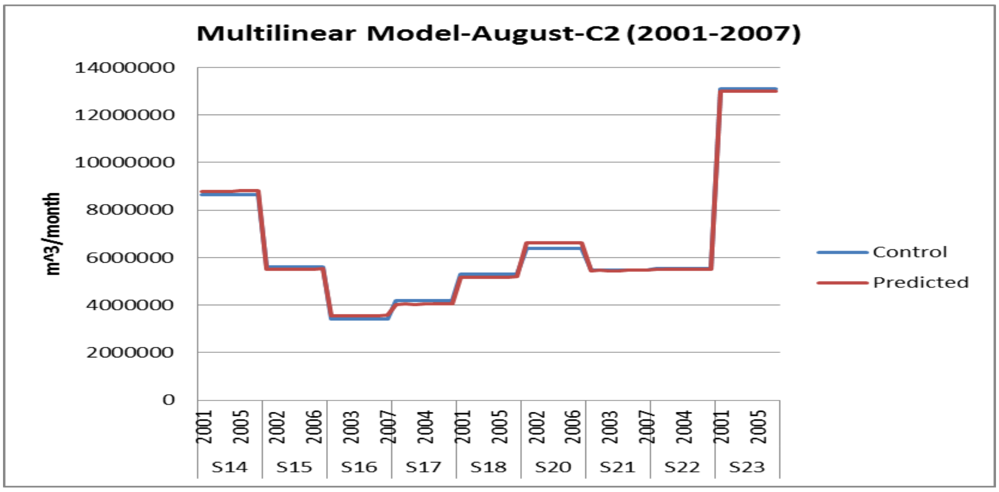

Figure 6-32 Multilinear Model- August- C2

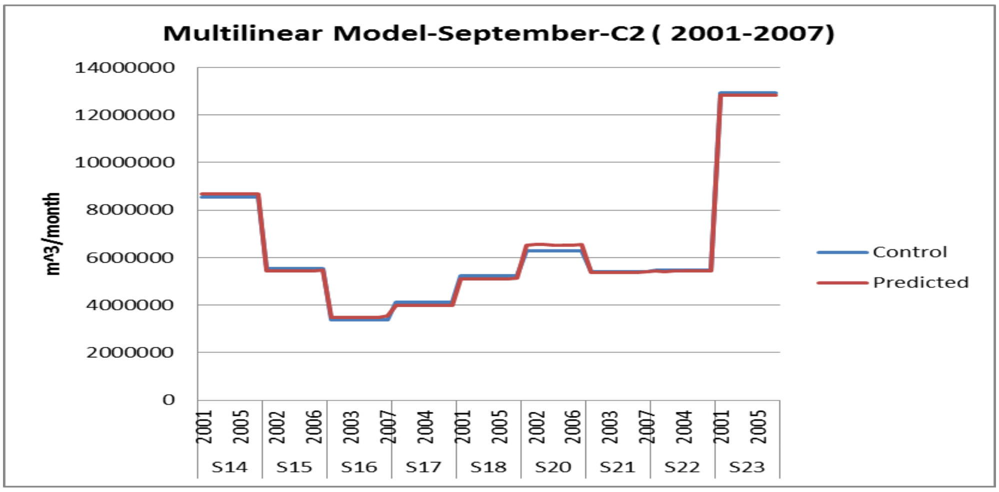

Figure 6-33 Multilinear Model- September- C2

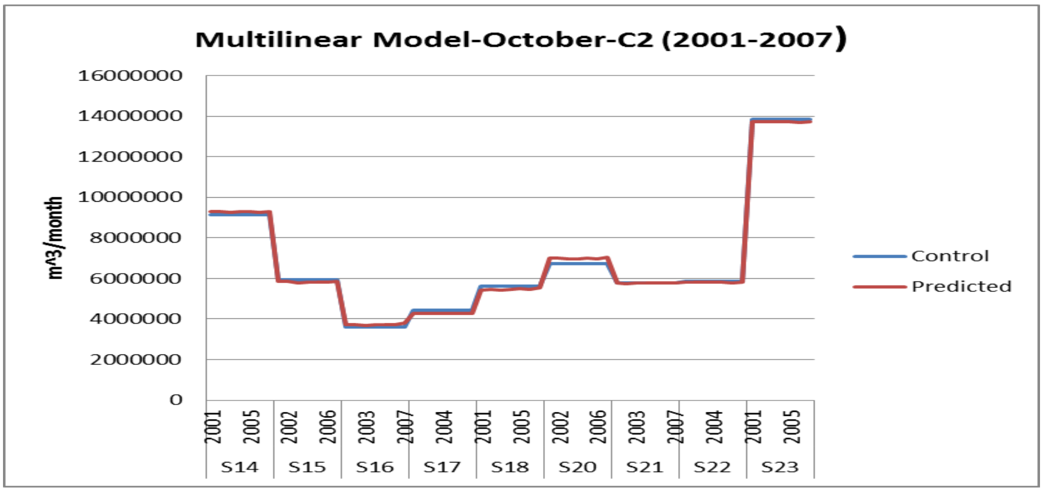

Figure 6-34 Multilinear Model- October-C2

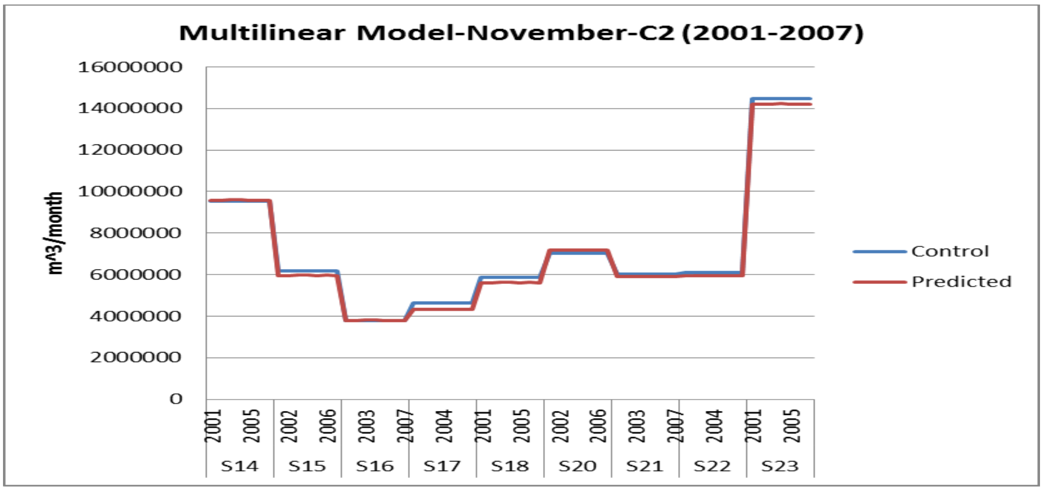

Figure 6-35 Multilinear Model- November-C2

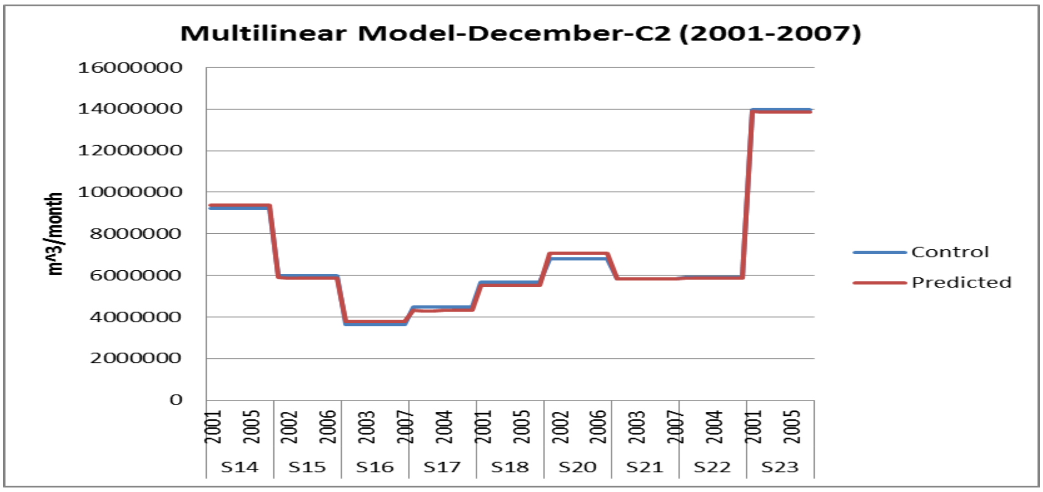

Figure 6-36 Multilinear Model- December- C2

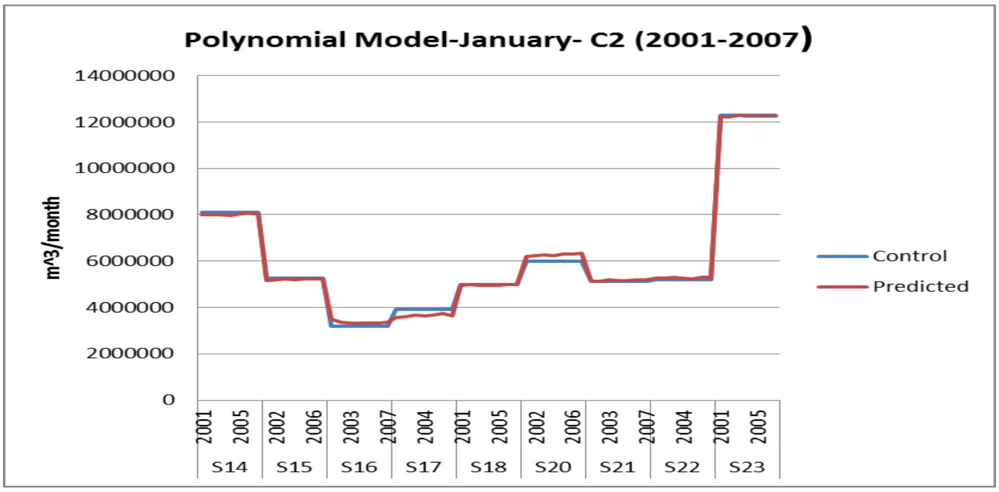

Figure 6-37 Polynomial Model- January-C2

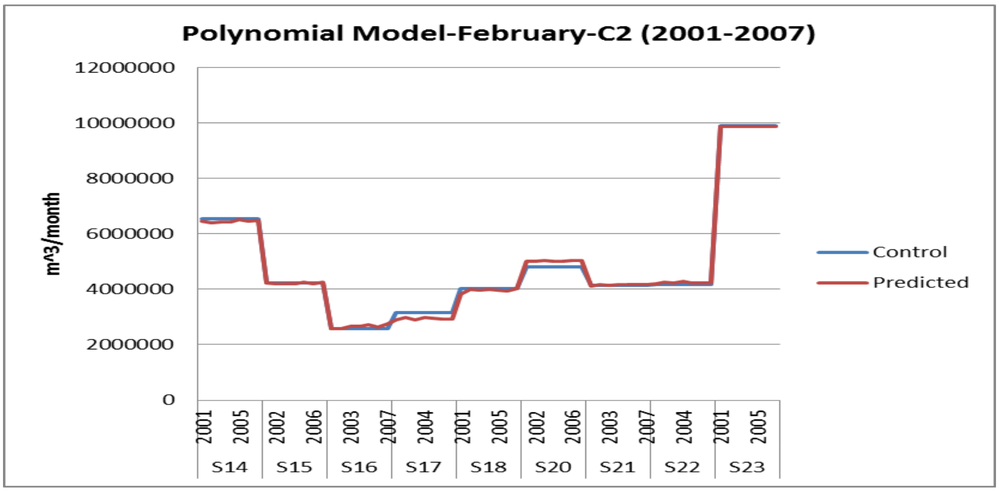

Figure 6-38 Polynomial Model- February- C2

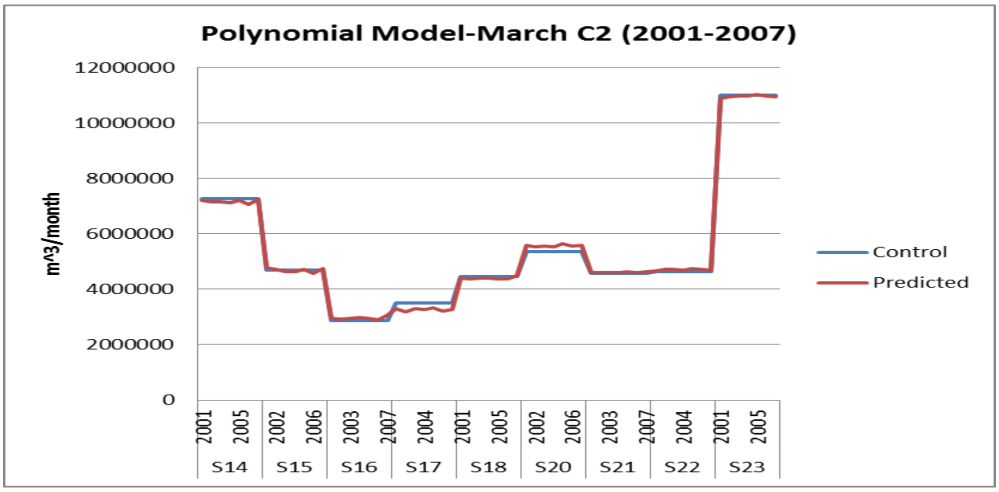

Figure 6-39 Polynomial Model- March- C2

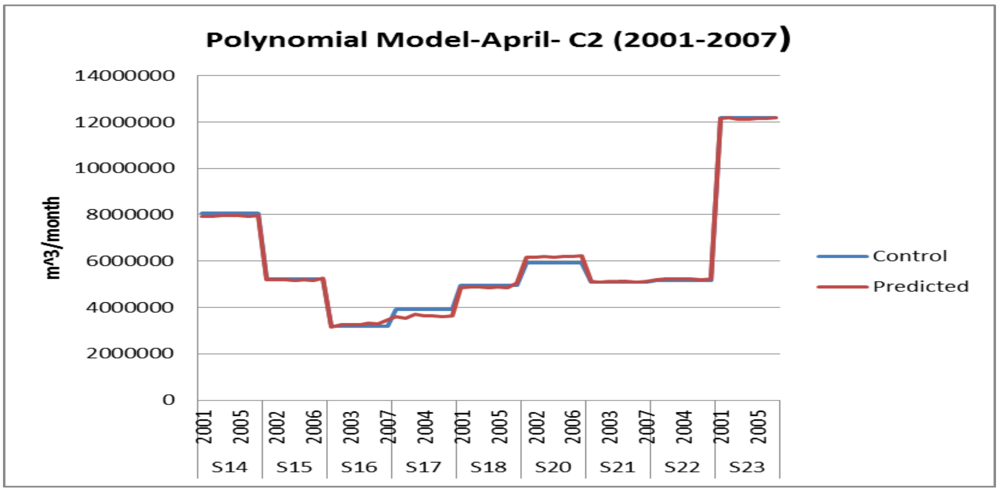

Figure 6-40 Polynomial Model- April-C2

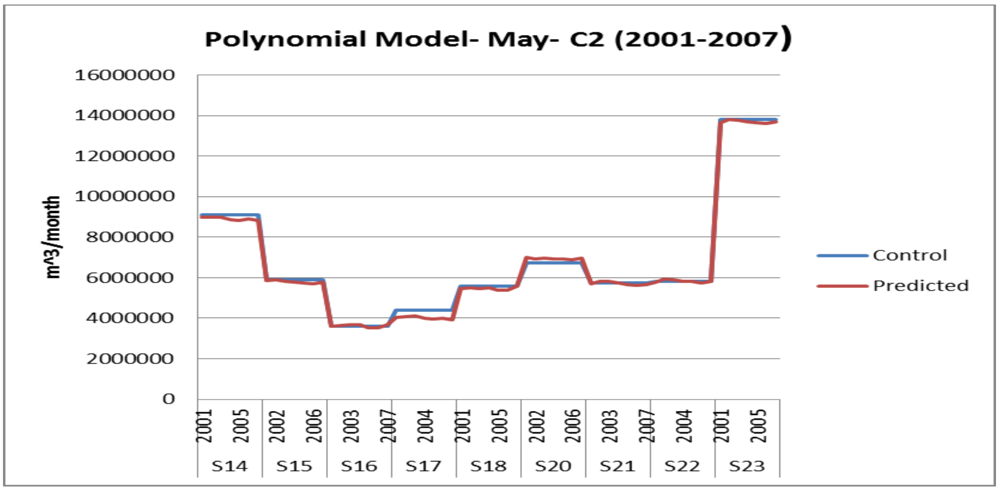

Figure 6-41 Polynomial Model- May- C2

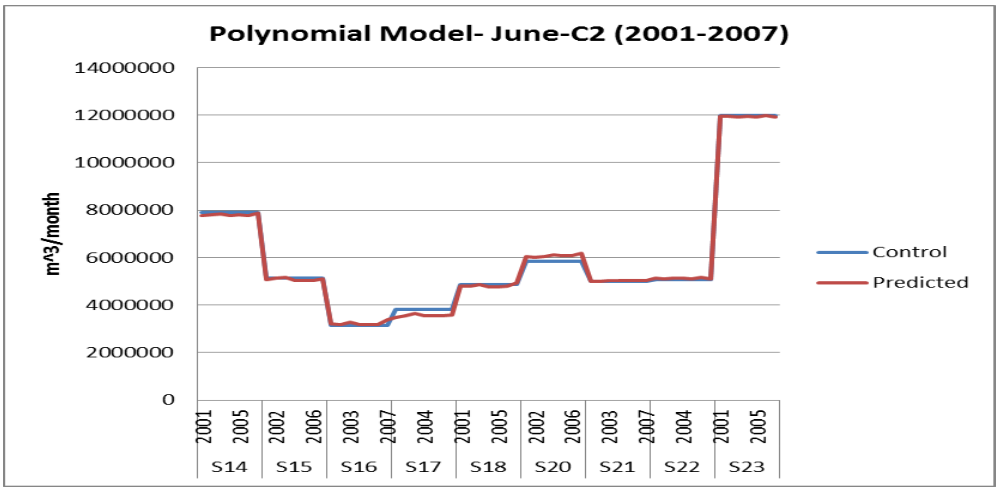

Figure 6-42 Polynomial Model- June- C2

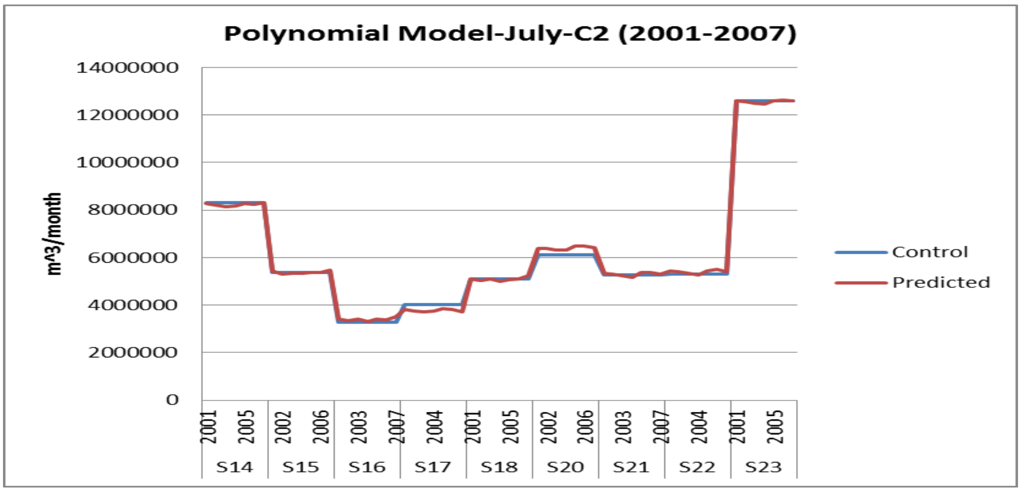

Figure 6-43 Polynomial Model- July- C2

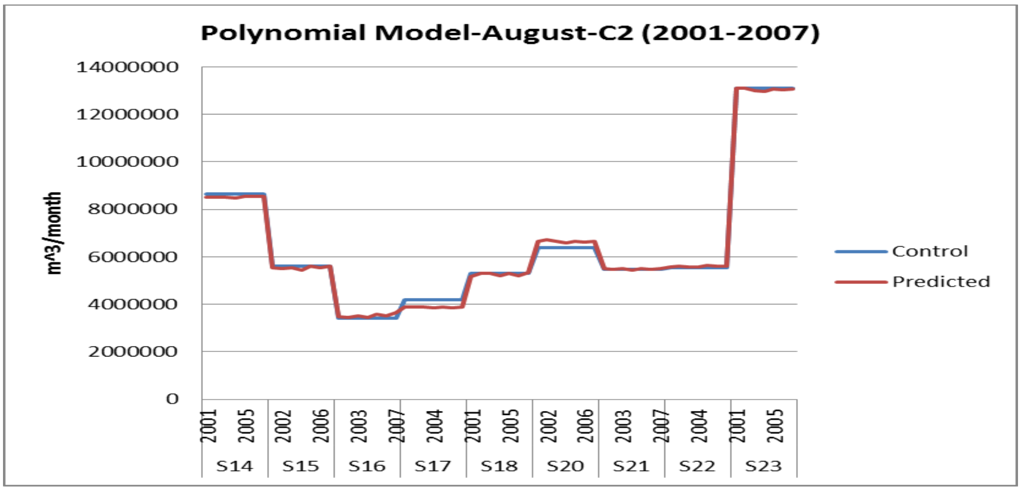

Figure 6-44 Polynomial Model- August- C2

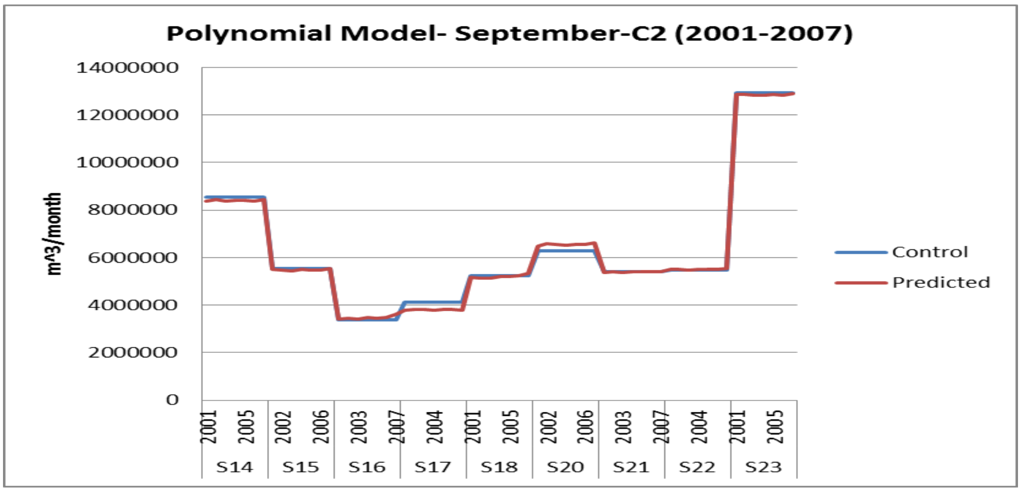

Figure 6-45 Polynomial Model- September- C2

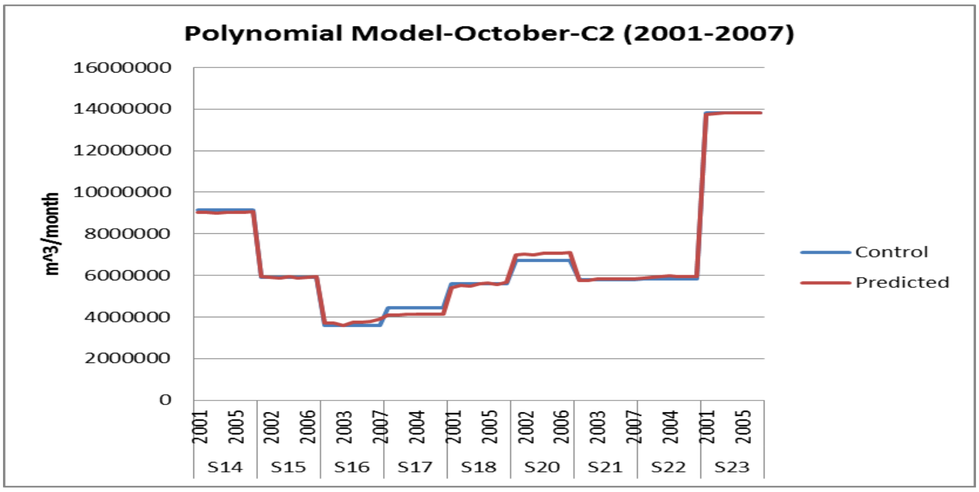

Figure 6-46 Polynomial Model- October- C2

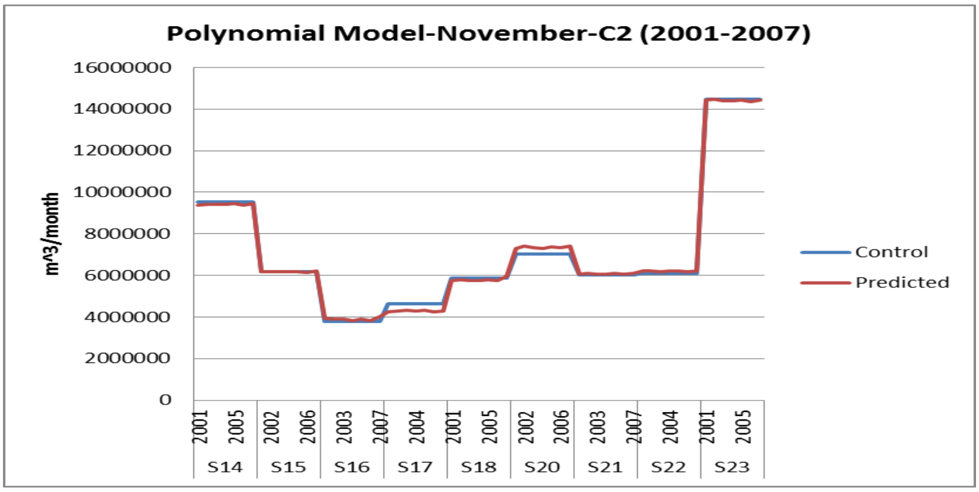

Figure 6-47 Polynomial Model- November- C2

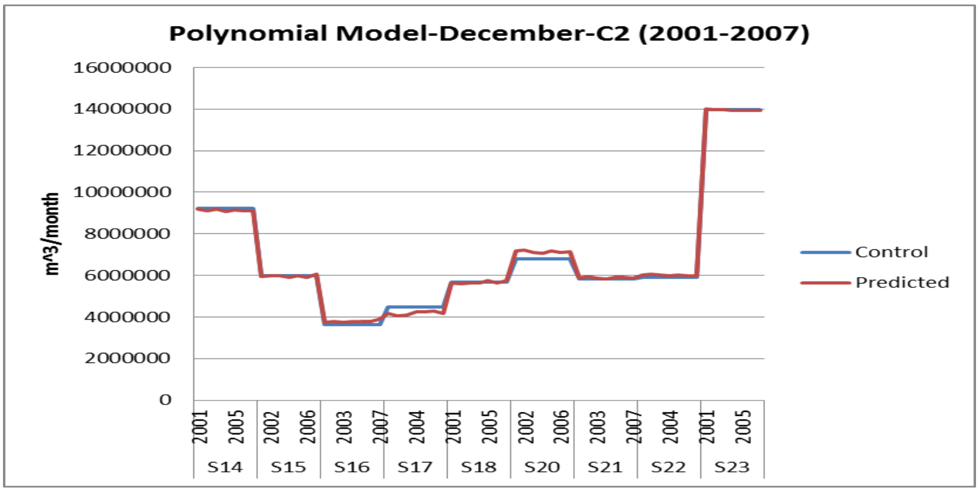

Figure 6-48 Polynomial Model- December- C2

Table 6-5 Summary of statistical performance

		Multi-linear regression			Polynomial regression		
		NSE	**PBIAS**	**RSR**	**NSE**	**PBIAS**	**RSR**
Category 1 (Flat)	**Jan**	0.932869	0.097069	0.259097	0.976955	-3.81624	0.151805
	Feb	0.932428	0.032203	0.259946	0.982453	0.6083	0.132467
	Mar	0.929791	-4.4485	0.26497	0.981543	0.124635	0.135858
	Apr	0.932272	-0.02967	0.260245	0.981677	0.155641	0.135362
	May	0.931716	0.023414	0.261312	0.981337	0.622844	0.136614
	Jun	0.933821	0.022675	0.257252	0.982	-0.17766	0.134164
	Jul	0.934256	0.019726	0.256405	0.98224	0.467527	0.133267
	Aug	0.933328	-0.00427	0.258208	0.981693	0.05941	0.135302
	Sep	0.936941	0.003844	0.251115	0.982271	-0.48307	0.13315
	Oct	0.934051	0.024921	0.256805	0.982258	0.461	0.1332
	Nov	0.937932	0.027235	0.249135	0.981809	0.275943	0.134872
	Dec	0.934236	0.015698	0.256444	0.981807	-0.19938	0.13488
Category 2 (Hilly)	**Jan**	0.996795	-1.05963	0.056612	0.996297	-0.23568	0.060855
	Feb	0.997552	0.005738	0.049478	0.996724	0.19771	0.057234
	Mar	0.997556	0.009396	0.049441	0.996767	0.070538	0.05686
	Apr	0.997549	-0.01515	0.049504	0.996699	0.053788	0.057458
	May	0.997134	-0.90477	0.05354	0.995596	1.191659	0.066362
	Jun	0.990645	-3.09406	0.096722	0.996709	0.172682	0.057366
	Jul	0.997549	0.007629	0.049507	0.996932	-0.23242	0.055393
	Aug	0.997562	-0.04204	0.04938	0.996587	0.232336	0.058418
	Sep	0.997569	-0.00333	0.049301	0.996567	0.375013	0.058594
	Oct	0.997612	0.000739	0.048867	0.996682	-0.11896	0.057603
	Nov	0.996063	1.637778	0.062746	0.996573	-0.04878	0.058539
	Dec	0.997554	-0.00594	0.049453	0.996569	-0.35105	0.058571

6.3 Model parameters

6.3.1 Multilinear regression model

The mesoscale deterministic model developed with the multilinear regression approach is not meant to address the temporal dynamics of the dependent variable. In order to deal with this limitation, optimum parameters were generated for each month and the summary is presented in table 6-3 above.

6.3.2 Polynomial regression model

Similarly, the deterministic model developed with the polynomial regression technique is not meant to address the temporal dynamics of the dependent variable that is the water generated within the Semliki subcatchments. And this shortfall was dealt with by genarating optimum parameters for each month and the summary is presented in table 6-4 above.

7 UNCERTAINTY AND SENSITIVITY ANALYSIS

7.1 Uncertainty

Previous reference is made to the table 2-3 on typology of uncertainty as formulated by the British Environmental Agency and as reported under 2.5.2. This study like most of the research work did not address uncertainties inherent to the system nor those associated with natural variability. This includes randomness of physiographic characteristics of the Semliki watershed as well as variation in natural hydrological response systems.

On the other hand, uncertainties associated with knowledge have been addressed in this study in three folds:

- Uncertainties linked to model input data
- Uncertainties associated with model structure
- Uncertainties linked to parameters

7.1.1 Uncertainties linked to model input data

The following uncertainties have been dealt with in this study by approaches that include the local calibration of satellite derived rainfall from FEWS/NOAA. The ground measurement used to correct the remotely sensed acquired rainfall data reduced uncertainty associated with such type of datasets. Moreover, the satellite derived rainfall used for this study presents the added advantage of providing a better spatial and temporal resolution for rainfall of the Semliki watershed despite the fact that the spatial resolution of the grid was 0.1degree.

The use of up-to-date GIS software, statistical packages and pre-processed Digital Elevation Model for hydrological applications from NASA, coupled with advance trainings in the above mentioned fields were also measures undertaken in this study in order to reduce uncertainty associated with data processing

7.1.2 Model structural uncertainties

The following can be reported on the deterministic and mesoscale models developed. In essence the deterministic models provide conceptual frameworks that do not adequately capture adequately temporal dynamics. However for this research work, that shortfall has been catered for in a quasi-temporal manner with model parameters being generated for each month. In addition to this approach, both the linear and the non-linear models were developed taking cognizance of physiographic similarities which to a great extent mitigate the uncertainties associated with their spatial representations as well as those linked to ambiguous boundary conditions.It is however worth mentioning that the approaches used to develop the two models did not address uncertainties associated with the actual hydrological processes of the catchment.

7.1.3 Parameters uncertainties

The parameters of the models in this study are lumped at the subcatchment scale. Thus lumping captures more faithfully the spatial dynamics than any previous study undertaken in this part of the equatorial Nile Basin. As a result, the scale of uncertainties associated with these parameters is reduced.

The concept of equifinality in parameter estimation process is documented to be one of the major causes for parameter uncertainty. For this study, as much as the performance achieved during the calibration stage (NSE above 95%) both for the linear and the nonlinear models, the concept of equifinality was not completely investigated and subsequently the uncertainty associated with the variability of parameters was not addressed.

7.2 Sensitivity analysis

Sensitivity analyses aims at determining how a model relates to its inputs, parameters, structure and underlying assumptions as alluded to under 2.5.2. As a result, sensitivity analysis can be viewed as part of uncertainty estimation methods by indicating where focus should be directed in order to reduce uncertainty. For this research work, the local technique that allows the response of outputs to deviation of individual inputs or variables, while fixing the other variables at their initial values, was used. Each physiographic attribute was varied in increment of 10% from 0 to ±30%. Beyond these lower and upper bounds of 30%, failure of the linear model is observed. To avoid distracting the essence of the analysis with too many graphs, summarised PBIAS graphical representation for selected month within a quarter are presented under 7.2.3, while the complete set of results can be found in Appendix C.

7.2.1 Multilinear model

The results of the sensitivity analysis of the multilinear model for the first group (Category 1) of subcatchments reveal that the stream length, the drainage density and the maximum elevation are respectively the most sensitive physiographic attributes for every month. Temporarily, the PBIAS for the months of March, April and May exhibit the greatest sensitivity to the above-mentioned group of physiographic attributes. Worth mentioning is the fact that the percentage Bias (PBIAS) index for this group of subcatchments indicates that flows within subcatchments are overestimated for each month for higher Rainfall and NDVI, and vice-versa.

For the second group of subcatchments (Category 2), the results of the step-wise sensitivity analysis indicates that for the months of January, May and June, the stream length is the most sensitive physiographic attribute followed by the Drainage density and then the maximum elevation. The month of June showed the highest level of sensitivity for the three landscape attributes. The group made of the following physiographic attributes, stream length, drainage density and Maximiun elevation, are respectively the most sensitive variables for January, May and June, with the month of June being the most sensitive for the three landscape attributes. For the remaining 9 months, stream length was again the most sensitive physiographic attribute, followed by drainage density and the weighted-average elevation. The month of August showed the highest level of sensitivity. However , in the month of November, Drainage density is the most sensitive physiographic attribute followed by the stream length and weighted-average elevation. The sensitivity analysis of the multilinear model did not show that rainfall, a primary driver of most hydrological processes, is very sensitive. This is explained by the conceptual and statistical (black-box) nature of this regression-based technique.

7.2.2 Polynomial model

The results of sensitivity analysis for the polynomial model for the first group (C1) of subcatchments indicate that for January and September, the stream length is most sensitive followed by the weighted-average elevation and the NDVI. For the remaining ten months of the year the weighted-average elevation is the most sensitive landscape attribute followed by the stream length then the drainage density. Moreover, the months of May and July showed the highest level of sensitivity for the above-mentioned variables.

For the second group of subcatchment (C2), the step-wise sensitivity analysis indicates in all the months of the year except May that the stream length is the most sensitive physiographic attribute followed by the drainage density and the weighted-average elevation. The level of sensitivity of these three landscape attributes is highest in December. In the month of May (one of the wettest), however, the following order is observed in the sensitivity of variables (Stream length, drainage density and rainfall). This observation remains true only for changes in variables up to the threshold of 10% beyond wich weighted-average elevation replaces rainfall. The sensitivity analysis of the polynomial model did not indicate that rainfall, a key driver of most hydrological processes is very sensitive, this is explained by conceptual and statistical (black-box) nature of this regression-based approach.

7.2.3 Performance indexes[8]

As alluded to earlier, the results of the sensitivity analyses in hilly subcatchments (category II) indicated that the stream length, the drainage density and the elevations generally were respectively the most sensitive landscape attributes both for the linear and the non-linear models. The PBIAS provides better schematic representation of the sensitivity analyses than the NSE and the RSR because it reflects whether or not the stream flow is over-predicted by the change in input variable. Hence, only the PBIAS is plotted and discussed in this section.

[8]Partly Sourced from Kileshye Onema and Taigbenu, 2011 (submitted).

Furthermore, presenting all the graphs of the sensitivity results would meant having 48 graphs for the two predictive models, two categories of sub-catchments and 12 monthly local flow estimates. Only a few of these plots are presented for a typical month in each quarter of the hydrological year.

For the hilly sub-catchments (category II), the flow predictions by the non-linear model are most affected by the stream length and followed by the drainage density (Figs. 7-1 to 7-3). The results of the PBIAS show that that a decrease in the stream length gives rise to an underestimation of the predicted flow, while the converse is the case for the drainage density. Furthermore, an increase in weighted-average elevation and NDVI brings about an over estimation of predicted flows. A similar trend is observed with the multi-linear model for the category II sub-catchments (Figs. 7-4 to 7-6).

Stream slope, NDVI and rainfall are the least sensitive physiographic and meteorological variables for these two models. This may come as a surprise, particularly for rainfall that is commonly considered one of the most important hydrological drivers. However, considering that the modeling approaches are essentially conceptual and with no causal mechanisms directly linked to the hydrological processes of the predicted flows, this result can be expected. Furthermore, it is conjectured that the humid nature of the study area which is the equatorial region may also conceal the sensitivity of rainfall on the models' predicted runoffs in contrast to arid regions.

For the flat sub-catchments (category I), the flow predictions of the non-linear model are influenced the most by the weighted-average elevation, followed by the stream length and then the drainage density (Figs. 7-10 to 7-12). All changes (increase and decrease) in the weighted-average elevation result in an underestimation for the predicted flows. The stream length and drainage density produce opposite effects on the predicted flows, with an increase in stream length resulting in overestimation of the flows and conversely for the drainage density (Figs. 7-10 to 7-12). The sensitivity analysis results from the multilinear model for category I sub-catchments that are presented in Figures 7-7 to 7-9 indicate that the stream length, drainage density, NDVI and maximum elevation are, in that order, the most sensitive input variables for the prediction of the monthly flows. The month of February showed however that the maximum elevation was more sensitive than the NDVI. Increases in the drainage density, the maximum, minimum and weighted-average elevations result in an underestimation of predicted flows, while an increase in stream length and NDVI produced the opposite effect (Figs. 7-7 to 7-9).

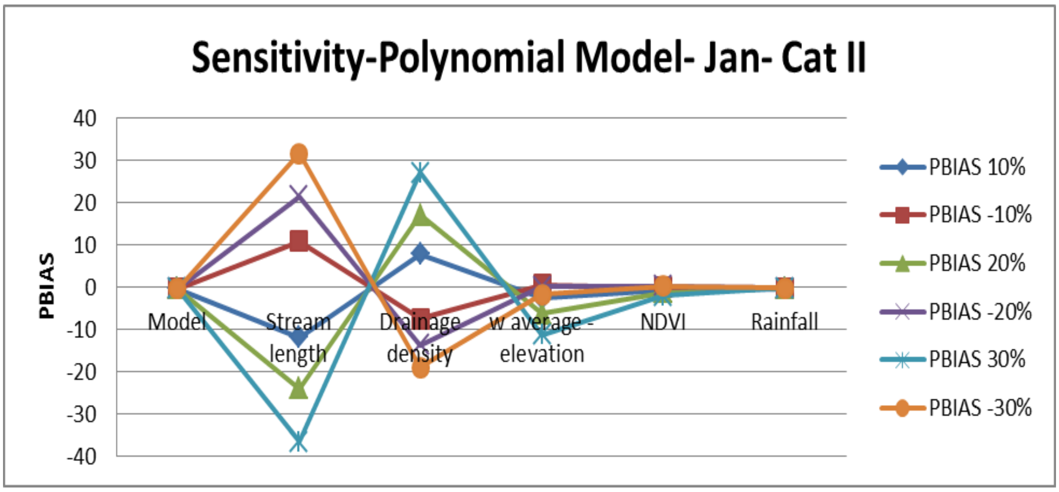

Figure 7-1 Sensitivity analysis for polynomial model in Hilly subcatchments- January

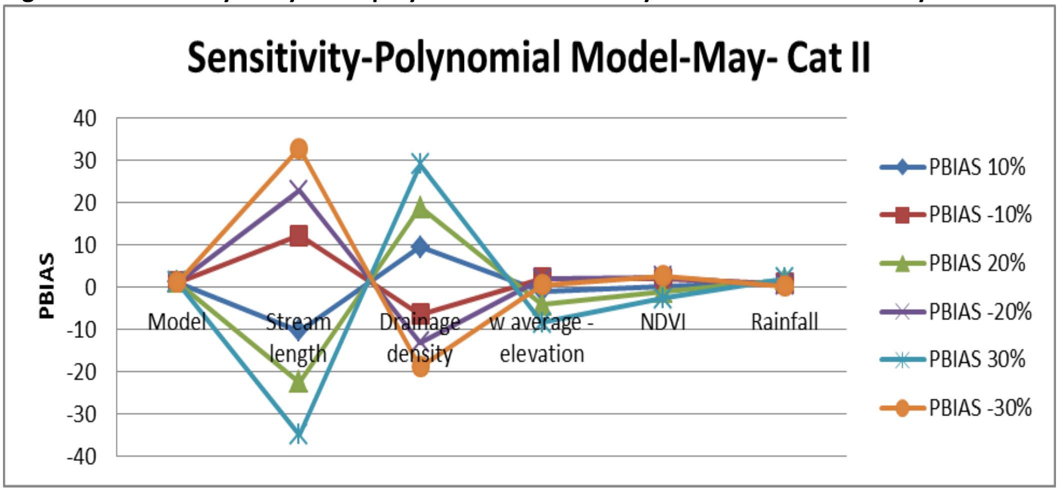

Figure 7-2 Sensitivity analysis for polynomial model in Hilly subcatchments- May

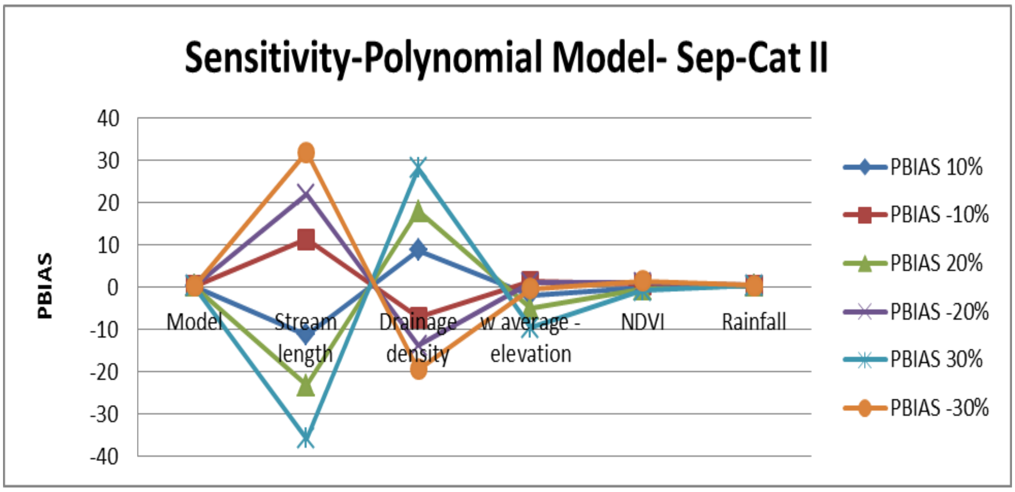

Figure 7-3 Sensitivity analysis for polynomial model in Hilly subcatchments- September

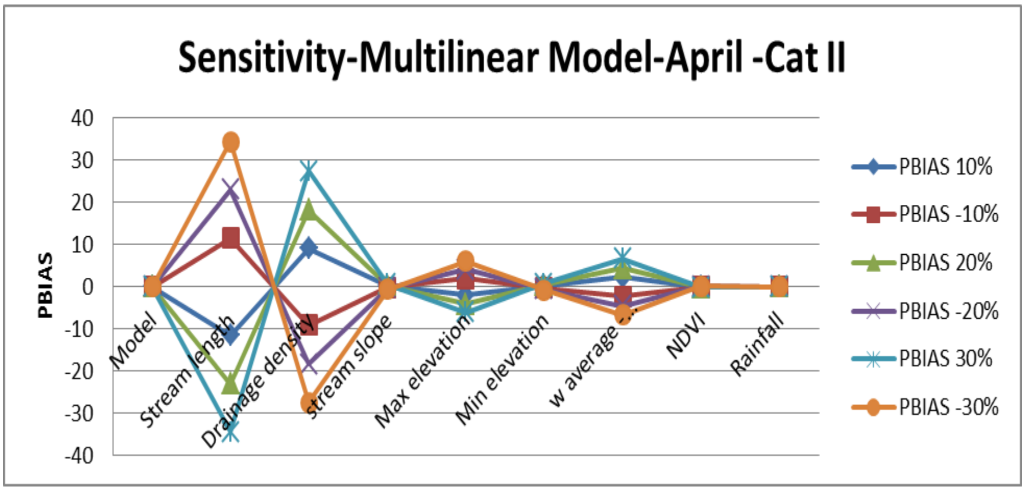

Figure 7-4 Sensitivity analysis for multilinear model in Hilly subcatchments- April

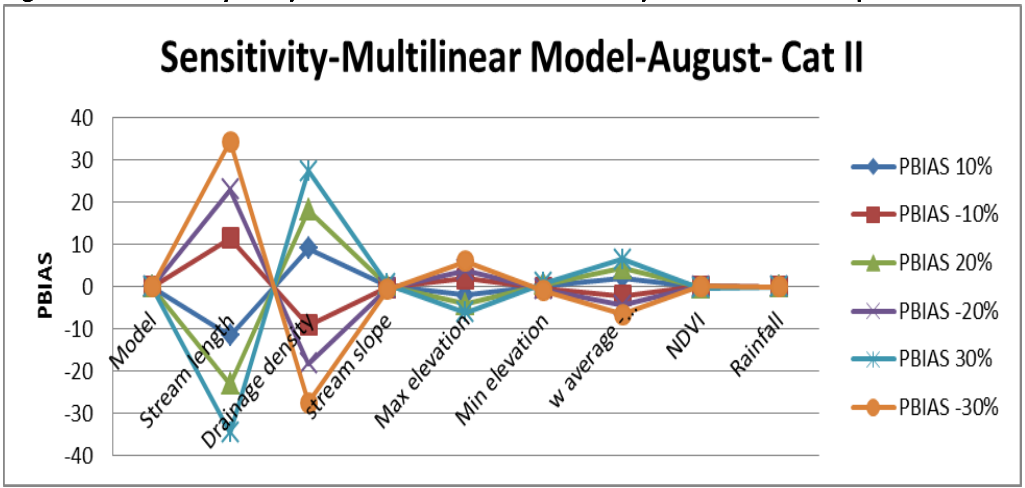

Figure 7-5 Sensitivity analysis for multilinear model in Hilly subcatchments- August

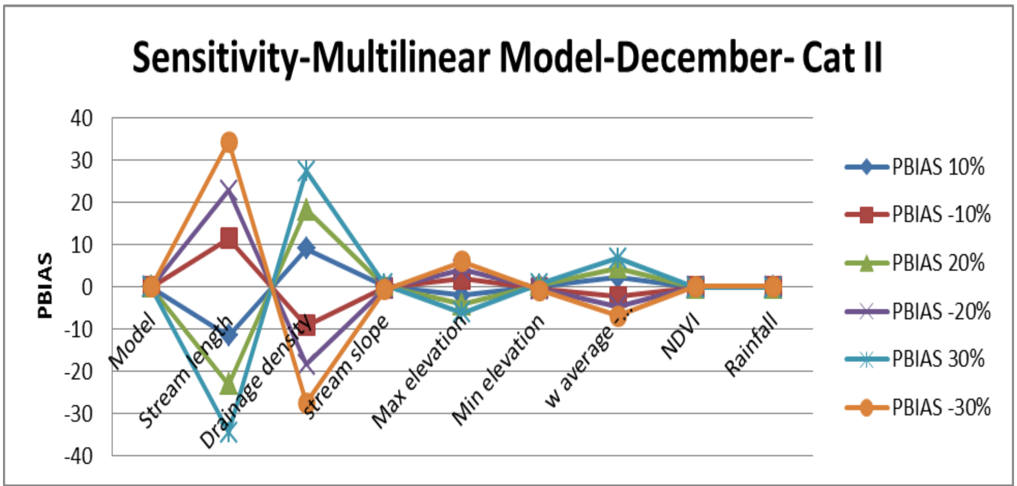

Figure 7-6 Sensitivity analysis for multilinear model in Hilly subcatchments- December

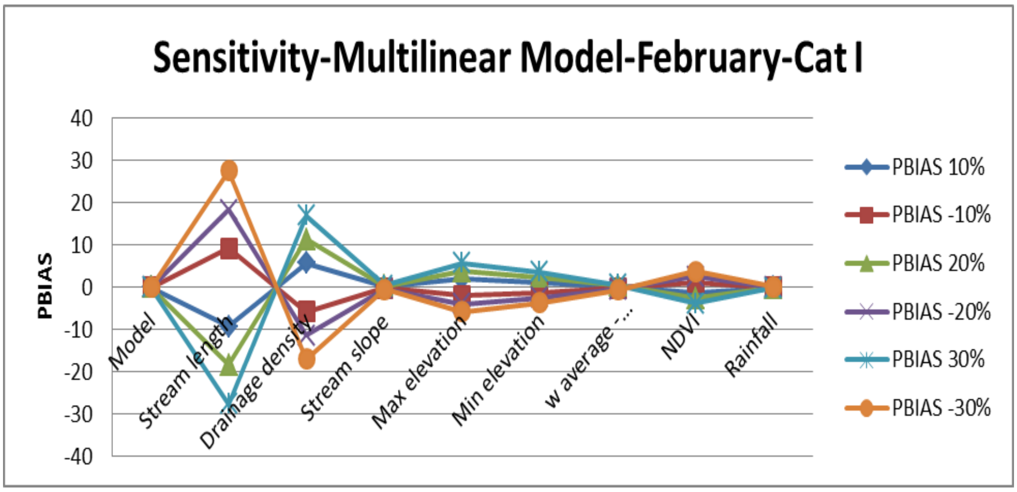

Figure 7-7 Sensitivity analysis for multilinear model in Flat subcatchments- February

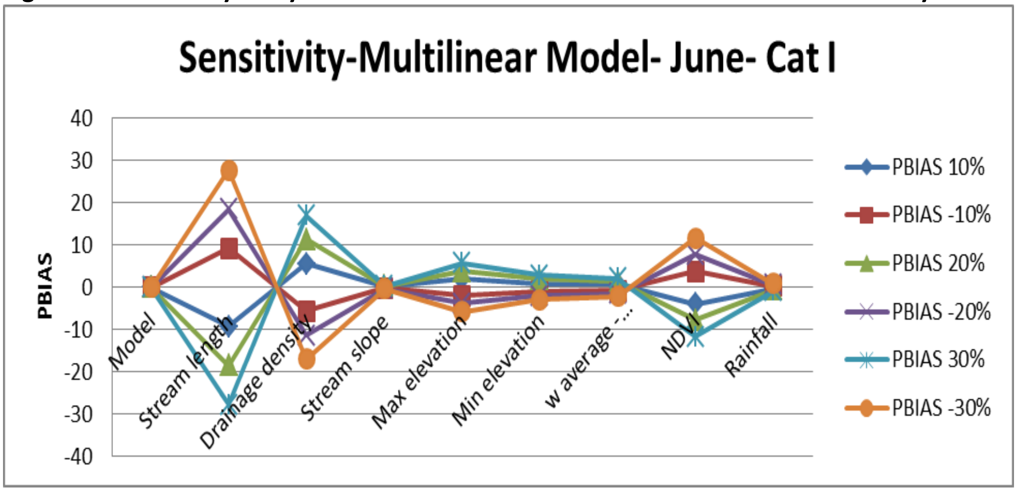

Figure 7-8 Sensitivity analysis for multilinear model in Flat subcatchments- June

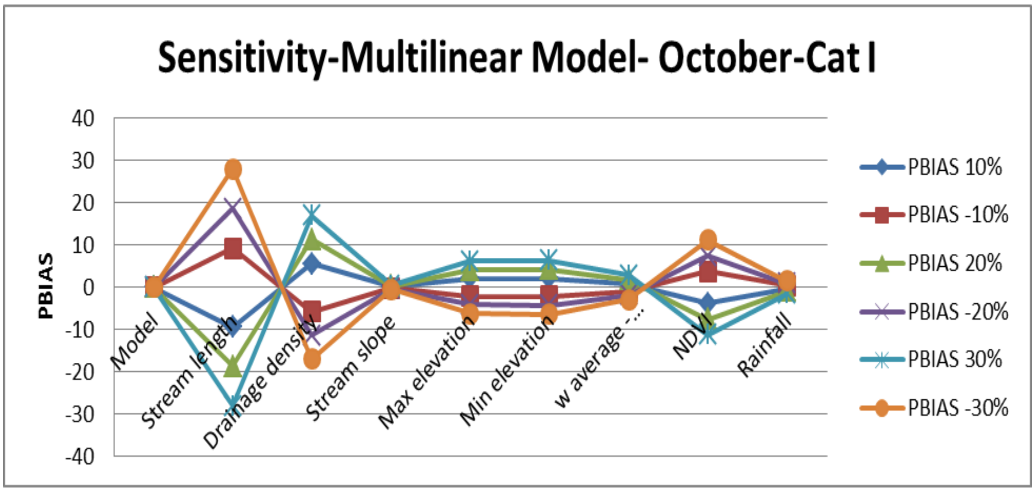

Figure 7-9 Sensitivity analysis for multilinear model in Flat subcatchments- October

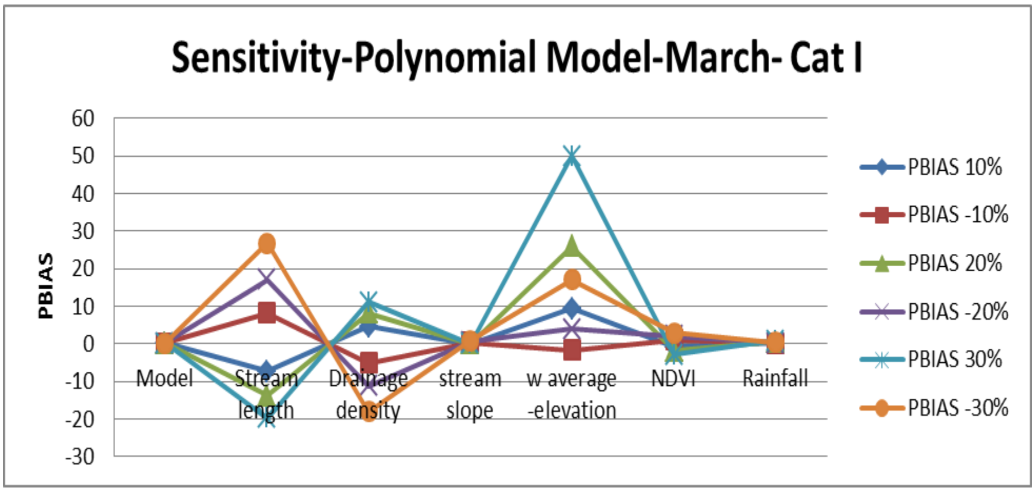

Figure 7-10 Sensitivity analysis for polynomial model in Flat subcatchments- March

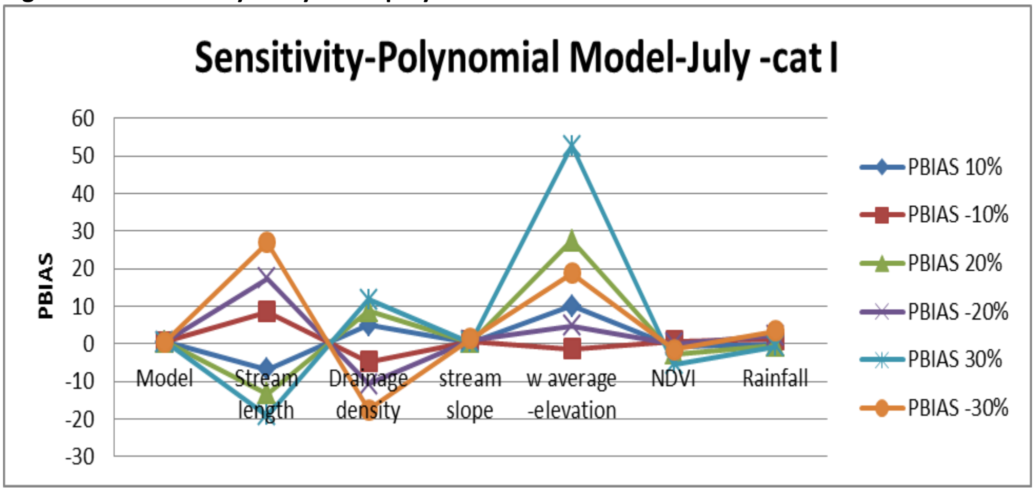

Figure 7-11 Sensitivity analysis for polynomial model in Flat subcatchments- July

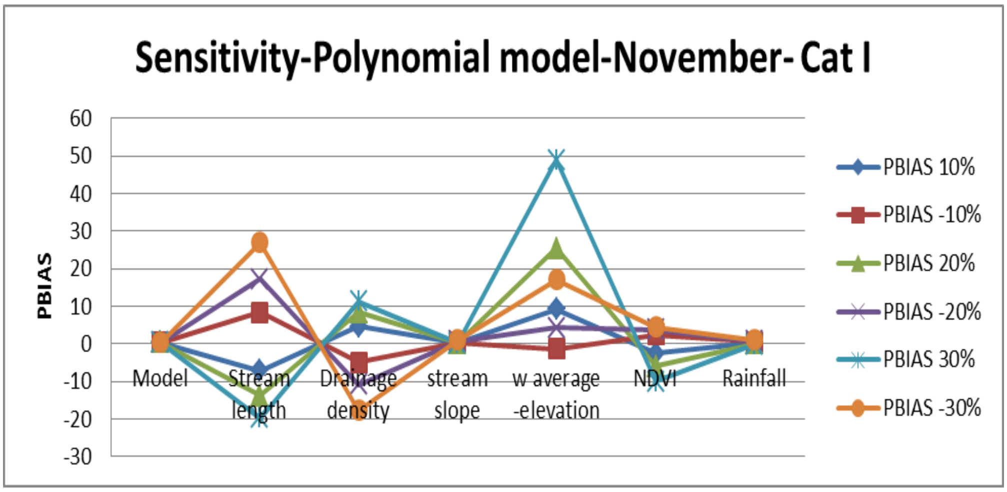

Figure 7-12 Sensitivity analysis for polynomial model in Flat subcatchments- November

8 CONCLUSIONS AND RECOMMENDATIONS

8.1 Conclusions

The objective of this study was to develop monthly models from landscape attributes for flow predictions in the data-scarce Semliki watershed of the equatorial Nile region. This approach is particularly important for the Nile basin where flows for the entire basin are generated by only 20% of the basin area. The Nile is the world's longest stream with water travel times varying from 20 days (Blue Nile tributary) to more than 45 days (White Nile tributary) depending on the seasons (Koutsoyiannis *et al.*, 2008). The Nile River is utilised for numerous water uses that include energy generation, water supply for agricultural, industrial and domestic use, flood mitigation and management as well as the provision of other environmental and ecosystem services (Said, 1993; Waterbury, 2002). Moreover long and intermediate flows information are crucial for the management and operation of water infrastructure from the Central and Eastern parts of Africa up to Egypt via the middle reaches of Sudan. This indicates the need for spatially and temporally appropriate monthly forecast of the flow of the Nile River. The underlying assumptions for this study were that landscape attributes have impacts on water resources of a basin, with considerable influence of upstream physiographic conditions on downstream flows and that lack of adequate information about the quantity of water resources can be overcome by a suitable combination of predictive methodologies. Furthermore it is assumed that the dynamic effects of anthropogenic activities are implicitly captured in the physiographic variable associated with land cover, which in our case is the NDVI.

Existing methods and approaches for flow prediction in data-poor and ungauged catchments were extensively reviewed in Chapter 2.

Hence, in our attempt to further advance knowledge in the area of predictions in data-scarce watersheds, the following approaches were used in this research work:

- From limited ground information, remotely sensed acquired data-sets watershed attributes for the Semliki were generated for 21 subcatchments that form the study area.
- An indirect ordination technique namely the Principal Component Analysis (PCA) in conjunction with the clustering analysis (tree diagram and two-way joining) were used to detect data structure and similiraties. The PCA further guided the determination of optimal model dimension by indicating redundant variables.
- Multilinear and polynomial regressions together with all the statistical techniques linked with the two approaches were performed to develop the mesoscale deterministic prediction models for the Semliki watershed.
- Several statistical performance indices were computed for the calibration of the developed models

The results have indicated the existence of two groups of subcatchments in the Semliki watershed with similar hydrological conditions. The first group (C1) is characterized by landscape that is flatter in contrast to the second group (C2) of subcatchments which are at higher elevations.

The predictions from the two models are in close range with estimates provided by Senay et al. (2009) in their attempt to document the overall basin dynamics of the Nile River.

Monthly parameters were generated for the multilinear and the polynomial models for both the first group (C1) and the second group (C2) of subcatchments. The statistical indexes of performance for the calibration process of the multlinear model are in the following ranges:

C1, NSE: 0.93 to 0.94; RSR: 0.26 to 0.25; PBIAS:-4.4 to 0.09

C2, NSE: 0.990 to 0.998; RSR 0.097 to 0.049; PBIAS:-3.09 to1.64

The polynomial performance indexes are as follow:

C1, NSE: 0.98; RSR: 0.15 to 0.13; PBIAS: -3.82 to 0.62

C2, NSE: 0.996, RSR: 0.066 to 0.055; PBIAS: -0.24 to 0.37

These indexes indicate that the non-linear model better predicts flows within subcatchments than the linear model. Whereas both models gave satisfactory predictions of the flows, their predictions in (C2) group of subcatchments were better than in (C1).

The step-wise sensitivity analyses indicated that the stream length was the most sensitive variable for both the linear and the non-linear models. Moreover, the results of the sensitivity analyses provide guidance to users on the variables that require higher accuracy when using both the linear and the non linear models.

Although the sensitivity analysis did not indicate that rainfall, a key driver of most hydrological processes is very sensitive in both models, it only underscores their conceptual and statistical nature.

This study constitutes the first documented and rational approach that has related physiographic attributes to flow generated in the Semliki watershed at this spatial and temporal scale.

8.2 Recommendations

This study has produced a rational approach for flow prediction in a data-scarce watershed. The approach is in essence deterministic and mesoscale. As with all regression-based methods that are constructed entirely or in part by data, the generalization and reliability could be enhanced by extending the database to better support the empirical approach. Some of the mathematical representations documented in this research work were calibrated on historical information due to lack on current data, therefore further field validation would be valuable.

The generation of catchment descriptors was done in GIS laboratory with limited ground truthing. Improvement in the accuracy of the geohydrological data from field investigations could be considered for further research.

The linear and the non-linear mesoscale and deterministic models do not directly address the hydrological processes in the subbasin. Hence a physically based approach could be coupled to this approach to provide greater understanding of the hydrology of the Semliki watershed. Similarly, this research work highlighted the need for serious steps to be initiated in obtaining Hydro meteorological data that can be used for further investigations into physically based modelling approaches that explicitly account for the interaction between landscape attributes and water resources in the Semliki watershed.

The sensitivity analyses resulted from a step-wise approach, that is local by nature, can be extended by the use of global techniques to further provide insight into the behaviors of the developed models.

REFERENCES

Ahmad, M., Bastiaanssen, W.G.M. and Feddes, R.A. 2005. A new technique to estimate net groundwater use across large irrigated areas by combining remote sensing and water balance approaches, Rechna Doab, Pakistan. *Hydrogeology Journal*, ***13***, *653-664.*

Ahmad, M.-D., Biggs, T., Turral, H. and. Scott, C.A., 2006. Application of SEBAL approach and MODIS time-series to map vegetation water use patterns in the data scarce Krishna river basin of India. *Water Science & Technology* ***53 (10)*** *83–90* IWA Publishing.

Andersen, J., Dybkjaer, G., Jensen, K.H., Refsgaard, J.C., Rasmussen, K., 2002. Use of remotely sensed precipitation and leaf area index in a distributed hydrological model. *Journal of Hydrology*, ***264***, *34-50.*

Andréassian, V., Perrin, C., Michel, C., Usart-Sanchez, I. and Lavabre, J., 2001. Impact of imperfect rainfall knowledge on the efficiency and the parameters of watershed models, *Journal of Hydrology*, **250**, 206-223.

Andréassian, V., Perrin, C., Michel, C., 2004. Impact of imperfect potential evapotranspiration knowledge on the efficiency and the parameters of watershed models, *Journal of Hydrology* **286**, 19-35.

Ardo, J., Pilesjo, P. and Skidmore, A.1997. Neural networks, multitemporal Landsat thematic mapper data and topographic data to classify forest damages in the Czech Republic. *Canadian Journal of Remote sensing,* ***23****, 3, 217-228*

Arnold, S. F., 1990**.** Mathematical Statistics, Prentice-Hall, Englewood cliffs, New Jersey.

Arnold, J.G. and Foster, N., 2005. SWAT2000. Current capabilities and research opportunities in applied watershed modeling. *Hydrological Processes,* ***19****, 563-572*.

Asadullah, A., McIntyre, N. and Kigobe, M., 2008. Evaluation of five satellite products for estimation of rainfall over Uganda. *Hydrological sciences Journal,* ***53(6)****, 1137-1150.*

Aspinal, R. and Pearson, D., 2000. Integrated geographical assessment of environmental condition in water catchments: Linking landscape ecology, environmental modeling and GIS. *Journal of Environmental Management* ***59****, 299-319.*

Bari, M and Smettem, K. R. J., 2004. Modelling monthly runoff generation processes following land use changes: groundwater–surface runoff interactions *Hydrology and Earth System Sciences*, ***8****, 903-922.*

Barker, R. and Molle, F., 2004. *Evolution of irrigation in South and Southeast Asia.* Comprehensive Assessment Research Report 4, International Water Management Institute, Colombo, 39p.

Bastiaanssen, W.G.M., Menenti, M., Feddes, R.A. and Holtslag, A.A.M., 1998. A remote sensing surface energy balance algorithm for land (SEBAL): 1. Formulation. *Journal of Hydrology*, ***212-213****, 198-212.*

Bastiaanssen, W.G.M., 2000. SEBAL-based sensible and latent heat fluxes in the irrigated Gediz Basin, Turkey. *Journal of Hydrology*, ***229****,87-100*

Bastiaanssen, W.G.M., Ahmad, M.D. and Chemin, Y., 2002. Satellite surveillance of evaporative depletion across the Indus Basin. *Water Resources Research,* ***38****, 1273, 1-9.*

Baumgartner, M.F., Schultz, G.A and Johnson A.I. (Editors). 1997. Remote sensing and Geographic Information Systems for Design and Operation of Water Resources Systems. IAHS, **242.**

Berger, K.P. and Enthekhabi, D., 2001. Basin hydrologic response relations to distributed physiographic descriptors and climate. *Journal of hydrology*, ***247***,*169-182*.

Beven, K.J. and Binley, A.M., 1992. The future of distributed models-model calibration and uncertainty prediction, *Hydrological Processes,* **6(3),** 279-298.

Beven, K., 1993. Prophecy, reality and uncertainty in distributed hydrological modelling. *Advances in Water Resources* ***16***, *41-51.*

Beven, K. and Freer, J., 2001. Equifinality, data assimilation, and uncertainty estimation in mechanistic modelling of complex environmental systems using the GLUE methodology, *Journal of Hydrology,* **249,** 11-29.

Binley, A.M., Beven, K.J., Calver, A. and Watts, L.G., 1991. Changing responses in hydrology: assessing uncertainty in physically based model predictions, *Water Resources. Research,* **27(6)**, 1253-1261.

Bishop, P.L., Hivley, W.D., Stedinger, J.R., Rafferty, M.R., Lojpersberger, J.L. and Bloomfield, J.A., 2005. Multivariate analysis of paired watershed data to evaluate agricultural best management practice effects on stream water phosphorous. *Journal of Environmental Quality*, ***34***, *1087-1101.*

Blöschl, G. and Sivapalan, M., 1997. Process controls on regional flood frequency: coefficient of variation and basin scale. *Water Resources Research*, ***33(12),*** *2967-2980***.**

Bobba, A.G., Bukata, R.P. and Jerome, J.H., 1992. Digitally processed satellite data as a tool in detecting potential groundwater flow systems. *Journal of Hydrology*, ***131***, *25-62*.

Boegh, E., & Soegaard, H., 2004. Remote sensing based estimation of evapotranspiration rates. *International Journal of Remote Sensing*, ***25(13)***, *2535−2551*.

Boegh, E., Soegaard, H., Christensen, J. H., Hasager, C. B., Jensen, N. O., Nielsen, N. W., and Rasmussen, M. S., 2004. Combining weather prediction and remote sensing data for the calculation of evapotranspiration rates: application to Denmark. *International Journal of Remote Sensing*, ***25 (13),*** *2553-2574.*

Bormann, H. and Diekkrüger, B., 2003. Possibilities and limitations of regional hydrological models applied within an environmental change study in Benin (West Africa). *Physics and Chemistry of the Earth*, ***28***, *1323-1332*.

Borradaile, G., 2003. Statistics of earth science data: their distribution in space, time, and orientation. Springer-verlag Berlin Heidelberg.

Boughton, W., 2005. Catchment water balance modelling in Australia 1960-2004. *Agricultural Water Management*, ***71***, *91-116*.

Butterworth, J.A., Mugabe, F., Simmonds, L.P. and Hodnett, M.G., 1999. Hydrological processes and water resources management in a dryland environment II: surface redistribution of rainfall within fields. *Hydrology and Earth Systems Sciences*, ***3***, *333-343*.

Butts, M.B., Payne, J.T., Kristensen, M. and Madsen, H., 2004. An evaluation of the impact of model structure on hydrological modelling uncertainty for streamflow simulation, *Journal of Hydrology,* **298**, 242-266.

Calder, I.R., Hall, R.L., Bastable, H.G., Gunston, H.M., Shela, O., Chirwa, A. and Kafundu, R., 1995. The impact of land use change on water resources in sub-Saharan Africa: a modelling study of Lake Malawi. *Journal of Hydrology*, ***170***, *123-135*.

Chammaillé-Jammes, S., Fritz, H., Murindagomo, F., 2006. Spatial patterns of the NDVI-rainfall relationship at the seasonal and interannual time scales in an African savanna. *International Journal of Remote Sensing, Vol. **27**, No.23, 5185-5200*.

Chiang, S.M, Tsay, T.K, Nix, S.J., 2002. Hydrologic regionalization of watersheds I: Methodology. *Journal of Water Resources Planning and Management 128 (1), 3-11*.

Chen, P.Y., Srinivasan, R., Fedosejevs, G., Kiniry, J. R., 2003. Evaluating different NDVI composite techniques using NOAA-14 AVHRR data. *International Journal of Remote Sensing Vol. **24** No. 17, 3403-3412.*

Cheng, Q., Ko, C., Yuan,Y., Ge, Y., Zhang, S., 2006. GIS modeling for predicting river runoff volume in ungauged drainages in the greater Toronto area, Canada. *Computers and Geosciences **32**, 1108-1119.*

Cole, S.J., Moore, R.J., 2008. Hydrological modeling using raingauge and radar-based estimators of areal rainfall. *Journal of hydrology **358,** 159-181.*

Collischonn, B., Collischonn, W., Tucci, C.E.M., 2008. Daily hydrological modelling in the Amazon basin using TRMM rainfall estimates. *Journal of hydrology **360**, 207-216.*

Conway, D., 2005. From headwater tributaries to international river: observing and adapting to climate variability and change in the Nile basin. *Global environment change* ***15****, 99-114*.

Crago, R.D., 1996. Conservation and variability of the evaporative fraction during the day time. *Journal of Hydrology*, ***180****, 173-194*

Croke, B.F.W., Merritt, W.S., Jakeman, A.J., 2004. A dynamic model for predicting hydrologic response to land cover changes in gauged and ungauged catchments. *Journal of hydrology* ***291,*** *115-131*.

Das,T., Bardossy, A., Zehe,E., He,Y., 2008. Comparison of conceptual model performance using different representations of spatial variability, *Journal of hydrology* ***356****, 106-118.*

Dawson, C.W., Abrahart, R.J., Shamseldin, A.Y., Wilby, R.L., 2006. Flood estimation at ungauged sites using artificial neural networks. *Journal of hydrology* ***319****, 391-409.*

Day, D.G**.,** 1978**.** Drainage density changes during rainfall. *Earth surface processes,* ***3****, 319-326.*

De Groen, M.M., 2002. *Modelling interception and transpiration at monthly time steps: introducing daily variability through Markov Chains*. Ph.D. dissertation, IHE Delft, Swets and Zeitlinger B.V., Netherlands, 211p

Dent, M.C., 2000. Strategic issues in modelling for integrated water resource management in Southern Africa. *Water SA, **26**, 513-520.*

Dewan, A.M., Yamaguchi, Y., 2009. Land use and land cover change in Greater Dhaka, Bangladesh: using remote sensing to promote sustainable urbanization. *Applied Geography*, Vol **29(3),** 390-401.

Dibella, C.M., Rebella, C.M., Paruelo, J.M., 2000 Evapotranspiration estimates using NOAA AVHRR imagery in the Pampa region of Argentina. *International Journal of Remote Sensing Vol. **21,** No. 4, 791–797.*

Dingman, S.L., 2002. Physical Hydrology, 2nd Edition. Prentice-Hall, New Jersey, 646pp.

Dooge, J.C.I., 2005. Bringing it all together. *Hydrology and Earth Systems Sciences, **9**, 3-14.*

Doore, I.D., Grayson, R.B., Ladson, A.R., 1991. Digital Terrain modeling: A review of hydrologiocal, geomorphological and biological applications. *Hydrological Processes, Vol **5**, 3-30.*

Droogers. P., 2000. Estimating of actual evapotranspirationtion using a detailed agro-hydrological model. *Journal of Hydrology, **229,** 50-58.*

Duan, Q., Schaake, J.C. and Koren, V.I., 2001. A prior estimation of land surface model parameters, Land surface hydrology, meteorology, and climate: Observations and Modelling. (ed. V. Lakshmi, J. Alberston and J.C. Schaake), American Geophysical Union, Water and Sci. Appl., 77-94.

Dunne, S. and Entekhabi, D., 2006. Land surface state and flux estimation using the ensemble Kalman smoother during the Southern Great Plains 1997 field experiment. *Water Resources Research*, ***42***, *W01407, doi: 10.1029/2005WR004334.*

El-Fadel, M., El-Sayegh, Y., El-Fadl, K. and Khorbotly, D., 2003.The Nile River Basin: A Case Study in Surface Water Conflict Resolution J. Nat. Resour. Life Sci. Educ. 32:107–117.

Engel, V., Jobbágy, E.G., Stieglitz, M., Williams, M. and Jackson, R.B. 2005. Hydrological consequences of Eucalyptus afforestation in the Argentine Pampas. *Water Resources Research*, **41**, W10409, doi:10.1029/2004WR003761.

FAO., 1997. Irrigation potential in Africa: A basin approach FAO LAND AND WATER BULLETIN 4.

Farah, H.O., Bastiaanssen, W.G.M. and Feddes, R.A., 2004. Evaluation of the temporal variability of the evaporative fraction in a tropical watershed. *International Journal of Applied Earth Observation and Geoinformation*, **5**, 129-140.

Fekete, B.M., Vörösmarty, C.J., Roads, J.O. and Willmott, C.J., 2004. Uncertainties in Precipitation and their Impacts on Runoff Estimates, *Journal of Climatology*, **17**, 294-304.

Fernandez, W., Vogel, R.M. and Sankarasubramanian, S., 2000. Regional calibration of watershed model. *Hydrological Sciences Journal* **45(5)**, 689-707.

Finch, J.W., 1998. Estimating direct groundwater recharge using a simple water balance model – sensitivity to land surface parameters. *Journal of Hydrology*, **211**, 112-125.

Fraser, R.H., Olthof, I., Pouliot, D., 2009. Monitoring land cover change and ecological integrity in Canada's National parks. *Remote Sensing of Environ*ment, **113(7),** 1397-1409.

Freer, J.E., Beven, K.J. and Ambroise, B., 1996. Bayesian estimation on uncertainty in runoff prediction and the value of data: an application of the GLUE approach, *Water Resources Research*, **32**, 2161-2173.

Gallart, F., Llorens, P., 2004. Observations on land cover changes and water resources in the headwaters of the Ebro catchment, Iberian Peninsula. *Physics and Chemistry of the Earth*, **29**, 769-773.

Gardiner, V., Gregory, K. J. and Walling, D. E., 1977. 'Further notes on the drainage density – basin area relationship', *Area*, ***9***, *117–121*.

Getirana, A.C.V., Bonnet, M-P., Calmant, S., Roux, E., Filho, O.C.R., Mansur, W.J., 2009. Hydrological monitoring of poorly gauged basins based on rainfall-runoff modeling and spatial altimetry. *Journal of Hydrology*, ***379***, *205-219*.

Georgakakos, A., 2007. Decision support systems for integrated water resources management with an application to the Nile. Ch.5 in: Topics on systems analysis and integrated water Resources management (ed. By A. Castelletti & R. Soncini-Sessa). Elsevier, The Netherlands.

Gordon, N.D., McMahon, T.A., Finlayson, B.L., Gippel, C.J., Nathan, R.J., 2004. Stream hydrology, an introduction for ecologists. Second edition. John Wiley & Sons Ltd, West Sussex, England.

Gourley, J.J. and Vieux, B.E., 2006. A method for identifying sources of model uncertainty in rainfall-runoff simulations, *Journal of Hydrology,* **327**, 68-80.

Groeneveld, D. P., Baugh, W.M., 2007. Correcting satellite data to detect vegetation signal for eco-hydrologic analyses. *Journal of Hydrology*, ***344****, 135-145.*

Gupta, H.V., Beven, K.J. and Wagener, T., 2006. Model Calibration and Uncertainty Estimation, *Encyclopedia of Hydrological Sciences*, (ed. M.G. Anderson), John Wiley and Sons, Chichester, UK, 2026.

Hall, M.J. and Minns, A.W., 1999. The classification of hydrologically homogeneous regions. *Hydrological sciences Journal*, ***44****, 8,639-704.*

Harr Milton, E., 1989. Probabilistic estimates for multivariate analysis, *Applied Mathematical Modelling,* **13**, 313-319.

Helton, J.C. and Davis, F.J., 2003. Latin hypercube sampling and propagation of uncertainty in analysis of complex systems, *Reliable Engineering and Systems Safety,* **81** (1), 23-69.

Heuvelmans, G., Muys, B. and Feyen, J., 2004. Evaluation of hydrological parameter transferability for simulating the impact of land use on catchment hydrology. *Physics and Chemistry of the Earth*, ***29***, *739-747.*

Heuvelmans, G., Muys, B., Feyen, J., 2006. Regionalization of the parameters of a hydrological model: comparison of linear regression models with artificial nets. *Journal of hydrology* ***319****, 245-265.*

Hoffmann, J., 2005. The future of satellite remote sensing in hydrogeology. *Hyydrogeology Journal*, ***13****, 247-250.*

Holmes, M.G.R., Young, A.R., Gustard, A. and Grew, R., 2002. A region of influence approach to predicting flow duration curves within ungauged catchments. *Hydrology and Earth System Sciences*, ***6****, 721-731.*

Horton, R.E., 1945. Erosional development of streams and their drainage basins; hydrophysical approach to quantitative morphology. *Geol. Soc. Am. Bull*. ***56****, 275–370.*

Huang, X and Niemann, J.D., 2008. How do streamflow generation mechanisms affect watershed hypsometry? *Earth surface Processes and Landforms* ***33****,751-772.*

Huisman, J.A., Breuer, J. and Frede, H.-G., 2004. Sensitivity of simulated hydrological fluxes towards changes in soil properties in response to land use change. *Physics and Chemistry of the Earth*, ***29***, *749-758.*

Hsu, K., Gupta, H.V., Gao, X., Sorooshian, S., 1999. Estimation of physical variables from multi-channel remotely sensed imagery using a neural network: Application to rainfall estimation. *Water Resources Research*, **35** ***(5)*** *1605-1618*.

Hughes, D.A., Smakhtin, V.Y., 1996. Daily flow time series patching or extension: a spatial interpolation approach based on flow duration curves. *Hydrological Sciences Journal* ***41 (6)****, 851-871.*

Immerzeel, W.W., Droogers, P., 2008. Calibration of a distributed hydrological model based on satellite evapotranspiration *Journal of Hydrology*, ***349****, 411-424.*

Iroumé, A., Huber, A. and Schulz, K., 2005. Summer flows in experimental catchments with different forest covers, Chile. *Journal of Hydrology*, ***300****, 300-313.*

Jena, S.K., Tiwari, K.N., 2006. Modeling synthetic unit hydrograph parameters with geomorphologic parameters of watersheds. *Journal of hydrology* ***319,*** *1-14.*

Ji, L., Peters., A.J., 2003. Assessing vegetation response to drought in the northern great plains using vegetation and drought indices. *Remote Sensing of Environment* **87,** 85-98.

Jiang, L., Islam, S., 2001. Estimation of surface evaporation map over southern great plains using remote sensing data. *Water Resources Research*, **37** (**2)** 329-340.

Jiménez-Muñoz, J. C., Sobrino, J. A., Gillespie, A., Sabol, D., Gustafson, W. T., 2006. Improved land surface emissivities over agricultural areas using ASTER NDVI. *Remote Sensing of Environment* **103,** 474–487.

Jolliffe, I. T., 2002. Principal Component Analysis, Springer series in statistics, ISBN 0-387-95442-2. New York, USA.

Jothityangkoon, C. and Sivapalan, M., 2001. Temporal scales of rainfall-runoff processes and spatial scaling of flood peaks: space-time connection through catchment water balance. *Advances in Water Research*, **24**, 1015-1036.

Kapangaziwiri, E., Hughes, D.A., (2008). Towards a physically-based parameter estimation methods for the Pitman monthly rainfall-runoff model. Water SA, **32**(2), 183-191.

Karyabwite, D., 2000. Water sharing in the Nile River valley. United Nations Environment Programme, Geneva, Switzerland.

Kawabata, A., Ichii, K., Yamaguchi, Y., 2001. Global monitoring of interannual changes in vegetation activities using NDVI and its relationships to temperature and precipitation. *International Journal of Remote Sensing Vol.* ***22,*** *No. 7, 1377-1382*.

Kebede, S., Travi, Y., Alemayehu, T., Marc, V., 2006. Water balance of Lake Tana and its sensitivity to fluctuations in rainfall, Blue Nile basin, Ethiopia. *Journal of hydrology* ***316****, 233-247*.

Kileshye Onema, J.-M., 2004. *A hydrological assessment of land use changes and human's effects on water resources in semi-arid Zimbabwe; the case of the Insiza sub-catchment.* M.Sc. thesis (unpublished), Water Resources Engineering and Management Programme, University of Zimbabwe, 81p.

Kileshye Onema, J-M., Mazvimavi, D., Love, D., Mul, M.L., 2006a. Effects of selected dams on river flows of Insiza River, Zimbabwe. *Physics and Chemistry of the Earth* ***31****,870-875.*

Kileshye Onema, J-M., Taigbenu, A.E., Twikirize, D., 2006b. *Challenges to the implementation of the Nile Basin Initiatives in the Equatorial region.* In proceedings of the 7th WATERNET-WARFSA-GWPSA symposium, Malawi.

Kileshye onema, J-M, Taigbenu, A.E., 2008. *Uncertainties in the use of NDVI for rainfall prediction in the data-scarce watershed of the equatorial Nile* . In proceedings of the NBI- workshop, Entebbe- Uganda.

Kileshye Onema, J-M., Katambara, Z., and Taigbenu, A.E., 2009a. *Shuffled complex evolution and multi-linear approaches to flow predictions in the Equatorial Nile Basin*. First Annual Nile Basin Research Conference. Dar Es Salaam, Tanzania.

Kileshye Onema, J-M., Taigbenu, A. E., 2009b. NDVI–rainfall relationship in the Semliki watershed of the equatorial Nile. *Physics and Chemistry of the Earth **34**, 711-721.*

Kileshye Onema, J-M., Taigbenu, A.E., Ndiritu, J., (2011) *submitted. Classification and flow prediction in a data-scarce watershed of the equatorial Nile region.*

Kileshye Onema, J-M., Taigbenu, A. E., (2011) *Submitted*. *Uncertainty and sensitivity analyses in the use of landscape attributes for flow prediction in a data-poor watershed.*

Kim, U., Kaluarachchi, J.J., 2008. Application of parameter estimation and regionalization methodologies to ungauged basins of the Upper Blue Nile River Basin, Ethiopia. *Journal of Hydrology **362**, 39– 56.*

Kite, G.W., 1981. Recent changes in level of Lake Victoria *Hydrological Sciences Journal*, **26,** 233-243.

Klemeš, V., 1986. Operational testing of hydrological simulation models, *Hydrological Sciences Journal* **31(1)**, 13-24.

Kling, H., Gupta, H., 2009. On the development of regionalization relationships of lumped watershed models : the impact of ignoring sub-basin scale variability. . *Journal of Hydrology **373,** 337-351***.**

Koloskov, G., Mukhamejanova, Kh., Tanton T.W., 2007. Monin–Obukhov length as a cornerstone of the SEBAL calculations of evapotranspiration. *Journal of Hydrology **335**, 170– 179.*

Koutsoyiannis, D., 2005a. Uncertainty, entropy, scaling and hydrological stochastics.1Marginal distributional properties of hydrological processes and state scaling *Hydrological Sciences Journal **50(3)**, 381-404.*

Koutsoyiannis, D., 2005b Uncertainty, entropy, scaling and hydrological stochastics. 2Time dependence of hydrological processes and time scaling *Hydrological Sciences Journal* ***50(3)****, 405-426*

Koutsoyiannis, D., 2006. An entropic-stochastic representation of rainfall intermittency: the origin of clustering and persistence. *Water Resources Research*, **42**, W01401, doi:10.1029/2005WR004175

Koutsoyiannis, D., Yao, H., Georgakakos, A., 2008 Medium-range flow prediction for the Nile: a comparison of stochastic and deterministic methods. *Hydrological sciences Journal* ***53(1)****,405-426*

Krause, S., Jacobs, J., and Bronstert, A., 2007**.** Modelling the impacts of land-use and drainage density on the water balance of a lowland–floodplain landscape in northeast Germany. *Ecological modelling* ***200****, 475–492*.

Kundzewicz, Z.W., 1995. New uncertainty concepts in hydrology and water resources, Cambridge University Press, New York.

Kundzewicz, Z.W., 2007. Prediction in ungauged basins-a systemic perspective. IAHS publication no. 309.

Kustas, W.P. and Norman, J.M., 1996. Use of remote sensing for evapotranspiration monitoring over land surfaces. *Hydrological Sciences Journal, **41**, 495-516.*

Kwon, H-H., Brown, C., Xu, K., Lall, U., 2009. seasonal and annual maximum streamflow forecasting using climate information: application to the Three Gorges dam in the Yangtze river basin, China. *Hydrological Sciences Journal **54(x)**, 606-622.*

Lahaa, G., Blöschl, G., 2006. A comparison of low flow regionalisation methods-catchment grouping. *Journal of hydrology **323***, 193-214.

Laudon, H., Sjöblom, V., Buffam, I., Seibert, J., Mörth, M., 2007. The role of catchment scale and landscape characteristics for runoff generation of boreal streams. *Journal of hydrology **344***, 198-209.

Laws, K.B., Janowiak, J.E., Huffman, G.J., 2004. Verification of rainfall estimates over Africa using RFE, NASA MPA-RT and CMORPH. Paper 2.2. *18th conference on hydrology. Ame. Met.soc*.11-15 January, Seattle.

Lee, H., McIntyre, N., Wheater, H., Young, A., 2005. Selection of conceptual models for regionalization of the rainfall-runoff relationship. *Journal of hydrology **312**, 125-147.*

LeMarie, M., Van der Zaag, P., Menting, G., Baquete, E., Schotanus, D., 2006. The use of remote sensing for monitoring environmental indicators: The case of the Incomati estuary, Mozambique. *Physics and Chemistry of the Earth **31**, 857-863.*

Lin, Z. and Oguchi, T., 2004. Drainage density, slope angle, and relative basin position in Japanese bare lands from high-resolution DEMs. *Geomorphology **63**, 159–173*.

Lindley, D. V., 2006. Understanding uncertainty, John Wiley & sons, Inc., Hoboken, New Jersey.

Looney, S.W., 1995. How to use tests for univariate normality to assess multivariate normality. *The American Statistician, Vol. **49,** 64-70*.

Lørup, J.K., Refsgaard, J.C. and Mazvimavi, D., 1998. Assessing the effect of land use change on catchment runoff by combined use of statistical test and hydrological modelling: case studies from Zimbabwe. *Journal of Hydrology, **205**, 147-163*.

Loucks, D.P., Stedingher, J.R. and Haith, D.A., 1981. Water resource systems planning and analysis. Prentice-Hall, Inc.Englewood Cliffs, New Jersey 07632.

Loucks, D.P. and Van Beek, E., 2005. Water Resources Systems Planning and Management. UNESCO publications. ISBN 92-3-103998-9, Delft Hydraulics, the Netherlands.

Ludwig, R., Probeck, M. and Mauser, W., 2003. Mesoscale water balance modelling in the Upper Danube watershed using sub-scale land cover information derived from NOAA-AVHRR imagery and GIS techniques. *Physics and Chemistry of the Earth*, **28**, 1351-1364

Luo, W and Harlin, J.M., 2003. A theoretical travel time based on watershed hypsometry. *J. of the American Water Resources Association* (JAWRA) **39**(4):785-792.

Ma, M. and Frank, V., 2006. Interannual variability of vegetation cover in the Chinese Heihe River Basin and its relation to meteorological parameters. *International Journal of Remote Sensing* Vol. **27** No.16, 3473–3486.

Madsen, H., Mikkelsen, P.S., Rosbjerg, B. and Harremöes, P., 2002. Regional estimation of rainfall intensity-duration-frequency curves using generalized least squares regression of partial duration series statistics. *Water Resources Research*, **38**, W01239, doi:10.1029/2001WR001125.

Madduma Bandara, C. M., 1974. Drainage density and effective precipitation, *Journal of Hydrology*, **21**, 187–190

Maidment, D.R., Handbook of Hydrology, McGraw-Hill, Inc, 1992.

Martiny, N., Camberlin, P., Richard, Y., Philippon, N., 2006. Compared regimes of NDVI and rainfall in semi-arid regions of Africa. *International Journal of Remote Sensing* Vol. **23** No.23, 5201-5223.

Maselli, F., Barbati, A., Chiesi, M., Chirici, G., Corona, P., 2006. Use of remotely sensed and ancillary data for estimating forest gross primary productivity in Italy. *Remote Sensing of Environment,* **100,** 563–575.

Mazvimavi, D., 2003. Estimation of flow Characteristics of ungauged catchment: case study in Zimbabwe, PhD Thesis, Wageningen University.

McIntyre, N., Lee, H., Wheater, H., Young, A., Wagener, T., 2005a. Ensemble predictions of runoff in ungauged catchments. *Water Resources Research,* **41**, W12434, doi:10.1029/2005WR004289.

McKinney, D.C., Cai, X., 2002. Linking GIS and water resources management models: an object-oriented method. *Environmental Modelling and Software* ***17****, 413-425.*

Meigh, J., 1995. The impact of small farm reservoirs on urban water supplies in Botswana. *Natural Resources Forum, **19**, 71-83*.

Meijerink, A.M.J., De Brouwer, H.A.M., Mannaerts, C.M., and Valenuala, C.R., 1994. Introduction to the use of geographical information systems for practical hydrology. Publication No 23, International Institute for Aerospace survey and Earth sciences, Enschede, Netherlands.

Melching, C.S., Yen, B.C. and Wenzel Jr, H.G., 1990. A reliability estimation in modelling watershed runoff uncertainty uncertainties, *Water Resources Research,* **26**, 2275-2286.

Melching, C.S., 1992. An improved first-order reliability approach for assessing uncertainties in hydrologic modeling, *Journal of Hydrology,* **132**, 157-177.

Melesse, A.M., 2004. Spatiotemporal dynamics of land surface parameters in the Red River of the North Basin. *Physics and Chemistry of the Earth,* **29**, 795-810.

Merz, R., Blöschl, G., 2004. Regionalization of catchment model parameters. *Journal of hydrology **287**, 95-123.*

Midgley, D.C., Pitman, W.V. and Middleton, B.J., 1994. *Surface Water Resources of South Africa 1990, Volumes I to VI*, Water Research Commission Reports, Pretoria.

Montanari, A., 2007. What do we mean by 'uncertainty'? The need for a consistent wording about uncertainty assessment in hydrology, *Hydrological Processes*, **21**, 841-845.

Moore, I. D., Grayson, R.B and Ladson, A.R., 1991. Digital terrain modelling: A review of hydrological, geomorphological, and biological applications. *Hydrological processes* ***5****, 3-30*.

Mugabe, F.T., 2005. *Comparative hydrological behaviour of two catchments in semi-arid Zimbabwe*. D.Phil. thesis (unpublished), University of Zimbabwe, Harare.

Muleta, M.K. and Nicklow, J.W., 2005. Sensitivity and uncertainty analysis coupled with automatic calibration for a distributed watershed model, *Journal of Hydrology,* **306**, 127-145.

Mumeka, A., 1986. Effect of deforestation and subsistence agriculture on runoff on the Kafue headwaters, Zambia. *Hydrological Sciences Journal,* ***31****(4), 543-554*.

Mutua, B.M., Klik, A., 2007. Predicting daily streamflow in ungauged rural catchments: the case of Masinga catchment, Kenya. *Hydrological Sciences journal **52**(2), 292-304.*

Mwakalila, S., 2003. Estimation of stream flows of ungauged catchments for river basin management. *Physics and Chemistry of the Earth* **28**, 935-942.

Naden, P. S**.,** 1992**.** Spatial variability in flood estimation for large catchments: the exploitation of channel network structure. *Hydrological Sciences Journal **37**, 53-71.*

Nandagiri, L., 2007. Calibrating hydrological models in unguaged basins: possible use of areal evapotranspiration instead of streamflows, *Predictions In Ungauged Basins: PUB Kick-off (Proceedings of the Kick-off meeting held in Brasilia, 20-22 November 2002)* IAHS.

Nash, J.E. and Sutcliffe, J.V., 1970. River flow forecasting through conceptual models part I — A discussion of principles, *Journal of Hydrology* **10(3)**, 282-290.

Nemani, R.R., and Running, S.W., 1989. Estimation of regional surface resistance to evapotranspiration from NDVI and thermal IR-AVHRR data. *Journal of applied meteorology***, 28**, 276-284.

Niadas, I.A., 2005. Regional flow duration curve estimation in small ungauged catchments using instantaneous flow measurements and a censored data approach. *Journal of hydrology* ***314,*** *48-66.*

Nicholson, S.E., 1998. Historical fluctuation of lake victoria and other lakes in the northern Rift Valley of East Africa.*In Environmental change and response in East African lakes* (ed.by J.T.Lehhman) Kluwer , Dordrecht, The Netherlands.

Nicol, A., 2003. The Nile: Moving beyond cooperation, UNESCO-IHP.

Nkomo, S. and van der Zaag, P., 2004. Equitable water allocation in a heavily committed international catchment area: the case of the Komati Catchment. *Physics and Chemistry of the Earth*, **29**, 1309-1317.

Nyabeze, W.R., 2003. Modification of a rainfall-runoff model for distributed modeling in a GIS and its validation. *Physics and Chemistry of the Earth*, **28**, 1025-1032.

Nyabeze, W.R., 2005. Calibrating a distributed model to estimate runoff for ungauged catchments in Zimbabwe. *Physics and Chemistry of the Earth*, **30**, 625-633.

Oguchi, T., 1997. Drainage density and relative relief in humid steep mountains with frequent slope failure. *Earth surface processes and landforms,* **22**, 107–120

Okidi, C.O., 1990. History of the Nile and Lake Victoria Basins through Treaties, in The Nile: Resource Evaluation, Resource Management, Hydropolitical and Legal issues. Eds. Howell and Allan. SOAS, University of London : London.

Ott, B. and Uhlenbrook, S., 2004. Quantifying the impact of land use changes at the event and seasonal time scale using a process-oriented catchment model. *Hydrology and Earth System Sciences*, **8**, 62-78.

Ouarda, T.B.M.J., Bâ, K.M., Diaz-Delgado, C., Cârsteanu, A, Chokmani, K., Gingras, H., Quentin, E., Trujillo, E., Bobée, B., 2008. Intercomparison of regional flood frequency estimation methods at ungauged sites for a Mexican case study. *Journal of hydrology* ***348,*** *40-58.*

Oudin, L., Michel, C. and Anctil, F., 2005. Which potential evapotranspiration input for a lumped rainfall-runoff model?: Part 1—Can rainfall-runoff models effectively handle detailed potential evapotranspiration inputs?, *Journal of Hydrology,* **303**, 275-289.

Oyebande, L., 2001.Water problems in Africa-how can sciences help? *Hydrological Sciences journal*, **46**(6): 947-961.

Pappenberger, F. and Beven, K.J., 2006. Ignorance is bliss: Or seven reasons not to use uncertainty analysis, *Water Resources Research.*, **42(5),**W05302, doi: 10.1029/ 2005 WR004820.

Parajka, J., Blöschl, G., 2008. The value of MODIS snow cover data in validating and calibrating conceptual hydrologic models. *Journal of hydrology* ***358,*** *240-258.*

Paturel, J.E., Barrau, C., Mahé, G., Dezetter, A., Servat, E., 2007. Modelling the impact of climatic of climatic variability on water resources in west and central Africa from non-calibrated hydrological model. *Hydrological Sciences journal* ***52****(1), 38-48.*

Pinzon, J., Brown, M.E., and Tucker, C. J., 2004. Satellite time series correction of orbital drift artifacts using empirical mode decomposition. In Hilbert-Huang Transform: Introduction and Applications, eds. N. Huang, pp. Chapter 10, Part II.

Piper, B.S., Plinston, D.T. and Sutcliffe, J.V., 1986 The water balance of the lake Victoria. *Hydrological sciences Journal*, **31**, 25-37.

Pitlick, J., 1994. Relation between peak flows, precipitation and physiography for five mountainous regions in the western USA. *Journal of hydrology,* **158**,219-240

Plumptre, A.J., Eilu, G., Ewango, C., Ssegawa, P., Nkuutu, D., Gereau, R.,Beentje, H., Poulsen, A. D., Fischer, E., Goyder, D., Pearce, T.R., Hafashimana, D., 2003. *The biodiversity of the Albertine rift.* World Conservation Society report.

Prince, S.D., Steininger, M.K., 1999. Biophysical stratification of the Amazon basin. *Global Change Biology*, **5**, 1-22.

Raynolds, M. K., Comiso, J. C., Walker, D. A., Verbyla, D., 2008. Relationship between satellite-derived land surface temperatures, arctic vegetation types, and NDVI. *Remote Sensing of Environment* **112,** 1884–1894.

Richard, Y., Poccard, I., 1998. A statistical study of NDVI sensitivity to seasonal and interannual rainfall variations in southern Africa. *International Journal of Remote Sensing.* Vol.**19**, 2907-2920.

Ritchie, J.C. and Rango, A., 1996. Remote sensing applications to hydrology. *Hydrological Sciences Journal,* ***41 (4)***, *429-431*.

Rodríguez-Iturbe, I., Gupta V.K. and Waymire, E., 1984. Scale considerations in the modelling of temporal rainfall. *Water Resources Research*, **20**, 1611-1619.

Rosenblueth, E., 1981. Two-point estimates in probabilities, *Applied Mathematical Modelling*, **5**, 329-335.

Rzòska, J., 1976.The Nile, Biology of an ancient river, Dr. W. Junk B.V., Publishers, the Hague, Netherlands.

Sahin, M., 1985. Hydrology of the Nile River Basin, Amsterdam.

Said, R., 1993. The river Nile, Geology, hydrology and utilization, Pergamon Press Ltd.Oxford, England.

Saltelli, A., 2000. What is senstivity analysis? *In: Sensitivity Analysis* (eds. A. Saltelli, K. Chan and E.M. Schott), Jonh Wiley and Sons, Chichester, UK, 3-12.

Sanborn, S. C., Bledsoe, B. P., 2006. Predicting streamflow regime metrics for ungauged streams in Colorado, Washington and Oregon. *Journal of hydrology **325,** 241-261.*

Savenije, H.H.G., 2004. The importance of interception and why we should delete the term evapotranspiration from our vocabulary. *Hydrological Processes*, **18**, 1507-1511.

Sawunyama, T., Hughes, D., 2008. Application of satellite-derived rainfall estimates to extend water resource simulation modelling in South Africa. *Water SA* **34 (1)** 1-9.

Schröder, B., 2006. Pattern, process, and function in landscape ecology and catchment hydrology-how can quantitative landscape ecology support predictions in ungauged basins? *Hydrology and Earth Systems Science **10**, 967-979.*

Schulze, R.E., 2003. On Land Cover, Land Use and Their Impacts on Hydrological Responses. *In*: Schulze, R.E. (Ed) *Modelling as a Tool in Integrated Water Resources Management: Conceptual Issues and Case Study Applications*. Water Research Commission, Pretoria, RSA, WRC Report 749/1/02. Chapter 4, 84-97.

Sefton, C. E. M., Howard, S. M., 1998. Relationship between dynamic response characteristics and physical descriptors of catchments in England and Wales. *Journal of hydrology **211**, 1-16.*

Senay, G.B., Asante, K and Artan, G., 2009. Water balance dynamics in the Nile Basin. *Hydrological Processes **23**, 3675-3681*.

Sene K.J., 2000. Theoretical estimates for influence of lake Victoria on flows in the upper White Nile. *Hydrological sciences Journal* **45**,125-145.

Servat, E., Dezetter, A., 1993. Rainfall-runoff modeling and water resources assesment in northwestern Ivory Coast. Tentative extension to ungauged catchments. *Journal of hydrology **148** ,231-248*

Sesnie et al.,2008

Shaban, A., Khawlie, M. and Abdallah, C., 2006. Use of remote sensing and GIS to determine recharge potential zones: the case of Occidental Lebanon. *Hydrogeology Journal*, **14**, 433-443.

Shankar, U., Pearson, C.P., Nikora, V.I. and Ibbitt, R.P., 2002. Heterogeneity in catchment properties: a case study of Grey and Buller catchments, News Zealand. *Hydrology and Earth System Sciences*, **6**, 167-183.

Shao, Q., Zhang, L., Chen, Y. D., Singh, V. P., 2009. A new method for modeling flow duration curves and predicting streamflow regimes under altered land-use conditions. *Hydrological sciences Journal* **54**, 582-595.

Sharda, V. N., Prasher, S. O., Patel, R. M., Ojasvi, P. R., Prakash, C., 2008. Performance of Multivariate Adaptive Regression Splines (MARS) in predicting runoff in mid-Himalayan micro-watersheds with limited data. *Hydrological sciences Journal* **53(6)**, 1165-1175.

Sivapalan, M., 2003: Prediction in ungauged basins: a grand challenge for theoretical hydrology. *Hydrological Processes **17**, 3163-3170.*

Sivapalan, M., Takeuchi, K., Franks, S. W., Gupta, V. K., Karambiri, H., Lakshmi, V., Liang, X., Mcdonnell, J. J., Mendiondo, E. M., O'connell, P. E., Oki, T., Pomeroy, J. W., Schertzer, D., Uhlenbrook, S. and Zehe, E., 2003. IAHS Decade on Predictions in Ungauged Basins(PUB), 2003–2012: Shaping an exciting future for the hydrological sciences. *Hydrological sciences Journal* **48(6)**, 857-880.

Sooroshian, S., Hsu, K.L., Gao, X., Gupta, H.V., Imam, B., Braithwaite, D., 2000. Evaluation of PERSIANN system satellite-based estimates of tropical rainfall. *Bulletin of American Meteorological Societies.* **81 (9)** 2035-2046.

Stehman, S.V., 2009. Sampling designs for accuracy assessment of landcover. *International Journal of Remote Sensing* Vol **30**, issue 20, 5243-5272.

Stoms, D. M., Hargrove, W.W., 2000. Potential NDVI as a baseline for monitoring ecosystem functioning. *International Journal of Remote Sensing* Vol. **21** No.2 401-407

Sutcliffe, J.V and Parks, Y.P., 1999.The hydrology of the Nile, IAHS special publication no.5

Symphorian, G.R., Madamombe, E. and van der Zaag, P., 2003. Dam operation for environmental releases: the case of Osborne Dam, Save catchment, Zimbabwe. *Physics and Chemistry of the Earth*, **28**, 985-993.

Tarboton, D.G., Bras, R.L. and Rodriguez-Iturbe, I., 1992. A physical basis for drainage density. *Geomorphology,* **5**, 59-76.

Tarnavsky, E., Garrigues, S., Brown, M. E., 2008. Multiscale geostatistical analysis of AVHRR, SPOT-VGT, and MODIS global NDVI products. *Remote Sensing of Environment* **112,** 535–549.

Tate, E.L., Sene, K.J and Sutcliffe, J.V., 2001. A water balance study of the upper White Nile basin flows in the late century *Hydrological sciences Journal* **46(2)**, 301-318.

Tate, E., Sutcliffe, J., Conway, D. and Farquharson, F., 2004. Water balance of Lake Victoria: update to 2000 and climate change modelling to 2100 *Hydrological sciences Journal* **49(4)**, 563-574.

Ter Braak, C.J.F. and Prentice, I.C., 1988. A theory of gradient analysis. *Advances in ecological research*, 18, 271-317

Thoma, D.P., Moran, M.S., Bryant, R., Rahman, M., Holifield-Collins, C.D., Skirvin, S., Sano, E.E. and Slocum, K., 2006. Comparison of four models to determine surface soil moisture from C-band radar imagery in a sparsely-vegetated semiarid landscape. *Water Resources Research*, **42**, W01418, doi:10.1029/2004WR003905.

Todd, M.C., Barret, E.C., Beaumont, M. J., Belleryby, T.J., 1999. Estimation of daily rainfall over the upper Nile River basin using a continuous calibrated satellite infrared technique. *Journal of applied meteorology***,** **6**, 201-210.

Todd, M.C., Kidd., C., Kniveton, D., Belleryby, T.J., 2001. A combined satellite and passive microwave technique for estimation of small-scale rainfall. *J. Atmos. Ocean. Technol.* **18,** 742-755.

Townley, L.R. 1998. Shallow groundwater systems. In: Dillon, P. and Simmers, I. (Eds.) International Contributions to Hydrogeology 18: Shallow Groundwater Systems. Balkema, Rotterdam, pp3-12.

Tsihrintzis, V.A., Hamid, R., Fuentes, H.R.. 1996. Use of Geographic Information Systems (GIS) in Water Resources: A review. *Water Resources Management **10**, 251-277.*

Tucci, C., Silviera, A. and Sanchez, J., 1995. Flow regionalization in the upper Paraguay basin, Brazil. *Hydrological Sciences Journal*, **40**, 4, 485-497.

Tucker, C. J., Sellers, P. J., 1986. Satellite remote sensing of primary vegetation. *International Journal of Remote Sensing* **7**, 1395-1416.

Tucker, G.E., Catani, F, Rinaldo, A., Bras, R.L., 2001. Statistical analysis of drainage density from digital terrain data. *Geomorphology **36**,187–202.*

Tucker C.J., Pinzon J.E., Brown M.E., Slayback D., Pak E.W., Mahoney R., Vermote E., El Saleous, N., 2005. An Extended AVHRR 8-km NDVI Data Set Compatible with MODIS and SPOT-Vegetation NDVI Data. *International Journal of Remote Sensing* **26 (20)**, 4485−4498.

Uhlenbrook, S., Frey, M., Leibundgut, C. and Maloszewski, P., 2002. Hydrograph separations in a mesoscale mountainous basin at event and seasonal timescales. *Water Resources Research*, **38**, 31-1

Uhlenbrook, S., Siebert, A., 2003. On the value of experimental data to reduce the prediction uncertainty of process-oriented catchment model. *Environmental modeling and software* ***20****, 19-3.*

UNEP-WCMC., 2003. World Conservation Monitoring Centre Protected Areas Database. http://www.wcmc.org.uk/protected_areas/data/wh/virunga.html.

Van Dijk, A.I.J.M., Meester, A.G.C.A., Schelekens, J. and Bruijnzeel, L.A., 2005. A two-parameter exponential rainfall depth-intensity distribution applied to runoff and erosion modelling. *Journal of Hydrology*, **300**, 155-171.

Varis, O., 2000. The Nile Basin in a global perspective: Natural, human, and Socioeconomic resource nexus. *Water International* **25(4)**:624–637.

Vivoni, E.R., Di Benetto, F., Grimaldi, S., Eltahir, E.A.B., 2008. Hypsometric control on surface and subsurface runoff. *Water Resources Research*, Vol **44**, W12502,doi:10.1029/2008WR006931.

Vrugt, J.A., Gupta, H.V., Bouten, W. and Sorooshian, S., 2003. A Shuffled Complex Evolution Metropolis algorithm for optimization and uncertainty assessment of hydrologic model parameters, *Water Resources Research,* **39(8)**, art. No.1201, doi:10.1029/2002WR001642.

Vrugt, J.A., Diks, C.G.H., Gupta, H.V., Bouten, E. and Verstraten, J.M., 2005. Improvement treatment of uncertainty in hydrologic modelling: combining the strengths of global optmisation and data assimilation, *Water Resources Research,* **41(1).** W01017, doi:10.1029/2004WR003059.

Wang, Q., Tenhunen, J., Dinh, Q. N., Reichstein, M.,Vesala, T., Keronen, P., 2004. Similarities in ground- and satellite-based NDVI time series and their relationship to physiological activity of a Scots pine forest in Finland. *Remote Sensing of Environment* **93,** 225–237.

Wang, Q., Adiku, S., Tenhunen, J., Granier, A., 2005. On the relationship of NDVI with leaf area index in a deciduous forest site. *Remote Sensing of Environment* **94,** 244–255.

Wagener, T., Wheater, H.S., 2006. Parameter estimation and regionalization for continuous rainfall-runoff models including uncertainty. *Journal of hydrology **320,** 132-154.*

Wagener, T. and Kollat, J., 2007. Numerical and visual evaluation of hydrological and environmental models using the Monte Carlo analysis toolbox, *Environmental Modelling Software, **22(7)**, 1021-1033.*

Wagenseil, H. and Samimi, C., 2006. Assessing spatio-temporal variations in plant phenology using Fourier analysis on NDVI time series: results from a dry savannah environment in Namibia. *International Journal of Remote Sensing* Vol. **27** No.16 3455–3471.

Wegehenkel, M., 2003. Longterm evaluation of land use changes on catchment water balance – a case study from North-East Germany. *Physics and Chemistry of the Earth*, **28**, 1281-1290.

Winsemius, H.C., Savenije, H.H.G., Gerrits, A.M.G., Zapreeva, E.A. and Klees, R., 2006. Comparison of two model approaches in the Zambezi river basin with regard to model reliability and identifiability. *Hydrology and Earth System Sciences*, **10**, 339-352.

Xie, P., Yarosh, Y., Love, T., Janowiak, J and Arkin, P., 2002. A real-time daily precipitation analysis over Africa as well as South Asia. *16th conference of hydrology, Orlando, Fl. American Meteorological Societies* 12-17 January.

Xu, C-Y., 2003. Testing the transferability of regression equations derived from small sub-catchments to a large area in central Sweden. *Hydrology and Earth System Sciences **7(3)**, 317-324.*

Yadav, M., Wagener., T., Gupta, H., 2007. Regionalization of constraints on expected watershed response behavior for improved predictions in ungauged basins. *Advance in Water Resources* **30,** 1756-1774.

Yapo, P.O., Gupta, H.V. and Sorooshian, S., 1998. Multi-objective global optimization for hydrologic models, *Journal of Hydrology,* **204**, 83-97.

Zeleke, T.B. and Si, B.C., 2005. Scaling relationships between saturated hydraulic conductivity and soil physical properties. *Soil Science Society of America Journal*, ***69***, *1691-1702.*

Zhang, Z., Wagener, T., Reed, P., Bhushan, R., 2008. Reducing uncertainty in prediction in ungauged basins by combining hydrologic indices regionalization and multiobjective optimization. *Water Resources Research*, **44**, W00B04, doi:10.1029/2008WR006833.

Zwart, S. J. and Bastiaanssen W.G.M., 2007. SEBAL for detecting spatial variation of water productivity and scope for improvement in eight irrigated wheat systems *Agricultural Water Management **89**, 287–296*

Appendix A Satellite generated NDVI

Table A-1: Satellite derived NDVI for the Semliki catchment (2001-2003) S3-S14

	S3	S4	S5	S6	S7	S8	S9	S10	S11	S12	S13	S14	
Jan-01	0.36	0.45	0.4	0.57	0.6	0.46	0.54	0.48	0.58	0.49	0.39	0.57	
Feb-01	0.38	0.43	0.44	0.67	0.73	0.49	0.73	0.55	0.69	0.73	0.69	0.58	
Mar-01	0.35	0.45	0.4	0.61	0.72	0.45	0.71	0.47	0.59	0.74	0.71	0.59	
Apr-01	0.58	0.65	0.61	0.76	0.77	0.61	0.76	0.64	0.76	0.76	0.75	0.63	
May-01	0.51	0.67	0.74	0.78	0.78	0.73	0.73	0.73	0.75	0.76	0.75	0.67	
Jun-01	0.59	0.59	0.51	0.61	0.68	0.63	0.67	0.63	0.66	0.67	0.57	0.51	
Jul-01	0.58	0.62	0.57	0.69	0.73	0.63	0.67	0.65	0.72	0.71	0.67	0.45	
Aug-01	0.48	0.57	0.58	0.44	0.6	0.59	0.6	0.59	0.6	0.61	0.61	0.32	
Sep-01	0.47	0.61	0.65	0.67	0.74	0.59	0.74	0.59	0.68	0.74	0.7	0.51	
Oct-01	0.45	0.56	0.57	0.66	0.71	0.53	0.72	0.55	0.63	0.69	0.68	0.55	
Nov-01	0.54	0.65	0.66	0.79	0.76	0.65	0.7	0.66	0.78	0.77	0.73	0.54	
Dec-01	0.57	0.61	0.65	0.82	0.79	0.65	0.67	0.67	0.78	0.76	0.69	0.67	
Jan-02	0.27	0.36	0.29	0.46	0.46	0.45	0.46	0.46	0.47	0.44	0.47	0.51	
Feb-02	0.28	0.45	0.35	0.59	0.62	0.4	0.59	0.47	0.59	0.61	0.62	0.45	
Mar-02	0.34	0.49	0.49	0.67	0.68	0.52	0.67	0.54	0.66	0.67	0.67	0.53	
Apr-02	0.47	0.62	0.66	0.76	0.8	0.68	0.76	0.69	0.76	0.78	0.72	0.64	
May-02	0.63	0.71	0.73	0.8	0.77	0.74	0.76	0.76	0.78	0.76	0.71	0.67	
Jun-02	0.58	0.66	0.63	0.7	0.75	0.63	0.72	0.65	0.73	0.74	0.71	0.63	
Jul-02	0.45	0.53	0.53	0.64	0.65	0.51	0.62	0.55	0.65	0.63	0.64	0.55	
Aug-02	0.43	0.54	0.51	0.62	0.65	0.5	0.64	0.5	0.62	0.65	0.65	0.42	
Sep-02	0.5	0.62	0.55	0.72	0.73	0.61	0.72	0.64	0.72	0.73	0.69	0.63	
Oct-02	0.5	0.62	0.59	0.67	0.61	0.57	0.63	0.62	0.65	0.61	0.57	0.6	
Nov-02	0.53	0.62	0.6	0.78	0.73	0.6	0.71	0.66	0.73	0.76	0.72	0.59	
Dec-02	0.56	0.63	0.62	0.73	0.74	0.59	0.69	0.63	0.73	0.74	0.62	0.61	
Jan-03	0.45	0.54	0.54	0.65	0.65	0.55	0.61	0.58	0.65	0.65	0.62	0.55	
Feb-03	0.36	0.52	0.4	0.7	0.68	0.49	0.65	0.56	0.64	0.65	0.61	0.57	
Mar-03	0.28	0.45	0.42	0.74	0.71	0.5	0.69	0.53	0.62	0.7	0.7	0.53	
Apr-03	0.35	0.53	0.42	0.71	0.72	0.57	0.71	0.6	0.68	0.69	0.75	0.61	
May-03	0.59	0.69	0.69	0.76	0.77	0.7	0.75	0.7	0.76	0.77	0.75	0.66	
Jun-03	0.53	0.62	0.56	0.69	0.72	0.59	0.71	0.59	0.69	0.72	0.69	0.51	
Jul-03	0.47	0.57	0.49	0.51	0.59	0.51	0.55	0.51	0.59	0.59	0.58	0.43	
Aug-03	0.39	0.51	0.43	0.48	0.47	0.46	0.48	0.46	0.54	0.51	0.52	0.35	
Sep-03	0.51	0.59	0.48	0.7	0.73	0.55	0.73	0.57	0.71	0.73	0.71	0.55	
Oct-03	0.45	0.55	0.46	0.7	0.7	0.52	0.64	0.57	0.61	0.7	0.67	0.53	
Nov-03	0.53	0.62	0.61	0.71	0.76	0.61	0.61	0.61	0.71	0.75	0.69	0.55	
Dec-03	0.52	0.62	0.63	0.77	0.73	0.65	0.69	0.67	0.73	0.73	0.67	0.67	

Table A-2 Satellite derived NDVI for the Semliki catchment (2001-2003) S15-S23

	S15	S16	S17	S18	S19	S20	S21	S22	S23
Jan-01	0.31		0.33	0.24	0.46	0.43	0.49	0.51	0.49
Feb-01	0.62	0.23	0.57	0.14	0.47	0.43	0.42	0.46	0.43
Mar-01	0.67	0.36	0.62	0.44	0.58	0.58	0.54	0.5	0.48
Apr-01	0.62	0.32	0.73	0.43	0.72	0.62	0.7	0.67	0.63
May-01	0.65	0.47	0.68	0.47	0.67	0.66	0.63	0.59	0.61
Jun-01	0.47	0.41	0.54	0.33	0.57	0.55	0.58	0.62	0.59
Jul-01	0.42	0.31	0.63	0.22	0.64	0.47	0.57	0.57	0.53
Aug-01	0.31	0.21	0.47	0.18	0.58	0.39	0.43	0.47	0.47
Sep-01	0.51	0.3	0.59	0.35	0.65	0.42	0.57	0.6	0.59
Oct-01	0.61	0.38	0.59	0.29	0.67	0.53	0.57	0.61	0.57
Nov-01	0.55	0.57	0.6	0.39	0.71	0.49	0.63	0.65	0.63
Dec-01	0.6	0.41	0.65	0.47	0.67	0.64	0.65	0.68	0.67
Jan-02	0.44	0.22	0.46	0.22	0.5	0.39	0.36	0.42	0.39
Feb-02	0.45	0.12	0.61	0.41	0.5	0.4	0.43	0.49	0.39
Mar-02	0.61	0.35	0.54	0.24	0.58	0.54	0.54	0.56	0.54
Apr-02	0.62	0.44	0.59	0.5	0.68	0.64	0.67	0.67	0.67
May-02	0.67	0.51	0.71	0.51	0.7	0.53	0.69	0.71	0.69
Jun-02	0.63	0.42	0.69	0.3	0.64	0.54	0.61	0.6	0.6
Jul-02	0.27	0.28	0.63	0.37	0.59	0.55	0.54	0.53	0.51
Aug-02	0.27	0.18	0.6	0.38	0.57	0.53	0.54	0.47	0.48
Sep-02	0.47	0.32	0.69	0.3	0.66	0.66	0.63	0.58	0.58
Oct-02	0.62	0.38	0.57	0.42	0.57	0.55	0.51	0.6	0.57
Nov-02	0.59	0.49	0.62	0.4	0.67	0.58	0.66	0.67	0.64
Dec-02	0.61	0.43	0.51	0.44	0.65	0.67	0.67	0.66	0.63
Jan-03	0.51	0.32	0.6	0.29	0.6	0.51	0.57	0.55	0.53
Feb-03	0.53	0.46	0.53	0.43	0.54	0.54	0.54	0.54	0.51
Mar-03	0.49	0.39	0.65	0.36	0.59	0.45	0.47	0.5	0.47
Apr-03	0.49	0.34	0.67	0.37	0.65	0.58	0.59	0.57	0.54
May-03	0.59	0.52	0.73	0.43	0.72	0.63	0.68	0.68	0.67
Jun-03	0.55	0.34	0.68	0.35	0.63	0.47	0.57	0.57	0.55
Jul-03	0.33	0.16	0.57	0.15	0.56	0.43	0.47	0.47	0.44
Aug-03	0.31	0.24	0.47	0.34	0.56	0.37	0.43	0.4	0.37
Sep-03	0.39	0.32	0.69	0.32	0.65	0.56	0.56	0.56	0.56
Oct-03	0.45	0.27	0.65	0.36	0.66	0.47	0.61	0.61	0.59
Nov-03	0.56	0.49	0.66	0.41	0.63	0.55	0.59	0.57	0.57
Dec-03	0.6	0.35	0.61	0.31	0.63	0.54	0.6	0.63	0.6

Table A-3 Satellite derived NDVI for the Semliki catchment (2004-2006) S3-S14

	S3	S4	S5	S6	S7	S8	S9	S10	S11	S12	S13	S14
Jan-04	0.31	0.49	0.4	0.7	0.69	0.49	0.59	0.54	0.65	0.73	0.65	0.48
Feb-04	0.23	0.38	0.31	0.57	0.6	0.4	0.57	0.46	0.56	0.65	0.58	0.5
Mar-04	0.28	0.45	0.38	0.65	0.55	0.46	0.54	0.51	0.57	0.62	0.62	0.46
Apr-04	0.51	0.66	0.59	0.75	0.75	0.65	0.72	0.65	0.71	0.76	0.72	0.62
May-04	0.56	0.68	0.66	0.69	0.65	0.65	0.63	0.64	0.68	0.69	0.7	0.47
Jun-04	0.56	0.63	0.59	0.65	0.69	0.64	0.68	0.64	0.66	0.71	0.69	0.57
Jul-04	0.39	0.51	0.46	0.61	0.64	0.54	0.64	0.56	0.6	0.66	0.68	0.51
Aug-04	0.49	0.54	0.48	0.54	0.64	0.51	0.63	0.52	0.56	0.64	0.64	0.39
Sep-04	0.5	0.57	0.46	0.67	0.71	0.57	0.7	0.59	0.67	0.7	0.68	0.55
Oct-04	0.51	0.64	0.51	0.78	0.79	0.61	0.77	0.64	0.78	0.77	0.72	0.6
Nov-04	0.58	0.68	0.58	0.77	0.74	0.65	0.73	0.69	0.76	0.76	0.65	0.57
Dec-04	0.47	0.59	0.52	0.74	0.75	0.59	0.75	0.63	0.73	0.76	0.71	0.55
Jan-05	0.27	0.45	0.31	0.62	0.66	0.48	0.64	0.57	0.63	0.65	0.63	0.59
Feb-05	0.27	0.43	0.25	0.68	0.67	0.47	0.62	0.56	0.63	0.65	0.61	0.65
Mar-05	0.42	0.59	0.49	0.74	0.74	0.56	0.73	0.63	0.7	0.76	0.78	0.6
Apr-05	0.53	0.67	0.65	0.79	0.8	0.69	0.75	0.7	0.75	0.78	0.8	0.67
May-05	0.59	0.67	0.68	0.73	0.77	0.67	0.73	0.67	0.71	0.78	0.78	0.58
Jun-05	0.56	0.66	0.7	0.71	0.67	0.68	0.66	0.68	0.73	0.72	0.71	0.59
Jul-05	0.46	0.65	0.59	0.72	0.7	0.63	0.69	0.66	0.73	0.73	0.71	0.61
Aug-05	0.5	0.59	0.56	0.71	0.69	0.58	0.66	0.62	0.69	0.69	0.67	0.57
Sep-05	0.51	0.62	0.56	0.71	0.71	0.61	0.69	0.62	0.7	0.71	0.7	0.57
Oct-05	0.5	0.64	0.59	0.75	0.75	0.62	0.73	0.64	0.72	0.75	0.74	0.56
Nov-05	0.55	0.63	0.59	0.78	0.78	0.64	0.76	0.71	0.76	0.78	0.76	0.67
Dec-05	0.45	0.59	0.53	0.72	0.71	0.63	0.68	0.67	0.7	0.73	0.7	0.67
Jan-06	0.35	0.52	0.4	0.73	0.71	0.59	0.69	0.64	0.68	0.72	0.71	0.64
Feb-06	0.32	0.55	0.38	0.66	0.67	0.53	0.61	0.55	0.59	0.69	0.63	0.49
Mar-06	0.39	0.56	0.39	0.65	0.65	0.51	0.6	0.53	0.6	0.7	0.61	0.49
Apr-06	0.58	0.71	0.68	0.82	0.8	0.69	0.78	0.7	0.76	0.8	0.78	0.65
May-06	0.6	0.71	0.67	0.8	0.8	0.67	0.78	0.69	0.77	0.8	0.75	0.65
Jun-06	0.47	0.66	0.62	0.72	0.76	0.67	0.71	0.67	0.72	0.76	0.71	0.56
Jul-06	0.41	0.62	0.52	0.69	0.7	0.61	0.69	0.63	0.69	0.7	0.69	0.53
Aug-06	0.45	0.58	0.53	0.67	0.67	0.57	0.67	0.62	0.63	0.69	0.67	0.49
Sep-06	0.43	0.53	0.49	0.74	0.74	0.57	0.71	0.61	0.72	0.75	0.75	0.52
Oct-06	0.52	0.64	0.59	0.68	0.69	0.6	0.69	0.63	0.72	0.72	0.67	0.55
Nov-06	0.52	0.64	0.59	0.68	0.69	0.6	0.69	0.63	0.72	0.72	0.67	0.55
Dec-06	0.52	0.57	0.62	0.65	0.67	0.61	0.66	0.62	0.7	0.71	0.7	0.58

Table A-4 Satellite derived NDVI for the Semliki catchment (2004-2006) S15-S23

	S15	S16	S17	S18	S19	S20	S21	S22	S23
Jan-04	0.47	0.41	0.54	0.35	0.58	0.49	0.5	0.51	0.46
Feb-04	0.41	0.26	0.58	0.37	0.49	0.41	0.45	0.46	0.43
Mar-04	0.33	0.25	0.61	0.33	0.57	0.39	0.49	0.49	0.47
Apr-04	0.53	0.39	0.68	0.42	0.69	0.57	0.56	0.51	0.51
May-04	0.5	0.3	0.63	0.44	0.7	0.53	0.63	0.63	0.59
Jun-04	0.51	0.35	0.66	0.39	0.67	0.63	0.62	0.63	0.61
Jul-04	0.49	0.28	0.66	0.35	0.57	0.55	0.48	0.46	0.45
Aug-04	0.27	0.22	0.57	0.33	0.54	0.37	0.42	0.49	0.41
Sep-04	0.53	0.42	0.6	0.45	0.65	0.51	0.6	0.59	0.53
Oct-04	0.61	0.39	0.66	0.47	0.68	0.57	0.6	0.66	0.58
Nov-04	0.6	0.43	0.64	0.39	0.67	0.49	0.56	0.6	0.61
Dec-04	0.46	0.35	0.69	0.33	0.66	0.49	0.57	0.61	0.6
Jan-05	0.51	0.39	0.59	0.33	0.61	0.56	0.55	0.57	0.54
Feb-05	0.58	0.45	0.54	0.37	0.54	0.5	0.46	0.53	0.51
Mar-05	0.61	0.43	0.68	0.37	0.64	0.64	0.58	0.58	0.57
Apr-05	0.58	0.49	0.73	0.48	0.71	0.65	0.67	0.66	0.64
May-05	0.61	0.43	0.7	0.47	0.71	0.67	0.67	0.68	0.66
Jun-05	0.47	0.43	0.67	0.39	0.68	0.63	0.65	0.63	0.59
Jul-05	0.48	0.45	0.69	0.43	0.66	0.65	0.61	0.6	0.58
Aug-05	0.46	0.35	0.65	0.36	0.64	0.61	0.6	0.57	0.56
Sep-05	0.45	0.35	0.66	0.4	0.65	0.55	0.6	0.59	0.57
Oct-05	0.49	0.41	0.68	0.54	0.67	0.56	0.6	0.62	0.59
Nov-05	0.58	0.47	0.73	0.46	0.71	0.63	0.67	0.67	0.64
Dec-05	0.61	0.5	0.69	0.63	0.68	0.67	0.65	0.65	0.63
Jan-06	0.55	0.4	0.66	0.57	0.65	0.6	0.58	0.6	0.57
Feb-06	0.44	0.34	0.59	0.37	0.63	0.63	0.59	0.57	0.54
Mar-06	0.43	0.35	0.59	0.36	0.63	0.59	0.59	0.57	0.53
Apr-06	0.57	0.48	0.72	0.46	0.71	0.69	0.68	0.65	0.64
May-06	0.57	0.51	0.72	0.49	0.68	0.62	0.63	0.63	0.62
Jun-06	0.48	0.34	0.67	0.32	0.68	0.6	0.63	0.67	0.65
Jul-06	0.45	0.37	0.66	0.41	0.63	0.59	0.55	0.56	0.54
Aug-06	0.4	0.29	0.64	0.33	0.61	0.63	0.57	0.54	0.55
Sep-06	0.45	0.44	0.7	0.46	0.67	0.55	0.6	0.6	0.54
Oct-06	0.55	0.43	0.62	0.43	0.65	0.54	0.59	0.59	0.55
Nov-06	0.55	0.43	0.62	0.43	0.65	0.54	0.59	0.59	0.55
Dec-06	0.5	0.45	0.71	0.34	0.68	0.55	0.63	0.61	0.59

Table A-5 Satellite derived NDVI for the Semliki catchment (2007) S3-S14

	S3	S4	S5	S6	S7	S8	S9	S10	S11	S12	S13	S14
Jan-07	0.53	0.57	0.54	0.6	0.59	0.56	0.59	0.59	0.6	0.6	0.59	0.61
Feb-07	0.62	0.65	0.62	0.68	0.67	0.64	0.67	0.67	0.67	0.68	0.67	0.68
Mar-07	0.51	0.57	0.49	0.63	0.63	0.54	0.63	0.59	0.61	0.64	0.63	0.62
Apr-07	0.72	0.74	0.71	0.76	0.75	0.73	0.75	0.74	0.75	0.76	0.76	0.75
May-07	0.58	0.63	0.6	0.66	0.65	0.61	0.65	0.63	0.64	0.66	0.66	0.66
Jun-07	0.59	0.61	0.6	0.64	0.61	0.61	0.6	0.61	0.61	0.61	0.61	0.69
Jul-07	0.55	0.59	0.55	0.59	0.58	0.58	0.6	0.59	0.6	0.59	0.59	0.62
Aug-07	0.57	0.61	0.59	0.6	0.68	0.61	0.68	0.61	0.68	0.74	0.68	0.74
Sep-07	0.57	0.62	0.59	0.7	0.62	0.6	0.63	0.63	0.64	0.64	0.64	0.65
Oct-07	0.59	0.62	0.59	0.65	0.65	0.61	0.65	0.64	0.65	0.66	0.65	0.65
Nov-07	0.73	0.62	0.66	0.68	0.63	0.62	0.61	0.63	0.63	0.69	0.7	0.68
Dec-07	0.57	0.59	0.57	0.63	0.62	0.59	0.62	0.62	0.63	0.63	0.62	0.64

Table A-6 Satellite derived NDVI for the Semliki catchment (2007) S15-S23

	S15	S16	S17	S18	S19	S20	S21	S22	S23
Jan-07	0.59	0.61	0.61	0.61	0.59	0.66	0.59	0.59	0.57
Feb-07	0.68	0.75	0.68	0.72	0.66	0.75	0.59	0.65	0.63
Mar-07	0.63	0.64	0.64	0.64	0.61	0.63	0.61	0.61	0.6
Apr-07	0.76	0.76	0.76	0.76	0.75	0.76	0.75	0.75	0.74
May-07	0.69	0.69	0.66	0.73	0.64	0.7	0.64	0.67	0.68
Jun-07	0.61	0.7	0.69	0.65	0.63	0.71	0.62	0.61	0.57
Jul-07	0.61	0.62	0.59	0.66	0.59	0.61	0.59	0.59	0.59
Aug-07	0.69	0.67	0.67	0.75	0.68	0.67	0.61	0.59	0.59
Sep-07	0.65	0.71	0.65	0.71	0.62	0.71	0.62	0.66	0.66
Oct-07	0.66	0.73	0.67	0.74	0.63	0.74	0.63	0.62	0.61
Nov-07	0.69	0.75	0.71	0.72	0.69	0.75	0.69	0.67	0.67
Dec-07	0.69	0.67	0.65	0.68	0.62	0.64	0.62	0.62	0.61

Appendix B Corrected satellite derived rainfall for the the Semliki Watershed

Table B-1 Semliki's Corrected Satellite derived rainfall (S3-S15)-2001/2003

	S3	S4	S5	S6	S7	S8	S9	S10	S11	S12	S13	S14	S15
Jan-01	27.02198	24.83552	29.27796	22.33698	22.50469	24.67718	24.90644	23.91385	20.08089	29.74251	32.8355	17.01651	21.50555
Feb-01	24.1603	34.30803	30.62714	41.83927	47.4976	39.28887	46.26588	38.91097	37.72542	55.14562	51.97596	37.14434	43.73134
Mar-01	130.941	126.514	126.846	167.7423	171.8919	122.8847	173.8354	133.3824	152.6165	185.0562	167.3303	125.3688	139.5359
Apr-01	182.9813	192.8083	182.8368	152.3186	136.7139	201.9439	120.9144	202.4756	158.2	126.0695	109.0029	142.3288	111.7523
May-01	106.8473	111.3516	103.7137	141.5215	140.6977	118.5676	134.2148	122.643	125.2487	140.866	129.3828	125.7497	120.8593
Jun-01	84.20562	105.5445	79.9079	135.2597	118.158	94.95298	102.2145	108.3043	112.2972	115.4567	99.90227	89.32217	85.02861
Jul-01	97.04514	114.0834	94.87078	131.4712	118.1406	107.2909	110.5899	123.4868	126.6162	102.0387	94.47743	115.319	106.2111
Aug-01	93.53798	116.9003	96.46831	131.5232	118.312	115.8998	100.6186	135.8244	121.7618	106.5874	105.2244	110.9579	100.8037
Sep-01	84.33969	103.7267	88.79452	132.5304	130.5144	97.22175	113.9212	106.4927	110.5548	152.2814	137.1494	96.17617	100.3092
Oct-01	136.4012	137.0188	121.6242	141.6625	130.6822	123.0175	119.0905	126.2146	129.4459	133.9966	131.4694	129.6949	122.0795
Nov-01	113.5139	103.2902	120.4919	158.7909	146.2386	109.6495	116.6931	110.6026	127.206	136.7895	117.3931	108.4384	102.1486
Dec-01	75.22534	80.11062	88.03522	98.74408	93.23545	77.86004	84.29145	76.45177	81.42309	95.19966	92.31014	80.05278	95.4068
Jan-02	35.3893	46.24568	42.18887	57.86672	54.70114	50.36549	51.12383	56.30331	56.49238	55.81012	56.17552	57.46798	56.89131
Feb-02	31.57194	33.46475	43.42521	36.21824	34.71294	41.81616	32.25496	38.18218	35.27158	39.78338	34.32621	40.99676	35.93971
Mar-02	204.8216	198.0965	215.137	151.0935	151.9183	218.2356	143.5187	195.5323	157.8764	157.0344	130.8252	150.8218	119.7692
Apr-02	160.1984	143.1822	157.3236	176.352	178.6023	139.5211	170.3944	145.1733	156.3456	182.6098	155.566	125.8573	137.0731
May-02	78.52494	85.54284	83.30369	128.2168	118.622	85.13496	109.3075	95.72022	111.0592	117.5321	114.3972	105.6666	106.6275
Jun-02	34.51165	52.56664	25.62007	58.08887	68.21328	30.9389	42.91801	40.02802	45.77163	52.1026	41.36046	32.05289	35.29788
Jul-02	67.4482	81.90371	61.62179	95.71963	85.6651	65.70497	76.86951	81.85643	84.0537	84.83461	77.79926	52.93719	56.02082
Aug-02	134.7515	150.4714	146.0096	167.0162	159.968	152.0752	152.2854	155.3041	163.7972	150.4929	143.0159	148.176	135.566
Sep-02	72.88822	89.95163	79.46873	134.5688	121.4585	88.90869	96.62745	100.1939	107.7286	108.636	92.76287	95.91622	84.52171
Oct-02	143.8179	162.6045	137.3806	172.958	172.8728	148.7989	161.7925	159.2831	167.1833	180.0602	173.2358	155.049	148.5279
Nov-02	130.2746	155.5107	128.7234	185.7413	163.5524	130.9293	126.4769	139.2286	138.0024	152.4313	123.0268	102.3815	101.9291
Dec-02	56.64674	87.1749	63.36571	93.81373	89.8618	70.95371	79.41491	82.03406	88.14943	86.72019	73.52903	82.21113	78.86902
Jan-03	46.62621	65.66309	44.47468	69.48462	74.33836	50.38884	75.29461	59.95589	55.2601	96.34038	85.7875	38.30354	59.43649
Feb-03	30.90951	36.22472	36.46622	47.47454	53.60499	39.5187	57.13568	40.91556	47.83754	57.09403	54.5785	51.08827	58.95626
Mar-03	66.6952	83.38324	79.64187	130.5089	145.7965	99.96093	154.2622	114.077	132.9804	165.9455	161.5134	134.0152	138.4008
Apr-03	176.5117	210.4541	164.9137	237.0938	225.1267	151.5036	207.778	174.1732	202.0113	228.5927	223.7831	175.3204	191.0244
May-03	120.9335	112.2244	118.5445	118.9327	110.5648	113.466	106.3285	122.1699	125.0077	106.8852	103.4841	115.3614	107.2676
Jun-03	70.83967	87.10336	80.06219	106.1391	103.646	86.17627	109.4663	101.5557	114.2679	105.3727	110.635	115.6871	115.8188
Jul-03	72.98043	93.01517	66.13014	98.62499	96.79022	64.27978	80.11419	70.74843	76.51355	106.637	83.82818	57.63043	65.80793
Aug-03	95.1534	92.50981	88.09239	113.4045	116.0973	87.20695	116.445	93.96834	107.6637	115.6337	112.0495	109.6273	111.4408
Sep-03	106.9787	149.4242	125.968	181.7614	177.0552	155.7137	166.7159	177.7733	178.4591	169.086	171.3523	172.9177	176.5948
Oct-03	74.08246	96.8464	75.11021	120.9428	111.2778	77.7647	97.13396	90.93887	100.9509	111.6108	109.5716	91.87854	98.26836
Nov-03	171.2929	186.2315	180.1108	186.2378	184.1305	180.3302	184.9035	180.0145	178.0778	186.7754	176.491	170.5737	176.3653

Table B-2 Corrected Satellite derived rainfall (S3-S15)-2003/2006 of Semliki

	S3	S4	S5	S6	S7	S8	S9	S10	S11	S12	S13	S14	S15
Dec-03	34.41104	53.19791	40.7071	64.54117	58.0432	53.37564	52.14303	60.74104	64.62264	49.36636	49.28261	67.09838	58.75992
Jan-04	76.92882	90.39801	75.17737	107.2395	98.24634	84.20885	88.79376	92.56458	101.7073	88.09462	85.06804	101.5569	88.902
Feb-04	52.57285	62.23088	58.40398	61.2022	60.78016	66.7666	61.3078	67.84832	63.75612	63.59181	67.70677	67.80569	71.14215
Mar-04	99.15252	98.24579	99.5931	126.3439	131.1825	98.81231	137.5274	104.7283	126.181	137.632	140.9838	129.5714	136.1141
Apr-04	159.4325	179.9428	180.0006	199.4369	193.126	184.8564	170.6147	180.5186	175.8447	198.3749	188.8765	170.392	161.2866
May-04	106.1583	117.7413	109.7471	140.3786	123.2934	112.2151	100.3101	117.9826	116.2713	112.2222	103.8655	95.918	90.19931
Jun-04	30.11857	38.17718	27.24946	52.18188	45.10092	26.39662	37.62959	34.30408	39.55197	41.36248	32.6926	27.30535	26.12687
Jul-04	38.83068	50.63885	36.19761	59.66046	62.99358	41.84803	66.78768	52.29163	63.34842	62.561	53.87011	57.02332	56.28989
Aug-04	74.037	101.2317	82.86149	111.9476	99.66891	87.7086	84.47778	91.55278	87.40621	99.97623	84.95337	75.59381	73.04768
Sep-04	77.51642	90.26187	81.5506	105.5575	108.5806	90.52056	110.2668	96.1271	107.3614	112.2789	108.2143	104.6637	106.8666
Oct-04	103.9672	107.0061	113.8281	103.3659	104.3732	113.4289	100.3479	98.33878	86.47936	115.2676	103.023	86.33863	85.63243
Nov-04	114.8444	117.896	115.8829	134.6251	134.5815	133.1487	143.3902	139.9074	151.703	133.1135	146.0015	157.5031	148.6
Dec-04	36.04235	63.40098	40.91381	119.2077	116.1392	49.08144	94.80683	67.70025	93.27533	119.6058	93.0612	74.30369	76.76912
Jan-05	43.0856	64.1485	45.79918	79.92309	87.73258	56.46785	86.06863	67.66348	76.54157	104.0086	87.24422	72.14142	77.83325
Feb-05	64.98674	98.27028	72.3846	115.0604	108.0198	84.25472	94.22084	94.66721	94.3145	102.6378	87.87994	74.74719	74.05131
Mar-05	117.4318	139.2627	133.2692	165.078	158.0846	143.2804	148.6973	153.4392	159.0726	159.2574	154.6124	143.3848	141.8253
Apr-05	132.7734	159.5973	157.4038	164.2659	164.0856	170.3436	161.7961	168.6106	165.701	161.5989	161.2156	161.6287	153.3314
May-05	152.6054	179.4362	163.866	227.2818	223.9176	175.5405	207.1256	188.6368	195.3668	220.7838	204.271	174.6251	174.864
Jun-05	83.83493	122.4072	85.48599	107.8043	102.3539	90.98297	92.30598	97.32595	96.54661	97.68233	87.62449	73.71388	67.83841
Jul-05	95.1253	94.0931	78.22692	82.44626	74.88707	71.47929	76.57271	76.48105	73.81879	77.5684	79.95004	58.66466	65.24254
Aug-05	88.25375	92.51119	94.03217	95.96157	100.0401	90.74326	101.4497	90.9178	96.00837	107.4299	107.234	90.97491	97.10855
Sep-05	94.72607	125.6116	103.6149	143.0163	140.4851	120.4032	135.0699	127.6881	124.9038	141.4273	137.1215	119.2147	116.5196
Oct-05	96.9849	96.79553	100.2377	123.9839	123.359	101.3229	115.2934	104.791	116.359	128.4213	124.4486	116.6528	116.9053
Nov-05	56.24746	78.40724	65.42407	109.4826	104.1165	75.84368	95.91245	85.84899	96.42049	109.1088	108.2072	91.98856	97.15238
Dec-05	38.8637	47.54553	41.28542	77.66456	77.2288	43.35155	72.20709	52.66541	64.78214	84.98869	80.95208	56.00301	62.74349
Jan-06	29.15891	34.18923	43.29317	45.35855	52.26145	42.67091	57.56525	40.90868	48.12137	60.55841	53.92676	56.13602	54.16236
Feb-06	53.9328	65.14149	56.81521	89.42351	87.00019	63.05077	79.82068	70.5814	77.90451	82.23366	72.58491	71.96588	69.64756
Mar-06	106.468	96.09733	110.9784	95.88451	98.64428	101.7008	97.56898	91.61857	87.84664	109.9099	102.736	91.71568	99.5622
Apr-06	82.5637	91.85028	92.84263	130.4418	132.9934	110.5228	125.5727	111.3779	118.5636	137.0861	120.8695	120.9806	113.1778
May-06	120.8999	150.917	143.2813	215.8987	217.0769	158.1669	206.1432	173.129	193.315	223.4817	204.998	167.3476	182.5392
Jun-06	19.54575	24.58548	18.92057	43.66289	31.6517	18.15458	25.62907	22.63798	26.29534	32.03856	27.42222	14.30548	16.96271
Jul-06	48.95318	58.17769	51.3254	78.44383	81.09549	56.20524	85.74506	66.22111	80.2927	93.38434	89.38855	69.29771	72.20452
Aug-06	78.53567	81.73365	82.89994	106.8094	108.528	87.66937	106.845	97.75175	105.7673	104.6978	99.05744	94.86465	87.87908
Sep-06	74.85549	91.76872	92.82798	128.9673	129.3755	100.7082	124.7669	107.5492	112.99	137.8814	133.3769	102.7636	107.9466
Oct-06	81.29169	95.39056	91.27698	103.6997	99.81894	105.4909	95.98967	99.69164	91.82863	106.9866	103.0096	87.16013	86.09702

Table B-3 Corrected Satellite derived rainfall (S16-S23)-2001/2003 of Semliki

	S16	S17	S18	S19	S20	S21	S22	S23	
Jan-01	28.9419	31.21557	29.30446	30.78088	29.02819	30.59397	29.69221	26.43792	
Feb-01	46.8423	49.32833	46.29958	58.15699	42.37928	47.31612	48.41265	40.23847	
Mar-01	137.5904	138.0604	122.4968	142.2925	111.4385	108.9066	92.84263	84.95182	
Apr-01	100.9621	100.6451	97.27291	102.0957	99.53238	106.0832	106.2948	100.7114	
May-01	119.5057	119.6709	115.632	130.4375	116.8733	132.7407	129.732	118.4765	
Jun-01	84.35046	85.00535	76.46384	85.97552	71.0203	77.91356	82.18554	71.57619	
Jul-01	92.70609	84.37769	72.94795	76.16615	63.81174	64.61114	65.94722	59.71811	
Aug-01	102.6859	106.9235	111.1491	129.5158	109.2683	127.3321	155.4695	139.1247	
Sep-01	110.257	120.0523	106.263	142.1515	102.3275	121.7572	126.906	112.3587	
Oct-01	120.2524	126.8165	146.7053	179.3739	173.3545	194.567	204.4174	189.7753	
Nov-01	100.2329	105.5205	106.8522	112.0164	113.7512	107.2395	100.1512	109.1402	
Dec-01	98.87514	94.28832	90.80433	94.0689	90.74501	98.9695	104.3353	97.15113	
Jan-02	54.02932	56.88617	61.68749	67.24429	65.25898	66.79832	71.1363	70.3704	
Feb-02	30.80663	31.48047	34.85266	40.37174	34.71298	33.5151	35.8962	35.01588	
Mar-02	104.1047	102.8425	98.04049	107.9229	96.03902	100.5392	104.42	95.79561	
Apr-02	130.5793	128.2251	119.3626	123.1341	131.6859	136.3453	137.5902	144.6491	
May-02	104.5505	103.0851	94.83461	112.7175	83.84232	91.38933	99.63824	83.58181	
Jun-02	36.49969	36.46139	31.10998	39.73351	26.15352	31.96451	29.88649	22.86516	
Jul-02	57.64065	63.4097	49.61432	79.94673	44.28255	61.64246	60.46842	45.52634	
Aug-02	121.4678	122.2762	115.3706	160.1617	121.9715	158.2364	150.9029	127.8952	
Sep-02	78.01072	78.41557	71.63044	92.86676	69.31712	78.12725	78.65208	77.37401	
Oct-02	152.2061	160.1997	154.3746	200.3601	146.1244	171.582	181.3108	153.3872	
Nov-02	101.1938	102.868	90.97459	109.281	85.79298	96.05799	105.7467	81.95251	
Dec-02	67.46159	64.75973	62.71877	67.25287	63.69601	71.42609	78.15208	73.05904	
Jan-03	67.35346	69.55003	56.80712	72.96331	51.18356	59.23924	70.0664	62.08003	
Feb-03	55.53826	52.91421	47.4882	50.92482	41.21795	48.93756	57.87077	43.38325	
Mar-03	147.7774	154.9037	145.1208	154.6912	130.6025	137.5957	143.7726	121.6891	
Apr-03	208.5416	218.3656	203.6459	225.4756	185.9063	191.2231	190.2277	158.2717	
May-03	102.9896	102.2897	100.3043	95.68079	96.91077	87.48669	90.90438	85.55619	
Jun-03	114.6412	112.5353	104.5006	118.2972	88.52641	96.59793	94.33645	68.97046	
Jul-03	71.33601	73.38911	59.96598	65.18625	47.49041	54.24447	54.69056	39.22809	
Aug-03	110.6544	110.8595	107.1552	114.9331	99.94251	97.93994	88.53614	74.28902	
Sep-03	178.9841	176.9384	173.3637	179.0176	166.2004	168.7122	183.1425	160.7481	
Oct-03	105.5209	110.4686	112.1012	126.4093	114.8304	126.0517	125.6378	107.8573	
Nov-03	169.6869	164.8979	148.8021	169.4469	141.1961	146.5636	145.48	138.0647	

Table B-4 Corrected Satellite derived rainfall (S16-S23)-2001/2003 of Semliki

	S16	S17	S18	S19	S20	S21	S22	S23	
Dec-03	54.09992	51.6964	55.13594	55.97276	65.08714	79.58813	86.795	72.9168	
Jan-04	88.18218	86.52019	89.91938	94.71083	92.52414	93.40317	93.4367	90.28886	
Feb-04	75.07976	74.37865	73.83416	75.24529	69.07784	71.39427	76.49446	66.7936	
Mar-04	134.1359	132.9301	125.2898	157.805	122.7798	141.5	150.8892	131.3558	
Apr-04	167.3466	174.0709	168.8601	215.6673	176.2724	206.4108	217.8127	185.8976	
May-04	91.70826	96.52795	89.04265	118.1941	83.75987	105.4023	107.6716	87.48637	
Jun-04	24.26705	24.30402	22.16692	23.52494	17.31154	17.75877	20.51547	15.87766	
Jul-04	50.71927	46.79467	36.60555	38.64379	26.747	27.43271	31.12615	21.17419	
Aug-04	75.73763	74.67406	71.14863	83.26995	70.1899	73.41098	70.86989	60.67185	
Sep-04	100.9481	100.9072	94.96514	107.3188	87.22776	98.58315	114.1709	98.12936	
Oct-04	84.72199	87.49369	78.14492	103.3447	75.17532	86.87805	93.40192	78.64806	
Nov-04	148.0522	153.0417	155.1878	156.8582	153.5955	160.4205	175.6876	148.6286	
Dec-04	71.84551	74.77251	71.49095	96.19383	77.1171	92.70716	95.7181	85.72473	
Jan-05	68.67099	71.36663	70.51612	97.431	76.94116	119.2177	152.2004	99.47878	
Feb-05	72.64311	74.07471	66.7918	78.83197	62.60311	67.90952	67.49941	58.52414	
Mar-05	146.8776	153.0034	155.3714	167.7718	153.956	155.7133	157.3244	146.598	
Apr-05	148.9205	151.6637	148.6044	175.0819	145.5932	156.6906	152.6192	135.9414	
May-05	180.0051	181.9982	166.1683	184.994	160.1799	168.328	161.0164	143.7468	
Jun-05	68.58507	74.24664	58.23953	74.67513	47.98543	53.21299	47.70072	36.95793	
Jul-05	73.25981	75.07137	60.66775	80.46968	49.0589	65.40318	56.67927	34.22038	
Aug-05	102.9087	106.0288	95.21628	106.6345	82.52963	89.82522	97.75648	79.43594	
Sep-05	120.7073	122.4113	108.243	124.999	103.6655	110.9873	106.0394	87.42953	
Oct-05	119.3075	122.6944	127.4132	146.9078	132.606	148.9985	151.9204	139.9761	
Nov-05	100.8536	105.8725	116.0868	141.021	123.6124	147.3441	154.2481	129.8085	
Dec-05	70.83247	74.78269	66.08723	79.90638	58.67683	62.68674	65.30269	53.31634	
Jan-06	48.98103	46.2459	42.06399	43.974	39.73247	42.62018	35.5217	27.52211	
Feb-06	64.97332	65.84549	61.43206	61.65165	54.90064	57.04356	63.23303	59.49661	
Mar-06	99.81044	100.5518	100.4632	96.29005	93.66452	95.75425	102.3926	104.8358	
Apr-06	108.6721	107.99	99.33387	123.8326	96.16807	111.4896	114.4882	91.54203	
May-06	186.5783	189.4971	173.4699	197.4745	163.9917	175.3555	175.0567	157.0154	
Jun-06	21.02568	23.34216	19.48085	25.3066	14.6662	17.52546	22.24788	11.96927	
Jul-06	73.61474	75.42591	71.92317	94.21057	69.44707	85.85015	90.6445	70.50234	
Aug-06	83.85073	82.60825	67.67972	80.76491	63.42841	75.28942	83.84946	67.4684	
Sep-06	118.9644	123.8007	118.5589	136.349	117.3243	125.9594	125.0266	103.2945	
Oct-06	95.31846	97.24214	96.99874	108.6913	100.8015	103.237	101.7017	93.13588	

Table B-5 Corrected Satellite derived rainfall (S3-S15)-2006/2007 of Semliki

	S3	S4	S5	S6	S7	S8	S9	S10	S11	S12	S13	S14	S15
Nov-06	153.5956	133.8806	162.6755	126.9297	124.2682	153.1958	116.1468	135.2413	122.9061	127.8537	122.9339	129.1831	119.8033
Dec-06	49.78594	46.78041	47.00125	52.24696	59.60739	51.23372	67.44118	53.32553	62.06143	61.9885	67.12807	75.88277	71.72712
Jan-07	16.86118	19.47706	23.64277	24.86219	27.27215	23.88687	27.13838	20.57761	22.99895	30.0926	22.90789	24.76221	23.50328
Feb-07	58.87096	56.89215	61.91289	58.16922	64.53763	60.81676	71.77255	61.01877	66.3485	65.74994	64.8366	71.55269	68.97485
Mar-07	104.6661	126.7461	105.4365	113.8123	115.0793	114.4628	113.7431	118.121	120.7267	106.0481	106.9218	127.7569	121.154
Apr-07	110.9756	109.007	123.7665	119.965	115.965	118.2959	113.5214	116.5777	119.076	117.0013	121.5315	117.9483	122.0639
May-07	108.6094	133.4033	129.8253	189.519	197.1174	168.7802	205.059	190.8306	209.836	196.873	197.3488	208.3864	205.2227
Jun-07	66.18591	67.17826	64.3758	59.68279	57.23444	63.50774	63.83511	59.96529	56.98774	63.88823	73.55066	63.73311	67.95382
Jul-07	94.11576	81.74319	95.0088	74.4131	70.78921	84.44105	68.73278	81.91536	75.03648	73.0295	68.38464	64.89327	63.44233
Aug-07	113.8753	116.8077	124.0124	119.0049	113.4169	118.0875	113.1191	118.2711	121.1052	100.5846	101.3561	117.5592	111.3525
Sep-07	122.8168	136.6023	126.5449	143.5667	143.8367	137.5635	148.0894	145.449	150.9064	159.3122	160.6275	144.0915	152.7088
Oct-07	83.82643	122.2976	116.3607	151.9343	139.2853	132.7449	117.6038	133.114	128.5633	144.731	125.0456	119.8437	110.9234
Nov-07	78.4127	119.4312	76.74939	145.861	140.3816	89.47586	120.1745	104.2062	117.4525	137.3185	123.1126	102.6863	110.9582
Dec-07	44.82184	46.38007	46.85955	62.97596	66.30857	50.92423	66.69364	56.37068	61.80633	73.80533	65.67521	57.57244	56.57449

Table B-6 Corrected Satellite derived rainfall (S16-S23)-2006/2007 of Semliki

	S16	S17	S18	S19	S20	S21	S22	S23
Nov-06	124.9129	128.3643	134.4934	133.2877	142.1009	141.8254	140.1962	137.1849
Dec-06	71.2386	71.82839	74.36434	71.46622	70.02619	68.00798	62.55987	55.29587
Jan-07	18.96411	18.60469	19.27424	21.35628	22.0759	22.54558	27.76136	22.84257
Feb-07	64.69785	64.6662	60.87172	60.16384	56.03694	57.90183	56.81802	50.84166
Mar-07	112.5141	108.7067	103.0487	92.82563	94.95173	91.80619	84.14685	83.93229
Apr-07	121.994	123.9782	126.2557	129.9902	125.253	128.1908	131.5572	122.5383
May-07	196.9717	192.7763	182.847	185.3284	169.2425	168.7762	158.7198	144.8496
Jun-07	74.62162	75.585	71.57454	78.75714	64.66927	69.61882	62.81796	54.75364
Jul-07	61.94399	58.7208	49.86948	55.81969	42.39298	40.1324	37.93582	35.55296
Aug-07	102.5139	99.42478	92.32865	91.75948	85.74414	84.87439	74.80159	71.05759
Sep-07	154.7865	157.2505	154.1992	176.968	150.8462	158.994	158.0352	142.389
Oct-07	108.0103	114.4829	119.7193	137.1152	134.3257	139.8514	129.831	122.9828
Nov-07	113.6597	116.4676	118.7725	126.0176	128.7246	137.2465	144.3041	133.6003
Dec-07	52.84366	54.56378	52.67471	62.50957	54.52103	54.51672	62.29085	52.98701

Appendix C: Step-wise Sensitivity analyses

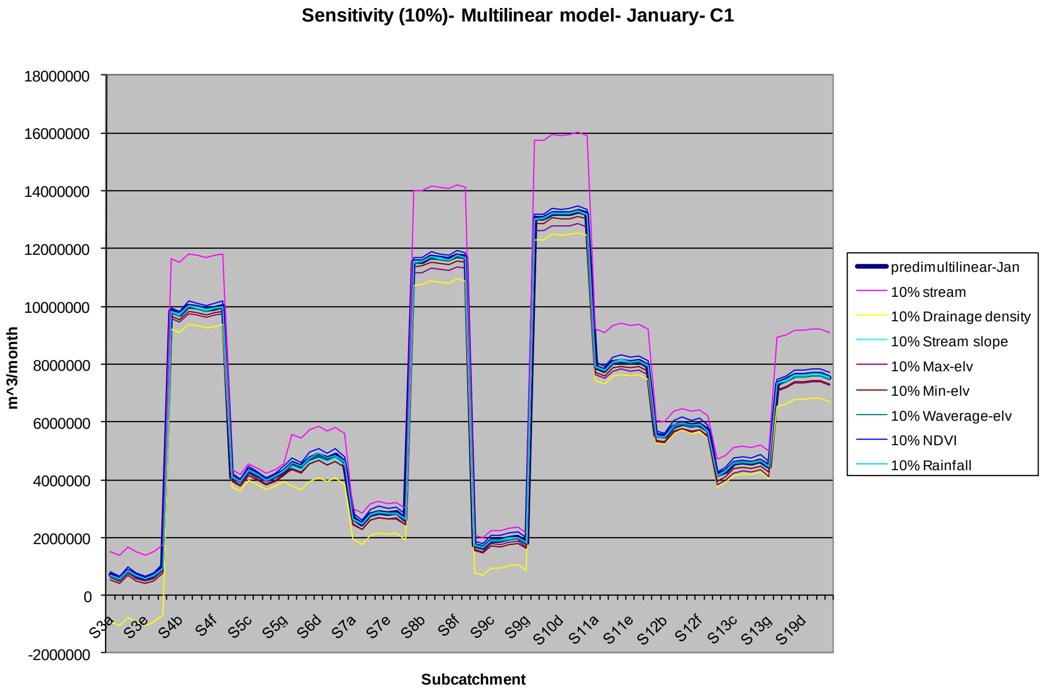

Figure C-1 Sensitivity (10%)-multilinear model-January C1

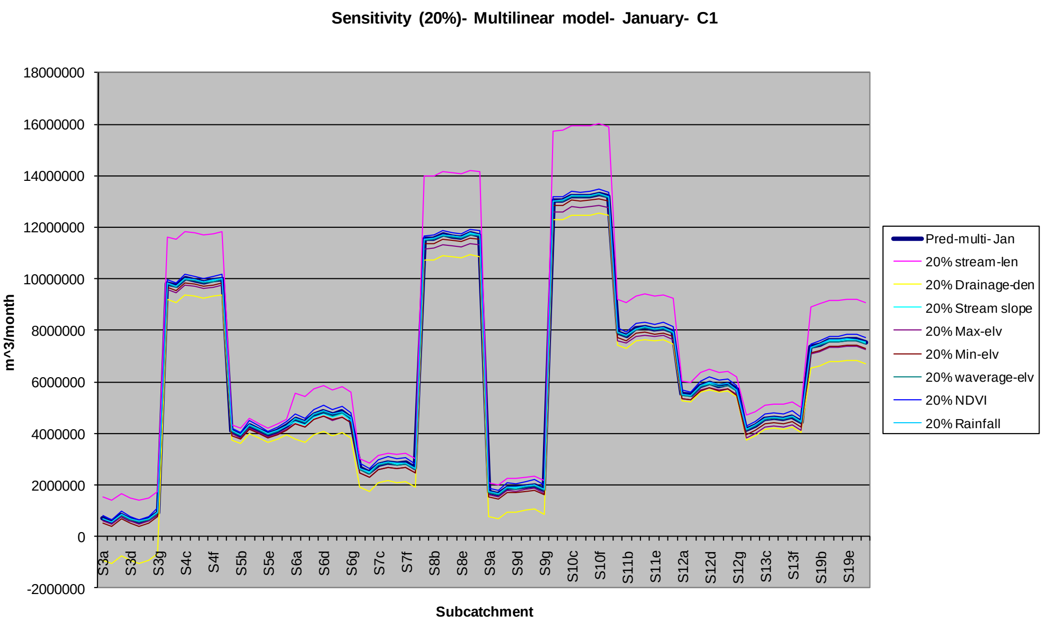

Figure C-2 Sensitivity (20%)- Multilinear model – January C1

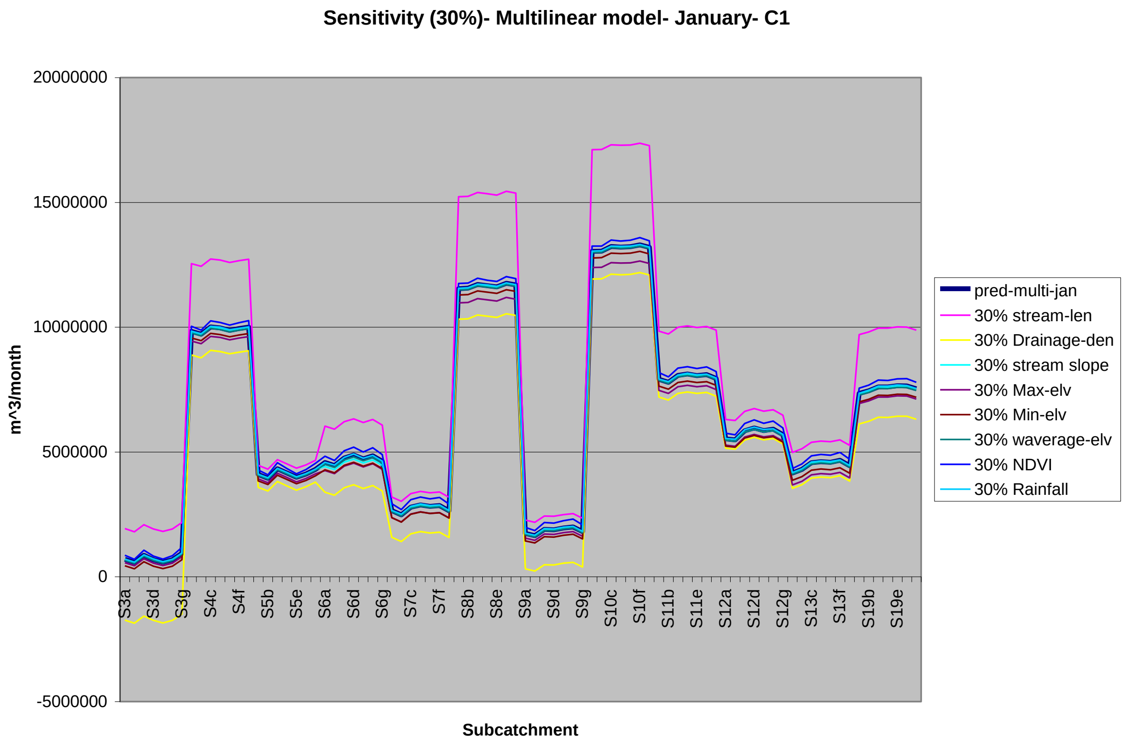

Figure C-3 Sensitivity (30%) – Multilinear model-January C1

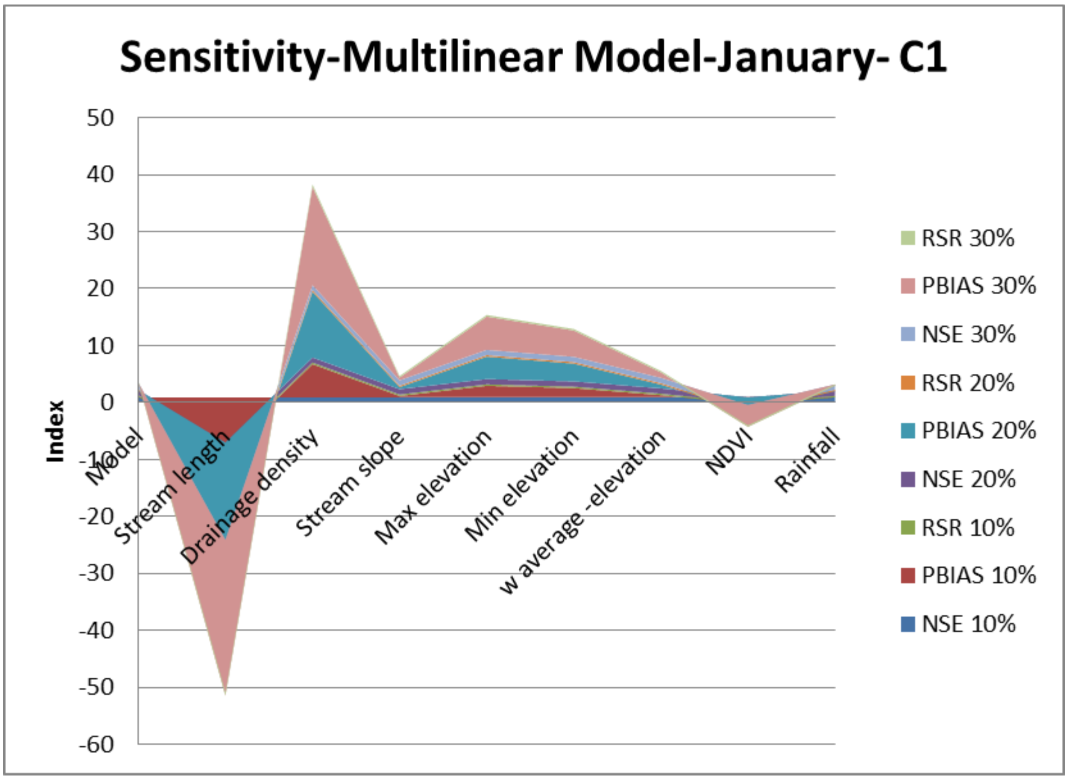

Figure C-4 Sensitivity Summary-January

Table C-1 Summary performance- Multilinear model- January C1

		10%							
	0%	**Stream length**	**Drainage density**	**Stream slope**	**Max elevation**	**Min elevation**	**w average - elevation**	**NDVI**	**Rainfall**
NSE	0.932869	0.900990406	0.922163182	0.932844437	0.931654	0.932202	0.932833594	0.932473	0.932871
PBIAS	0.097069	-9.040859069	5.820381115	0.227243567	2.01267	1.605031	0.379792982	-1.2121	-0.00936
RSR	0.259097	0.314657899	0.278992505	0.259143903	0.261432	0.26038	0.259164824	0.259859	0.259093
		20%							
	0%	**Stream length**	**Drainage density**	**Stream slope**	**Max elevation**	**Min elevation**	**w average - elevation**	**NDVI**	**Rainfall**
NSE	0.932869	0.804452673	0.890614969	0.932784112	0.928198	0.930354	0.93275597	0.931154	0.932865
PBIAS	0.097069	-18.17878726	11.54369311	0.35741801	3.92827	3.112994	0.66251684	-2.52127	-0.1158
RSR	0.259097	0.442207334	0.330734079	0.25926027	0.267958	0.263904	0.259314538	0.262384	0.259104
		30%							
	0%	**Stream length**	**Drainage density**	**Stream slope**	**Max elevation**	**Min elevation**	**w average - elevation**	**NDVI**	**Rainfall**
NSE	0.932869	0.643255718	0.838224277	0.932687942	0.922504	0.927325	0.932636046	0.928913	0.932853
PBIAS	0.097069	-27.31671545	17.2670051	0.487592454	5.84387	4.620956	0.945240699	-3.83044	-0.22223
RSR	0.259097	0.59728074	0.402213529	0.259445675	0.278382	0.269583	0.259545668	0.266622	0.259128

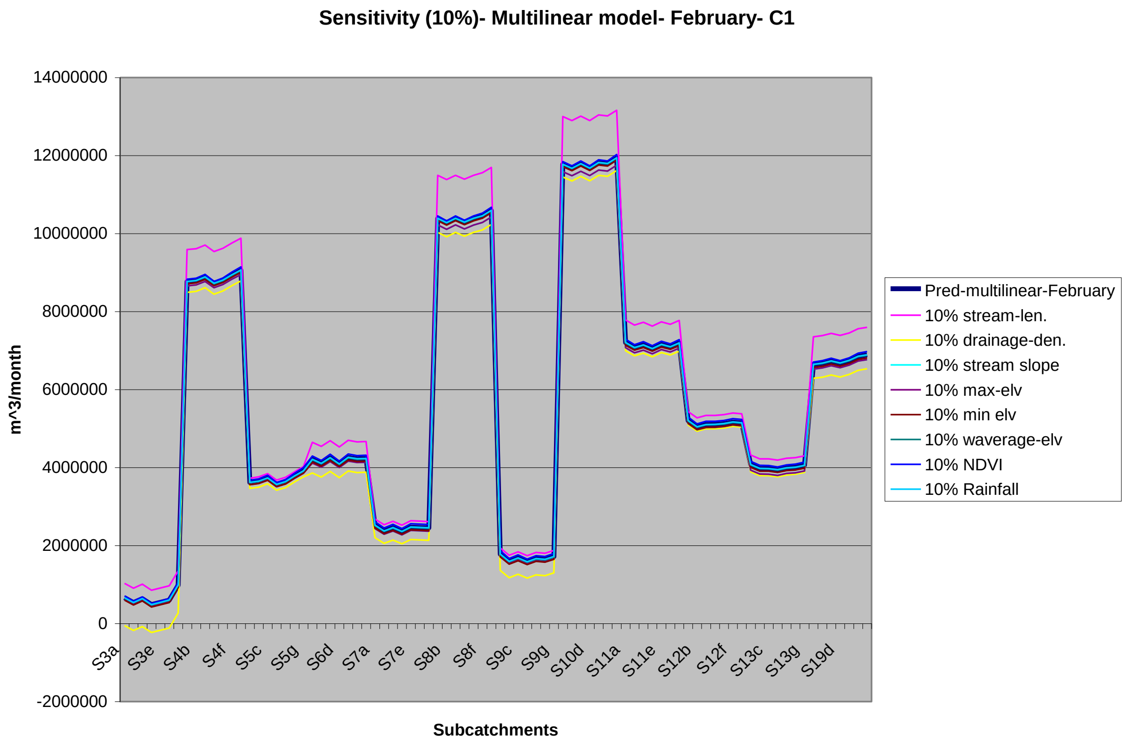

Figure C-5 Sensitivity (10%)- Multilinear model – February C1

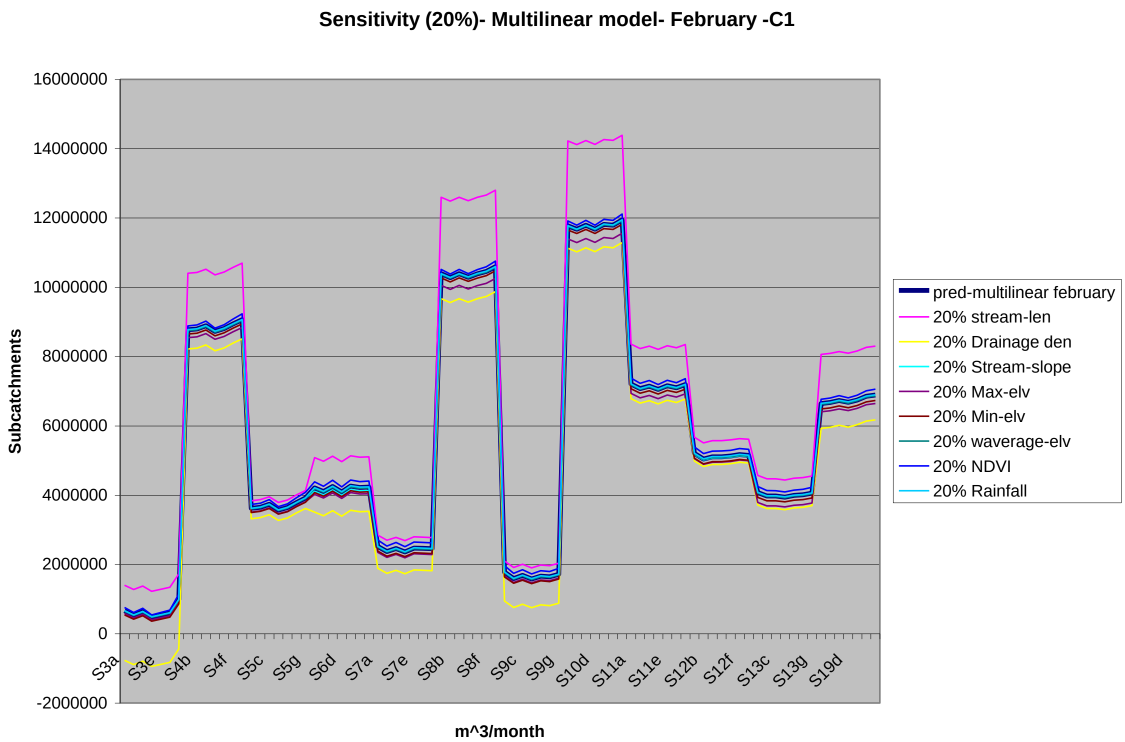

Figure C-6 Sensitivity (20%)- Multilinear model – February C1

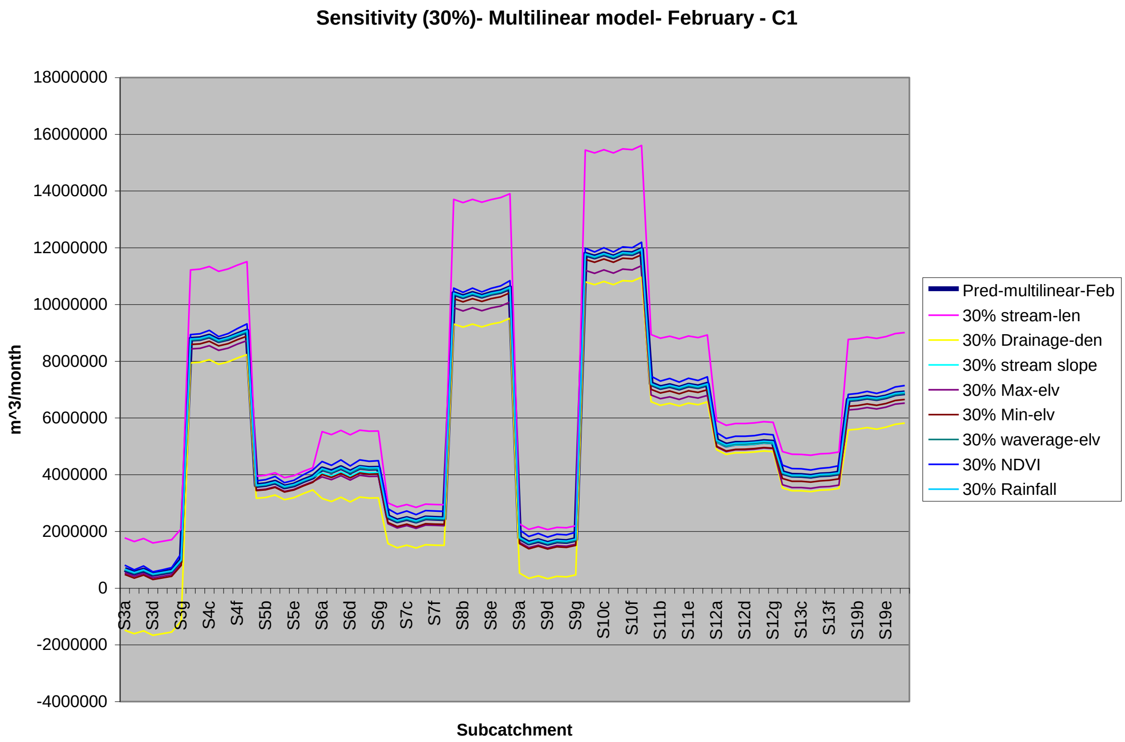

Figure C-7 Sensitivity (30%)- Multilinear model –February C1

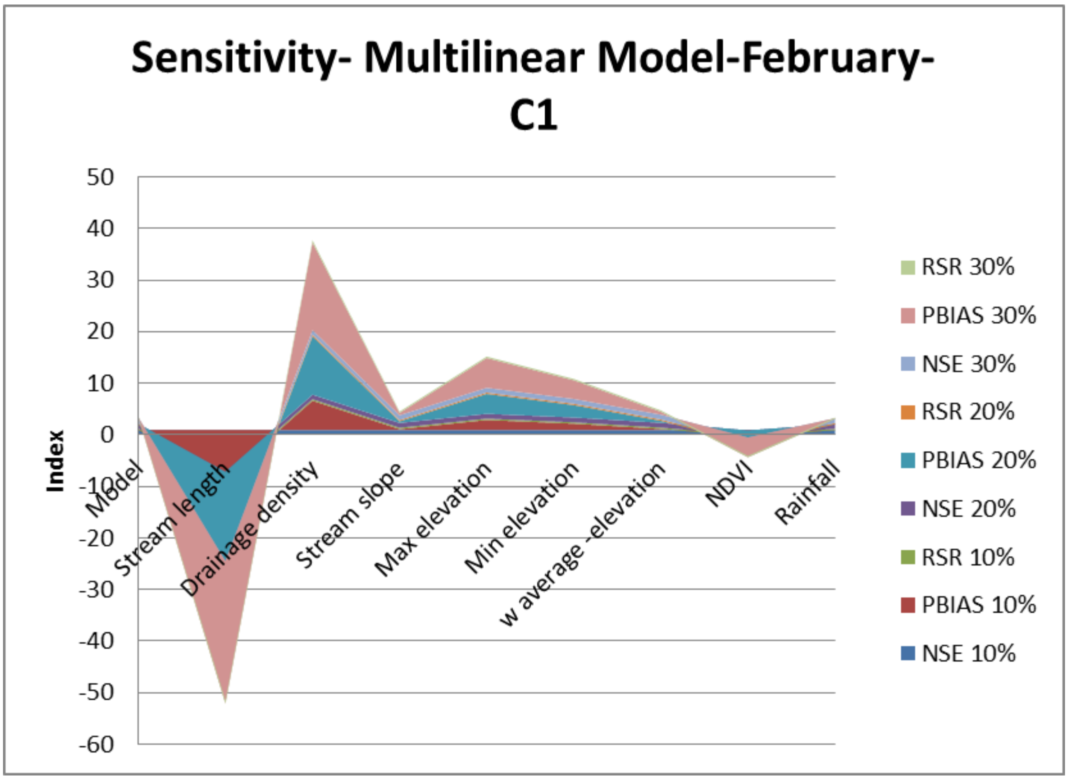

Figure C-8 Summary Sensitivity- Multilinear model –February C1

Table C-2 Summary performance- Multilinear model- February C1

		10%							
	0%	Stream length	Drainage density	Stream slope	Max elevation	Min elevation	w average - elevation	NDVI	Rainfall
NSE	0.932428	0.899683	0.922178	0.932405	0.931285	0.932039	0.932417	0.932	0.932428
PBIAS	0.032203	-9.17745	5.684491	0.170175	1.94554	1.224079	0.207829	-1.26161	-0.02312
RSR	0.259946	0.316729	0.278966	0.259989	0.262135	0.260693	0.259967	0.260767	0.259946
		20%							
	0%	**Stream length**	**Drainage density**	**Stream slope**	**Max elevation**	**Min elevation**	**w average - elevation**	**NDVI**	**Rainfall**
NSE	0.932428	0.801259	0.8916	0.932343	0.927907	0.930912	0.93239	0.930673	0.932427
PBIAS	0.032203	-18.3871	11.33678	0.308146	3.858878	2.415955	0.383454	-2.55543	-0.07845
RSR	0.259946	0.445803	0.329242	0.26011	0.268501	0.262846	0.26002	0.2633	0.259949
		30%							
	0%	**Stream length**	**Drainage density**	**Stream slope**	**Max elevation**	**Min elevation**	**w average - elevation**	**NDVI**	**Rainfall**
NSE	0.932428	0.637157	0.840693	0.932239	0.922296	0.929046	0.932346	0.928445	0.932423
PBIAS	0.032203	-27.5968	16.98907	0.446117	5.772215	3.607831	0.559079	-3.84925	-0.13378
RSR	0.259946	0.602364	0.399133	0.260309	0.278755	0.266371	0.260104	0.267497	0.259956

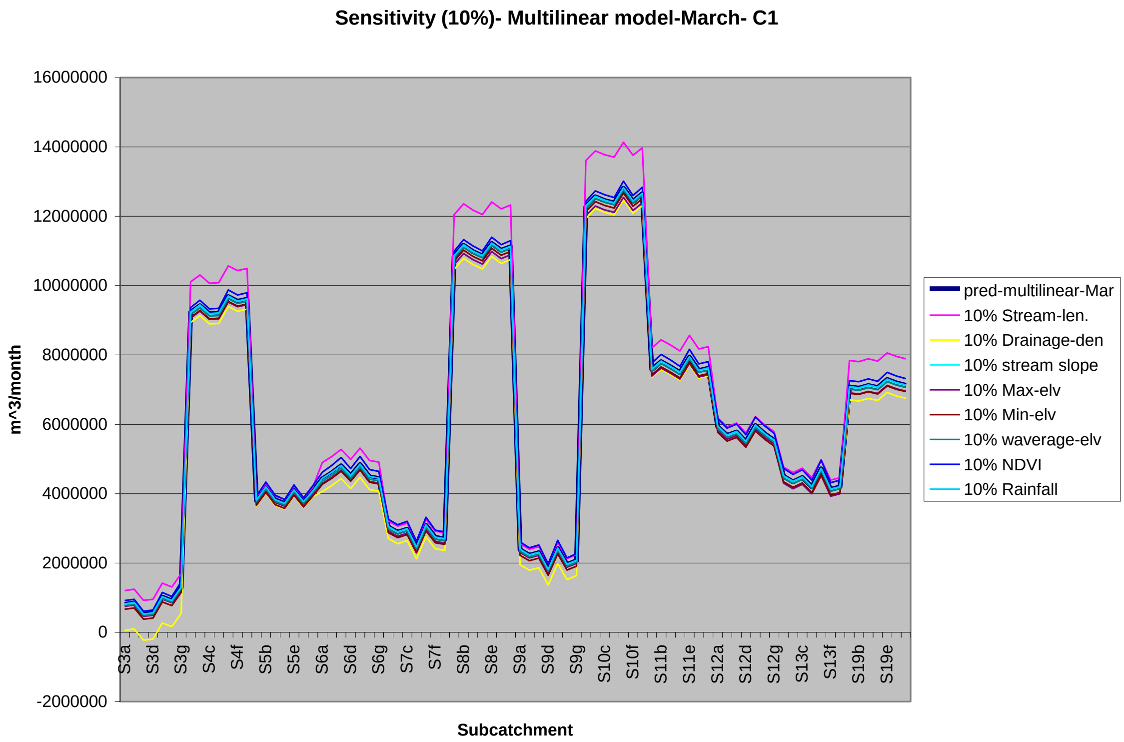

Figure C-9 Sensitivity (10%) – Multilinear model –March C1

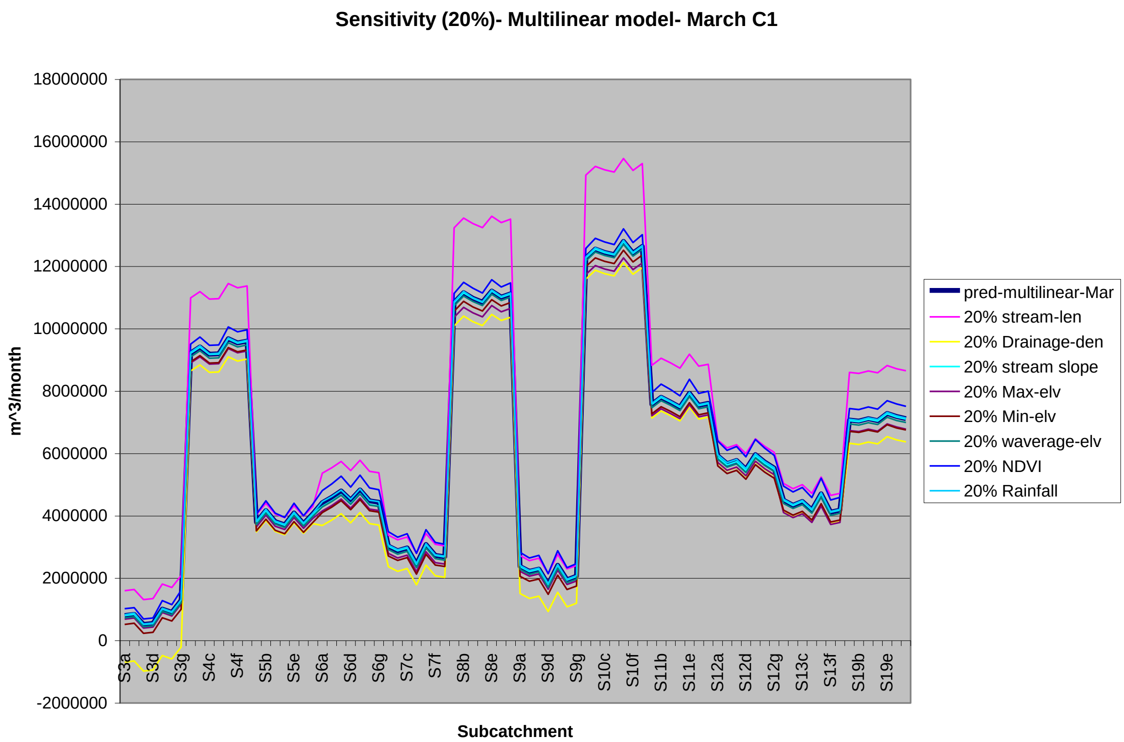

Figure C-10 Sensitivity (20%) – Multilinear model –March C1

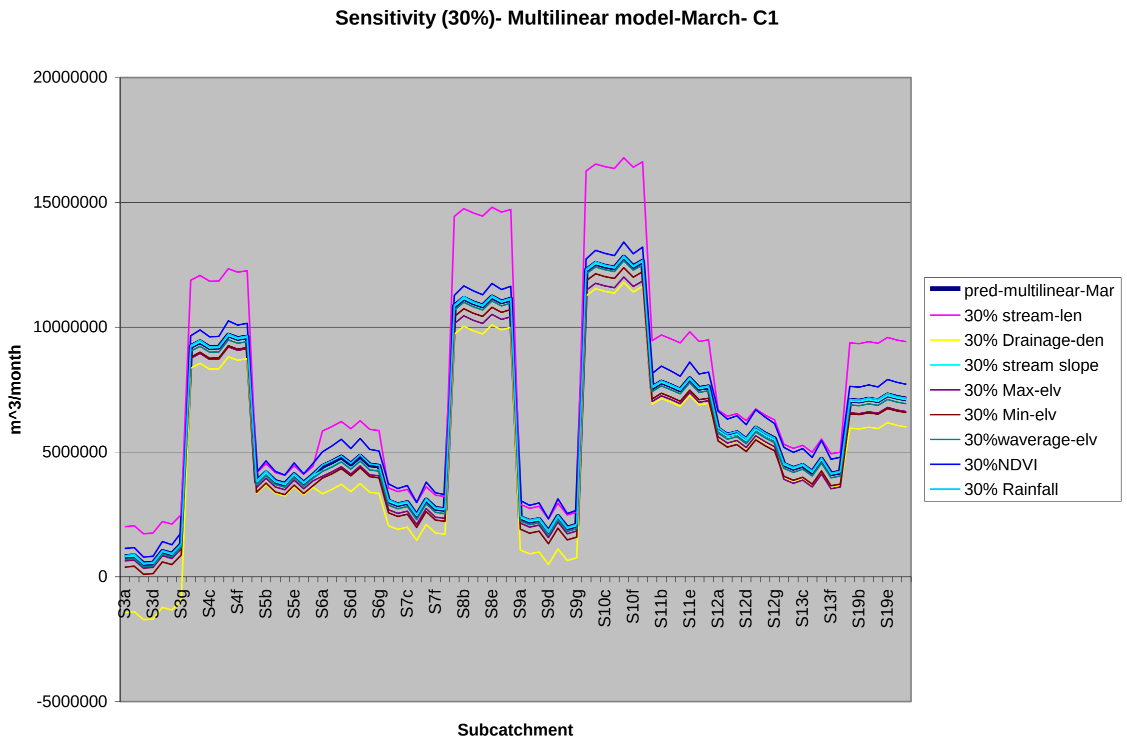

Figure C-11 Sensitivity (30%) – Multilinear model –March C1

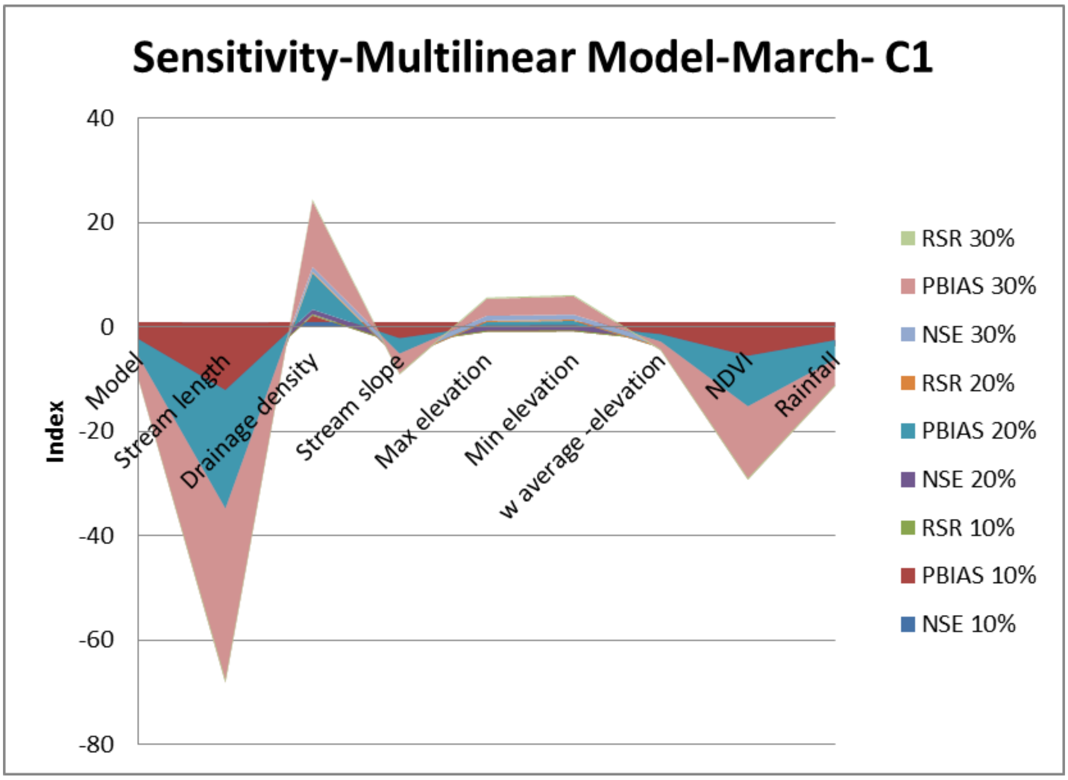

Figure C-12 Sensitivity summary – Multilinear model –March C1

Table C-3 Summary performance- Multilinear model- March C1

		10%							
	0%	Stream length	Drainage density	Stream slope	Max elevation	Min elevation	w average - elevation	NDVI	Rainfall
NSE	0.929791	0.871918	0.932367	0.930134	0.933687	0.934065	0.931686	0.919551	0.929243
PBIAS	-4.4485	-14.0904	1.247723	-4.29255	-1.88064	-1.80209	-3.52872	-7.6552	-4.66861
RSR	0.26497	0.357886	0.260063	0.264323	0.257513	0.256778	0.261369	0.283636	0.266001
		20%							
	0%	Stream length	Drainage density	Stream slope	Max elevation	Min elevation	w average - elevation	NDVI	Rainfall
NSE	0.929791	0.742056	0.914298	0.930425	0.933558	0.9347	0.933134	0.903797	0.928669
PBIAS	-4.4485	-23.7324	6.943949	-4.1366	0.687226	0.844328	-2.60893	-10.8619	-4.88871
RSR	0.26497	0.507882	0.292749	0.263772	0.257763	0.255539	0.258585	0.310167	0.267078
		30%							
	0%	Stream length	Drainage density	Stream slope	Max elevation	Min elevation	w average - elevation	NDVI	Rainfall
NSE	0.929791	0.540205	0.875583	0.930664	0.929405	0.931695	0.934133	0.882529	0.928068
PBIAS	-4.4485	-33.3743	12.64018	-3.98065	3.255091	3.490743	-1.68914	-14.0686	-5.10882
RSR	0.26497	0.678082	0.352728	0.263317	0.265698	0.261352	0.256645	0.342741	0.268201

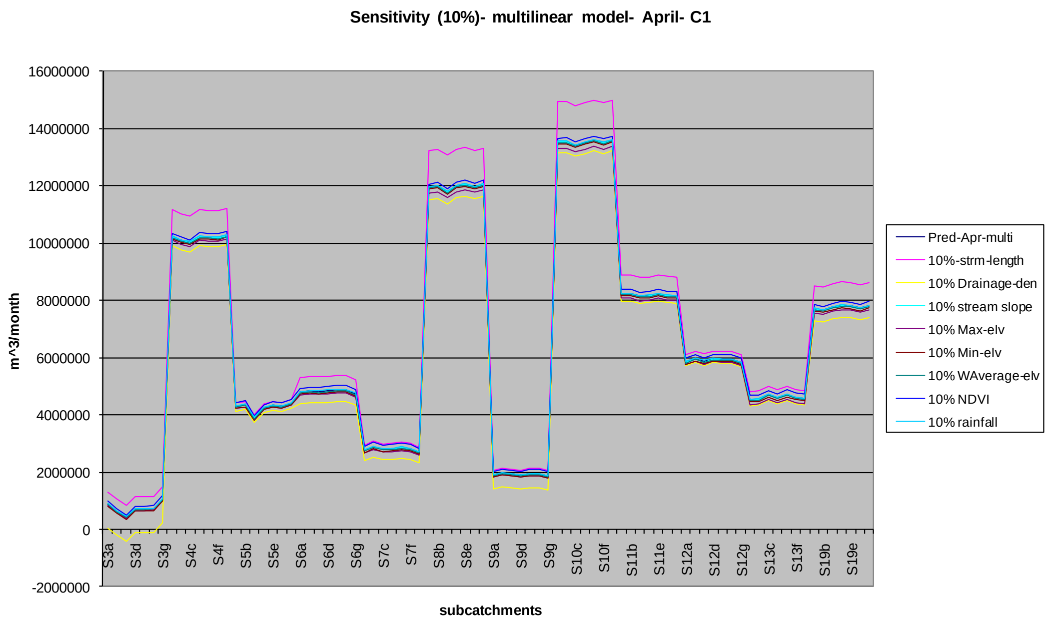

Figure C-13 Sensitivity (10%) – Multilinear model -April C1

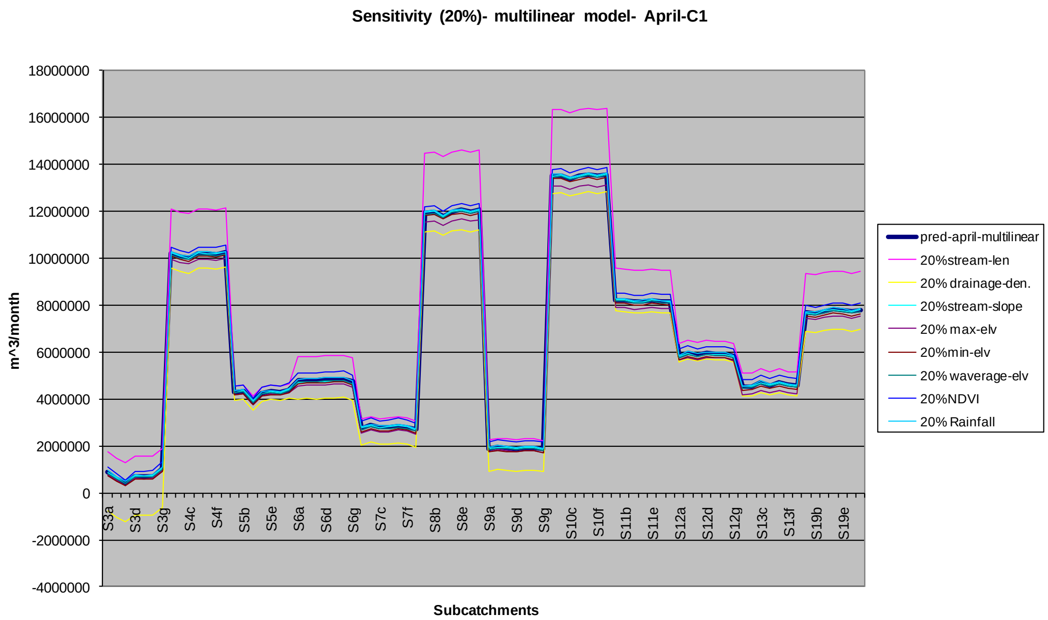

Figure C-14 Sensitivity (20%) – Multilinear model –April C1

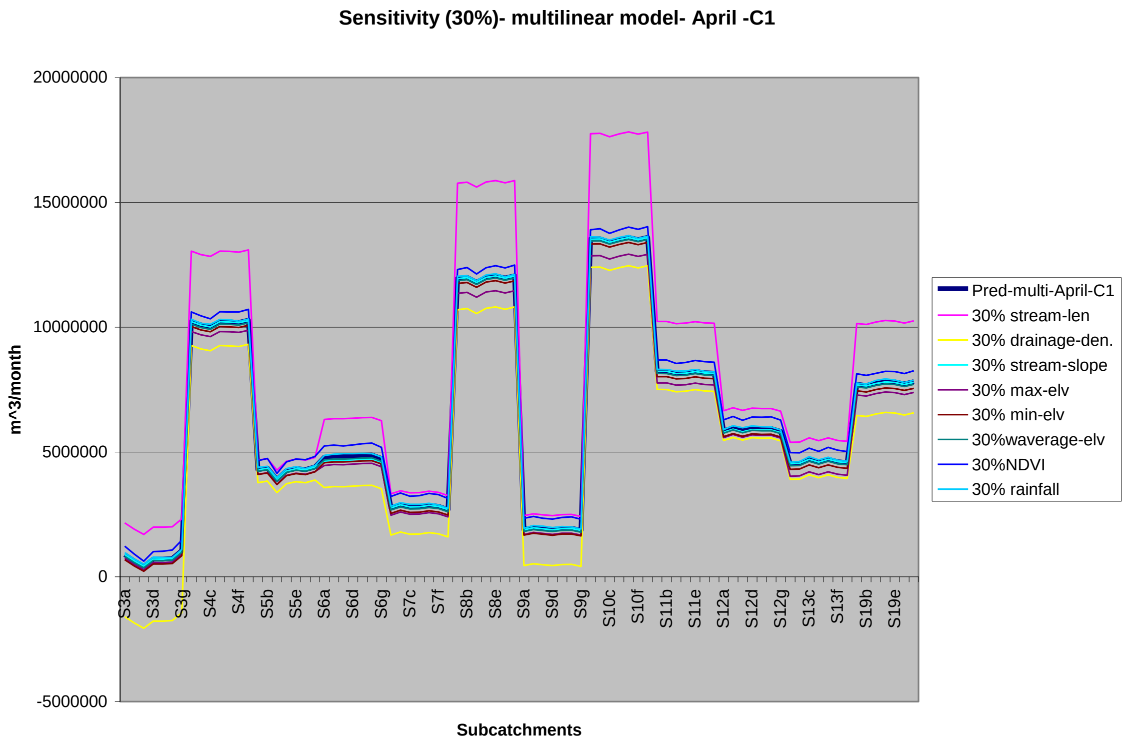

Figure C-15 Sensitivity (30%) – Multilinear model –April C1

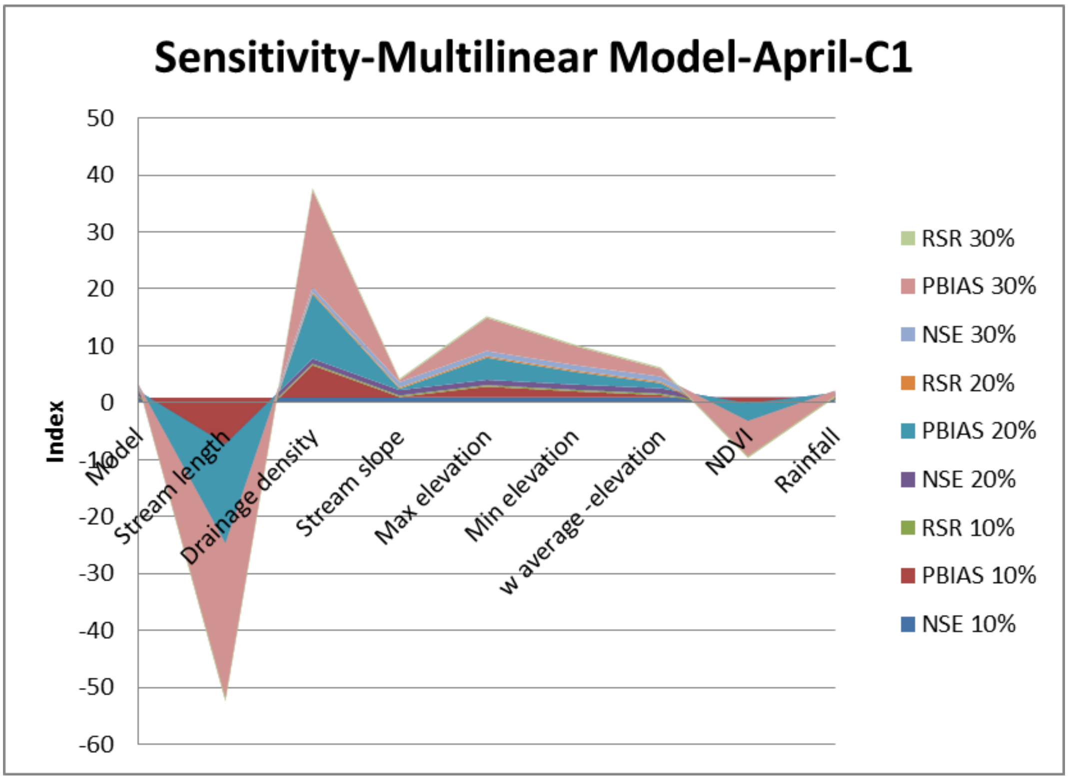

Figure C-16 Sensitivity summary – Multilinear model –April C1

Table C-4 Summary performance- Multilinear model- April C1

		10%							
	0%	**Stream length**	**Drainage density**	**Stream slope**	**Max elevation**	**Min elevation**	**w average – elevation**	**NDVI**	**Rainfall**
NSE	0.932272	0.899114	0.92204019	0.93225637	0.931141947	0.931955717	0.932224313	0.931036	0.932228
PBIAS	-0.02967	-9.2591945	5.665678356	0.100243982	1.923492956	1.104000049	0.427024826	-2.17258	-0.40577
RSR	0.260245	0.317624038	0.27921284	0.260276065	0.262408179	0.260852992	0.26033764	0.26261	0.26033
		20%							
	0%	**Stream length**	**Drainage density**	**Stream slope**	**Max elevation**	**Min elevation**	**w average - elevation**	**NDVI**	**Rainfall**
NSE	0.932272	0.799995586	0.891168671	0.932204643	0.927683142	0.930971215	0.932065856	0.927391	0.932107
PBIAS	-0.02967	-18.48871811	11.36102777	0.230159019	3.876656968	2.237671153	0.883720708	-4.31548	-0.78186
RSR	0.260245	0.447218531	0.329895936	0.260375415	0.26891794	0.262733296	0.260641792	0.26946	0.260563
		30%							
	0%	**Stream length**	**Drainage density**	**Stream slope**	**Max elevation**	**Min elevation**	**w average - elevation**	**NDVI**	**Rainfall**
NSE	0.932272	0.63491424	0.839657838	0.932117214	0.921895977	0.929318891	0.931797024	0.921339	0.931909
PBIAS	-0.02967	-27.71824164	17.05637718	0.360074056	5.829820979	3.371342257	1.340416589	-6.45838	-1.15796
RSR	0.260245	0.60422327	0.400427474	0.260543252	0.279470969	0.265859191	0.261156995	0.280465	0.260942

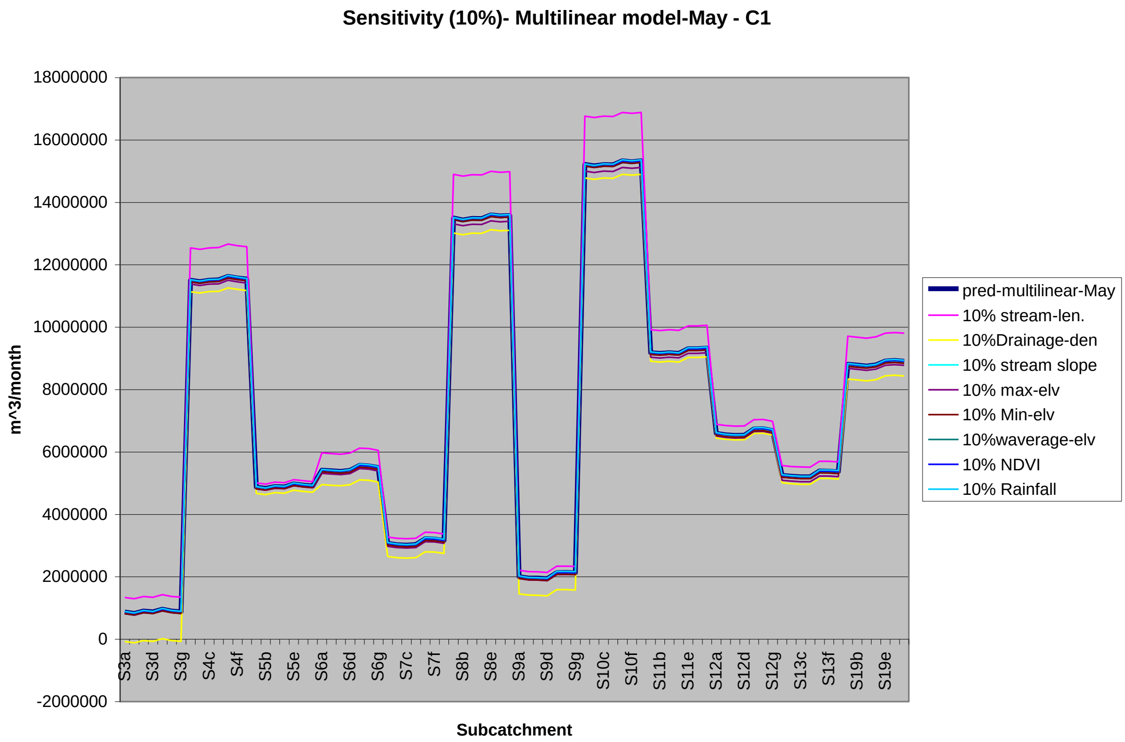

Figure C-17 Sensitivity (10%) – Multilinear model –May C1

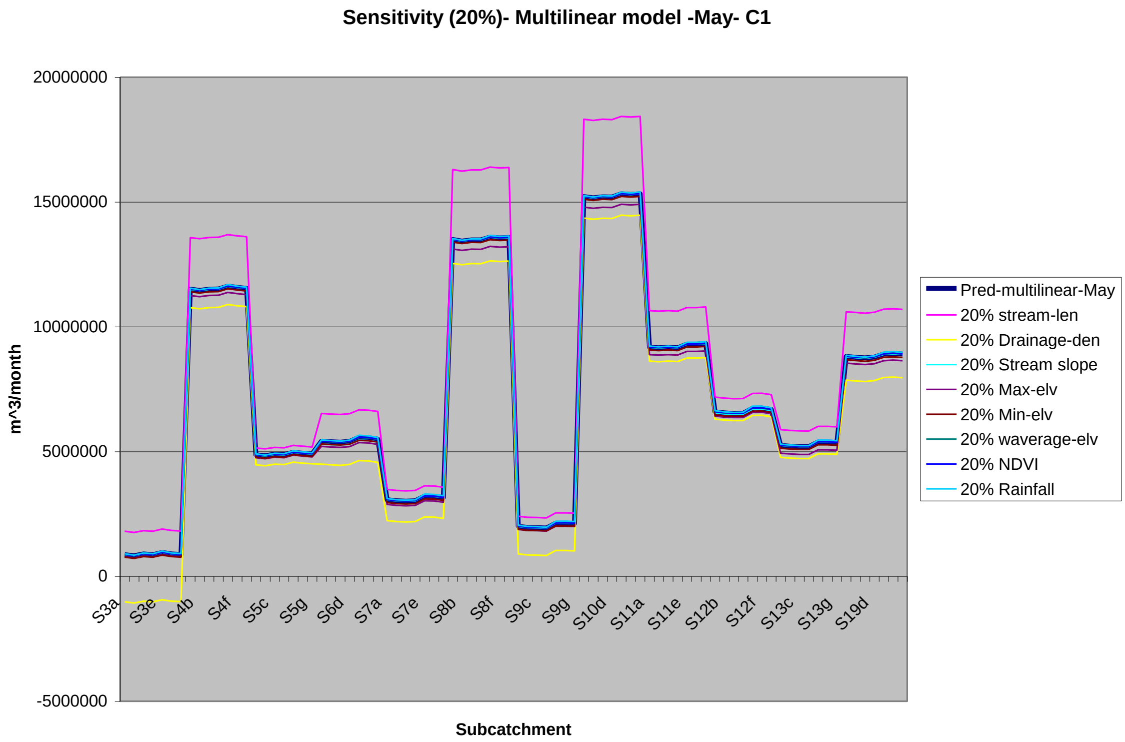

Figure C-18 Sensitivity (20%) – Multilinear model –May C1

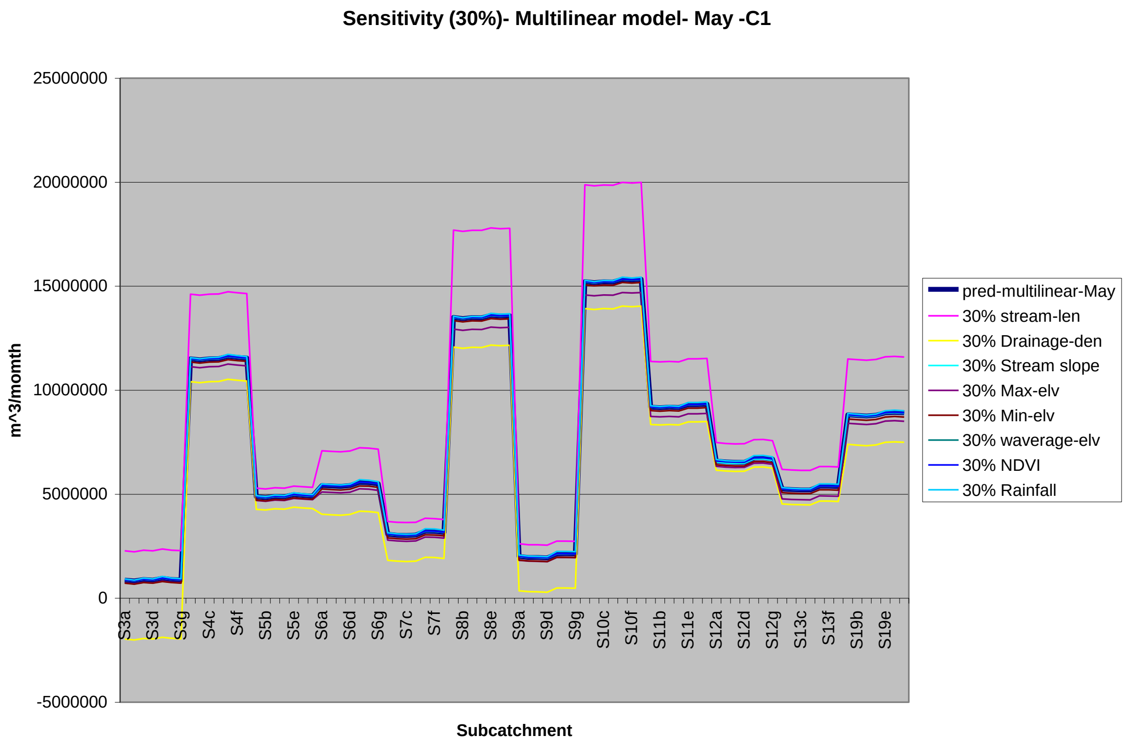

Figure C-19 Sensitivity (30%) – Multilinear model –May C1

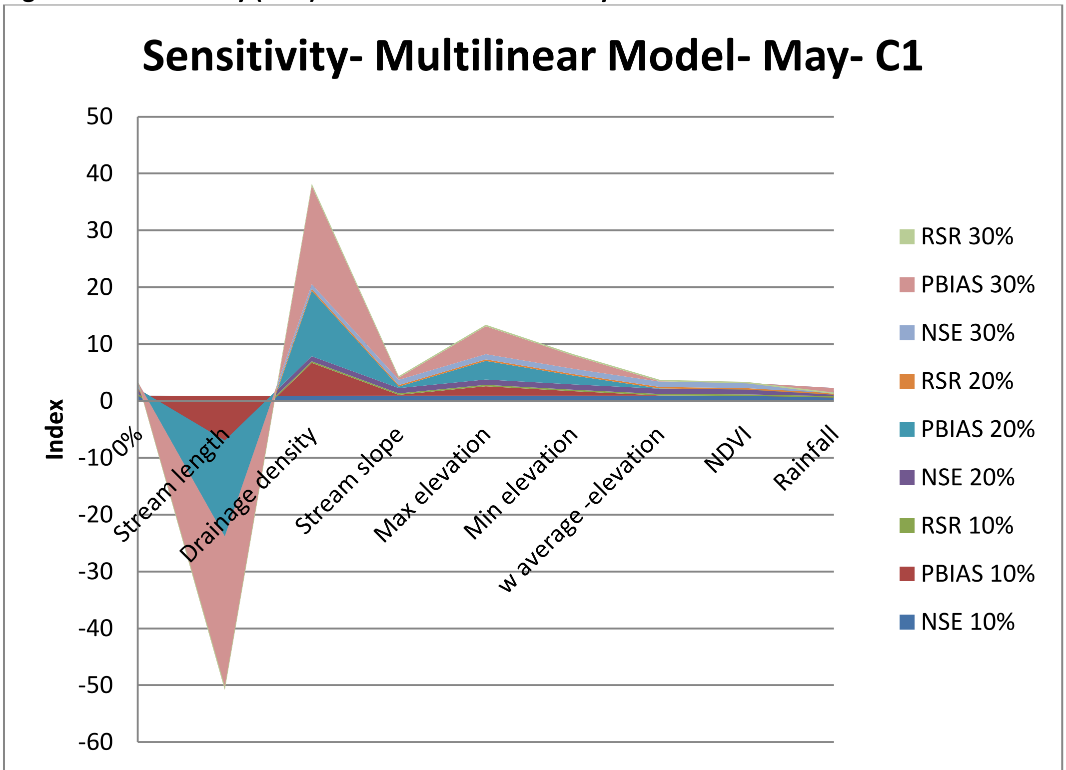

Figure C-20 Sensitivity summary – Multilinear model –May C1

Table C-5 Summary performance- Multilinear model- May C1

		10%							
	0%	Stream length	Drainage density	Stream slope	Max elevation	Min elevation	w average - elevation	NDVI	Rainfall
NSE	0.931716	0.900545	0.921146	0.9317	0.930888	0.931553	0.931716	0.931716	0.931684
PBIAS	0.023414	-8.9691	5.768793	0.142811	1.648416	0.792878	0.035563	-0.03501	-0.33618
RSR	0.261312	0.315366	0.28081	0.261343	0.262892	0.261623	0.261312	0.261312	0.261373
		20%							
	0%	**Stream length**	**Drainage density**	**Stream slope**	**Max elevation**	**Min elevation**	**w average - elevation**	**NDVI**	**Rainfall**
NSE	0.931716	0.806755	0.889572	0.931653	0.928448	0.931082	0.931716	0.931714	0.93158
PBIAS	0.023414	-17.9616	11.51417	0.262208	3.273417	1.562341	0.047711	-0.09344	-0.69578
RSR	0.261312	0.439596	0.332308	0.261432	0.267492	0.262522	0.261313	0.261316	0.261572
		30%							
	0%	**Stream length**	**Drainage density**	**Stream slope**	**Max elevation**	**Min elevation**	**w average - elevation**	**NDVI**	**Rainfall**
NSE	0.931716	0.650348	0.836994	0.931577	0.924396	0.930304	0.931715	0.931718	0.931404
PBIAS	0.023414	-26.9541	17.25955	0.381606	4.898419	2.331804	0.059859	-0.09394	-1.05538
RSR	0.261312	0.591314	0.40374	0.261579	0.274961	0.264	0.261313	0.261307	0.261909

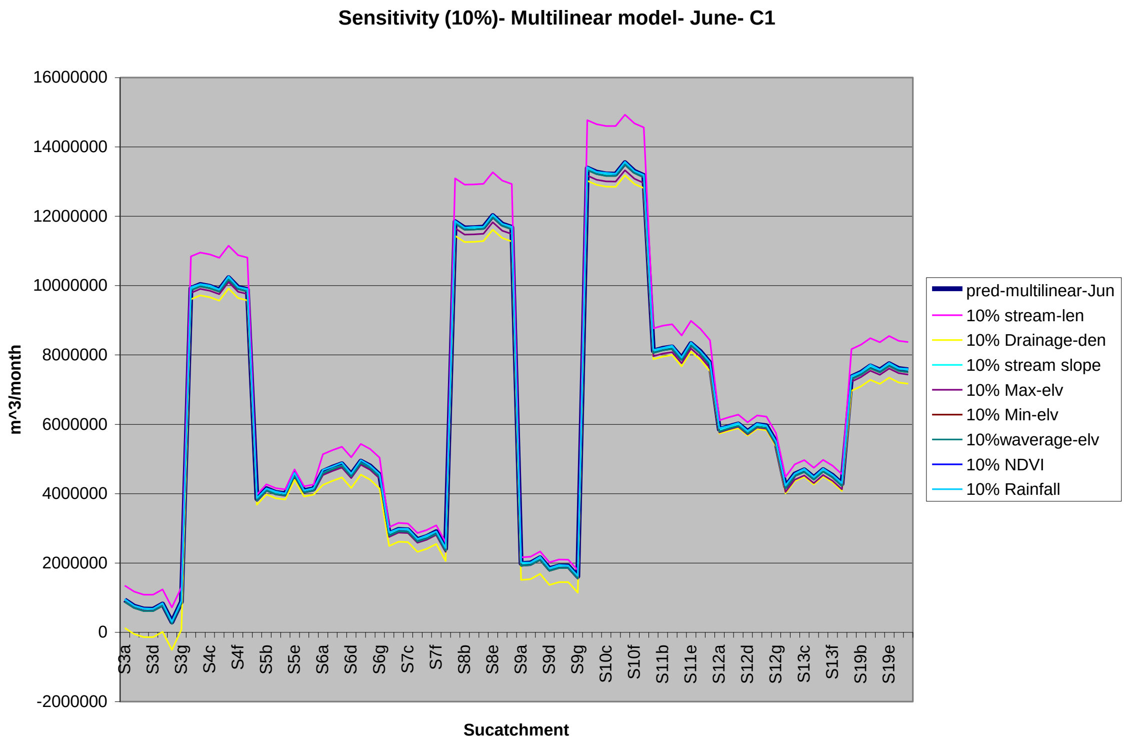

Figure C-21 Sensitivity (10%) – Multilinear model –June C1

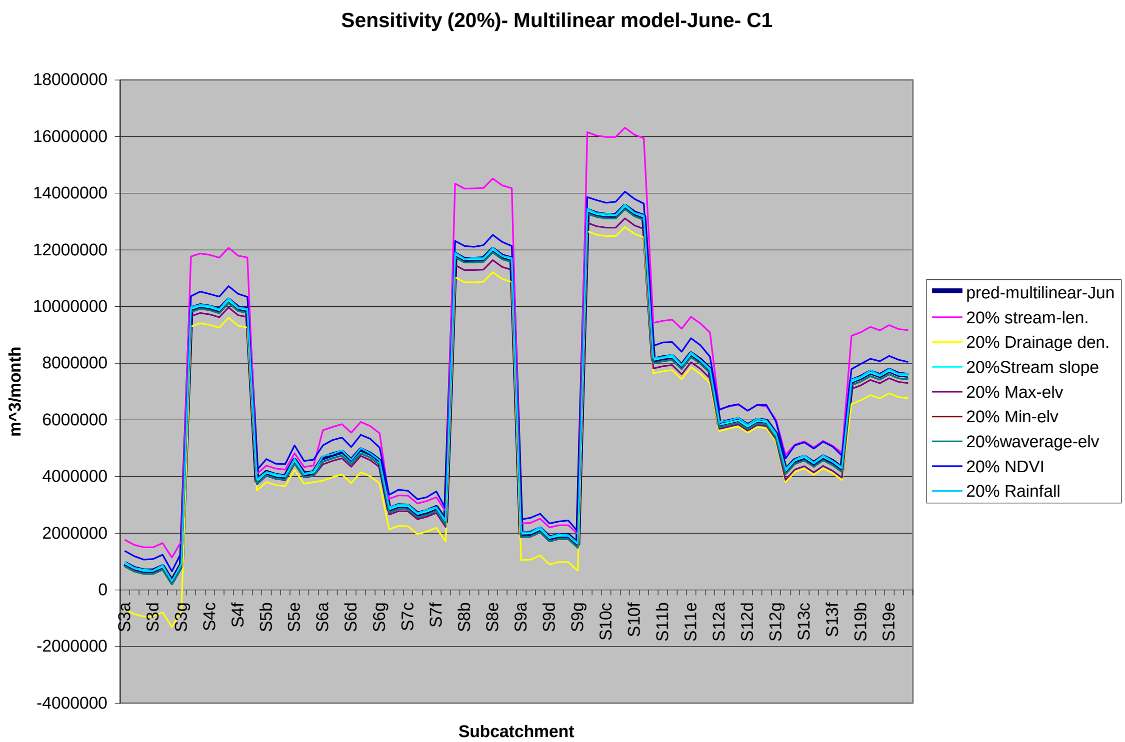

Figure C-22 Sensitivity (20%) – Multilinear model –June C1

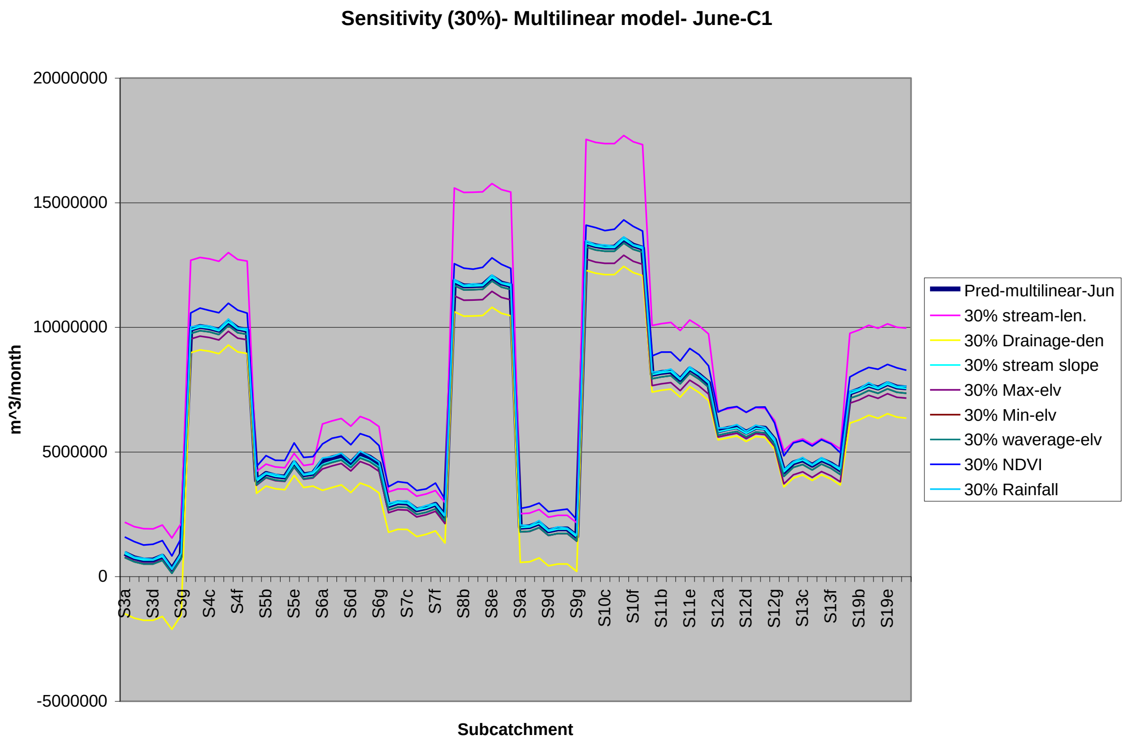

Figure C-23 Sensitivity (30%) – Multilinear model –June C1

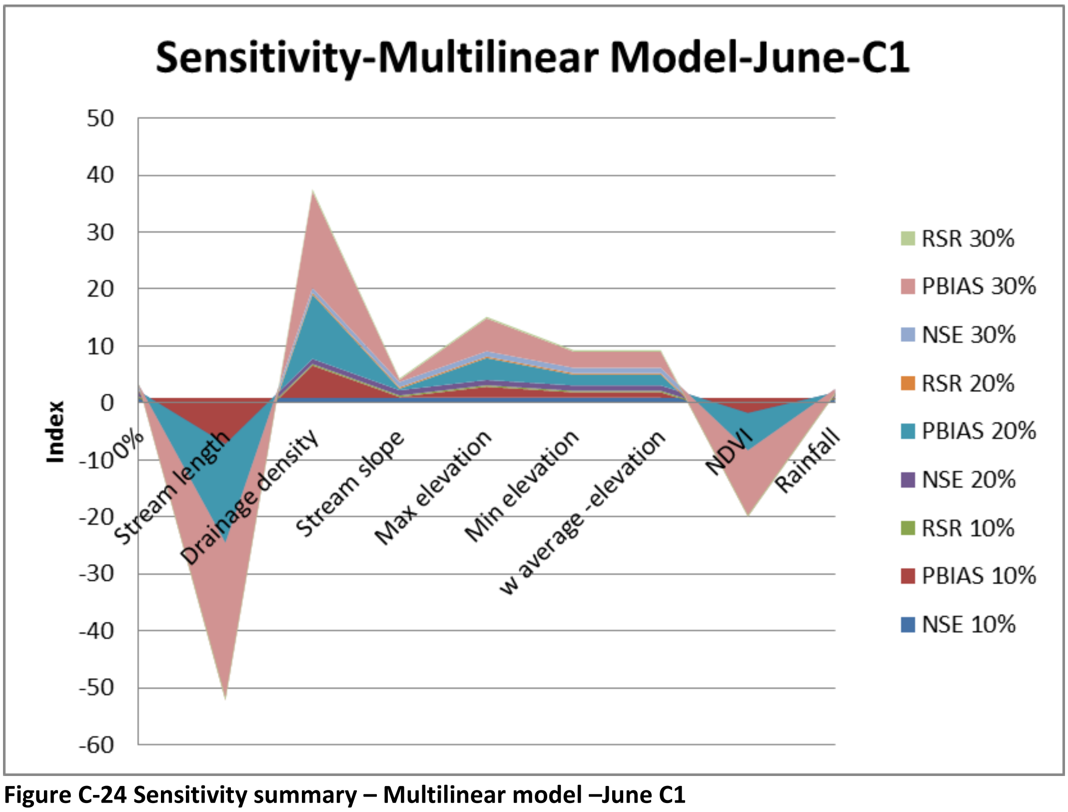

Figure C-24 Sensitivity summary – Multilinear model –June C1

Table C-6 Summary performance- Multilinear model- June C1

		10%							
	0%	Stream length	Drainage density	Stream slope	Max elevation	Min elevation	w average - elevation	NDVI	Rainfall
NSE	0.933821	0.901036	0.923641	0.933806	0.932675	0.933581	0.933581	0.929938	0.933796
PBIAS	0.022675	-9.20406	5.659955	0.138826	1.935876	0.96157	0.96157	-3.86254	-0.27835
RSR	0.257252	0.314585	0.276332	0.257282	0.259471	0.257718	0.257718	0.264692	0.257302
		20%							
	0%	Stream length	Drainage density	Stream slope	Max elevation	Min elevation	w average - elevation	NDVI	Rainfall
NSE	0.933821	0.802329	0.89324	0.933762	0.929294	0.932883	0.932883	0.9182	0.933713
PBIAS	0.022675	-18.4308	11.29723	0.254976	3.849076	1.900465	1.900465	-7.74775	-0.57937
RSR	0.257252	0.444602	0.326742	0.257368	0.265905	0.259069	0.259069	0.286008	0.257462
		30%							
	0%	Stream length	Drainage density	Stream slope	Max elevation	Min elevation	w average - elevation	NDVI	Rainfall
NSE	0.933821	0.637699	0.842618	0.933689	0.92368	0.931728	0.931728	0.898605	0.933573
PBIAS	0.022675	-27.6575	16.93451	0.371126	5.762277	2.83936	2.83936	-11.633	-0.88039
RSR	0.257252	0.601914	0.396714	0.257509	0.276261	0.26129	0.26129	0.318425	0.257734

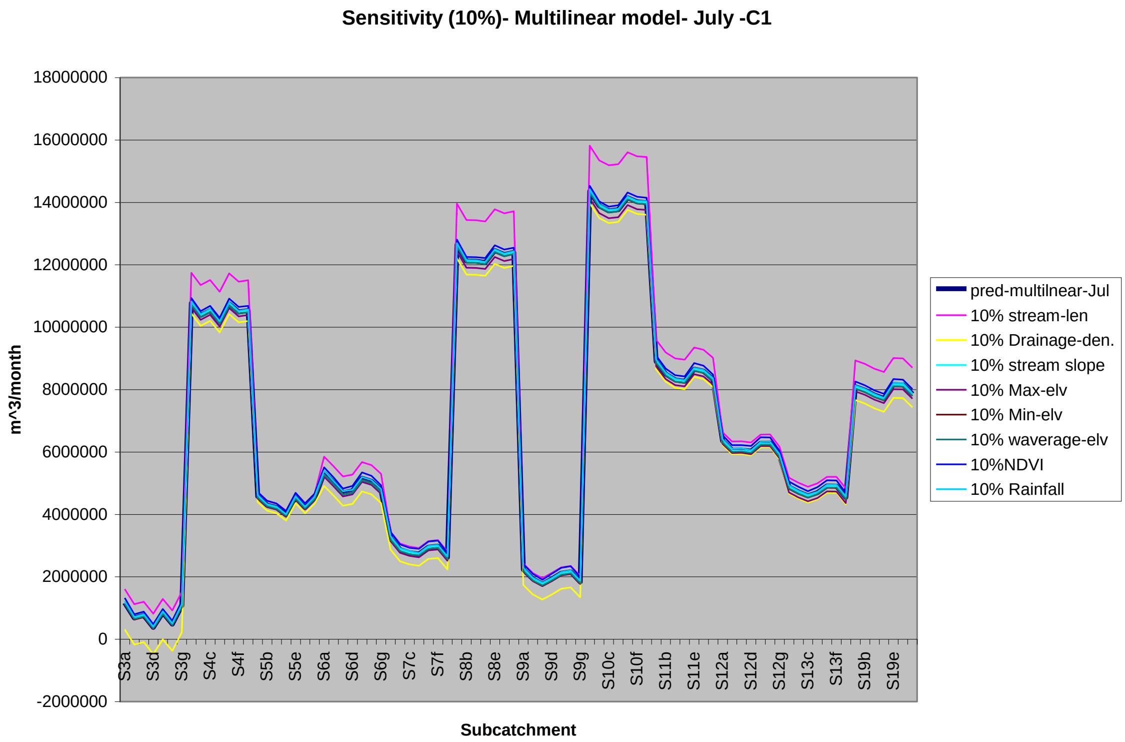

Figure C-25 Sensitivity (10%) – Multilinear model –July C1

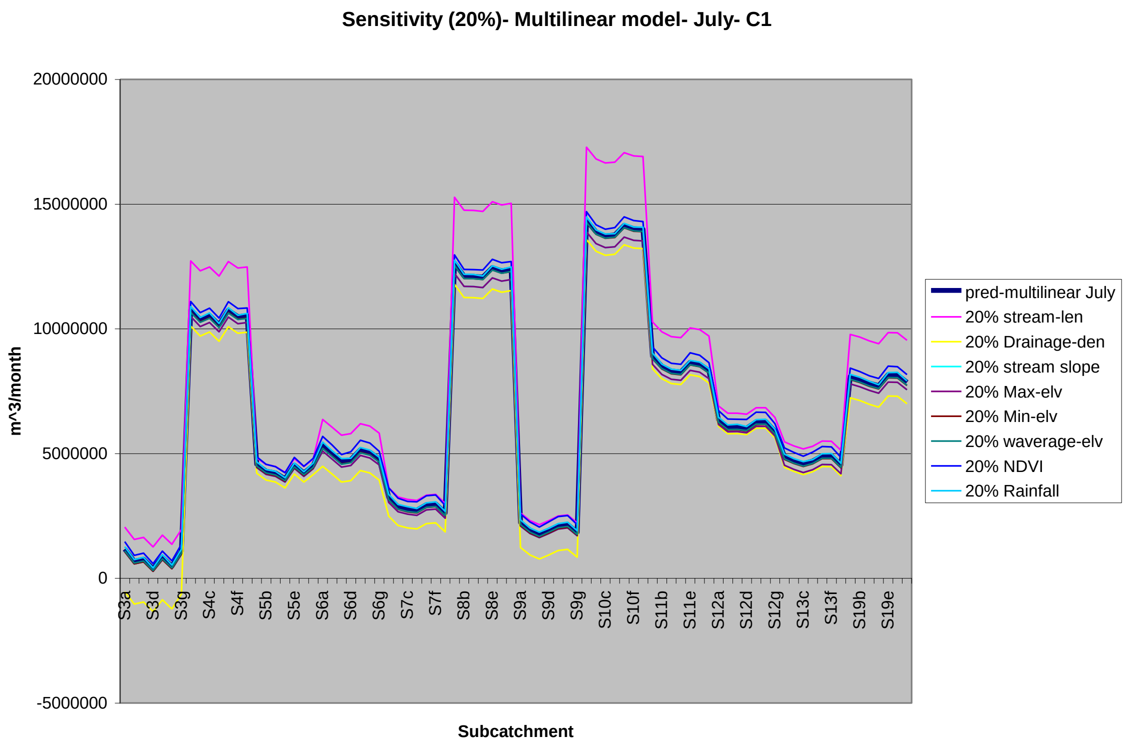

Figure C-26 Sensitivity (20%) – Multilinear model –July C1

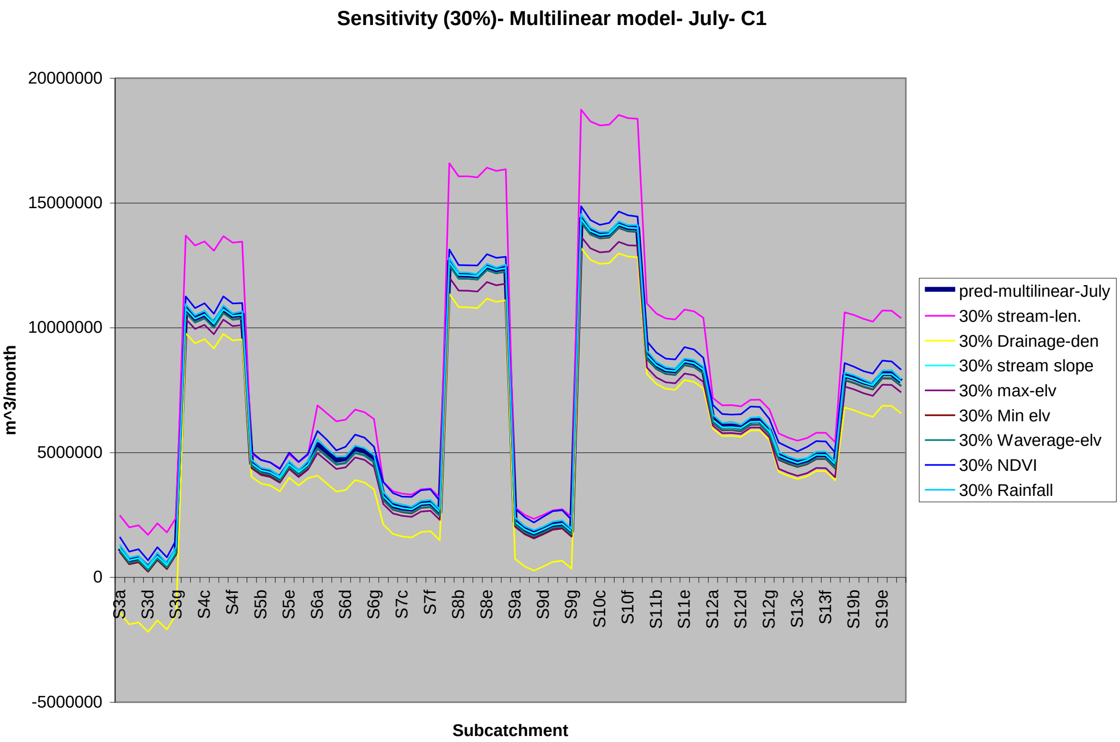

Figure C-27 Sensitivity (30%) – Multilinear model –July C1

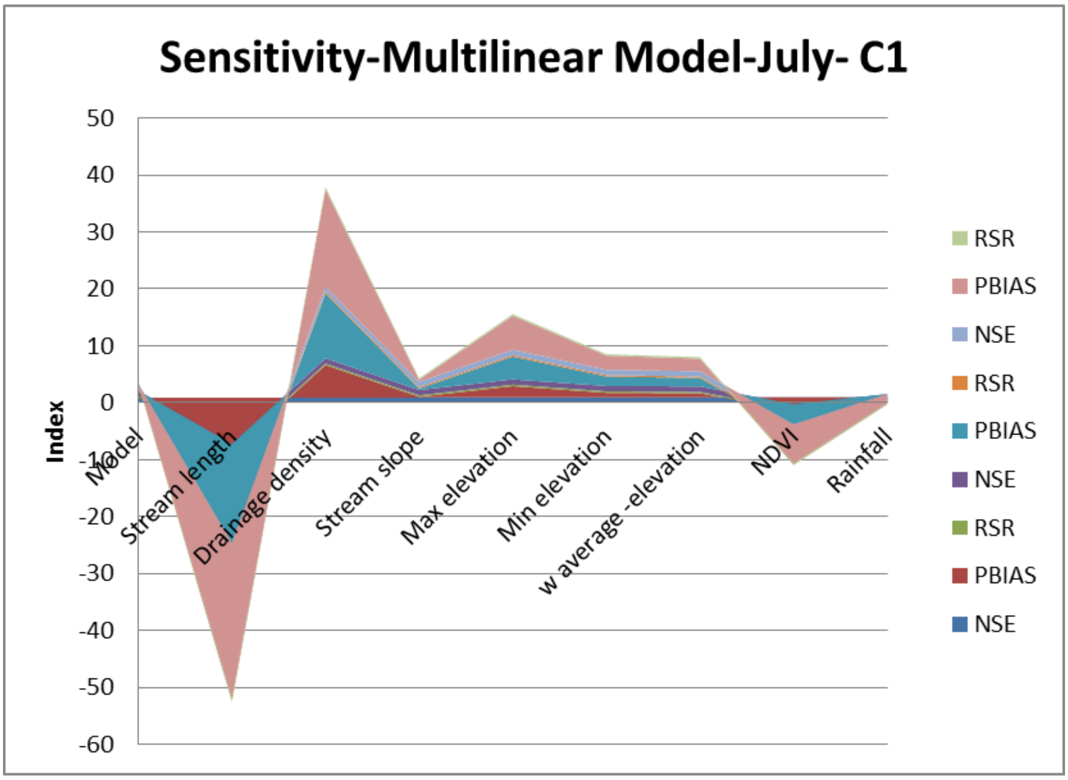

Figure C-28 Sensitivity summary – Multilinear model –July C1

Table C-7 Summary performance- Multilinear model- July C1

		10%							
	0%	**Stream length**	**Drainage density**	**Stream slope**	**Max elevation**	**Min elevation**	**w average - elevation**	**NDVI**	**Rainfall**
NSE	0.934256	0.901139	0.923873	0.934241	0.933028	0.934073	0.934107	0.932798	0.934161
PBIAS	0.019726	-9.24589	5.715001	0.134163	2.007058	0.839338	0.75066	-2.35821	-0.58851
RSR	0.256405	0.314421	0.275912	0.256434	0.258789	0.256762	0.256696	0.259234	0.256591
		20%							
	0%	**Stream length**	**Drainage density**	**Stream slope**	**Max elevation**	**Min elevation**	**w average - elevation**	**NDVI**	**Rainfall**
NSE	0.934256	0.801544	0.892851	0.934199	0.92939	0.933542	0.933676	0.928373	0.933863
PBIAS	0.019726	-18.5115	11.41028	0.2486	3.99439	1.65895	1.481594	-4.73614	-1.19674
RSR	0.256405	0.445485	0.327337	0.256518	0.265726	0.257795	0.257535	0.267631	0.25717
		30%							
	0%	**Stream length**	**Drainage density**	**Stream slope**	**Max elevation**	**Min elevation**	**w average - elevation**	**NDVI**	**Rainfall**
NSE	0.934256	0.635469	0.84119	0.934128	0.923341	0.932661	0.932961	0.920984	0.933363
PBIAS	0.019726	-27.7771	17.10555	0.363036	5.981722	2.478561	2.212527	-7.11408	-1.80498
RSR	0.256405	0.603764	0.39851	0.256655	0.276874	0.259498	0.258918	0.281098	0.258141

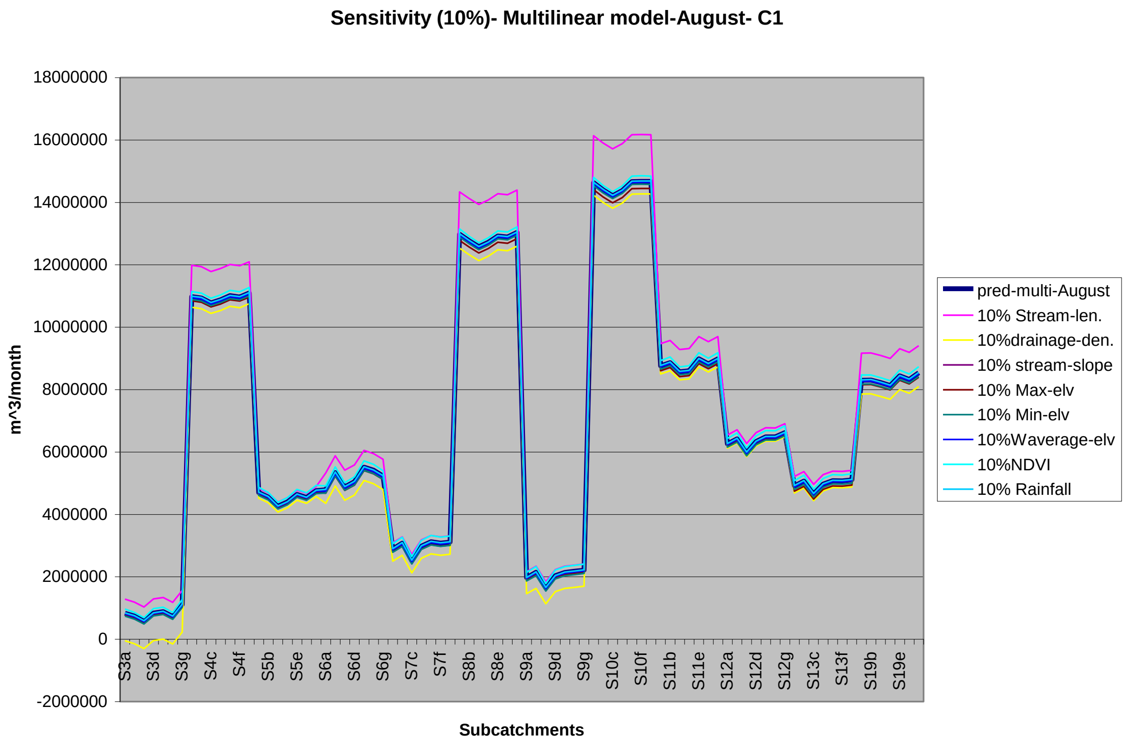

Figure C-29 Sensitivity (10%) – Multilinear model –August C1

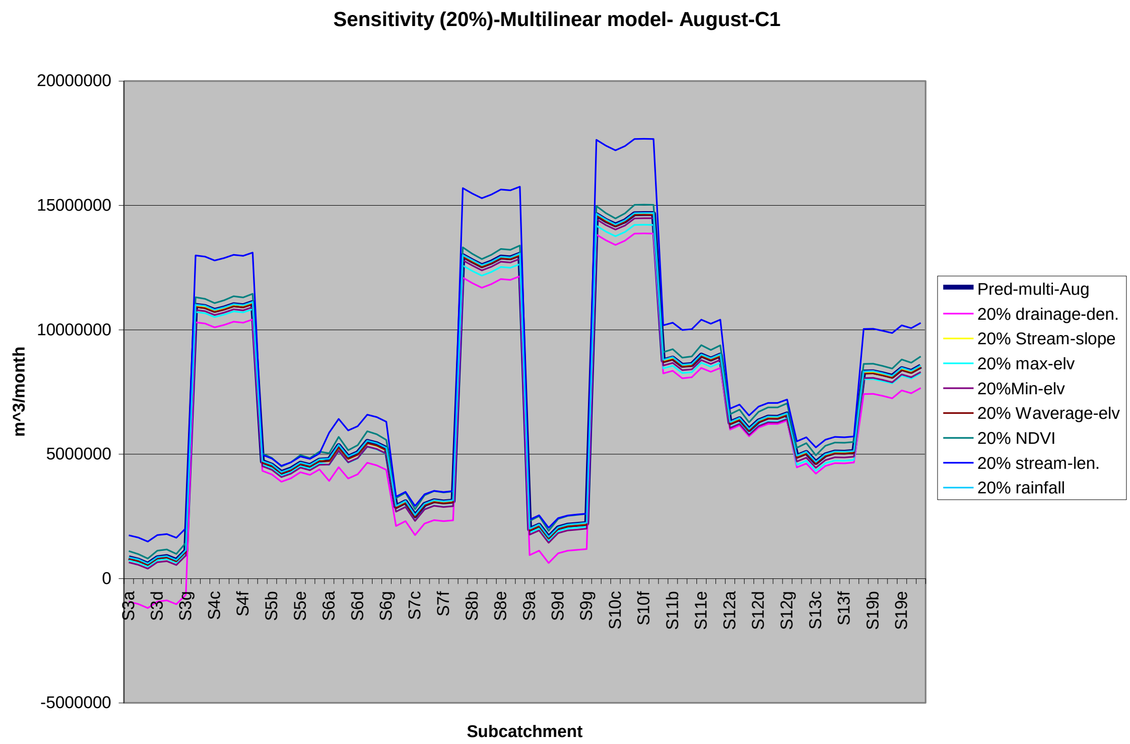

Figure C-30 Sensitivity (20%) – Multilinear model –August C1

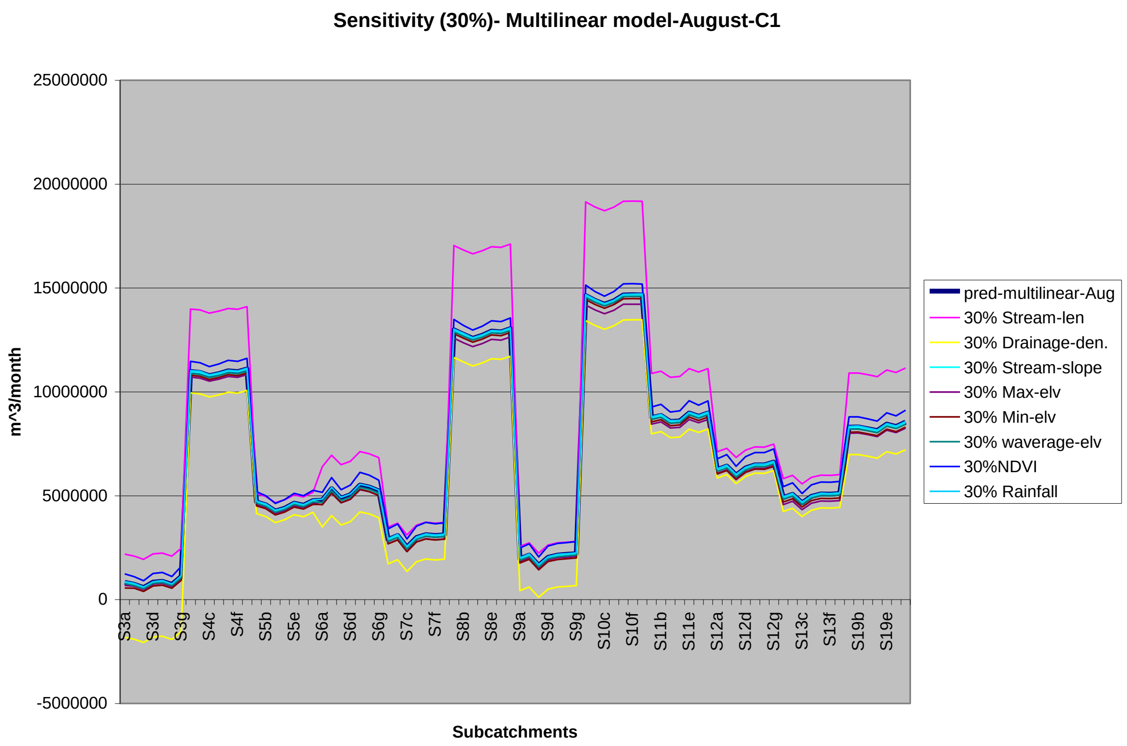

Figure C-31 Sensitivity (30%) – Multilinear model –August C1

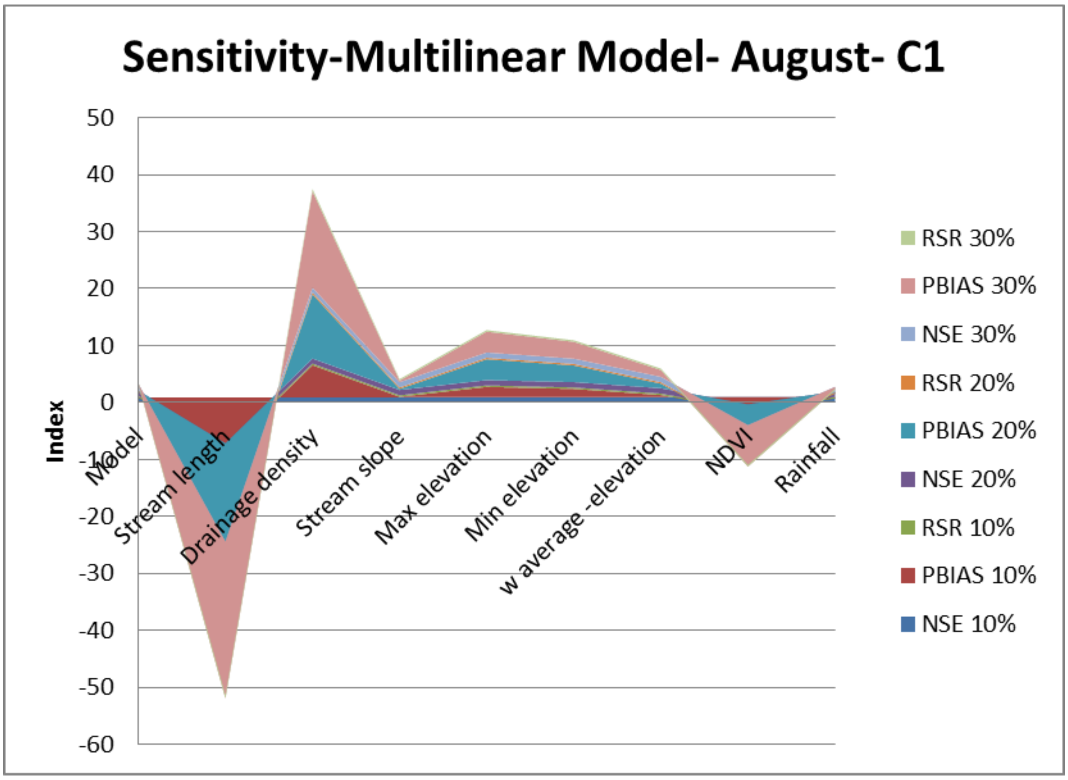

Figure C-32 Sensitivity summary – Multilinear model –August C1

Table C-8 Summary performance- Multilinear model- August C1

		10%							
	0%	**Stream length**	**Drainage density**	**Stream slope**	**Max elevation**	**Min elevation**	**w average - elevation**	**NDVI**	**Rainfall**
NSE	0.933328	0.900767554	0.923215642	0.933319594	0.932312111	0.932770168	0.933286298	0.931785	0.933319
PBIAS	-0.00427	-9.171824288	5.638004839	0.088042014	1.82405379	1.465756731	0.39873335	-2.42377	-0.18976
RSR	0.258208	0.315011818	0.277099906	0.258225494	0.260168962	0.259287161	0.258289958	0.261179	0.258227
		20%							
	0%	**Stream length**	**Drainage density**	**Stream slope**	**Max elevation**	**Min elevation**	**w average - elevation**	**NDVI**	**Rainfall**
NSE	0.933328	0.803127526	0.892846457	0.933292762	0.929255596	0.931089045	0.933158246	0.927166	0.933291
PBIAS	-0.00427	-18.33937966	11.28027859	0.180352945	3.652376496	2.935782379	0.801735616	-4.84328	-0.37525
RSR	0.258208	0.443703137	0.327343158	0.258277444	0.265978203	0.262508961	0.258537722	0.269877	0.258282
		30%							
	0%	**Stream length**	**Drainage density**	**Stream slope**	**Max elevation**	**Min elevation**	**w average - elevation**	**NDVI**	**Rainfall**
NSE	0.933328	0.640408317	0.842220845	0.933247904	0.929174855	0.930920998	0.932944247	0.919472	0.933244
PBIAS	-0.00427	-27.50693503	16.92255235	0.272663876	3.660784994	2.951884313	1.204737883	-7.26278	-0.56074
RSR	0.258208	0.599659639	0.397214243	0.258364269	0.26612994	0.262828845	0.258951256	0.283775	0.258372

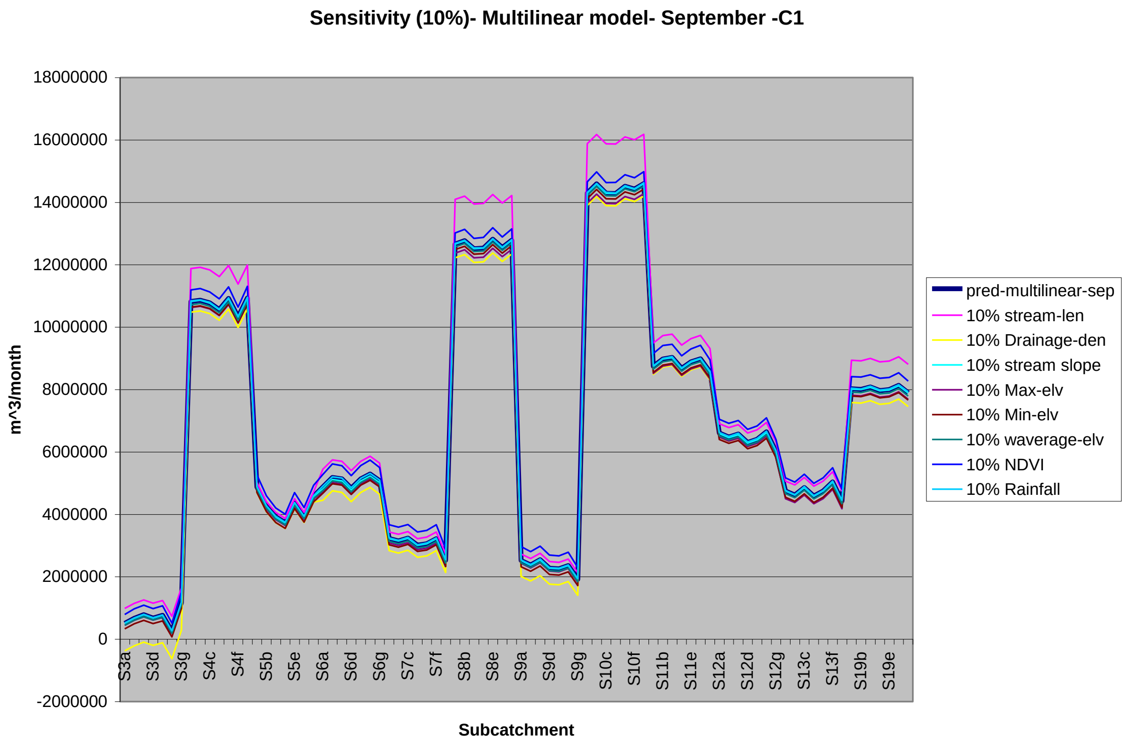

Figure C-33 Sensitivity (10%) – Multilinear model –September C1

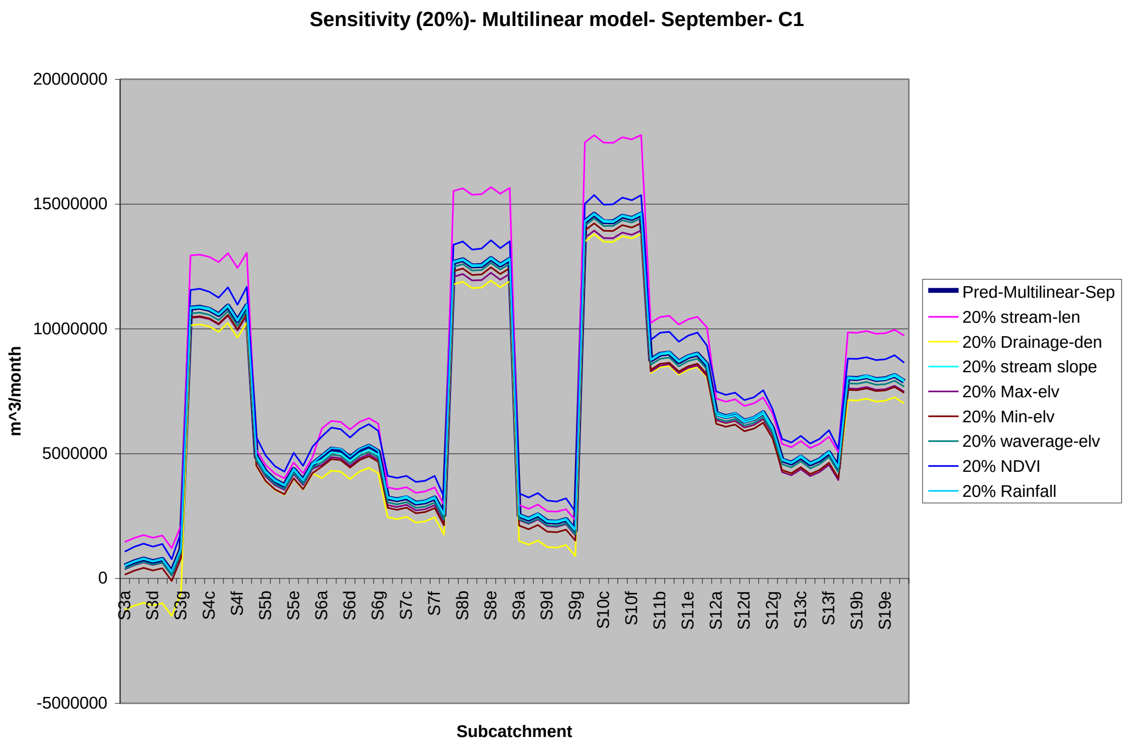

Figure C-34 Sensitivity (20%) – Multilinear model –September C1

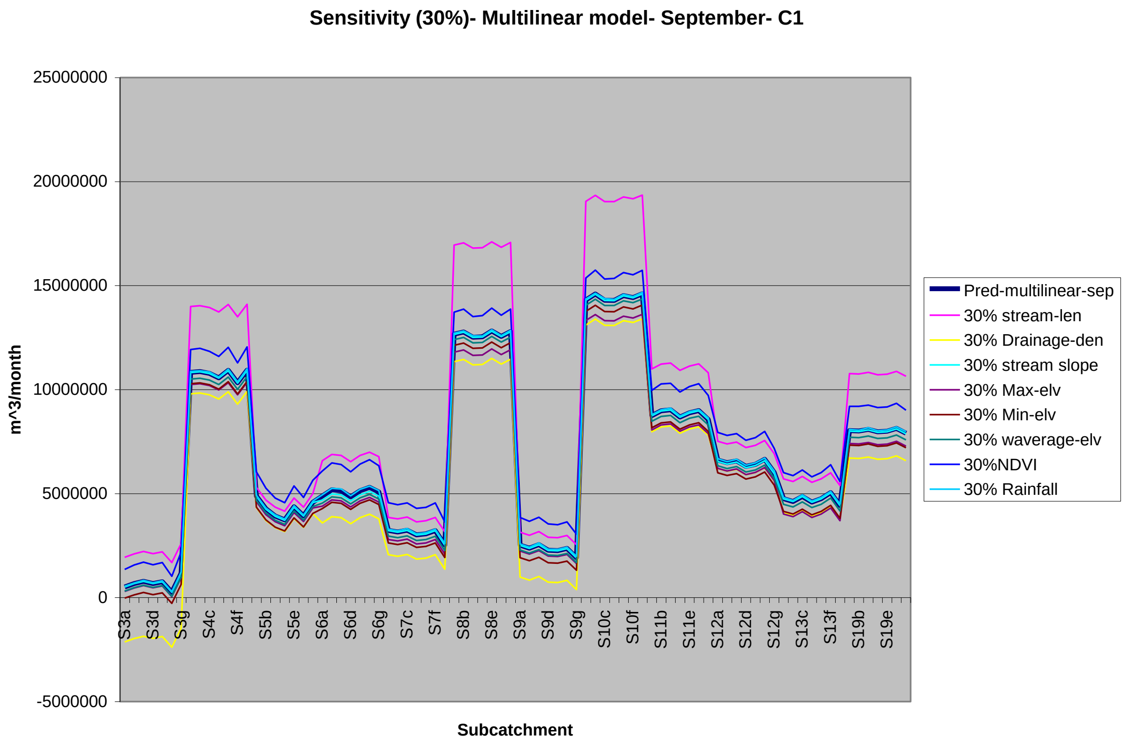

Figure C-35 Sensitivity (30%) – Multilinear model –September C1

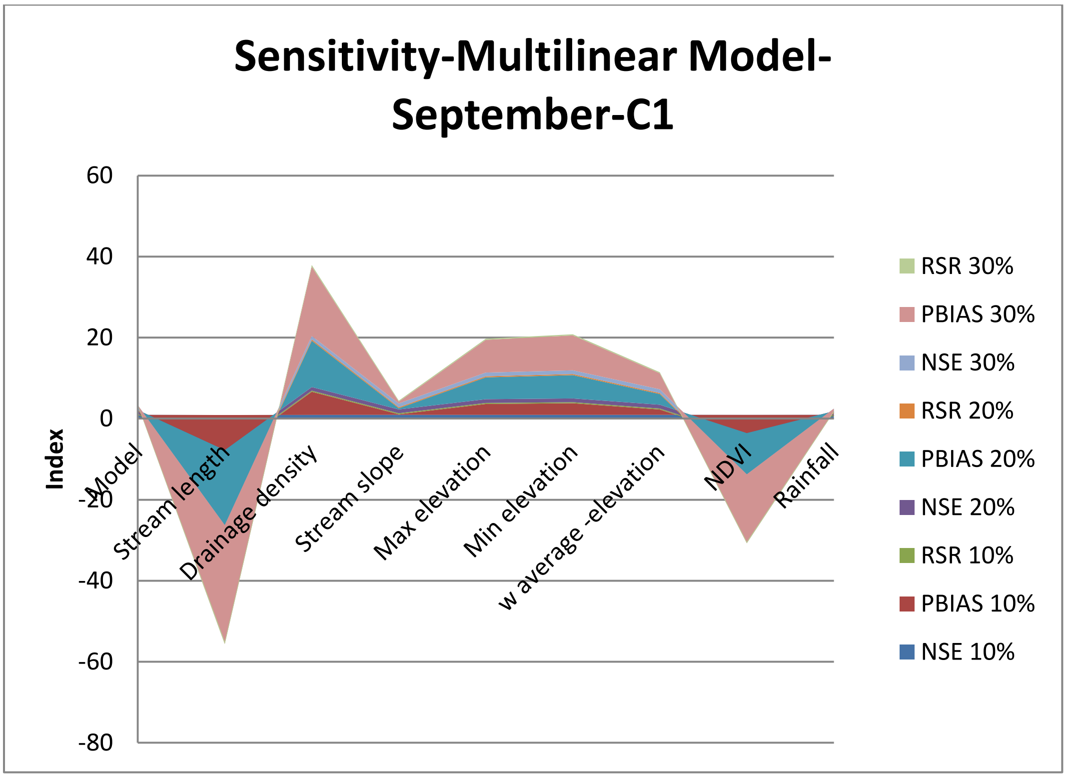

Figure C-36 Sensitivity summary – Multilinear model –September C1

Table C-9 Summary performance- Multilinear model- September C1

		10%							
	0%	**Stream length**	**Drainage density**	**Stream slope**	**Max elevation**	**Min elevation**	**w average - elevation**	**NDVI**	**Rainfall**
NSE	0.936941	0.899871	0.926557	0.936918	0.934732	0.934793	0.936482	0.928519	0.93692
PBIAS	0.003844	-9.78161	5.713096	0.149843	2.692549	2.875457	1.317273	-5.66939	-0.27768
RSR	0.251115	0.316432	0.271004	0.251161	0.255475	0.255357	0.252027	0.26736	0.251157
		20%							
	0%	**Stream length**	**Drainage density**	**Stream slope**	**Max elevation**	**Min elevation**	**w average - elevation**	**NDVI**	**Rainfall**
NSE	0.936941	0.788653	0.895432	0.93685	0.928112	0.92836	0.935111	0.903229	0.936856
PBIAS	0.003844	-19.5671	11.42235	0.295842	5.381255	5.747071	2.630701	-11.3426	-0.55921
RSR	0.251115	0.459725	0.32337	0.251296	0.26812	0.267657	0.254734	0.31108	0.251284
		30%							
	0%	**Stream length**	**Drainage density**	**Stream slope**	**Max elevation**	**Min elevation**	**w average - elevation**	**NDVI**	**Rainfall**
NSE	0.936941	0.603288	0.843567	0.936737	0.917078	0.917642	0.932826	0.861072	0.936749
PBIAS	0.003844	-29.3525	17.1316	0.441841	8.06996	8.618684	3.94413	-17.0159	-0.84073
RSR	0.251115	0.629851	0.395516	0.251521	0.287961	0.286981	0.25918	0.37273	0.251497

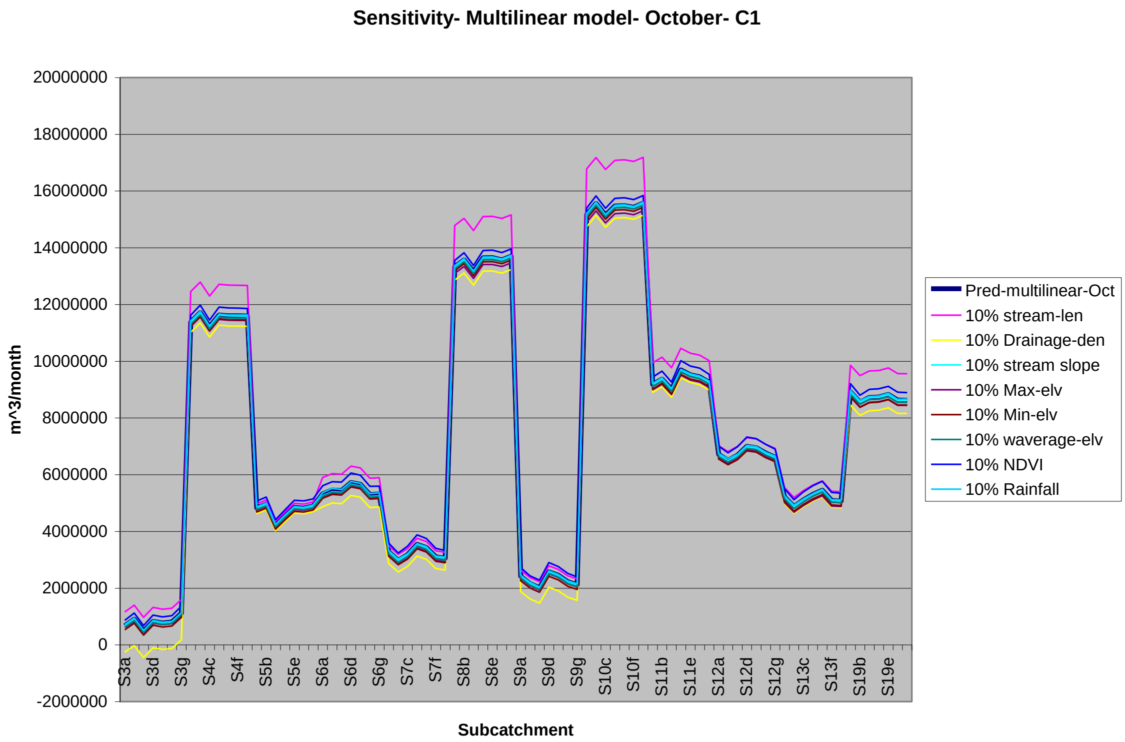

Figure C-37 Sensitivity (10%) – Multilinear model –October C1

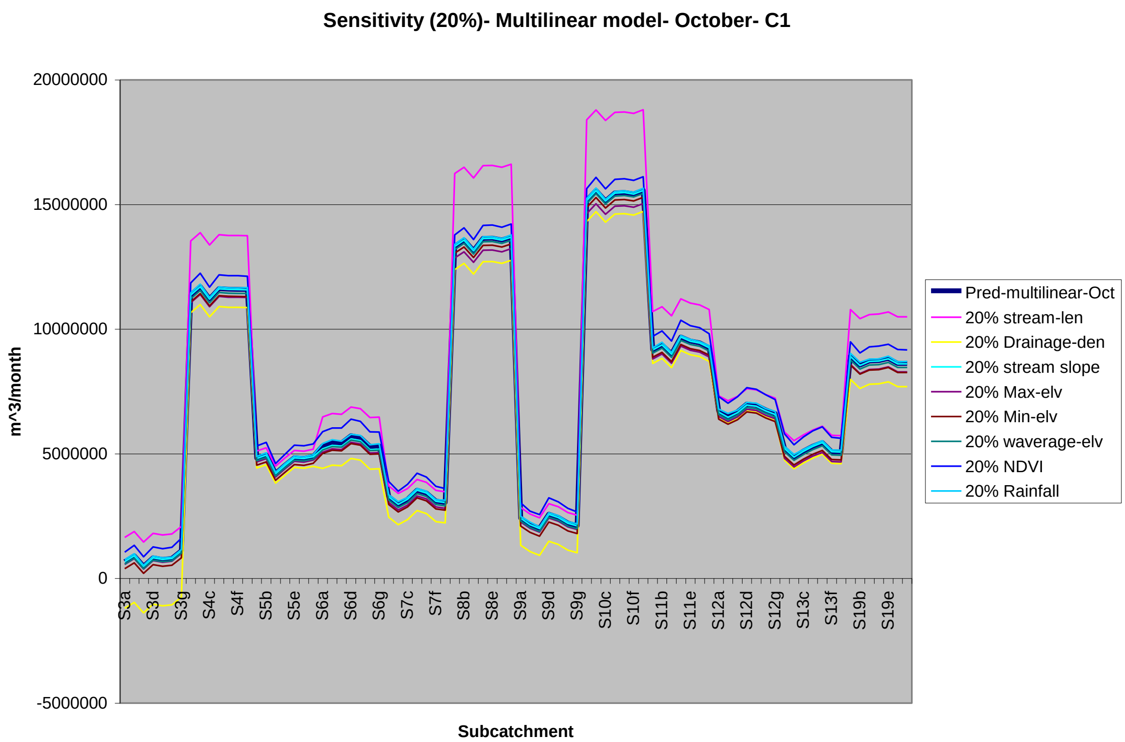

Figure C-38 Sensitivity (20%) – Multilinear model –October C1

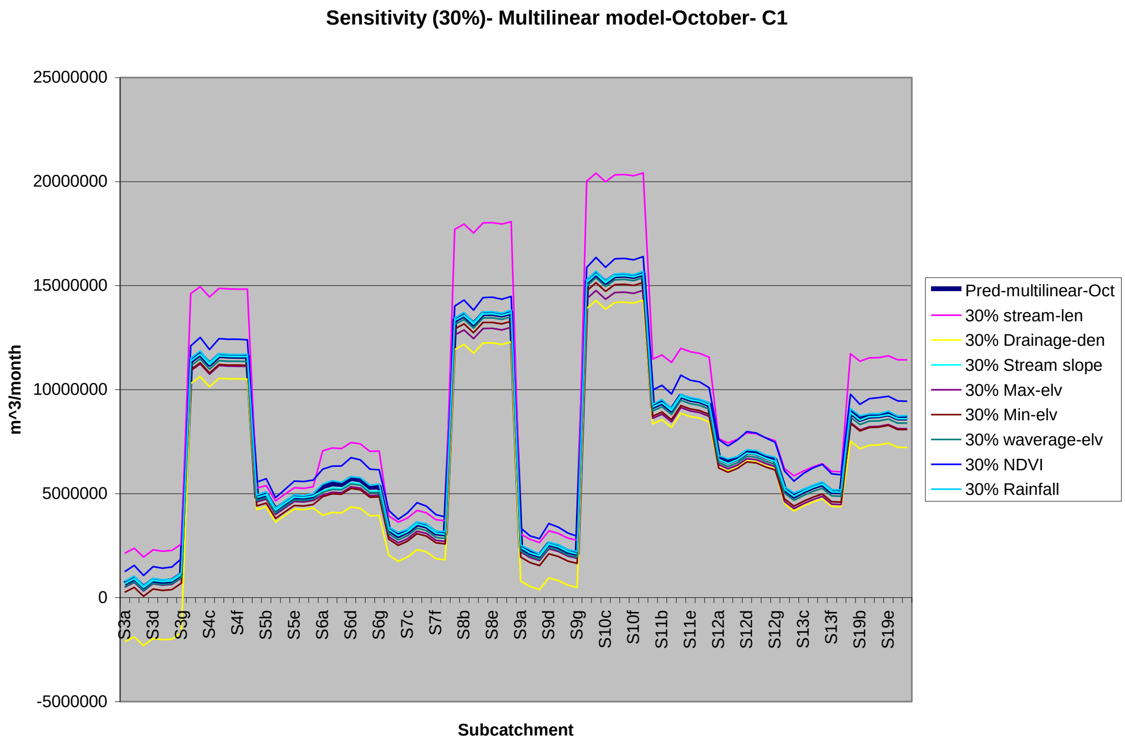

Figure C-39 Sensitivity (30%) – Multilinear model –October C1

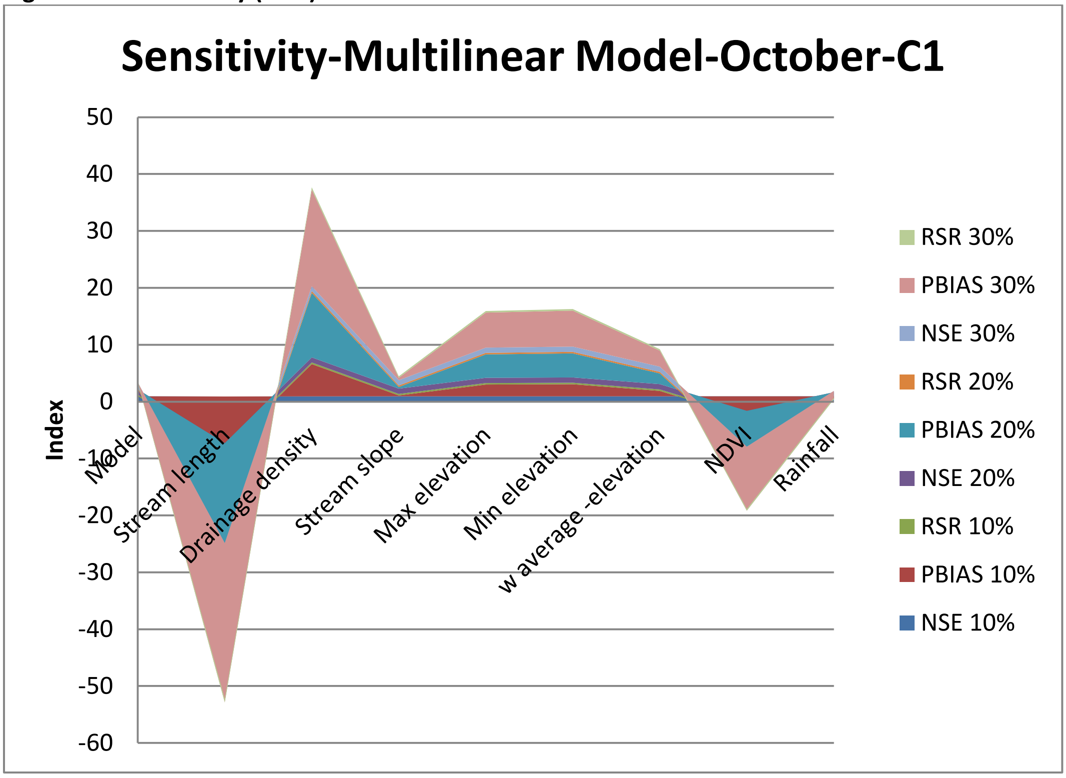

Figure C-40 Sensitivity summary – Multilinear model –October C1

Table C-10 Summary performance- Multilinear model- October C1

		10%							
	0%	Stream length	Drainage density	Stream slope	Max elevation	Min elevation	w average - elevation	NDVI	Rainfall
NSE	0.934051	0.900462	0.923795	0.934031	0.932744	0.932877	0.933811	0.930401	0.933991
PBIAS	0.024921	-9.31391	5.680752	0.158502	2.068755	2.126886	0.953262	-3.73227	-0.47176
RSR	0.256805	0.315496	0.276052	0.256844	0.259337	0.259081	0.257272	0.263817	0.256922
		20%							
	0%	**Stream length**	**Drainage density**	**Stream slope**	**Max elevation**	**Min elevation**	**w average - elevation**	**NDVI**	**Rainfall**
NSE	0.934051	0.799339	0.893185	0.933973	0.928888	0.929406	0.933115	0.919355	0.933797
PBIAS	0.024921	-18.6527	11.33658	0.292083	4.112589	4.228851	1.881602	-7.48947	-0.96843
RSR	0.256805	0.447952	0.326826	0.256957	0.266668	0.265694	0.258622	0.283981	0.257299
		30%							
	0%	**Stream length**	**Drainage density**	**Stream slope**	**Max elevation**	**Min elevation**	**w average - elevation**	**NDVI**	**Rainfall**
NSE	0.934051	0.630683	0.842221	0.933877	0.922482	0.92364	0.931962	0.900913	0.93347
PBIAS	0.024921	-27.9916	16.99241	0.425664	6.156423	6.330815	2.809943	-11.2467	-1.46511
RSR	0.256805	0.607715	0.397214	0.257144	0.27842	0.276333	0.26084	0.314782	0.257934

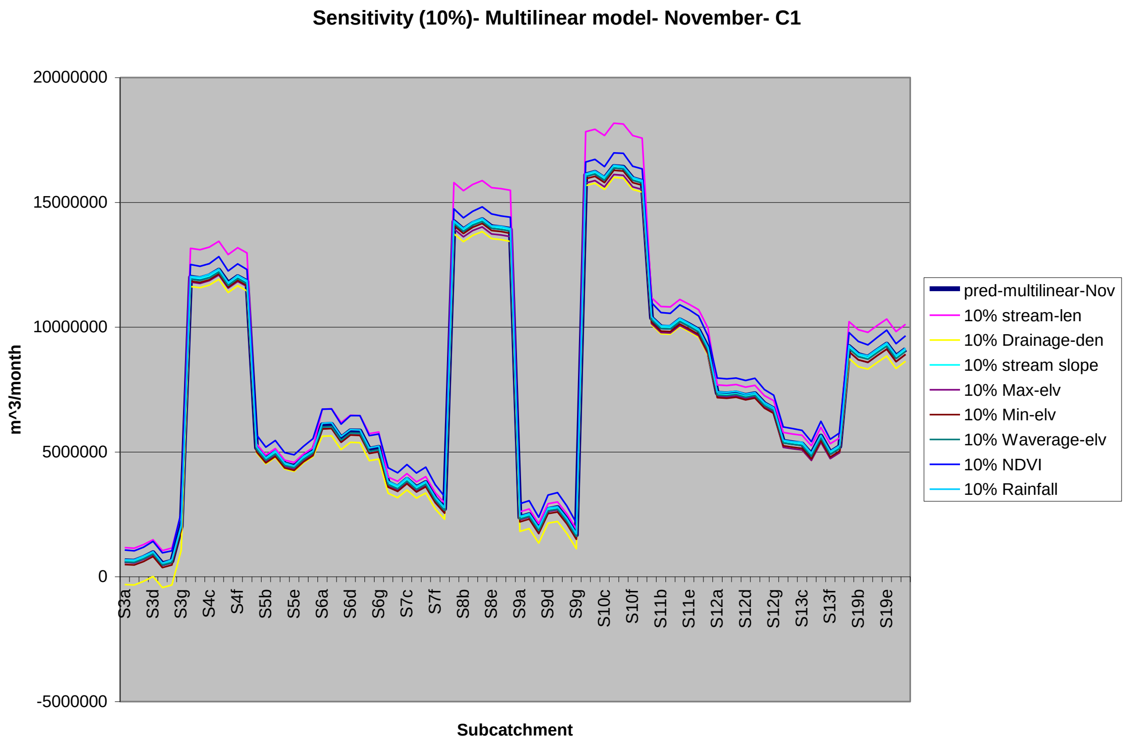

Figure C-41 Sensitivity (10%) – Multilinear model –November C1

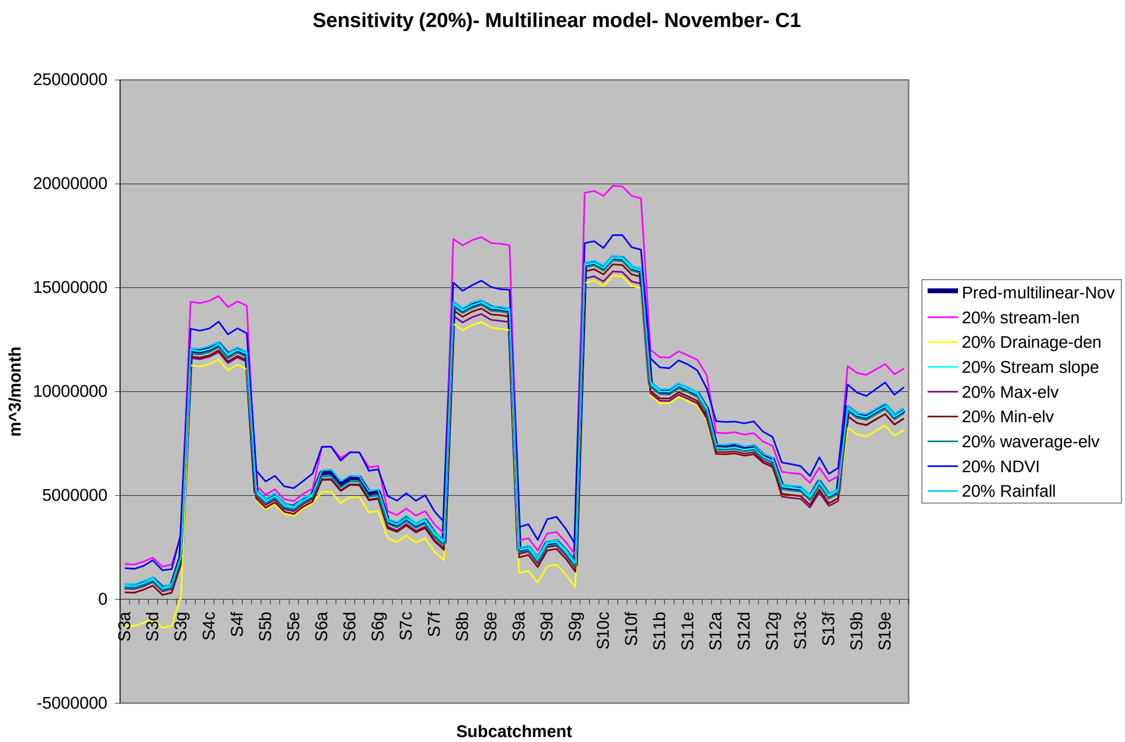

Figure C-42 Sensitivity (20%) – Multilinear model –November C1

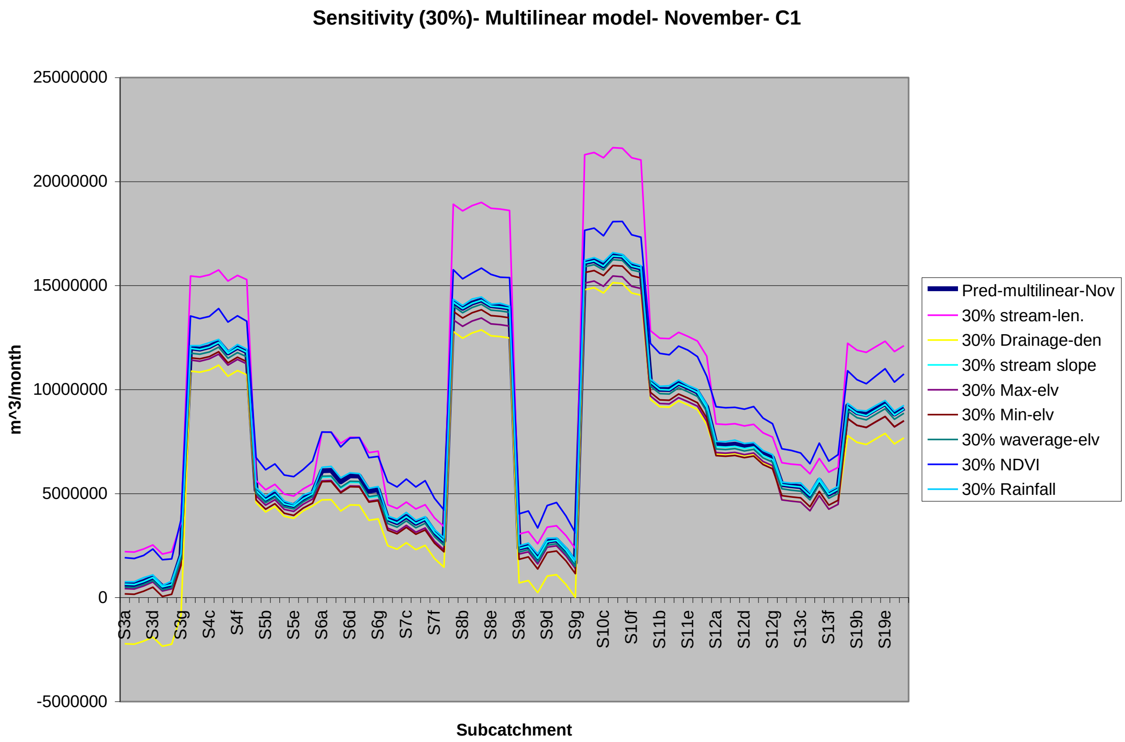

Figure C-43 Sensitivity (30%) – Multilinear model –November C1

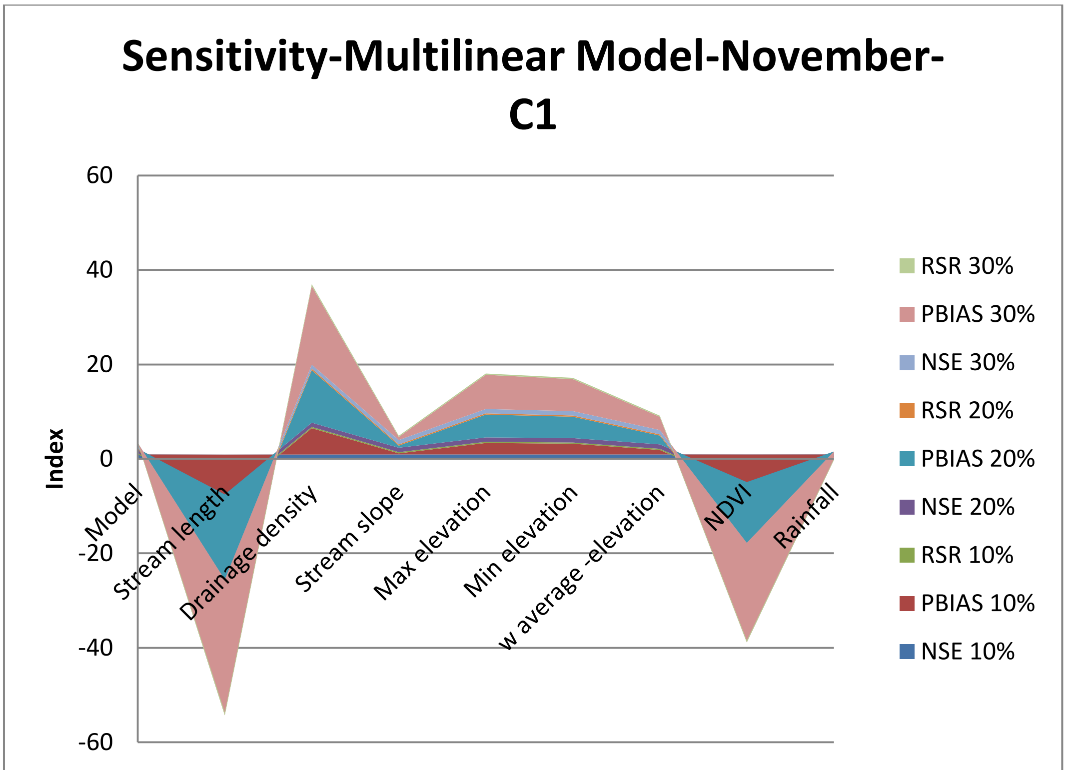

Figure C-44 Sensitivity Summary – Multilinear model –November C1

Table C-11 Summary performance- Multilinear model- November C1

		10%							
	0%	**Stream length**	**Drainage density**	**Stream slope**	**Max elevation**	**Min elevation**	**w average - elevation**	**NDVI**	**Rainfall**
NSE	0.937932	0.902645	0.928089	0.937883	0.936132	0.936585	0.937696	0.925146	0.937839
PBIAS	0.027235	-9.54472	5.567544	0.235273	2.428303	2.277294	0.944695	-7.00187	-0.58417
RSR	0.249135	0.312018	0.268162	0.249232	0.252722	0.251823	0.249608	0.273594	0.249321
		20%							
	0%	**Stream length**	**Drainage density**	**Stream slope**	**Max elevation**	**Min elevation**	**w average - elevation**	**NDVI**	**Rainfall**
NSE	0.937932	0.796411	0.898715	0.937743	0.930813	0.932608	0.937014	0.886594	0.937543
PBIAS	0.027235	-19.1167	11.10785	0.443311	4.829372	4.527353	1.862156	-14.031	-1.19558
RSR	0.249135	0.451209	0.318253	0.249513	0.263034	0.2596	0.250969	0.336758	0.249914
		30%							
	0%	**Stream length**	**Drainage density**	**Stream slope**	**Max elevation**	**Min elevation**	**w average - elevation**	**NDVI**	**Rainfall**
NSE	0.937932	0.619229	0.849811	0.937512	0.921976	0.926	0.935887	0.822274	0.937044
PBIAS	0.027235	-28.6886	16.64816	0.651349	7.230441	6.777411	2.779617	-21.0601	-1.80699
RSR	0.249135	0.617067	0.387543	0.249976	0.279328	0.27203	0.253205	0.421576	0.25091

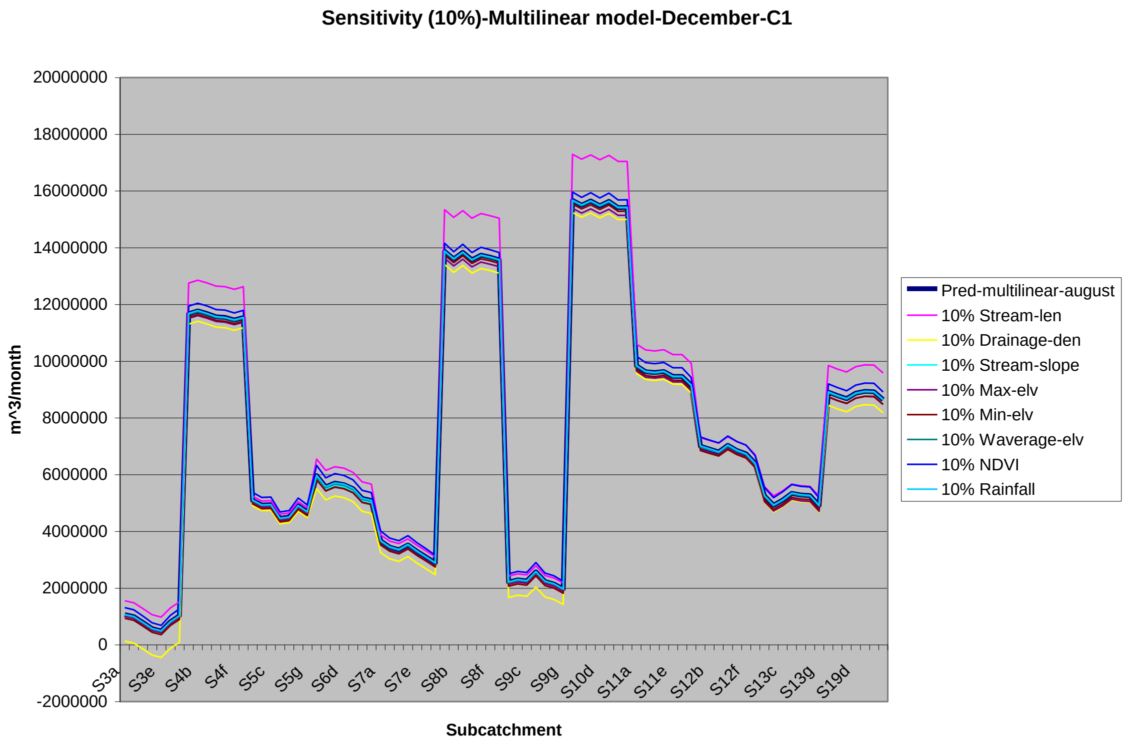

Figure C-45 Sensitivity (10%) – Multilinear model –December C1

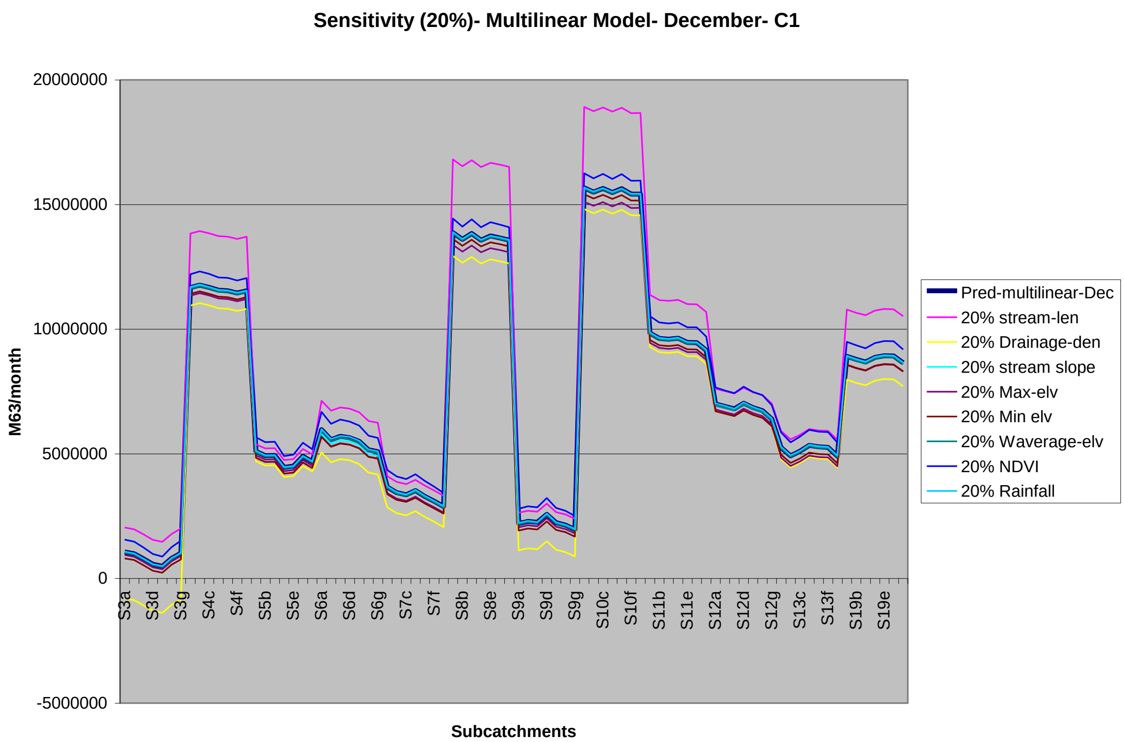

Figure C-46 Sensitivity (20%) – Multilinear model –December C1

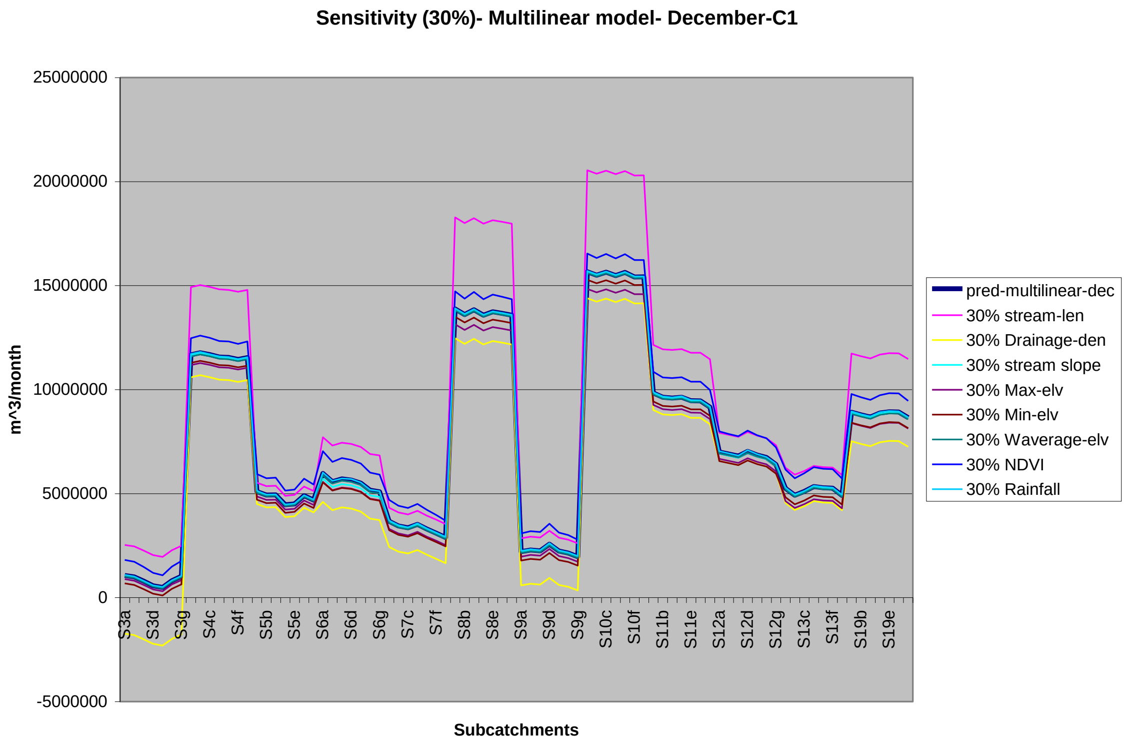

Figure C-47 Sensitivity (30%) – Multilinear model –December C1

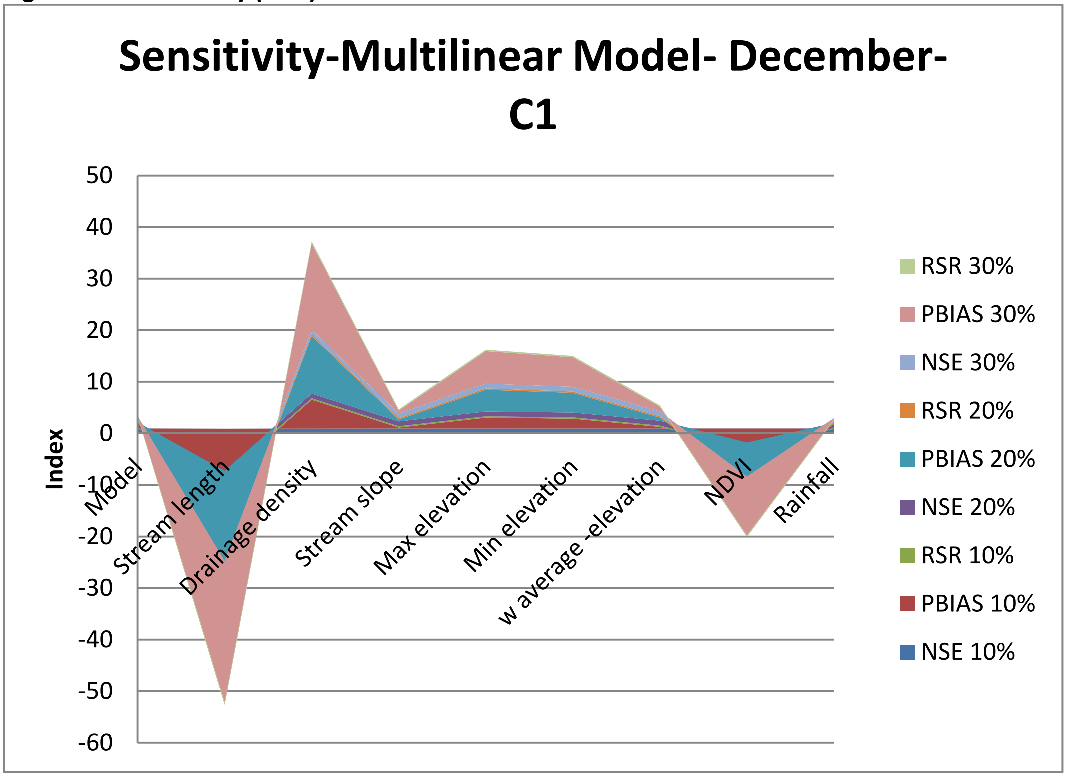

Figure C-48 Sensitivity summary – Multilinear model –December C1

Table C-12 Summary performance- Multilinear model- December C1

		10%							
	0%	**Stream length**	**Drainage density**	**Stream slope**	**Max elevation**	**Min elevation**	**w average - elevation**	**NDVI**	**Rainfall**
NSE	0.934236	0.900882	0.924246	0.934203	0.932875	0.933285	0.93421	0.93029	0.934232
PBIAS	0.015698	-9.27737	5.605553	0.189337	2.113897	1.913426	0.316731	-3.88587	-0.11646
RSR	0.256444	0.31483	0.275234	0.256509	0.259084	0.258292	0.256496	0.264026	0.256452
		20%							
	0%	**Stream length**	**Drainage density**	**Stream slope**	**Max elevation**	**Min elevation**	**w average - elevation**	**NDVI**	**Rainfall**
NSE	0.934236	0.800654	0.894375	0.934106	0.928827	0.930463	0.934135	0.91839	0.934219
PBIAS	0.015698	-18.5704	11.19541	0.362976	4.212097	3.811153	0.617765	-7.78744	-0.24861
RSR	0.256444	0.446481	0.325001	0.256699	0.266782	0.263699	0.256641	0.285675	0.256478
		30%							
	0%	**Stream length**	**Drainage density**	**Stream slope**	**Max elevation**	**Min elevation**	**w average - elevation**	**NDVI**	**Rainfall**
NSE	0.934236	0.633554	0.844621	0.933945	0.922093	0.925769	0.934013	0.898535	0.934196
PBIAS	0.015698	-27.8635	16.78526	0.536614	6.310297	5.708881	0.918798	-11.689	-0.38077
RSR	0.256444	0.605348	0.394181	0.257012	0.279119	0.272453	0.256879	0.318536	0.256524

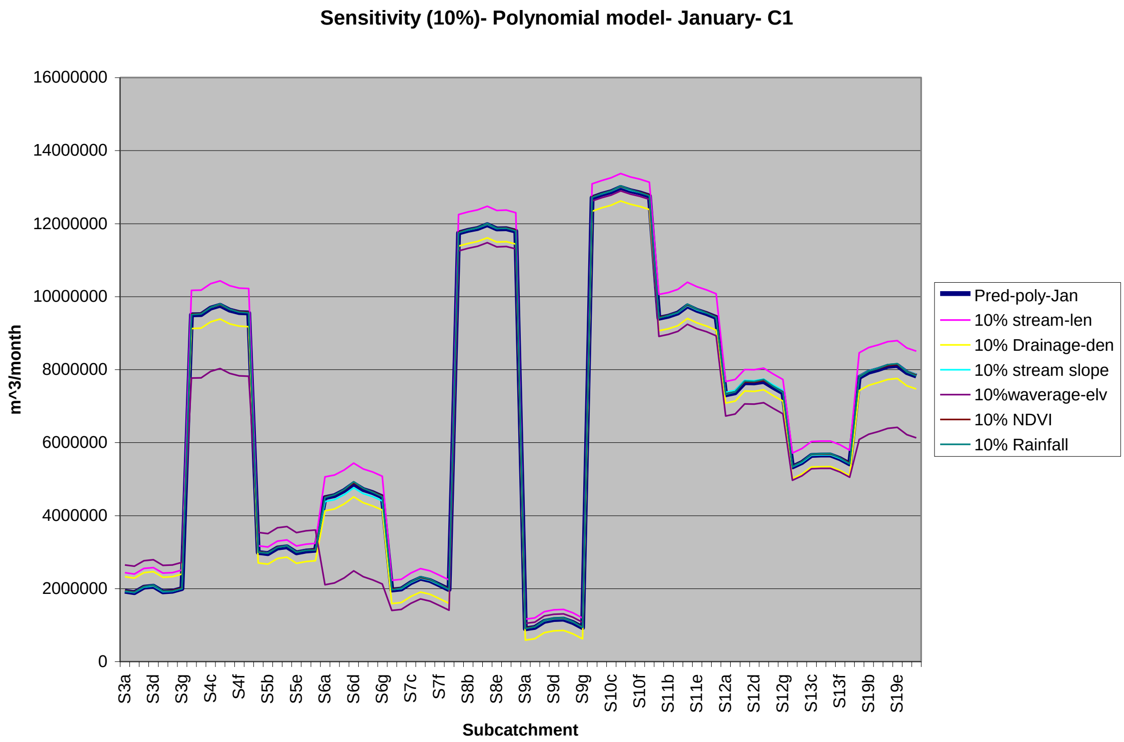

Figure C-49 Sensitivity (10%) – Polynomial model –January C1

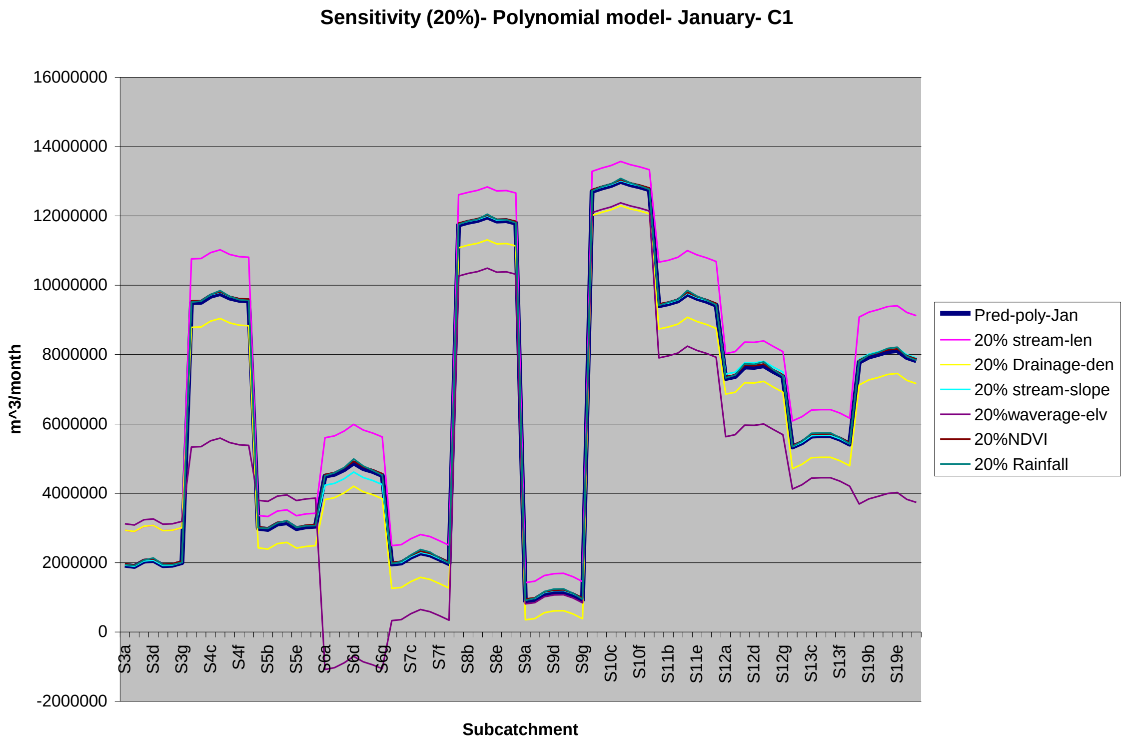

Figure C-50 Sensitivity (20%) – Polynomial model –January C1

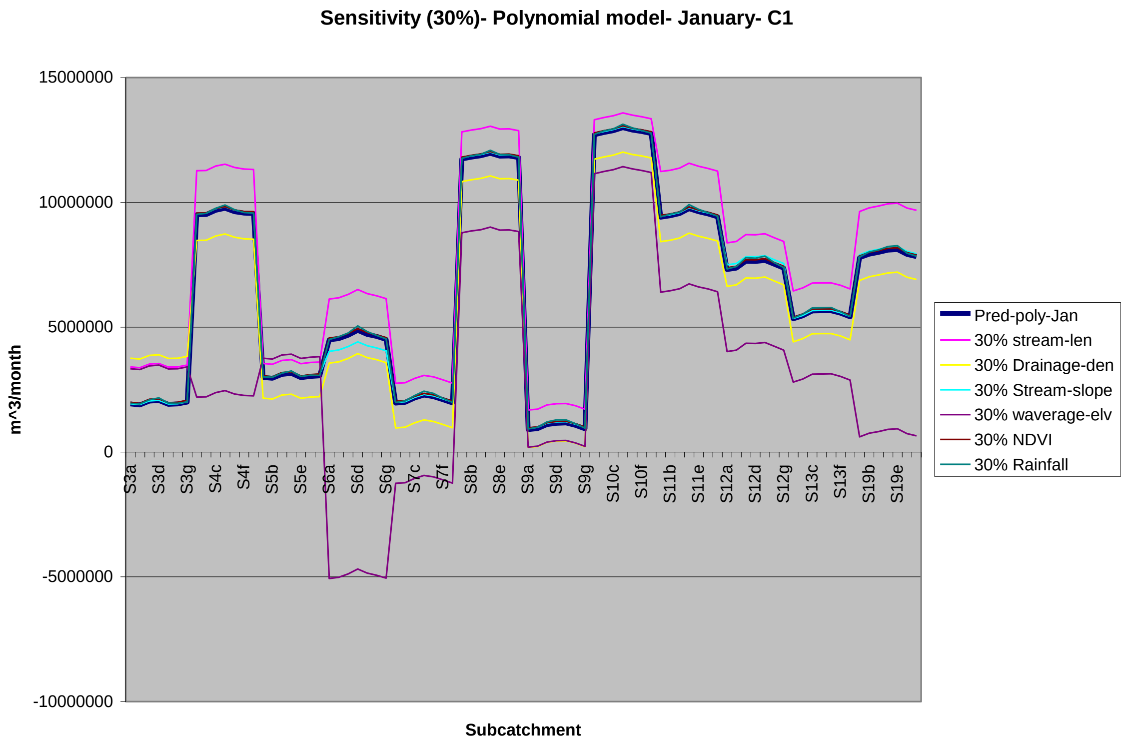

Figure C-51 Sensitivity (30%) – Polynomial model –January C1

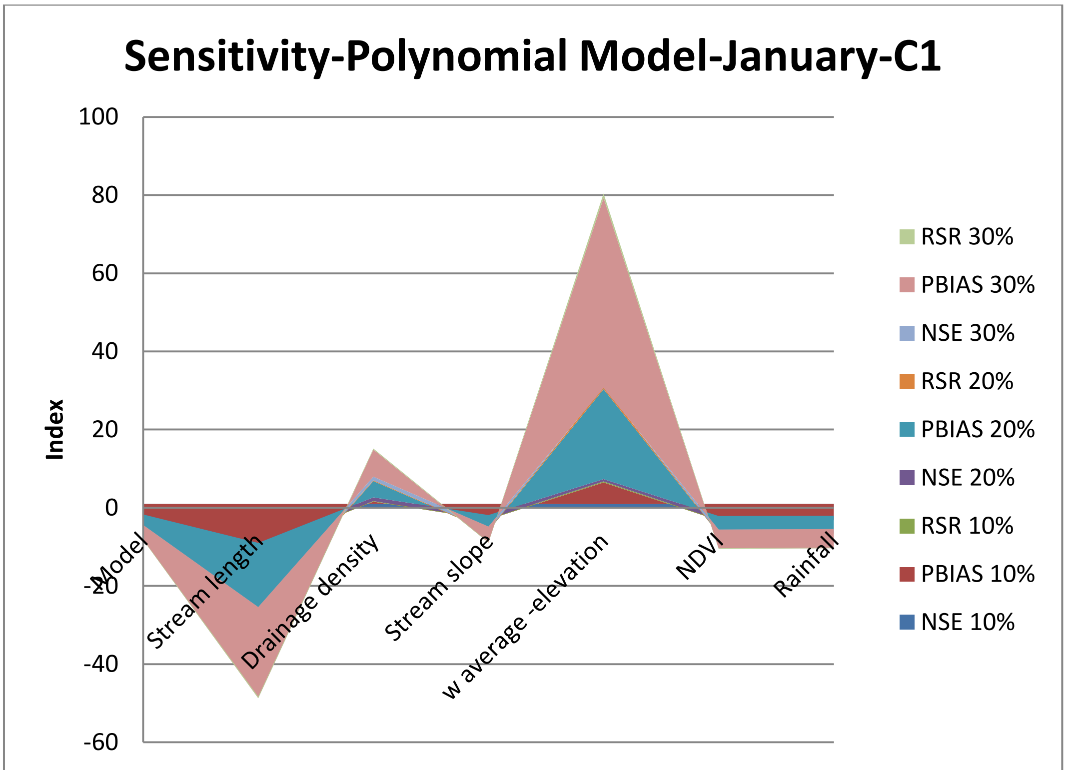

Figure C-52 Sensitivity (30%) – Polynomial model –January C1

Table C-13 Summary performance- Polynomial model- January C1

		10%					
	0%	Stream length	Drainage density	Stream slope	w average - elevation	NDVI	Rainfall
NSE	0.976955	0.947312	0.978291	0.976528	0.921443	0.97611	0.976046
PBIAS	-3.81624	-11.0686	0.576081	-3.97595	5.539698	-4.22211	-4.16079
RSR	0.151805	0.22954	0.147341	0.153204	0.280281	0.154564	0.154771
		20%					
	0%	Stream length	Drainage density	Stream slope	w average - elevation	NDVI	Rainfall
NSE	0.976955	0.894517	0.963307	0.975921	0.595984	0.975272	0.974996
PBIAS	-3.81624	-17.5636	4.159719	-4.06845	22.99985	-4.59108	-4.5219
RSR	0.151805	0.324781	0.191553	0.155175	0.635623	0.157253	0.158127
		30%					
	0%	Stream length	Drainage density	Stream slope	w average - elevation	NDVI	Rainfall
NSE	0.976955	0.826039	0.931623	0.974919	-0.28398	0.974461	0.97379
PBIAS	-3.81624	-23.3013	6.934674	-4.09375	48.56423	-4.92315	-4.89956
RSR	0.151805	0.417086	0.261489	0.158368	1.13313	0.159809	0.161895

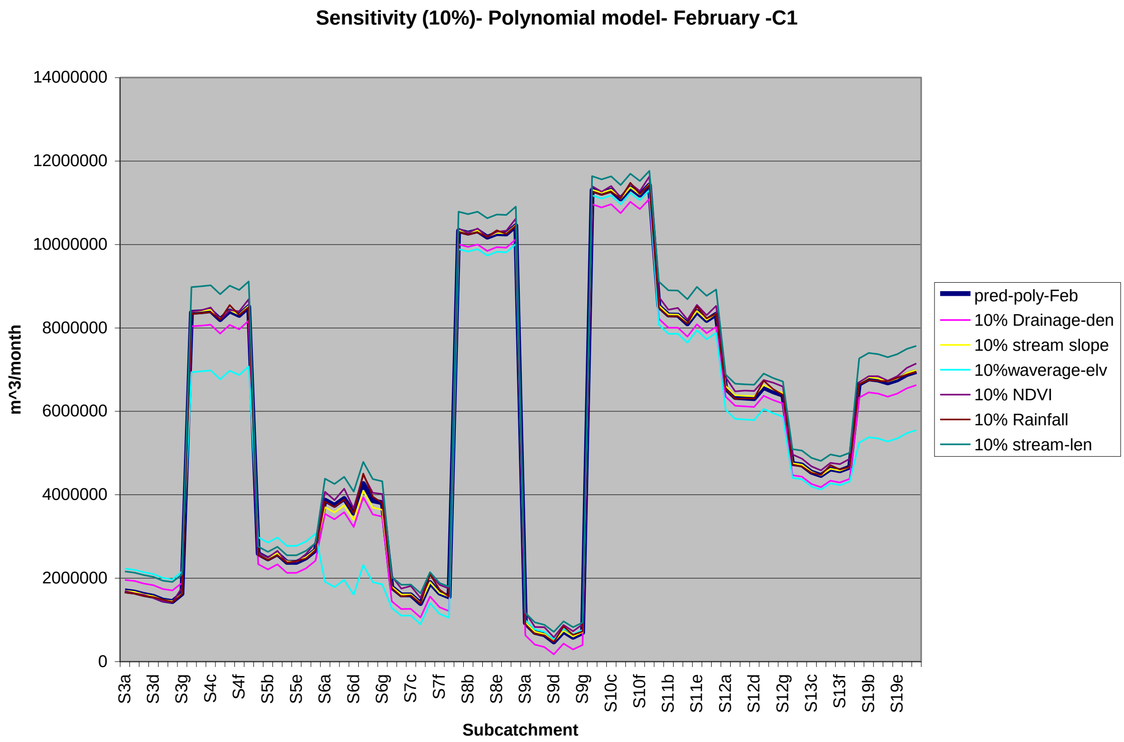

Figure C-53 Sensitivity (10%) Polynomial model –February C1

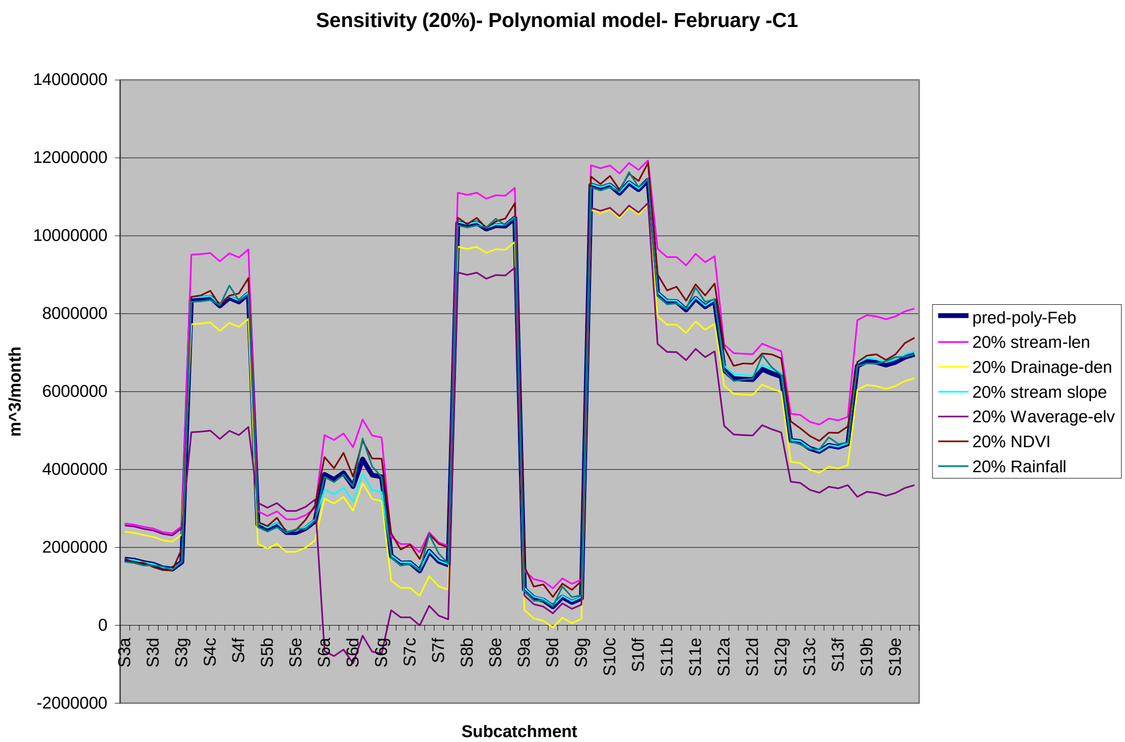

Figure C-54 Sensitivity (20%) – Polynomial model –February C1

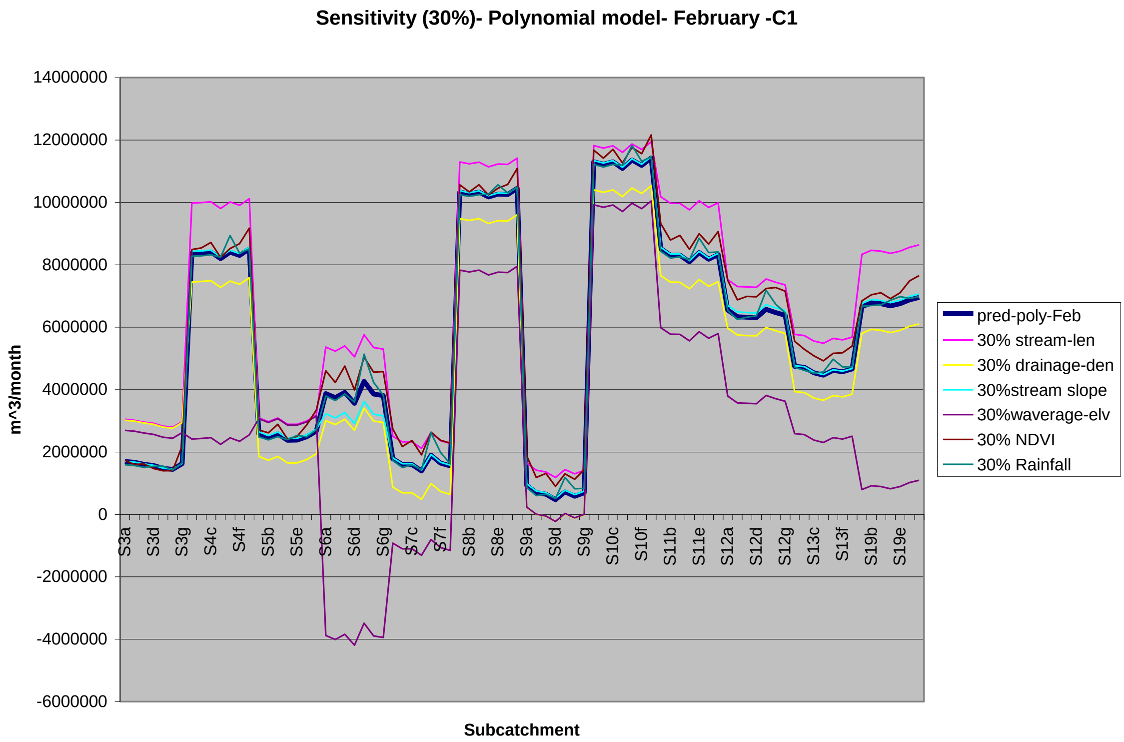

Figure C-55 Sensitivity (30%) – Polynomial model –February C1

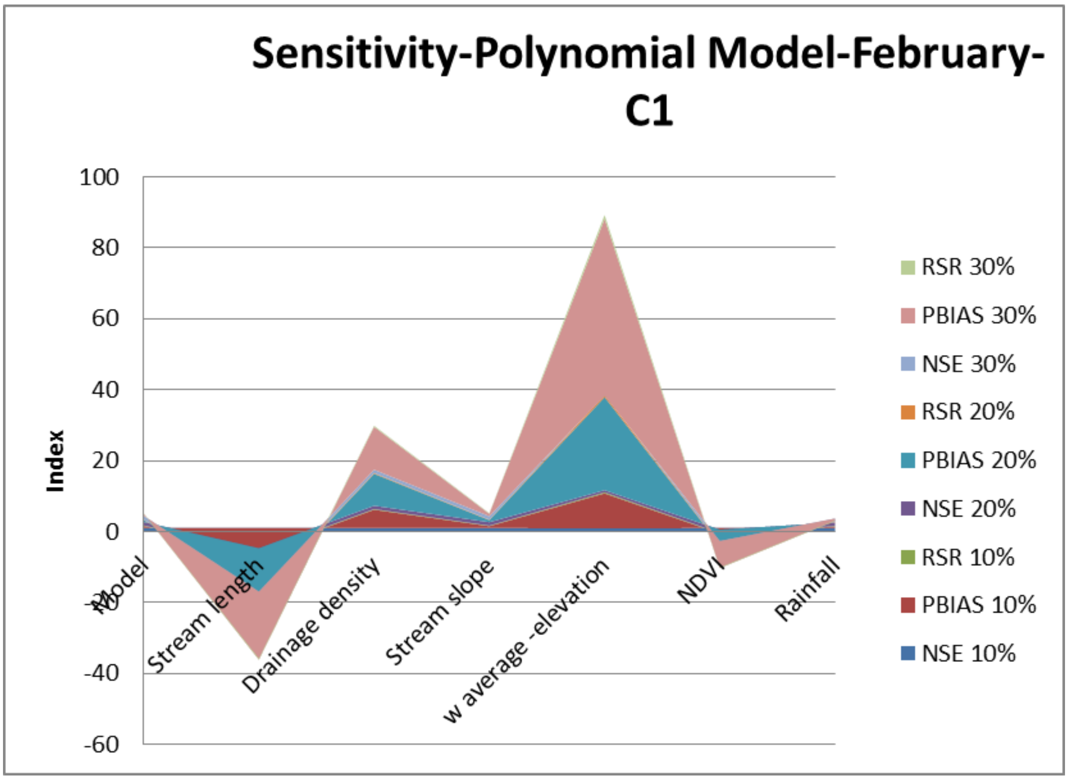

Figure C-56 Sensitivity summary – Polynomial model –February C1

Table C-14 Summary performance- Polynomial model- February C1

		10%					
	0%	Stream length	Drainage density	Stream slope	w average - elevation	NDVI	Rainfall
NSE	0.982453	0.968991	0.973324	0.982211	0.914003	0.981425	0.982244
PBIAS	0.6083	-6.77103	5.187027	0.549225	9.841163	-1.5492	0.442976
RSR	0.132467	0.176095	0.163327	0.133377	0.293253	0.136289	0.13325
		20%					
	0%	Stream length	Drainage density	Stream slope	w average - elevation	NDVI	Rainfall
NSE	0.982453	0.929849	0.950492	0.981224	0.601211	0.975388	0.981333
PBIAS	0.6083	-13.371	9.016435	0.572247	26.24005	-4.30399	0.017574
RSR	0.132467	0.264861	0.222504	0.137025	0.631497	0.156882	0.136626
		30%					
	0%	Stream length	Drainage density	Stream slope	w average - elevation	NDVI	Rainfall
NSE	0.982453	0.872749	0.914504	0.979072	-0.18959	0.96125	0.979232
PBIAS	0.6083	-19.1916	12.09652	0.677364	49.80496	-7.65606	-0.66791
RSR	0.132467	0.356723	0.292397	0.144665	1.090681	0.19685	0.144111

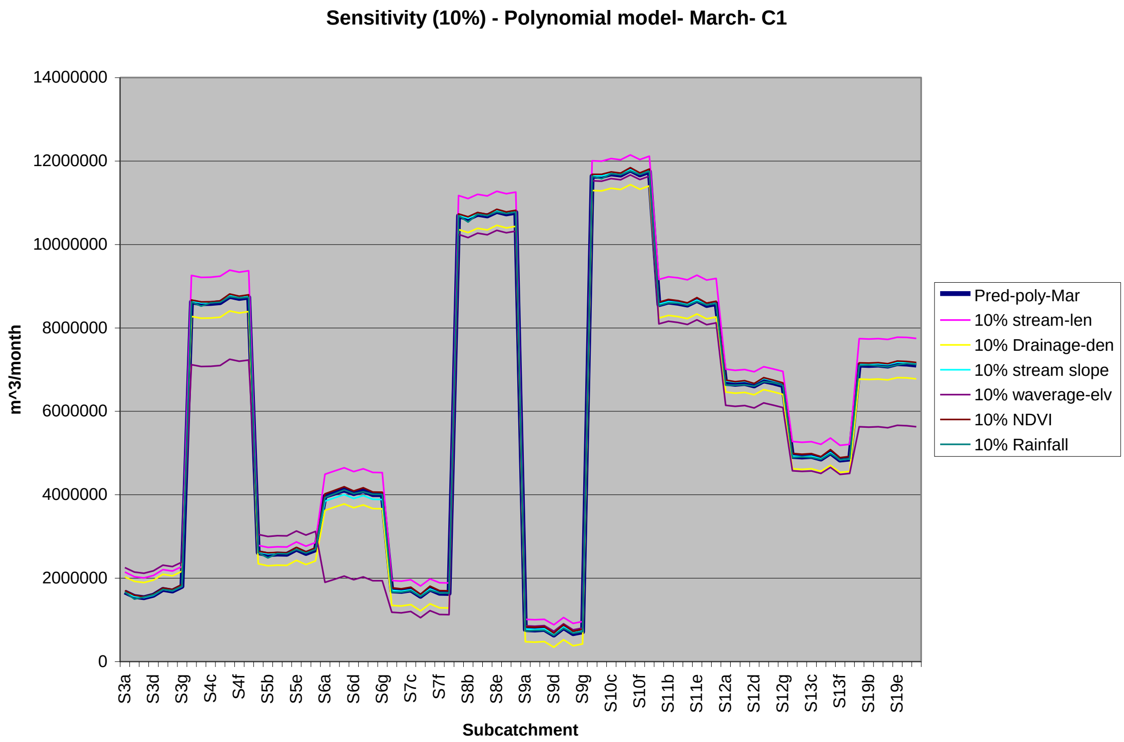

Figure C-57 Sensitivity (10%) – Polynomial model –March C1

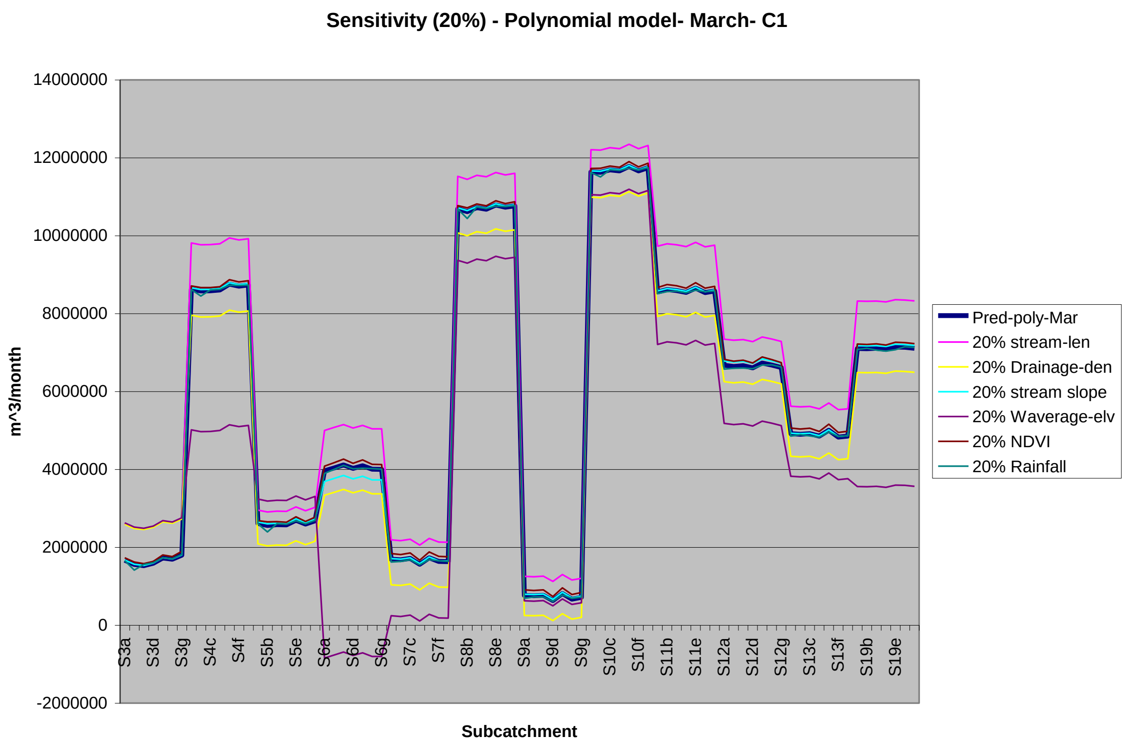

Figure C-58 Sensitivity (20%) – Polynomial model –March C1

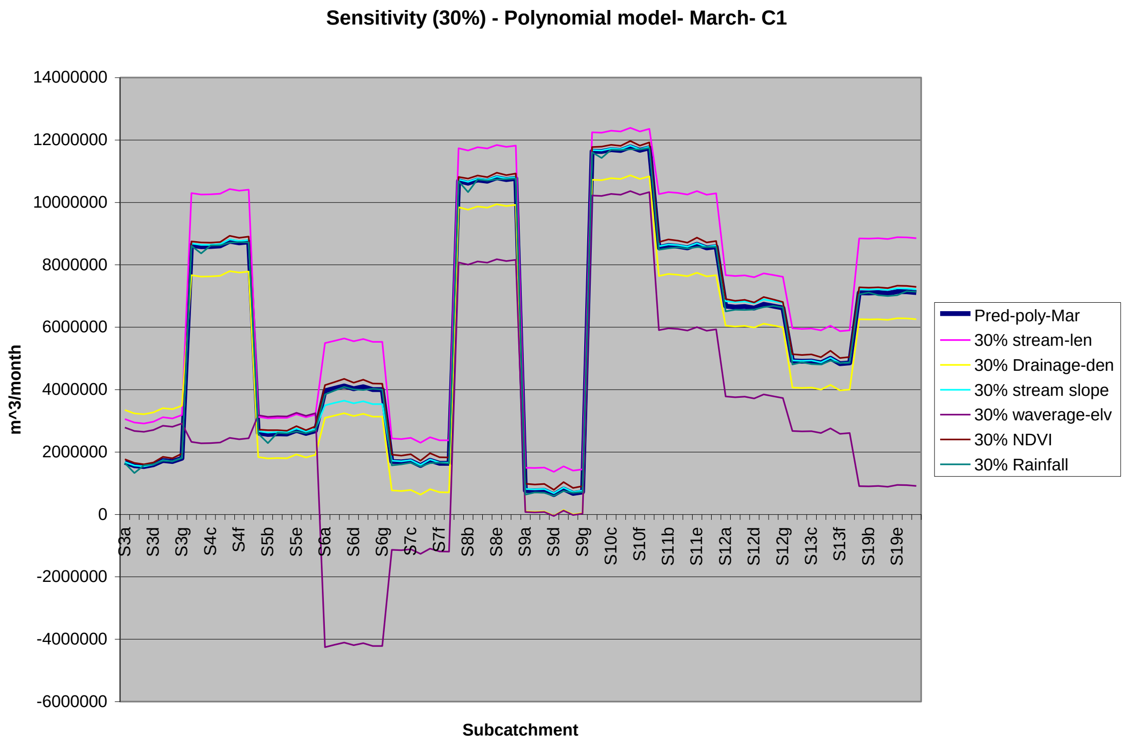

Figure C-59 Sensitivity (30%) – Polynomial model –March C1

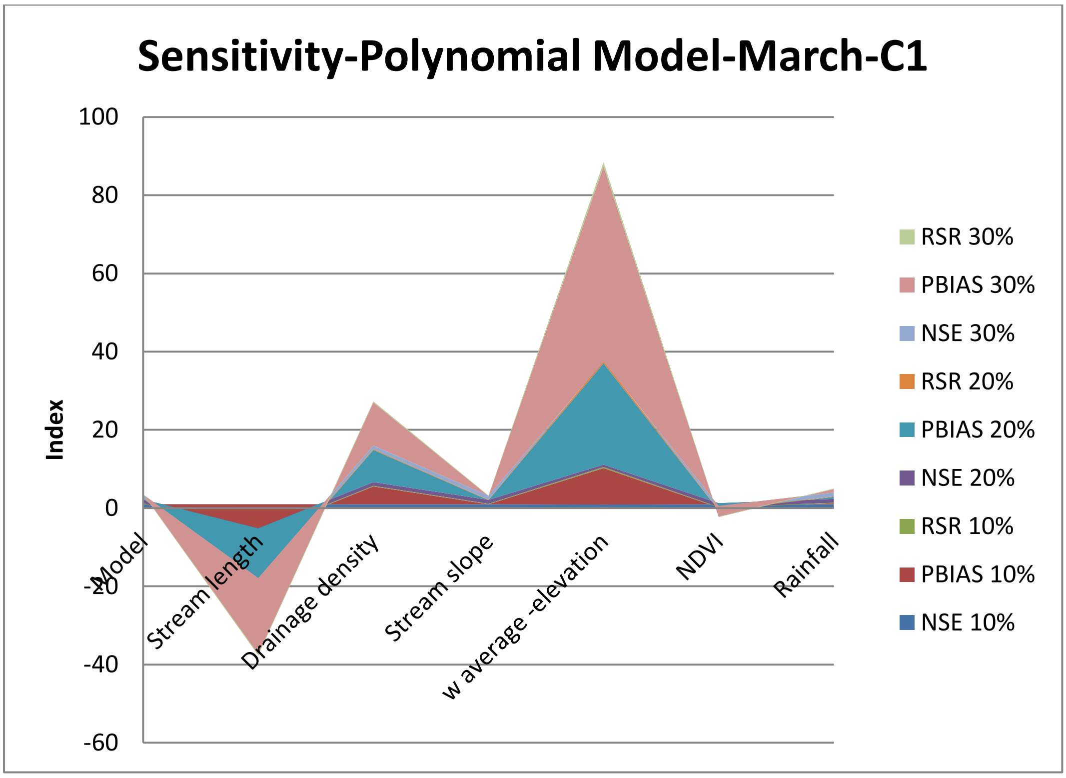

Figure C-60 Sensitivity summary – Polynomial model –March C1

Table C-15 Summary performance- Polynomial model- March C1

		10%					
	0%	Stream length	Drainage density	Stream slope	w average - elevation	NDVI	Rainfall
NSE	0.981543	0.966195	0.973323	0.981424	0.913704	0.981352	0.981498
PBIAS	0.124635	-7.24372	4.564972	-0.0029	9.307153	-0.84262	0.259346
RSR	0.135858	0.18386	0.163331	0.136293	0.293762	0.136557	0.13602
		20%					
	0%	Stream length	Drainage density	Stream slope	w average - elevation	NDVI	Rainfall
NSE	0.981543	0.92539	0.950164	0.980923	0.594049	0.980636	0.981334
PBIAS	0.124635	-13.8565	8.195386	-0.06237	25.89573	-1.827	0.512521
RSR	0.135858	0.273148	0.223239	0.138119	0.637143	0.139153	0.136623
		30%					
	0%	Stream length	Drainage density	Stream slope	w average - elevation	NDVI	Rainfall
NSE	0.981543	0.866845	0.911759	0.979799	-0.22268	0.979367	0.980967
PBIAS	0.124635	-19.7136	11.01587	-0.05378	49.89035	-2.82851	0.884162
RSR	0.135858	0.364904	0.297054	0.142129	1.105747	0.143642	0.137959

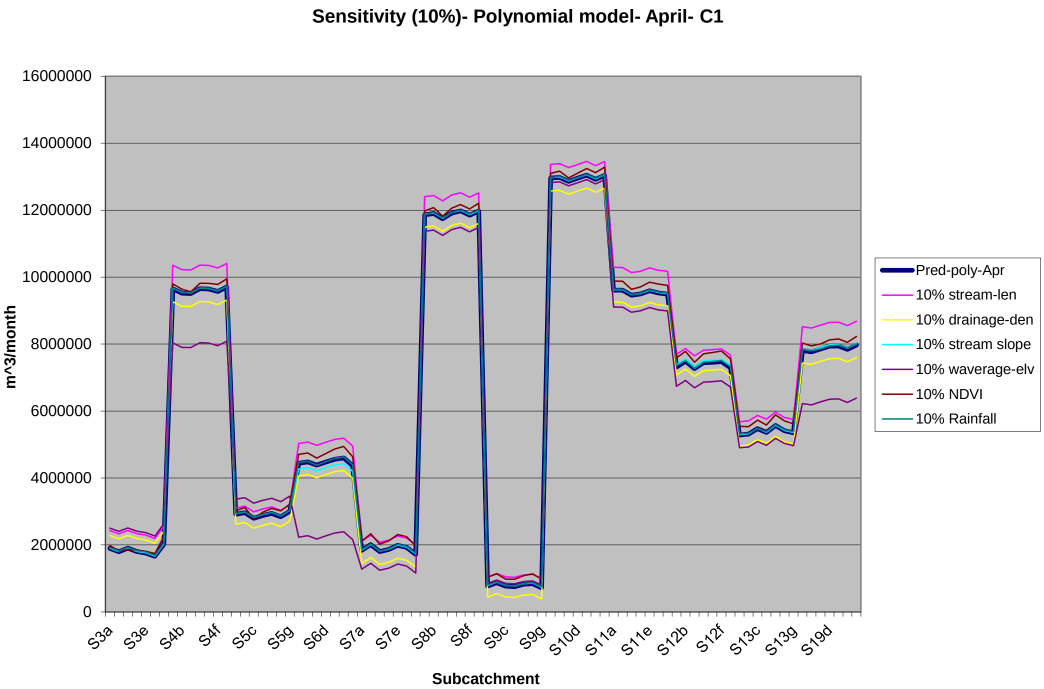

Figure C-61 Sensitivity (10%) – Polynomial model –April C1

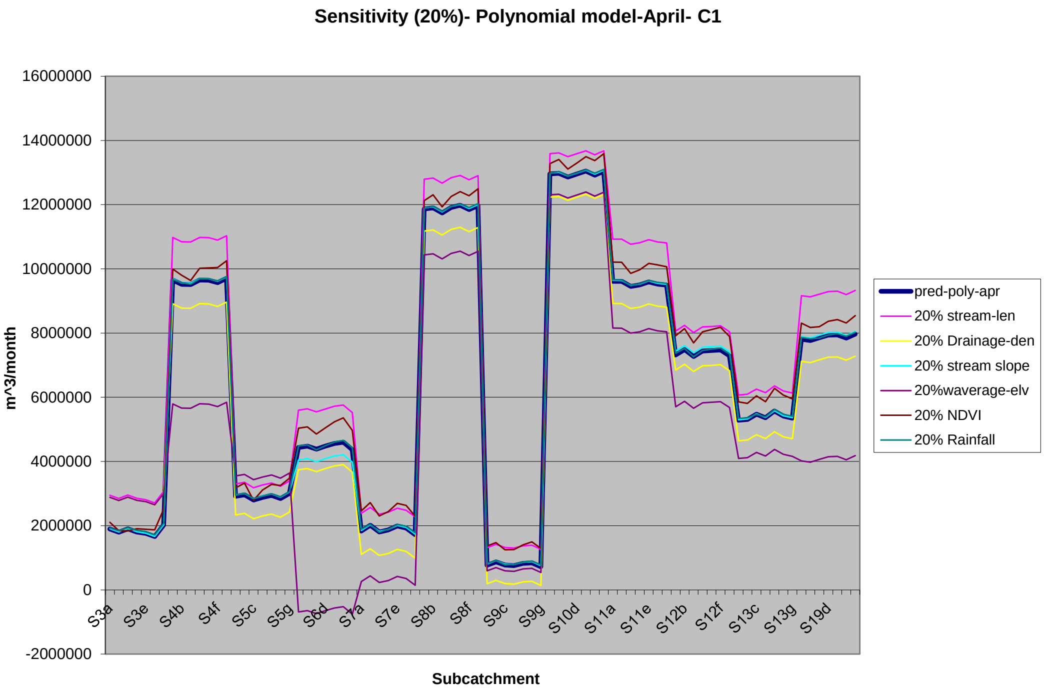

Figure C-62 Sensitivity (20%) – Polynomial model -April C1

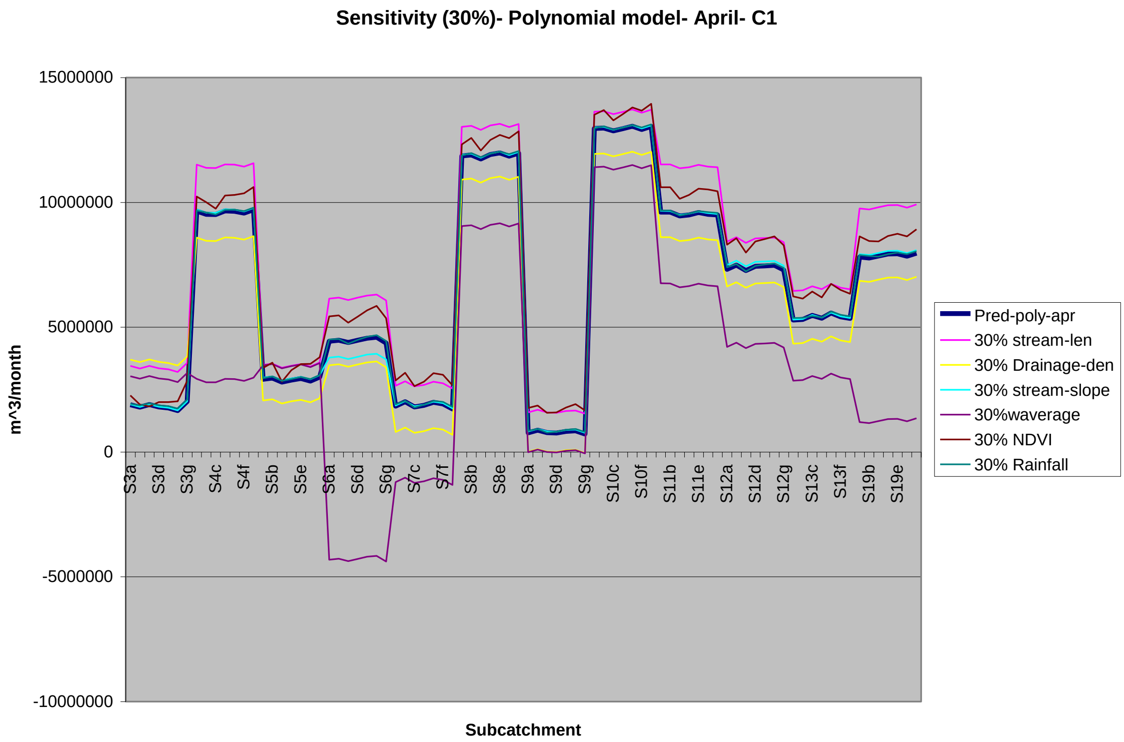

Figure C-63 Sensitivity (30%) – Polynomial model –April C1

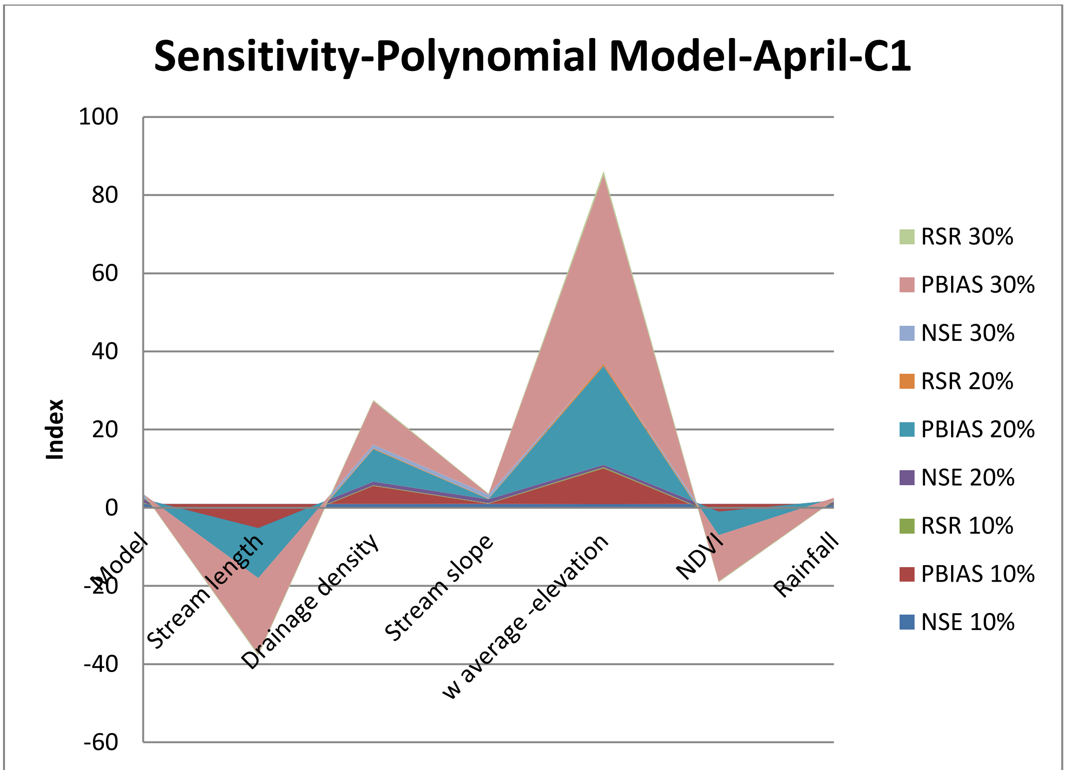

Figure C-64 Sensitivity summary – Polynomial model –April C1

Table C-16 Summary performance- Polynomial model- April C1

		10%					
	0%	Stream length	Drainage density	Stream slope	w average - elevation	NDVI	Rainfall
NSE	0.981677	0.966265	0.973447	0.981485	0.918272	0.978843	0.981668
PBIAS	0.155641	-7.2597	4.620044	0.075781	9.174816	-3.06959	-0.20969
RSR	0.135362	0.183672	0.162951	0.136068	0.285881	0.145455	0.135396
		20%					
	0%	Stream length	Drainage density	Stream slope	w average - elevation	NDVI	Rainfall
NSE	0.981677	0.92506	0.950513	0.980714	0.620998	0.966655	0.9816
PBIAS	0.155641	-13.9135	8.285757	0.072202	25.25092	-7.13047	-0.48774
RSR	0.135362	0.273751	0.222457	0.138876	0.615631	0.182607	0.135645
		30%					
	0%	Stream length	Drainage density	Stream slope	w average - elevation	NDVI	Rainfall
NSE	0.981677	0.86588	0.912733	0.979016	-0.13591	0.939436	0.981503
PBIAS	0.155641	-19.8058	11.15278	0.144906	48.38394	-12.027	-0.67849
RSR	0.135362	0.366224	0.29541	0.144859	1.065791	0.246098	0.136005

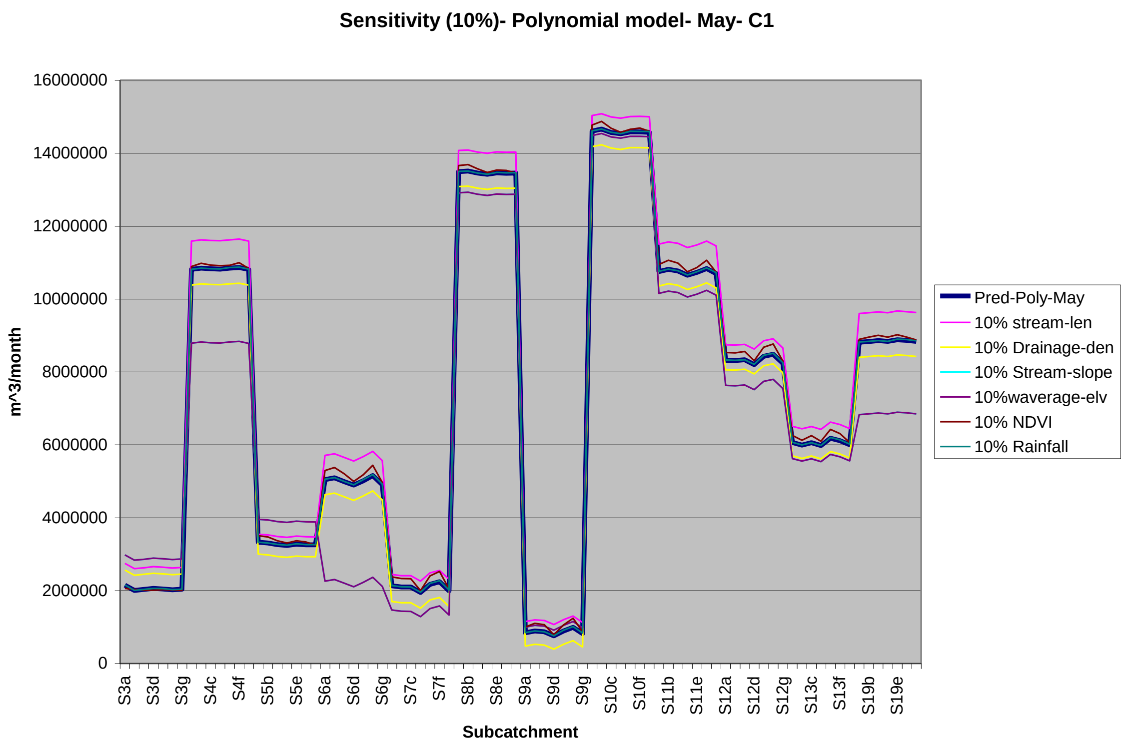

Figure C-65 Sensitivity (10%) – Polynomial model –May C1

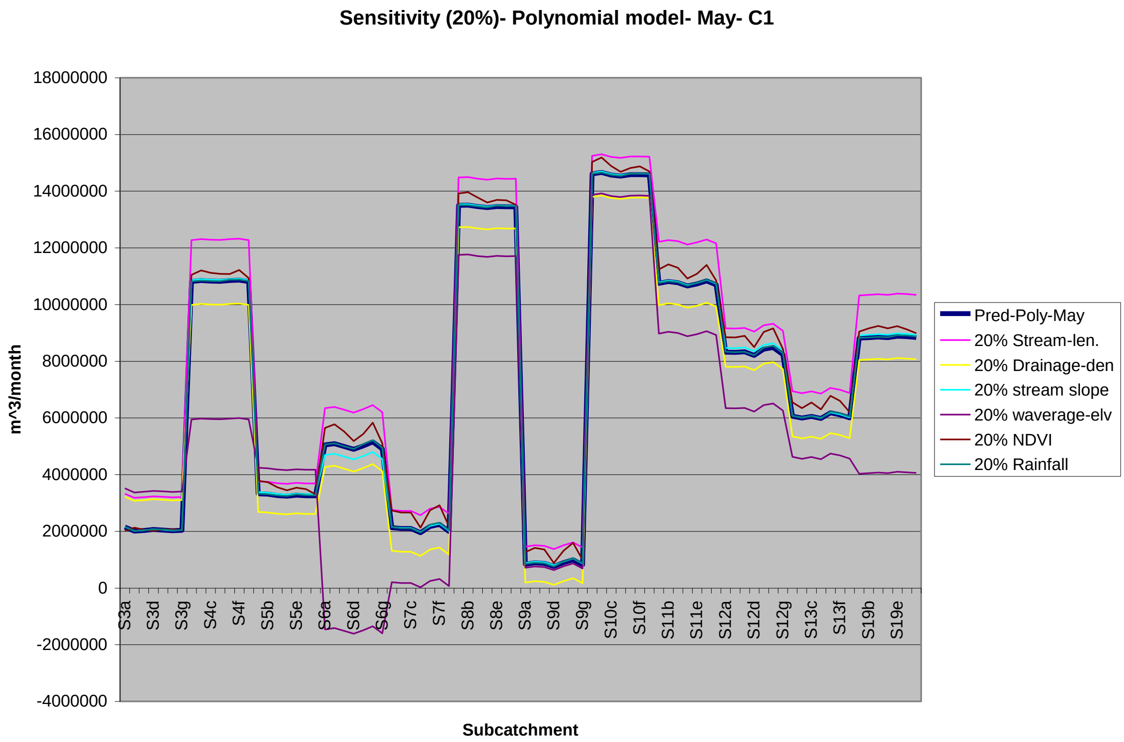

Figure C-66 Sensitivity (20%) – Polynomial model –May C1

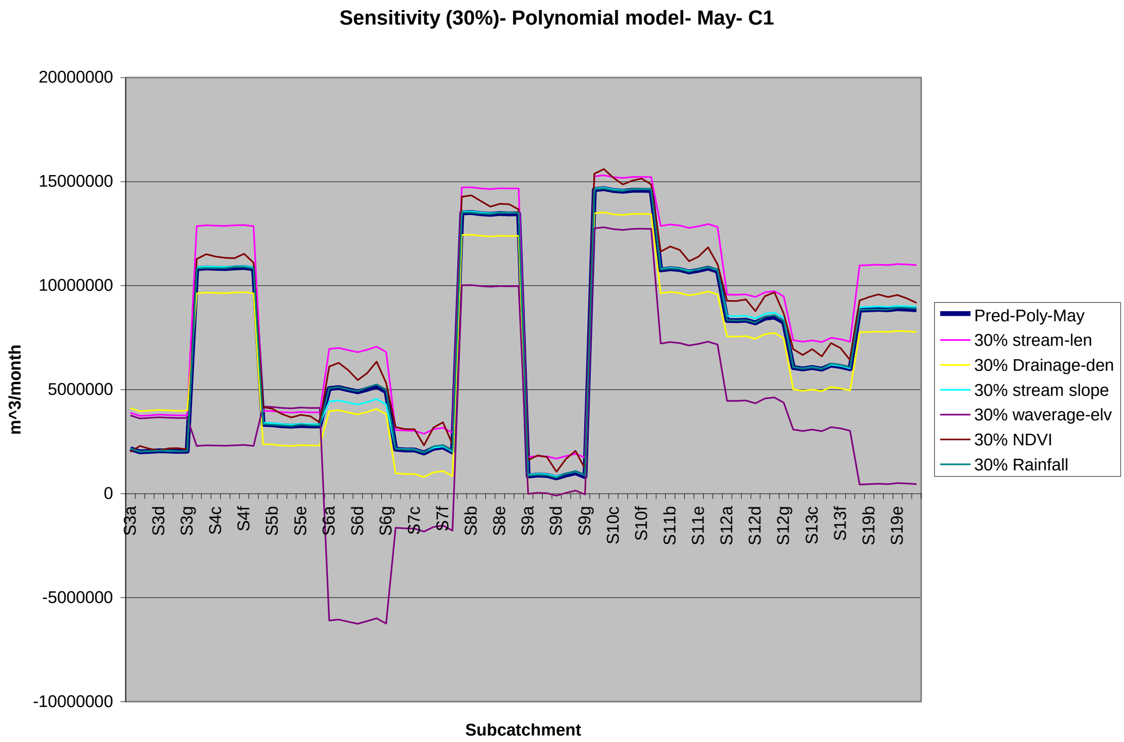

Figure C-67Sensitivity (30%) – Polynomial model –May C1

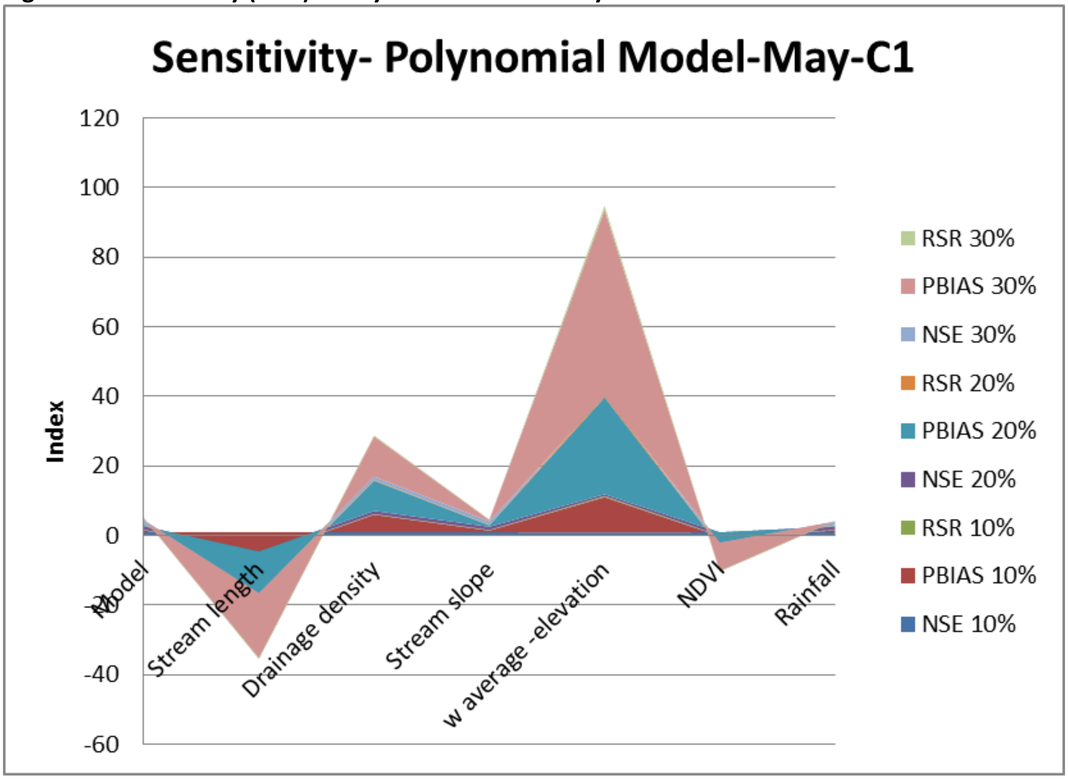

Figure C-68 Sensitivity summary – Polynomial model –May C1

Table C-17 Summary performance- Polynomial model- May C1

		10%					
	0%	Stream length	Drainage density	Stream slope	w average - elevation	NDVI	Rainfall
NSE	0.981337	0.96843	0.972207	0.981228	0.900135	0.980742	0.981371
PBIAS	0.622844	-6.63124	5.048861	0.482617	10.17687	-1.13075	0.493806
RSR	0.136614	0.17768	0.166711	0.137012	0.316014	0.138773	0.136486
		20%					
	0%	Stream length	Drainage density	Stream slope	w average - elevation	NDVI	Rainfall
NSE	0.981337	0.930699	0.949074	0.980672	0.525821	0.975368	0.981394
PBIAS	0.622844	-13.115	8.694566	0.414537	27.83323	-4.08481	0.338938
RSR	0.136614	0.263251	0.225667	0.139025	0.688606	0.156946	0.136404
		30%					
	0%	Stream length	Drainage density	Stream slope	w average - elevation	NDVI	Rainfall
NSE	0.981337	0.875601	0.911918	0.979403	-0.42867	0.959265	0.981395
PBIAS	0.622844	-18.8284	11.55996	0.418602	53.5919	-8.23932	0.158239
RSR	0.136614	0.352703	0.296785	0.143516	1.19527	0.20183	0.136402

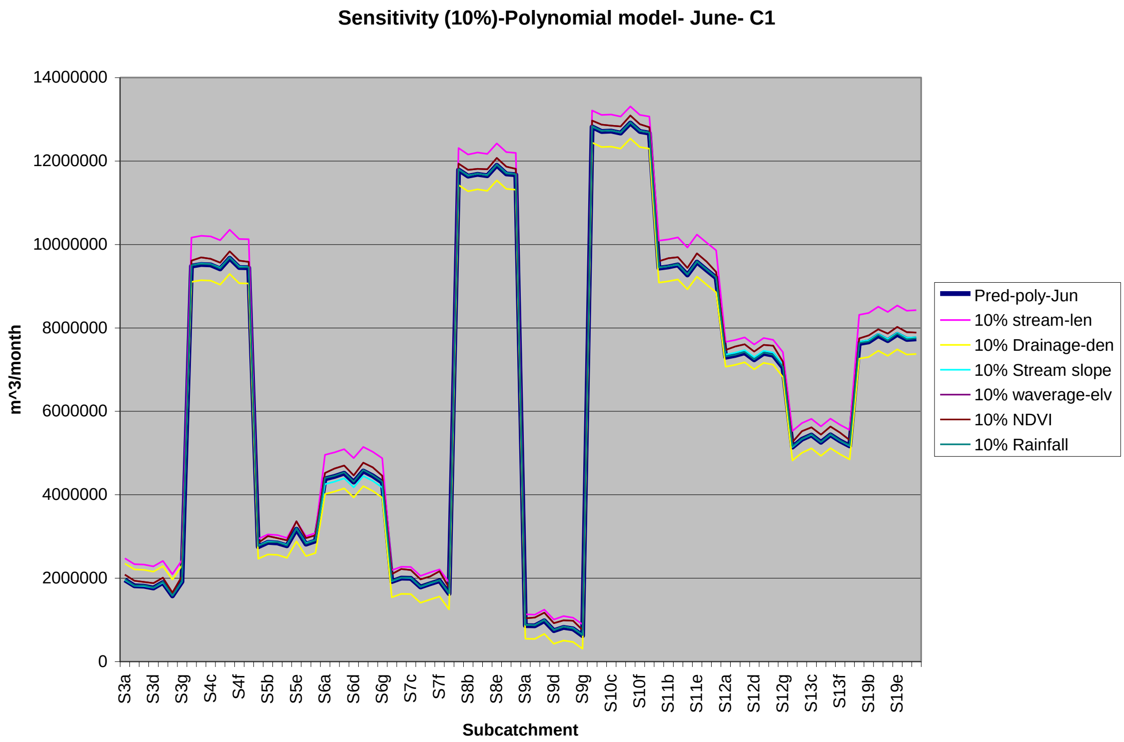

Figure C-69 Sensitivity (10%) – Polynomial model –June C1

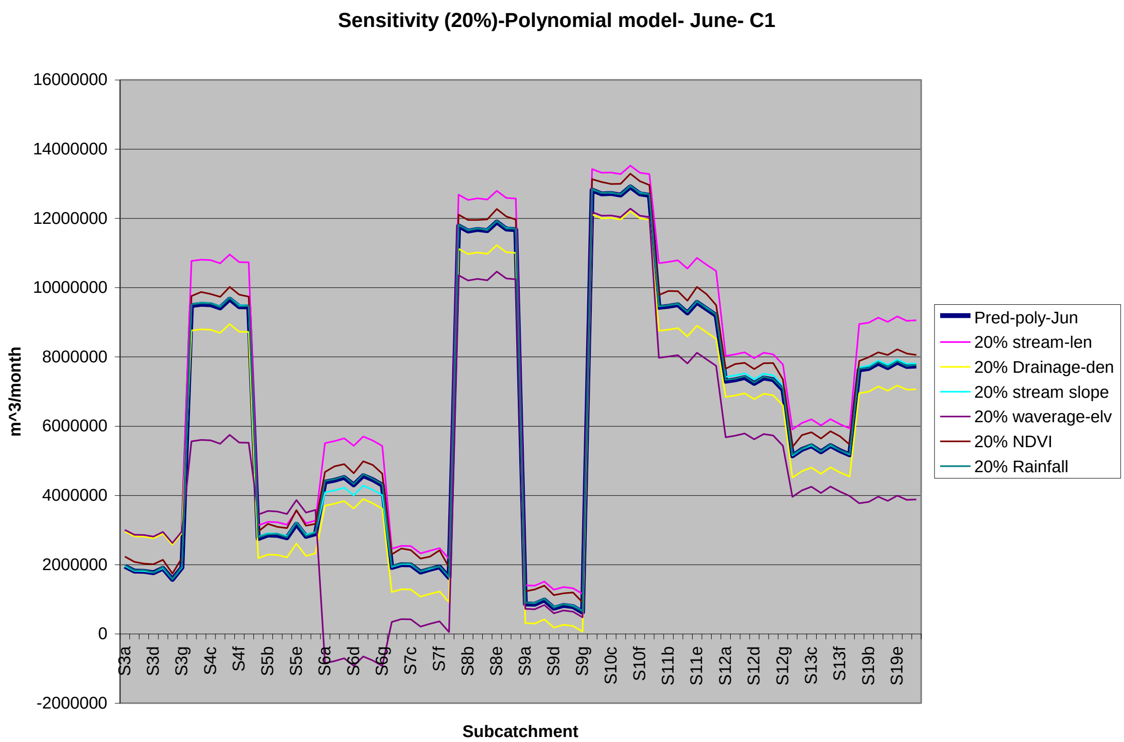

Figure C-70 Sensitivity (20%) – Polynomial model –June C1

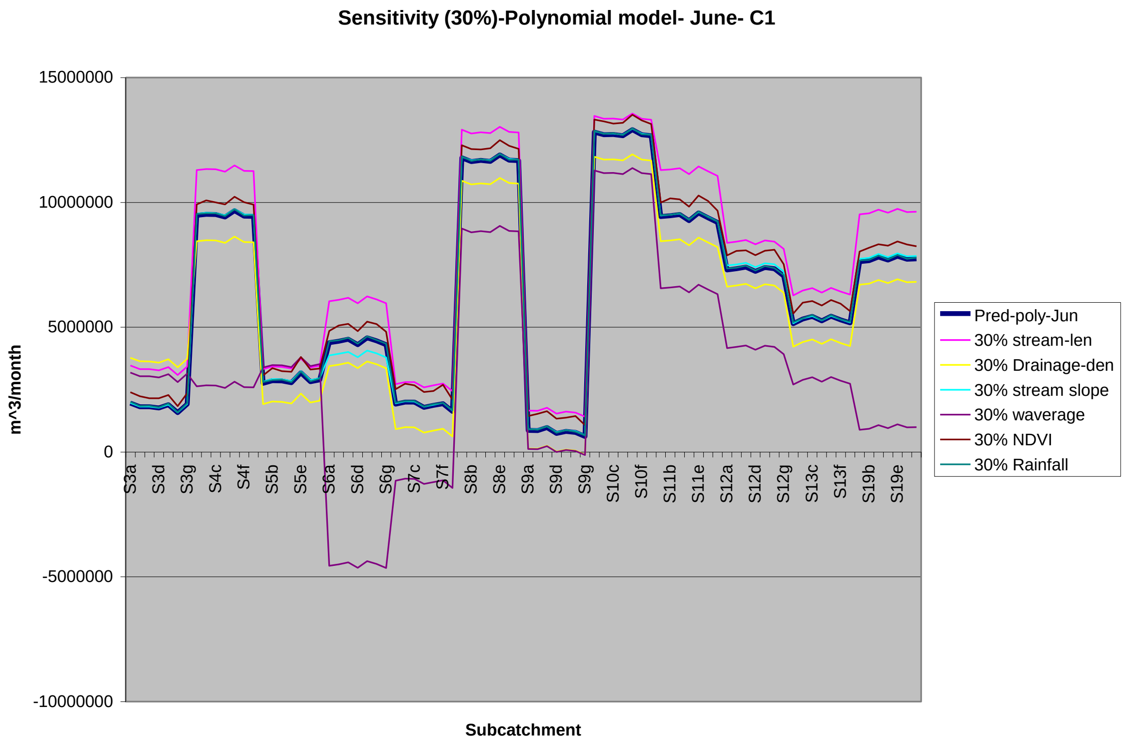

Figure C-71 Sensitivity (30%) – Polynomial model –June C1

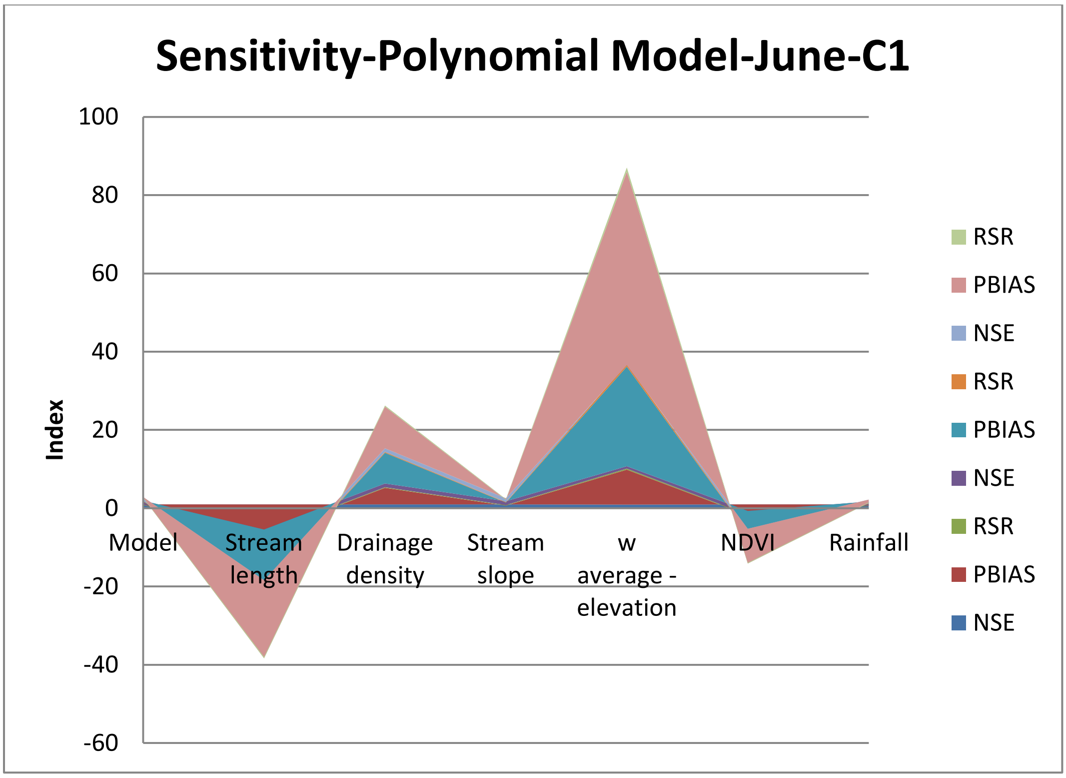

Figure C-72 Sensitivity (30%) – Polynomial model –June C1

Table C-18 Summary performance- Polynomial model- June C1

		10%					
	0%	Stream length	Drainage density	Stream slope	w average - elevation	NDVI	Rainfall
NSE	0.982	0.965603	0.974615	0.981867	0.916339	0.979942	0.981964
PBIAS	-0.17766	-7.5187	4.235067	-0.30631	8.931822	-2.7827	-0.40398
RSR	0.134164	0.185464	0.159327	0.134657	0.289243	0.141625	0.134297
		20%					
	0%	Stream length	Drainage density	Stream slope	w average - elevation	NDVI	Rainfall
NSE	0.982	0.924061	0.952375	0.981368	0.601789	0.973382	0.981903
PBIAS	-0.17766	-14.1031	7.843519	-0.36697	25.44051	-5.68347	-0.62099
RSR	0.134164	0.275571	0.218231	0.1365	0.63104	0.163151	0.134527
		30%					
	0%	Stream length	Drainage density	Stream slope	w average - elevation	NDVI	Rainfall
NSE	0.982	0.865031	0.914985	0.980262	-0.20567	0.960946	0.981819
PBIAS	-0.17766	-19.9307	10.6477	-0.35964	49.3484	-8.87996	-0.82867
RSR	0.134164	0.367381	0.291574	0.140492	1.098032	0.197621	0.134838

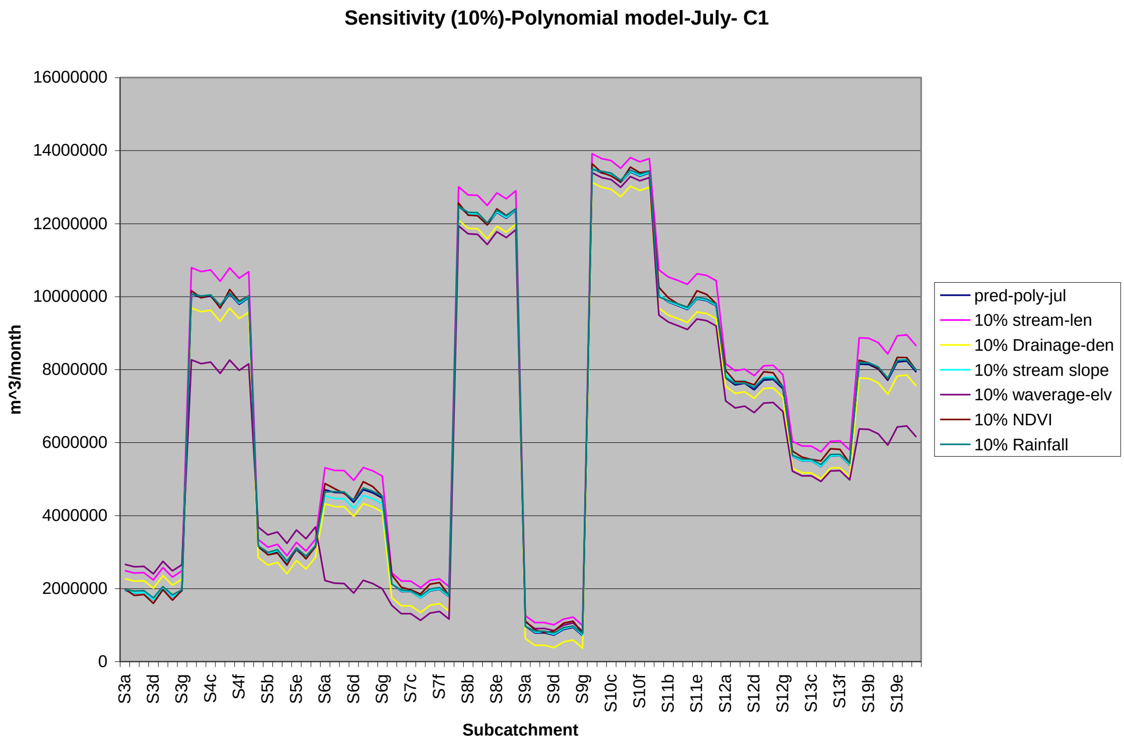

Figure C-73 Sensitivity (10%) – Polynomial model –July C1

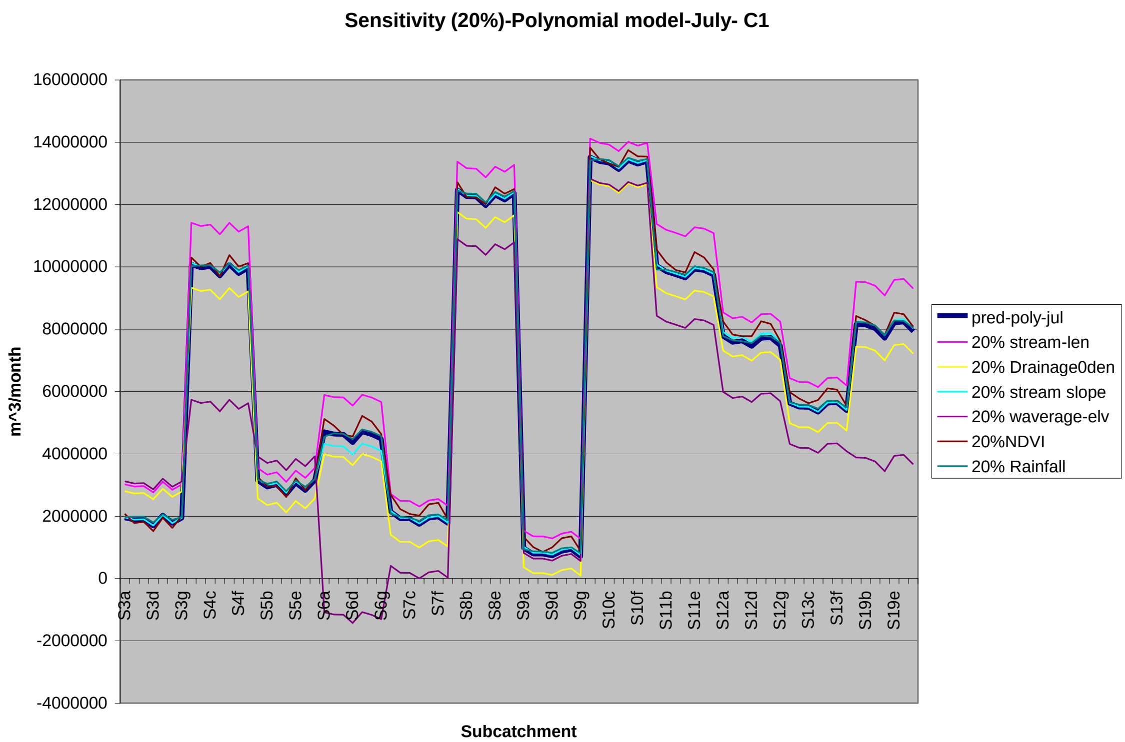

Figure C-74 Sensitivity (20%) – Polynomial model –July C1

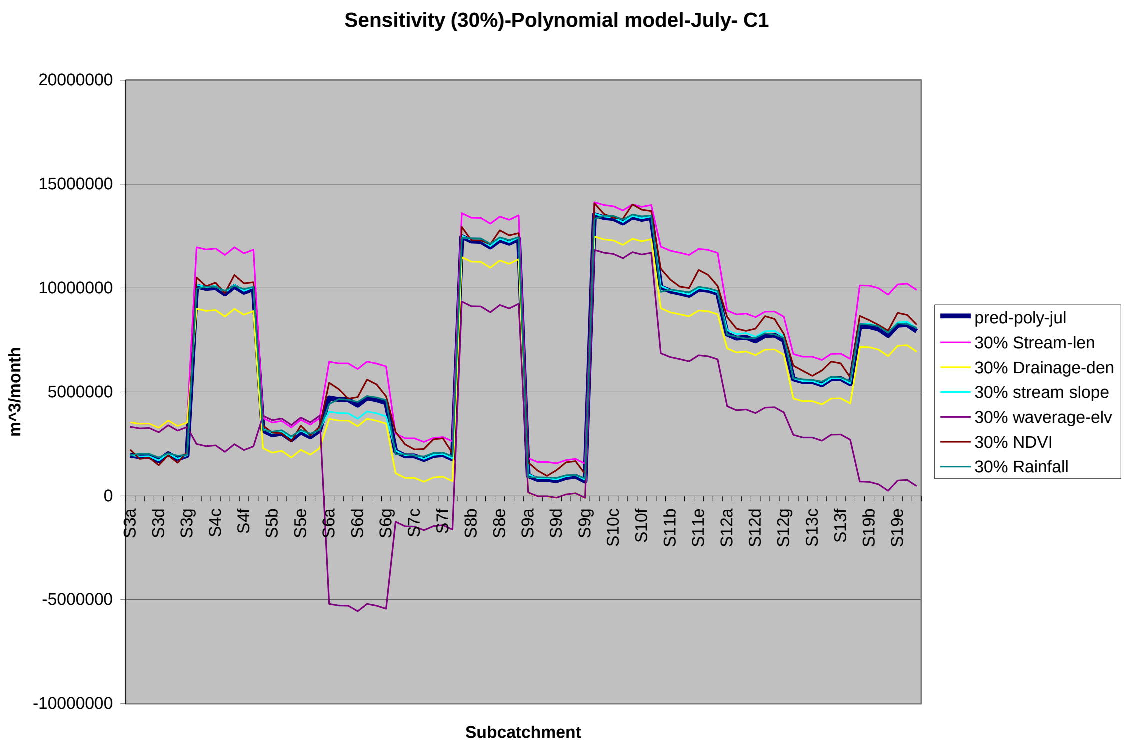

Figure C-75 Sensitivity (30%) – Polynomial model –July C1

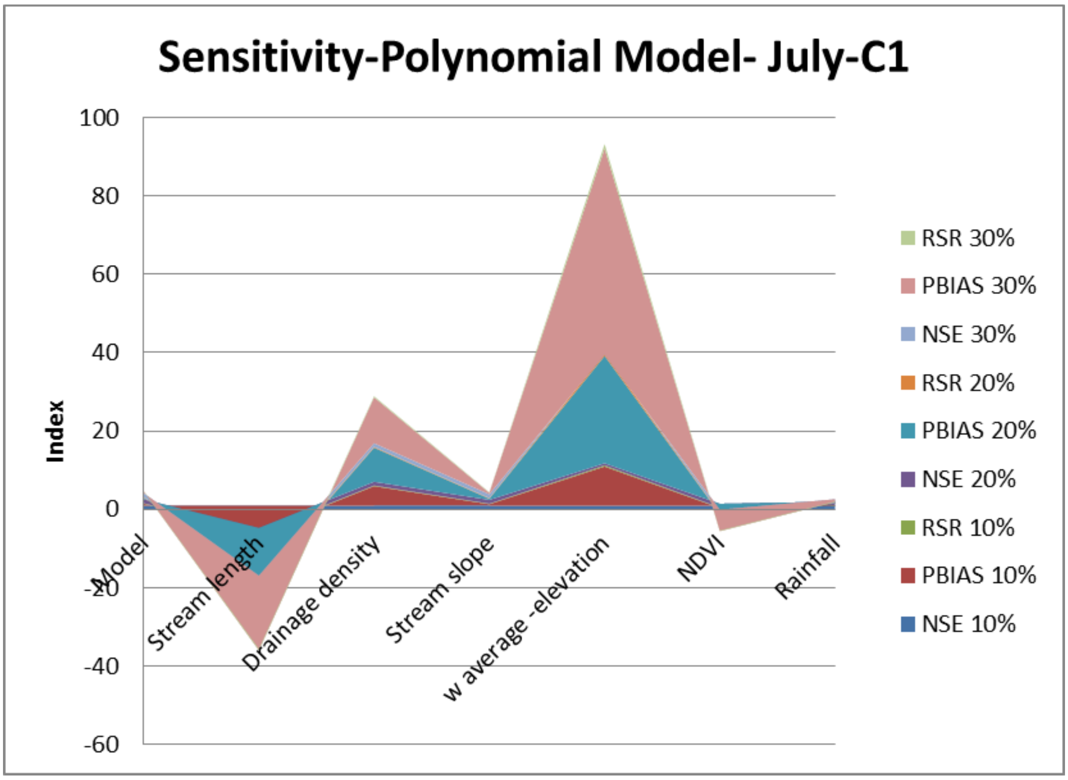

Figure C-76 Sensitivity summary – Polynomial model –July C1

Table C-19 Summary performance- Polynomial model- July C1

		10%					
	0%	Stream length	Drainage density	Stream slope	w average - elevation	NDVI	Rainfall
NSE	0.98224	0.968615	0.973678	0.982077	0.905373	0.981831	0.982257
PBIAS	0.467527	-6.80997	4.963047	0.346666	10.02822	-0.64092	-0.11478
RSR	0.133267	0.177157	0.162239	0.133877	0.307616	0.134794	0.133204
		20%					
	0%	Stream length	Drainage density	Stream slope	w average - elevation	NDVI	Rainfall
NSE	0.98224	0.93007	0.95166	0.981345	0.549068	0.978771	0.982052
PBIAS	0.467527	-13.3183	8.71326	0.304566	27.40999	-2.62912	-0.50681
RSR	0.133267	0.264444	0.219863	0.136583	0.671515	0.145703	0.133971
		30%					
	0%	Stream length	Drainage density	Stream slope	w average - elevation	NDVI	Rainfall
NSE	0.98224	0.874112	0.916628	0.979703	-0.35845	0.969888	0.981677
PBIAS	0.467527	-19.0575	11.71816	0.341227	52.61285	-5.49708	-0.70859
RSR	0.133267	0.354807	0.288742	0.142466	1.165527	0.173527	0.135362

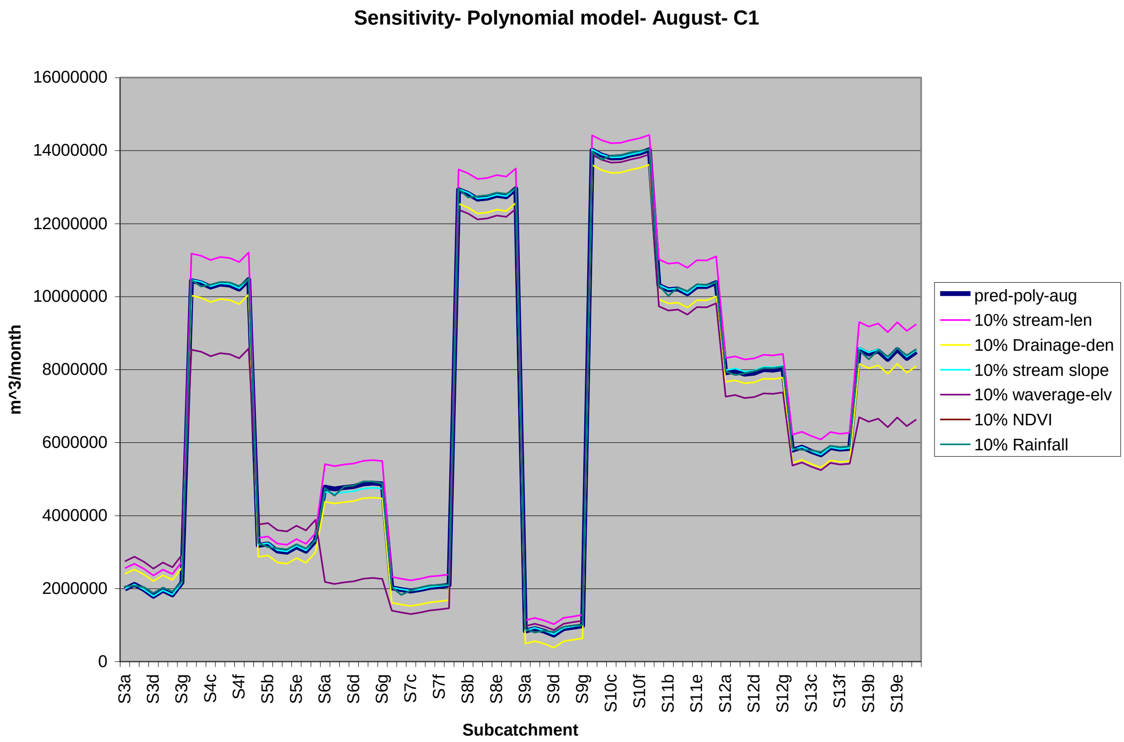

Figure C-77 Sensitivity (10%) – Polynomial model –August C1

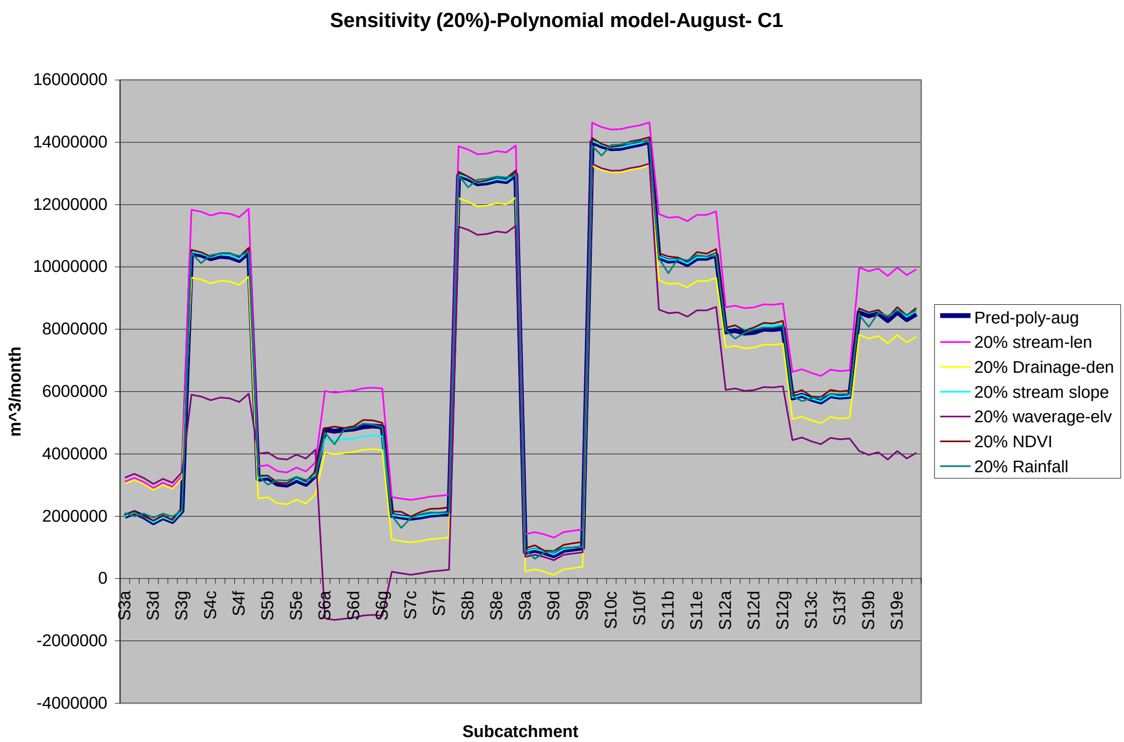

Figure C-78 Sensitivity (20%) – Polynomial model –August C1

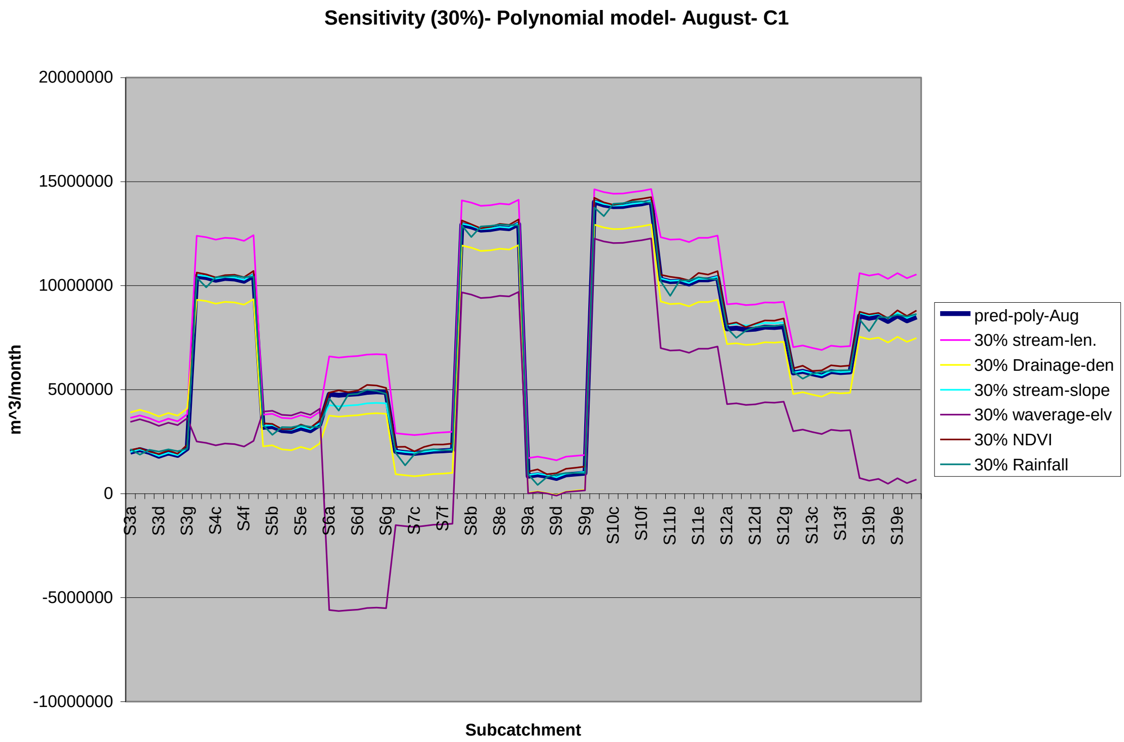

Figure C-79 Sensitivity (30%) – Polynomial model –August C1

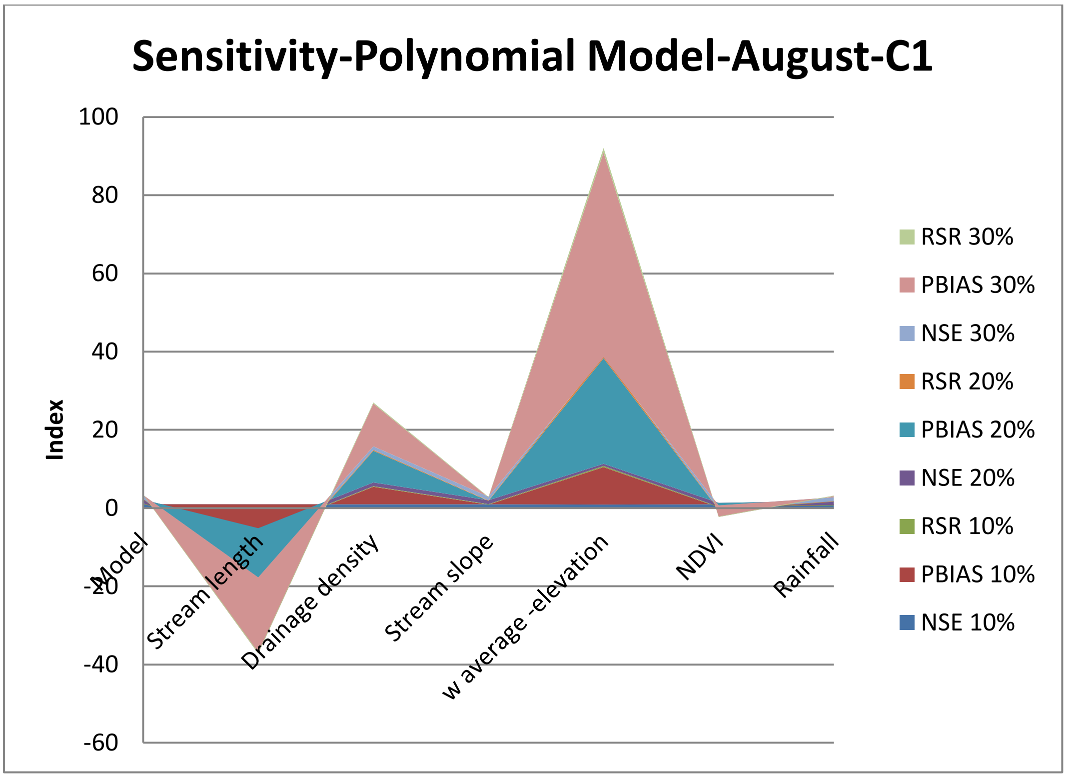

Figure C-80 Sensitivity summary – Polynomial model –August C1

Table C-20 Summary performance- Polynomial model- August C1

		10%					
	0%	Stream length	Drainage density	Stream slope	w average - elevation	NDVI	Rainfall
NSE	0.981693	0.966511	0.973866	0.98158	0.906642	0.981513	0.98145
PBIAS	0.05941	-7.21615	4.470302	-0.09538	9.568702	-0.7644	-0.27954
RSR	0.135302	0.183	0.16166	0.135721	0.305546	0.135966	0.136198
		20%					
	0%	Stream length	Drainage density	Stream slope	w average - elevation	NDVI	Rainfall
NSE	0.981693	0.926583	0.951622	0.981109	0.551358	0.980752	0.980611
PBIAS	0.05941	-13.7211	8.090966	-0.18124	26.97677	-1.76619	-0.19485
RSR	0.135302	0.270957	0.219951	0.137446	0.669807	0.138736	0.139244
		30%					
	0%	Stream length	Drainage density	Stream slope	w average - elevation	NDVI	Rainfall
NSE	0.981693	0.869411	0.914811	0.98005	-0.35948	0.979107	0.978814
PBIAS	0.05941	-19.4556	10.9214	-0.19816	52.28362	-2.94595	0.313479
RSR	0.135302	0.361371	0.291871	0.141245	1.165969	0.144544	0.145553

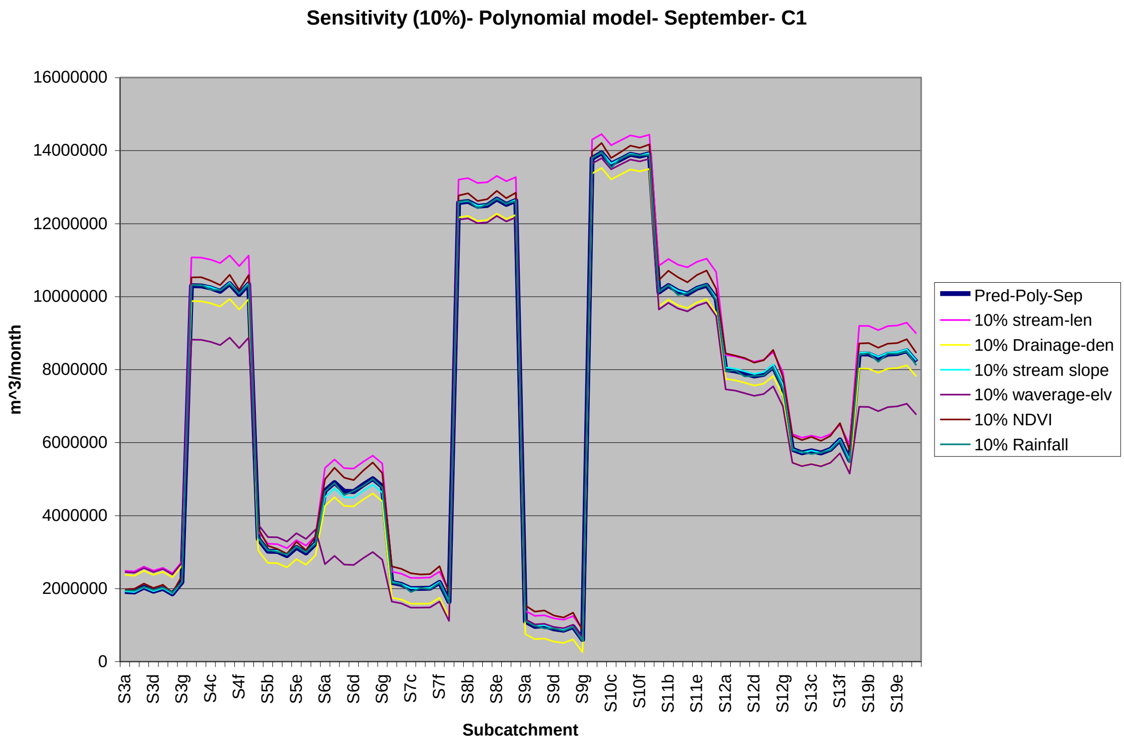

Figure C-81 Sensitivity (10%) – Polynomial model –September C1

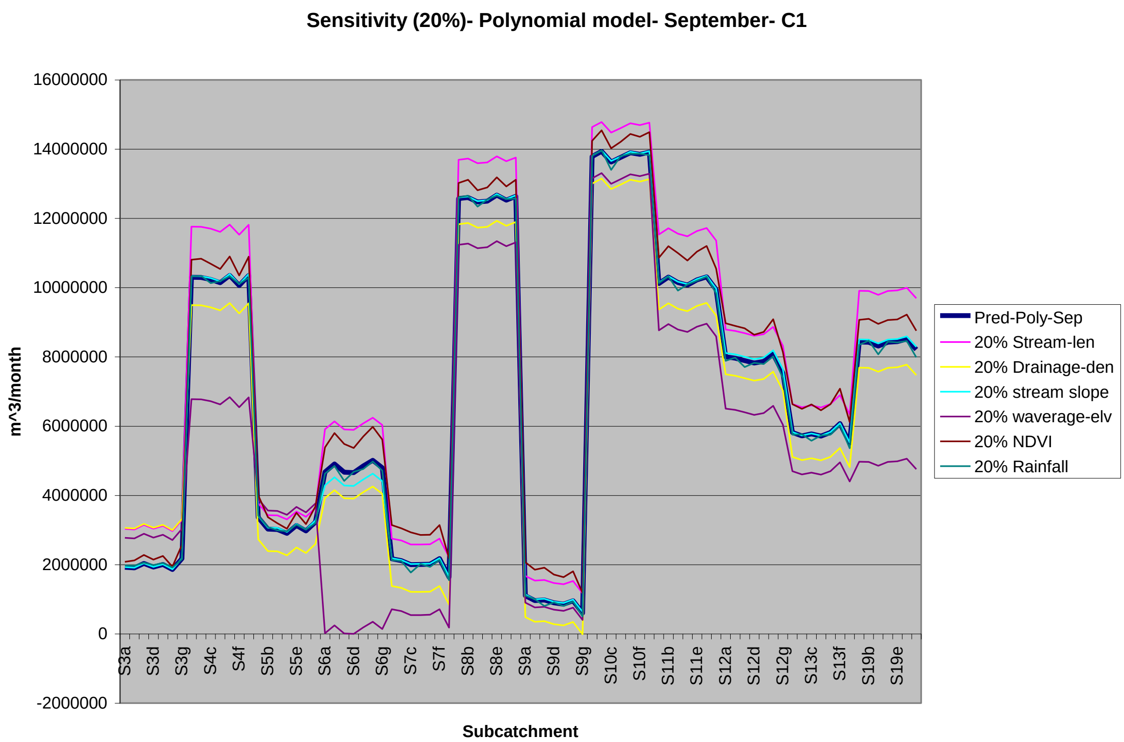

Figure C-82 Sensitivity (20%) – Polynomial model –August C1

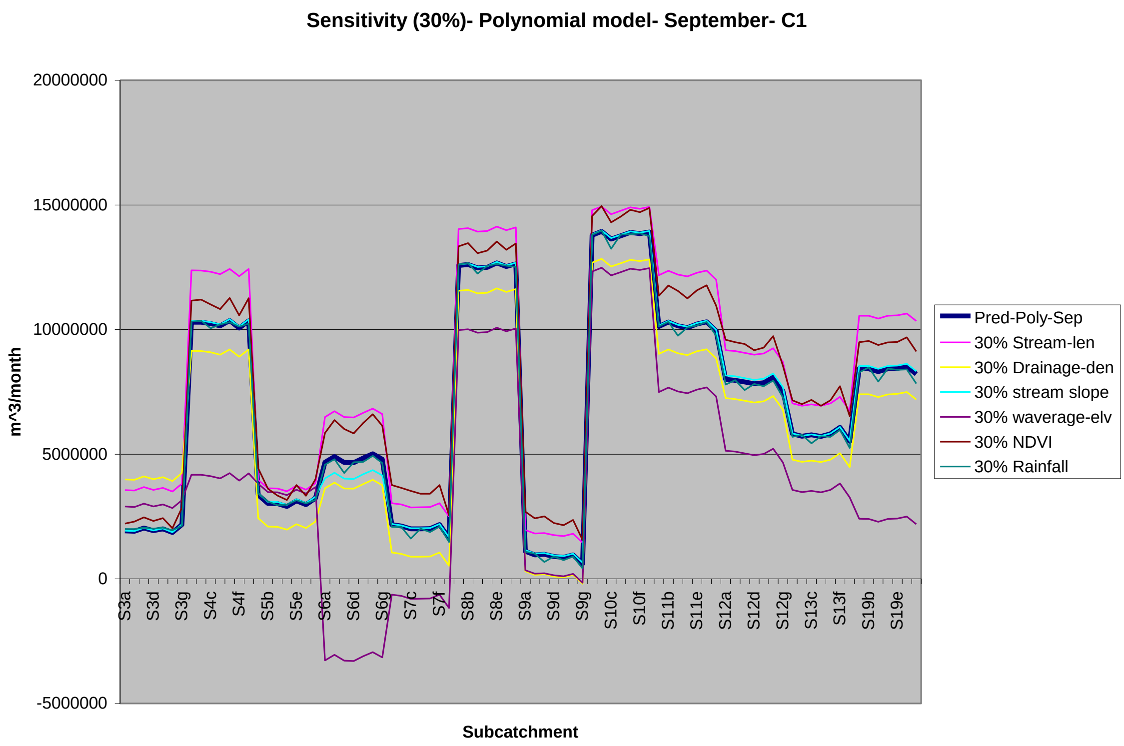

Figure C-83 Sensitivity (30%) – Polynomial model –August C1

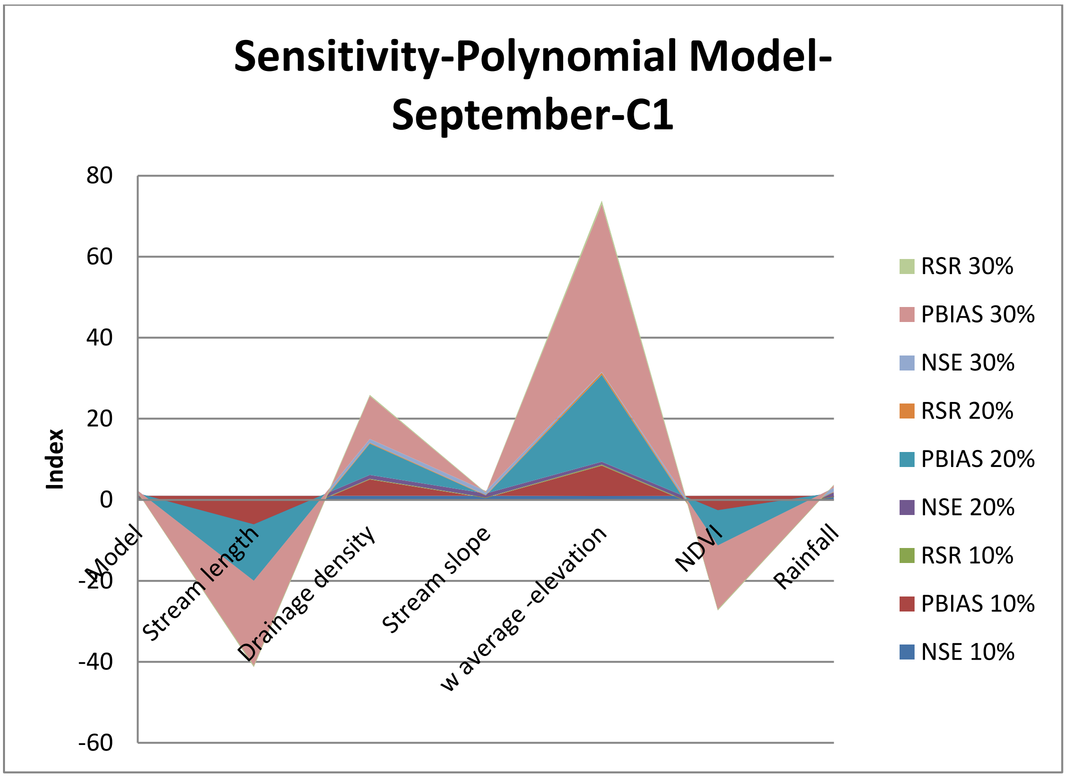

Figure C-84 Sensitivity summary – Polynomial model –August C1

Table C-21 Summary performance- Polynomial model- September C1

		10%					
	0%	Stream length	Drainage density	Stream slope	w average - elevation	NDVI	Rainfall
NSE	0.982271	0.963189	0.975119	0.982108	0.938151	0.975989	0.982231
PBIAS	-0.48307	-8.13089	4.049043	-0.53684	7.493012	-4.6481	-0.32293
RSR	0.13315	0.191863	0.157736	0.133762	0.248694	0.154955	0.1333
		20%					
	0%	Stream length	Drainage density	Stream slope	w average - elevation	NDVI	Rainfall
NSE	0.982271	0.916555	0.95189	0.98148	0.722559	0.953975	0.981965
PBIAS	-0.48307	-15.0633	7.744019	-0.52233	21.45214	-9.82848	0.05892
RSR	0.13315	0.288869	0.219341	0.136087	0.526726	0.214535	0.134296
		30%					
	0%	Stream length	Drainage density	Stream slope	w average - elevation	NDVI	Rainfall
NSE	0.982271	0.850653	0.912144	0.980101	0.170012	0.907381	0.98124
PBIAS	-0.48307	-21.2802	10.60185	-0.43954	41.3943	-16.0242	0.662475
RSR	0.13315	0.386455	0.296406	0.141064	0.911037	0.304334	0.136968

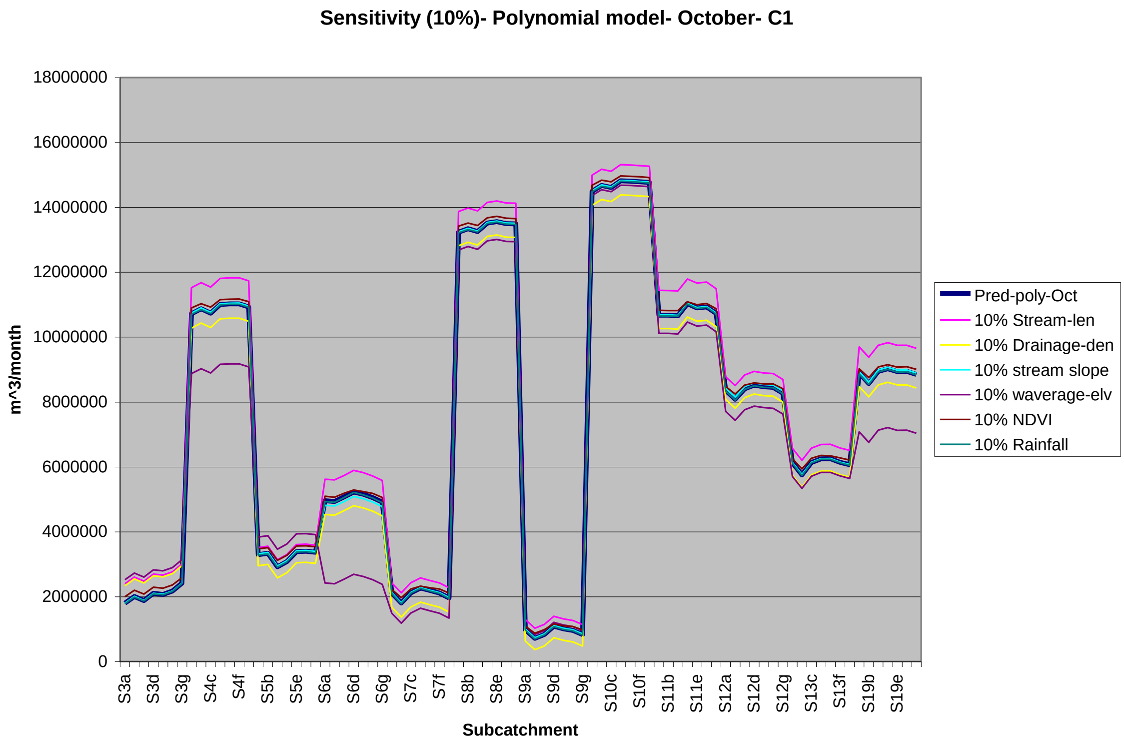

Figure C-85 Sensitivity (10%) – Polynomial model –October C1

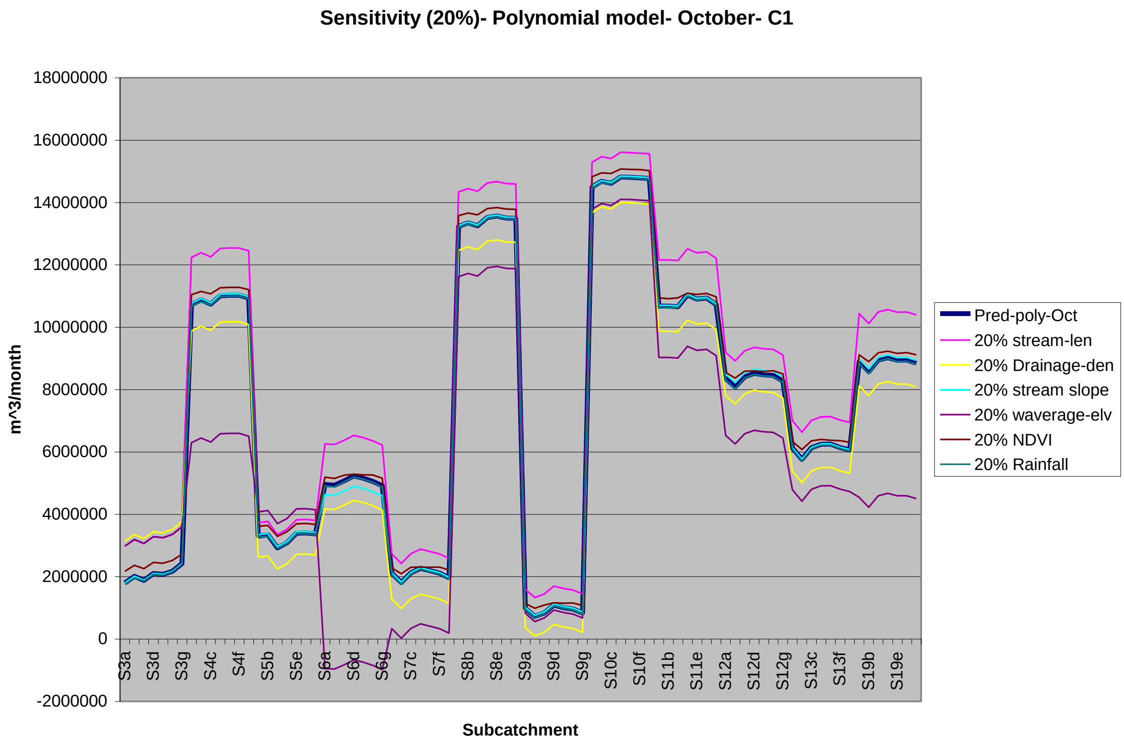

Figure C-86 Sensitivity (20%) – Polynomial model –October C1

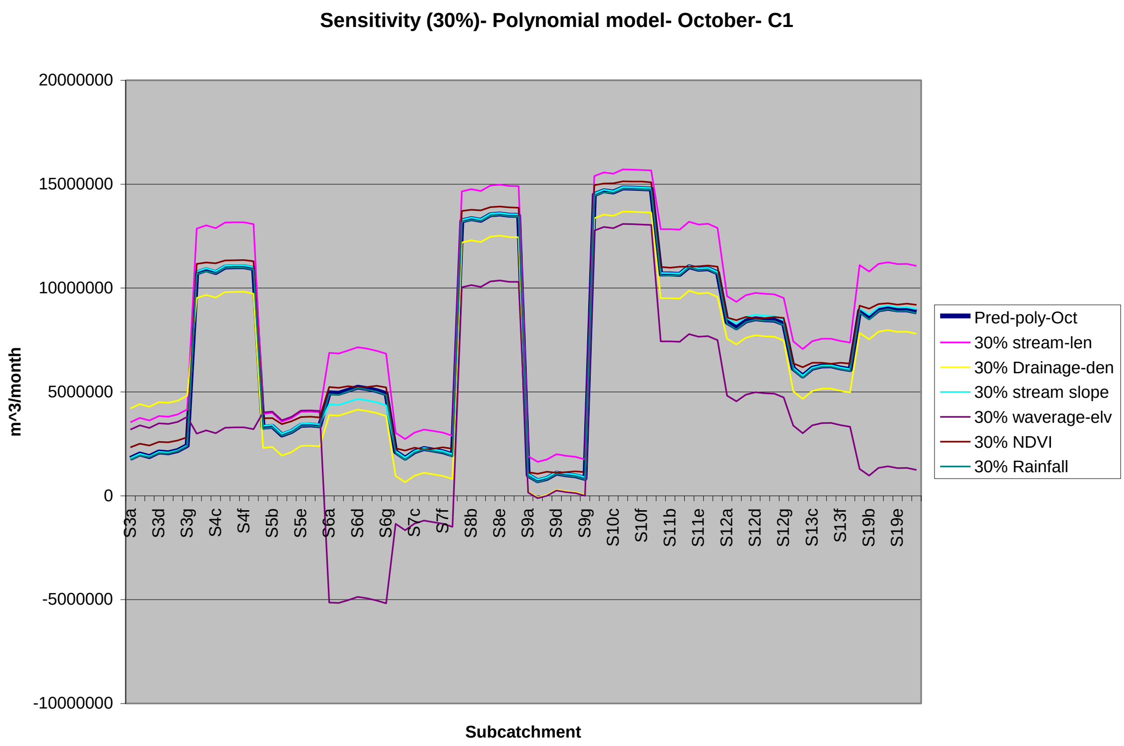

Figure C-87 Sensitivity (30%) – Polynomial model –October C1

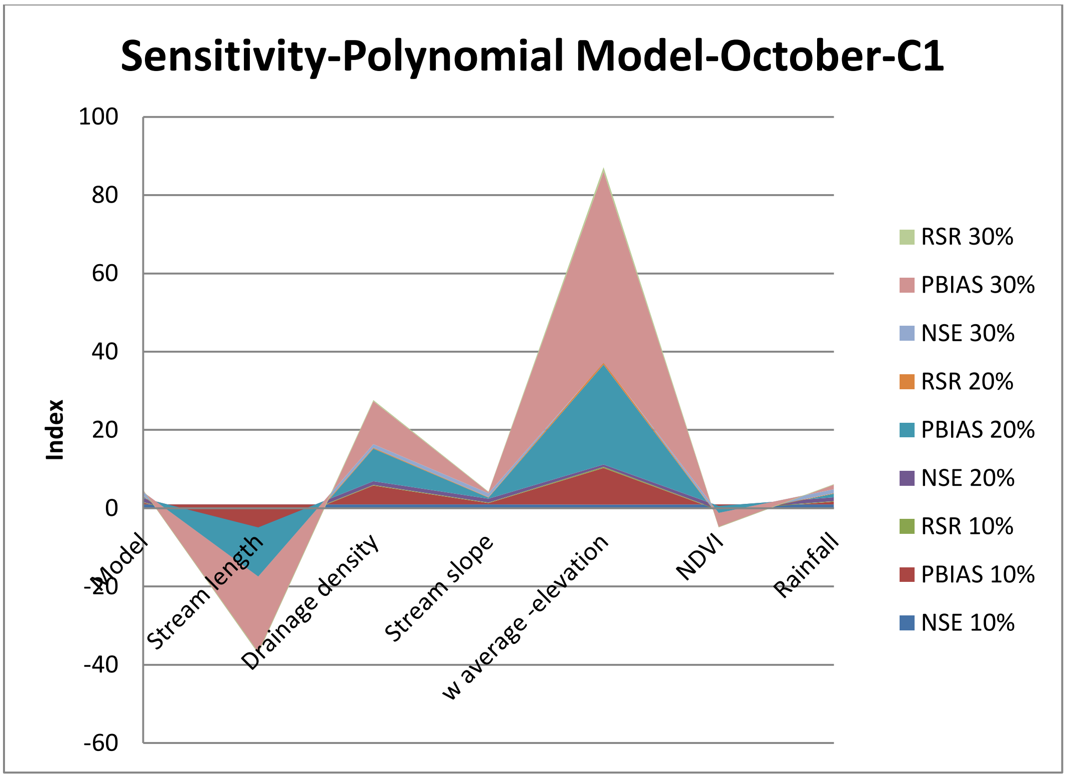

Figure C-88 Sensitivity summary – Polynomial model –October C1

Table C-22 Summary performance- Polynomial model- October C1

		10%					
	0%	Stream length	Drainage density	Stream slope	w average - elevation	NDVI	Rainfall
NSE	0.982258	0.967936	0.972856	0.982165	0.915877	0.981653	0.982187
PBIAS	0.461	-6.97804	4.820442	0.338337	9.366808	-1.51516	0.693014
RSR	0.1332	0.179063	0.164755	0.133547	0.29004	0.135452	0.133466
		20%					
	0%	Stream length	Drainage density	Stream slope	w average - elevation	NDVI	Rainfall
NSE	0.982258	0.927415	0.94759	0.98171	0.608814	0.979816	0.982083
PBIAS	0.461	-13.6834	8.323453	0.280747	25.51386	-2.89514	0.930496
RSR	0.1332	0.269417	0.228932	0.135242	0.625449	0.14207	0.133853
		30%					
	0%	Stream length	Drainage density	Stream slope	w average - elevation	NDVI	Rainfall
NSE	0.982258	0.868562	0.905455	0.980672	-0.17254	0.977888	0.981945
PBIAS	0.461	-19.6552	10.97003	0.288231	48.90215	-3.67897	1.173444
RSR	0.1332	0.362544	0.307481	0.139025	1.082838	0.148701	0.134369

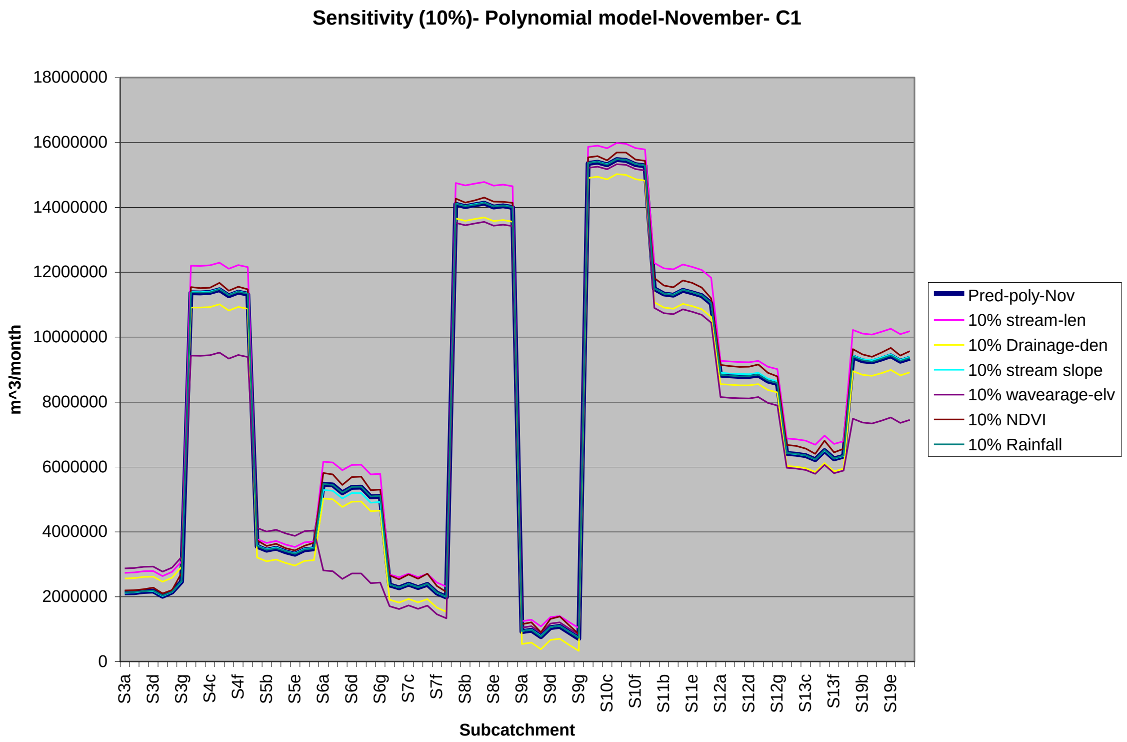

Figure C-89 Sensitivity (10%) – Polynomial model –November C1

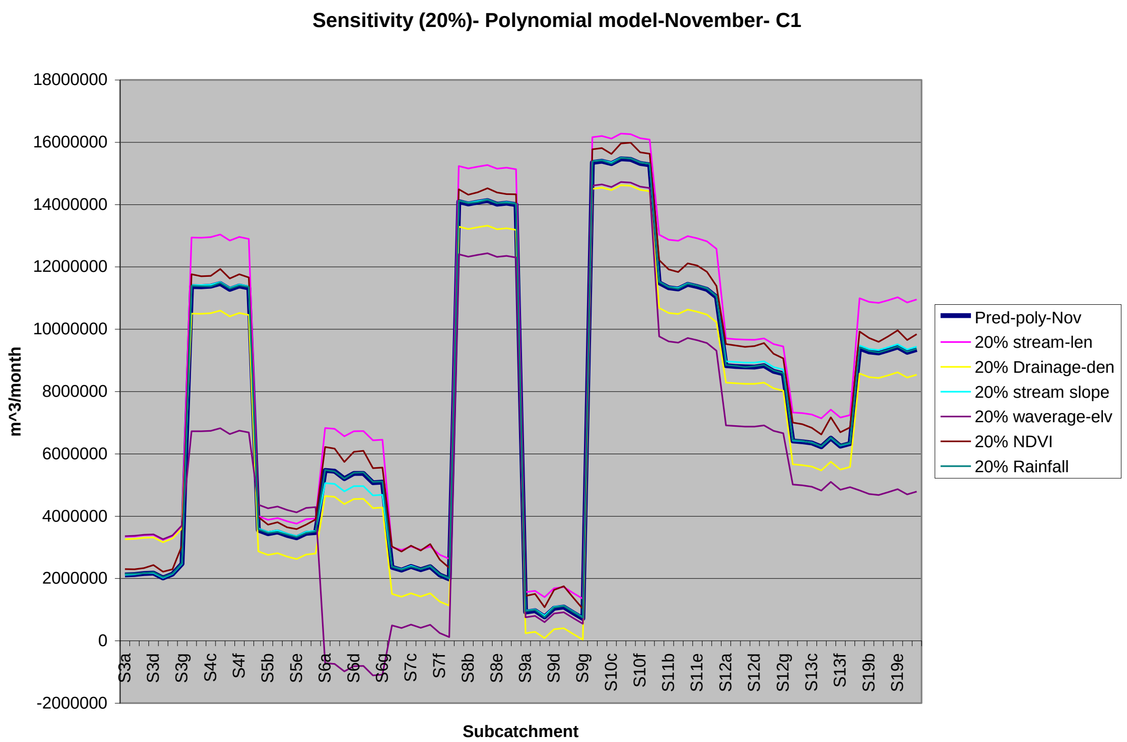

Figure C-90 Sensitivity (20%) – Polynomial model –November C1

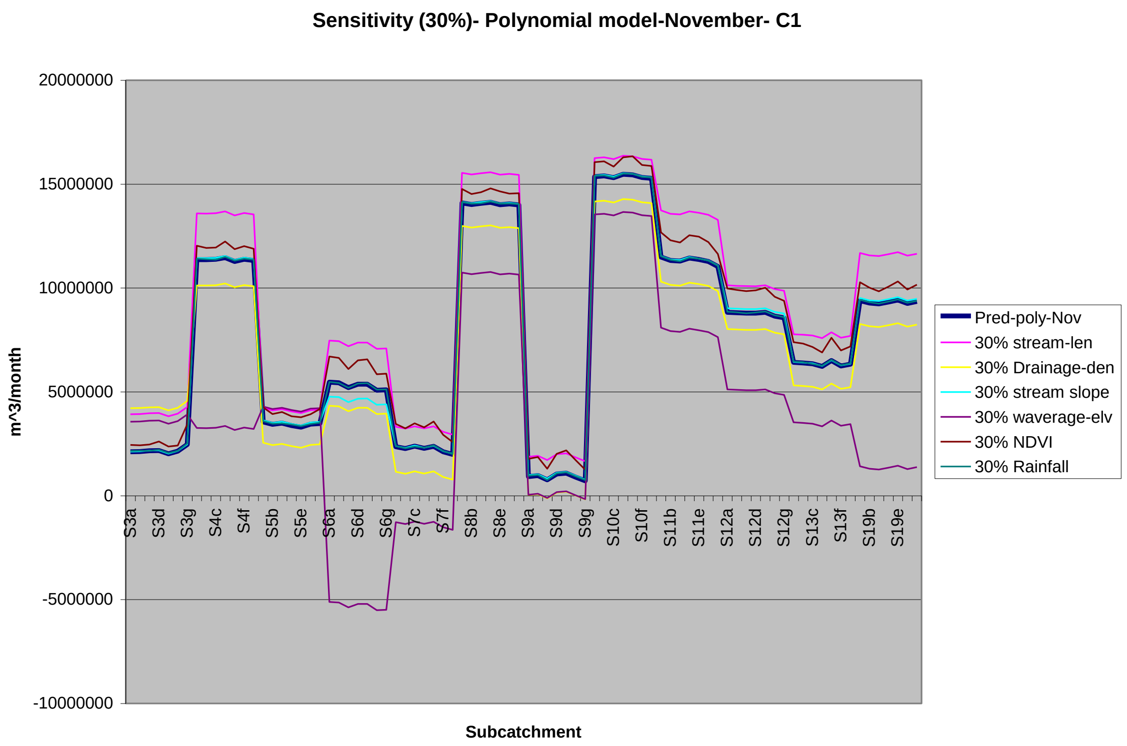

Figure C-91 Sensitivity (30%) – Polynomial model –November C1

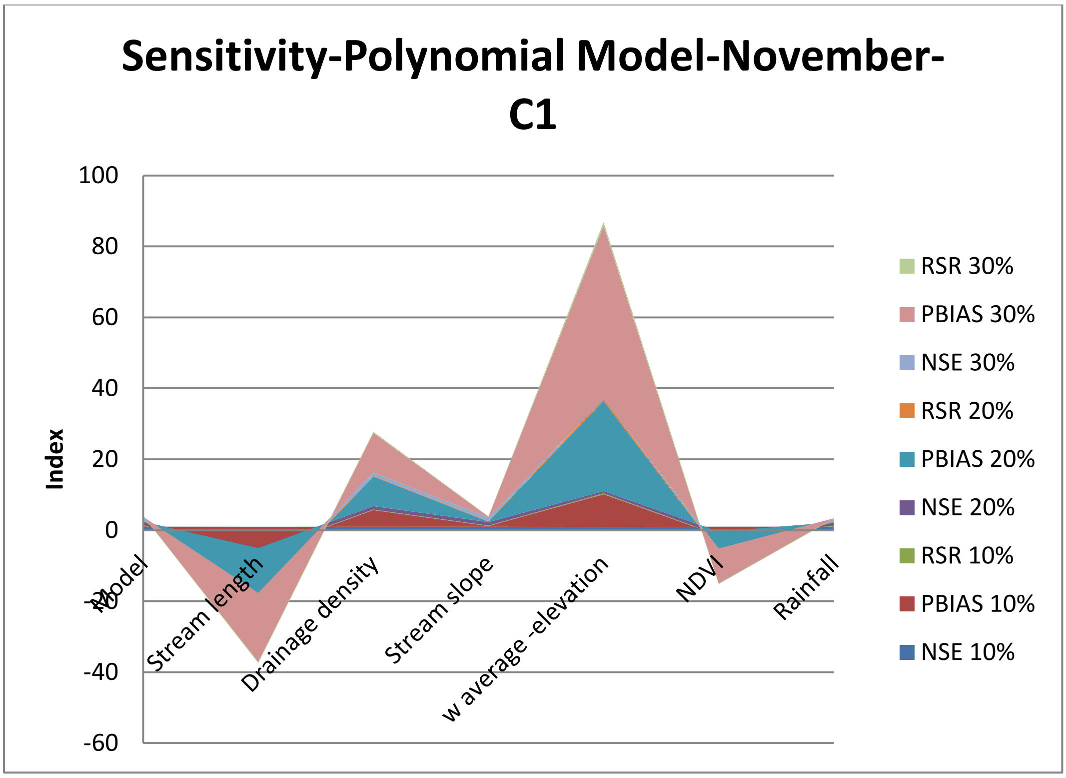

Figure C-92 Sensitivity summary – Polynomial model –November C1

Table C-23 Summary performance- Polynomial model- November C1

		10%					
	0%	Stream length	Drainage density	Stream slope	w average - elevation	NDVI	Rainfall
NSE	0.981809	0.966948	0.97346	0.981663	0.915997	0.980018	0.981825
PBIAS	0.275943	-7.12076	4.700438	0.186178	9.211672	-2.47469	0.113569
RSR	0.134872	0.181803	0.162912	0.135415	0.289833	0.141359	0.134816
		20%					
	0%	Stream length	Drainage density	Stream slope	w average - elevation	NDVI	Rainfall
NSE	0.981809	0.926278	0.950804	0.981045	0.608599	0.971777	0.981824
PBIAS	0.275943	-13.7813	8.337213	0.166582	25.41322	-5.89841	-0.00767
RSR	0.134872	0.271517	0.221801	0.137678	0.62562	0.167998	0.134818
		30%					
	0%	Stream length	Drainage density	Stream slope	w average - elevation	NDVI	Rainfall
NSE	0.981809	0.867583	0.913746	0.979673	-0.17558	0.953294	0.981813
PBIAS	0.275943	-19.7057	11.18627	0.217156	48.88058	-9.99524	-0.08777
RSR	0.134872	0.363892	0.293691	0.142571	1.08424	0.216117	0.134858

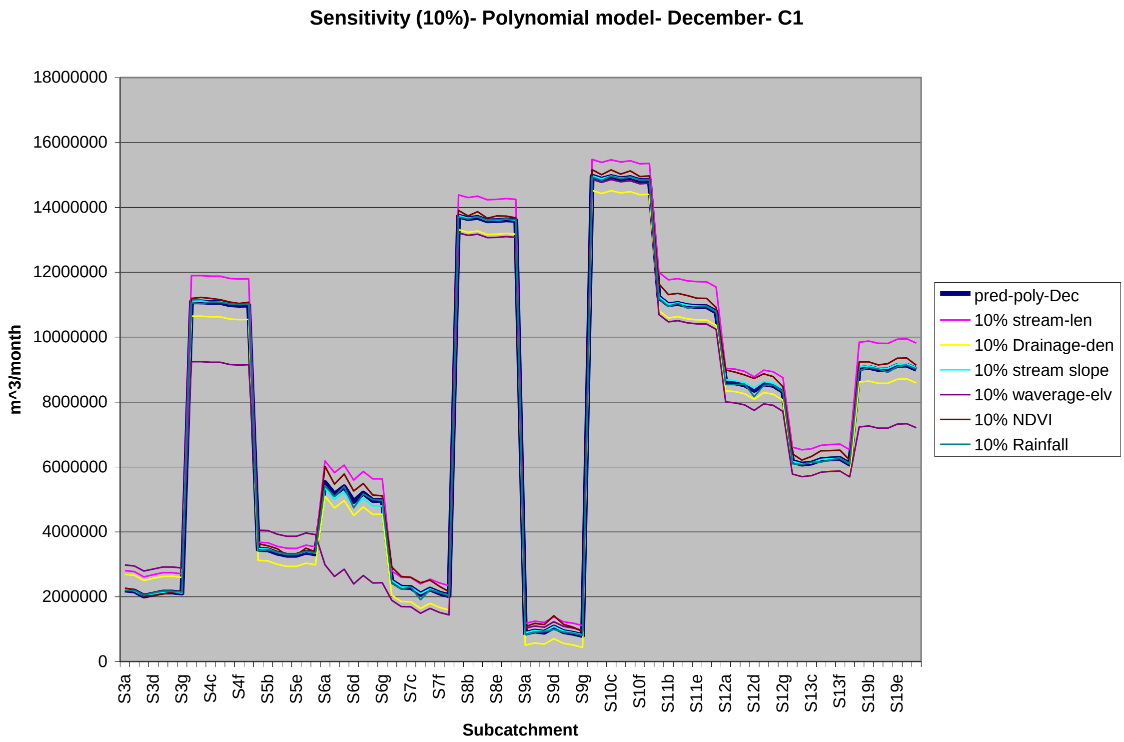

Figure C-93 Sensitivity (10%) – Polynomial model –December C1

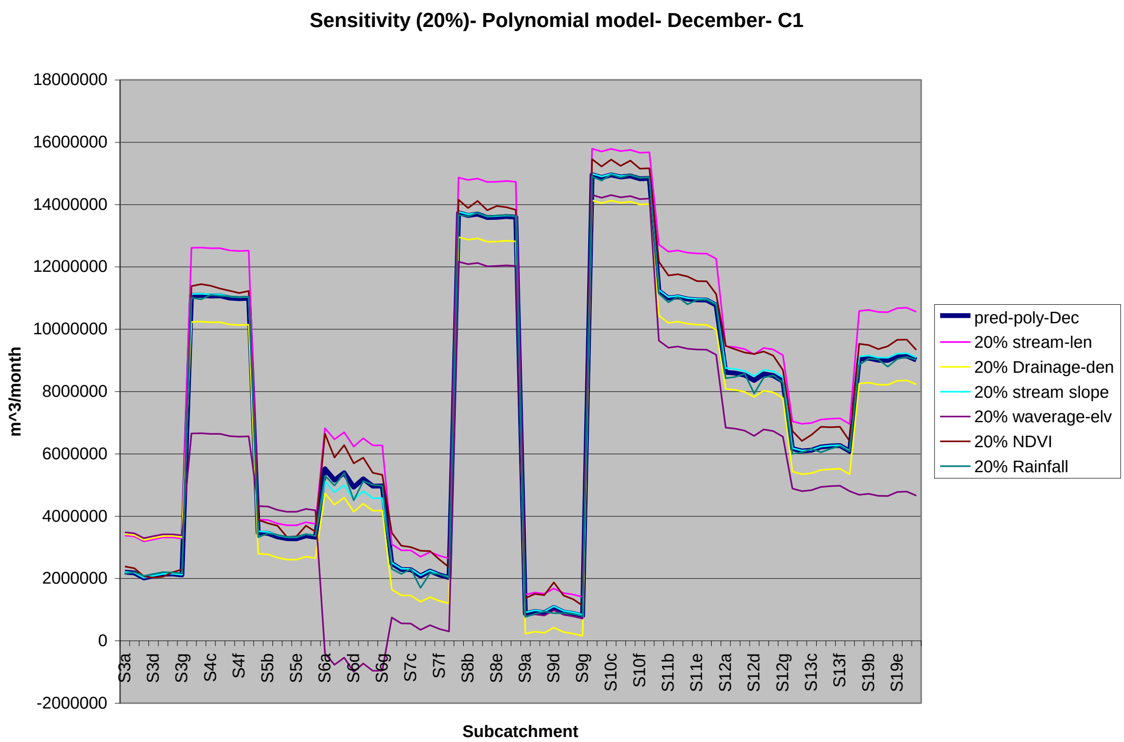

Figure C-94 Sensitivity (20%) – Polynomial model –December C1

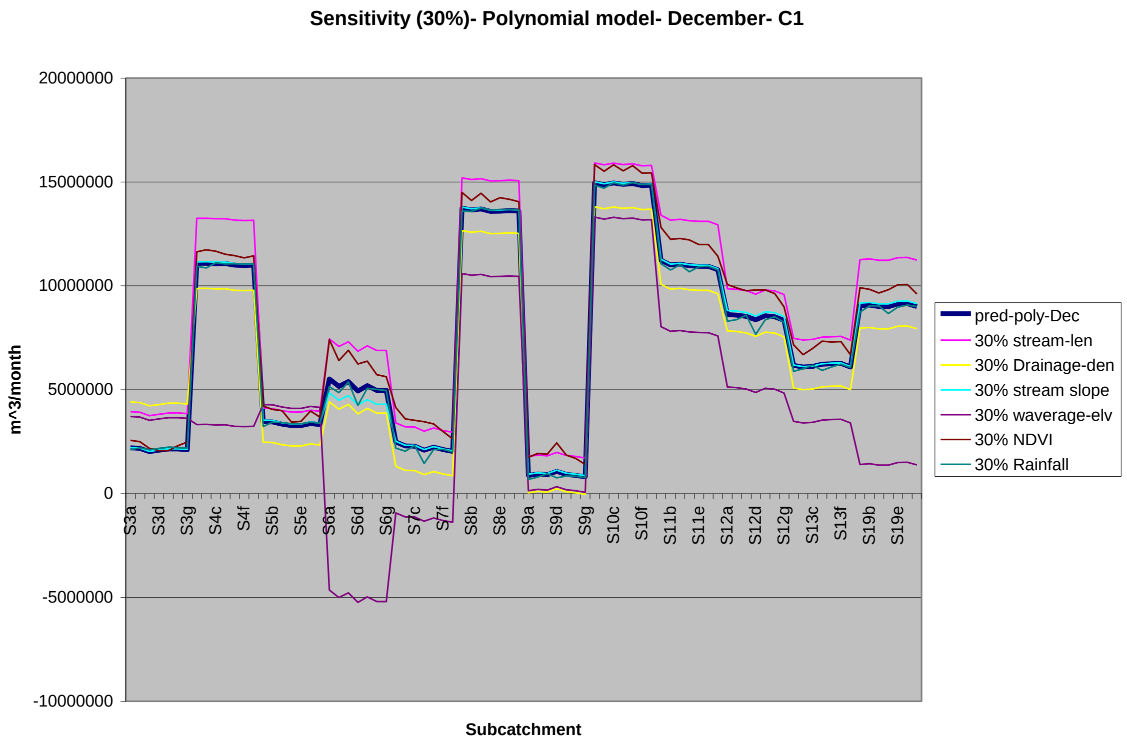

Figure C-95 Sensitivity (30%) – Polynomial model –December C1

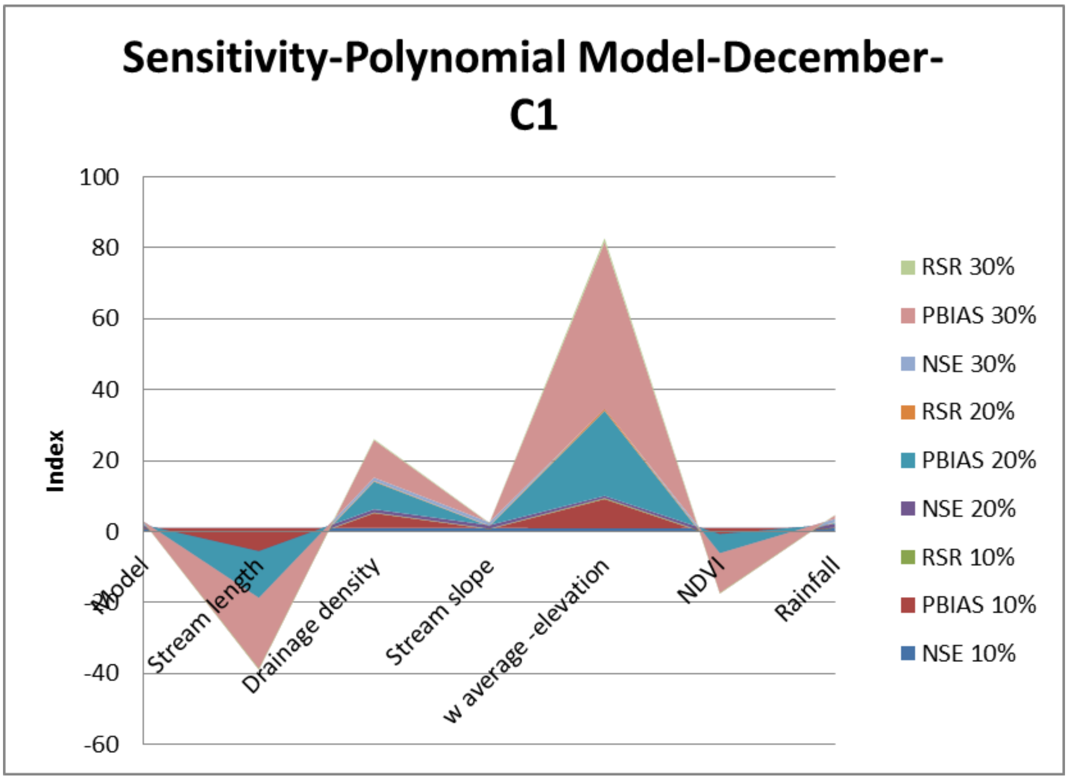

Figure C-96 Sensitivity summary – Polynomial model –December C1

Table C-24 Summary performance- Polynomial model- December C1

		10%					
	0%	Stream length	Drainage density	Stream slope	w average - elevation	NDVI	Rainfall
NSE	0.981807	0.964978	0.974344	0.981653	0.920746	0.979187	0.981706
PBIAS	-0.19938	-7.607	4.204558	-0.29115	8.23484	-2.7885	-0.00841
RSR	0.13488	0.187142	0.160174	0.135451	0.28152	0.144266	0.135254
		20%					
	0%	Stream length	Drainage density	Stream slope	w average - elevation	NDVI	Rainfall
NSE	0.981807	0.922351	0.951661	0.981053	0.626628	0.967977	0.981248
PBIAS	-0.19938	-14.2989	7.78942	-0.31284	24.00262	-6.51696	0.384112
RSR	0.13488	0.278657	0.219862	0.137647	0.611042	0.17895	0.136939
		30%					
	0%	Stream length	Drainage density	Stream slope	w average - elevation	NDVI	Rainfall
NSE	0.981807	0.86172	0.91328	0.979728	-0.13318	0.940922	0.980172
PBIAS	-0.19938	-20.2751	10.55521	-0.26444	47.10396	-11.3847	0.978179
RSR	0.13488	0.37186	0.294483	0.142379	1.06451	0.243059	0.140812

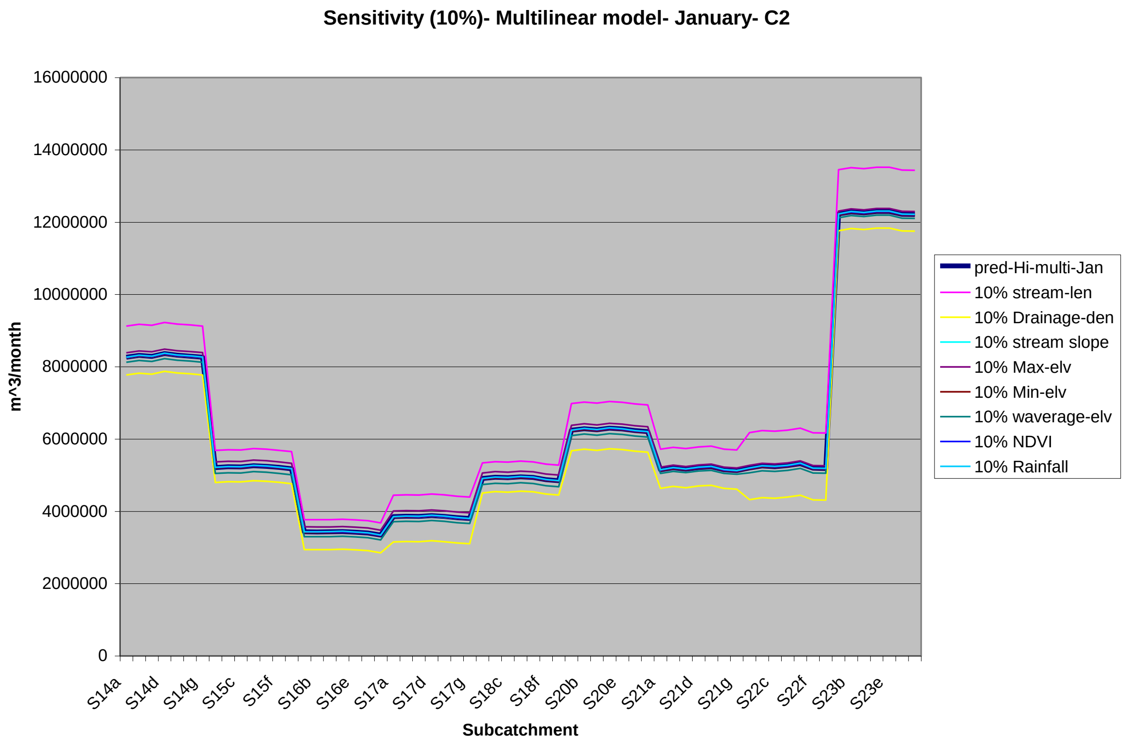

Figure C-97 Sensitivity (10%) – Multilinear model –January C2

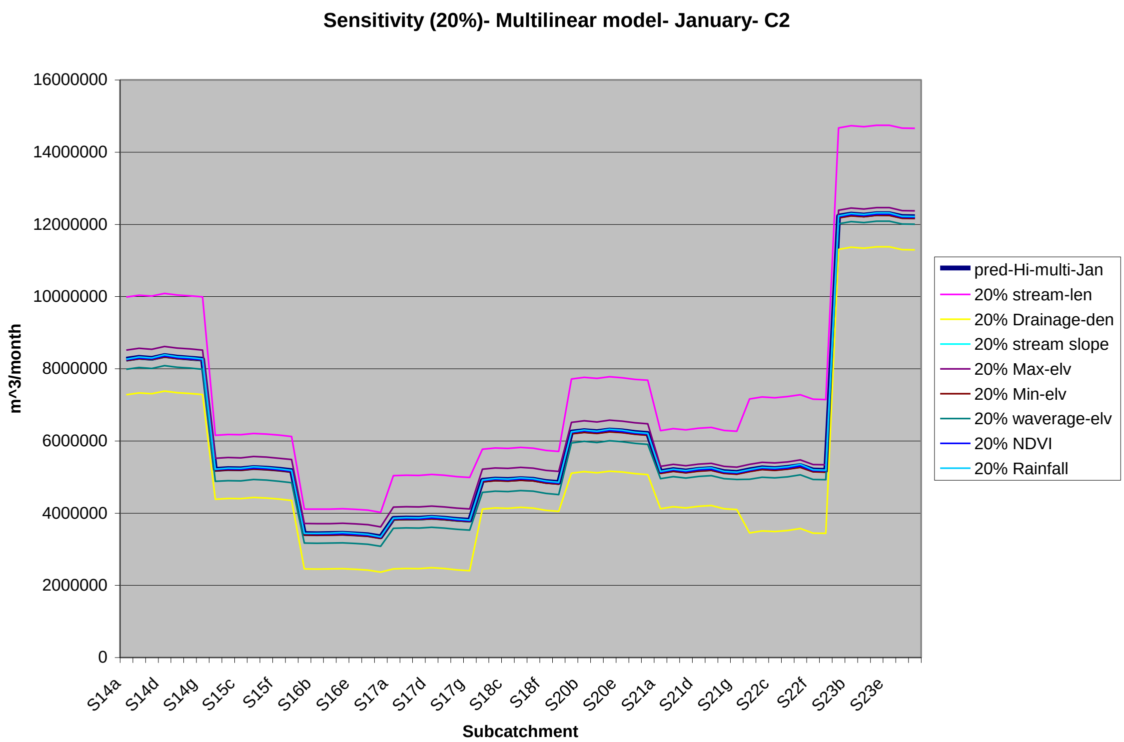

Figure C-98 Sensitivity (20%) – Multilinear model –January C2

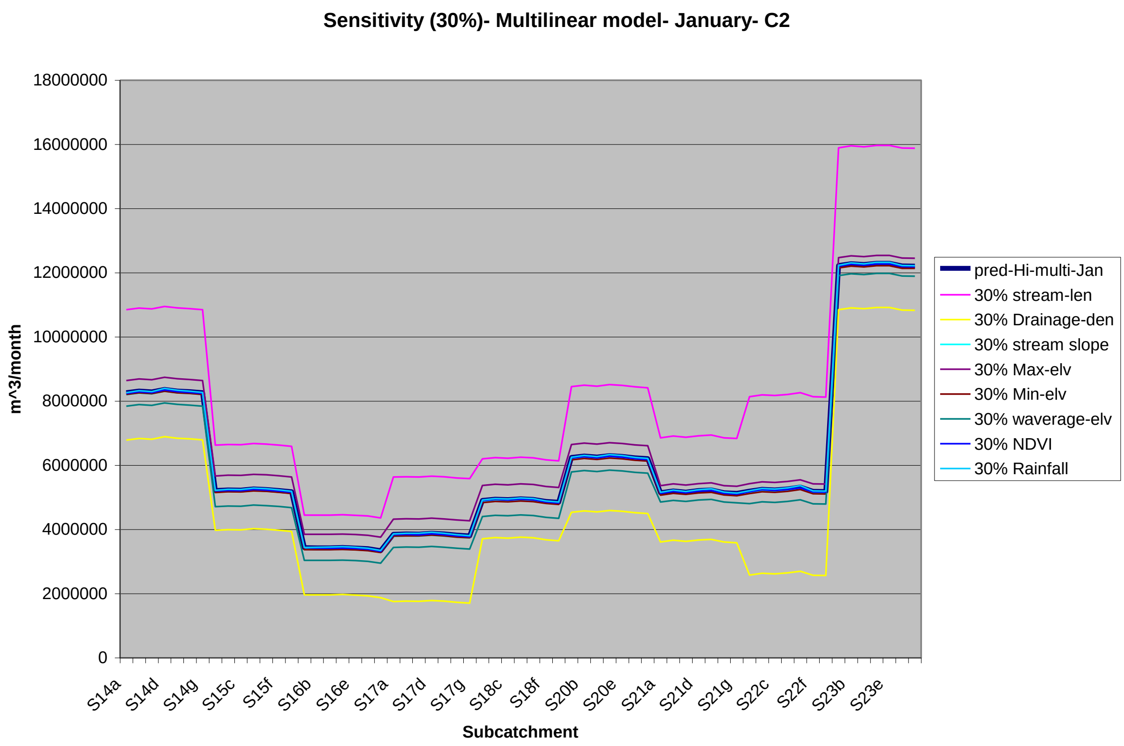

Figure C-99 Sensitivity (30%) – Multilinear model –January C2

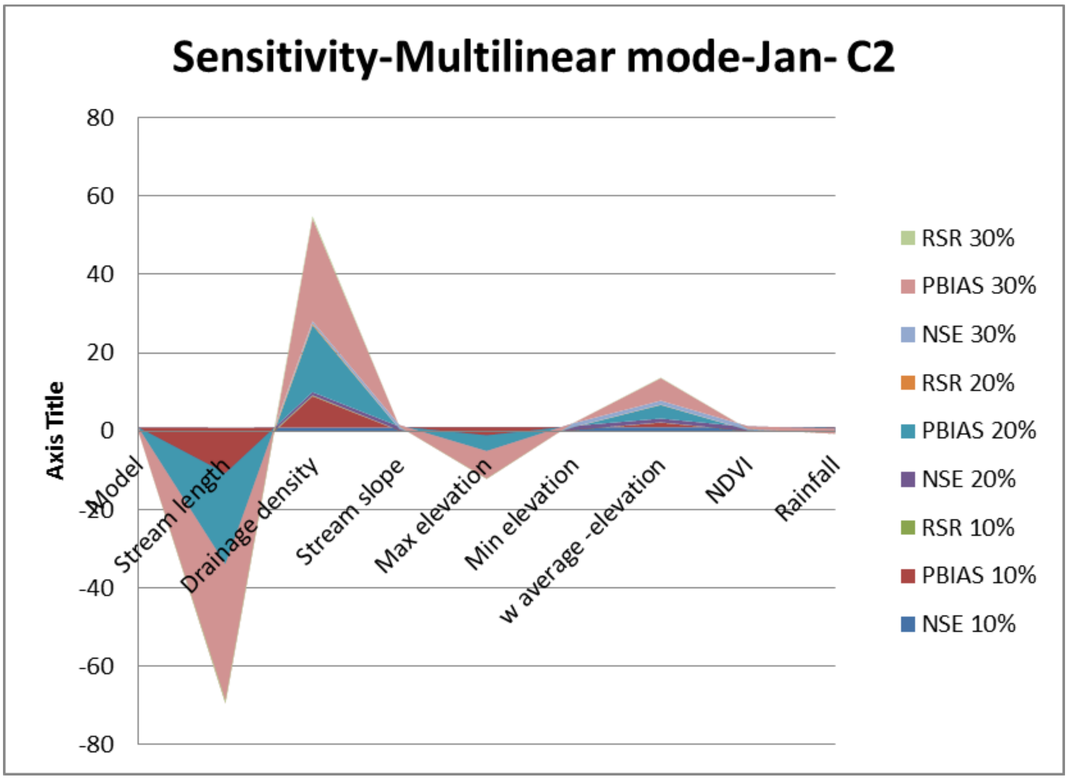

Figure C-100 Sensitivity summary – Multilinear model –January C2

Table C-25 Summary performance- Multilinear model- January C2

		10%							
	0%	Stream length	Drainage density	Stream slope	Max elevation	Min elevation	w average - elevation	NDVI	Rainfall
NSE	0.996795	0.899859	0.959116	0.996998	0.992043	0.997152	0.996511	0.996905	0.996648
PBIAS	-1.05963	-12.5483	8.015616	-0.85503	-3.08629	-0.68745	1.206406	-0.95307	-1.15922
RSR	0.056612	0.31645	0.202198	0.054789	0.089203	0.05337	0.059067	0.055629	0.057898
		20%							
	0%	Stream length	Drainage density	Stream slope	Max elevation	Min elevation	w average - elevation	NDVI	Rainfall
NSE	0.996795	0.635504	0.824727	0.99714	0.98245	0.997354	0.990431	0.997002	0.996487
PBIAS	-1.05963	-24.0371	17.09087	-0.65043	-5.11295	-0.31527	3.472447	-0.8465	-1.25881
RSR	0.056612	0.603735	0.418656	0.053477	0.132476	0.051438	0.097823	0.05475	0.059271
		30%							
	0%	Stream length	Drainage density	Stream slope	Max elevation	Min elevation	w average - elevation	NDVI	Rainfall
NSE	0.996795	0.203728	0.593629	0.997221	0.968017	0.997402	0.978554	0.997086	0.996312
PBIAS	-1.05963	-35.5258	26.16612	-0.44583	-7.13961	0.056907	5.738487	-0.73994	-1.3584
RSR	0.056612	0.892341	0.637473	0.052714	0.178839	0.050967	0.146445	0.05398	0.060726

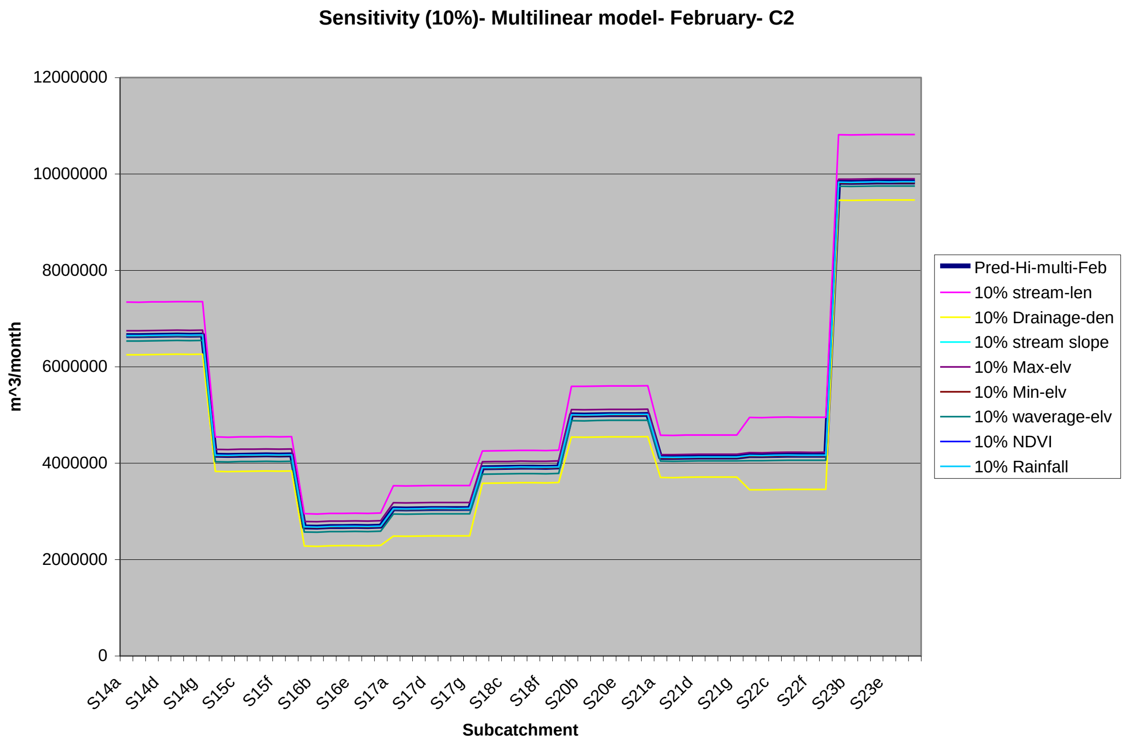

Figure C-101 Sensitivity (10%) – Multilinear model –February C2

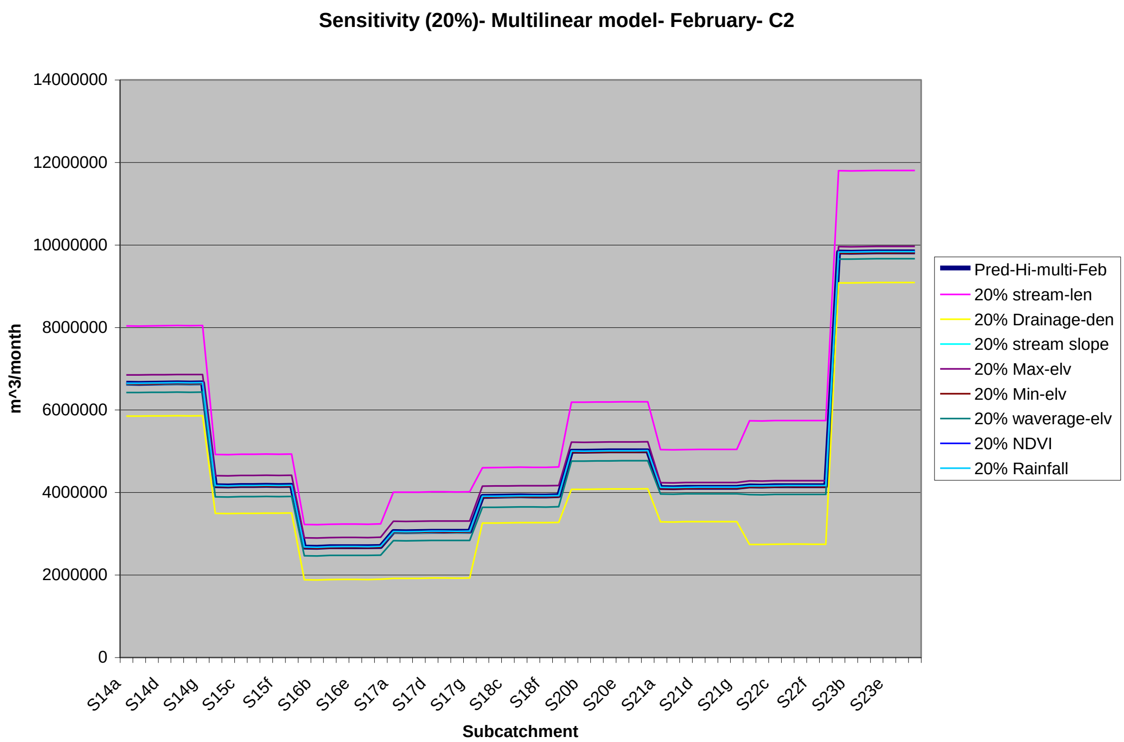

Figure C-102 Sensitivity (20%) – Multilinear model –February C2

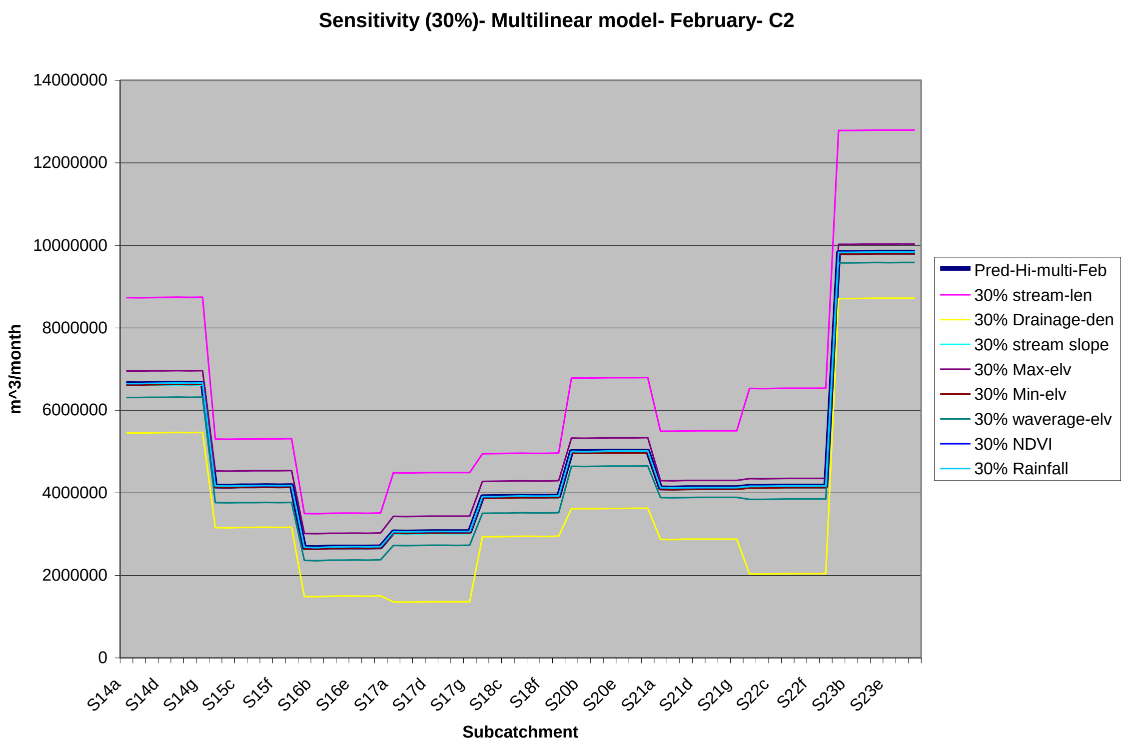

Figure C-103 Sensitivity (30%) – Multilinear model –February C2

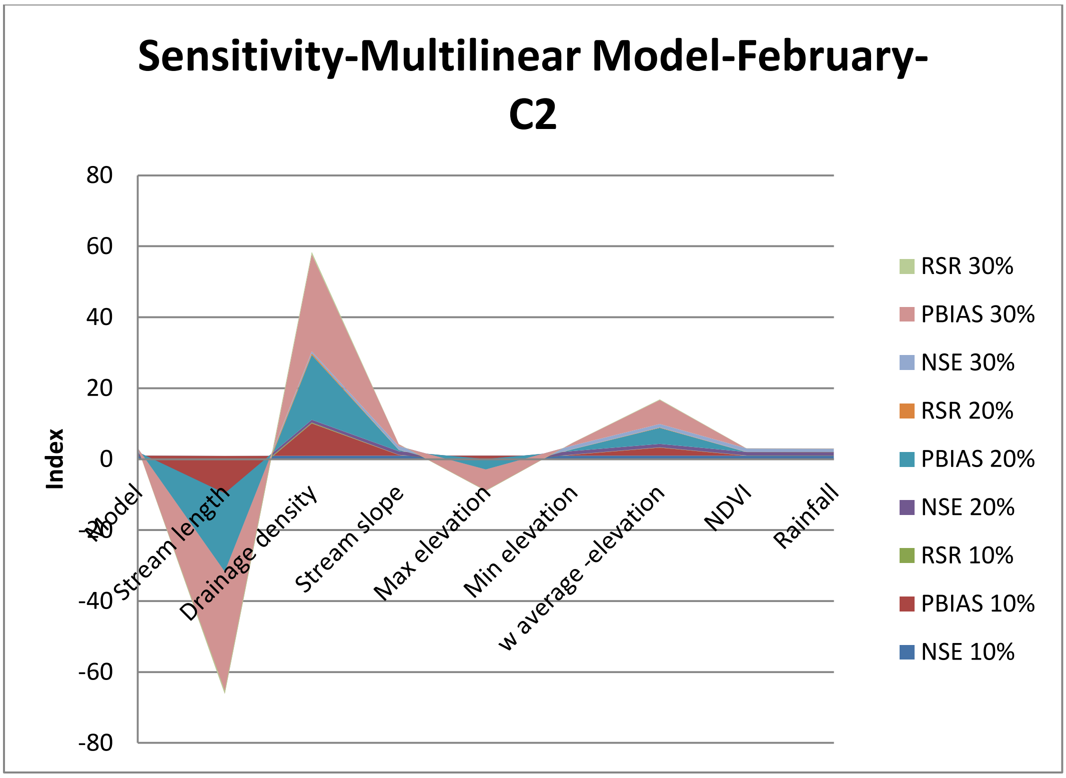

Figure C-104 Sensitivity summary – Multilinear model –February C2

Table C-26 Summary performance- Multilinear model- February C2

		10%							
	0%	Stream length	Drainage density	Stream slope	Max elevation	Min elevation	w average - elevation	NDVI	Rainfall
NSE	0.997552	0.914082	0.948579	0.997525	0.995168	0.997515	0.994668	0.997552	0.997552
PBIAS	0.005738	-11.4707	9.133676	0.192415	-2.01128	0.258817	2.260598	-0.01589	-0.02344
RSR	0.049478	0.293118	0.226763	0.049746	0.069513	0.049853	0.073023	0.04948	0.049481
		20%							
	0%	Stream length	Drainage density	Stream slope	Max elevation	Min elevation	w average - elevation	NDVI	Rainfall
NSE	0.997552	0.663547	0.801769	0.997448	0.987989	0.997406	0.986044	0.997551	0.99755
PBIAS	0.005738	-22.9472	18.26161	0.379092	-4.0283	0.511896	4.515458	-0.03753	-0.05262
RSR	0.049478	0.580045	0.445231	0.050518	0.109593	0.05093	0.118135	0.049487	0.049494
		30%							
	0%	Stream length	Drainage density	Stream slope	Max elevation	Min elevation	w average - elevation	NDVI	Rainfall
NSE	0.997552	0.24595	0.557124	0.99732	0.976016	0.997226	0.971681	0.99755	0.997548
PBIAS	0.005738	-34.4237	27.38955	0.56577	-6.04532	0.764975	6.770318	-0.05916	-0.08179
RSR	0.049478	0.868361	0.665489	0.051771	0.154868	0.052665	0.168283	0.049499	0.049517

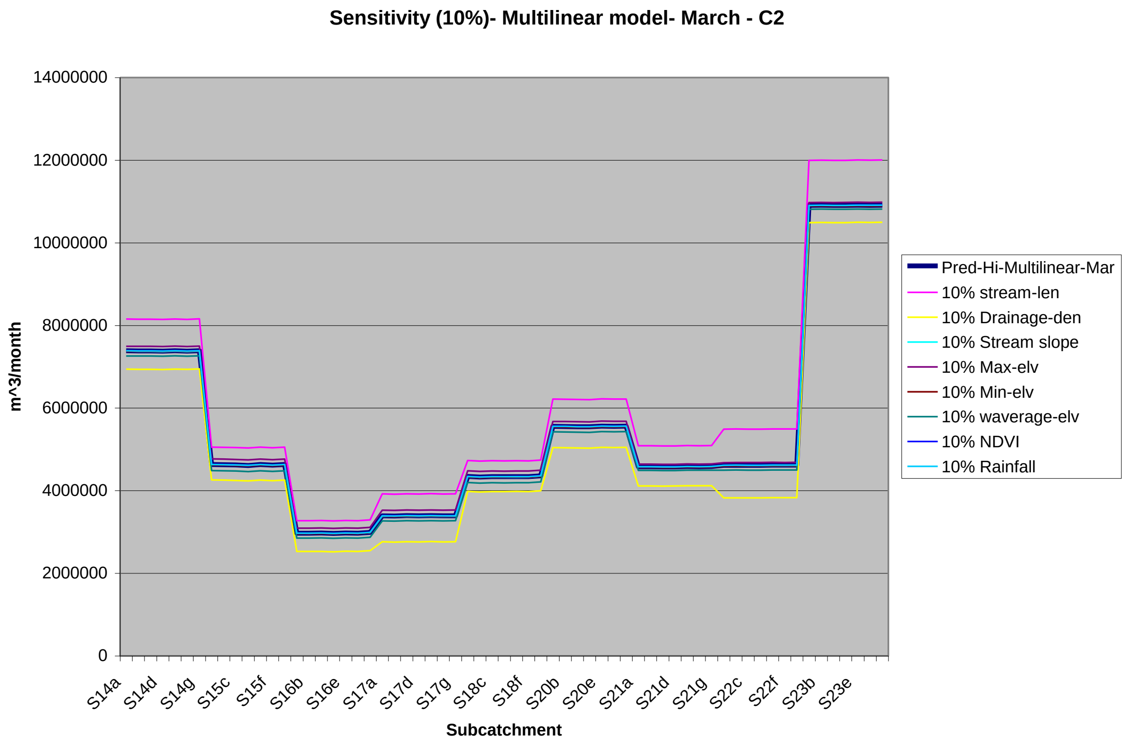

Figure C-105 Sensitivity (10%) – Multilinear model –March C2

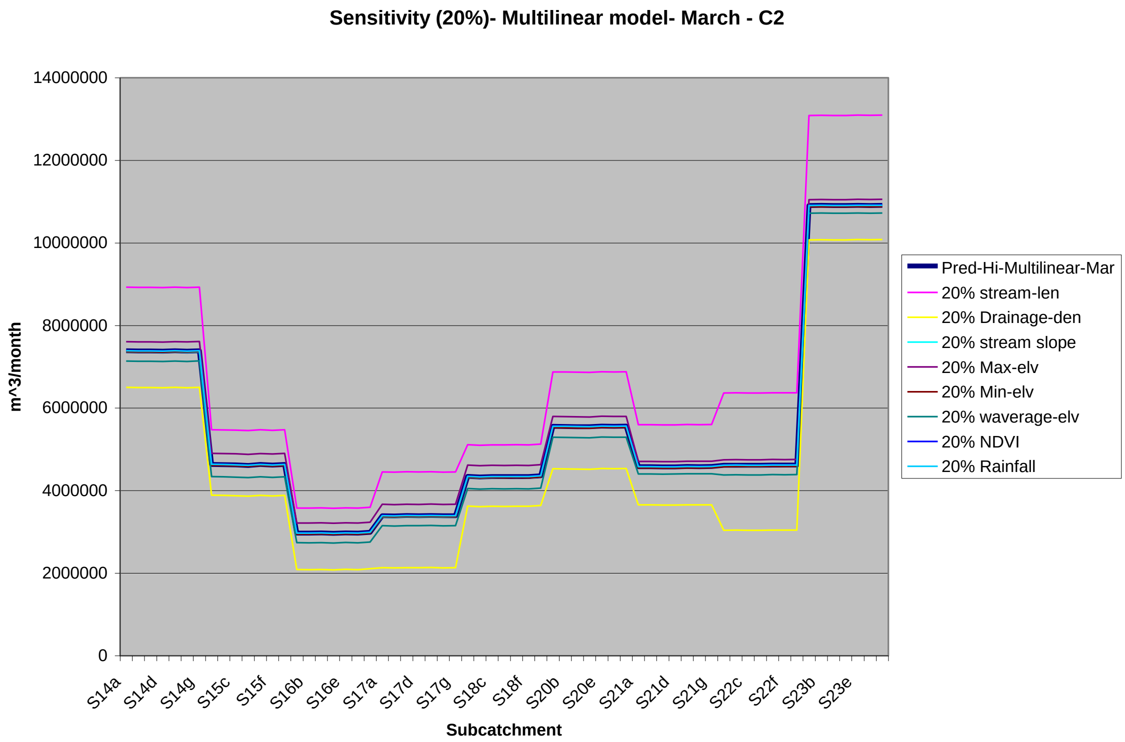

Figure C-106 Sensitivity (20%) – Multilinear model –March C2

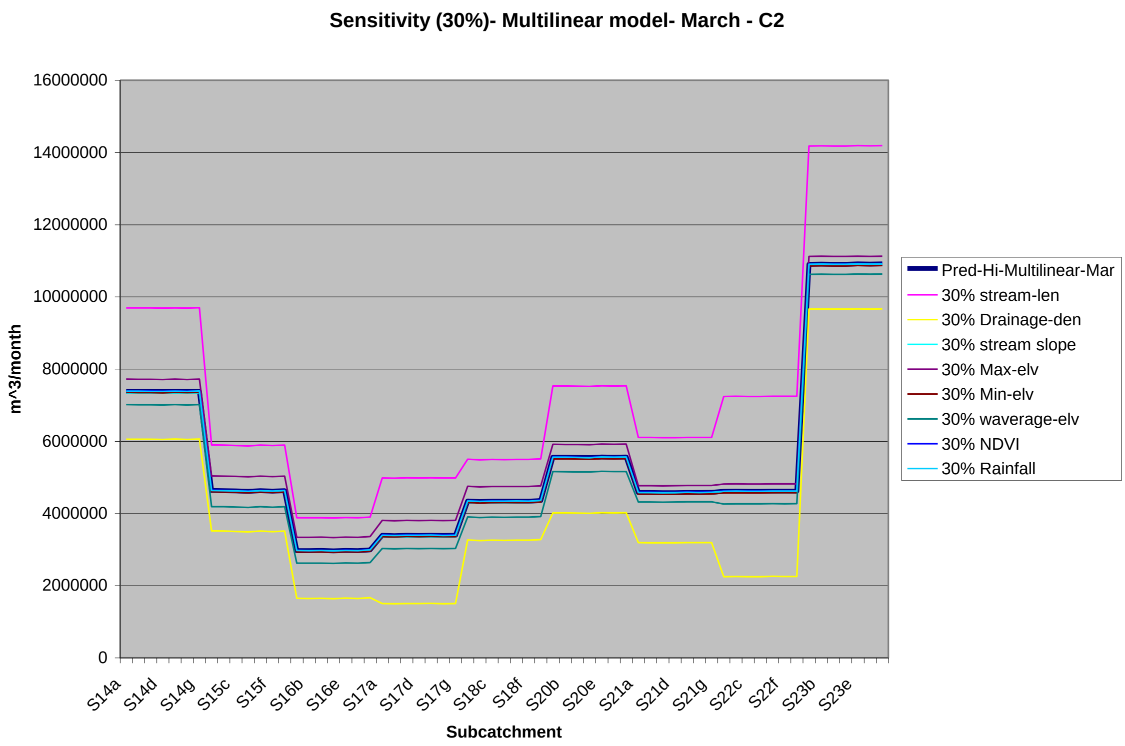

Figure C-107 Sensitivity (30%) – Multilinear model –March C2

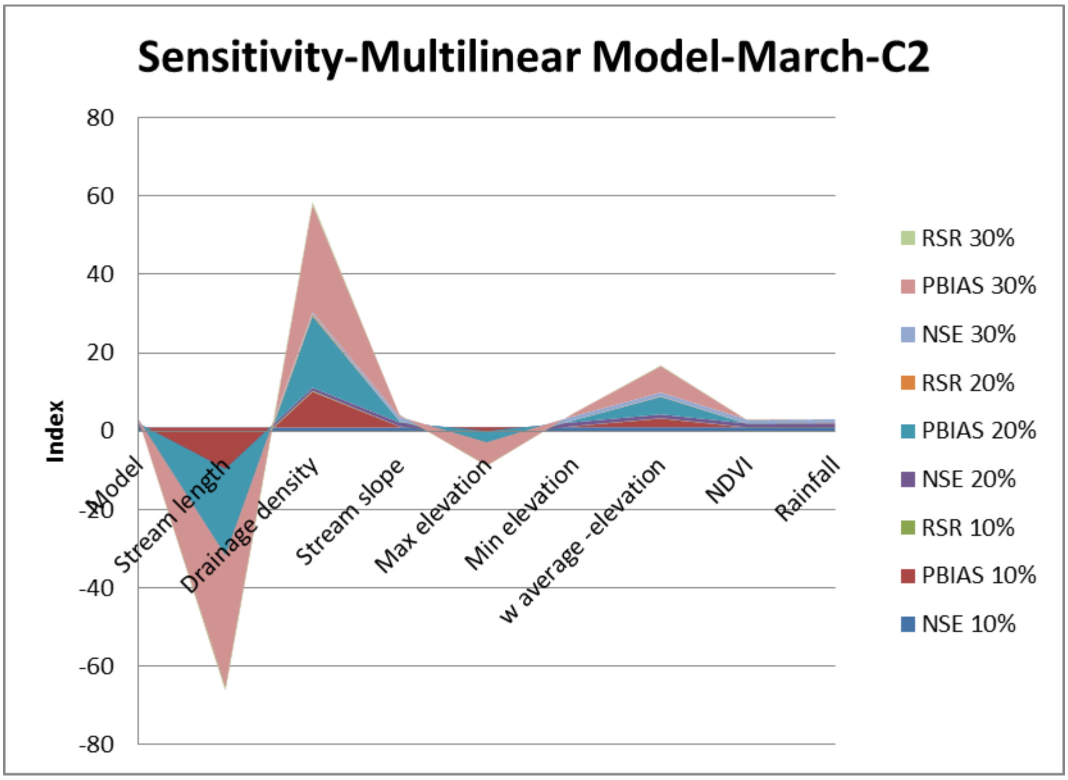

Figure C-108 Sensitivity Summary – Multilinear model –March C2

Table C-27 Summary performance- Multilinear model- March C2

		10%							
	0%	Stream length	Drainage density	Stream slope	Max elevation	Min elevation	w average - elevation	NDVI	Rainfall
NSE	0.997556	0.914344	0.948326	0.997531	0.995228	0.997519	0.994689	0.997554	0.997556
PBIAS	0.009396	-11.4549	9.157044	0.188028	-1.98595	0.256844	2.254087	-0.0575	0.00243
RSR	0.049441	0.292671	0.227318	0.049694	0.069078	0.049811	0.072874	0.04946	0.049441
		20%							
	0%	Stream length	Drainage density	Stream slope	Max elevation	Min elevation	w average - elevation	NDVI	Rainfall
NSE	0.997556	0.664423	0.800838	0.997459	0.988209	0.997414	0.986136	0.997547	0.997556
PBIAS	0.009396	-22.9192	18.30469	0.366661	-3.98129	0.504293	4.498778	-0.12439	-0.00454
RSR	0.049441	0.57929	0.446275	0.050409	0.108588	0.050853	0.117747	0.04953	0.049441
		30%							
	0%	Stream length	Drainage density	Stream slope	Max elevation	Min elevation	w average - elevation	NDVI	Rainfall
NSE	0.997556	0.247793	0.555091	0.997341	0.976497	0.997241	0.971894	0.997535	0.997556
PBIAS	0.009396	-34.3835	27.45234	0.545294	-5.97663	0.751742	6.74347	-0.19128	-0.0115
RSR	0.049441	0.867299	0.667015	0.051567	0.153307	0.052526	0.167648	0.049652	0.049442

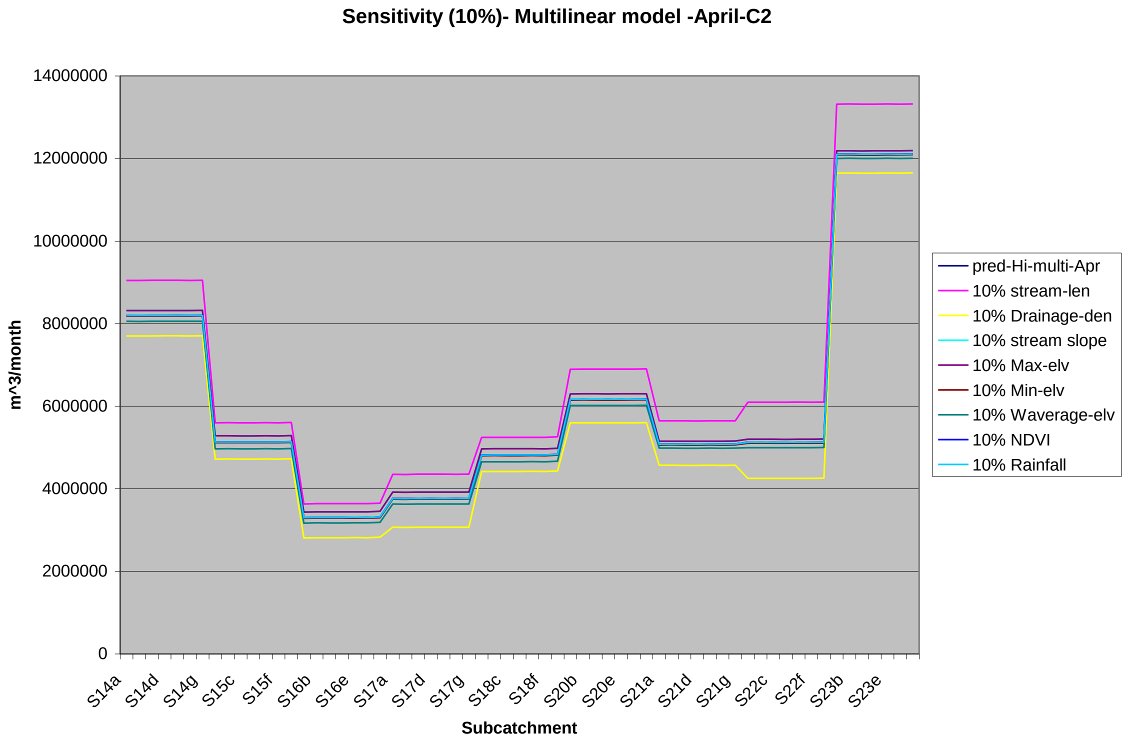

Figure C-109 Sensitivity (10%) – Multilinear model –April C2

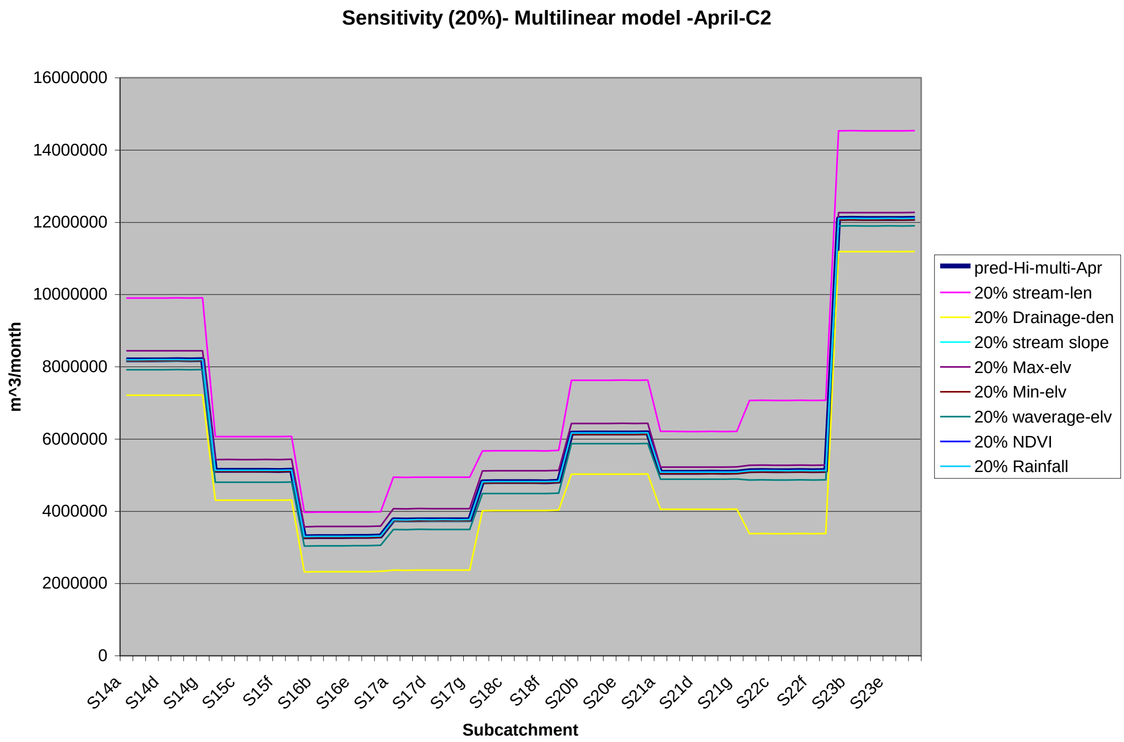

Figure C-110 Sensitivity (20%) – Multilinear model –April C2

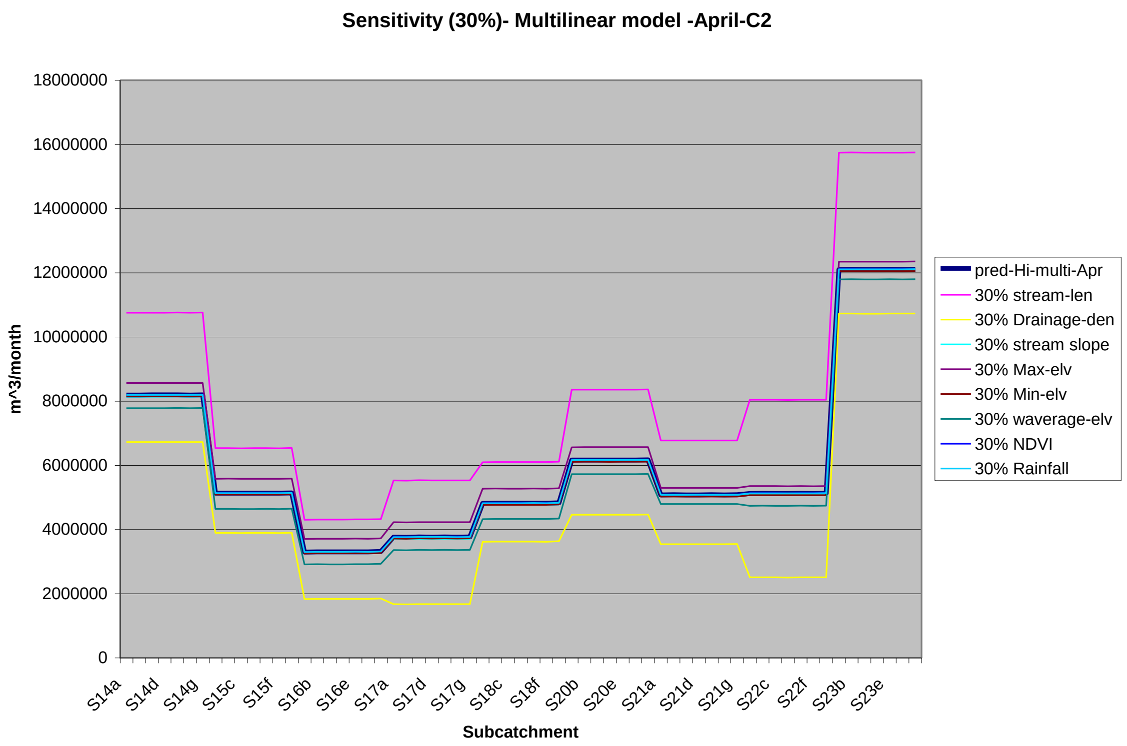

Figure C-111 Sensitivity (30%) – Multilinear model –April C2

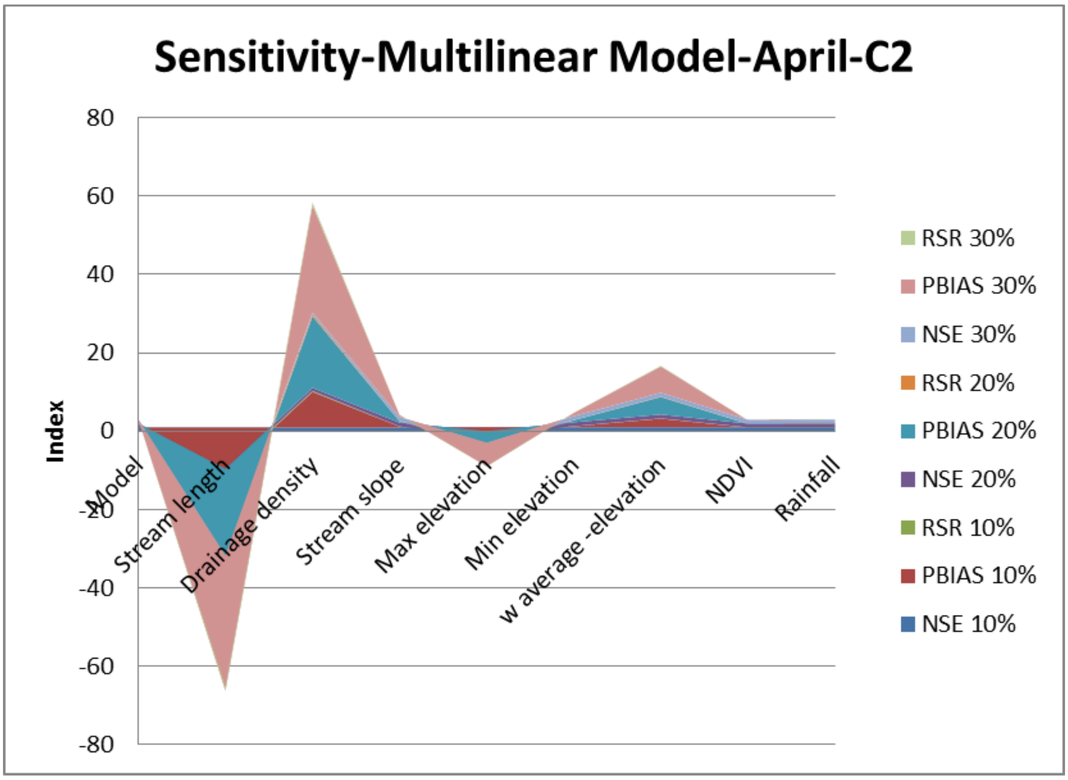

Figure C-112 Sensitivity summary – Multilinear model –April C2

Table C-28 Summary performance- Multilinear model- April C2

		10%							
	0%	Stream length	Drainage density	Stream slope	Max elevation	Min elevation	w average - elevation	NDVI	Rainfall
NSE	0.997549	0.913868	0.948788	0.997527	0.995138	0.997513	0.994758	0.997548	0.997549
PBIAS	-0.01515	-11.488	9.112765	0.172346	-2.02455	0.257555	2.223277	-0.05739	-0.02659
RSR	0.049504	0.293483	0.226301	0.049731	0.069731	0.049875	0.072401	0.049522	0.049507
		20%							
	0%	Stream length	Drainage density	Stream slope	Max elevation	Min elevation	w average - elevation	NDVI	Rainfall
NSE	0.997549	0.663228	0.802191	0.997453	0.987967	0.997393	0.986311	0.997544	0.997549
PBIAS	-0.01515	-22.9609	18.24068	0.359838	-4.03395	0.530256	4.461699	-0.09963	-0.03802
RSR	0.049504	0.58032	0.444758	0.050467	0.109694	0.051059	0.117	0.04956	0.049511
		30%							
	0%	Stream length	Drainage density	Stream slope	Max elevation	Min elevation	w average - elevation	NDVI	Rainfall
NSE	0.997549	0.24563	0.557758	0.997328	0.976038	0.997191	0.972208	0.997538	0.997548
PBIAS	-0.01515	-34.4337	27.36859	0.54733	-6.04336	0.802957	6.700121	-0.14187	-0.04946
RSR	0.049504	0.868545	0.665013	0.05169	0.154796	0.053004	0.16671	0.049618	0.049517

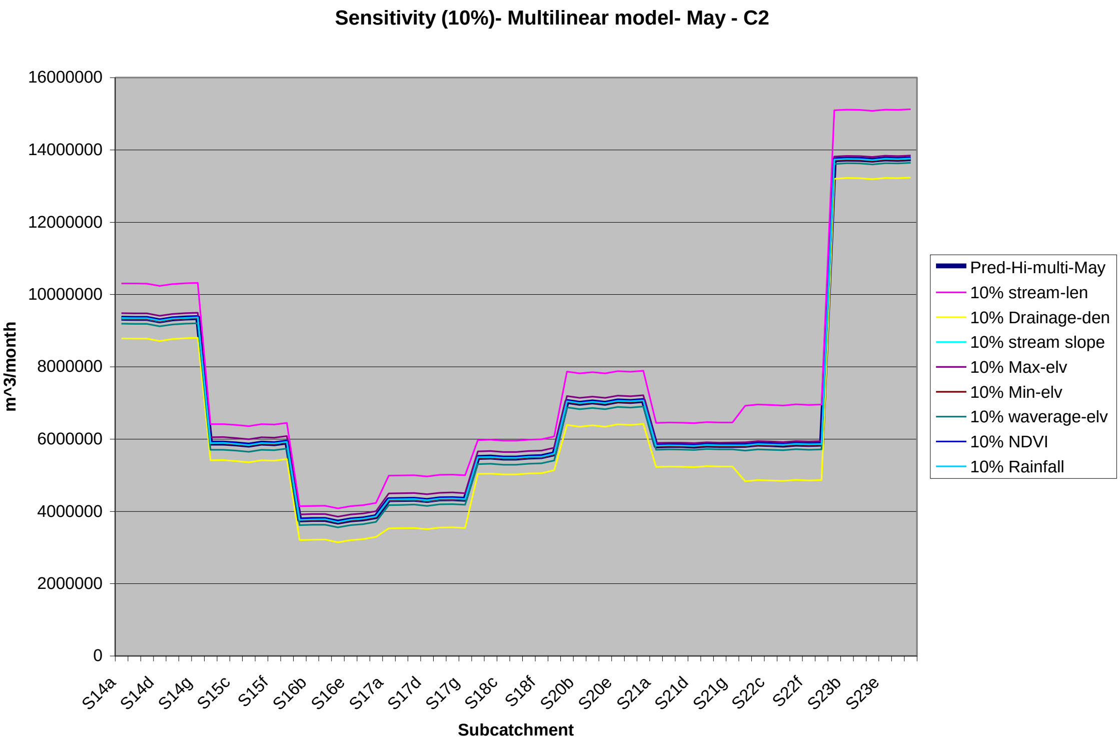

Figure C-113 Sensitivity (10%) – Multilinear model –May C2

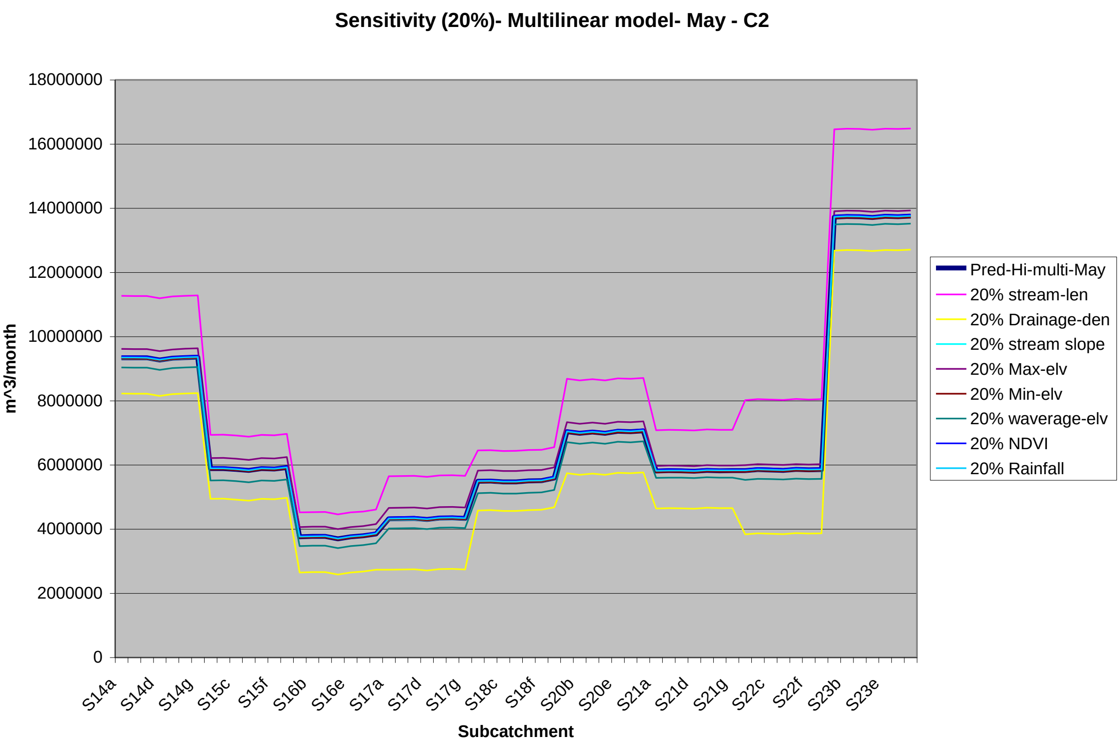

Figure C-114 Sensitivity (20%) – Multilinear model –May C2

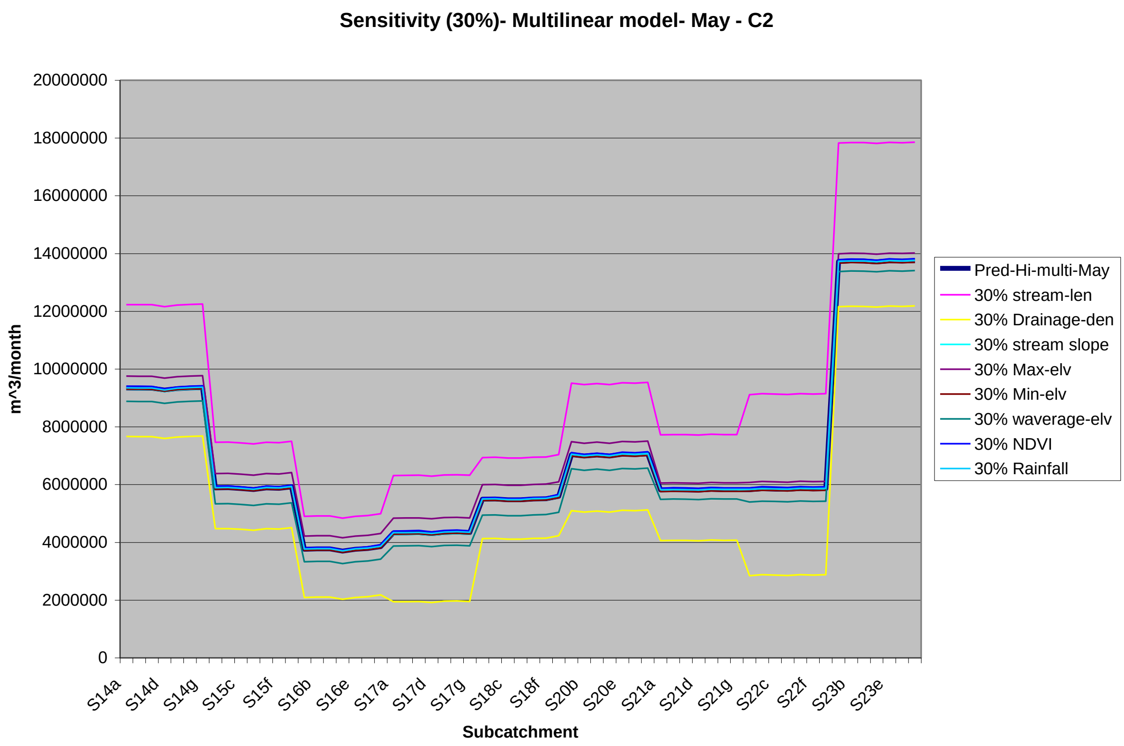

Figure C-115 Sensitivity (30%) – Multilinear model –May C2

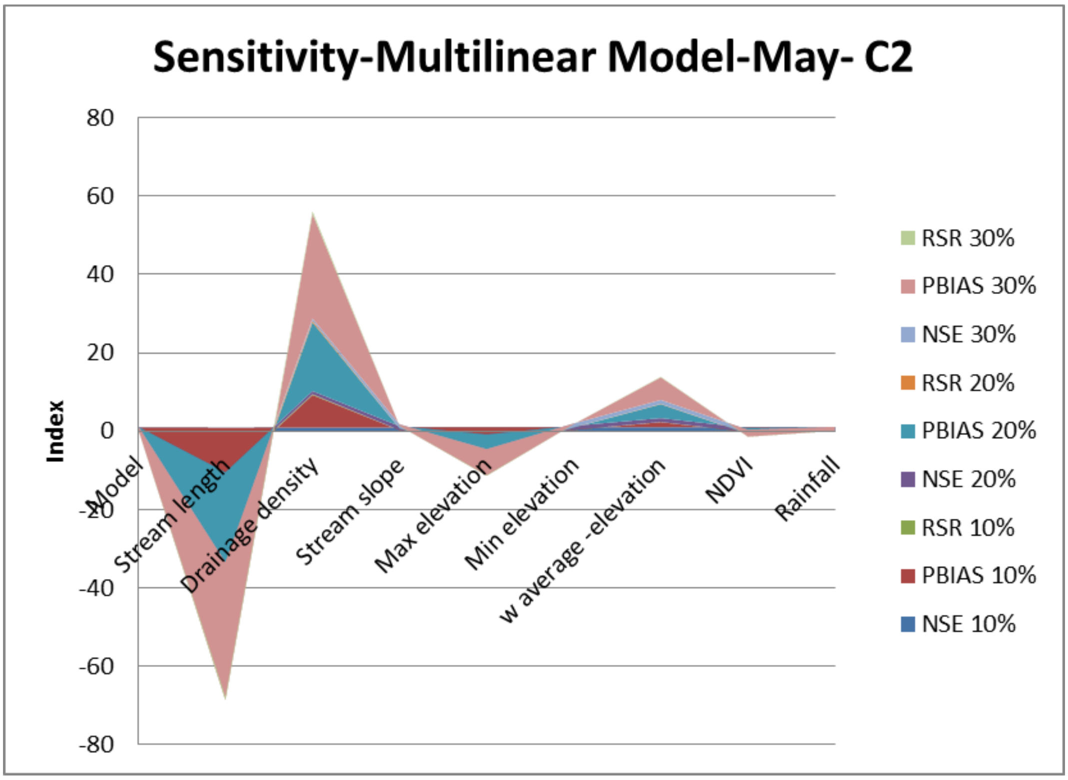

Figure C-116 Sensitivity summary – Multilinear model –May C2

Table C-29 Summary performance- Multilinear model- May C2

		10%							
	0%	Stream length	Drainage density	Stream slope	Max elevation	Min elevation	w average - elevation	NDVI	Rainfall
NSE	0.997134	0.903103	0.956599	0.997278	0.992895	0.997337	0.996562	0.996785	0.997085
PBIAS	-0.90477	-12.3336	8.294133	-0.74303	-2.86801	-0.6672	1.318082	-1.2023	-0.94928
RSR	0.05354	0.311283	0.20833	0.052173	0.084291	0.051605	0.058635	0.056697	0.053995
		20%							
	0%	Stream length	Drainage density	Stream slope	Max elevation	Min elevation	w average - elevation	NDVI	Rainfall
NSE	0.997134	0.643392	0.816701	0.997384	0.984114	0.997477	0.990413	0.996338	0.997033
PBIAS	-0.90477	-23.7625	17.49303	-0.5813	-4.83124	-0.42963	3.540929	-1.49983	-0.99379
RSR	0.05354	0.597167	0.428135	0.051143	0.126039	0.050225	0.097914	0.060515	0.054468
		30%							
	0%	Stream length	Drainage density	Stream slope	Max elevation	Min elevation	w average - elevation	NDVI	Rainfall
NSE	0.997134	0.218	0.57744	0.997453	0.970791	0.997555	0.978686	0.995791	0.99698
PBIAS	-0.90477	-35.1914	26.69193	-0.41957	-6.79448	-0.19206	5.763777	-1.79737	-1.0383
RSR	0.05354	0.884307	0.650046	0.050471	0.170907	0.049445	0.145993	0.064877	0.054959

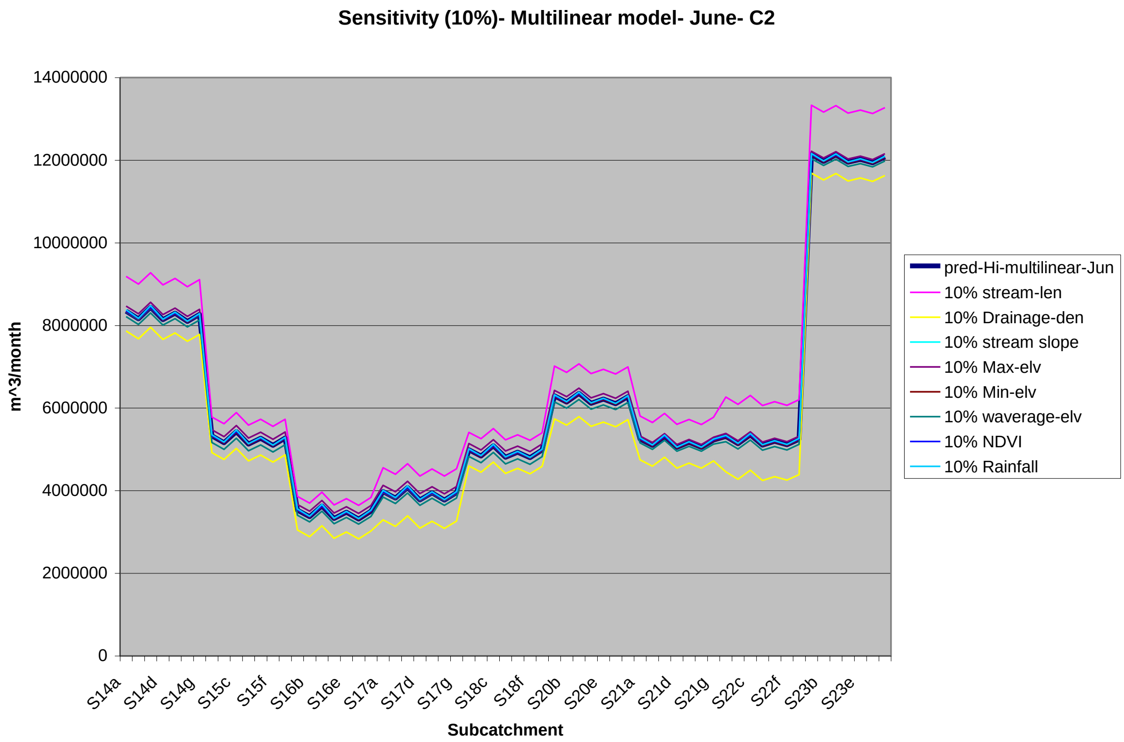

Figure C-117 Sensitivity (10%) – Multilinear model –June C2

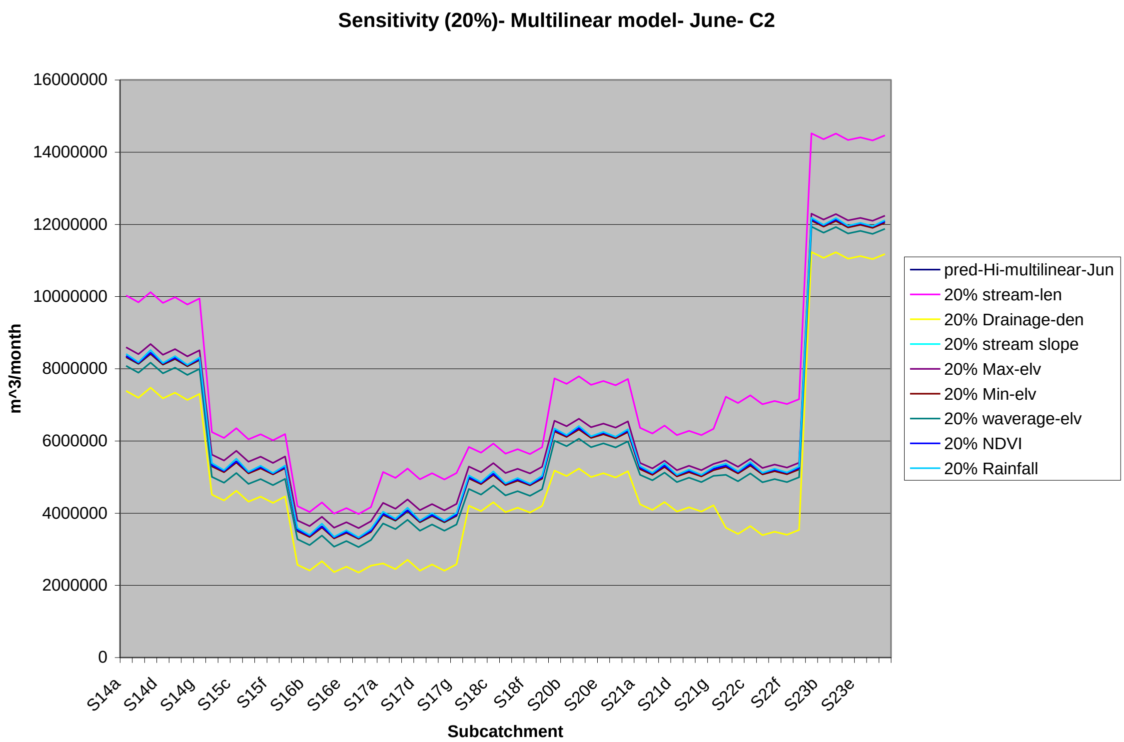

Figure C-118 Sensitivity (20%) – Multilinear model –June C2

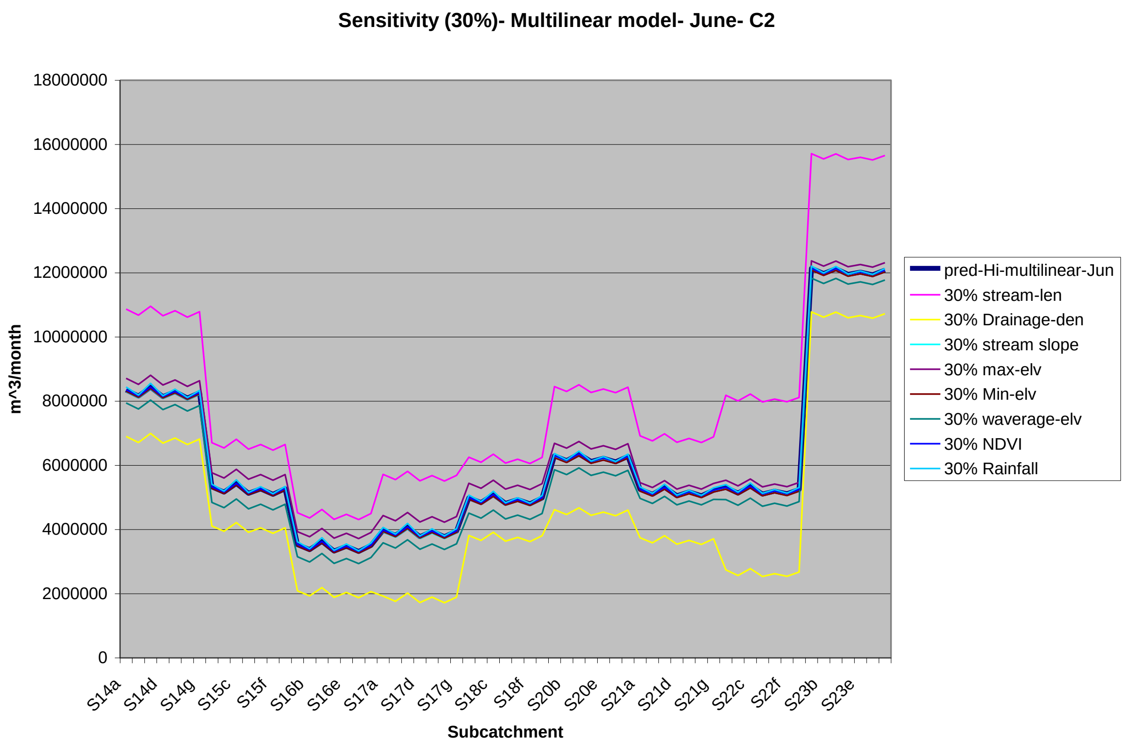

Figure C-119 Sensitivity (30%) – Multilinear model –June C2

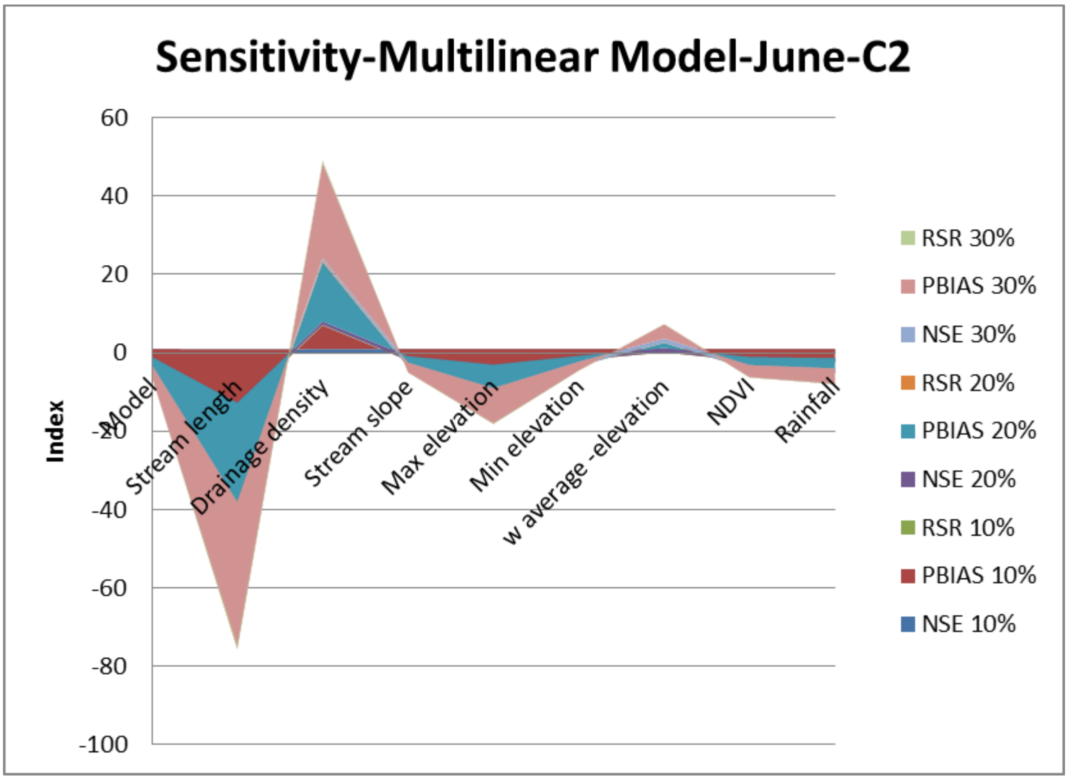

Figure C-120 Sensitivity (30%) – Multilinear model –June C2

Table C-30 Summary performance- Multilinear model- June C2

		10%							
	0%	Stream length	Drainage density	Stream slope	Max elevation	Min elevation	w average - elevation	NDVI	Rainfall
NSE	0.990645	0.869461	0.972729	0.991276	0.981306	0.991509	0.995493	0.990557	0.989186
PBIAS	-3.09406	-14.5684	6.035891	-2.9086	-5.10136	-2.82476	-0.85441	-3.12022	-3.405
RSR	0.096722	0.361301	0.165141	0.093403	0.136725	0.092148	0.067134	0.097177	0.103992
		20%							
	0%	Stream length	Drainage density	Stream slope	Max elevation	Min elevation	w average - elevation	NDVI	Rainfall
NSE	0.990645	0.581275	0.856933	0.991857	0.967219	0.992292	0.994679	0.990467	0.987587
PBIAS	-3.09406	-26.0428	15.16584	-2.72315	-7.10867	-2.55547	1.385238	-3.14638	-3.71595
RSR	0.096722	0.64709	0.378242	0.090241	0.181055	0.087796	0.072945	0.097635	0.111416
		30%							
	0%	Stream length	Drainage density	Stream slope	Max elevation	Min elevation	w average - elevation	NDVI	Rainfall
NSE	0.990645	0.126086	0.643259	0.992387	0.948383	0.992994	0.988203	0.990377	0.985848
PBIAS	-3.09406	-37.5172	24.29578	-2.5377	-9.11598	-2.28618	3.624885	-3.17255	-4.0269
RSR	0.096722	0.934833	0.597278	0.087251	0.227193	0.0837	0.108615	0.098094	0.118963

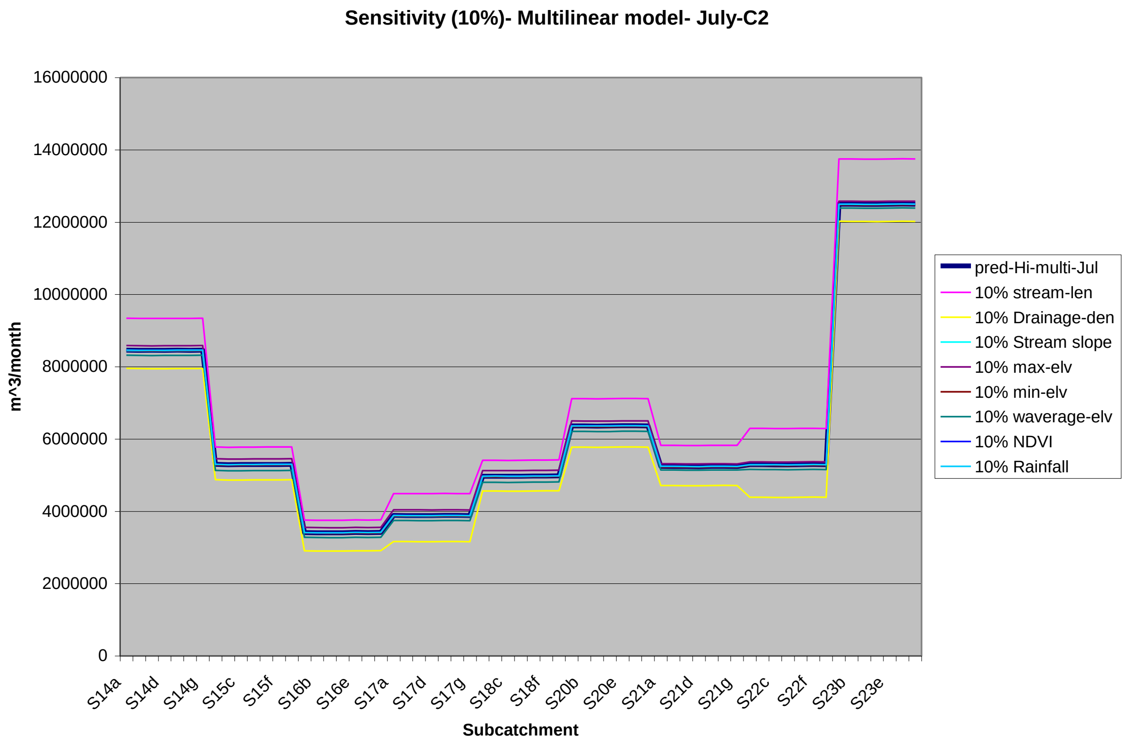

Figure C-121 Sensitivity (10%) – Multilinear model –July C2

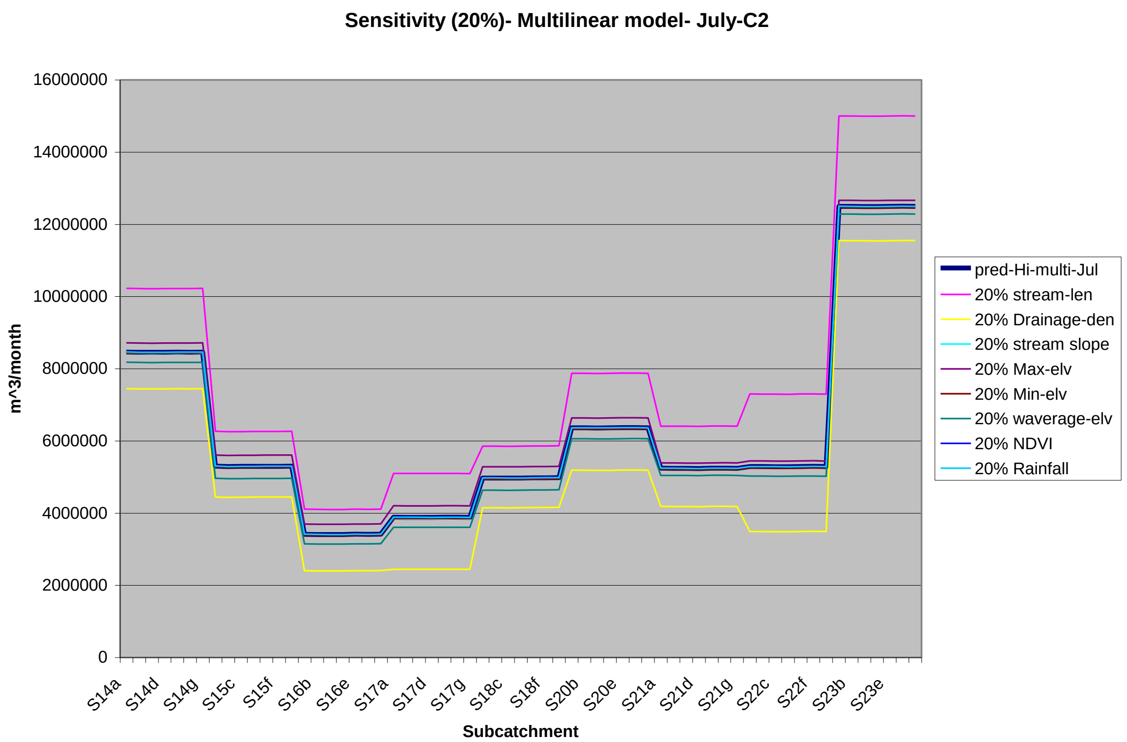

Figure C-122 Sensitivity (20%) – Multilinear model –July C2

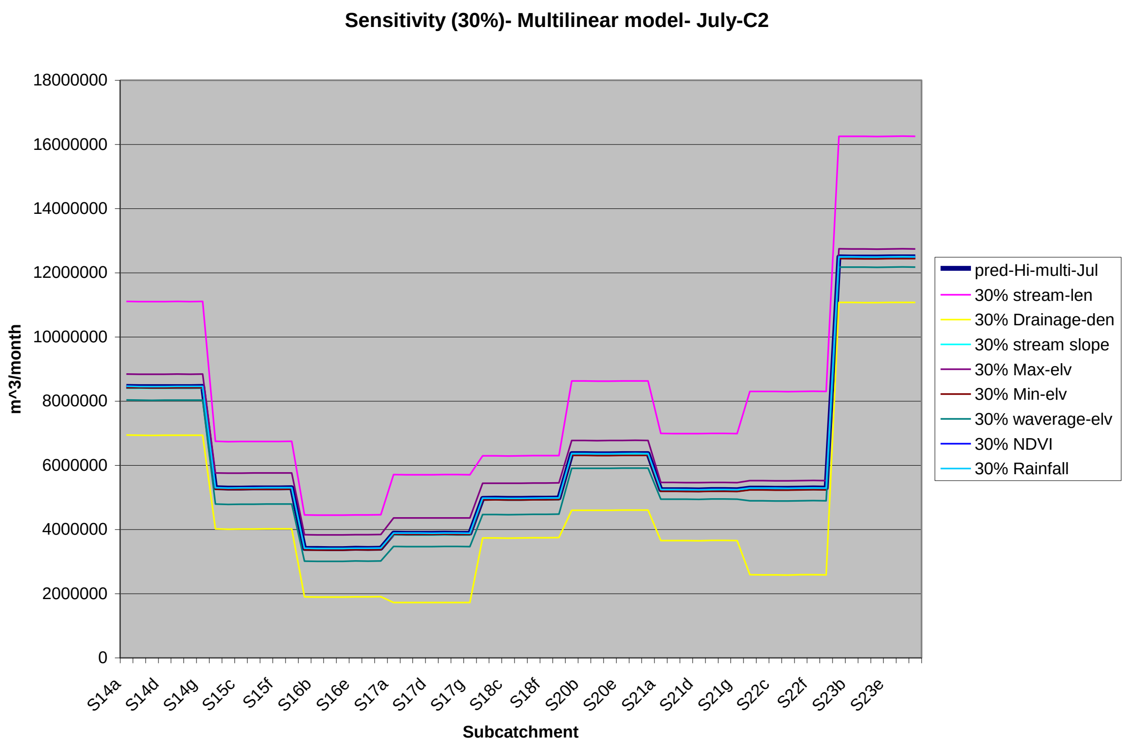

Figure C-123 Sensitivity (30%) – Multilinear model –July C2

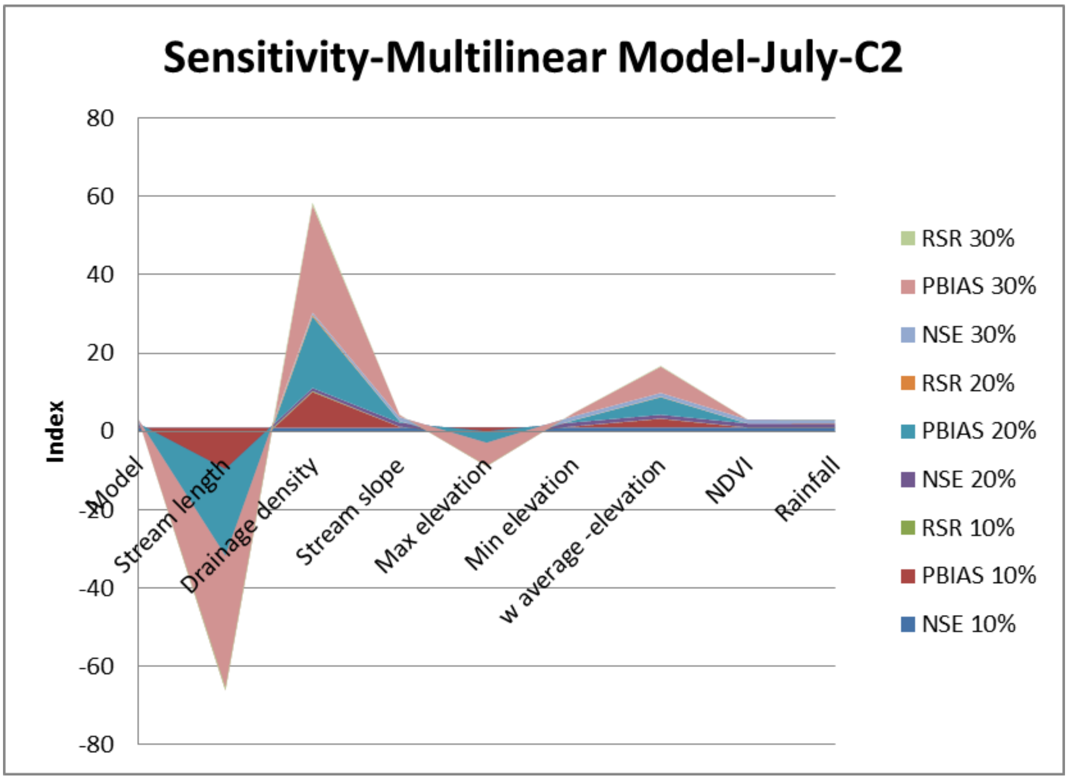

Figure C-124 Sensitivity summary – Multilinear model –July C2

Table C-31 Summary performance- Multilinear model- July C2

		10%							
	0%	Stream length	Drainage density	Stream slope	Max elevation	Min elevation	w average - elevation	NDVI	Rainfall
NSE	0.997549	0.914146	0.948545	0.997522	0.995193	0.997507	0.994718	0.997549	0.997549
PBIAS	0.007629	-11.4676	9.136099	0.196341	-1.99853	0.275711	2.239883	-0.01571	-0.00511
RSR	0.049507	0.293009	0.226837	0.049784	0.069332	0.049932	0.072674	0.049508	0.049507
		20%							
	0%	Stream length	Drainage density	Stream slope	Max elevation	Min elevation	w average - elevation	NDVI	Rainfall
NSE	0.997549	0.663717	0.801693	0.997442	0.988094	0.997384	0.986263	0.997548	0.997549
PBIAS	0.007629	-22.9427	18.26457	0.385052	-4.00468	0.543793	4.472136	-0.03905	-0.01784
RSR	0.049507	0.579899	0.445316	0.050575	0.109115	0.051142	0.117205	0.049516	0.049509
		30%							
	0%	Stream length	Drainage density	Stream slope	Max elevation	Min elevation	w average - elevation	NDVI	Rainfall
NSE	0.997549	0.246262	0.556994	0.997311	0.976251	0.997182	0.972183	0.997547	0.997548
PBIAS	0.007629	-34.4179	27.39304	0.573764	-6.01084	0.811875	6.70439	-0.06239	-0.03058
RSR	0.049507	0.868181	0.665587	0.051857	0.154106	0.053083	0.166785	0.04953	0.049513

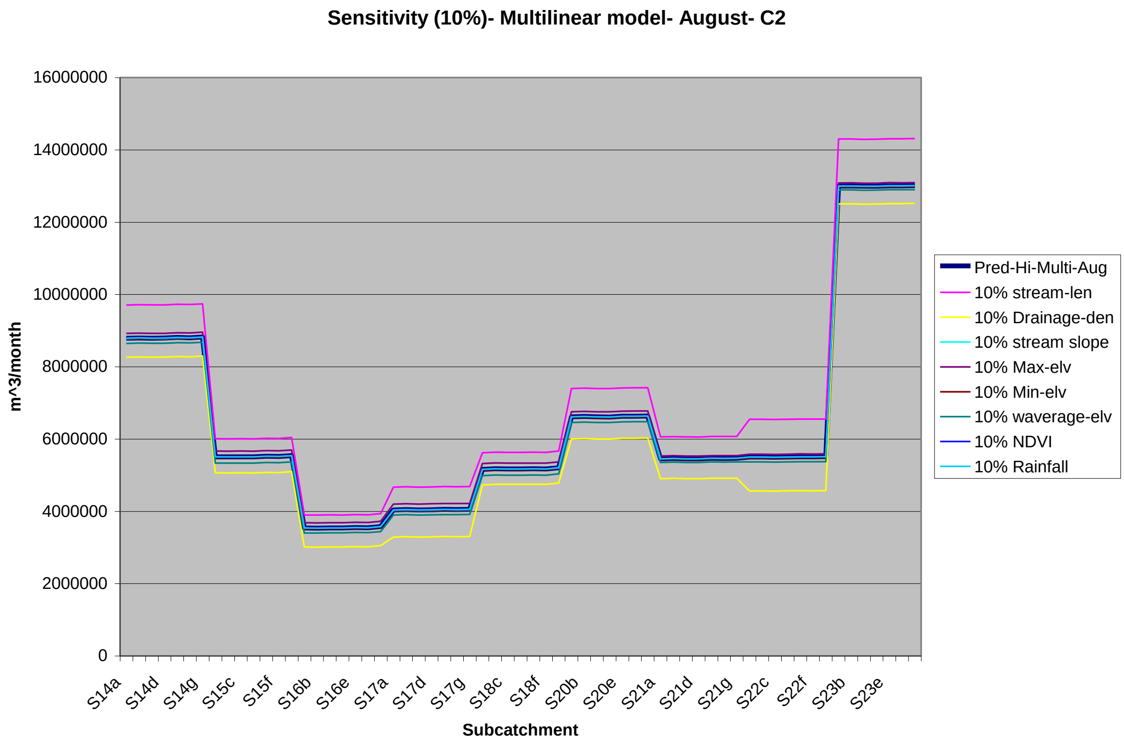

Figure C-125 Sensitivity (10%) – Multilinear model –August C2

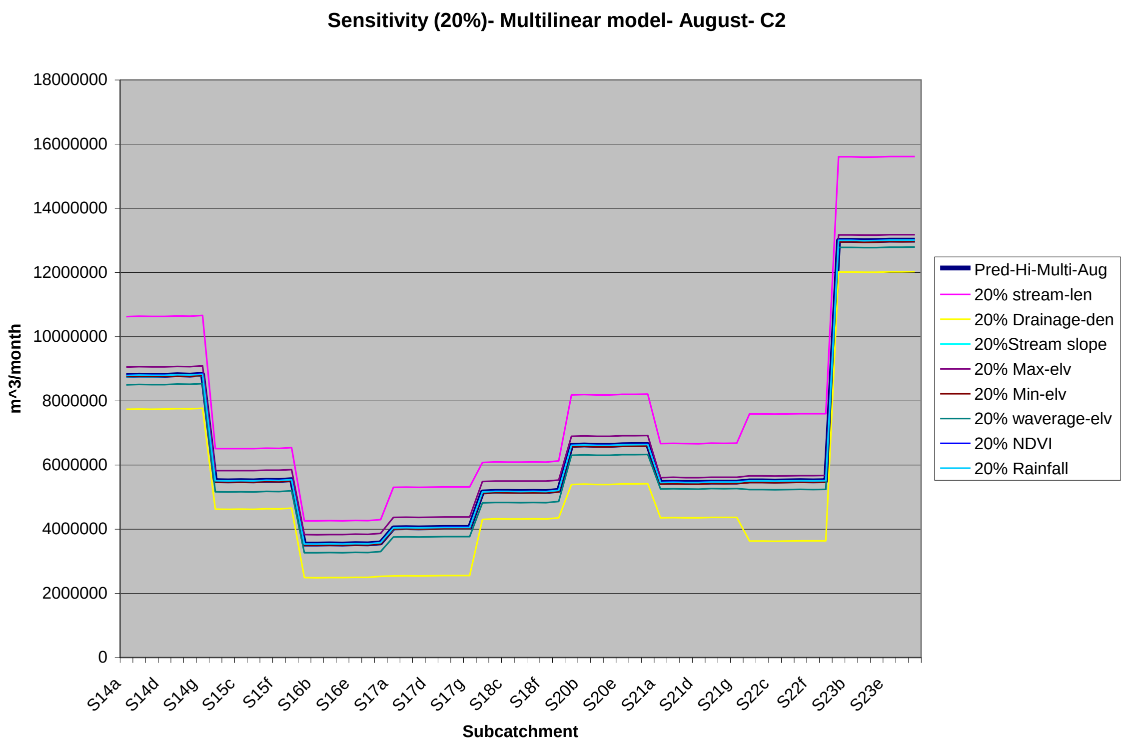

Figure C-126 Sensitivity (20%) – Multilinear model –August C2

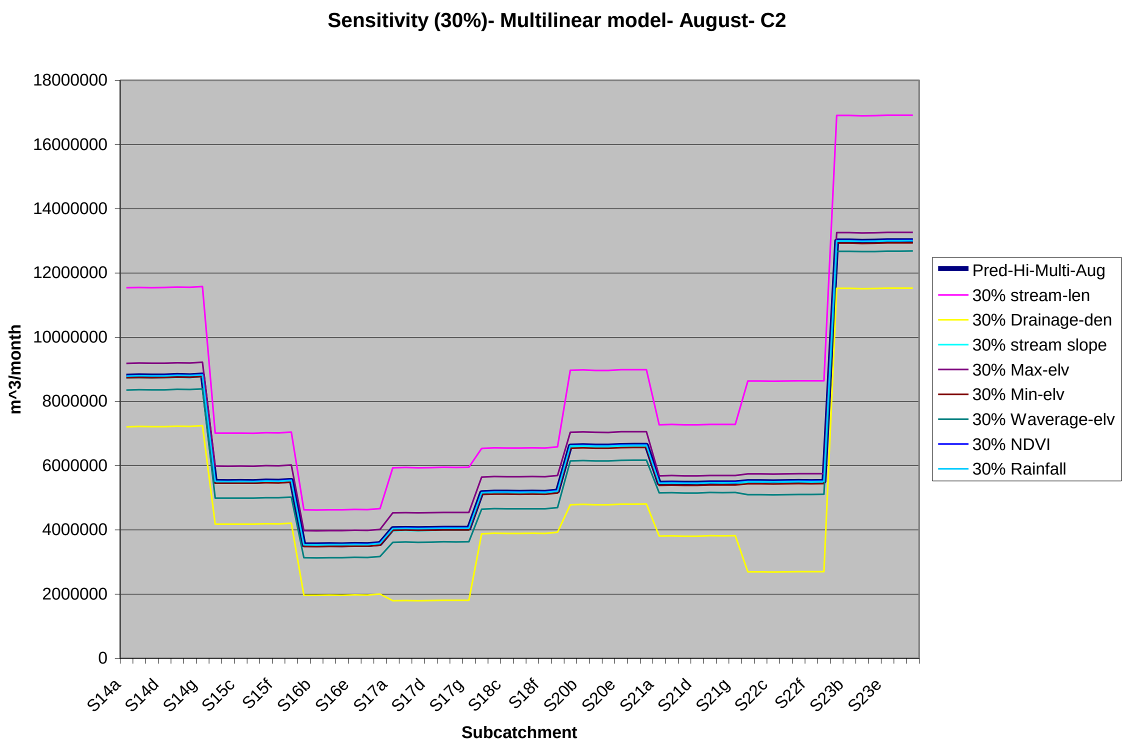

Figure C-127 Sensitivity (30%) – Multilinear model –August C2

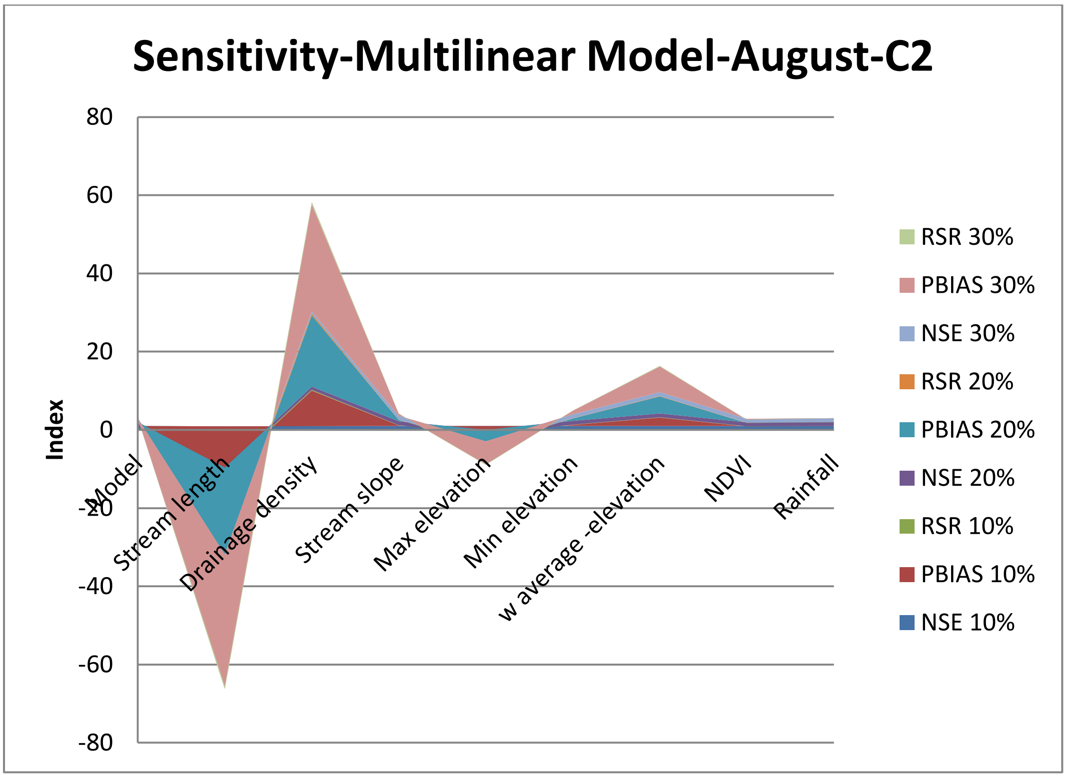

Figure C-128 Sensitivity summary – Multilinear model –August C2

Table C-32 Summary performance- Multilinear model- August C2

		10%							
	0%	Stream length	Drainage density	Stream slope	Max elevation	Min elevation	w average - elevation	NDVI	Rainfall
NSE	0.997562	0.913665	0.949067	0.997543	0.995145	0.997519	0.994939	0.997557	0.997562
PBIAS	-0.04204	-11.5086	9.085837	0.153052	-2.02767	0.279431	2.155302	-0.10224	-0.04408
RSR	0.04938	0.293829	0.225683	0.049567	0.069675	0.049811	0.071143	0.04943	0.049381
		20%							
	0%	Stream length	Drainage density	Stream slope	Max elevation	Min elevation	w average - elevation	NDVI	Rainfall
NSE	0.997562	0.662994	0.802738	0.997469	0.988082	0.997361	0.986865	0.997547	0.997561
PBIAS	-0.04204	-22.9751	18.21371	0.348142	-4.0133	0.600899	4.352641	-0.16244	-0.04612
RSR	0.04938	0.580522	0.444142	0.050307	0.109167	0.051371	0.114607	0.049524	0.049382
		30%							
	0%	Stream length	Drainage density	Stream slope	Max elevation	Min elevation	w average - elevation	NDVI	Rainfall
NSE	0.997562	0.24555	0.558574	0.99734	0.976373	0.997088	0.973342	0.997534	0.997561
PBIAS	-0.04204	-34.4416	27.34158	0.543231	-5.99893	0.922367	6.54998	-0.22264	-0.04816
RSR	0.04938	0.868591	0.664399	0.051578	0.153711	0.053961	0.163274	0.049661	0.049383

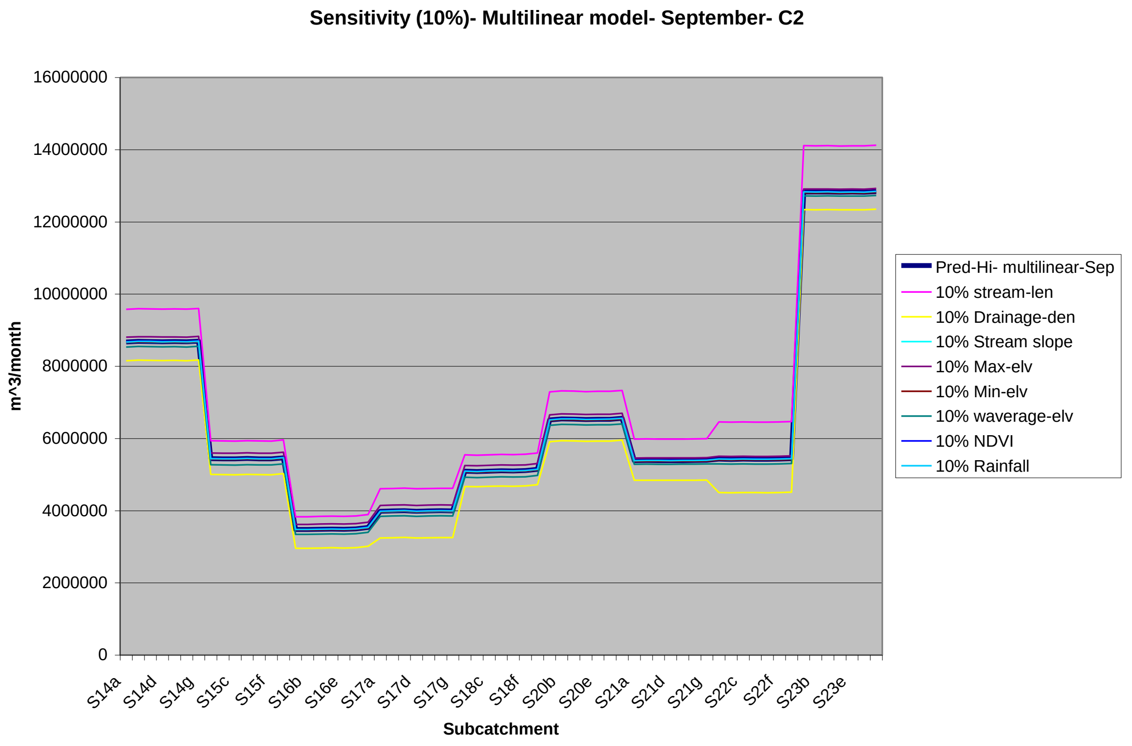

Figure C-129 Sensitivity (10%) – Multilinear model –September C2

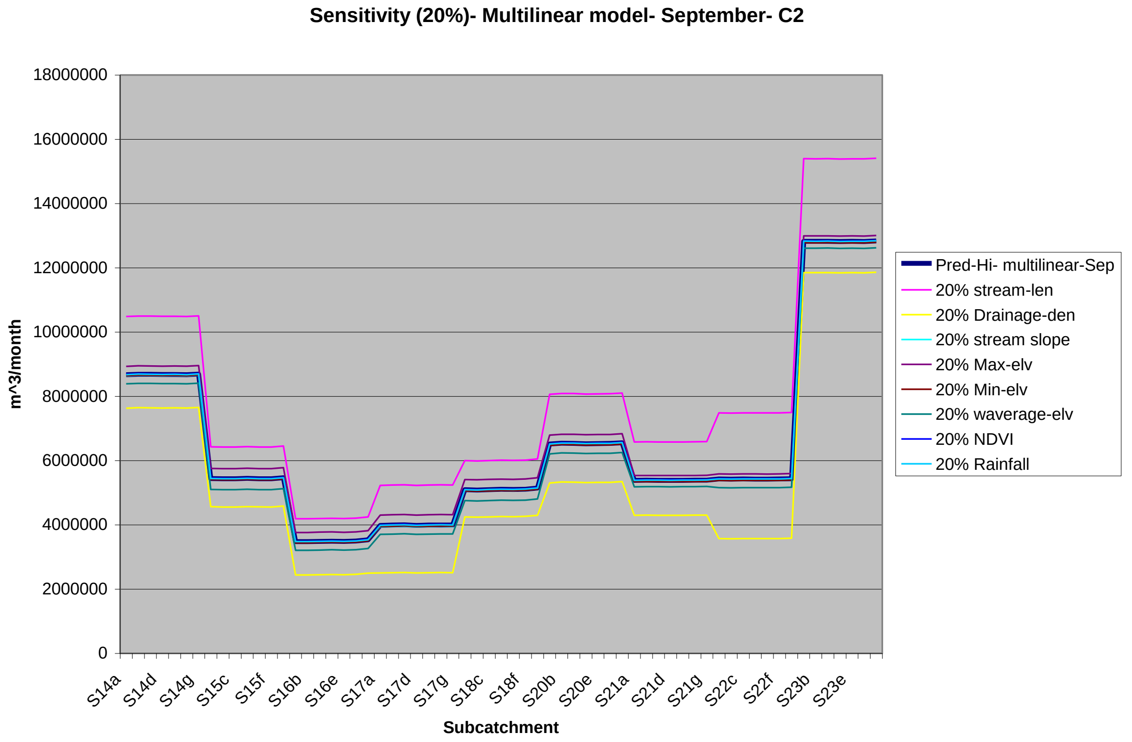

Figure C-130 Sensitivity (20%) – Multilinear model –September C2

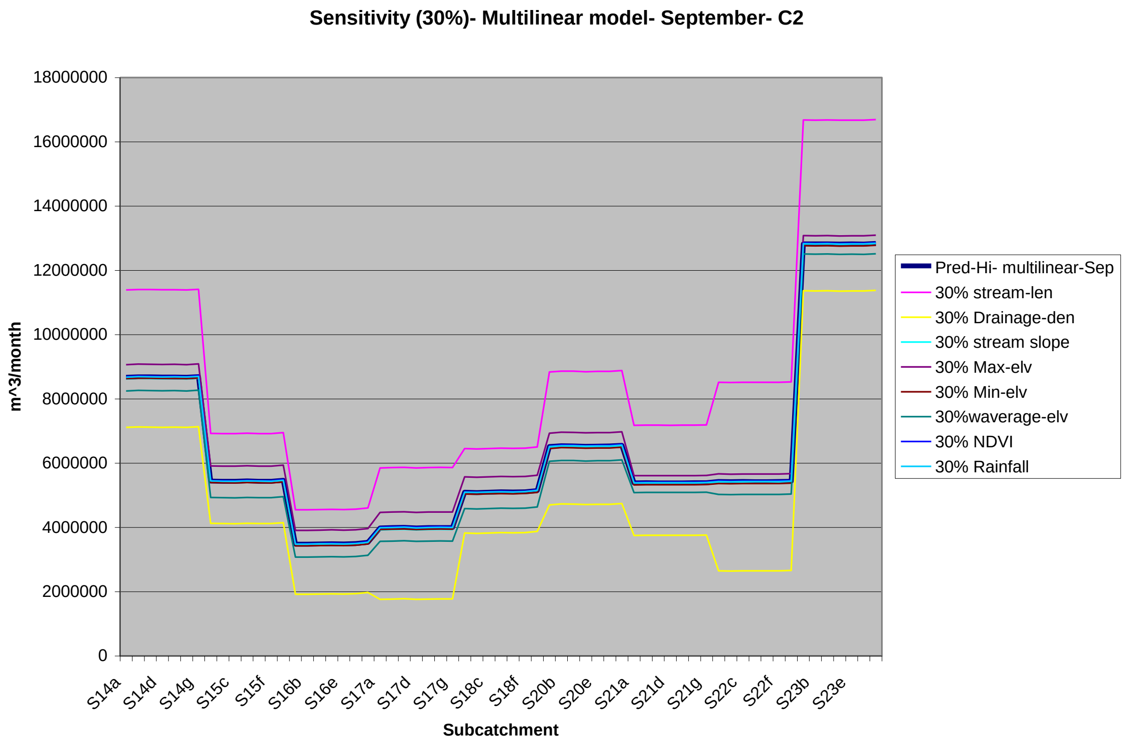

Figure C-131 Sensitivity (30%) – Multilinear model –September C2

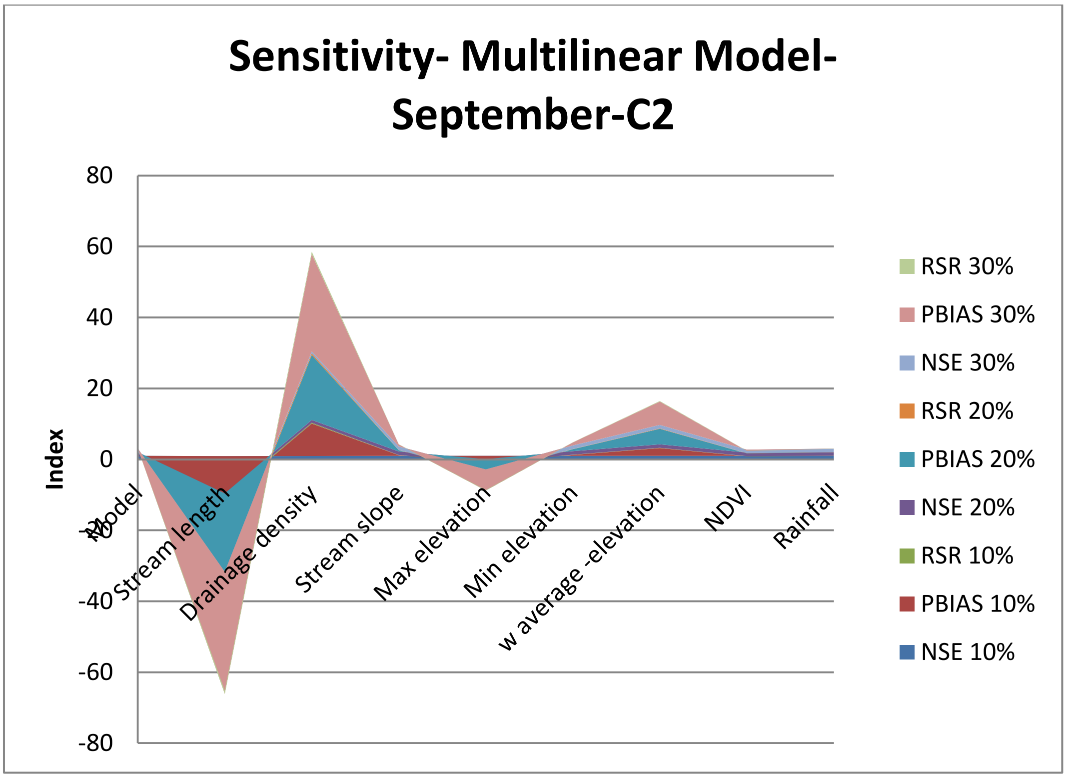

Figure C-132 Sensitivity summary – Multilinear model –September C2

Table C-33 Summary performance- Multilinear model- September C2

		10%							
	0%	Stream length	Drainage density	Stream slope	Max elevation	Min elevation	w average - elevation	NDVI	Rainfall
NSE	0.997569	0.914207	0.948442	0.997544	0.995239	0.997526	0.994864	0.997562	0.997569
PBIAS	-0.00333	-11.4645	9.147155	0.185728	-1.98923	0.278093	2.189106	-0.11606	-0.01933
RSR	0.049301	0.292904	0.227063	0.049558	0.069002	0.049735	0.071665	0.049379	0.049303
		20%							
	0%	Stream length	Drainage density	Stream slope	Max elevation	Min elevation	w average - elevation	NDVI	Rainfall
NSE	0.997569	0.664226	0.800996	0.997466	0.98826	0.997395	0.986733	0.997539	0.997569
PBIAS	-0.00333	-22.9257	18.29764	0.374784	-3.97512	0.559515	4.38154	-0.2288	-0.03533
RSR	0.049301	0.57946	0.446099	0.050334	0.10835	0.051037	0.115183	0.049604	0.049308
		30%							
	0%	Stream length	Drainage density	Stream slope	Max elevation	Min elevation	w average - elevation	NDVI	Rainfall
NSE	0.997569	0.247626	0.555229	0.997337	0.976634	0.997176	0.973176	0.997503	0.997568
PBIAS	-0.00333	-34.3869	27.44812	0.56384	-5.96102	0.840937	6.573974	-0.34153	-0.05132
RSR	0.049301	0.867395	0.666912	0.051605	0.15286	0.053143	0.163781	0.049973	0.049316

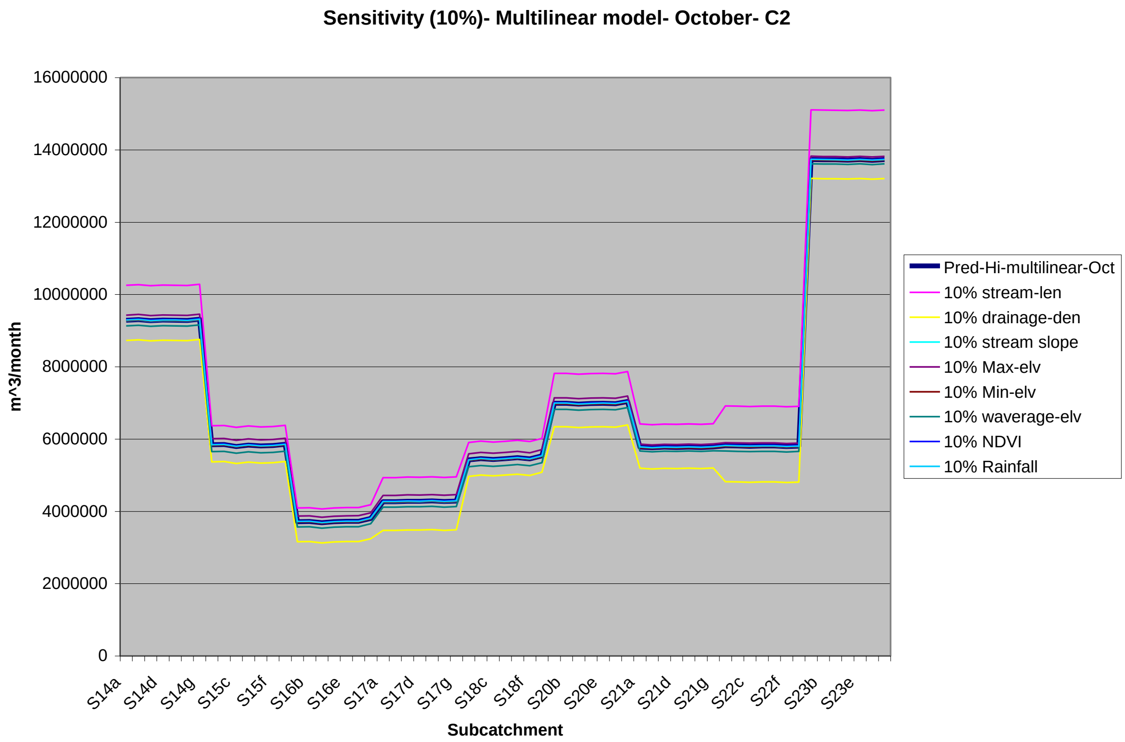

Figure C-133 Sensitivity (10%) – Multilinear model –October C2

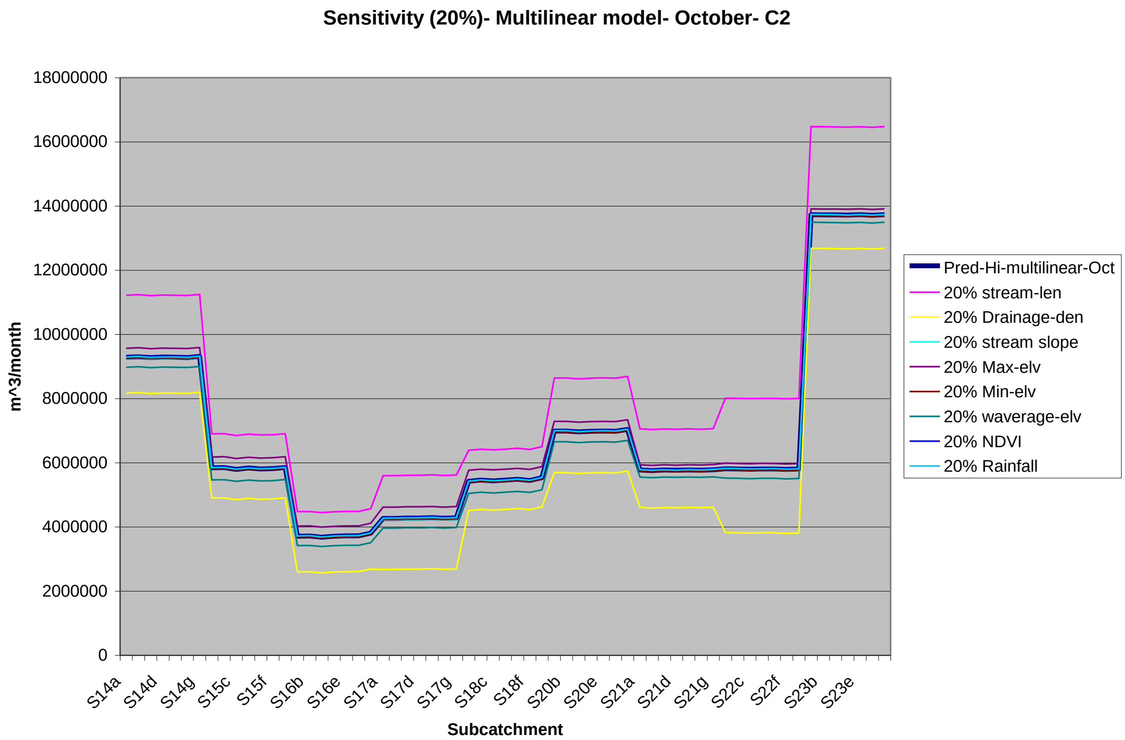

Figure C-134 Sensitivity (20%) – Multilinear model –October C2

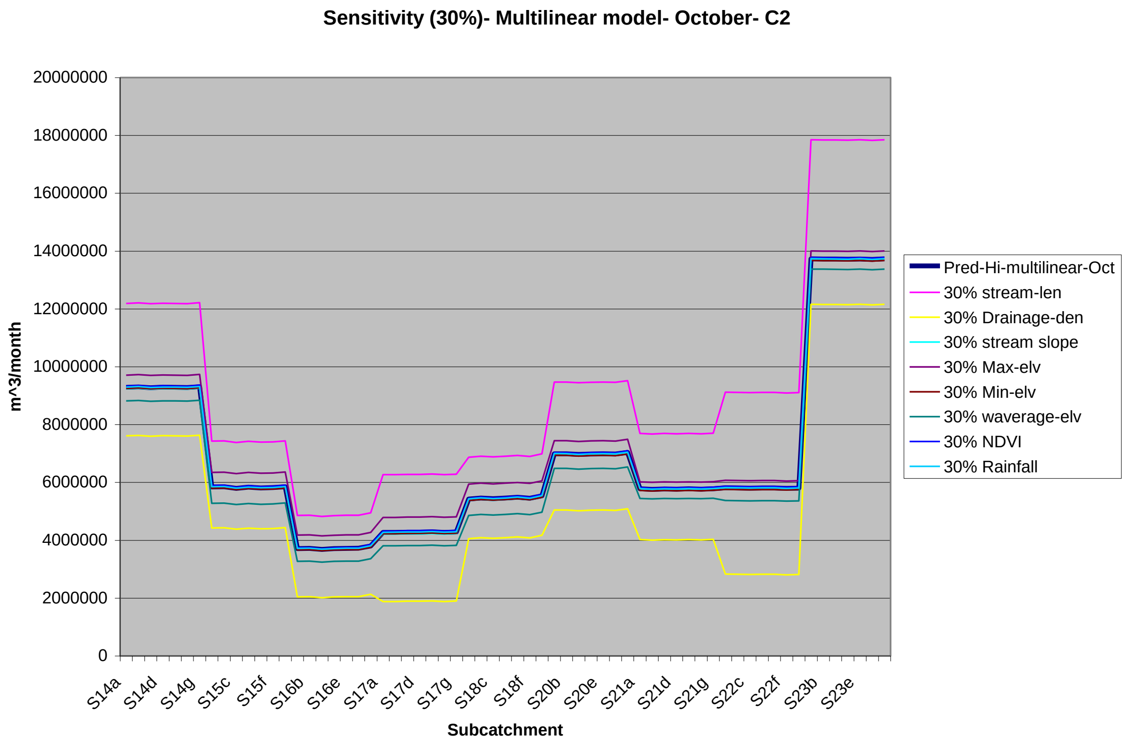

Figure C-135 Sensitivity (30%) – Multilinear model –October C2

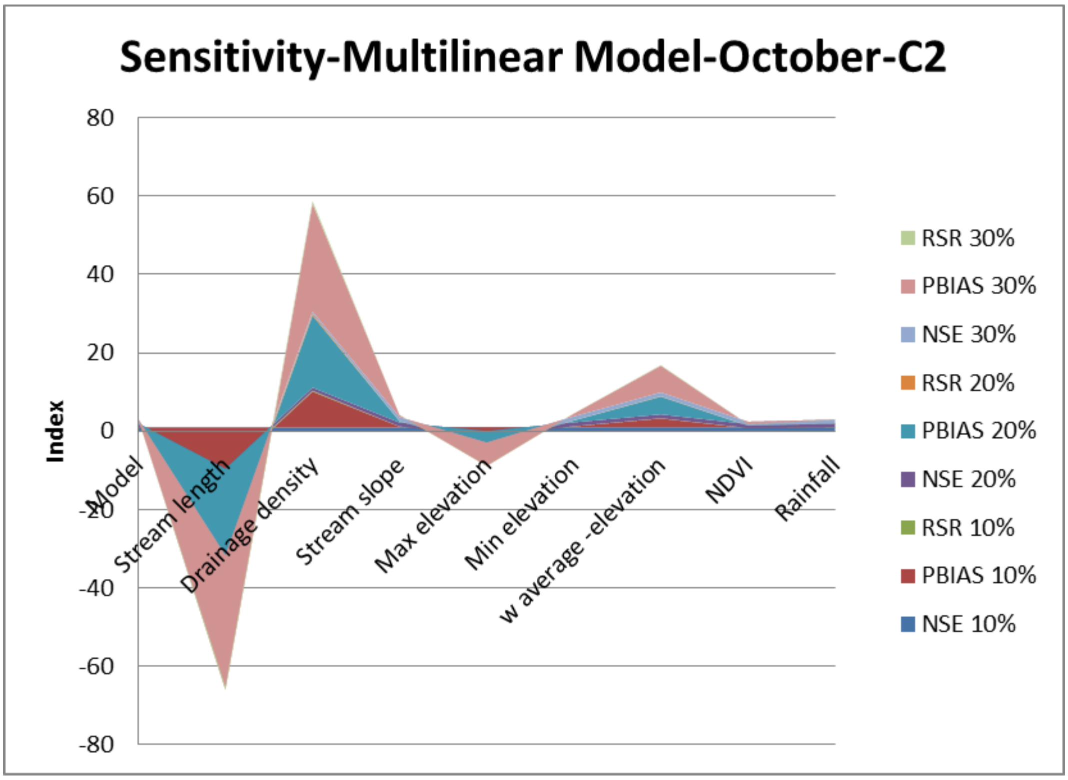

Figure C-136 Sensitivity summary – Multilinear model –October C2

Table C-34 Summary performance- Multilinear model- October C2

		10%							
	0%	Stream length	Drainage density	Stream slope	Max elevation	Min elevation	w average - elevation	NDVI	Rainfall
NSE	0.997612	0.91454	0.948067	0.99759	0.995248	0.997581	0.994727	0.997586	0.997611
PBIAS	0.000739	-11.4446	9.186199	0.172904	-2.00285	0.236455	2.26093	-0.21474	-0.03102
RSR	0.048867	0.292335	0.227888	0.04909	0.068932	0.049184	0.072617	0.049134	0.048873
		20%							
	0%	Stream length	Drainage density	Stream slope	Max elevation	Min elevation	w average - elevation	NDVI	Rainfall
NSE	0.997612	0.66531	0.799449	0.997525	0.988154	0.997488	0.986075	0.997507	0.99761
PBIAS	0.000739	-22.8899	18.37166	0.345069	-4.00644	0.472171	4.521121	-0.43021	-0.06278
RSR	0.048867	0.578524	0.447829	0.049747	0.108841	0.05012	0.118004	0.049928	0.04889
		30%							
	0%	Stream length	Drainage density	Stream slope	Max elevation	Min elevation	w average - elevation	NDVI	Rainfall
NSE	0.997612	0.249921	0.551759	0.997417	0.976328	0.997333	0.971657	0.997376	0.997607
PBIAS	0.000739	-34.3353	27.55712	0.517234	-6.01002	0.707887	6.781311	-0.64569	-0.09454
RSR	0.048867	0.866071	0.669508	0.050823	0.153858	0.051641	0.168355	0.051227	0.04892

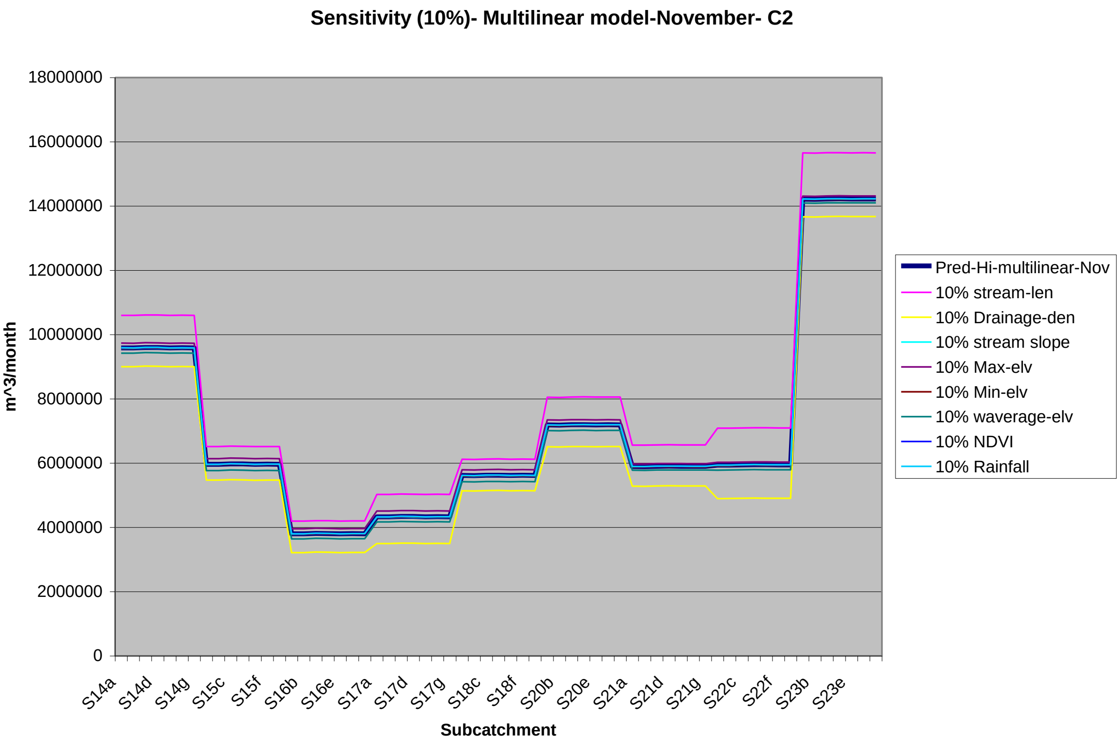

Figure C-137 Sensitivity (10%) – Multilinear model –November C2

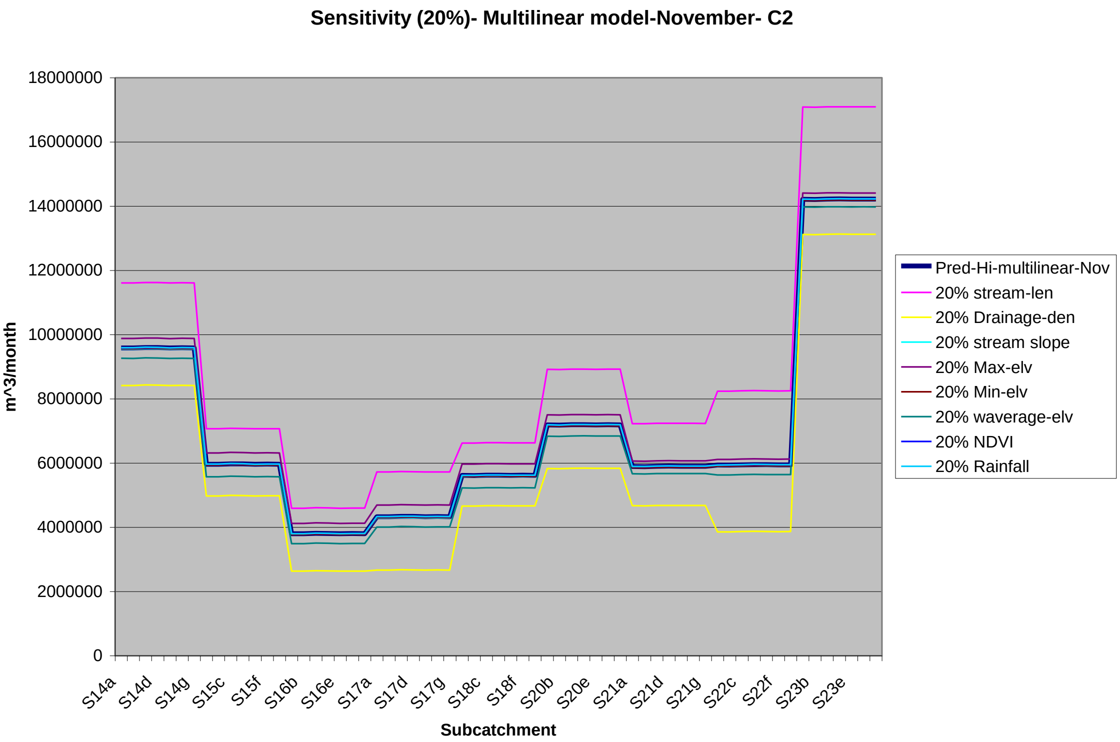

Figure C-138 Sensitivity (20%) – Multilinear model –November C2

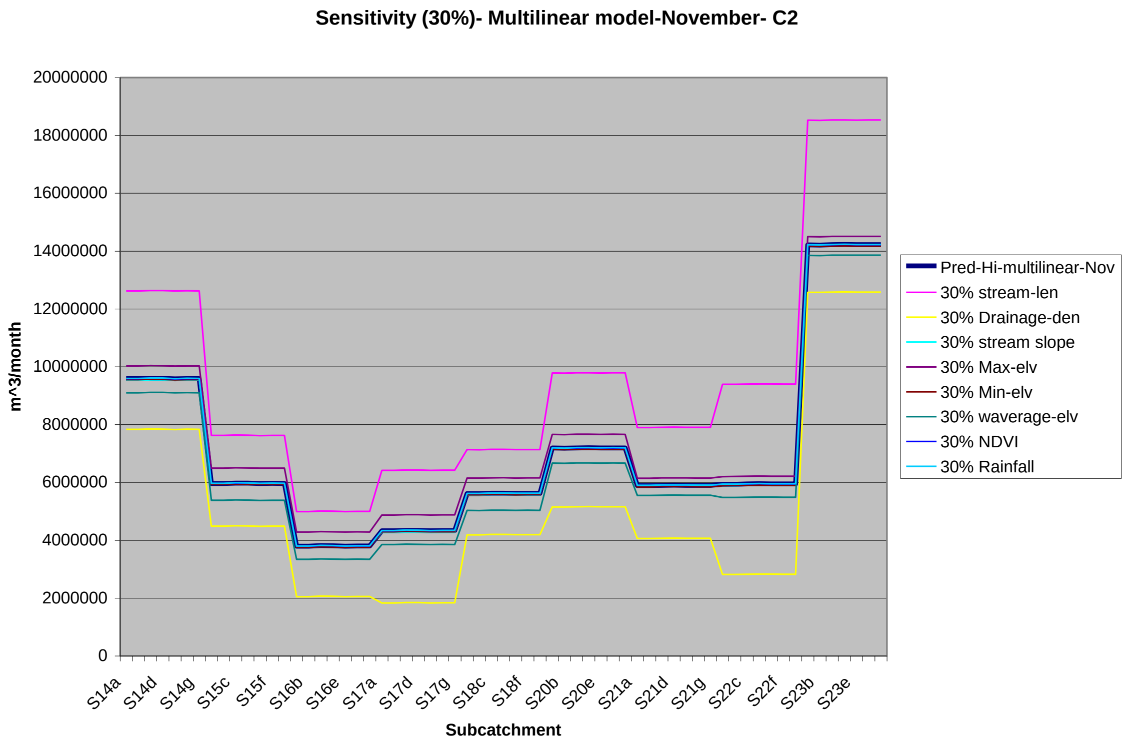

Figure C-139 Sensitivity (30%) – Multilinear model –November C2

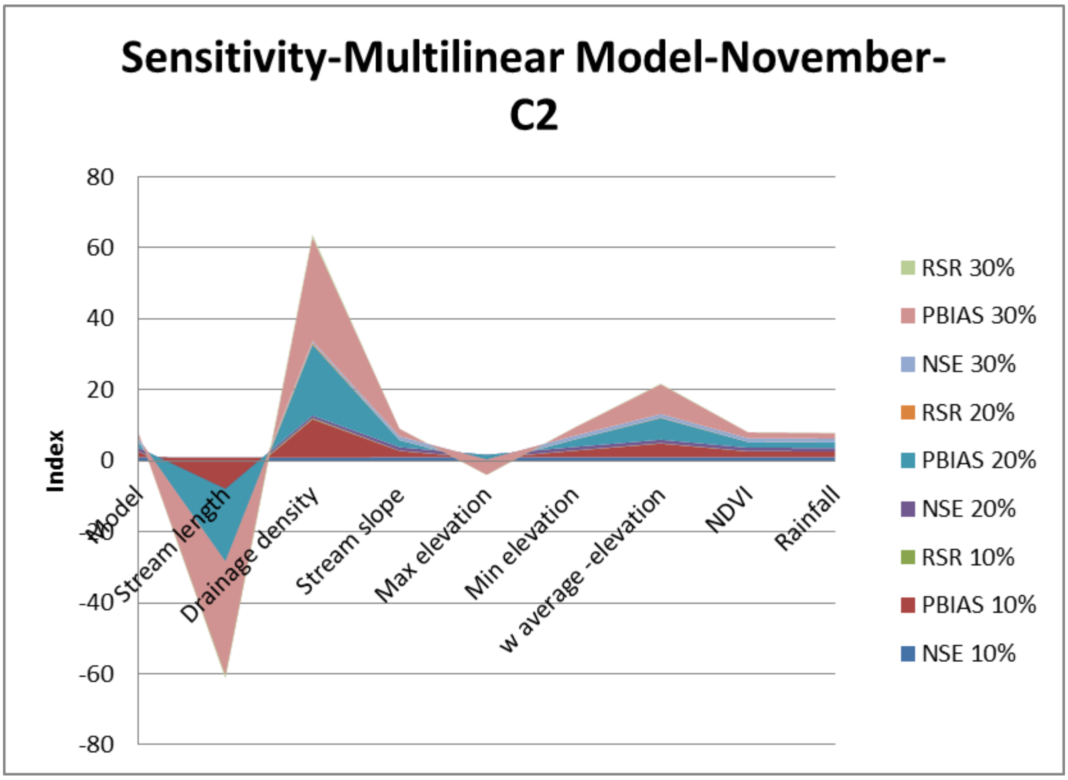

Figure C-140 Sensitivity summary – Multilinear model –November C2

Table C-35 Summary performance- Multilinear model- November C2

		10%							
	0%	Stream length	Drainage density	Stream slope	Max elevation	Min elevation	w average - elevation	NDVI	Rainfall
NSE	0.996063	0.933778	0.929771	0.995751	0.99726	0.995681	0.989234	0.996063	0.996133
PBIAS	1.637778	-9.82294	10.8222	1.801534	-0.36075	1.837304	3.878289	1.637761	1.59825
RSR	0.062746	0.257335	0.265008	0.065186	0.052343	0.065717	0.10376	0.062746	0.062186
		20%							
	0%	Stream length	Drainage density	Stream slope	Max elevation	Min elevation	w average - elevation	NDVI	Rainfall
NSE	0.996063	0.704889	0.764428	0.9954	0.99375	0.995255	0.976738	0.996063	0.996201
PBIAS	1.637778	-21.2837	20.00663	1.96529	-2.35928	2.03683	6.1188	1.637745	1.558723
RSR	0.062746	0.543241	0.485358	0.067827	0.079056	0.068883	0.152518	0.062745	0.061635
		30%							
	0%	Stream length	Drainage density	Stream slope	Max elevation	Min elevation	w average - elevation	NDVI	Rainfall
NSE	0.996063	0.309394	0.500035	0.995009	0.985533	0.994785	0.958576	0.996063	0.996267
PBIAS	1.637778	-32.7444	29.19105	2.129046	-4.35782	2.236357	8.359312	1.637728	1.519196
RSR	0.062746	0.831027	0.707082	0.070646	0.120279	0.072216	0.203528	0.062745	0.061094

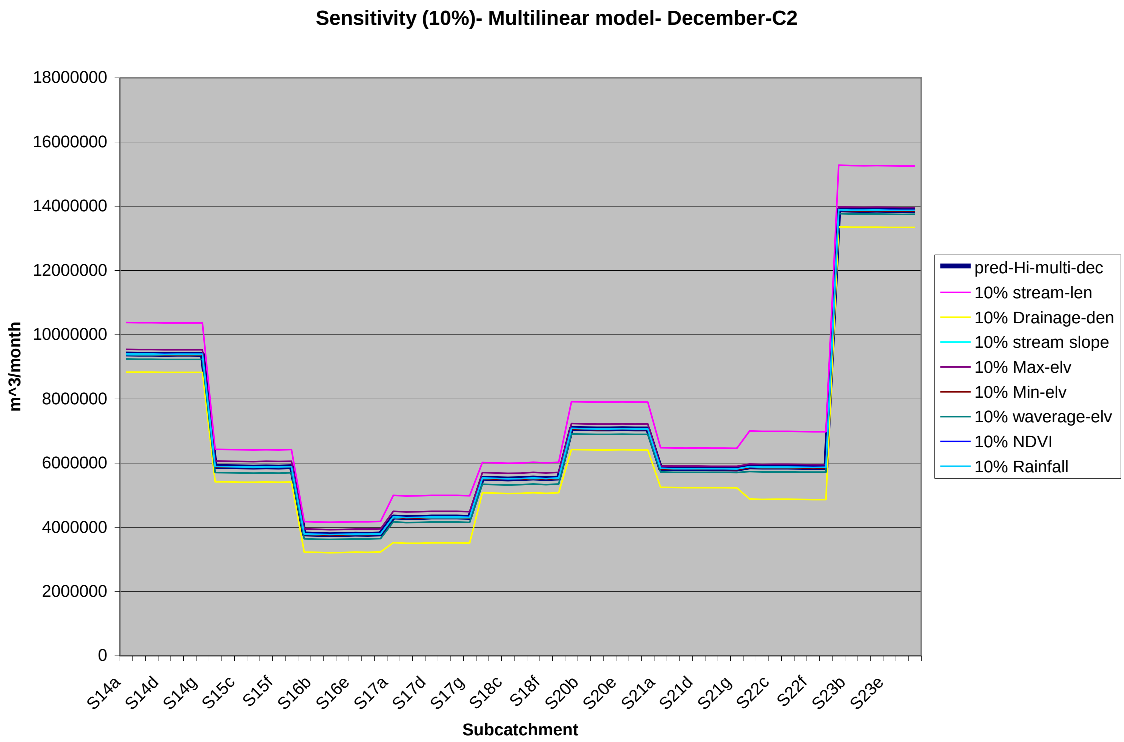

Figure C-141 Sensitivity (10%) – Multilinear model –December C2

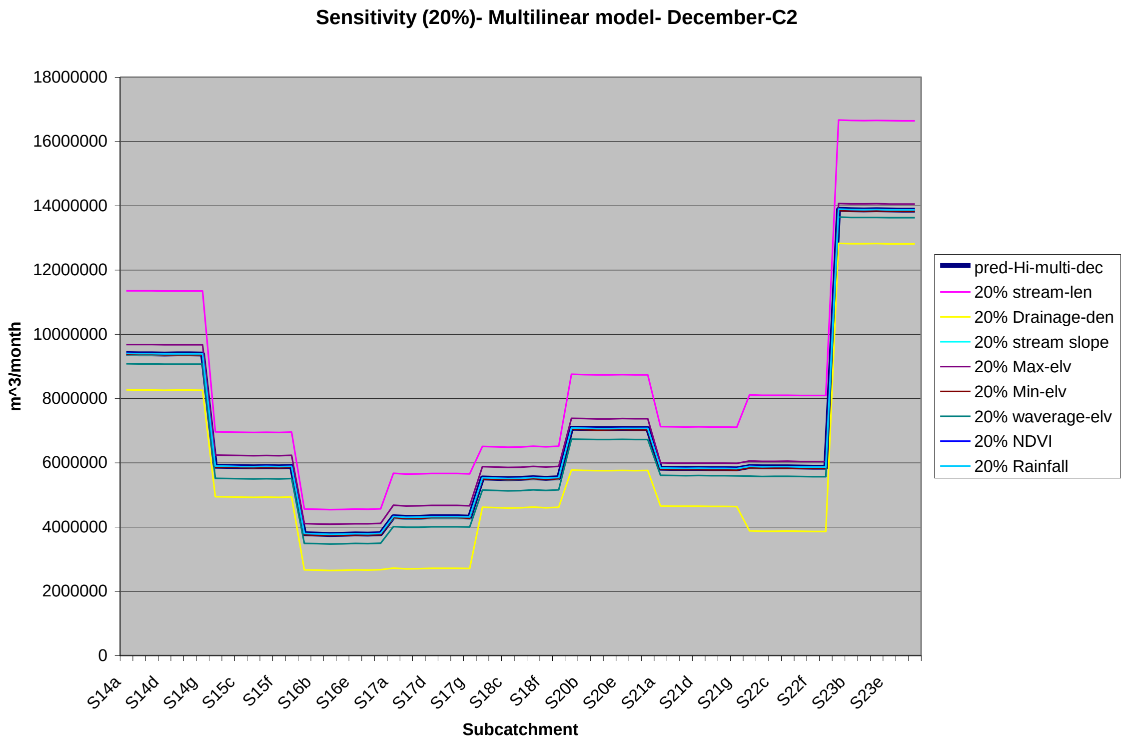

Figure C-142 Sensitivity (20%) – Multilinear model –Decemebr C2

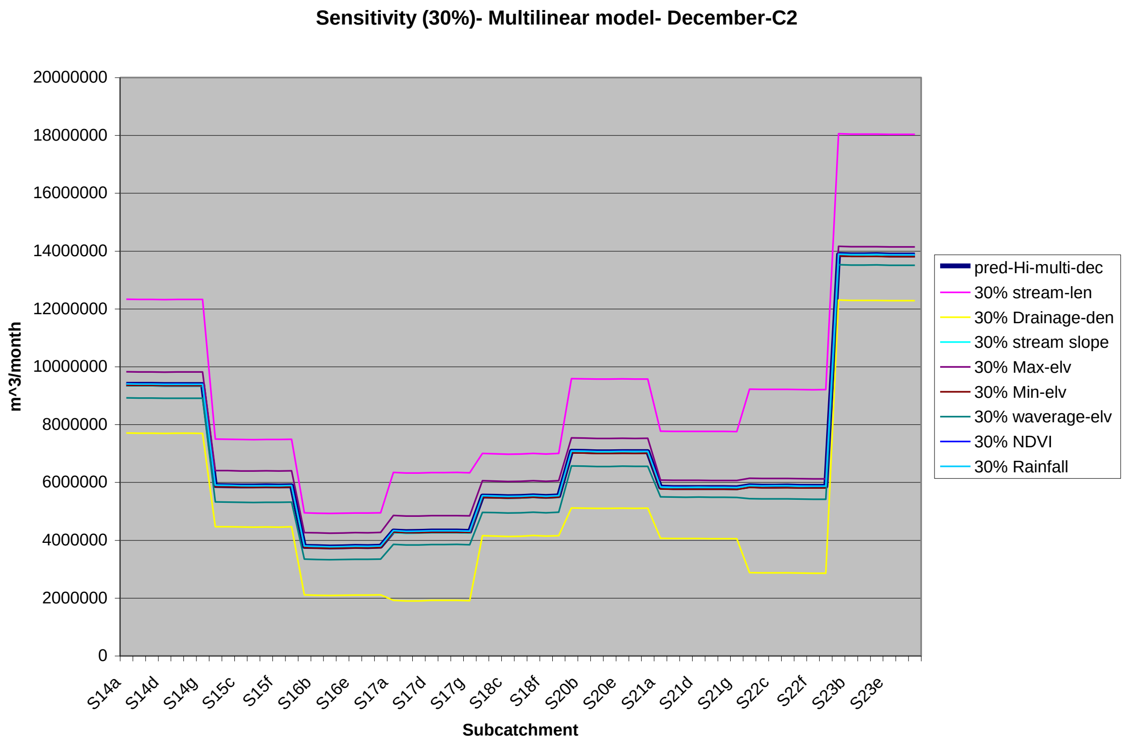

Figure C-143 Sensitivity (30%) – Multilinear model –December C2

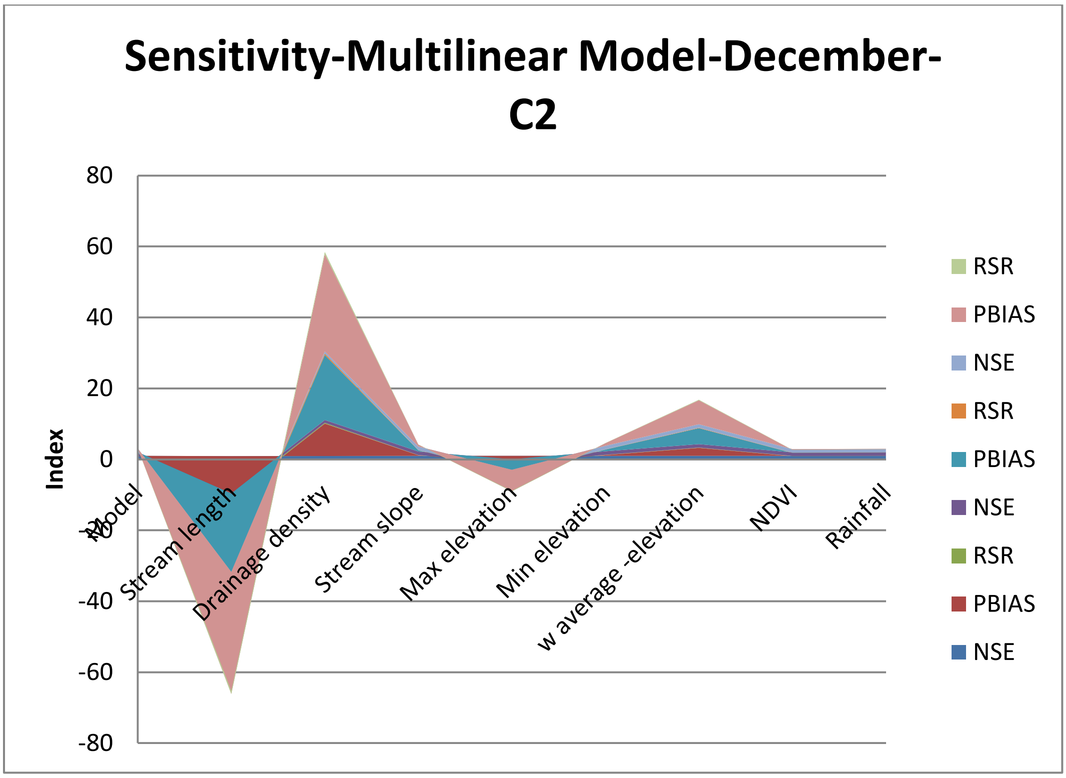

Figure C-144 Sensitivity summary – Multilinear model –December C2

Table C-36 Summary performance- Multilinear model- December C2

		10%							
	0%	Stream length	Drainage density	Stream slope	Max elevation	Min elevation	w average - elevation	NDVI	Rainfall
NSE	0.997554	0.914095	0.94855	0.997532	0.995133	0.997522	0.9947	0.997551	0.997553
PBIAS	-0.00594	-11.4731	9.135509	0.175943	-2.02729	0.241374	2.249033	-0.07278	-0.04242
RSR	0.049453	0.293096	0.226827	0.049684	0.069765	0.04978	0.072804	0.049482	0.049463
		20%							
	0%	Stream length	Drainage density	Stream slope	Max elevation	Min elevation	w average - elevation	NDVI	Rainfall
NSE	0.997554	0.663843	0.801419	0.99746	0.987896	0.997421	0.986105	0.997543	0.997551
PBIAS	-0.00594	-22.9402	18.27696	0.35783	-4.04864	0.48869	4.504009	-0.13962	-0.07889
RSR	0.049453	0.579791	0.445624	0.050394	0.110018	0.050779	0.117878	0.049563	0.049488
		30%							
	0%	Stream length	Drainage density	Stream slope	Max elevation	Min elevation	w average - elevation	NDVI	Rainfall
NSE	0.997554	0.246799	0.556162	0.997341	0.975844	0.997253	0.97177	0.99753	0.997547
PBIAS	-0.00594	-34.4074	27.41842	0.539717	-6.06999	0.736007	6.758985	-0.20646	-0.11536
RSR	0.049453	0.867872	0.666211	0.051565	0.155423	0.052413	0.168018	0.049695	0.049529

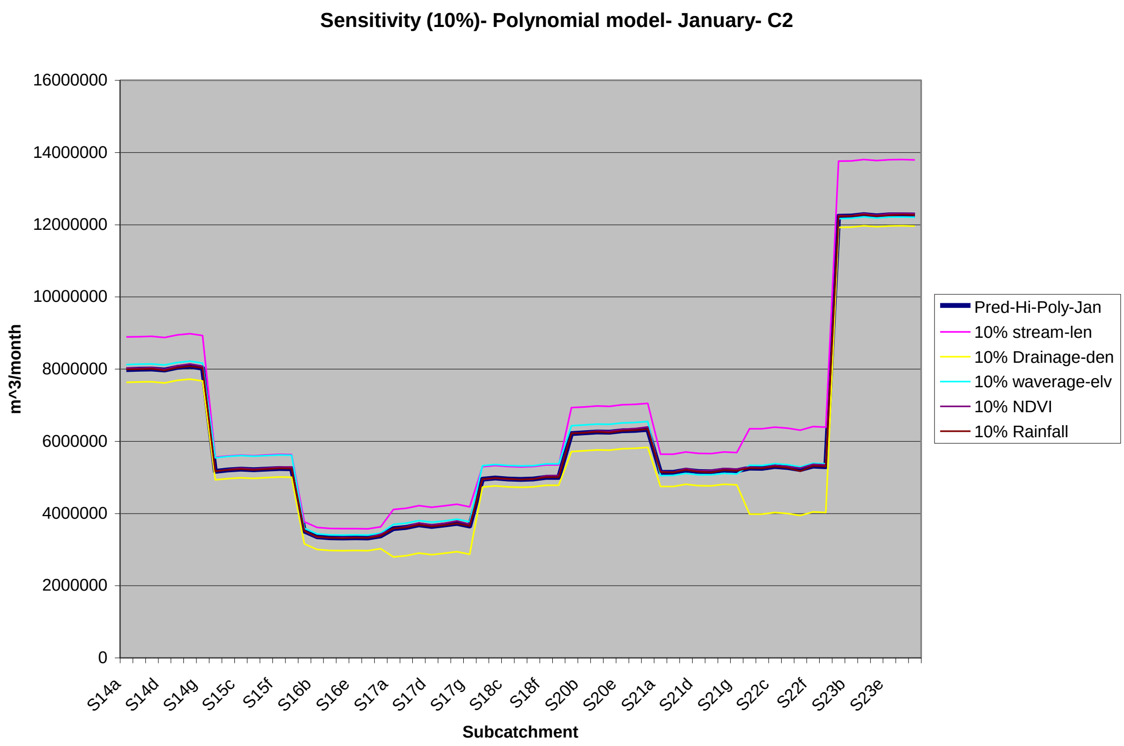

Figure C-145 Sensitivity (10%) – Polynomial model –January C2

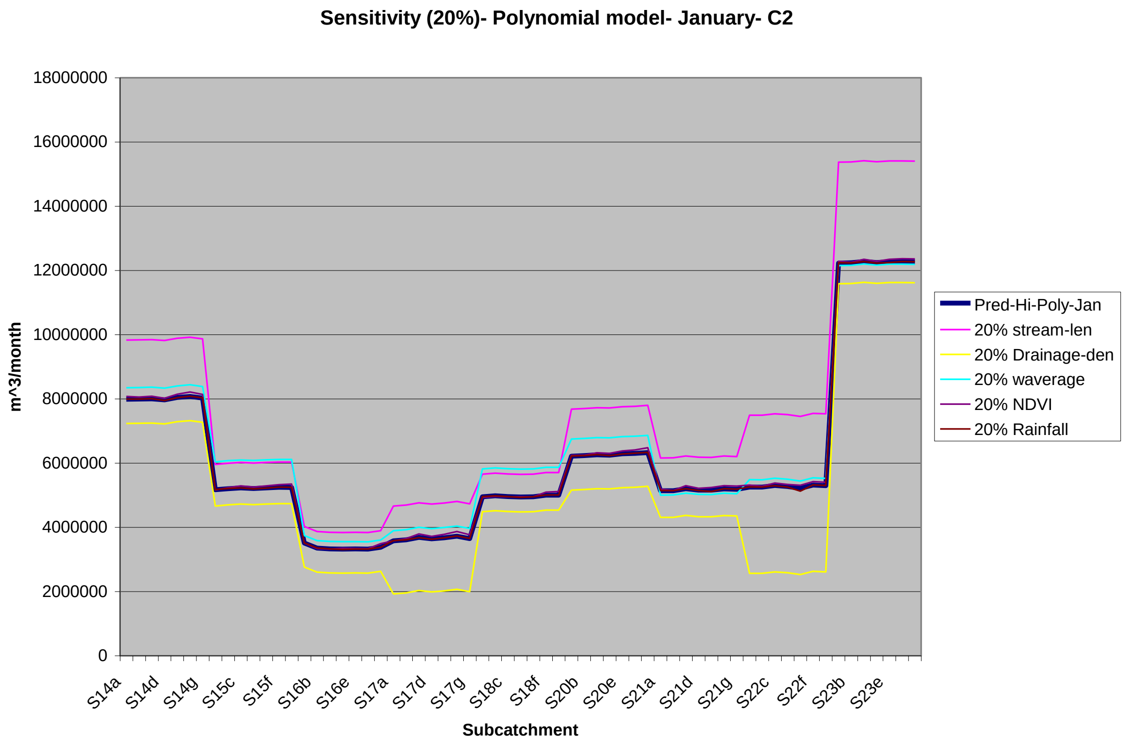

Figure C-146 Sensitivity (20%) – Polynomial model –January C2

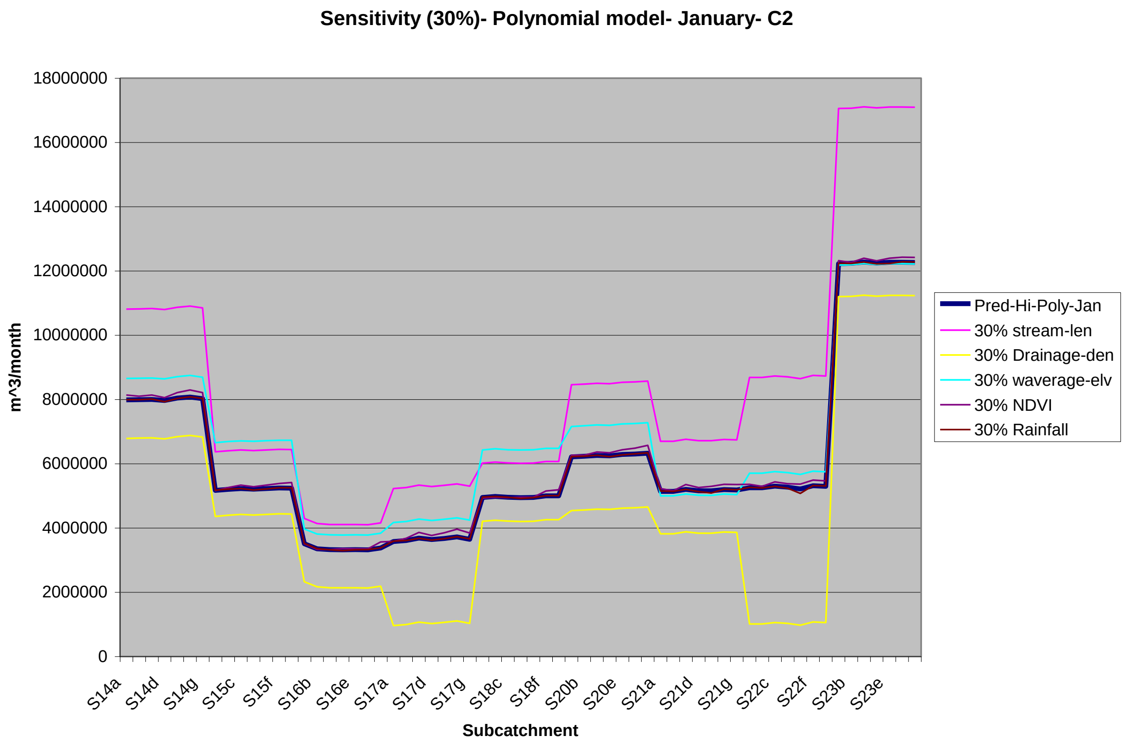

Figure C-147 Sensitivity summary – Polynomial model –January C2

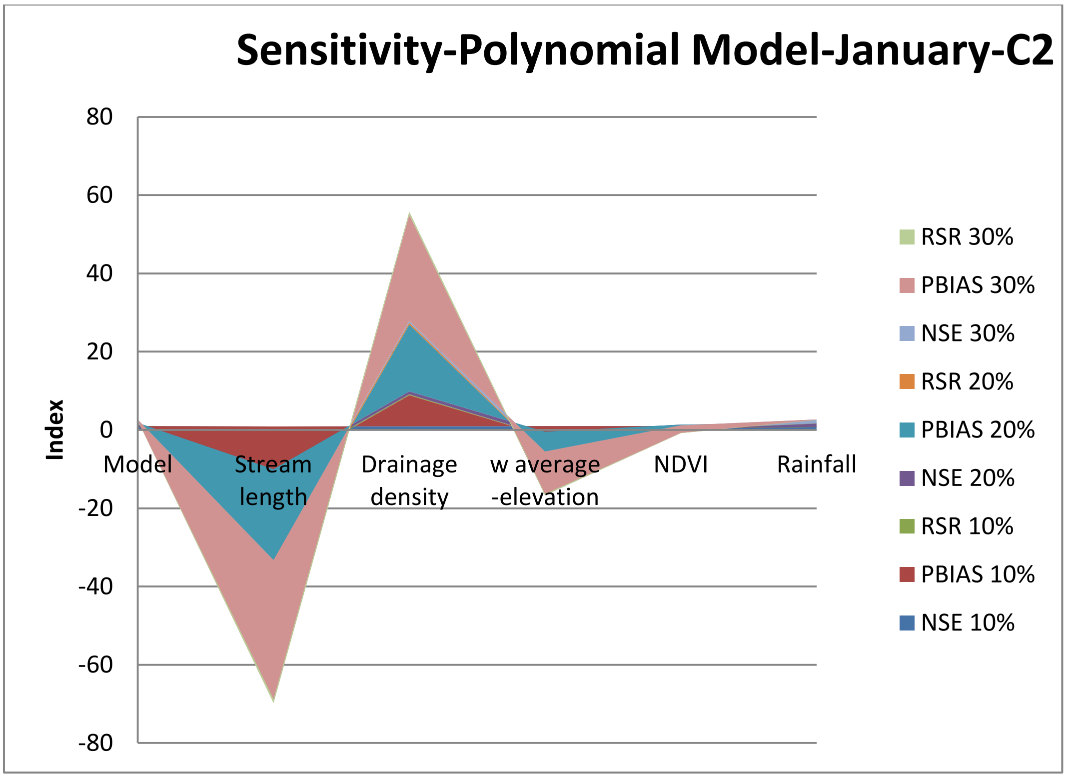

Figure C-148 Sensitivity summary – Polynomial model –January C2

Table C-37 Summary performance- Polynomial model- January C2

		10%				
	0%	Stream length	Drainage density	w average - elevation	NDVI	Rainfall
NSE	0.996297	0.897041	0.946023	0.98922	0.996048	0.996286
PBIAS	-0.23568	-11.8253	7.928948	-2.50337	-0.68215	-0.22687
RSR	0.060855	0.320873	0.23233	0.103827	0.062863	0.060943
		20%				
	0%	Stream length	Drainage density	w average - elevation	NDVI	Rainfall
NSE	0.996297	0.58556	0.767067	0.958341	0.995251	0.99626
PBIAS	-0.23568	-23.9076	17.06364	-6.14451	-1.26028	-0.1984
RSR	0.060855	0.64377	0.482631	0.204107	0.068914	0.061157
		30%				
	0%	Stream length	Drainage density	w average - elevation	NDVI	Rainfall
NSE	0.996297	0.03362	0.419445	0.882833	0.993584	0.996208
PBIAS	-0.23568	-36.4827	27.16838	-11.1591	-1.97007	-0.15028
RSR	0.060855	0.983046	0.761941	0.342297	0.0801	0.061576

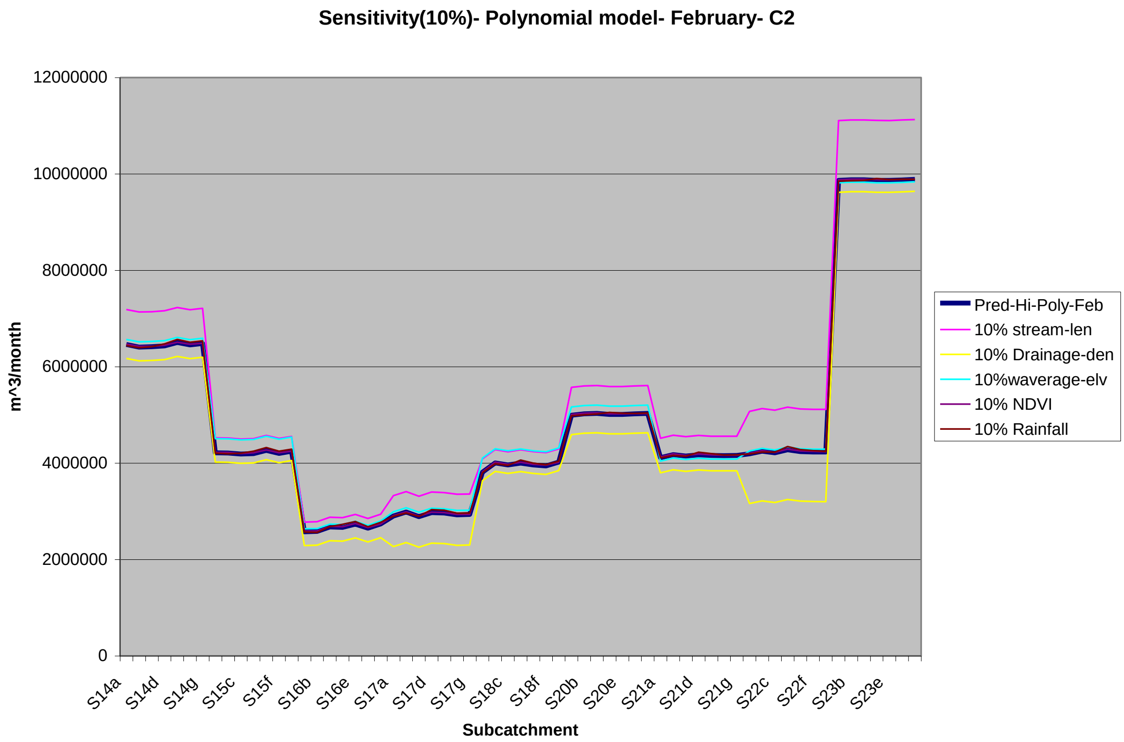

Figure C-149 Sensitivity (10%) – Polynomial model –February C2

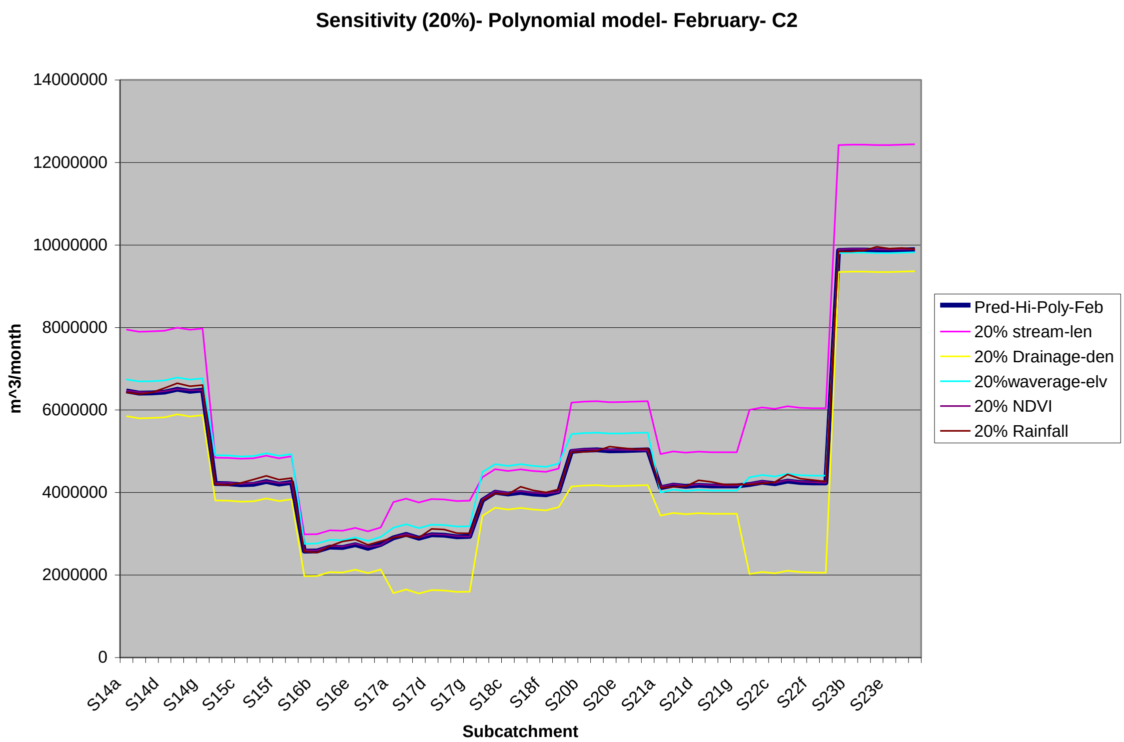

Figure C-150 Sensitivity (20%) – Polynomial model –February C2

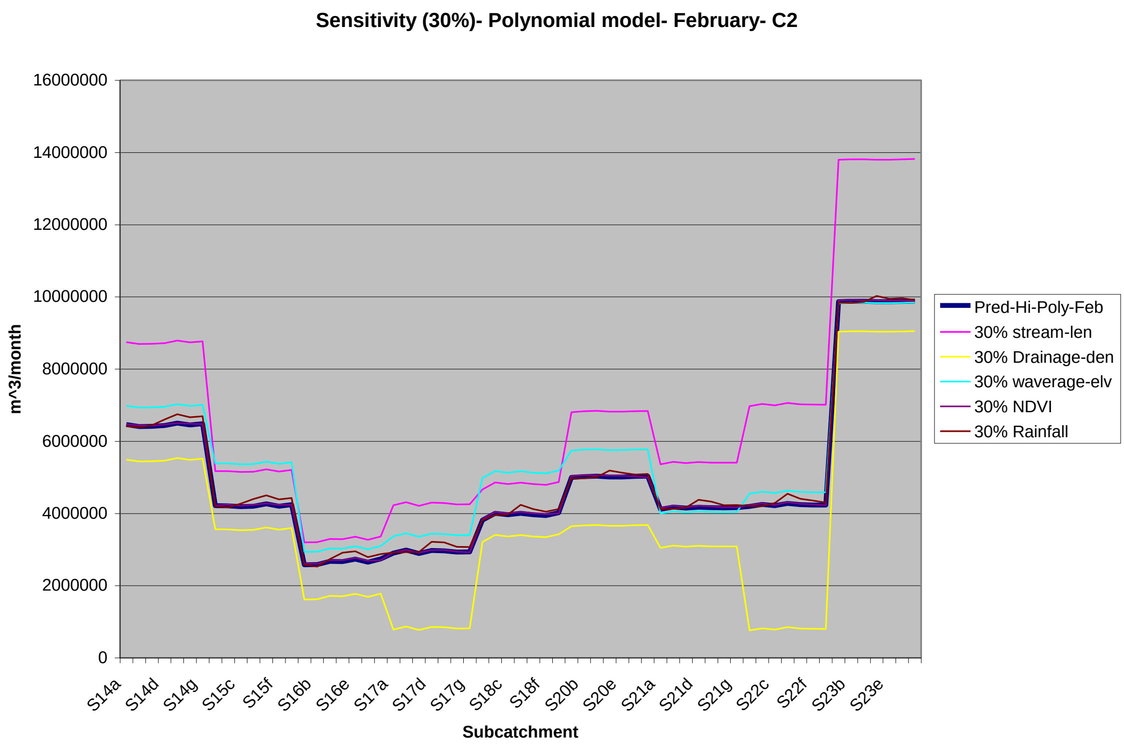

Figure C-151 Sensitivity (30%) – Polynomial model -February C2

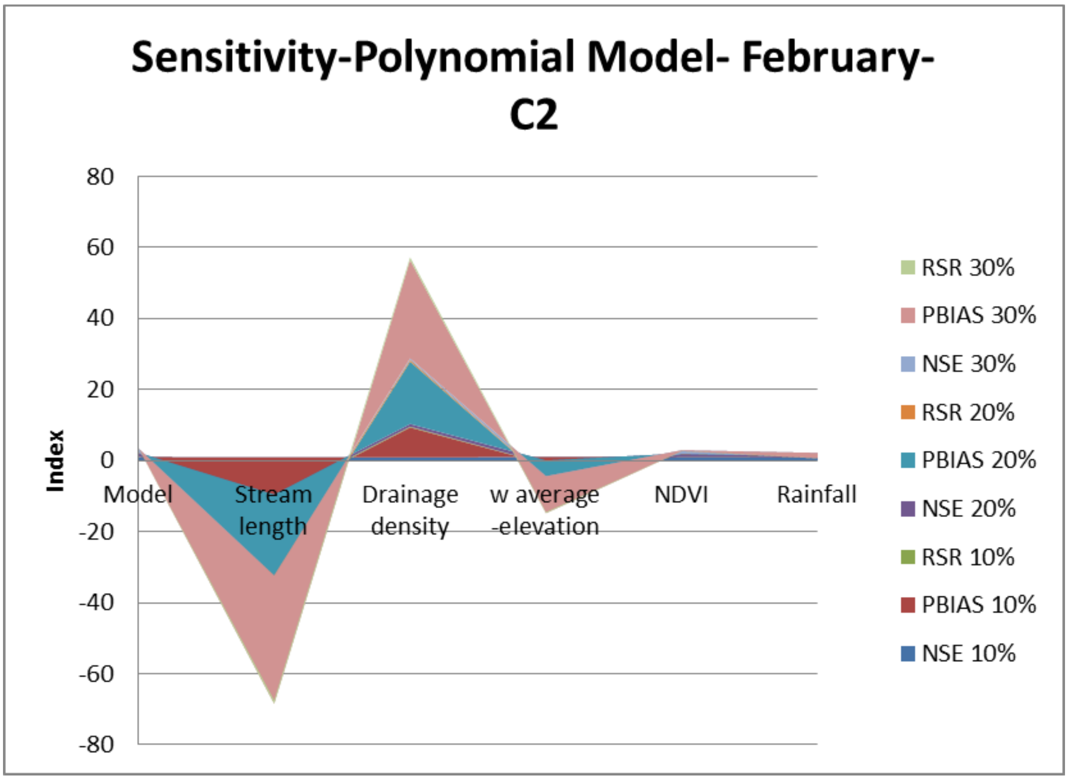

Figure C-152 Sensitivity (30%) – Polynomial model -February C2

Table C-38 Summary performance- Polynomial model- February C2

		10%				
	0%	Stream length	Drainage density	w average - elevation	NDVI	Rainfall
NSE	0.996724	0.901641	0.942541	0.991181	0.99674	0.996553
PBIAS	0.19771	-11.3786	8.385853	-1.98851	-0.01648	-0.16419
RSR	0.057234	0.313622	0.239705	0.09391	0.057099	0.058712
		20%				
	0%	Stream length	Drainage density	w average - elevation	NDVI	Rainfall
NSE	0.996724	0.592754	0.758484	0.963644	0.996703	0.995578
PBIAS	0.19771	-23.4701	17.5471	-5.52685	-0.16739	-0.75881
RSR	0.057234	0.638158	0.491443	0.190672	0.057424	0.066502
		30%				
	0%	Stream length	Drainage density	w average - elevation	NDVI	Rainfall
NSE	0.996724	0.040394	0.404324	0.894147	0.996633	0.993117
PBIAS	0.19771	-36.0768	27.68144	-10.4173	-0.25501	-1.58616
RSR	0.057234	0.979595	0.7718	0.32535	0.058024	0.082966

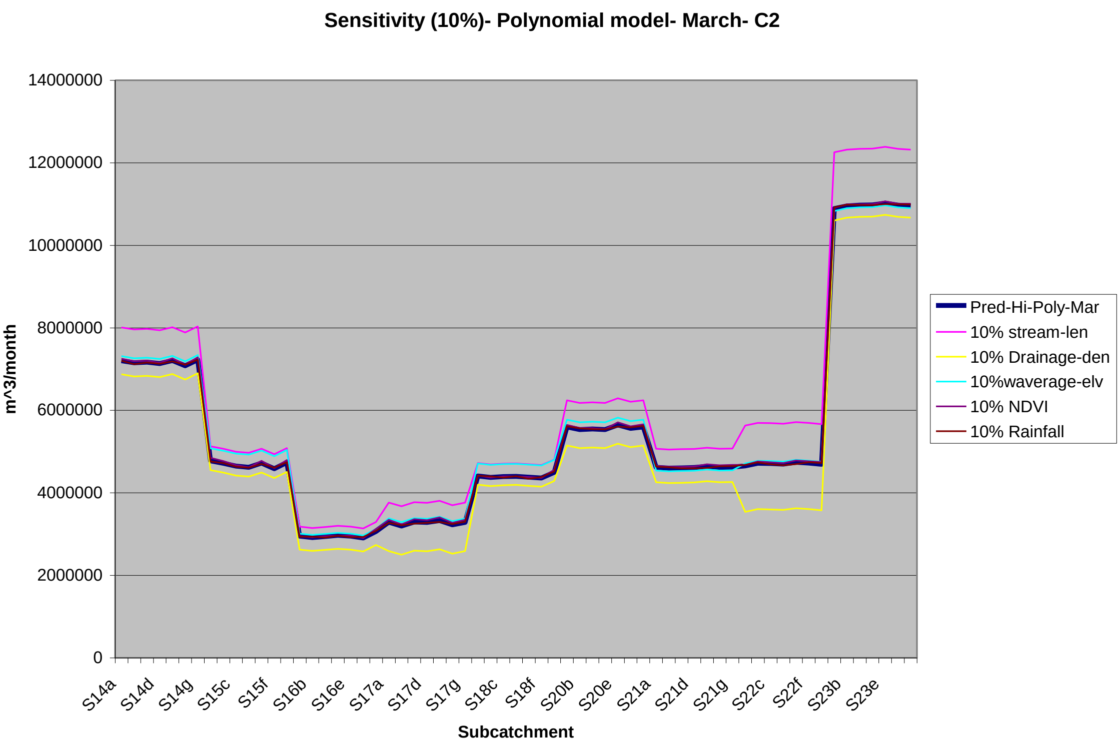

Figure C-153 Sensitivity (10%) – Polynomial model –March C2

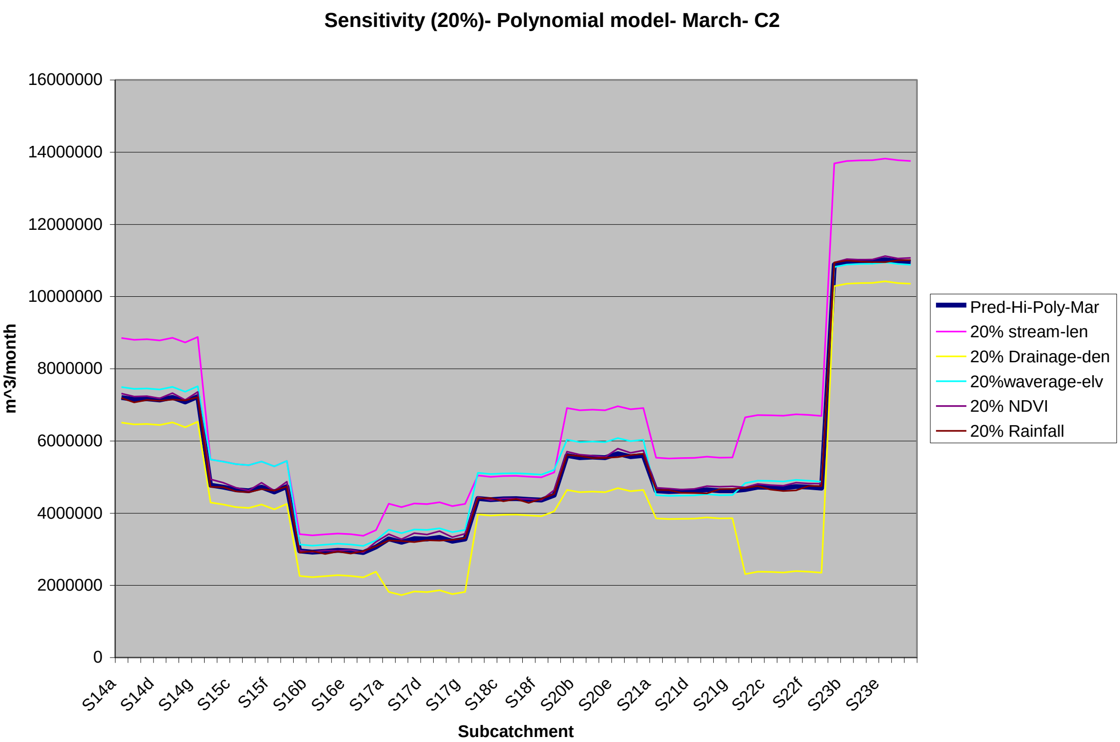

Figure C-154 Sensitivity (20%) – Polynomial model –March C2

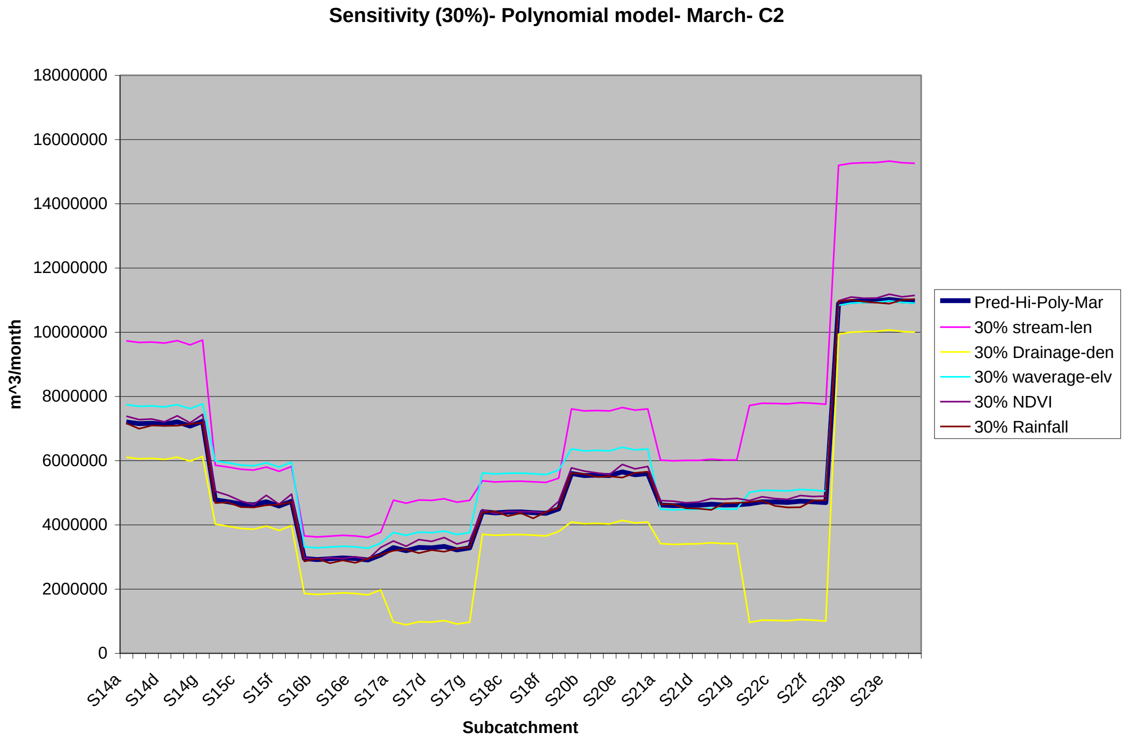

Figure C-155 Sensitivity (30%) – Polynomial model –March C2

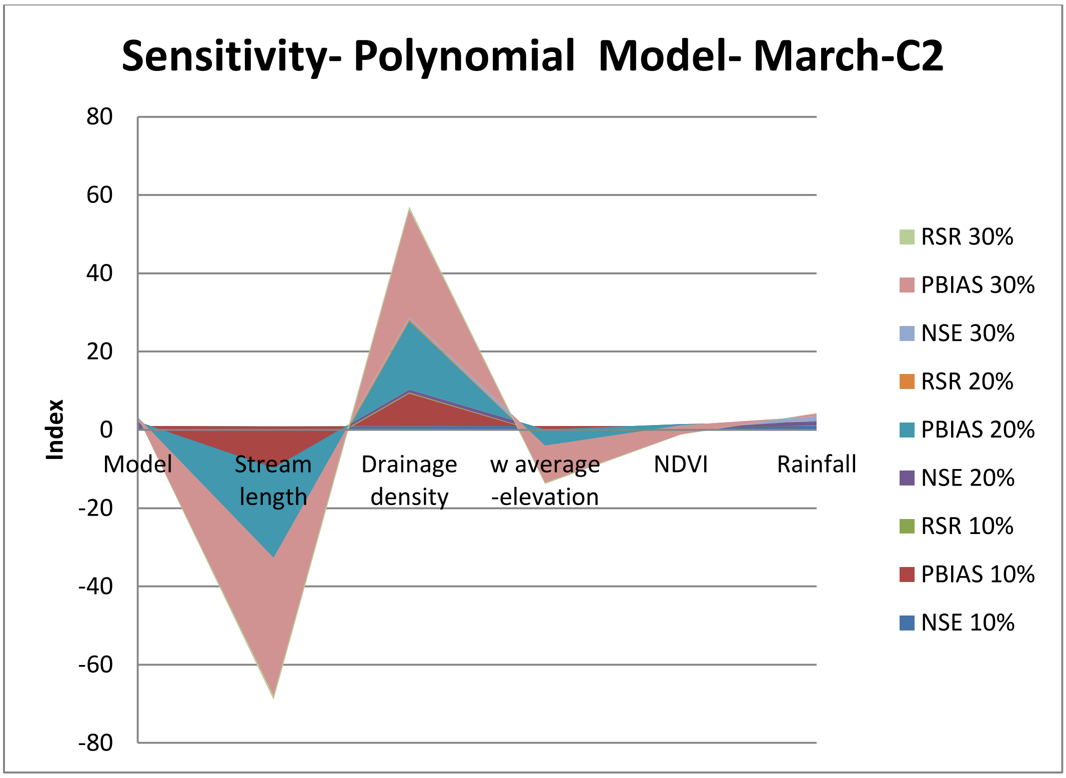

Figure C-156 Sensitivity summary – Polynomial model –March C2

Table C-39 Summary performance- Polynomial model- March C2

		10%				
	0%	Stream length	Drainage density	w average - elevation	NDVI	Rainfall
NSE	0.996767	0.900567	0.944296	0.991707	0.996489	0.996669
PBIAS	0.070538	-11.5346	8.350084	-1.93428	-0.57335	0.061662
RSR	0.05686	0.315331	0.236016	0.091066	0.059251	0.057719
		20%				
	0%	Stream length	Drainage density	w average - elevation	NDVI	Rainfall
NSE	0.996767	0.592742	0.765487	0.967407	0.995264	0.996252
PBIAS	0.070538	-23.6223	17.52079	-5.21341	-1.38318	0.288095
RSR	0.05686	0.638168	0.484266	0.180536	0.068815	0.061221
		30%				
	0%	Stream length	Drainage density	w average - elevation	NDVI	Rainfall
NSE	0.996767	0.045683	0.423962	0.906377	0.992552	0.995205
PBIAS	0.070538	-36.1927	27.58264	-9.76686	-2.35896	0.749837
RSR	0.05686	0.976891	0.758972	0.305978	0.086303	0.069244

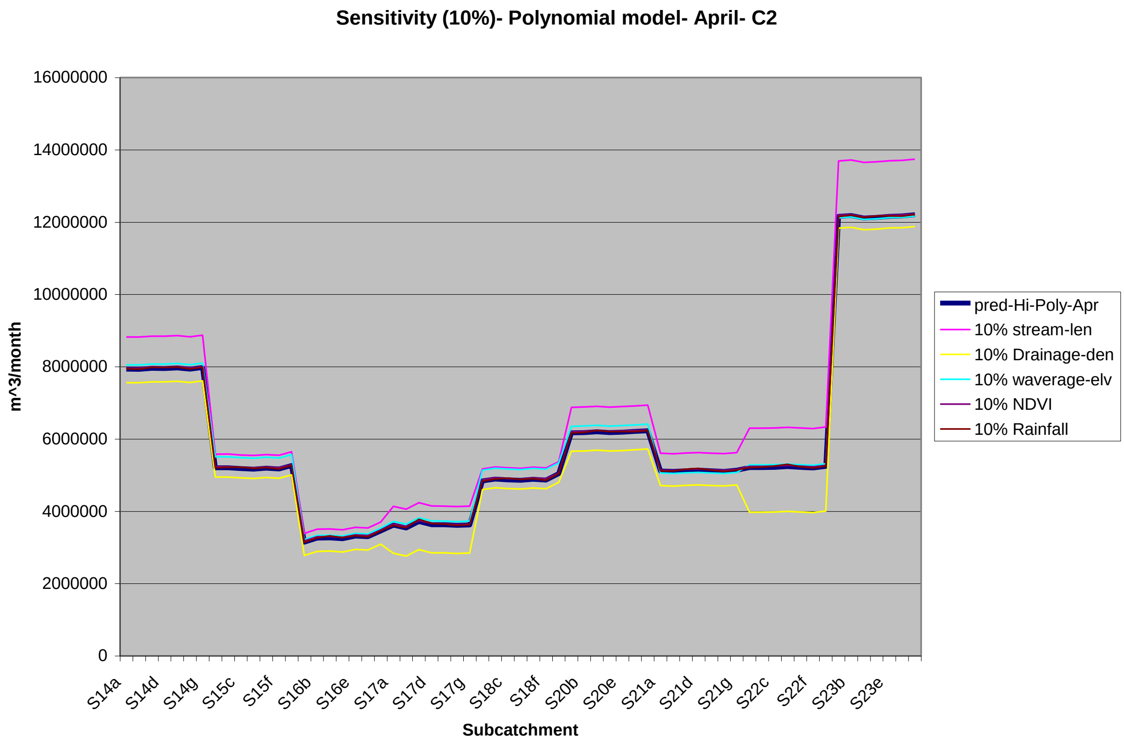

Figure C-157 Sensitivity (10%) – Polynomial model -April C2

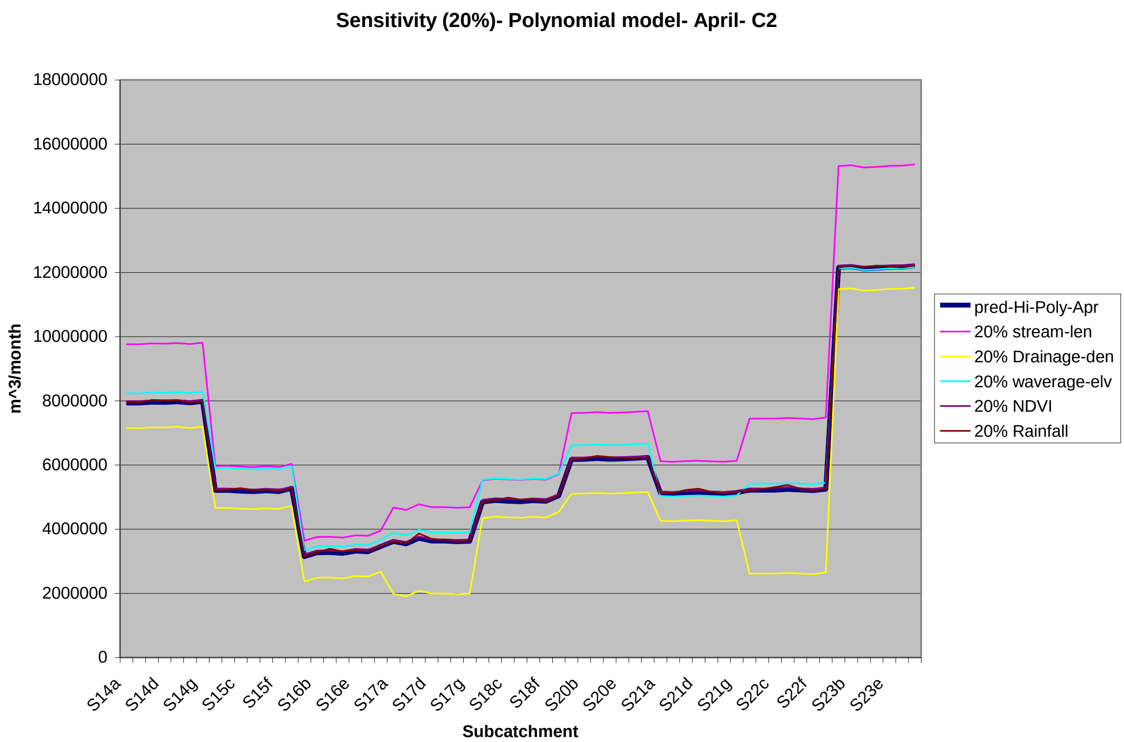

Figure C-158 Sensitivity (20%) – Polynomial model –April C2

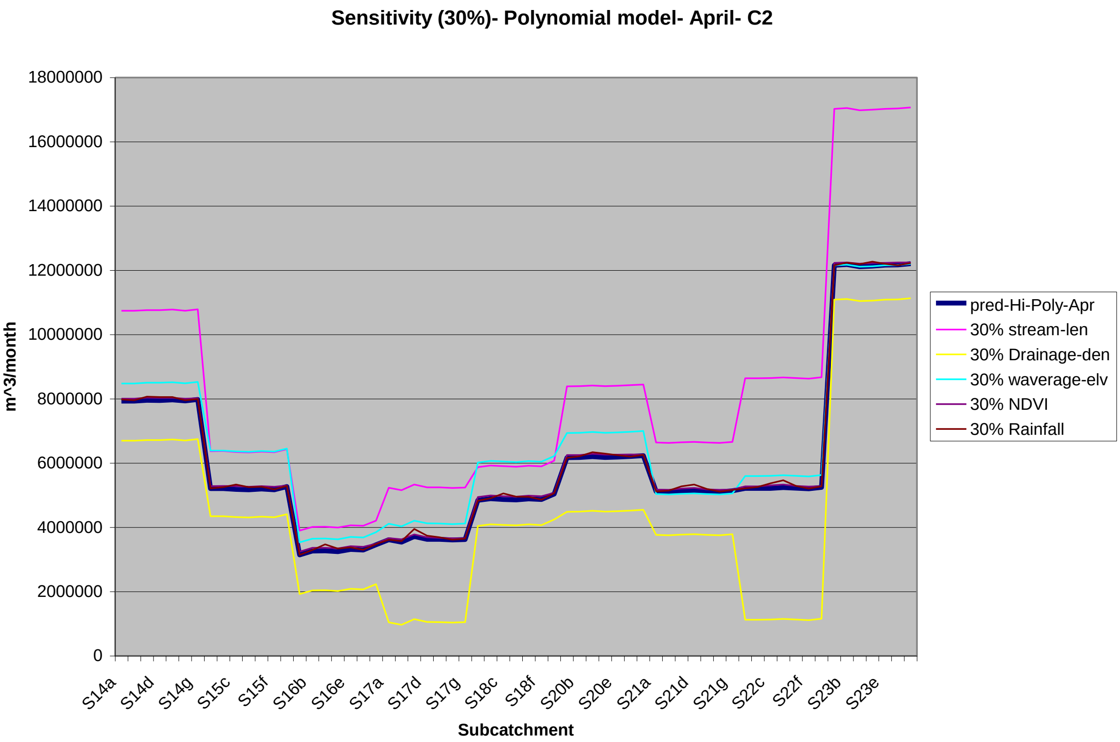

Figure C-159 Sensitivity (30%) – Polynomial model –April C2

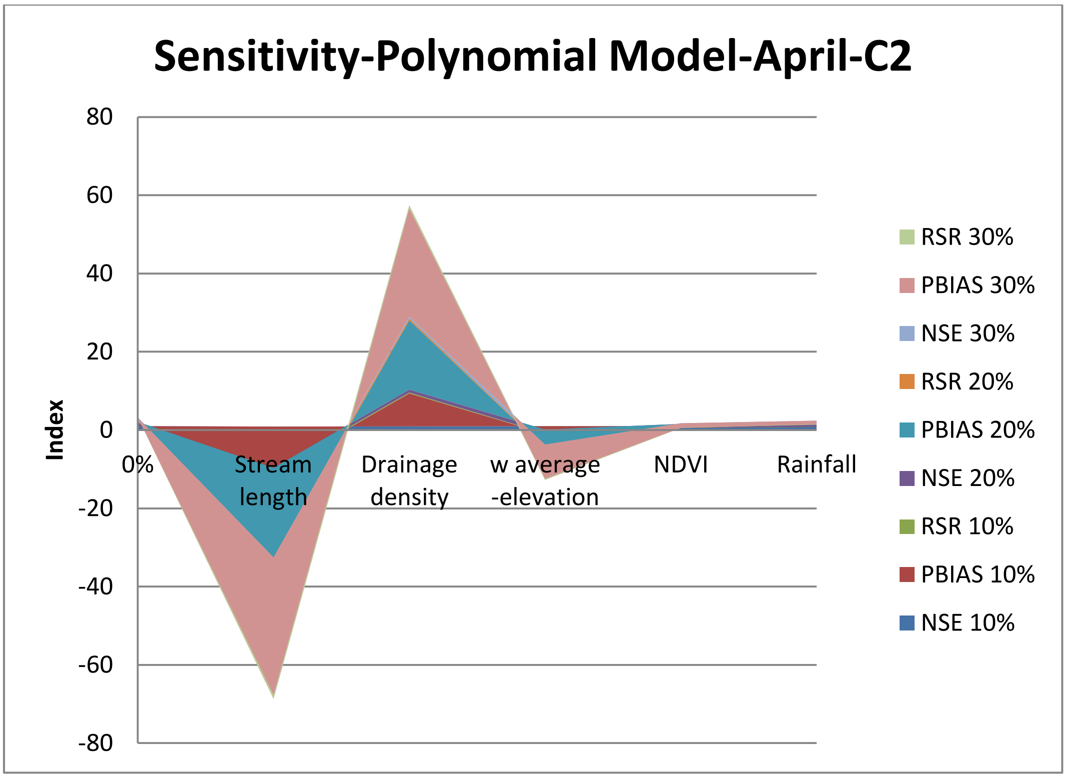

Figure C-160 Sensitivity summary – Polynomial model –April C2

Table C-40 Summary performance- Polynomial model- April C2

		10%				
	0%	Stream length	Drainage density	w average - elevation	NDVI	Rainfall
NSE	0.996699	0.900294	0.94366	0.992432	0.996573	0.996629
PBIAS	0.053788	-11.4732	8.419585	-1.90927	-0.47357	-0.18603
RSR	0.057458	0.315763	0.23736	0.086995	0.058543	0.058056
		20%				
	0%	Stream length	Drainage density	w average - elevation	NDVI	Rainfall
NSE	0.996699	0.589883	0.763261	0.972773	0.996239	0.996311
PBIAS	0.053788	-23.533	17.66162	-4.92851	-0.89169	-0.52271
RSR	0.057458	0.640404	0.486558	0.165005	0.061324	0.060736
		30%				
	0%	Stream length	Drainage density	w average - elevation	NDVI	Rainfall
NSE	0.996699	0.03475	0.419587	0.924604	0.995835	0.995582
PBIAS	0.053788	-36.1255	27.77989	-9.00394	-1.20057	-0.95626
RSR	0.057458	0.982471	0.761849	0.274583	0.064537	0.066467

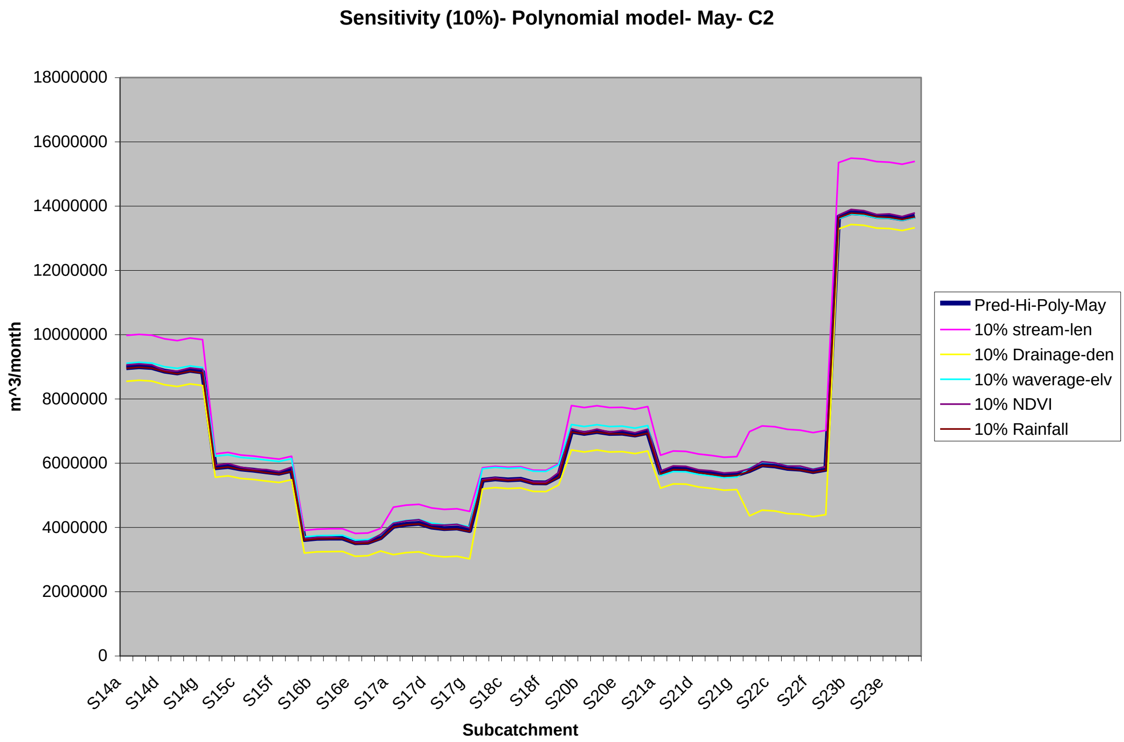

Figure C-161 Sensitivity (10%) – Polynomial model –May C2

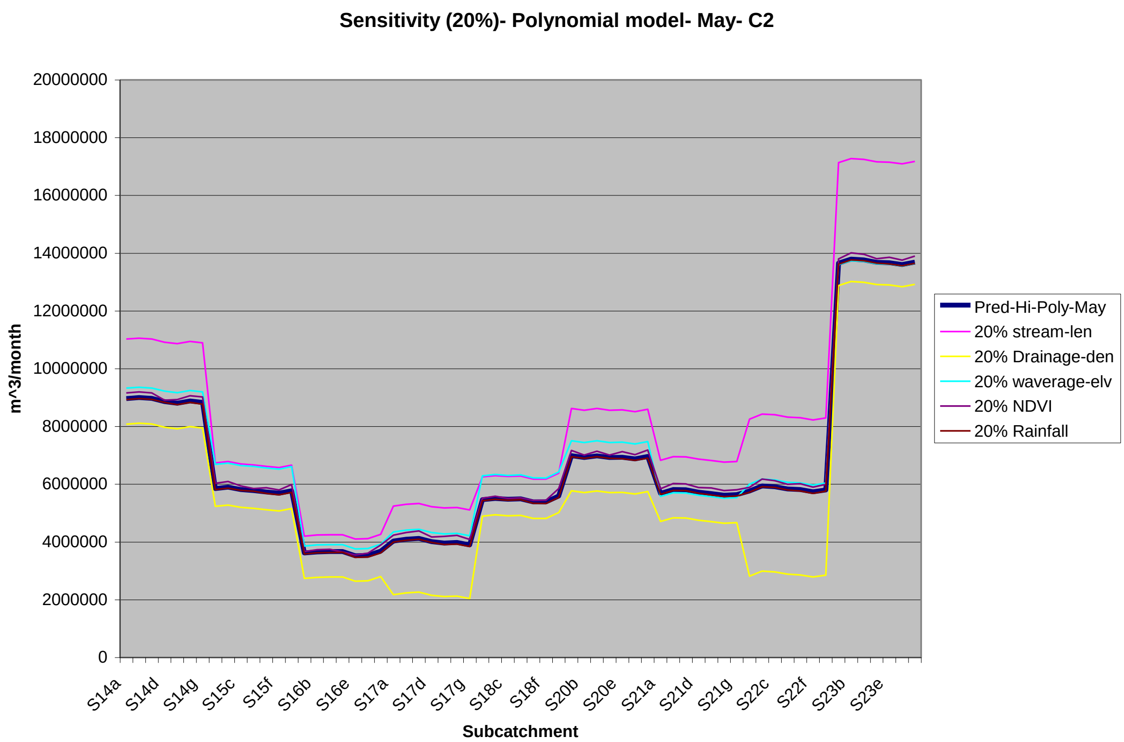

Figure C-162 Sensitivity (20%) – Polynomial model –May C2

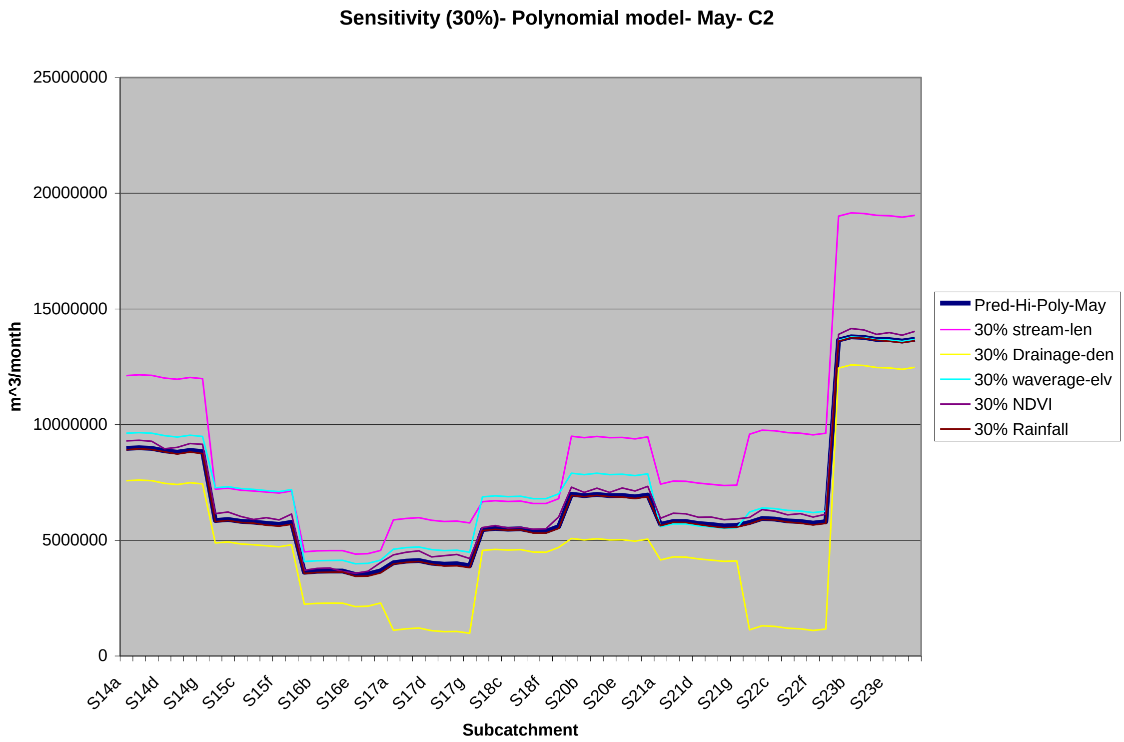

Figure C-163 Sensitivity (30%) – Polynomial model –May C2

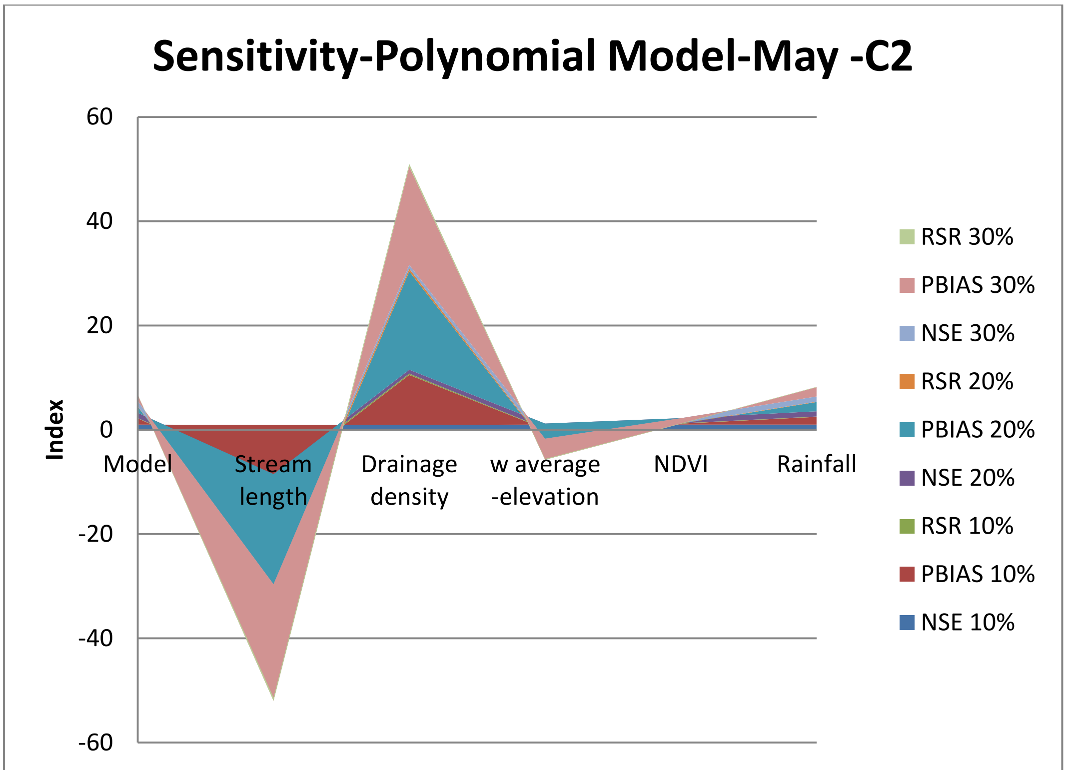

Figure C-164 Sensitivity summary – Polynomial model –May C2

Table C-41 Summary performance- Polynomial model- May C2

		10%				
	0%	Stream length	Drainage density	w average - elevation	NDVI	Rainfall
NSE	0.995596	0.914552	0.931689	0.993403	0.99634	0.995089
PBIAS	1.191659	-10.3384	9.583617	-0.85646	0.182211	1.483684
RSR	0.066362	0.292315	0.261363	0.081222	0.060495	0.070079
		20%				
	0%	Stream length	Drainage density	w average - elevation	NDVI	Rainfall
NSE	0.995596	0.625607	0.738459	0.975464	0.995427	0.99448
PBIAS	1.191659	-22.3434	18.85548	-4.03121	-1.07001	1.775709
RSR	0.066362	0.611876	0.511411	0.15664	0.067621	0.074295
		30%				
	0%	Stream length	Drainage density	w average - elevation	NDVI	Rainfall
NSE	0.995596	0.101798	0.379719	0.927031	0.991743	0.99377
PBIAS	1.191659	-34.8234	29.00725	-8.3326	-2.56502	2.067734
RSR	0.066362	0.947735	0.787579	0.270128	0.09087	0.078928

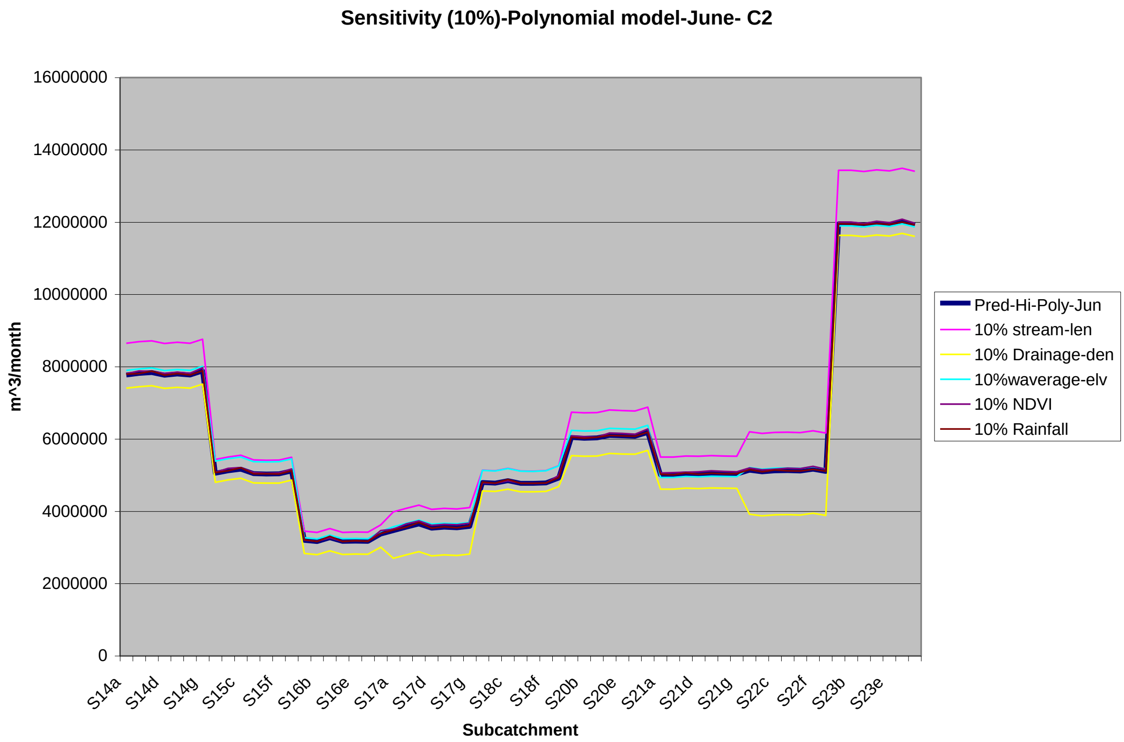

Figure C-165 Sensitivity (10%) – Polynomial model –June C2

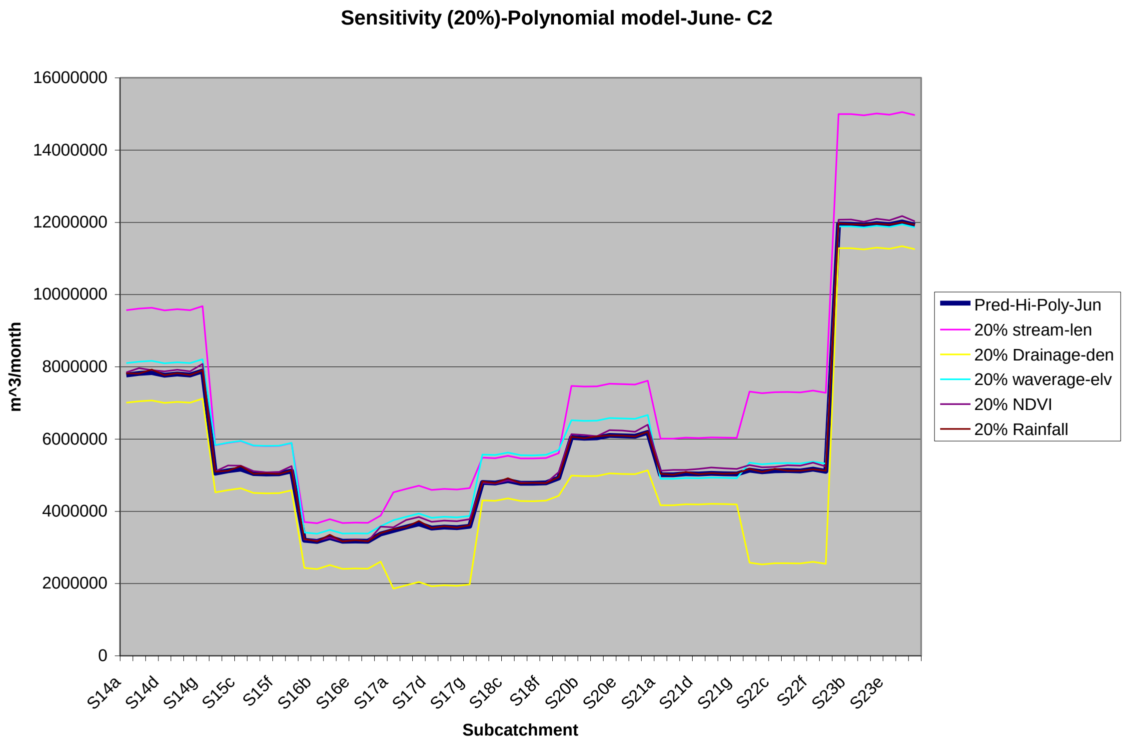

Figure C-166 Sensitivity (20%) – Polynomial model –June C2

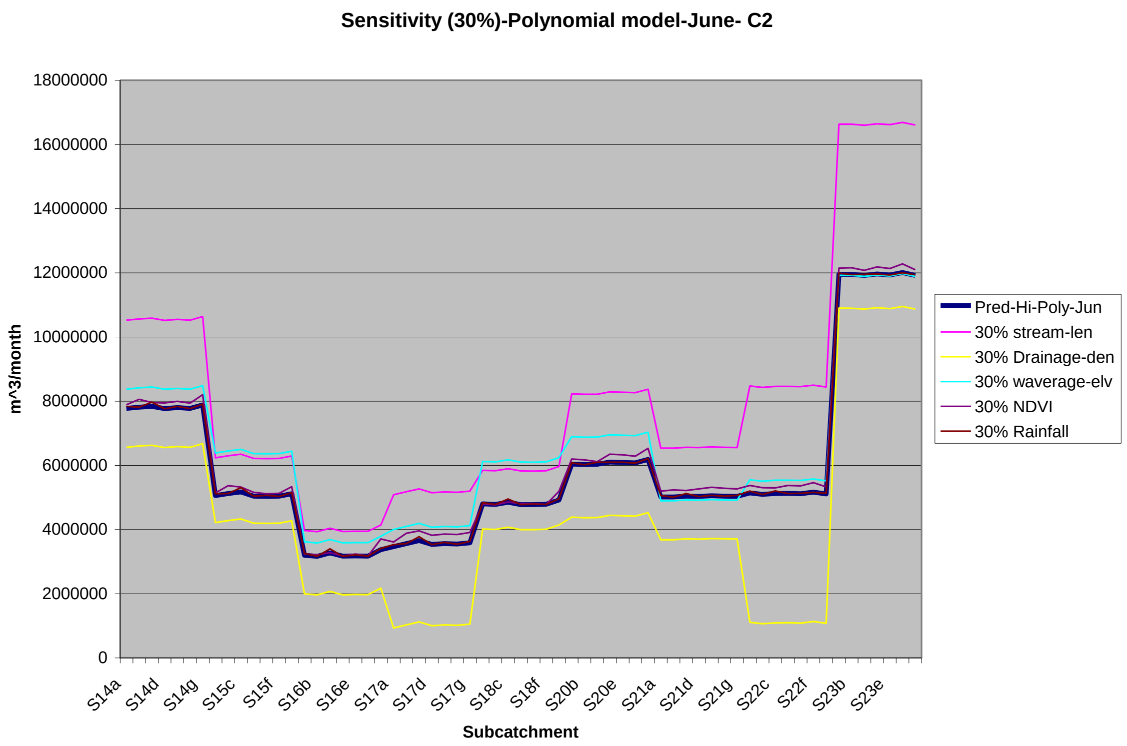

Figure C-167 Sensitivity (30%) – Polynomial model –June C2

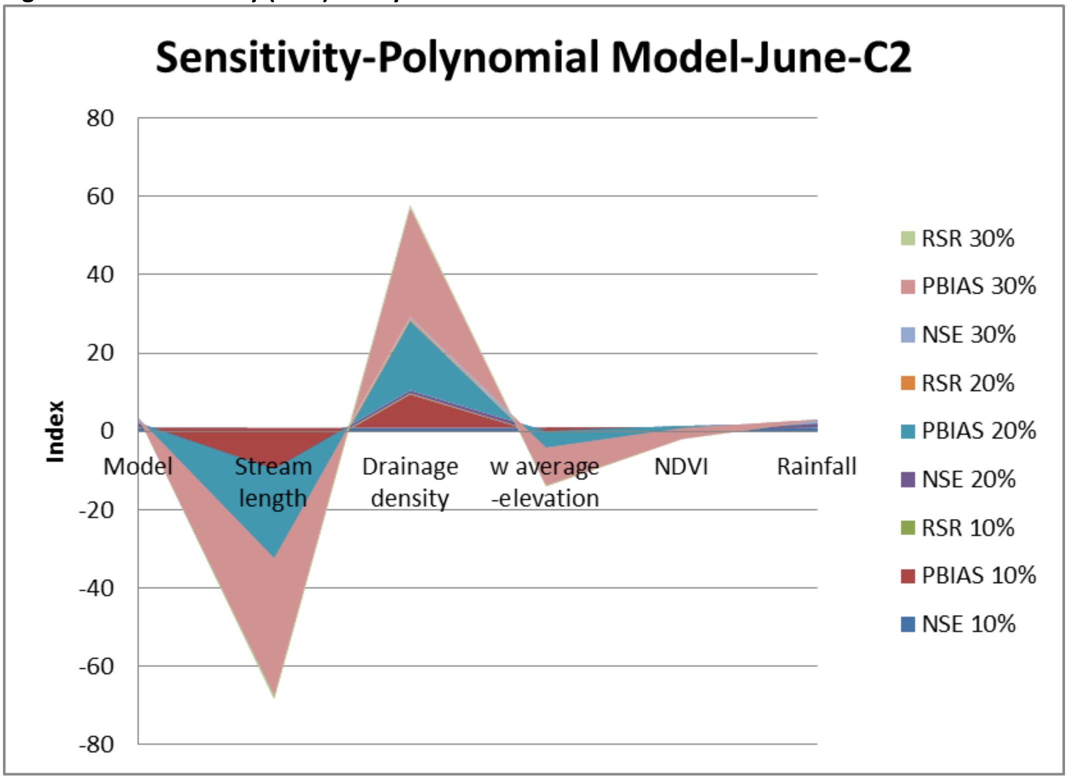

Figure C-168 Sensitivity summary – Polynomial model –June C2

Table C-42 Summary performance- Polynomial model- June C2

		10%				
	0%	Stream length	Drainage density	w average - elevation	NDVI	Rainfall
NSE	0.996709	0.902329	0.94246	0.991764	0.996367	0.996706
PBIAS	0.172682	-11.4004	8.54753	-1.93961	-0.62576	0.048761
RSR	0.057366	0.312523	0.239875	0.090751	0.060273	0.057393
		20%				
	0%	Stream length	Drainage density	w average - elevation	NDVI	Rainfall
NSE	0.996709	0.597627	0.760121	0.967338	0.994635	0.996634
PBIAS	0.172682	-23.454	17.80479	-5.29724	-1.62907	-0.10267
RSR	0.057366	0.634329	0.489774	0.180725	0.073243	0.058019
		30%				
	0%	Stream length	Drainage density	w average - elevation	NDVI	Rainfall
NSE	0.996709	0.055199	0.413437	0.906068	0.990704	0.99646
PBIAS	0.172682	-35.9879	27.94446	-9.90021	-2.83725	-0.28161
RSR	0.057366	0.972009	0.765874	0.306484	0.096418	0.059495

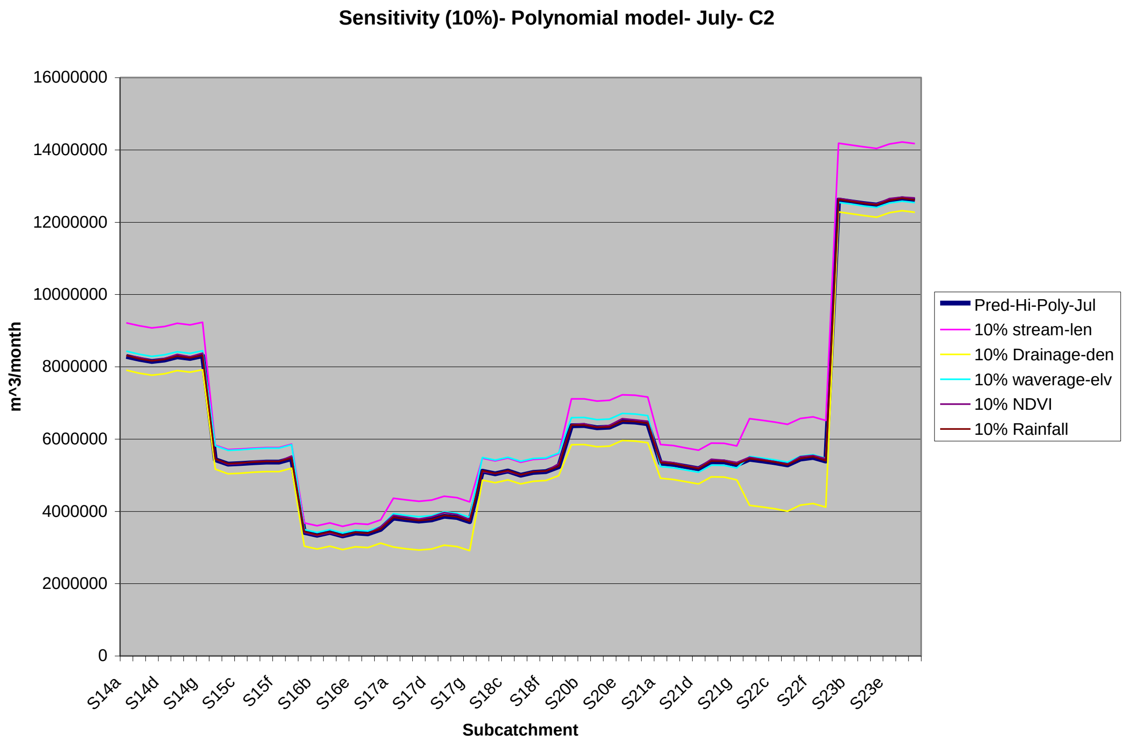

Figure C-169 Sensitivity (10%) – Polynomial model –July C2

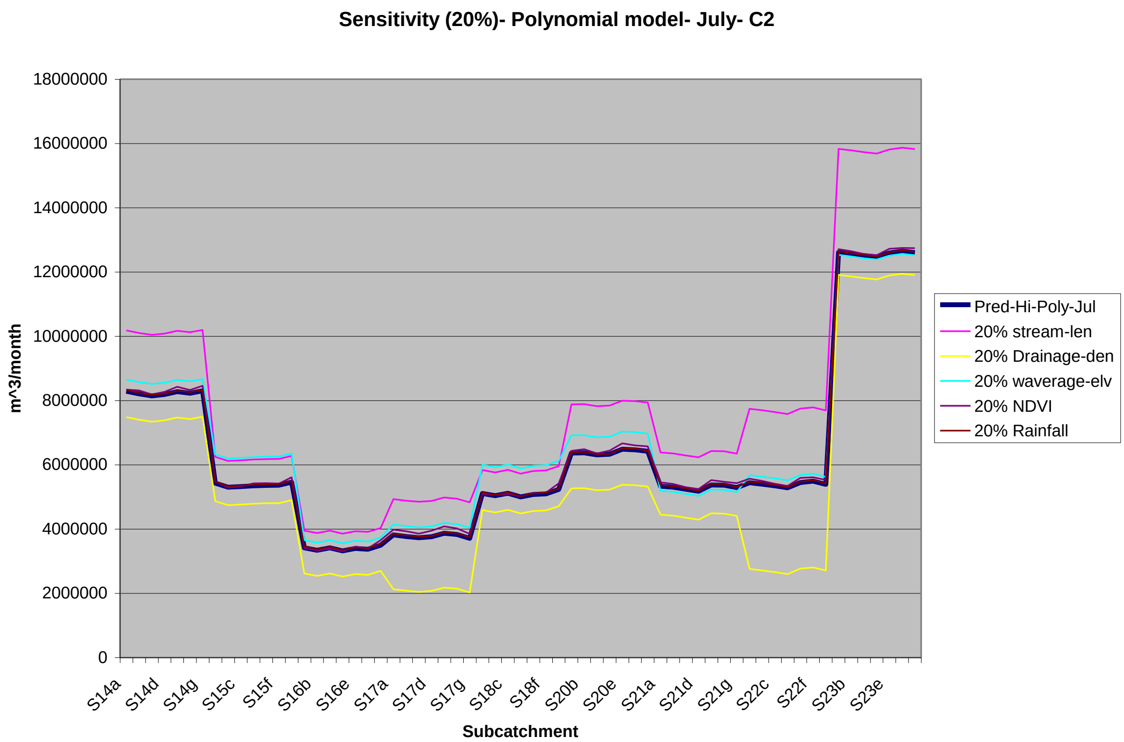

Figure C-170 Sensitivity (20%) – Polynomial model –July C2

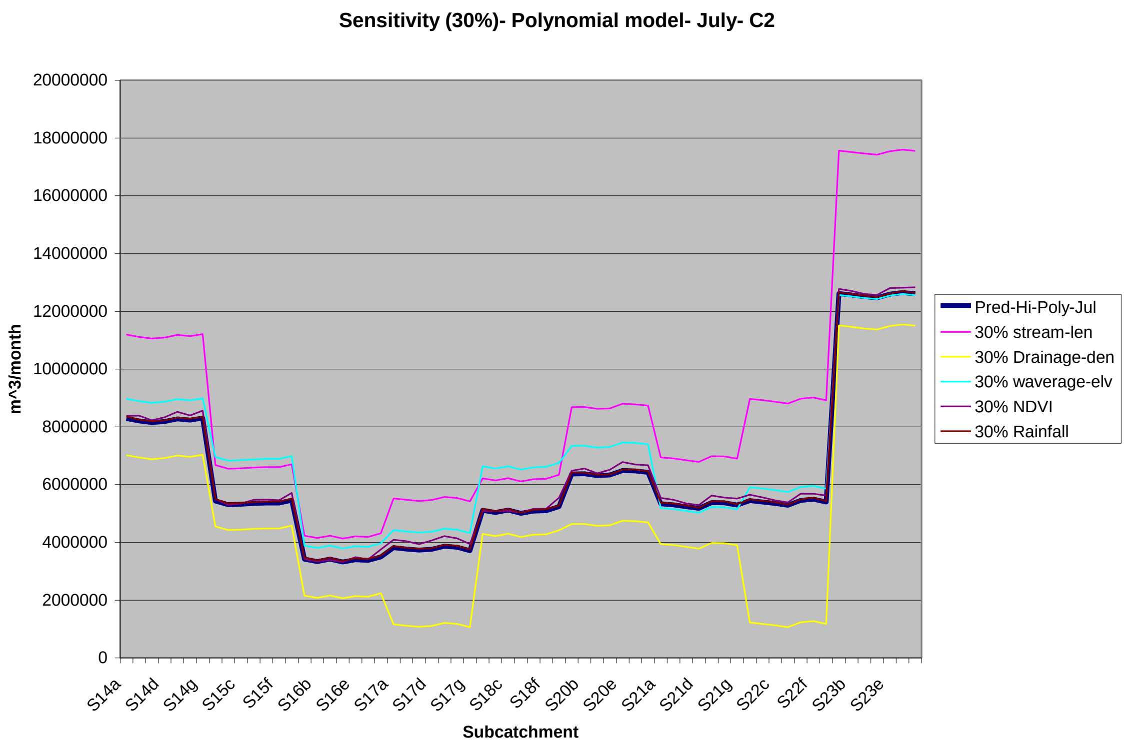

Figure C-171 Sensitivity (30%) – Polynomial model –July C2

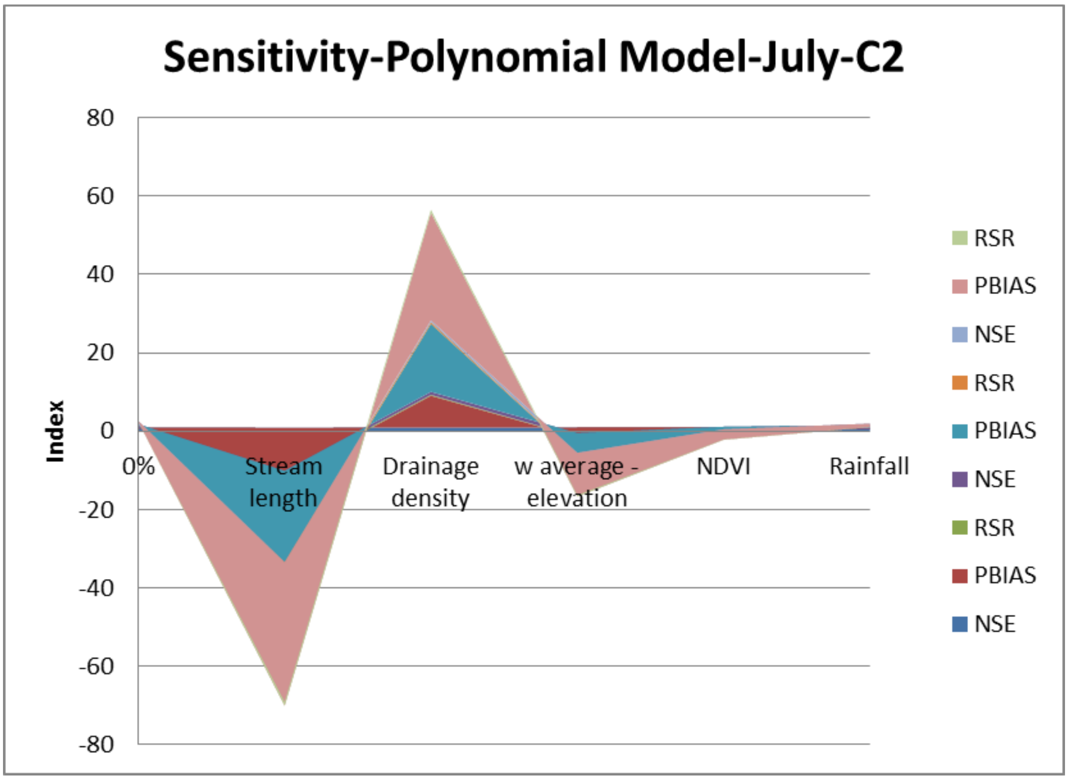

Figure C-172 Sensitivity summary – Polynomial model –July C2

Table C-43 Summary performance- Polynomial model- July C2

		10%				
	0%	Stream length	Drainage density	w average – elevation	NDVI	Rainfall
NSE	0.996932	0.896433	0.946649	0.98973	0.996415	0.996841
PBIAS	-0.23242	-11.8795	8.114652	-2.49098	-0.89412	-0.46248
RSR	0.055393	0.321818	0.230979	0.10134	0.059879	0.056201
		20%				
	0%	Stream length	Drainage density	w average – elevation	NDVI	Rainfall
NSE	0.996932	0.582619	0.769515	0.958658	0.994849	0.996692
PBIAS	-0.23242	-24.011	17.34106	-6.13002	-1.70999	-0.68969
RSR	0.055393	0.64605	0.480089	0.203327	0.071768	0.057519
		30%				
	0%	Stream length	Drainage density	w average – elevation	NDVI	Rainfall
NSE	0.996932	0.027669	0.429521	0.882775	0.991711	0.996484
PBIAS	-0.23242	-36.6271	27.4468	-11.1495	-2.68001	-0.91406
RSR	0.055393	0.986068	0.7553	0.342381	0.091046	0.059293

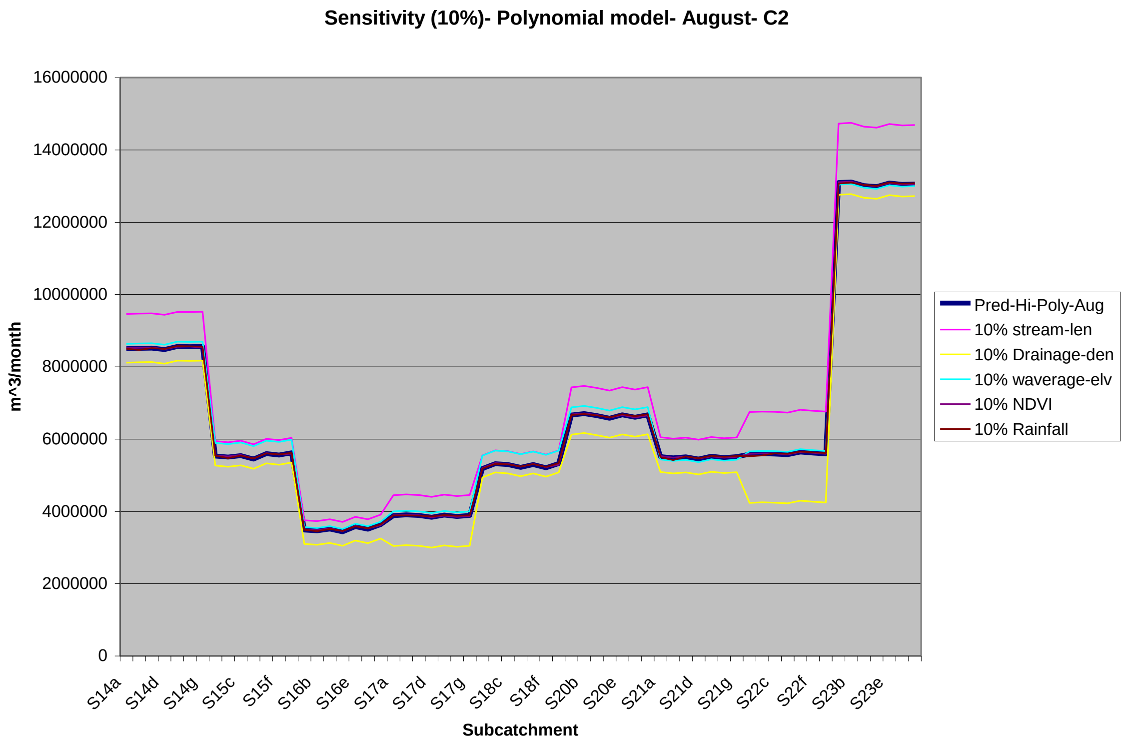

Figure C-173 Sensitivity (10%) – Polynomial model –August C2

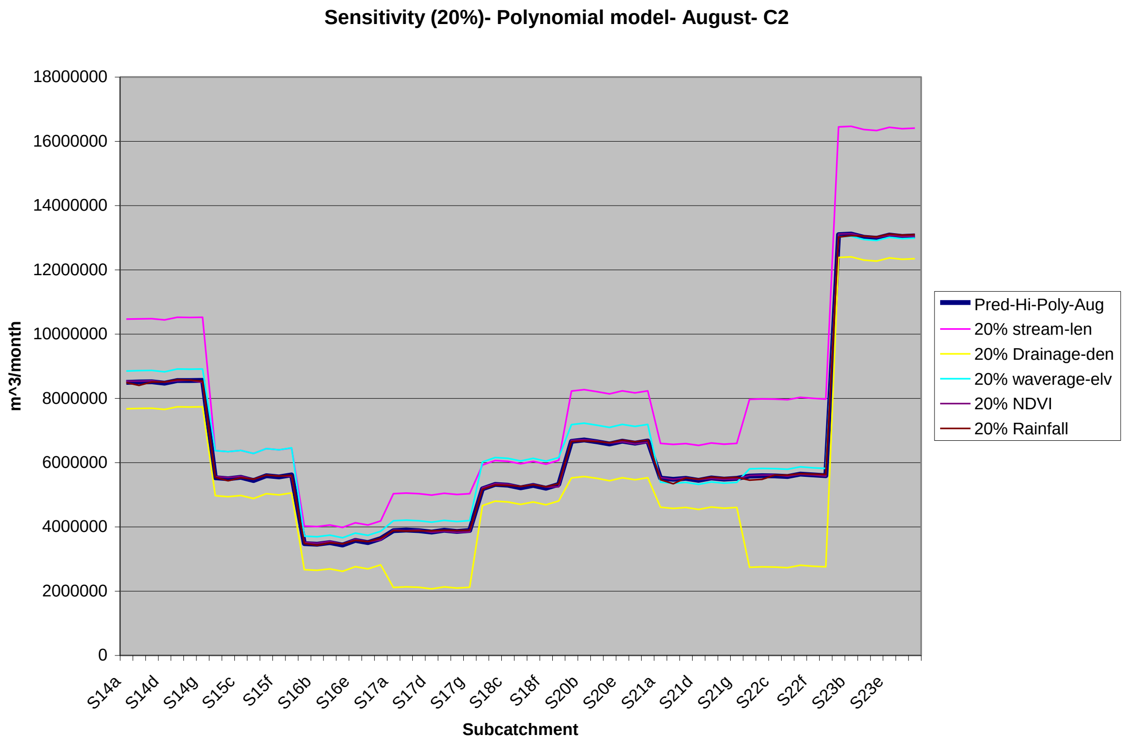

Figure C-174 Sensitivity (20%) – Polynomial model –August C2

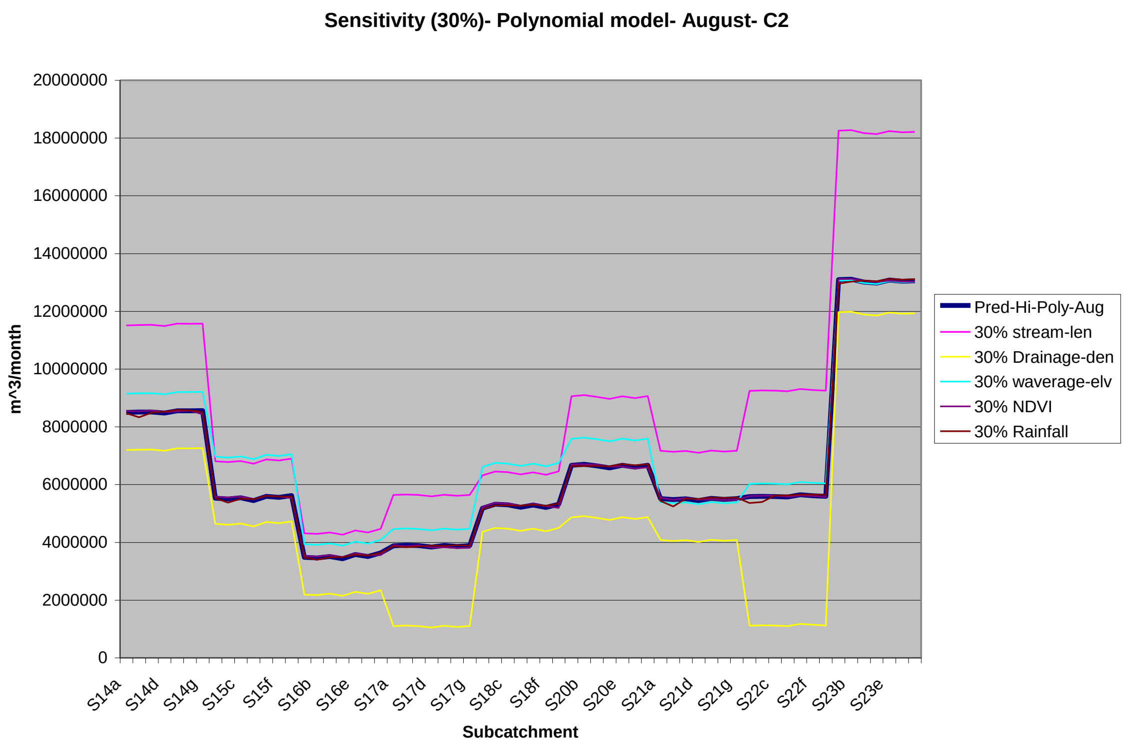

Figure C-175 Sensitivity (30%) – Polynomial model –August C2

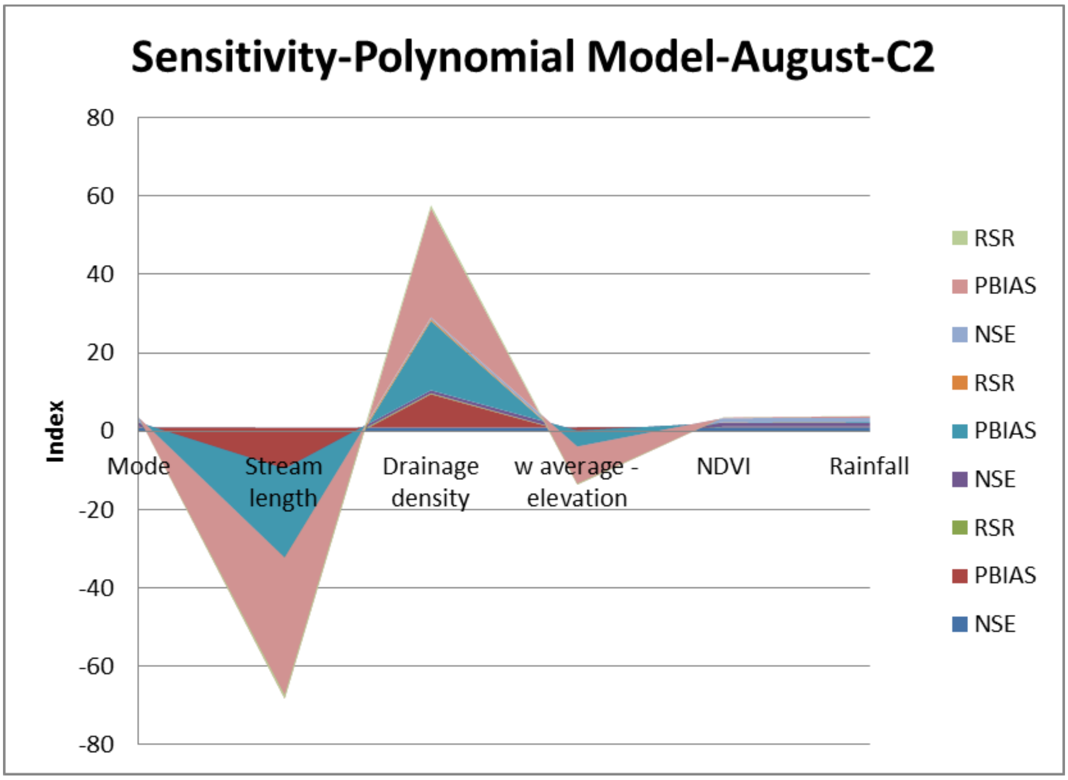

Figure C-176 Sensitivity summary – Polynomial model –August C2

Table C-44 Summary performance- Polynomial model- August C2

		10%				
	0%	Stream length	Drainage density	w average - elevation	NDVI	Rainfall
NSE	0.996587	0.902444	0.941986	0.99189	0.996588	0.996554
PBIAS	0.232336	-11.344	8.508969	-1.85606	0.130325	0.153587
RSR	0.058418	0.31234	0.240862	0.090054	0.058412	0.058702
		20%				
	0%	Stream length	Drainage density	w average - elevation	NDVI	Rainfall
NSE	0.996587	0.596194	0.758432	0.968201	0.996511	0.996352
PBIAS	0.232336	-23.4183	17.71427	-5.17769	0.106138	0.195809
RSR	0.058418	0.635457	0.491495	0.178323	0.059064	0.060397
		30%				
	0%	Stream length	Drainage density	w average - elevation	NDVI	Rainfall
NSE	0.996587	0.049287	0.407662	0.908506	0.99633	0.995895
PBIAS	0.232336	-35.9907	27.84825	-9.73253	0.159777	0.359003
RSR	0.058418	0.975045	0.769635	0.30248	0.060583	0.064073

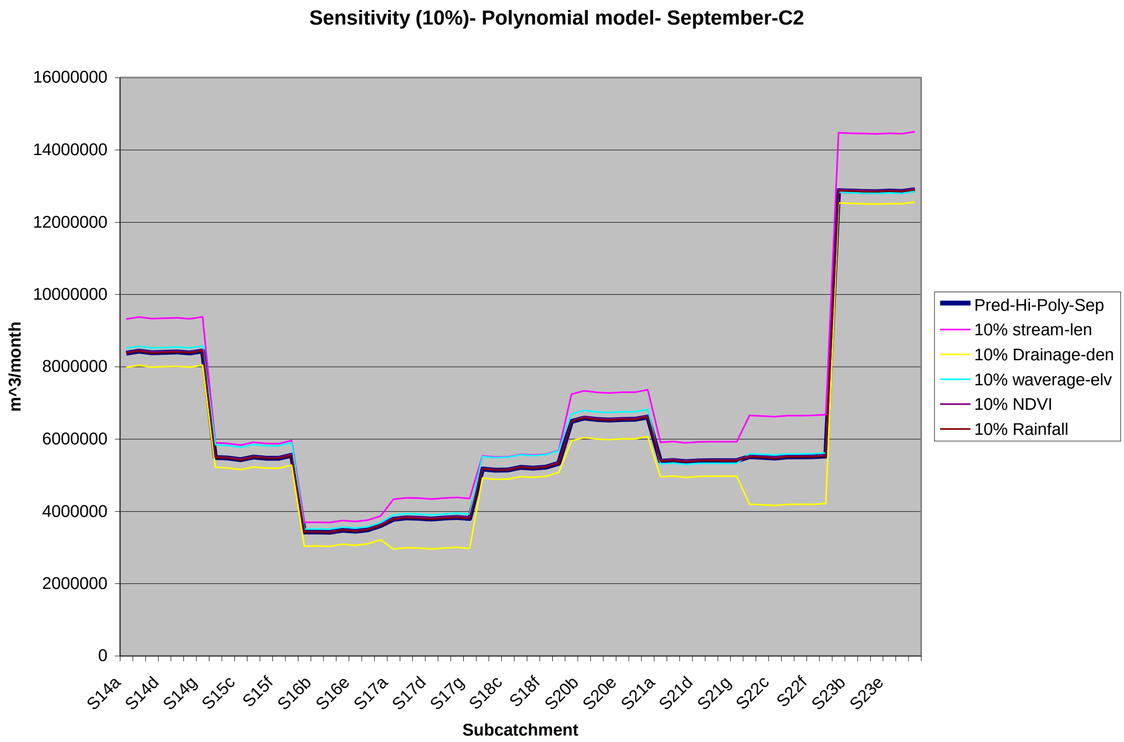

Figure C-177 Sensitivity (10%) – Polynomial model –September C2

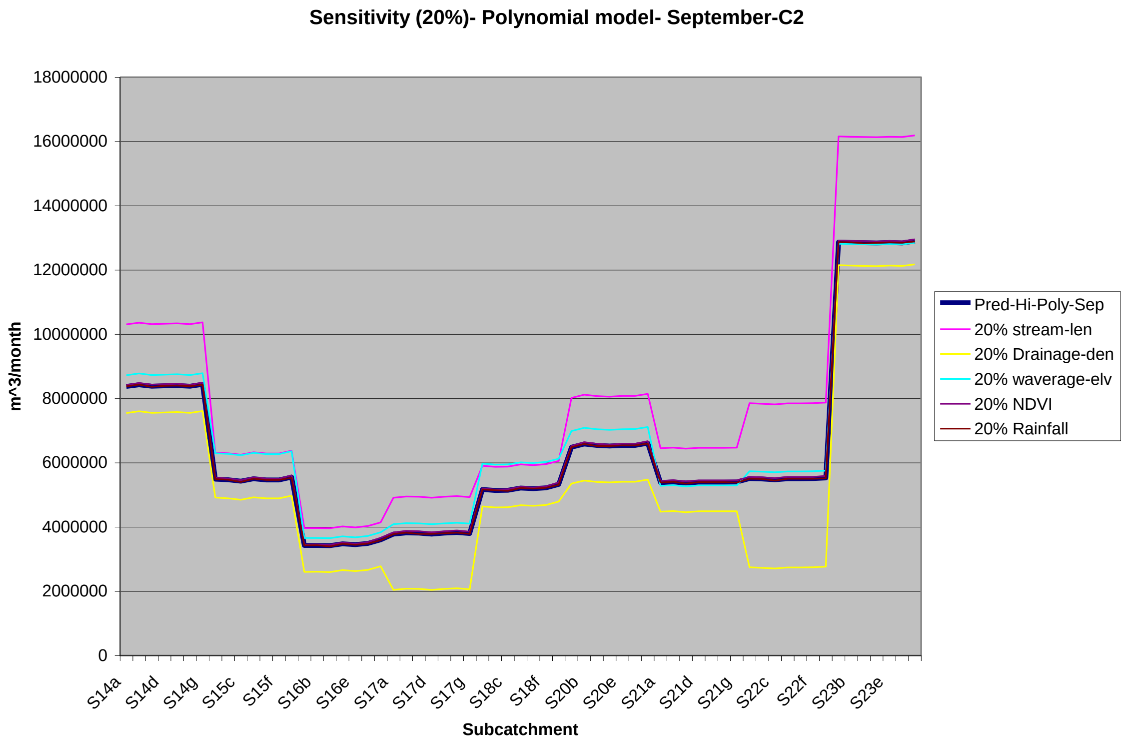

Figure C-178 Sensitivity (20%) – Polynomial model –September C2

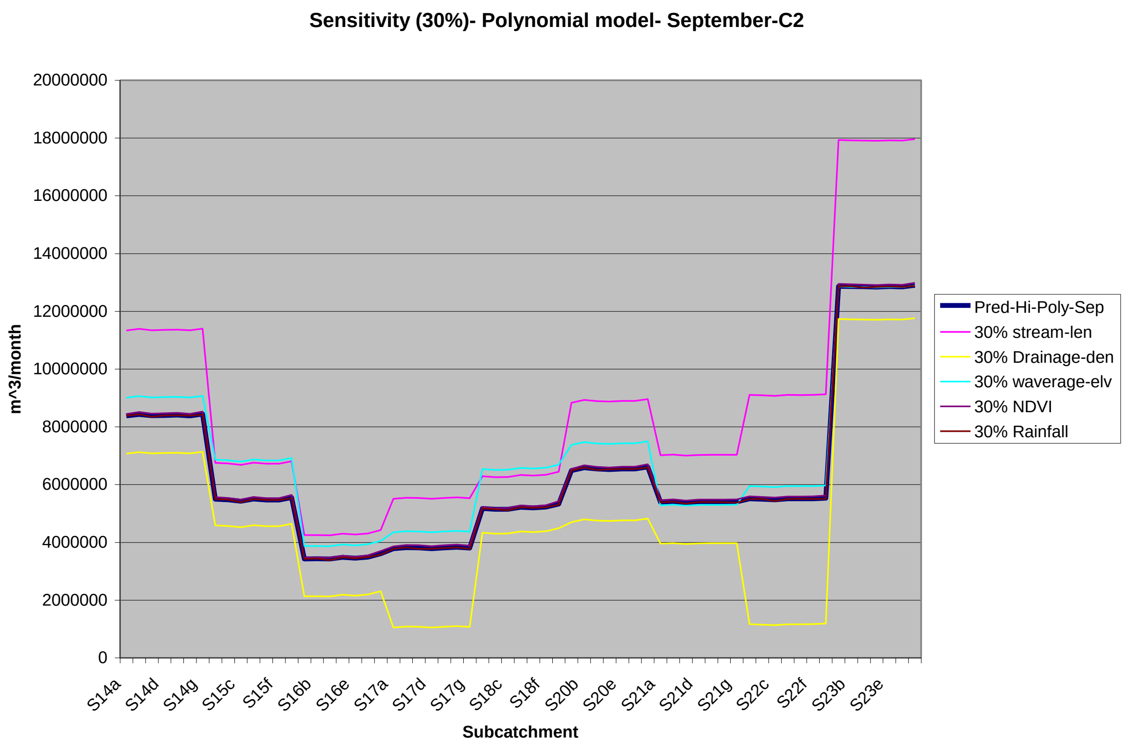

Figure C-179 Sensitivity (30%) – Polynomial model –September C2

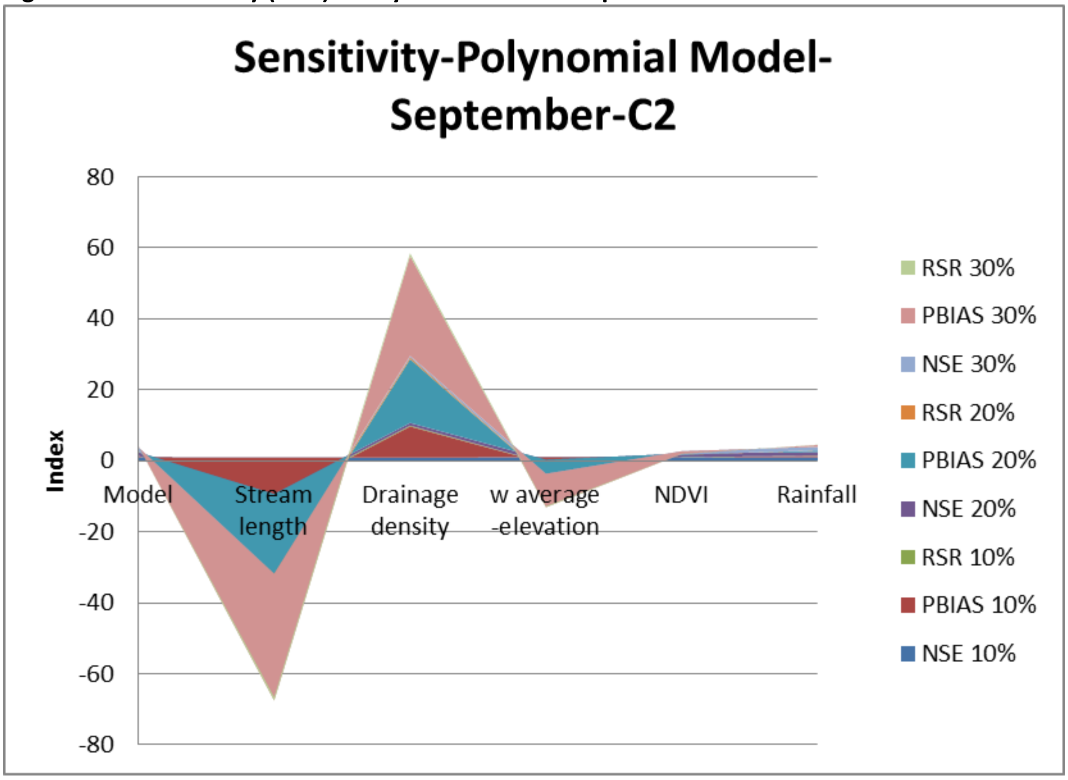

Figure C-180 Sensitivity (30%) – Polynomial model –September C2

Table C-45 Summary performance- Polynomial model- September C2

		10%				
	0%	Stream length	Drainage density	w average - elevation	NDVI	Rainfall
NSE	0.996567	0.90593	0.939935	0.991937	0.996662	0.996551
PBIAS	0.375013	-11.1587	8.738603	-1.74094	-0.00564	0.400386
RSR	0.058594	0.306709	0.245083	0.089792	0.057775	0.058726
		20%				
	0%	Stream length	Drainage density	w average - elevation	NDVI	Rainfall
NSE	0.996567	0.605216	0.755167	0.969375	0.996592	0.996519
PBIAS	0.375013	-23.185	17.98536	-5.01968	-0.38629	0.446809
RSR	0.058594	0.628318	0.494806	0.175001	0.058382	0.059004
		30%				
	0%	Stream length	Drainage density	w average - elevation	NDVI	Rainfall
NSE	0.996567	0.066314	0.406008	0.913161	0.996355	0.996463
PBIAS	0.375013	-35.7041	28.1153	-9.46122	-0.76695	0.514282
RSR	0.058594	0.966274	0.770709	0.294685	0.060372	0.059475

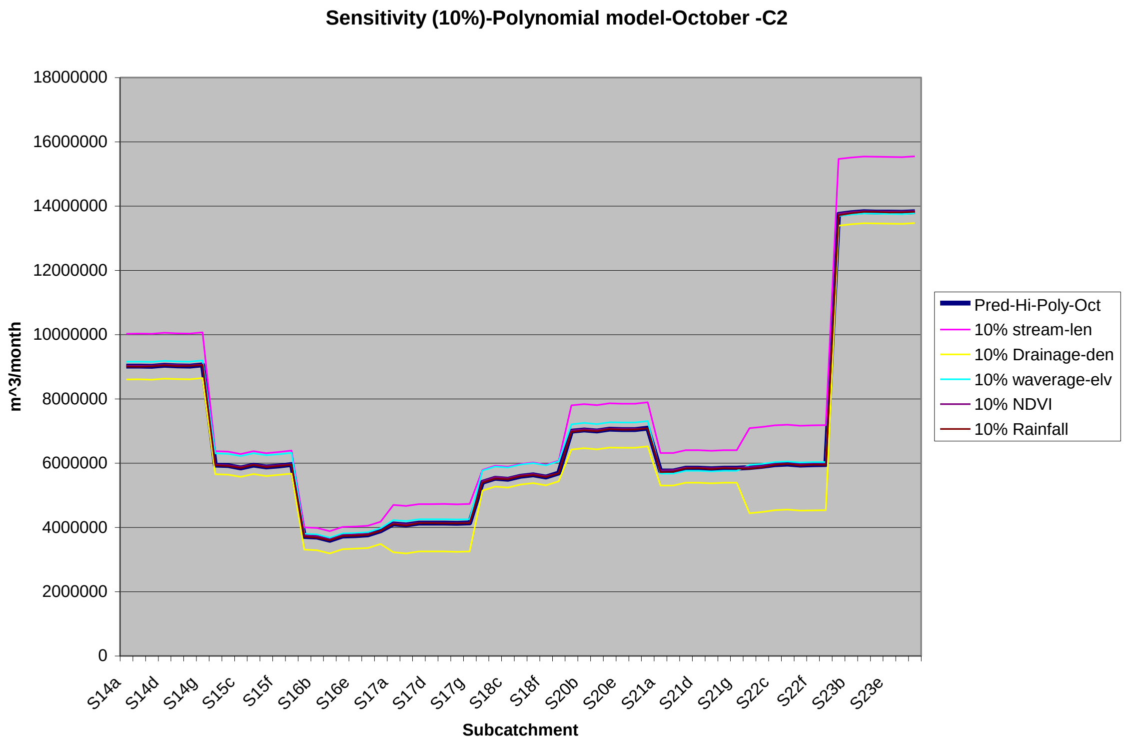

Figure C-181 Sensitivity (10%) – Polynomial model –October C2

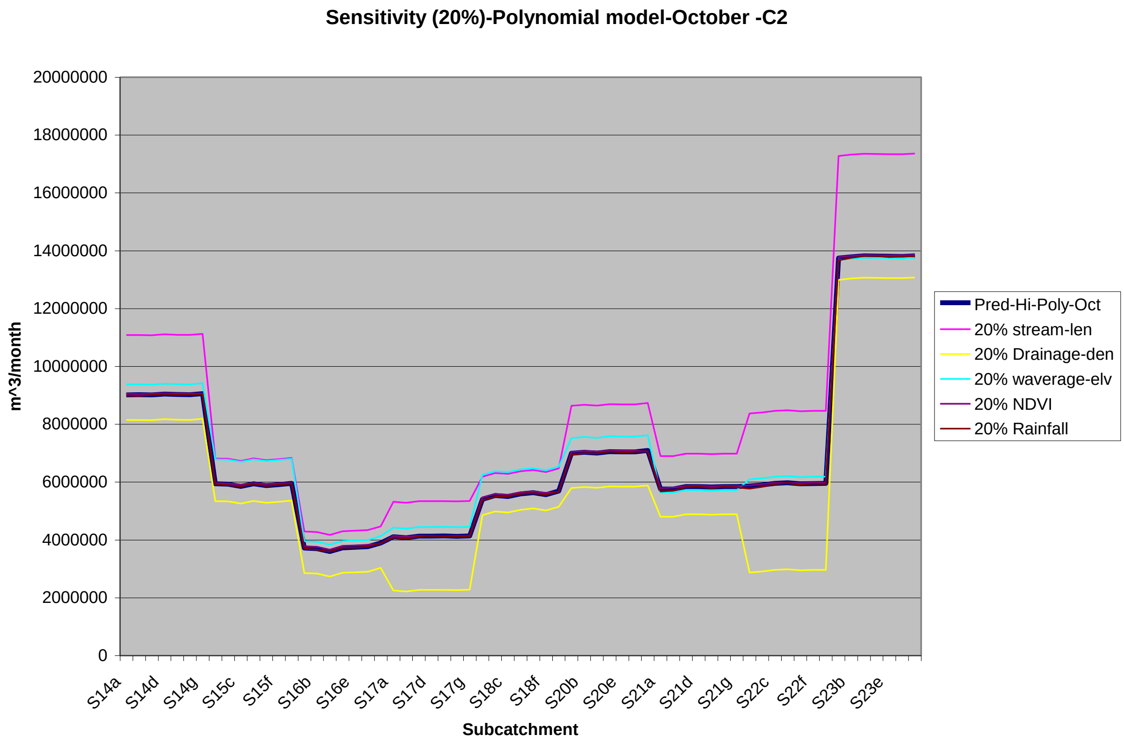

Figure C-182 Sensitivity (20%) – Polynomial model –October C2

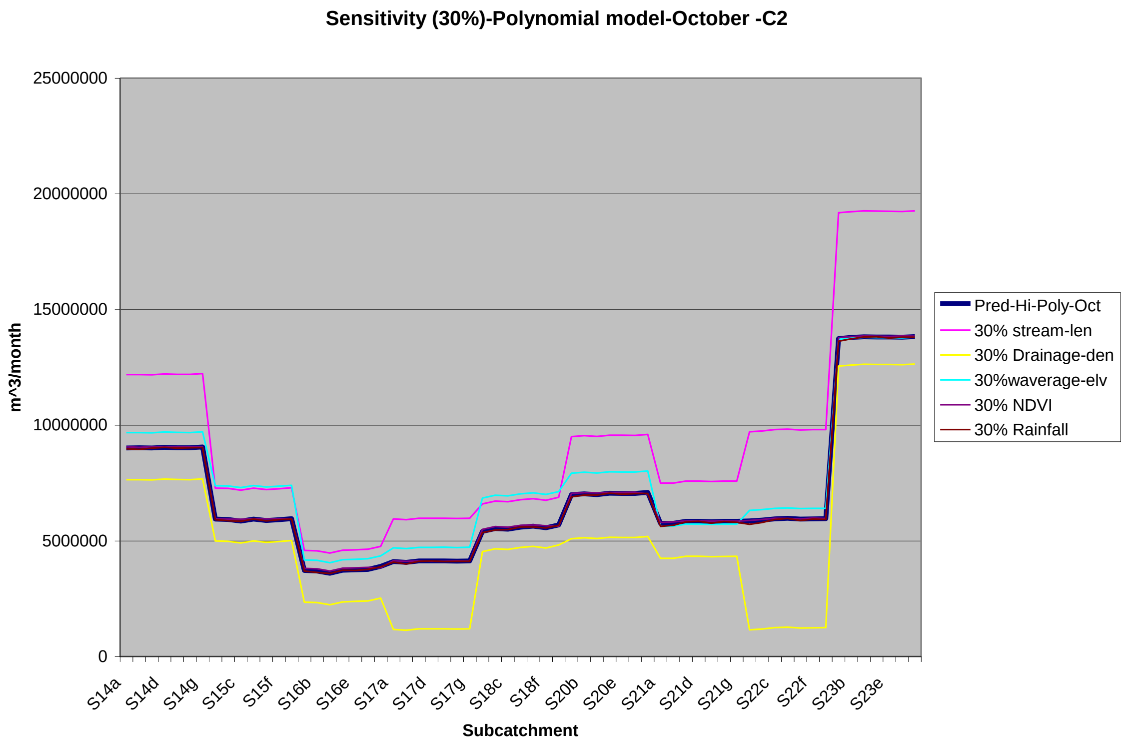

Figure C-183 Sensitivity (30%) – Polynomial model –October C2

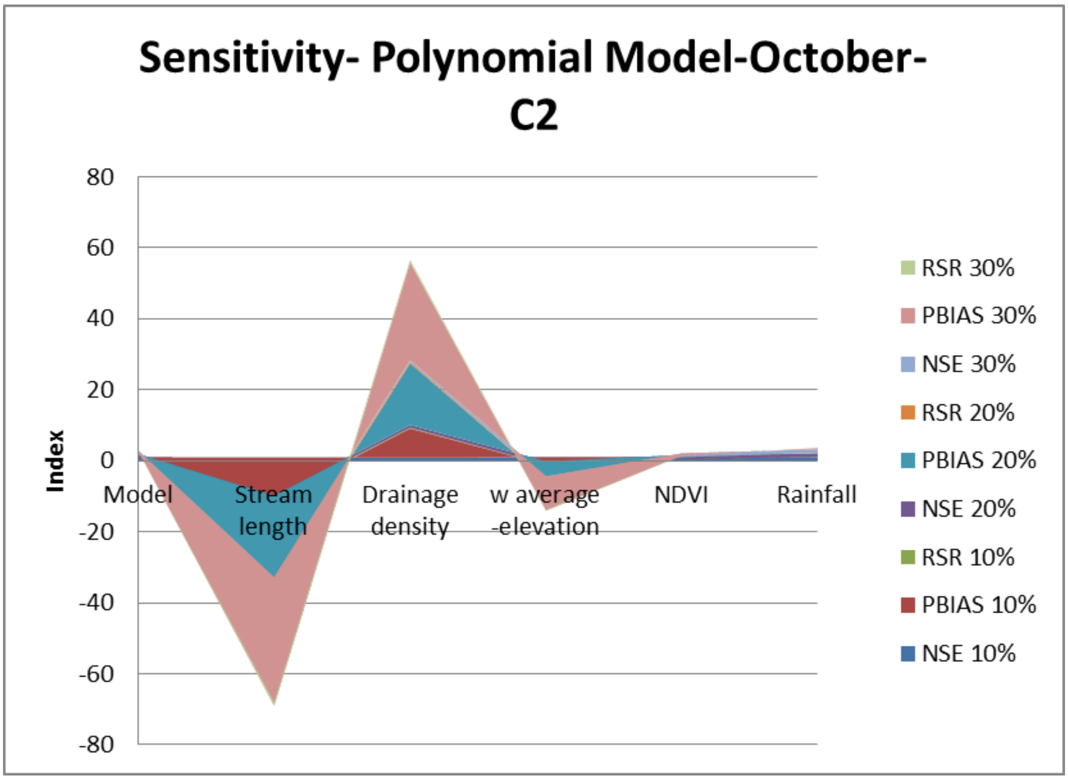

Figure C-184 Sensitivity summary – Polynomial model –October C2

Table C-46 Summary performance- Polynomial model- October C2

		10%				
	0%	Stream length	Drainage density	w average - elevation	NDVI	Rainfall
NSE	0.996682	0.899107	0.94529	0.991401	0.996581	0.996677
PBIAS	-0.11896	-11.6417	8.159502	-2.14271	-0.41864	-0.00502
RSR	0.057603	0.317637	0.233902	0.092733	0.058468	0.057645
		20%				
	0%	Stream length	Drainage density	w average - elevation	NDVI	Rainfall
NSE	0.996682	0.590729	0.765702	0.968254	0.996437	0.996621
PBIAS	-0.11896	-23.6651	17.35996	-5.33427	-0.59193	0.151245
RSR	0.057603	0.639743	0.484043	0.178173	0.059694	0.058128
		30%				
	0%	Stream length	Drainage density	w average - elevation	NDVI	Rainfall
NSE	0.996682	0.042939	0.419987	0.9118	0.996295	0.996481
PBIAS	-0.11896	-36.1892	27.4824	-9.69364	-0.63882	0.349846
RSR	0.057603	0.978295	0.761586	0.296985	0.060865	0.059323

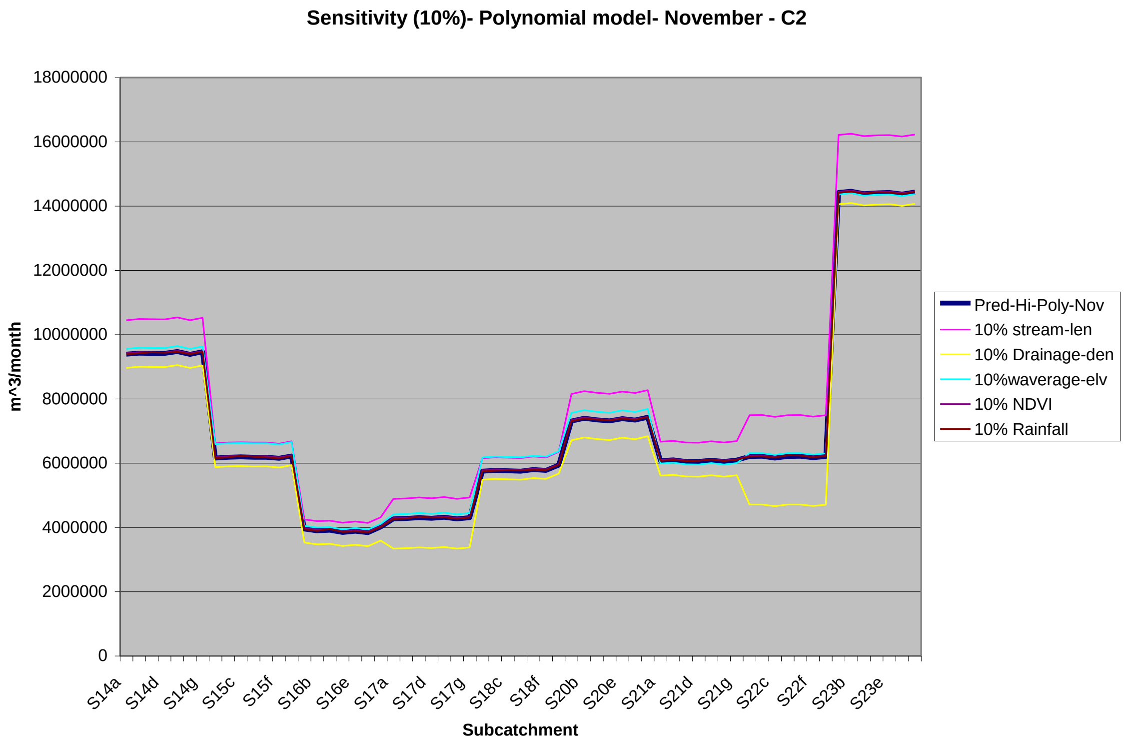

Figure C-185 Sensitivity (10%) – Polynomial model –November C2

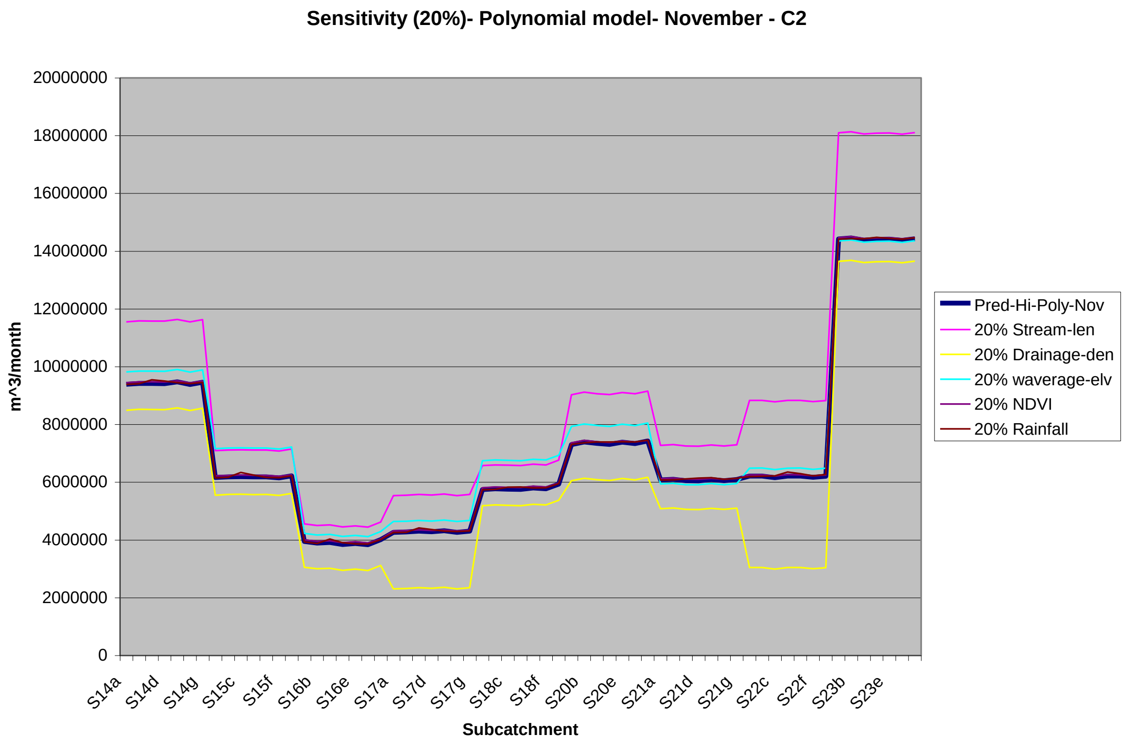

Figure C-186 Sensitivity (20%) – Polynomial model –November C2

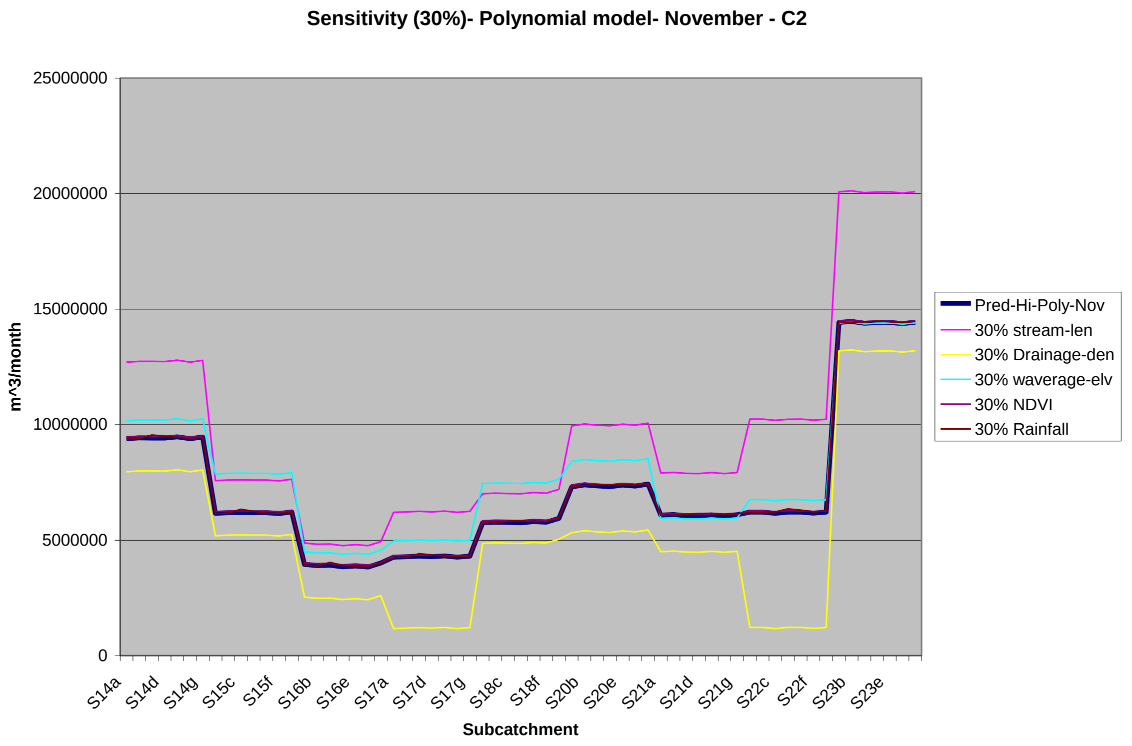

Figure C-187 Sensitivity (30%) – Polynomial model –November C2

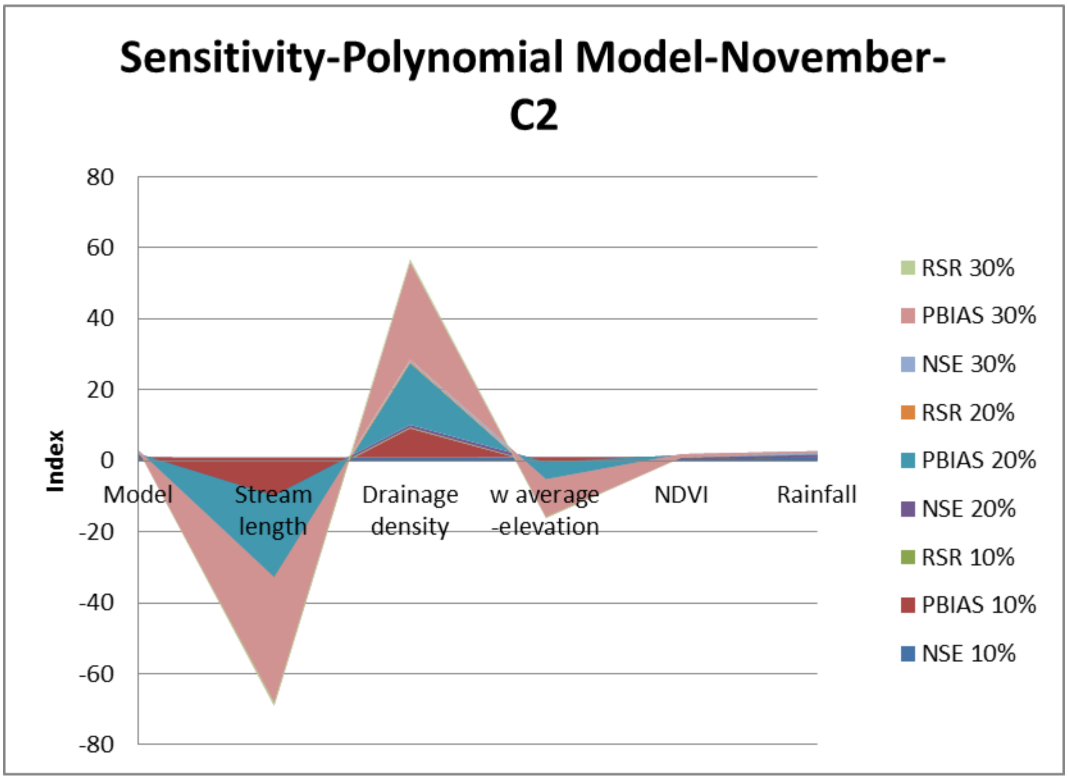

Figure C-188 Sensitivity summary – Polynomial model –November C2

Table C-47 Summary performance- Polynomial model- November C2

		10%				
	0%	Stream length	Drainage density	w average - elevation	NDVI	Rainfall
NSE	0.996573	0.899594	0.944123	0.990076	0.996465	0.99655
PBIAS	-0.04878	-11.6155	8.208269	-2.35802	-0.44032	-0.10601
RSR	0.058539	0.316869	0.236384	0.099619	0.059453	0.058734
		20%				
	0%	Stream length	Drainage density	w average - elevation	NDVI	Rainfall
NSE	0.996573	0.592005	0.761539	0.960903	0.996253	0.996454
PBIAS	-0.04878	-23.6666	17.42226	-5.97595	-0.7479	-0.2505
RSR	0.058539	0.638745	0.488325	0.197729	0.06121	0.059551
		30%				
	0%	Stream length	Drainage density	w average - elevation	NDVI	Rainfall
NSE	0.996573	0.046158	0.409175	0.889472	0.996015	0.996218
PBIAS	-0.04878	-36.2021	27.59318	-10.9026	-0.97152	-0.48225
RSR	0.058539	0.976648	0.768652	0.332457	0.063124	0.061495

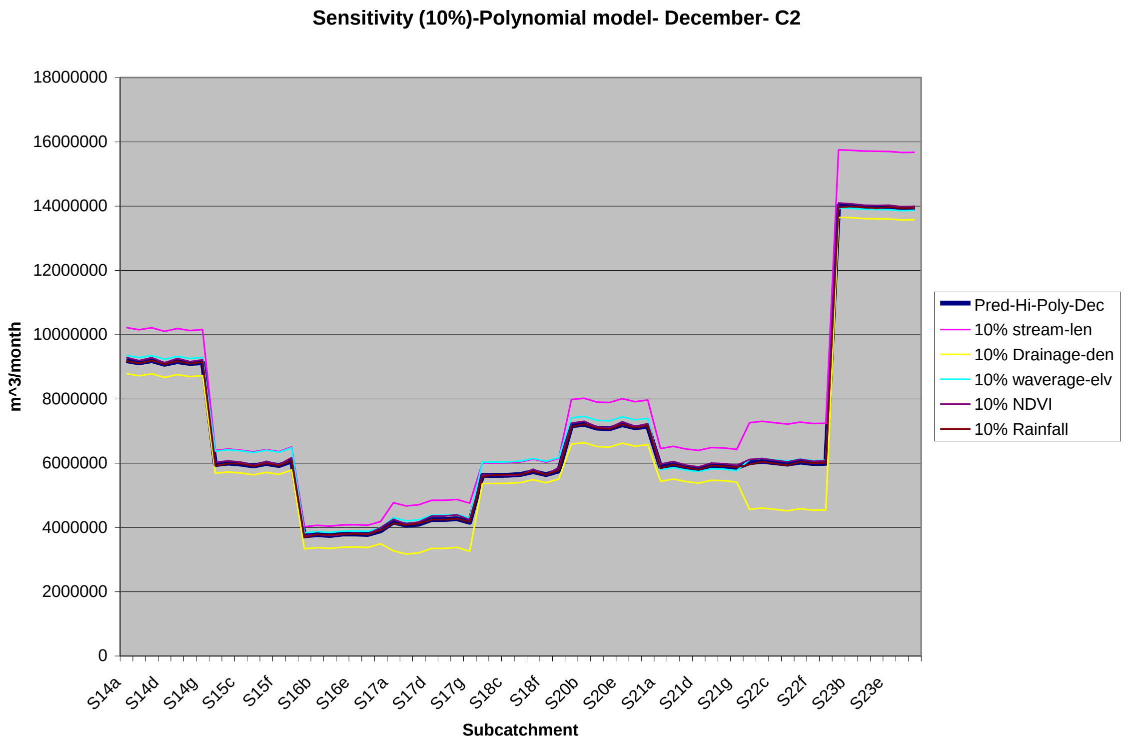

Figure C-189 Sensitivity (10%) – Polynomial model –December C2

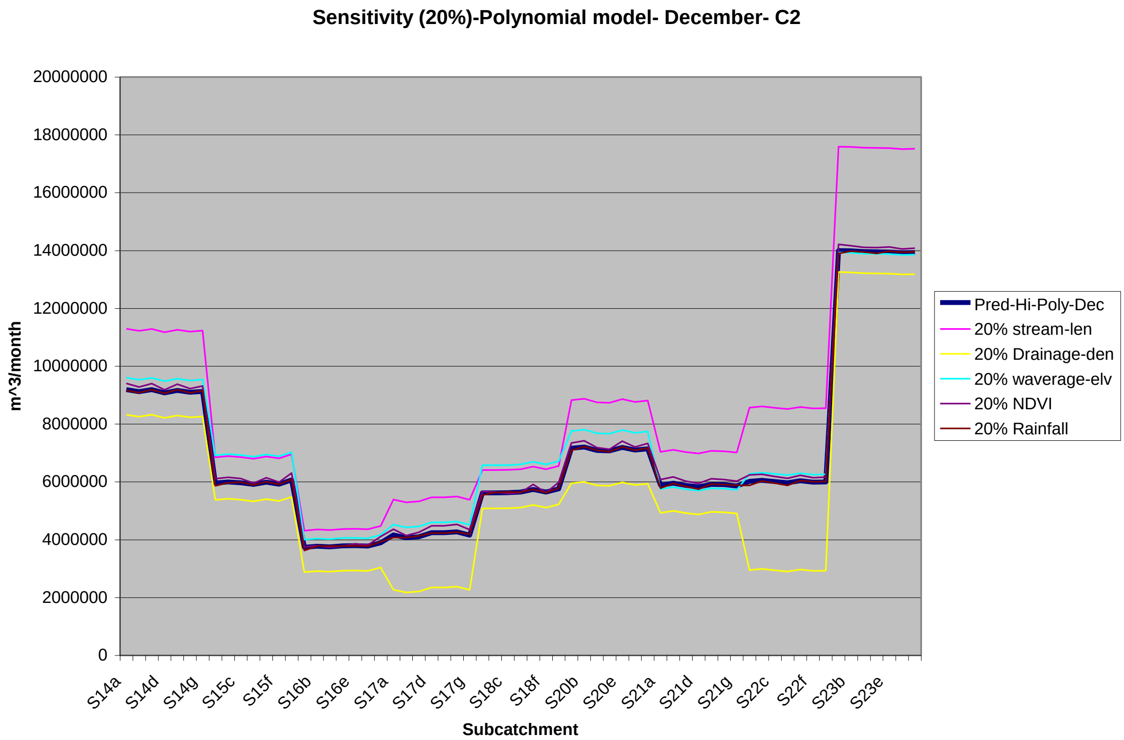

Figure C-190 Sensitivity (20%) – Polynomial model –December C2

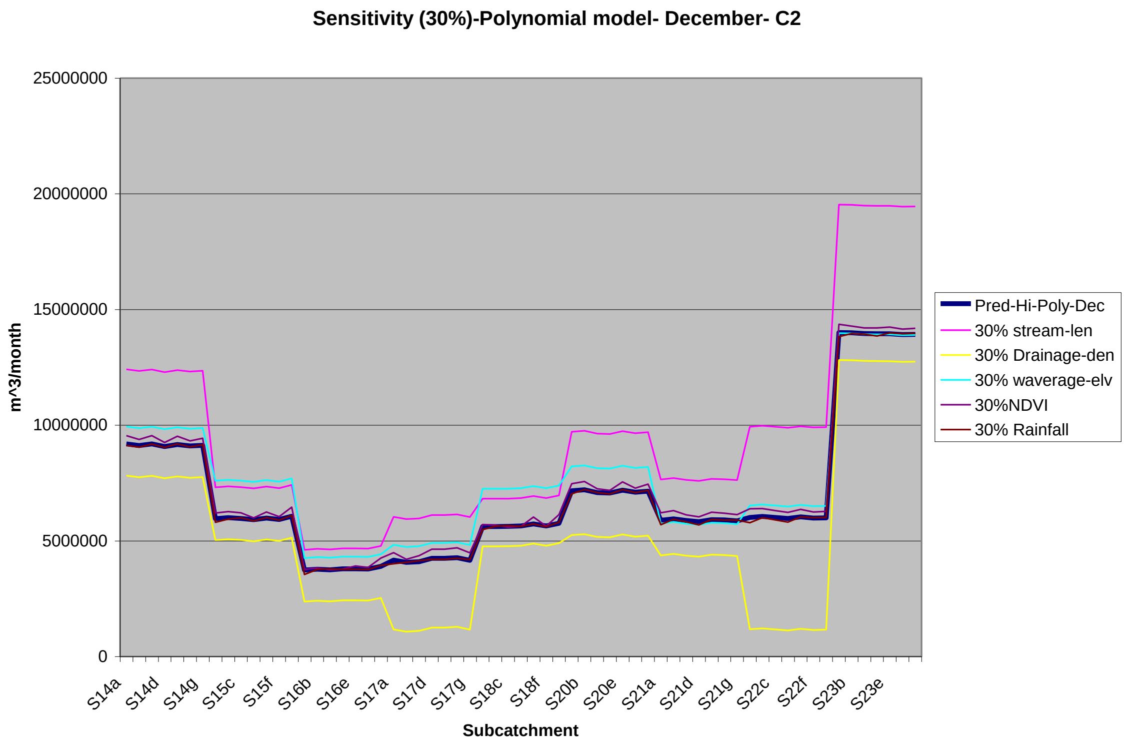

Figure C-191 Sensitivity (30%) – Polynomial model –December C2

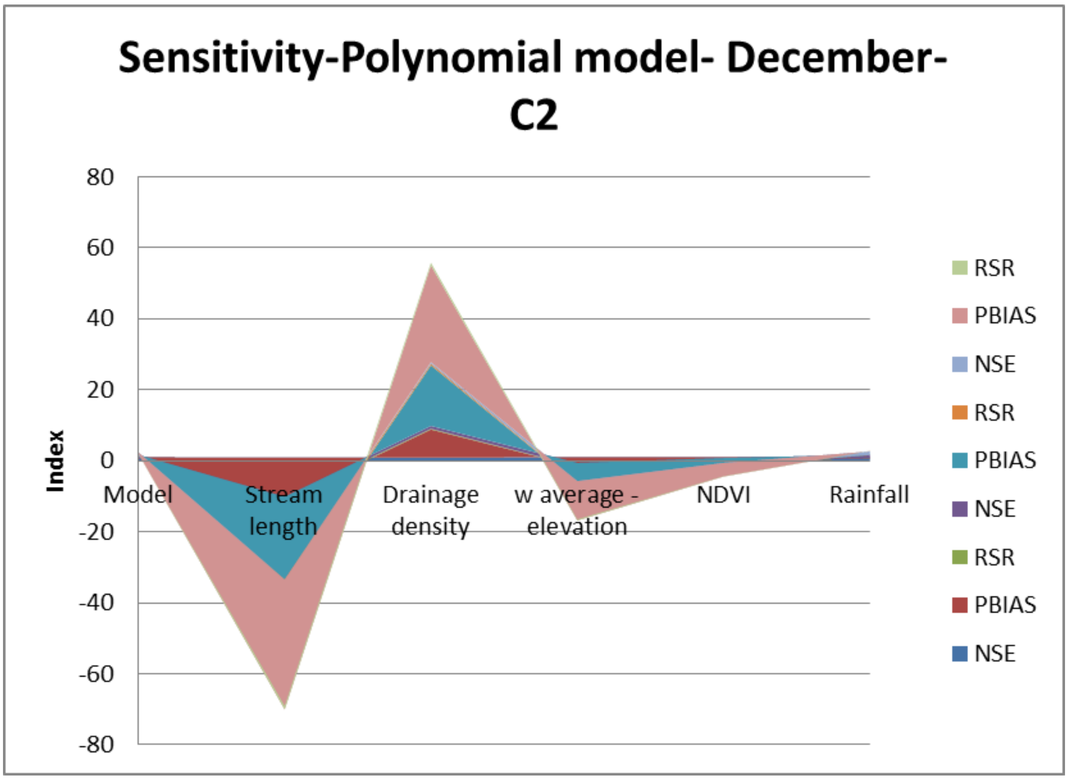

Figure C-192 Sensitivity summary – Polynomial model –December C2

Table C-48 Summary performance- Polynomial model- December C2

		10%				
	0%	Stream length	Drainage density	w average - elevation	NDVI	Rainfall
NSE	0.996569	0.895327	0.946896	0.989234	0.995628	0.996535
PBIAS	-0.35105	-11.9216	7.875805	-2.63457	-1.26522	-0.31821
RSR	0.058571	0.323532	0.230443	0.103759	0.066122	0.058868
		20%				
	0%	Stream length	Drainage density	w average - elevation	NDVI	Rainfall
NSE	0.996569	0.580897	0.767475	0.959117	0.992737	0.99641
PBIAS	-0.35105	-24.0001	17.06889	-6.21998	-2.43752	-0.1571
RSR	0.058571	0.647382	0.482208	0.202196	0.085225	0.059919
		30%				
	0%	Stream length	Drainage density	w average - elevation	NDVI	Rainfall
NSE	0.996569	0.024089	0.418291	0.886901	0.986746	0.996071
PBIAS	-0.35105	-36.5866	27.22821	-11.1073	-3.86797	0.132288
RSR	0.058571	0.987882	0.762698	0.336303	0.115126	0.062679